UNITED STATES
NUCLEAR REGULATORY COMMISSION
WASHINGTON, D.C. 20555-0001

ppr: per C. Lui

November 21, 1996

MEMORANDUM TO: John H. Austin, Chief
Performance Assessment and HLW
Integration Branch, DWM
Office of Nuclear Material Safety and Safeguards

David J. Brooks, Acting Chief
Engineering and Geosciences Branch, DWM
Office of Nuclear Material Safety and Safeguards

FROM: Christiana H. Lui
Performance Assessment and Integration Section
Performance Assessment and HLW
Integration Branch, DWM
Office of Nuclear Material Safety and Safeguards

Philip S. Justus for P. Justus
Geosciences and Hydrology Review Section
Engineering and Geosciences Branch, DWM
Office of Nuclear Material Safety and Safeguards

SUBJECT: TRIP REPORT FOR PROBABILISTIC SEISMIC HAZARD ANALYSIS - SEISMIC SOURCE CHARACTERIZATION WORKSHOP #2, SALT LAKE CITY, UTAH, OCTOBER 16-18, 1996

DOE held a second workshop on seismic source characterization (SSC) for the proposed high-level waste repository at Yucca Mountain (YM), Nevada, on October 16-18, 1996. SSC is part of the probabilistic seismic hazard analysis (PSHA) study being conducted by DOE. The objective of this PSHA study is to provide the annual probability with which various levels of vibratory ground motion and fault displacement may be exceeded at the YM site. These results will be used as a basis for developing seismic design inputs and in assessing the pre- and post-closure performance of the YM site and facilities.

The main goals of this second SSC workshop were to review the data that are available for the YM region, and to identify available methodologies for characterizing seismic sources for the YM site. Philip Justus and Christiana Lui attended this workshop as observers from NRC. John Stamatakos (CNWRA) also attended and was invited to present relevant and new data from studies conducted by the CNWRA.

The workshop started with an introductory session. Tim Sullivan (DOE) gave a brief update of the related YM programs since the first workshop which was held in April 1995. Carl Stepp (Woodward-Clyde) followed. He presented the schedule and related milestones for PSHA, and introduced members of the PSHA peer review panel. He also stated that a participatory peer review process where the reviewers attend each workshop and provide their informal inputs to Carl Stepp after each workshop has been adopted for this study.

NH16

WM-11 46 15.3

102

Deletion

Kevin Coppersmith (Geomatrix) wrapped up this introductory session by providing a process overview, guidelines for the workshop, a list of SSC subject-matter experts and facilitation team members, and the goals for the upcoming SSC workshops. The agenda, list of attendees and reprints of presentations by Tim Sullivan, Carl Stepp and Kevin Coppersmith are included as Attachment 1, Attachment 2, Attachment 3, Attachment 4 and Attachment 5, respectively. The remainder of this workshop was devoted to the presentation and discussion of relevant data and methodologies. Attachment 6 contains reprints of these technical presentations as enumerated in the workshop agenda and other relevant technical articles that were available to the NRC staff during the workshop.

DOE has chosen to implement a formal expert elicitation process for the performance of PSHA. For SSC, six subject-matter experts were selected from each of three disciplines: seismology/geophysics, tectonics/regional geology and Quaternary geology/paleoseismology. Tim Sullivan provided a copy of biographical sketch of each of the subject-matter experts to the NRC. Note that due to the long lag time between the first and second SSC workshops, Anthony J. Crone is no longer on the panel. He has been replaced by Peter L.K. Knuepfer. All biographical sketches are included as Attachment 7. During this SSC workshop, six three-member expert teams were formed by random drawing. Each team contains one subject-matter expert from each of the three disciplines. The membership of these expert teams is listed in Attachment 8. Members of individual teams are expected to collaborate such that only one assessment will be elicited from each team during the elicitation session.

Prior to the conclusion of this workshop, a copy of the Management Procedures Manual on "Scientific Expert Elicitation" (YMP-USGS-QMP-3.16, R0) was distributed. All subject-matter experts were asked to sign a statement certifying that they have received and read the procedure during the workshop. A copy of this procedure is included as Attachment 9.

During the feedback sessions at the end of each day, the NRC and CNWRA provided technical inputs to the group as appropriate. Philip Justus clarified aspects of QA as required to support a license application, and emphasized distinctions between Type I faults in NUREG-1451 and faults as a Type I seismic source in "Recommendations for Probabilistic Seismic Hazard Analysis: Guidance on Uncertainty and Use of Experts" (also known as the "SSHAC" report). John Stamatakos announced the impending availability of CNWRA's list of Type I faults.

DOE and NRC also met to discuss issues related to the implementation of an expert judgment elicitation process outside the main workshop. Issues discussed were: (1) status of DOE's decision criteria and procedure for updating the elicited judgments; (2) the need to document changes made to the elicited judgments based on the feedback; (3) status of the SSHAC report; (4) the various expert roles as delineated in the SSHAC report (i.e., proponent, evaluator and technical facilitator/integrator); (5) robustness of the final results with regard to the use of individual experts versus expert teams; and (6) documenting and disclosing potential conflict of interest (COI). Christiana Lui and Tim Sullivan exchanged view points regarding the first five issues. For the last issue, DOE is seeking input on acceptable

approaches to disclosing and documenting potential COIs because, by design, NRC's "Branch Technical Position on the Use of Expert Elicitation in the High-Level Waste Program" does not recommend any specific means for accomplishing this goal.

The third SSC workshop will be held at Amargosa Valley, Nevada, on November 18-21, 1996. The main goal of this third workshop will be to discuss alternative models, hypotheses, and interpretations that are important to the characterization of seismic sources for vibratory ground motion hazard and fault displacement hazard. Several field trips to the YM region will be included as part of this third workshop. The elicitations are currently scheduled to take place during February and March 1997, followed by a feedback workshop in April 1997. The final PSHA report is due to DOE from its contractor at the end of August 1997.

Attachments: As stated

Contact: C. Lui, DWM/PAHL
415-6200
P. Justus, DWM/ENGB
415-6745

approaches to disclosing and documenting potential COIs because, by design, NRC's "Branch Technical Position on the Use of Expert Elicitation in the High-Level Waste Program" does not recommend any specific means for accomplishing this goal.

The third SSC workshop will be held at Amargosa Valley, Nevada, on November 18-21, 1996. The main goal of this third workshop will be to discuss alternative models, hypotheses, and interpretations that are important to the characterization of seismic sources for vibratory ground motion hazard and fault displacement hazard. Several field trips to the YM region will be included as part of this third workshop. The elicitations are currently scheduled to take place during February and March 1997, followed by a feedback workshop in April 1997. The final PSHA report is due to DOE from its contractor at the end of August 1997.
Attachments: As stated

Contact: C. Lui, DWM/PAHL
415-6200
P. Justus, DWM/ENGB
415-6745

DISTRIBUTION: w/o att
Central File NMSS r/f JThoma PAHL r/f JHickey
JHolonich MBell JSurmeier DWM r/f

s:\dwm\pahl\cxl\ssc2.rpt
Mark Small Boxes in Concurrence Block to Define Distribution Copy Preference.
In small Box on "OFC:" line enter: C = Cover E = Cover & Enclosure N = No Copy

OFC	PAHL	C	PAHL	C						
NAME	CLui/wd		KMcConnell							
DATE	11/21/96	H	11/21/96						/ /96	

OFFICIAL RECORD COPY
In small Box on "DATE:" line enter: M = E-Mail Distribution Copy H = Hard Copy

PDR : YES X NO ___ Category: Proprietary ___ or CF Only X
ACNW: YES ___ NO X
IG : YES ___ NO X Delete file after distribution: Yes X No ___

Received 11/21/96

AGENDA
SEISMIC SOURCE CHARACTERIZATION (SSC) HAZARD METHODOLOGIES WORKSHOP

October 16-18, 1996
Doubletree Hotel, Salt Lake City, Utah

GOAL OF THE WORKSHOP:

The workshop has two principal goals: to review the data that are available for the Yucca Mountain region, and to identify available methodologies for characterizing seismic sources for the Yucca Mountain seismic hazard analysis. The first goal is a follow-on to the first SSC workshop held in April of last year, because additional data have become available and/or synthesized in summary reports since that time.

APPROACH:

The approach used in this workshop to accomplish the above goals is to divide seismic source characterization into two parts: SSC related to vibratory ground motion hazard analysis and related to fault displacement hazard analysis. SSC is then divided into three components: seismic source location and geometry, maximum earthquake magnitude, and earthquake recurrence assessment. Each of these topics is first introduced by overview presentations that focus on the *methods and approaches* that are available to characterize them. These talks are then followed by a series of talks that describe the available *data bases and data interpretations* that relate to these topics. Although the presentations will undoubtedly entail some interpretations, the next workshop (Workshop #3 Alternative Models and Interpretations) will provide a forum for debating alternative interpretations of the available data. In the meantime, it is important that each member of the expert panel have an opportunity to understand the available methodologies and the available data bases for conducting the SSC.

WEDNESDAY, OCTOBER 16

8:30 - 10:00	**INTRODUCTION**
8:30 - 8:45	Welcome (T. Sullivan)
8:45 - 9:15	Yucca Mountain PSHA Project (C. Stepp)
9: 15 - 10:00	Overview of Process and Guidelines for Workshops (K. Coppersmith)
10:00 -10:15	BREAK

103

Attachment 1

9611260175

WEDNESDAY, OCTOBER 16 (CONT.)

10:15 - 4:15	**SEISMIC SOURCE CHARACTERIZATION FOR ASSESSING VIBRATORY GROUND MOTIONS—LOCATION AND GEOMETRY**
10:15 - 11:15	General Approach and Key Issues (W. Arabasz)
11:15 - 12:00	Methods for Assessing Location and Geometry of Seismic Sources (R. Bruhn)
12:00 - 1:00	**LUNCH**
1:00 - 1:45	Quaternary Fault Studies in the Site Area (C. Menges)
1:45 - 2:30	Quaternary Fault Studies in the Yucca Mountain Region (L. Anderson/E. Anderson)
2:30 - 2:45	**BREAK**
2:45 - 3:30	New Deep Seismic Reflection Line Data (T. Brocher)
3:30 - 4:15	Geometry Information from Seismicity Data (K. Smith)
4:15 - 4:30	Information on November Field Trip (K. Coppersmith)
4:30 - 5:00	**STATEMENTS FROM OBSERVERS**

THURSDAY, OCTOBER 17

8:30 - 11:45	**MAXIMUM EARTHQUAKE MAGNITUDE EVALUATION**
8:30 - 9:15	Methods for Assessing Maximum Magnitudes (K. Coppersmith)
9:15 - 10:00	Data Related to Segmentation and Displacement per Event on Site Area Faults (S. Pezzopane)
10:00 - 10:15	**BREAK**
10:15 - 11:00	Relation between Rupture Length, Slip Rate, and Magnitude (J. Anderson)
11:00 - 4:30	**EARTHQUAKE RECURRENCE EVALUATION**
11:00 - 11:45	Methods for Assessing Earthquake Recurrence (J. McCalpin)
11:45 - 12:45	**LUNCH**
12:45 - 1:30	Yucca Mountain Slip Rate and Recurrence Interval Data (J. Whitney)
1:30 - 2:15	Evidence for Temporal Clustering on the Solitario Canyon Fault (A. Ramelli)
2:15 - 3:00	CNWRA Fault Studies in the Yucca Mountain Region (J. Stamatakos)
3:00 - 3:15	**BREAK**
3:15 - 3:45	Global Positioning System Data (CNWRA data - J. Stamatakos; USGS data - S. Pezzopane)
3:45 - 4:30	Earthquake Catalog Analysis (I. Wong)
4:30 - 5:00	**STATEMENTS FROM OBSERVERS**

FRIDAY, OCTOBER 18

8:30 - 2:30	**SEISMIC SOURCE CHARACTERIZATION FOR FAULT DISPLACEMENT ANALYSIS**
8:30 - 9:30	Methods for Assessing Fault Displacement Hazard (R. Youngs)
9:30 - 10:15	Mapping of Yucca Mountain Block (W. Day)
10:15 - 10:30	**BREAK**
10:30 - 11:00	Fractures and Faults Mapped in the ESF (R. Lung)
11:00 - 11:45	Yucca Mountain Geophysical Data (M. Feighner)
11:45 - 12:15	Ghost Dance Fault Paleoseismic Data (J. Whitney)
12:15 - 1:15	**LUNCH**
1:15 - 1:45	Average and Maximum Fault Displacements (B. Slemmons)
1:45 - 2:30	Basin and Range Secondary Faulting Data (S. Pezzopane)
2:30 - 2:45	Where we go from here (K. Coppersmith)
2:45 - 3:00	**COMMENTS FROM OBSERVERS**

YUCCA MOUNTAIN SEISMIC SOURCE CHARACTERIZATION
WORKSHOP #2 - HAZARD METHODOLOGIES

Registration List for
OCTOBER 16, 1996

Typed Name	Signature	Affiliation
1. Ake, Jon		U.S. Bureau of Reclamation (USBR)
2. Allen, Clarence		Nuclear Waste Technical Review Board (NWTRB)
3. Anderson, Ernie		U.S. Geological Survey (USGS)
4. Anderson, John		University of Nevada at Reno (UNR)
5. Anderson, Larry		USBR
6. Arabasz, Walter		University of Utah (UU)
7. Bell, John		UNR
8. Brocher, Tom		USGS
9. Bruhn, Ron		UU
10. Brune, James		UNR
11. Coppersmith, Kevin		Geomatrix
12. Cornell, Allin		Consultant
13. Day, Warren		USGS
14. dePolo, Craig		UNR
15. Doser, Diane		University of Texas, El Paso
16. Feighner, Mark		Lawrence Berkeley National Laboratory
17. Fridrich, Chris		USGS
18. Hanks, Tom		USGS
19. Justus, Phil		U.S. Nuclear Regulatory Commission (NRC)
20. Kimball, Jeff		U.S. Department of Energy (DOE)
21. King, Jerry		M&O/SAIC
22. Knuepfer, Peter		State University of New York at Binghamton
23. Lui, Christiana		NRC
24. Lung, Rob		USBR
25. McCalpin, Jim		GEO-HAZ Consulting, Inc.
26. McGuire, Robin		Risk Engineering
27. Menges, Chris		USGS
28. O'Leary, Dennis		USGS
29. Olig, Susan		Woodward-Clyde Federal Services (WCFS)

Attachment 2

YUCCA MOUNTAIN SEISMIC SOURCE CHARACTERIZATION
WORKSHOP #2 - HAZARD METHODOLOGIES

Registration List for
OCTOBER 16, 1996

30. Perman, Roseanne	Roseanne Perman	Geomatrix
31. Pezzopane, Silvio		USGS
32. Pomeroy, Paul		Advisory Committee on Nuclear Waste
33. Quittmeyer, Richard	R.C. Quittmeyer	WCFS
34. Ramelli, Alan		UNR
35. Reiter, Leon		NWTRB
36. Robert Smith		UU
37. Rogers, Al		EQE International
38. Savy, Jean		Lawrence Livermore National Laboratory
39. Schwartz, David		USGS
40. Slemmons, Burt		WCFS
41. Smith, Ken		UNR
42. Soeder, Daniel	Daniel J. Soeder	USGS
43. Stamatakos, John		CNWRA
44. Stepp, Carl		WCFS
45. Sullivan, Tim	T. Timothy Sullivan	DOE
46. Swan, Bert		Geomatrix
47. Tillson, David	David W. Tillson	Nevada Agency for Nuclear Projects
48. Toro, Gabe		Risk Engineering
49. Whitney, John		USGS
50. Wong, Ivan	IGWong	WCFS
51. Youngs, Robert		Geomatrix
52. Yount, Jim		UNR
44 53. Robert B. Smith		
40 54. David B Slemmons		
55.		
56. Tom O'Hanley		USGS
57.		
58. Chris Potter		USGS
59.		
60.		
61.		

YUCCA MOUNTAIN PROJECT

Studies

Introduction

Presented by:
Tim Sullivan
U.S. Department of Energy

October, 1996

U.S. Department of Energy
Office of Civilian Radioactive
Waste Management

Attachment 3

DOE Objectives

- Complete a probabilistic seismic hazard assessment
- Incorporate multiple scientific interpretations of data and associated uncertainties in defining input parameters to the seismic hazard calculation
- Based on the results of the hazard calculation define design bases for ground motion and fault displacement for the Viability Assessment design in 1998.

Update from 4/95

- Repository program downsizing -- budget cut ~50% in FY 96 resulting in PSHA deferral
- Reorientation in program milestones; site suitability process abandoned
- Viability assessment in 1998
- Interim storage not authorized; not likely in 1997
- ESF tunnel now ~6.5 km (map and some pictures after this)

Viability Assessment

- Now mandated in FY 97/98 congressional appropriation
- Interim step to site recommendation in 2001 (NWPA)
- Site recommendation involves stakeholders (include NRC, NV)
- Viability assessment is a DOE assessment consisting of
  - Comprehensive description of design and operations concept
  - Assessment of performance of the concept in the geologic setting
  - Cost estimate
  - Licensing plan
- Does not constitute a final evaluation of the site, but an interim evaluation to focus on remaining uncompleted work and unresolved issues

Viability Assessment

- Now mandated in FY 97/98 congressional appropriation
- Interim step to site recommendation in 2001 (NWPA)
- Site recommendation involves stakeholders
- Viability assessment is a DOE assessment consisting of
  - Comprehensive description of design and operations concept
  - Assessment of performance of the concept in the geologic setting
  - Cost estimate
  - Licensing plan
- Does not constitute a final evaluation of the site, but an interim evaluation to focus on remaining uncompleted work and unresolved issues

DOE NRC Issue Resolution

- DOE Topical Report *Methodology to Assess Fault Displacement and Vibratory Ground Motion Hazards at Yucca Mountain* has been accepted by NRC pending review of final results of the seismic hazard analysis

- DOE Topical Report *Seismic Design Methodology for a Geologic Repository at Yucca Mountain* is in final review at the NRC

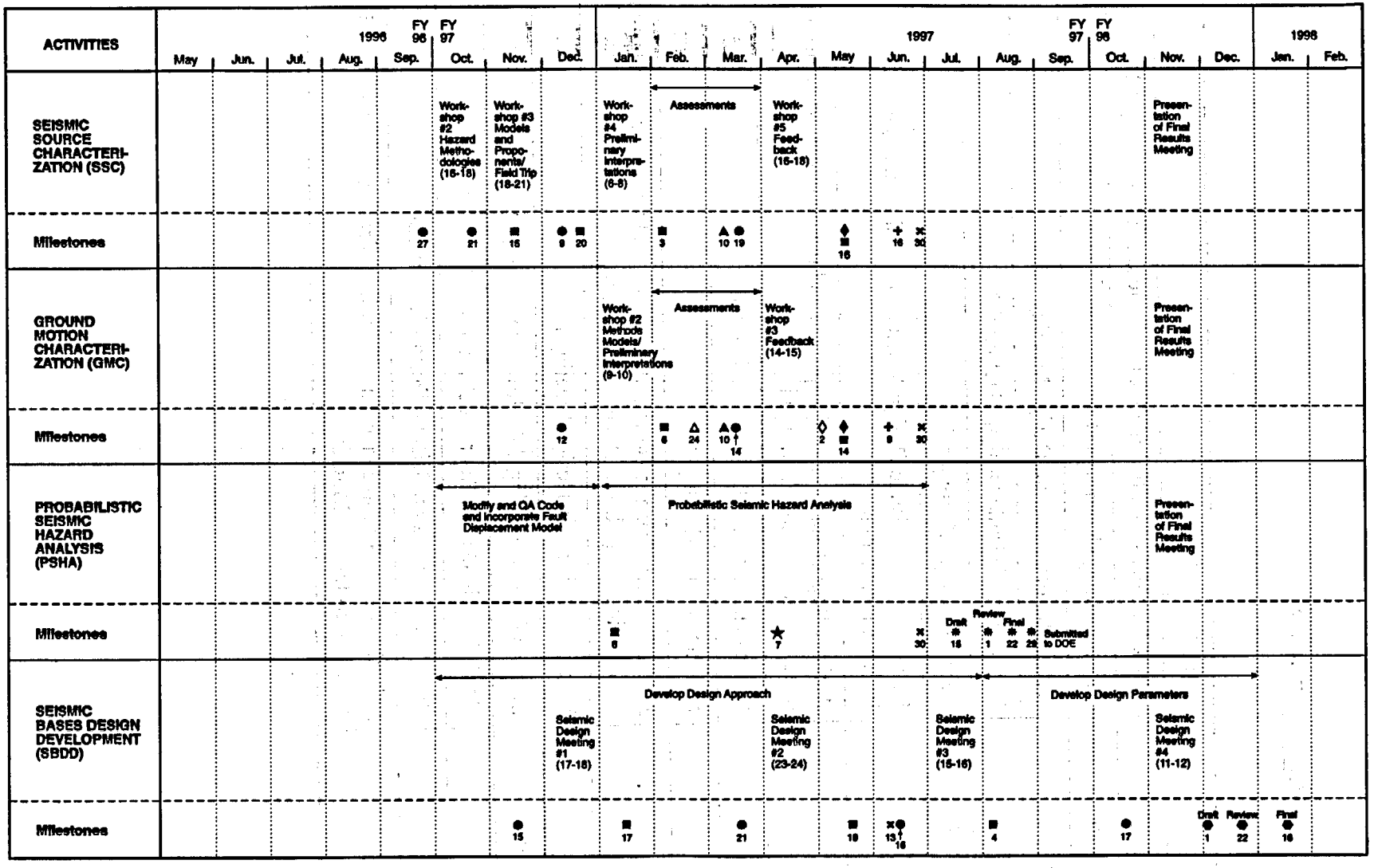

9001A-661/091296/gce

Attachment 4

SEISMIC DESIGN SCHEDULE

DATE	MILESTONE
15 Oct 96	Work Plan delivered to M&O for Seismic Design Meeting # 1
17-18 Dec 96	Seismic Design Meeting # 1
17 Jan 97	Letter Report: Seismic Design Meeting # 1
21 Mar 97	Work Plan: Seismic Design Meeting # 2
23-24 Apr 97	Seismic Design Meeting # 2
19 May 97	Letter Report: Seismic Design Meeting # 2 and requirements for PSHA Calculations
13 Jun 97	Activity Report summarizing approach and methodology to be used in development of seismic design bases
16 Jun 97	Work Plan: Seismic Design Meeting # 3
15-16 Jul	Seismic Design Meeting # 3
4 Aug	Letter Report: Seismic Design Meeting # 3 and final annotated outline of Seismic Design Basis Development Report
17 Oct 97	Work Plan: Seismic Design Meeting # 4
11-12 Nov 97	Seismic Design Meeting # 4 - Review working draft
01 Dec 97	Draft Seismic Design Report delivered to M&O for review
22 Dec 97	Review Comments on Seismic Design Report due
16 Jan 98	Seismic Design Report Finalized; resolution of review comments and submittal to DOE/YMSCO

PSHA SCHEDULE

DATE	MILESTONE
27-Sep-96	Workshop Plan delivered to the M&O for the Seismic Hazard Methodologies Workshop
16 thru 18-Oct-96	Workshop: Seismic Hazards Methodologies for Seismic Source and Fault Displacement Characterization
21-Oct-96	Workshop Plan delivered to the M&O for the Tectonic Models and Seismic Source Interpretations Workshop and Field Trip
15-Nov-96	Letter Report: Seismic Hazards Methodologies for Seismic Source and Fault Displacement Characterization Workshop delivered to the M&O.
18 thru 21-Nov-96	Field Trip and Workshop: Tectonic Models and Seismic Source Interpretations
9-Dec-96	Workshop Plan delivered to the M&O for the Seismic Source Preliminary Interpretations Workshop
12-Dec-96	Workshop Plan delivered to the M&O for the Ground Motion Models and Interpretations Workshop
20-Dec-96	Letter Report: Tectonic Models and Seismic Source Interpretations Field Trip and Workshop delivered to the M&O.
06-Jan-97	Letter Report on Modifications and QA of PSHA computer code including fault displacement model
6 thru 8-Jan-97	Workshop: Preliminary Interpretations for Seismic Source and Fault Displacement Characterization
9 thru 10-Jan-97	Workshop: Models and Interpretations for Ground Motion Characterization
3-Feb-97	Letter Report: Preliminary Interpretations for Seismic Source and Fault Displacement Characterization delivered to the M&O
6-Feb-97	Letter Report: Ground Motion Models and Interpretations delivered to the M&O
24-Feb-97	Preliminary Ground Motion Interpretations provided to the Facilitation Team by the Experts
10-Mar-97	Preliminary seismic source logic trees and ground motion interpretations provided to the Hazard Calculations Team

PSHA SCHEDULE

DATE	MILESTONE
14-Mar-97	Workshop Plan delivered to the M&O for the Ground Motion Feedback Workshop
19-Mar-97	Workshop Plan delivered to the M&O for the Seismic Source Feedback Workshop
07-Apr-97	Preliminary PSHA calculations to facilitation teams for feedback workshops
14 thru 15-Apr-97	Workshop: Feedback on Ground Motion Interpretations
16 thru 18-Apr-97	Workshop: Feedback on Seismic Source Interpretations
2-May-97	Final Ground Motion Interpretations delivered to the Facilitation Team
14 May-97	Final Ground Motion Interpretations delivered to the Calculations Team
14-May-97	Letter Report: Ground Motion Feedback Workshop delivered to the M&O
16-May-97	Letter Report: Seismic Source Feedback Workshop delivered to the M&O
16-May-97	Final Seismic Source Logic Trees delivered to the Calculation Team
9-Jun-97	Final interpretation documentation due to the Facilitation Team from ground motion experts
16-Jun-97	Final interpretation documentation due to the Facilitation Team from the seismic source expert teams.
30-Jun-97	Activity Report: Ground Motion Characterization (including experts' documentation of interpretations) delivered to the M&O
30-Jun-97	Activity Report: Seismic Source Characterization (including expert teams' documentation of interpretations) delivered to the M&O
30-Jun-97	Activity Report: Seismic Hazard Calculations for Yucca Mountain delivered to the M&O
15-Jul-97	Draft PSHA Report: Probabilistic Seismic Hazard Assessment for Yucca Mountain delivered to the USGS for formal review
01-Aug-97	Review Comments due on PSHA Report
22-Aug-97	PSHA Report finalized; resolution of review comments complete
29-Aug-97	PSHA Report Submitted to the DOE/YMSCO

Yucca Mountain PSHA Project
Peer Review

Reviewer	Review Areas
Jim Brune	seismicity aspects of seismic source characterization and vibratory ground motion
Allin Cornell	PSHA methodology, process, and seismic design basis hazard
Tom Hanks	vibratory ground motion
David Schwartz	tectonic aspects of seismic source characterization and fault displacement hazard

Process

- Participatory Peer Review
- Informal comments following each workshop
- Formal review of draft project reports

OVERVIEW OF PROCESS AND GUIDELINES FOR WORKSHOPS

Kevin J. Coppersmith

SEISMIC SOURCE CHARACTERIZATION (SSC) HAZARD METHODOLOGIES WORKSHOP

October 16-18, 1996
Doubletree Hotel, Salt Lake City, Utah

Attachment 5

SEISMIC SOURCE CHARACTERIZATION (SSC)
HAZARD METHODOLOGIES WORKSHOP

GOALS OF THE WORKSHOP:

- To review the data that are available for the Yucca Mountain region

- To identify available methodologies for characterizing seismic sources for the Yucca Mountain seismic hazard analysis.

Significant issues important to SSC were identified at the first workshop, as were the available data bases at that time (April, 1995)

APPROACH:

1. Consider the two purposes of seismic source characterization:

    - Vibratory ground motion hazard analysis
    - Fault displacement hazard analysis

2. SSC is divided into three components:

    - Seismic source location and geometry
    - Maximum earthquake magnitude
    - Earthquake recurrence assessment.

3. Each topic is first introduced by overview presentations that focus on the *methods and approaches* that are available to characterize them.

4. A series of talks describe the available *data bases and data interpretations* that relate to these topics.

GROUND RULES FOR WORKSHOPS

1. The workshops are an opportunity for the Expert Panel to:

- Exchange data
- Present interpretations
- Challenge and defend technical hypotheses
- Be trained in elicitation procedures
- Gain information on the project
- Interact and ask questions

Therefore, the focus of each workshop is the *Expert Panel*

2. The SSC Facilitation Team runs the workshops and is responsible for keeping to the schedule, logistics, etc.

3. The conduct of the technical discussions at the workshops will be at the highest professional level. Personal attacks or confrontations will not be permitted (especially those directed at the Facilitation Team)

4. Discussions will be among the Expert Panel and the Presenters

5. Observers are provided with a period each day for brief statements or questions (3 minutes each)

6. If an Observer has a burning question, please write it down and give to a member of the Facilitation team; they will attempt to have it answered during the course of the discussions

7. The data bases supplied to the Expert Panel will not be supplied to the Presenters or Observers; a list of all materials supplied will be available
8. A workshop summary will be supplied to all workshop participants who have signed in

TYPES OF PARTICIPATION
YM-SSC PROJECT

- **Members of Expert Teams**
- **Workshop Presenters/Data Specialists**
- **SSC Facilitation Team**
- **Observers**

YM-SSC PROJECT
MEMBERS OF EXPERT PANEL

EXPERT	AFFILIATION
J. Ake	U.S. Bureau of Reclamation
E. Anderson	U.S. Geological Survey
L. Anderson	U.S. Bureau of Reclamation
W. Arabasz	University of Utah
R. Bruhn	University of Utah
C. dePolo	University of Nevada, Reno
D. Doser	University of Texas, El Paso
C. Fridrich	U. S. Geological Survey
P. Knuepfer	SUNY Binghamton
J. McCalpin	Geo-Haz Consulting
C. Menges	U.S. Geological Survey
A. Ramelli	University of Nevada, Reno
A. Rogers	U.S. Geological Survey
B. Slemmons	Consultant
K. Smith	University of Nevada, Reno
R. Smith	University of Utah
B. Swan	Geomatrix Consultants
J. Yount	U.S. Geological Survey

YM-SSC FACILITATION TEAM MEMBERS

Member	Affiliation
K. Coppersmith	Geomatrix Consultants
P. Morris	Applied Decision Analysis
S. Olig	Woodward-Clyde Consultants
R. Perman	Geomatrix Consultants
S. Pezzopane	U.S. Geological Survey
J. Whitney	U.S. Geological Survey
R. Youngs	Geomatrix Consultants

YUCCA MOUNTAIN SEISMIC SOURCE CHARACTERIZATION

SCHEDULE

WORKSHOP #1 DATA NEEDS: April 17-19, 1995

- Discuss hazard methodologies, technical issues, and Yucca Mountain data bases
- Arrive at detailed list of data required by experts: scales, formats, processing
- Schedule for delivery of data to experts

WORKSHOP #2 HAZARD METHODOLOGIES (AND DATA): October 16-18, 1996

- Discuss methodologies for both ground motion and fault displacement: pros and cons, data requirements, applicability to Yucca Mountain
- Present all pertinent data bases that have become available since the first workshop

Note: Experts will be grouped into teams prior to the third workshop; the data delivery should be essentially complete prior to Workshop #3

WORKSHOP #3 MODELS AND PROPONENTS/FIELD TRIP November 18-21, 1996

- Focus of workshop is encouraging individual experts and invited presenters to act as `proponents' (advocates of a single model/hypothesis), making a distinction with `evaluators' (who consider alternative models/hypotheses)

- Proponents for key technical issues: (e.g., clustering, detachments, recurrence models, displacement models, synchroneity of faulting, etc.) and for various hazard methodologies

- Field trip to observe local faults, field relationships, and the ESF; opportunity to debate alternative interpretations in the field

- Elicitation training

WORKSHOP #4 PRELIMINARY SSC INTERPRETATIONS: January 6-8, 1996

- Full, preliminary characterization of inputs for both ground motion and displacement SSC

- Discussions by each team of their uncertainties and credibilities of alternative models and methods.

- Technical challenge of interpretations and their basis

ELICITATIONS: February -- March

- Teams meet in multi-day session with representatives from Facilitation team
- Expert teams document assessments and technical basis

WORKSHOP #5 FEEDBACK April 16-18, 1996

- Sensitivities, dominant contributors to ground motions and fault displacement
- Significant contributors to uncertainty
- Interpretations for each team presented, discussed, challenged, and defended

FINAL ASSESSMENTS June 16, 1996

- Experts make any changes they feel appropriate in light of discussions at workshop #5
- Expert team documentation delivered to Facilitation Team

IMPORTANT ASPECTS OF THE YM-SSC PROJECT

A key aspect of your evaluation is the identification and quantification of uncertainty

- Expert-to-expert diversity of interpretation; modeling uncertainties; parameter uncertainties; aleatory and epistemic uncertainties
- Sensitivity analyses: individual expert-team assessments, relative contribution to mean hazard, contribution to uncertainty/variance (all fed back to expert teams)

Probabilistic treatment of hazard allows for full consideration of alternatives without invoking `conservatism'

- We are not choosing the best or correct answer, or defining a conservative answer.
- The choice of alternative models and parameters should reflect true differences of interpretation, not perceptions of conservatism
- Conservatism will be considered by others in the context of risk

YM-SSC experts are not required to be statistical experts; methods to capture uncertainty will be spoon-fed

- Facilitation will assist with all calculations and statistical interpretations
- Simple methods (e.g., logic trees) are designed to be intuitively obvious

The procedures to be used in this study are consistent with recent guidance regarding multiple-expert studies

- NRC Branch Technical Position on the Use of Expert Elicitation in the High-Level Radioactive Waste Management Program
- Recommendations for Probabilistic Seismic Hazard Analysis: Guidance on Uncertainty and Use of Experts, NUREG/CR-6372 (SSHAC Study)

EXPERT *ROLES**

EVALUATOR

An evaluator is capable of listening to, understanding, interpreting, and evaluating the relative credibility of alternative models and interpretations. An evaluator recognizes that uncertainties exist and he/she expresses those uncertainties by assigning weights to alternative models and parameter values, based on his/her interpretation of the available data.

PROPONENT

A proponent is an advocate of a particular model, hypothesis, or point of view. It is common for scientists to act as proponents for ideas that they believe are most consistent with the available data. A proponent does not recognize the credibility of alternative hypotheses and does not focus on quantifying uncertainties.

INTEGRATOR

An integrator is responsible for integrating or combining the interpretations of multiple experts. In some cases, an integrator will aggregate the interpretations of multiple evaluators; or he/she will integrate the interpretations of the larger technical community.

TECHNICAL FACILITATOR/INTEGRATOR (TFI)

A TFI is an individual or small team that is responsible for facilitating the interactions of multiple evaluator experts and for integrating their interpretations.

**Terminology consistent with SSHAC*

GUIDELINES FOR SELECTION OF YM-SSC EXPERTS

- Strong relevant expertise as demonstrated by professional reputation, academic training, relevant experience, and peer-reviewed publications and reports

- Willingness to forsake the role of proponent of any model, hypothesis or theory, and perform as an impartial expert who considers all hypotheses and theories and evaluates their relative credibility as determined by the data

- Availability and willingness to commit the time required to perform the evaluations needed to complete the study

- Specific knowledge of the Yucca Mountain area, the Basin and Range Province, or ground motion characterization

- Willingness to participate in a series of open workshops, diligently prepare required evaluations and interpretations, and openly explain and defend technical positions in interactions with other experts participating in the project

- Personal attributes that include strong communications skills, interpersonal skills, flexibility and impartiality, and the ability to simplify and explain the basis for interpretations and technical positions

YUCCA MOUNTAIN PSHA PROJECT
CRITERIA FOR REMOVAL OF AN EXPERT
OR
1/CRITERIA FOR CONTINUED PARTICIPATION AS AN EXPERT

- Role of expert is to evaluate data and develop and document interpretations of seismic sources including uncertainty in the interpretations

- Experts were selected based on reasoned criteria

- The need to consider removing an expert can only arise for failure to perform according to the commitments and demands of the project as stated in the expert selection criteria

One or more of the following could prompt the need to consider removing an expert:

1) The person demonstrates unwillingness to perform as an expert evaluating credible models, hypotheses, or theories relative to the degree they are supported by data. This might be considered to be demonstrated if a person becomes a proponent of a single model, theory, or hypothesis to the exclusion of all others, or is unwilling to be guided by the data in making interpretations or expressing uncertainty.

2) The person is unwilling or finds it impossible to commit the time required to perform the evaluations needed to complete the study. This might be reflected in the person consistently being unprepared for workshops or meetings with the Facilitation Team and/or consistently failing to meet established schedules for deliverables.

3) The person is unwilling to interact with other members of the project in an open and professional manner. This might be demonstrated by the person assuming a hostile and aggressive posture toward other members of the project or being uncooperative and disruptive in the workshops or interactions with the Facilitation Team.

PROCEDURE

1) The Facilitation Team is primary point of interaction with the experts and is responsible for managing the technical activities.

2) The Facilitation Team will identify a non-performing expert and inform the Project Management of the situation.

3) The Facilitation Team with the support of the Project Management will meet with the expert and determine whether the unacceptable performance can be brought into conformance with the requirements of the expert selection criteria.

4) If after due consideration it is determined that this cannot be done, the Project Management will take formal action to remove the non-performing expert from further participation as an expert in the project.

GUIDELINES FOR EXPERT TEAMS

The SSC will be conducted by six three-person *teams:*

- Each team is multi-disciplinary, including expertise in Quaternary geology/paleoseismology, seismology/geophysics, and regional geology/tectonics.

- Each team should act as a virtual individual expert; each team should identify all approaches, tools, and data relevant to each evaluation

- For some elements of the SSC several data sets and/or overlapping discipline tools may apply, for others a single data set or discipline tools may dominate the evaluation; the full expertise/experience of the team should be drawn out rather than deferring to a single team member

- All informed interpretations should be freely explored and properly represented; there is no intention to mute an extreme interpretation within a team.

- Within the team dynamic each expert should provide interpretations within his/her discipline across all models/evaluations recognizing that the resolving power of discipline tools and data may vary among models; the team integrates across disciplines and fully assesses uncertainty

- Each team should achieve within-team aggregation through interactions, and across teams using equal weights

- All team members should be comfortable that their views are properly represented in the final interpretation; acting together, they will be asked to defend their interpretations

AGGREGATION OF EXPERT ASSESSMENTS

A goal of the YM-SSC project is to have a defensible basis for combining the assessments of the expert teams using equal weights. To do so, the following steps are being taken:

- A careful process of expert selection was conducted
- Experts are allowed to identify the data they require and all experts are given equal access to the data
- Experts are encouraged to interact, ask questions, and attain a high level of knowledge about data and methods
- The Facilitation team will assist in peripheral areas requiring support (e.g., statistics, computer coding and calculations, probability encoding)
- All significant data sets and interpretations will be presented to the expert panel in workshops and field trips; opportunity will be given to question the proponents of hypotheses and data presenters
- Every effort will be made to maintain a high level of commitment by each expert on the panel
- Feedback will be provided to ensure there are no unintentional disagreements; reviews and technical challenges will promote common understanding of issues and terminology
- The experts are required to play the role of an `evaluator' and, unless asked to do so, forsake the role of a `proponent'

All of these attributes are consistent with encouraging interdependence among the teams (i.e., establishing a common knowledge of data sets, definitions, methods, and alternative interpretations)

SEISMIC SOURCE CHARACTERIZATION
— SSC —
FOR ASSESSING
VIBRATORY GROUND MOTIONS

GENERAL APPROACH AND KEY ISSUES

Walter J. Arabasz

October 16, 1996

Attachment 6

Perspective ...

"Probabilistic seismic hazard analysis is an input to a larger decision-making process, not an end in itself."

—Robin McGuire

for example:

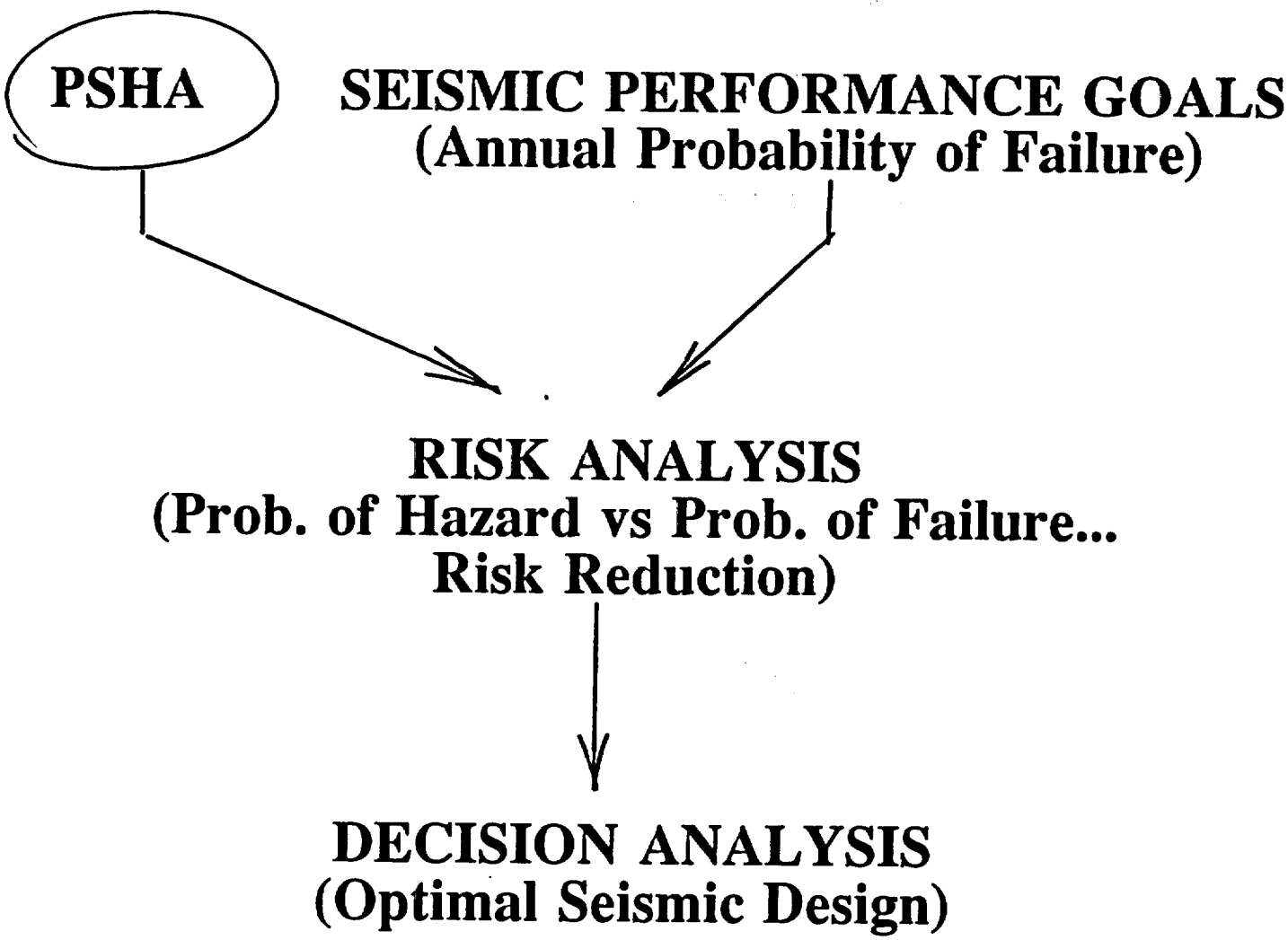

FOR BACKGROUND INFORMATION

UCRL-ID-122160

Recommendations for Probabilistic Seismic Hazard Analysis: Guidance on Uncertainty and Use of Experts

Prepared by the Senior Seismic Hazard Analysis Committee (SSHAC)

September 1995

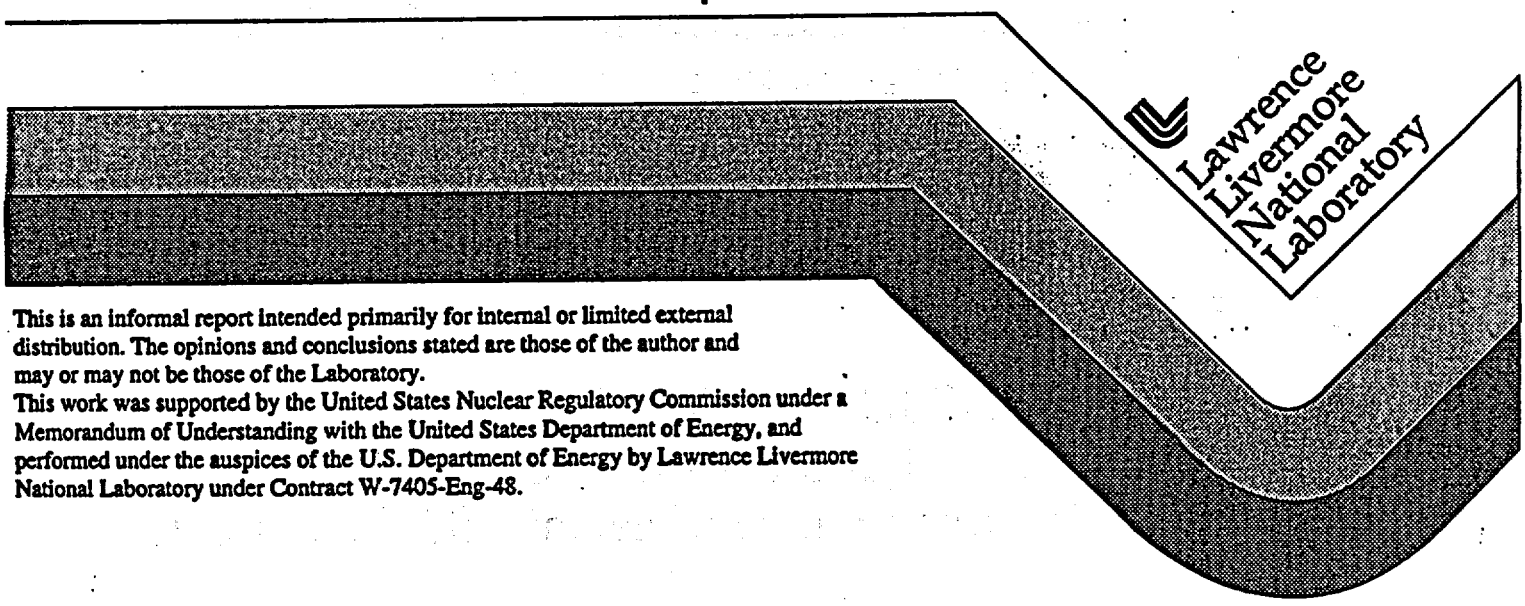

This work was supported by the United States Nuclear Regulatory Commission under a Memorandum of Understanding with the United States Department of Energy, and performed under the auspices of the U.S. Department of Energy by Lawrence Livermore National Laboratory under Contract W-7405-Eng-48.

OUTLINE

SEISMIC SOURCES

WHAT HAS TO BE DONE FOR EACH SOURCE

- Quantify Depiction
- Characterize Future Seismicity

SEISMICITY ☞ RECURRENCE EVALUATION

- $f_M(m)$
- Exponential vs Characteristic Models
- Importance of Frequencies in PSHA
- Careful "Conditioning" of EQ Catalogs
  - — common magnitude measure
  - — estimate completeness as a function of magnitude and location
  - — removal of dependent events (foreshocks and aftershocks)

ISSUES

- Issues for SSC from Workshop #1
- Issues from NRC review of SSHAC Rept
- Relative importance of certain SSC parameters

SEISMIC SOURCES

(Sources—faults and volumetric zones—of future seismic events that will affect site)

SEISMIC SOURCE = A region of the earth's crust that has relatively uniform seismicity characteristics, distinct from neighboring sources

[Can allow for some variation of seismicity parameters (a-, b-values), but Mmax and the probability of activity generally assumed to be uniform within a seismic source]

CANDIDATE SEISMIC SOURCES

- **Quaternary faults**
  - **— exposed**
  - **— buried (mapped or imaged)**
  - **— hidden (suspected)**
- **Zones of historical seismicity**
- **Sites of Underground Nuclear Explosions (UNE's)**
- **Localized regions of young magmatism that could produce volcanic earthquakes**

FOUR BASIC TYPES OF SEISMIC SOURCES (FROM SSHAC, 1995)

Type 1 Faults, represented by lines or planes

Type 2 Area sources enclosing concentrated zones of seismicity

Type 3 Area sources defined by regional seismotectonic characteristics

Type 4 Background area sources [note scale]

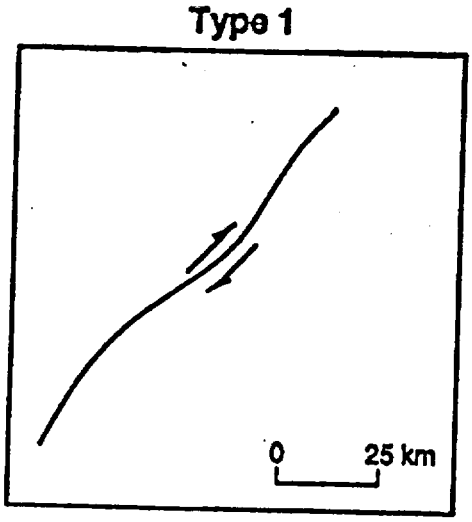

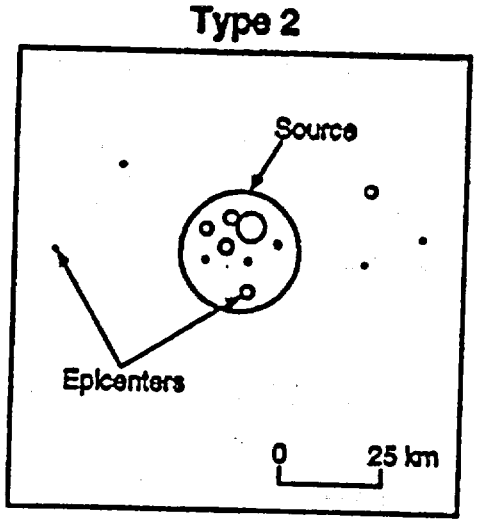

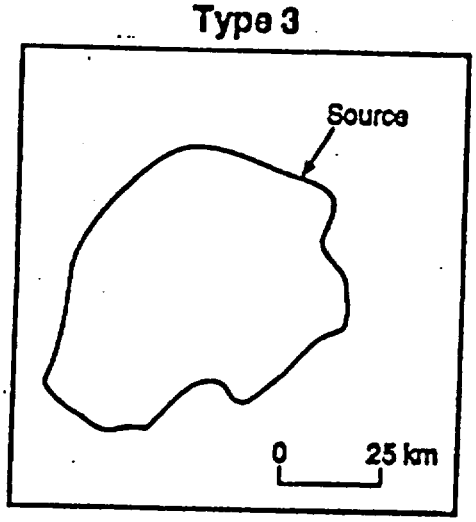

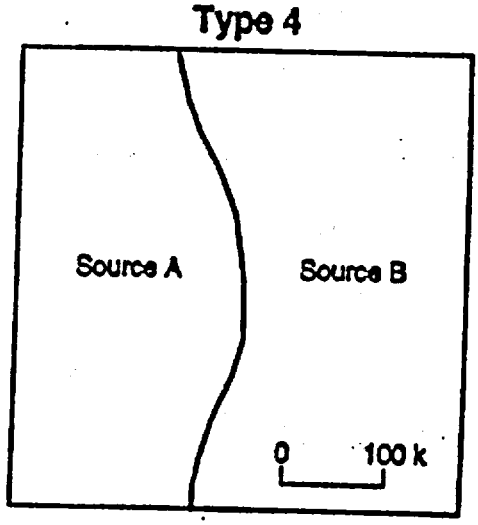

ISSUE OF ASSUMING HOMOGENEOUS SEISMICITY WITHIN AREA SOURCES (SSHAC, 1995)

eq = earthquake

Implication: Over enough time, one would observe the same density of eq's (events per unit area) in any small area within the given source . . .

1. **All sites within a homogeneous area source will have the same mean hazard due to this source, regardless of distribution of historical seismicity.**

2. **Statistical uncertainty in a- and b-values will be lower than if the source is subdivided into two or more smaller sources.**

WHAT HAS TO BE DONE FOR EACH SOURCE

1. QUANTIFY DEPICTION

- 3-D Geometry (and any variability, due to uncertainty, in the depiction)
- Probability That Source is Active
- Dependency With Other Sources

2. CHARACTERIZE FUTURE SEISMICITY

- Magnitude Distribution
- Rate of EQ Occurrence
- Maximum Magnitude

TO WHAT DISTANCE FROM A SITE IS "DETAILED" SOURCE CHARACTERIZATION NECESSARY?

General Guidance from SSHAC (1995) for Western U.S.:

- **Max distance for source identification ☞300 km**
- **Distance for detailed source characterization:**

  If fault sources within 50 km of site ☞ 100 km

  If no fault sources within 50 km of site ☞ 150 km

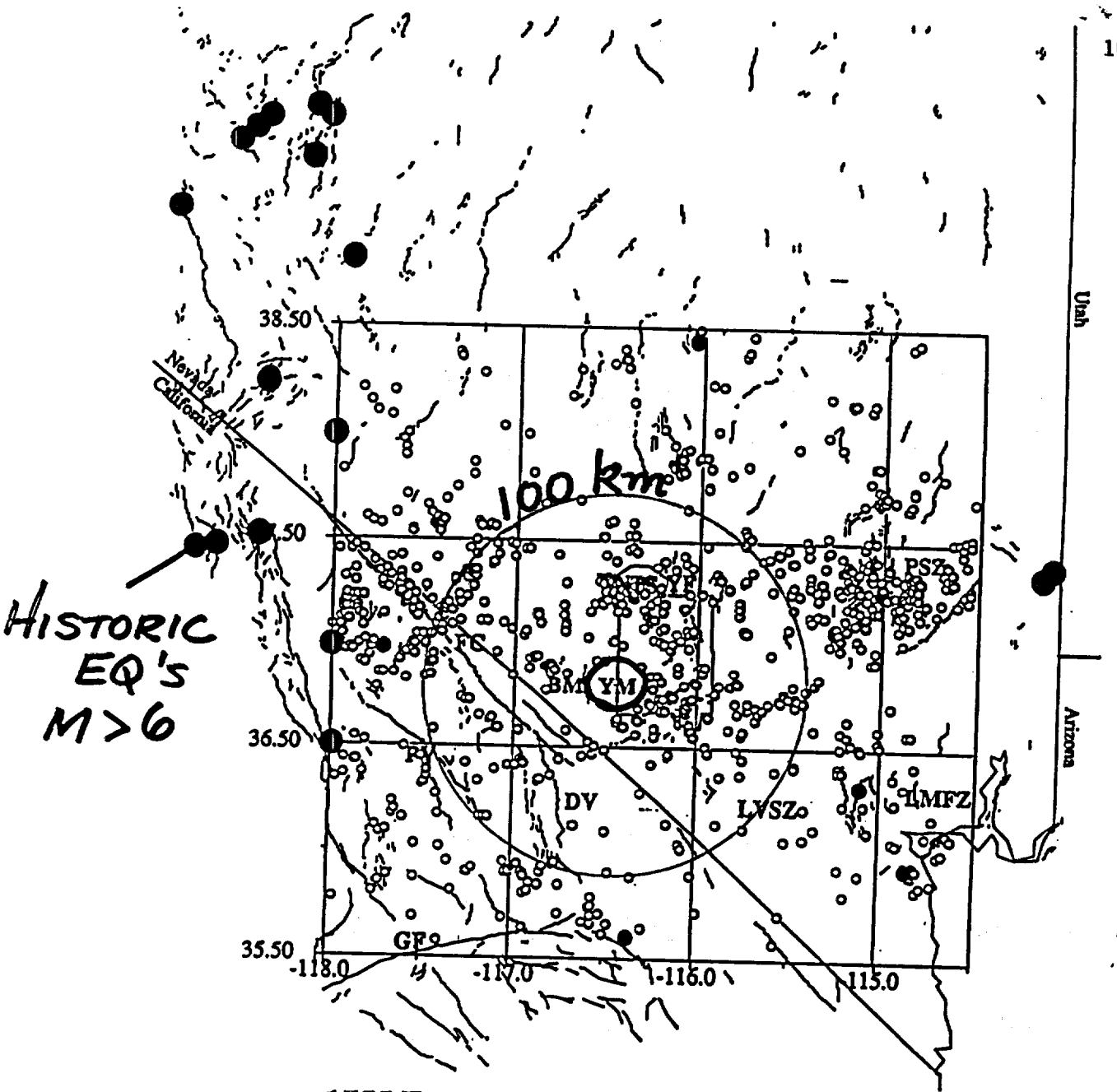

Fig. 2. Map of the area covered by the Southern Great Basin Seismic Network. Curved line segments are Quaternary fault scarps and lineaments inferred from geologic information [*Nakata et al.*, 1982]. Large solid circles are historic earthquake epicenters with magnitudes greater than approximately 6.0 [*Gawthrop and Carr*, 1988]. Epicenters of events recorded on the SGBSN between 1983 and 1989 are shown by the smaller solid circles for events recorded with local magnitude greater than 3.4 (the largest is 4.3), and open ovals are for events with magnitude greater than or equal to 1.6. Abbreviations are FC, Furnace Creek Fault; DV, Death Valley Fault Zone; LVSZ, Las Vegas Shear Zone; PSZ, Pahranagat Shear Zone; PV, Panamint Valley Fault Zone; GF, Garlock Fault; LMFZ, Lake Mead Fault Zone; YF, Yucca Fault; BM, Bear Mountain Fault; NTS, Nevada Test Site ; and YM, Yucca Mountain.

Representative seismicity map for the Yucca Mountain region; large black dots are historic EQ's with M > 6 (from Gomberg, 1991)

Data Used to Assess Seismic Source Locations & Geometry and Their Relative Usefulness (from SSHAC, 1995)

TYPE OF SOURCE	DATA/BASIS FOR SOURCE	RELATIVE USEFULNESS/ CREDIBILITY (1: high, 3: low)
Type 1: Faults	Mapped fault with historical rupture	1
	Mapped Quaternary fault at surface	1
	Mapped localized Quaternary deformation, inferred fault at depth	2
	Borehole evidence for fault, especially in young units	2
	Geophysical evidence (e.g. seismic reflection) of fault at depth	2
	Map of pre-Quaternary faults	3
Type 2: Concentrated Zone	Concentrated zone of well-located instrumental seismicity	1
	Mapped fault(s) at surface or subsurface in proximity to seismicity	1
	Zone of historical/poorly located seismicity	2
	Structural features/trends parallel to seismicity zone	2
	Focal mechanisms/stress orientation	3
	Rapid lateral changes in structures/tectonic features	3
Type 3: Regional Zone	Changes in spatial distribution/concentration/density of seismicity	1
	Regions of genetically-related tectonic history	1
	Regions of similar structural styles	2
	Changes in crustal thickness or crustal composition	2
	Regions of different geophysical signature	3
	Changes in regional stresses	3
	Changes in regional physiography	3
Type 4: Background Zones	Regional differences in structural styles/tectonic history	1
	Major physiographic/geologic provinces	1
	Changes in character of seismicity	3

RECURRENCE EVALUATION

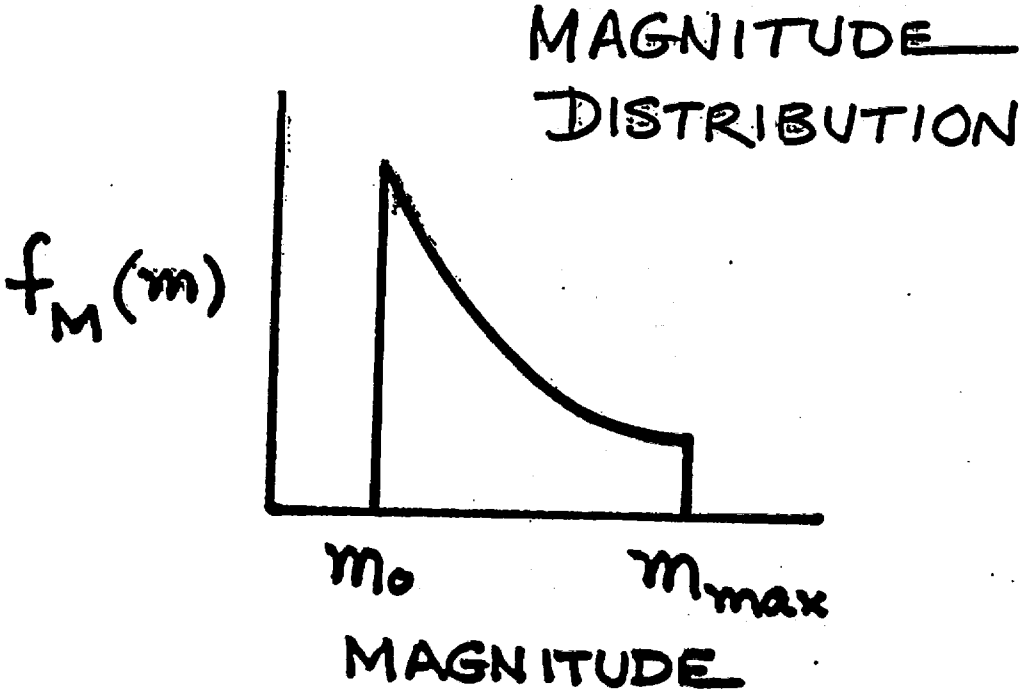

Probability (per unit of magnitude) that an event of magnitude m occurs, given an earthquake of $m_0 \leq m \leq m_{max}$ within Source i

FAULT-SPECIFIC SOURCES

Gutenberg-Richter (truncated exponential)?
Characteristic earthquake model?
Other model?

Seismicity on fault for recurrence estimation?
Generally, NO . . .

Can estimate recurrence rates using either

- **slip rate plus assumed b-value**
- **Average return time for the maximum or characteristic event plus assumed b-value**

(e.g., Youngs and Coppersmith, 1985)

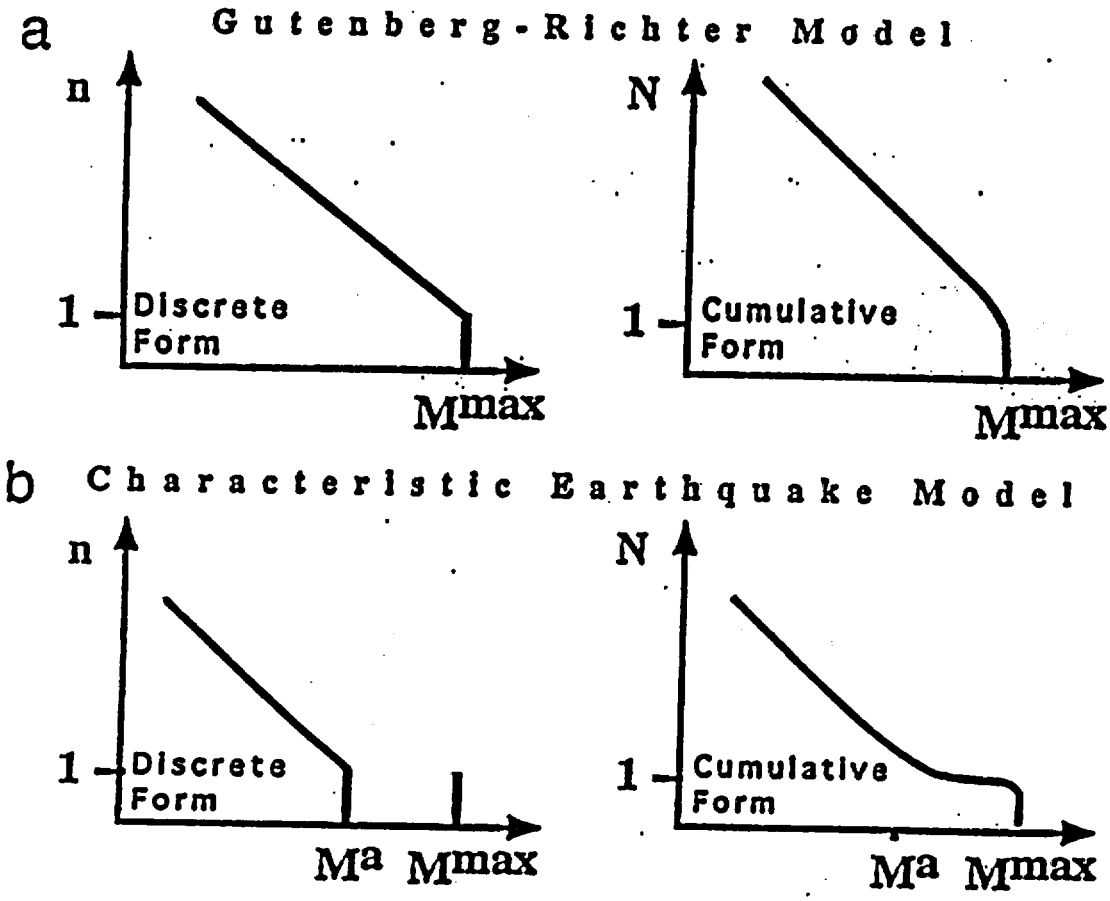

Figure 1. The distribution of the number of events versus magnitude implied by the assumption of either (a) the Gutenberg–Richter or (b) the characteristic earthquake model of fault behavior during the repeat time of one maximum magnitude (M^{max}) event along a fault. Both the discrete and cumulative forms of the expected magnitude distribution, where n equals the number of events equal to a given magnitude and N equals the number of events greater than or equal to a given magnitude, are provided in (a) and (b). For the characteristic earthquake model, the largest earthquake during the repeat time of a maximum-size event is defined to equal the size of the largest aftershock (M^a), and the size distribution of aftershocks is assumed to satisfy the Gutenberg–Richter relationship.

(from Wesnousky, 1994)

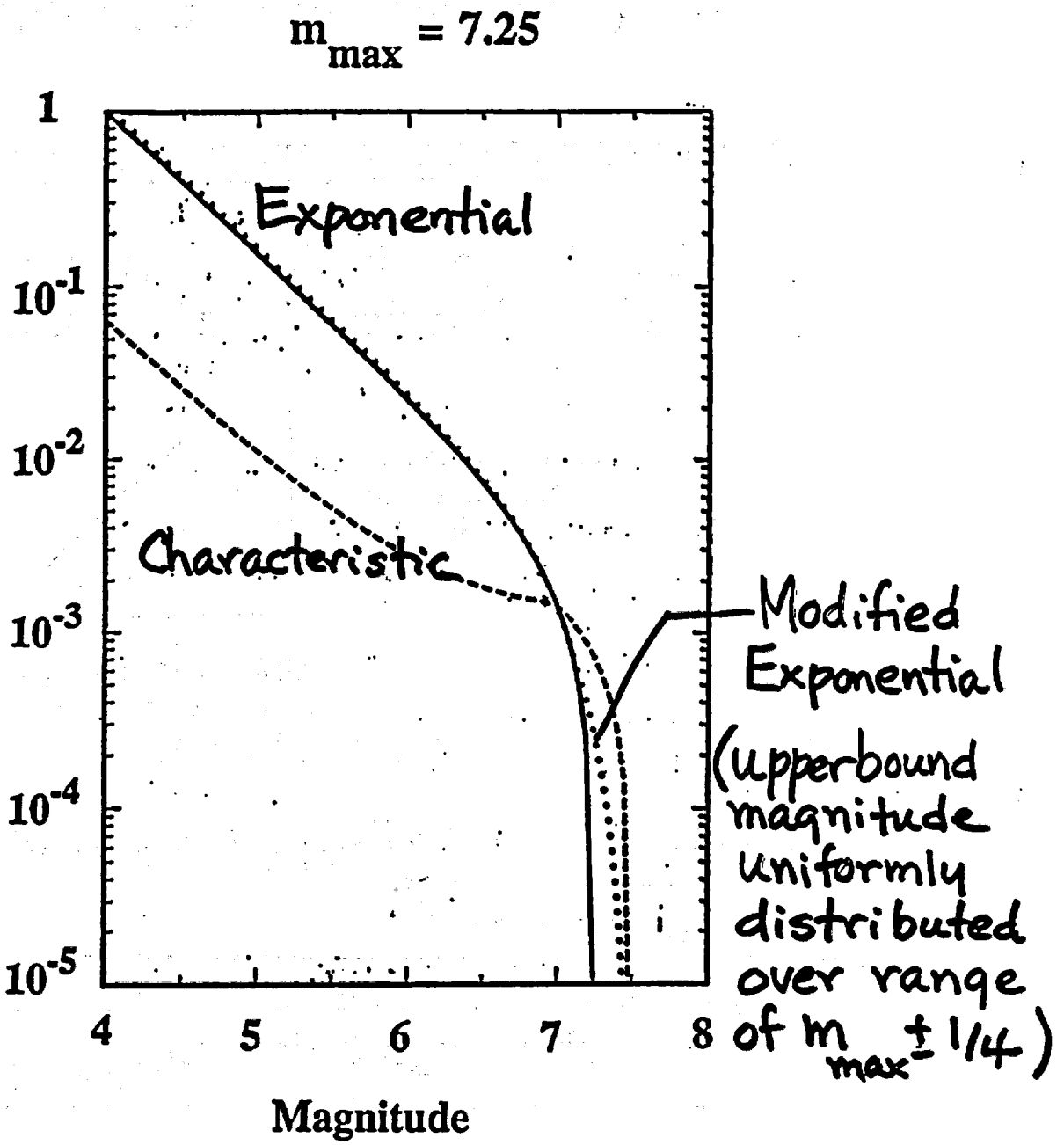

Example of recurrence modeling for m_{max} = 7.25, assuming b = 0.8 and with the frequency of events > M 7 held constant (from Youngs et al., 1987).

IMPORTANCE OF FREQUENCIES IN PSHA
(Keep your eye on the ball!)

In practice, <u>frequencies are a big deal in PSHA.</u>

Consider a seismic hazard curve.
How often does "bad" happen?

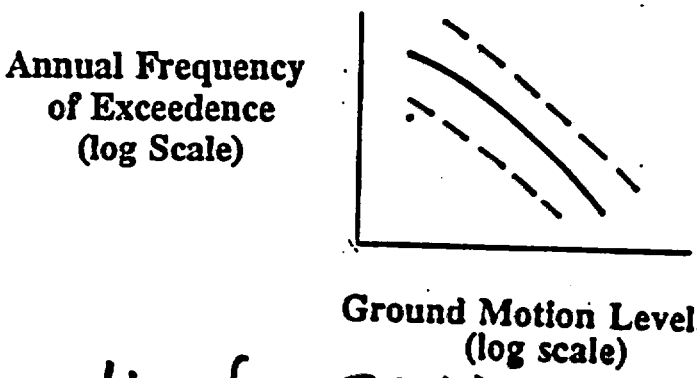

Typical Equation for PSHA

$$\text{Annual Frequency of Exceedence} = \sum_i \nu_i \iint G_{A|m,r}(a^*) f_M(m)\, f_R(r|m)\, dm\, dr$$

ν_i = annual number of EQ's in Source i with magnitude $\geq m_{threshold}$

Note the form of the equation ...

Expected Frequency = Number of Trials x Prob. [of the event]

OR

Frequency/yr of "bad" = N (events/yr) x Prob. ["bad"]

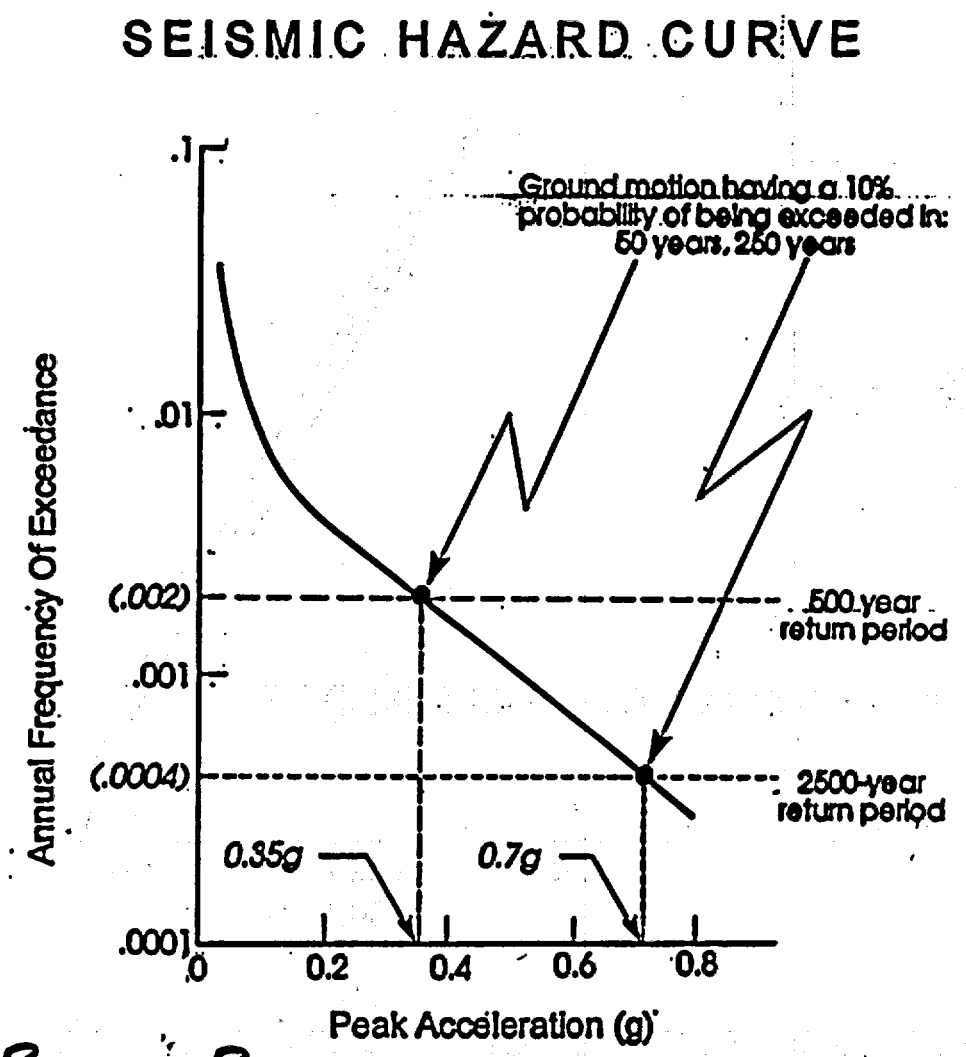

For a Poisson Process,
$P[1 \text{ or more events}] = 1 - P[\text{zero events}] = 1 - e^{-\lambda t}$

Figure 15. Graph of a simplified seismic hazard curve for a hypothetical site. From the procedure outlined in Figure 14, the curve gives the mean annual number of times (vertical axis) that a certain level of ground shaking (horizontal axis) is expected to be exceeded. The inverse (i.e., 1 divided by) an annual frequency is called a "return period." The ground motions having a 10 percent probability of being exceeded (or equivalently a 90 percent probability of not being exceeded) for some specified "exposure periods" are based on the Poisson model for random occurrence of events.

Example of simplified seismic hazard curve for a hypothetical site (from Arabasz, 1994)

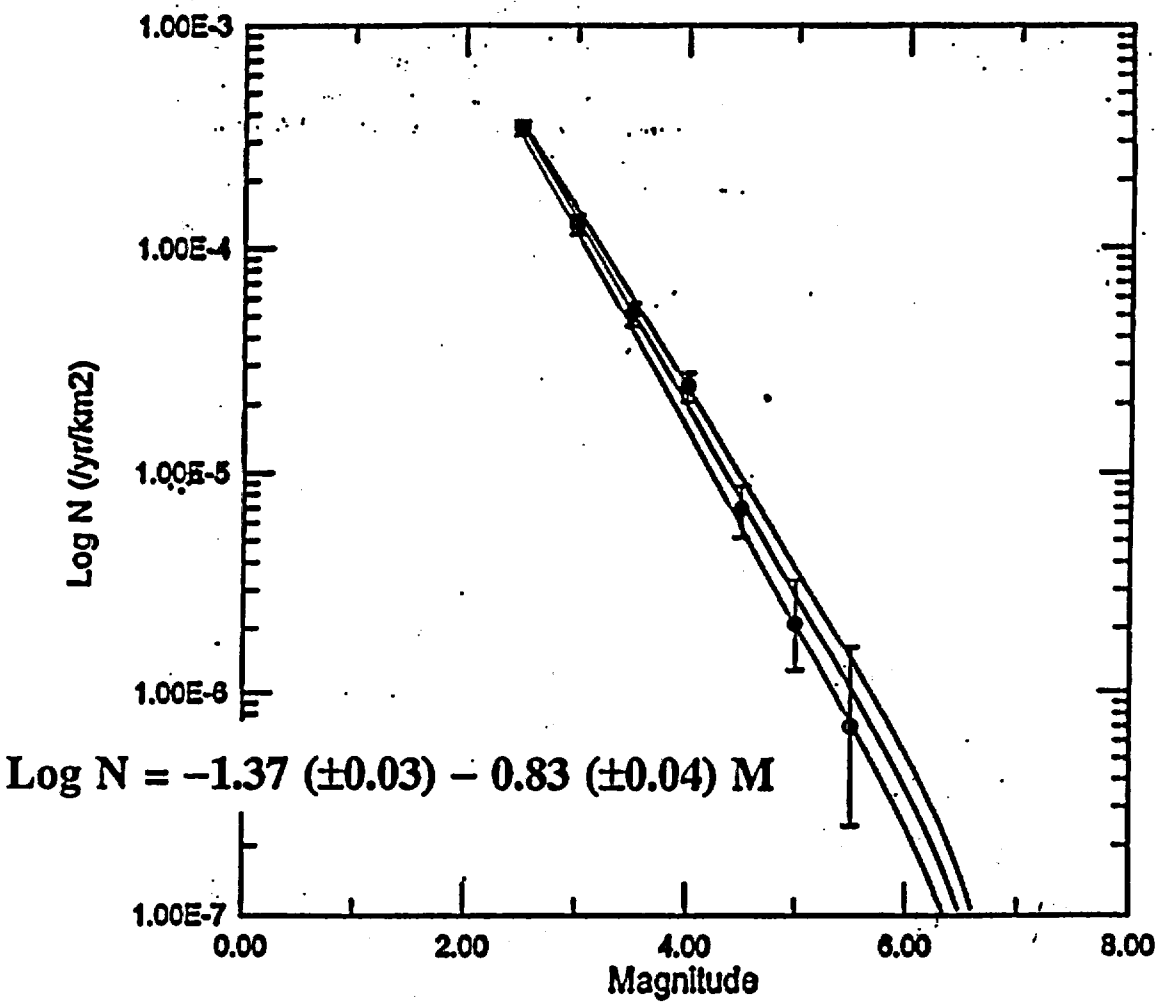

Example of recurrence modeling of seismicity within an areal source zone using the Gutenberg-Richter truncated exponential model and methodology described by Weichert (1980) [from 1994 report for Exploratory Studies Facility at Yucca Mountain].

(ASSUMES SEISMICITY DATA HAVE BEEN CAREFULLY AND APPROPRIATELY PROCESSED, AS DISCUSSED NEXT)

CAREFUL "CONDITIONING" OF EQ CATALOG

Common Magnitude Measure

- Reliable estimation of size for pre-instrumental events
- Check for inadvertent changes in instrumental magnitude reporting with time (e.g., Zuniga and Wyss, 1995)
- Systematic conversion to and use of Moment Magnitude

Completeness as a Function of Magnitude & Location

- Varying threshold of completeness with time (Stepp, 1972; EPRI, 1986)
- Spatially-varying threshold model of completeness for Southern Great Basin seismic network analyzed by Gomberg (1991)
- ZMAP (Wiemer and Zuniga, 1994)

Identification of Secondary Events—"Declustering" (Foreshocks, Aftershocks, Swarms)

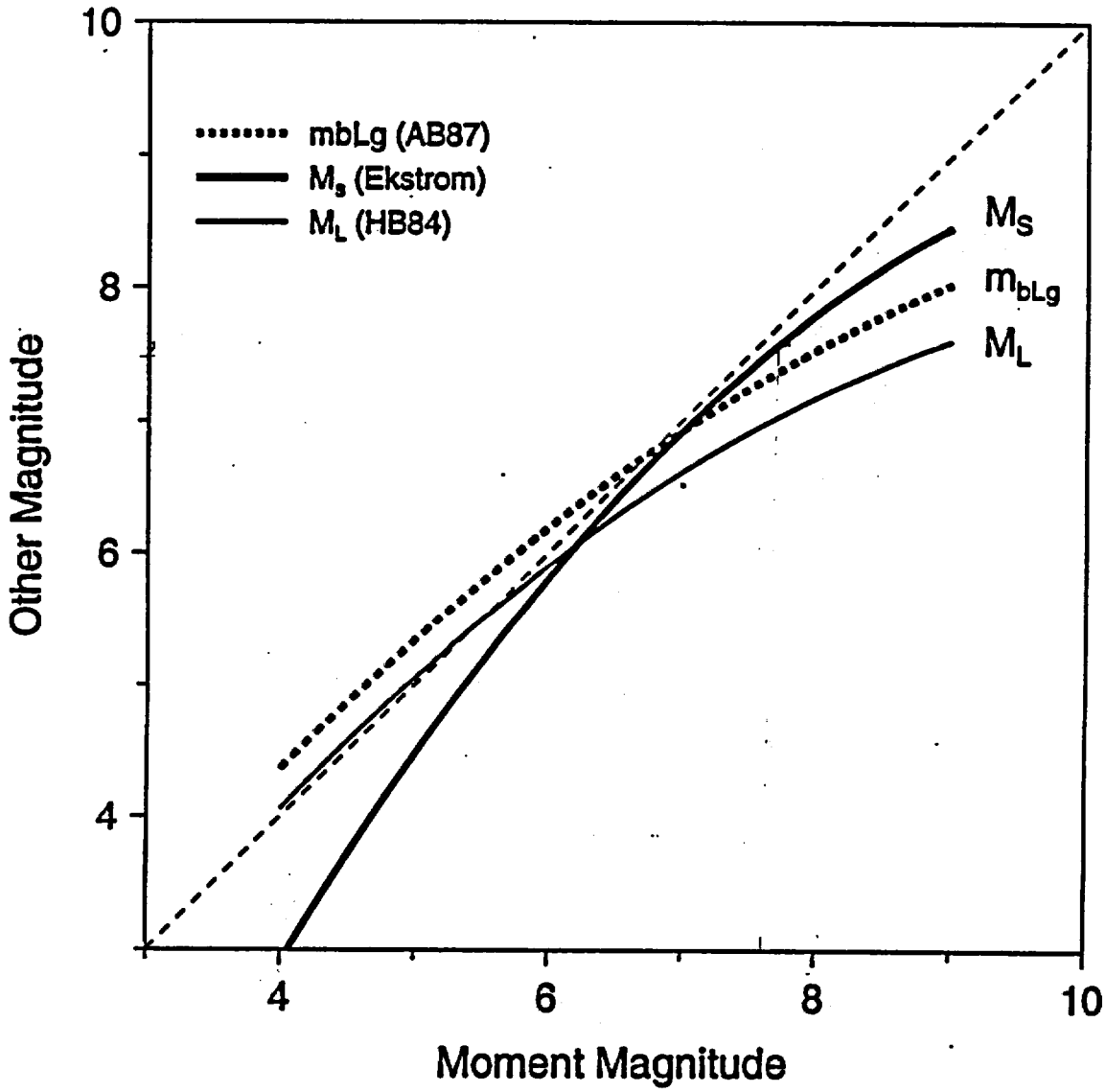

Figure 1. The functional dependence of various magnitudes on moment magnitude. The relation for m_{bLg} comes from Atkinson and Boore (1987). For M_S and M_L the relations came from fitting a quadratic to the data compiled by Ekström (1987) and Hanks and Boore (1984), respectively.

Comparison of various magnitude scales to moment magnitude (from Boore and Joyner, 1994)

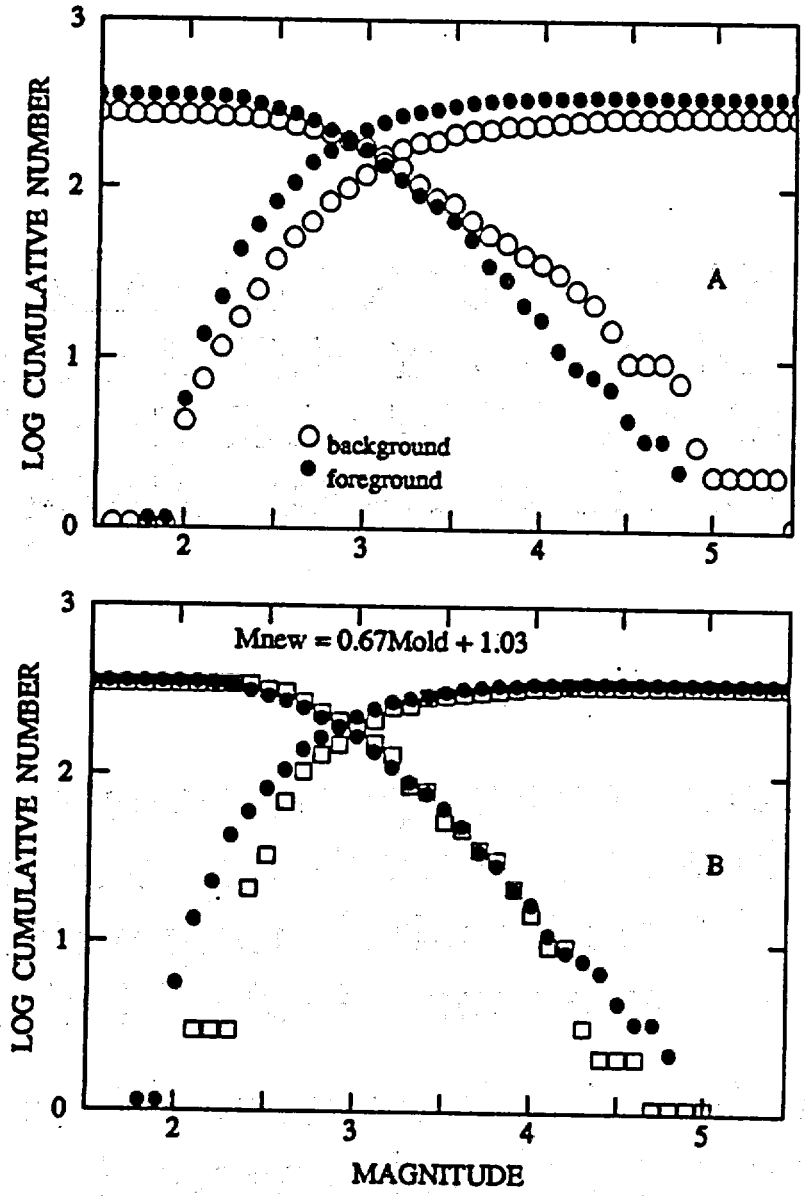

Figure 8. Frequency-magnitude relationship cumulated from above and below for the earthquake catalog for Italy for the periods 78.87 to 80.21 (background) and 80.21 to 81.5 (foreground). (a) The difference in *b* value noticed in these data is probably not due to a real change affecting all of Italy. (b) The background data with magnitudes transformed by the equation found using the *b*-value fitting method (open squares) yield a good fit to the observed foreground distribution.

Example analysis of inadvertent change in instrumental magnitude with time (from Zuniga and Wyss, 1995).

MOST EARTHQUAKE CATALOGS ARE FUNDAMENTALLY HETEROGENEOUS AND POSE CHALLENGES FOR SEISMIC HAZARD ANALYSIS

"[An] incorrect assumption made by many is that catalogs can be made homogeneous as a function of time by eliminating all events below a minimum magnitude, Mmin. . . .

However, this simple approach does not work [if changes in] assigned magnitudes occur inadvertently. Thus, earthquakes with true magnitude Mmin will be accepted in the culled catalog during one time period, but they will be excluded during another if a cut-off in magnitude is employed."

— Zuniga and Wyss (1995, p. 1859)

Clustered Catalog 1934–1991

Declustered Catalog 1934–1991

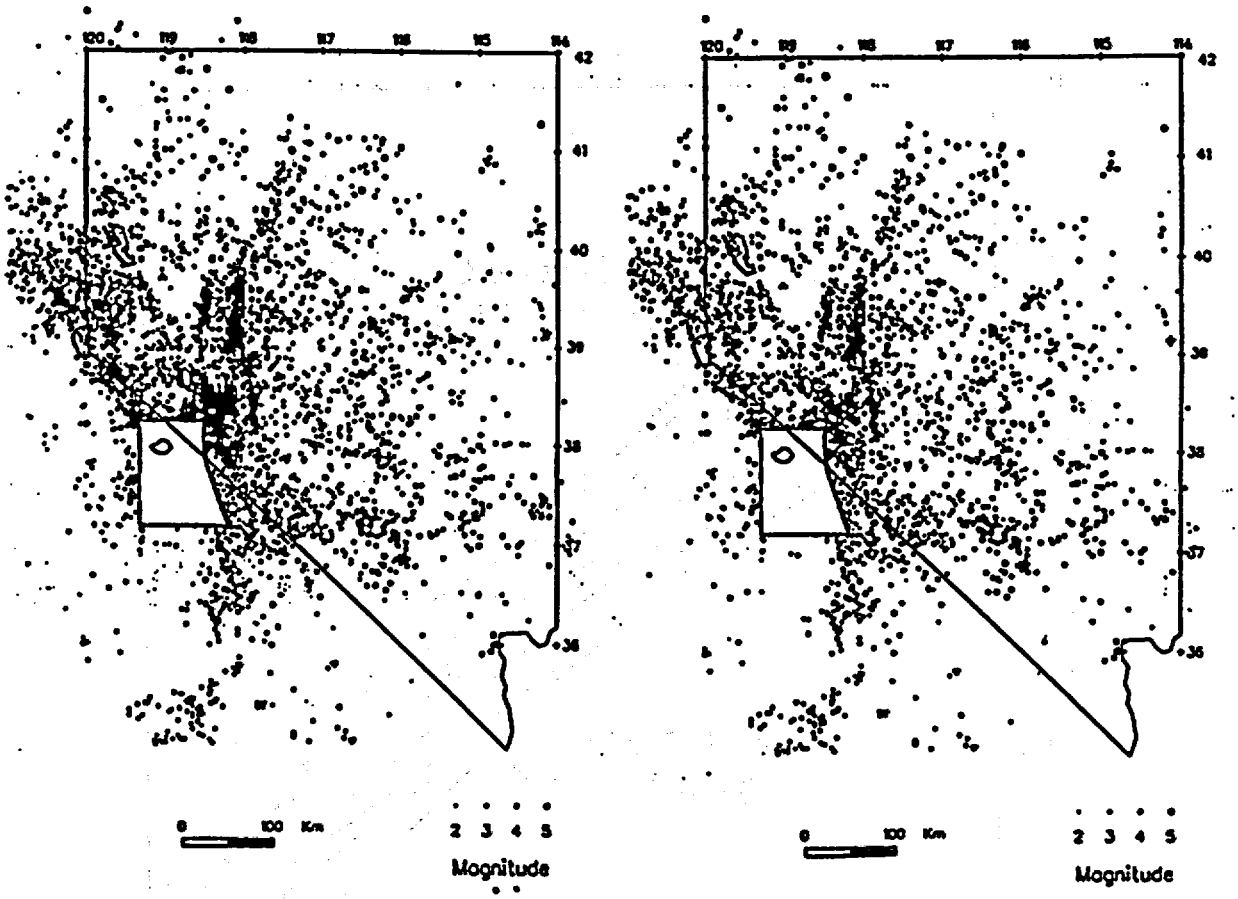

Example of declustering of Nevada earthquake catalog using Reasenberg's (1985) algorithm (from Savage and dePolo, 1993).

Illustration of significant difference between aftershock behavior in California and Utah—and why the declustering algorithm of Reasenberg (1985) must by "tuned" carefully for applications outside California (from Arabasz and Hill, 1994)

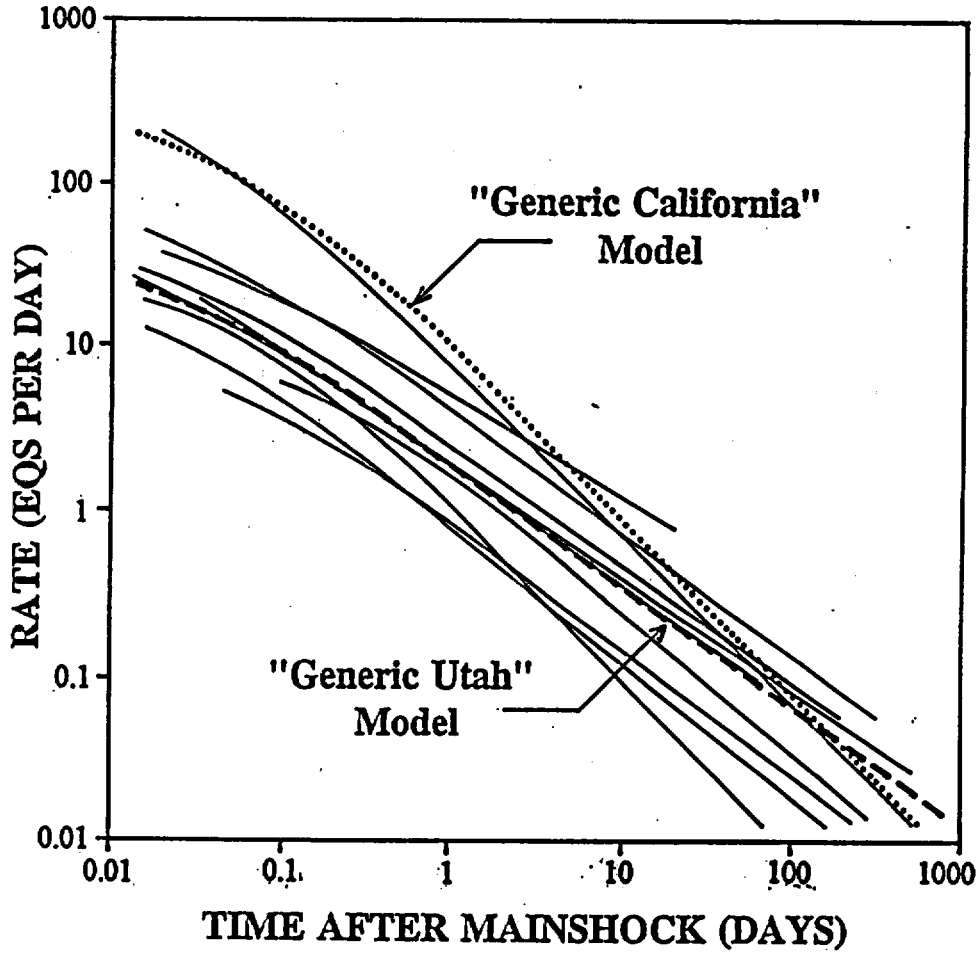

Rate decay and relative productivity of aftershock sequences, normalized to a cutoff magnitude 3.0 units below the mainshock magnitude. A median curve, labeled "Generic Utah" Model for 10 aftershock sequences in the Utah region is compared to a similarly derived "Generic California" Model of Reasenberg and Jones (1989). On average, the Utah aftershock sequences decay more slowly than the California model and are less "productive" by a factor of 4 to 5 in terms of aftershock rates after 1 day and the cumulative number of aftershocks during the first 30 days. Median values for the Utah Omori parameters are: p=0.75, b=0.87, c=0.02, a=-2.31 (from Arabasz and Hill, 1994).

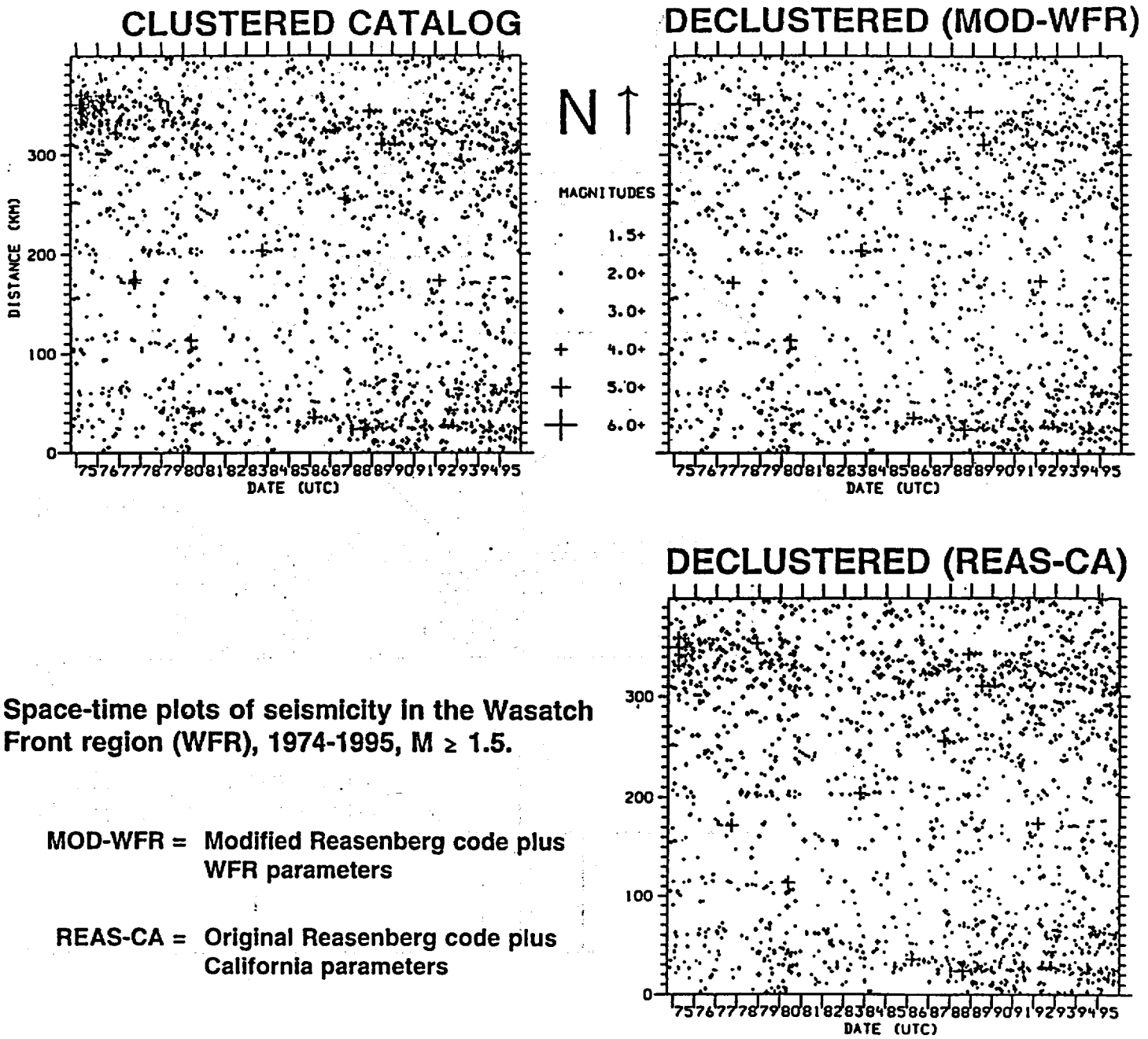

Space-time plots of seismicity in the Wasatch Front region (WFR), 1974-1995, M ≥ 1.5.

MOD-WFR = Modified Reasenberg code plus WFR parameters

REAS-CA = Original Reasenberg code plus California parameters

Illustration of improved declustering of seismicity in Utah's Wasatch Front region achieved by modifying the declustering algorithm of Reasenberg (1985) to account for differences in aftershock behavior compared to California (from Arabasz and Hill, 1996).

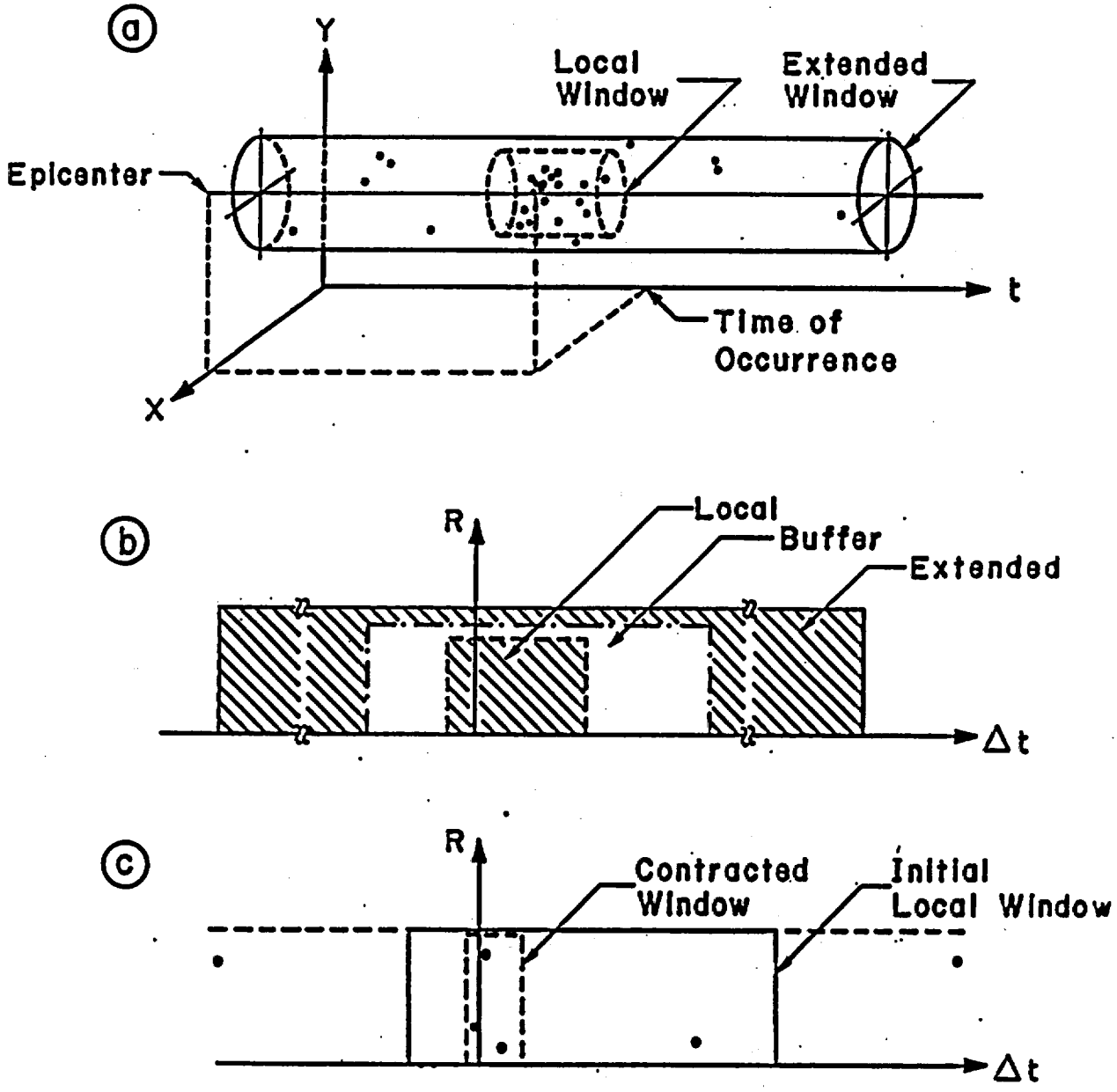

WINDOWS USED FOR CLUSTER ANALYSIS

Details of space-time windows used by Veneziano and Van Dyck (1985) to statistically discriminate secondary events in an earthquake catalog.

ISSUES FOR SSC IN THE YUCCA MTN REGION (From Workship #1 April 1995)

1. Candidate seismic sources for the background eq? Relative importance of volcanic earthquakes?

2. Size of maximum background earthquake?

3. Are rates of eq occurrence significantly affected by remotely triggered and "encouraged" mainshocks or are the effects insignificant when averaged over long periods of time?

4. Relative weighting of exponential vs characteristic vs maximum-magnitude eq recurrence models for fault-specific sources.

(more)

ISSUES FROM W'SHOP #1 (cont)

5. Developing fault segmentation models that define likely rupture segments.

6. Characterizing fault geometry and kinematics.

7. Characterizing distributive faulting.

8. Non-stationarity and possible temporal clustering of large earthquakes.

National Research Council

SSC ISSUES FROM NRC REVIEW OF SSHAC REPORT

- "Practitioners of PSHA should, in the judgement of the Panel, be aware of and free to use alternative valid approaches to SSC."

- "Classification of seismic source types is non-unique and admitted to be arbitrary."

- "Those who utilize the SSHAC procedures should be aware of . . . requirements for preparation of their earthquake catalog for PSHA. To the Panel's knowledge, a comprehensive study of the effects of systematic changes in earthquake catalogs on the results of a PSHA has not been done."

THE RELATIVE IMPORTANCE OF CERTAIN SSC PARAMETERS

[Relative to Best-Estimate Hazard & Contributions to the Uncertainty in the Hazard]

(SSHAC, 1995)

- **Uncertainty in fault location causes a moderate sensitivity for most sites for high-frequency ground motions, and less sensitivity at low frequencies. For source zones, this applies to sites located outside the source, but especially near the source boundary.**

- **Sensitivity to depth distribution is negligible except at small source-to-site distances (less than 50 km)**

(more)

- **Sensitivity to Mmax is largest at large source-to-site distances. It increases with ground motion amplitude, and is largest when the mean Mmax values are lower. (The sensitivity is greater when the mean Mmax is 6.0 rather than 7.5 for fixed a- and b-values.)**

- **Sensitivity to the b-value is moderate, except at small source-to-site distances (less than 25 km).**

- **Sensitivity to whether an exponential or characteristic magnitude distribution is used depends on whether a slip-rate constraint or a seismicity constraint is used to fix the rate of activity (a-value).**

  If a slip-rate constraint is used, the maximum sensitivity occurs for very close or very distant sites. If a seismicity constraint is used, calculations at all distances are sensitive to the choice of the model.

REFERENCES

Arabasz, W.J., 1994, Fundamentals of the Wasatch Front's earthquake threat: Proceedings, Seminar 1: Economic Impacts of a Large Earthquake, Earthquake Engineering Research Institute Wasatch Front Seismic Risk Regional Seminar; Salt Lake City, Utah, November 1994, p. 1-1 to 1-25.

Arabasz, W.J., and Hill, S.J., 1994, Aftershock temporal behavior and earthquake clustering in the Utah region (abstract): Seismological Research Letters, vol. 65, no. 1, p. 32.

Arabasz, W.J., and Hill, S.J., 1996, Applying Reasenberg's cluster-analysis algorithm to regional earthquake catalogs outside California (abstract): Seismological Research Letters, vol. 67, no. 2, p. 30.

Boore, D.M., and W.B. Joyner, 1994, Prediction of ground motion in North America, in Proceedings of ATC-35 seminar on new developments in earthquake ground motion estimation and implications for engineering design practice: Applied Technoloy Council Seminar TEchnical Papers ATC-35-1, p. 6-1 to 6-41.

EPRI, 1986, Seismic hazard methodology for the central and eastern United States, Vol. 1: Methodology, Electric Power Research Institute, Report NP-4726, July, p. 4-7.

Gomberg, J., 1991, Seismicity and detection/location threshold in the Southern Great Basin seismic network: Journal of Geophysical Research, vol. 96, no. B-10, p. 16,401-16,414.

Reasenberg, P., 1985, Second-order moment of central California seismicity, 1969-1982: Journal of Geophysical Research, vol. 90, p. 5479-5495.

Savage, M.K., and D.M. dePolo, 1993, Foreshock probabilities in the western Great Basin-eastern Sierra Nevada: Bulletin of the Seismological Society of America, vol. 83, p. 1910-1938.

SSHAC (Senior Seismic Hazard Analysis Committee), 1995, Recommendations for probabilistic seismic hazard analysis: Guidance on uncertainty and use of experts: NUREG/CR-6372.

Stepp, J.C., 1972, Analysis of completeness of the earthquake sample in the Puget Sound area and its effect on the statistical estimates of earthquake hazard: Proceedings of the International Conference on Microzonation, vol. 2, p. 897-910.

Veneziano, D., and J. Van Dyck, 1985, Main and secondary events in the EPRI catalog, in Seismic Hazard Methodology for Nuclear Facilities in the Eastern United States, Vol. 2, Appendix A: EPRI Research Project Number P101-29, Electric Power Research Institute, p. A-187 to A-219.

Weichert, D.H., 1980, Estimation of the arthquake recurrence parameters for unequal observation periods for different magnitudes: Bulletin of the Seismological Society of America, vol. 70, p. 1337-1346.

Weimer, S., and Zuniga, R.F., 1994, ZMAP—a software package to analyze seismicity (abstract): Eos, Trans. American Geophysical Union, vol. 75, p. 456.

Wesnousky, S.G., 1994, The Gutenberg-Richter or characteristic earthquake distribution, which is it?: Bulletin of the Seismological Society of America, vol. 84, p. 1940-1959.

Youngs, R.R., and Coppersmith, K.J., 1985, Implications of fault slip rates and earthquake recurrence models to probabilistic seismic hazard estimates: Bulletin of the Seismological Society of America, vol. 75, p. 939-964.

Youngs, R.R., Swan, F.H., Power, M.S., Schwartz, D.P., and Green, R.K., 1987, Probabilistic analysis of earthquake ground shaking hazard along the Wasatch Front, Utah, in Gori, P.L., and Hays, W.W., eds., Assessment of regional earthquake hazards and risk along the Wasatch Front, Utah, Vol. 2: U.S. Geological Survey Open-File Report 87-585, p. M1-110.

Zuniga, F.R., and Wyss, M., 1995, Inadvertent changes in magnitude reported in earthquake catalogs through of b-value estimates: Bulletin of the Seismological Society of America, vol. 85, p. 1858-1866. p. 53.

STRUCTURE AND GEOMETRY OF SEISMIC SOURCES

BY

RONALD L. BRUHN
DEPT. OF GEOLOGY AND GEOPHYSICS
UNIVERSITY OF UTAH
SALT LAKE CITY, UTAH
84109

OCT. 16, 1996

STRUCTURE AND GEOMETRY OF FAULT SYSTEMS
(Applications to Earthquake Studies)

Goals

Estimate Fault Location & Parameters Required for Seismic Moment Calculation
(Fault Area & Average Slip)
-> Estimate Geometry of Source in the Subsurface
-> Determine Kinematics
-> Infer Long - Term (STATIC) vs Transient Rupture Termination Points

Segmentation: Structural & Geometrical vs Earthquake

Definitions

Fault Scaling Parameters

Length vs Earthquake Displacement
Length vs Net (Long-Term) Displacement
Fault Size - Frequency Relationships

Fault Scarp & Bedrock Map Traces

Intersection with topography: Bedrock -> Surficial Deposit -> Surface Interactions
Trace curvature - listric faults vs fault terminations
Roughness - origin and interpretation
Fault spacing and length distributions

Down-dip Geometry

Fault tip-lines, branch-lines and intersections
Hanging and footwall rotation and flexure
Inferences from the 'Frictional / Quasi-plastic transition

Rupture extent and displacement field

Kinematic analysis - use of stress / strain field to constrain fault kinematics
Reading the rupture: Stationary versus transient rupture termination points
Barriers - slip-conservative and slip-divergent
Insight from Tectonic Geomorphology
Fault interactions - echelon segments, overlapping, underlapping, depth extent, anti-thetic faults
Fault zone rheology - slip strengthening versus weakening material, slip-distribution with depth

NEW TEXTBOOKS OF INTEREST

Active Tectonics, Earthquakes, Uplift and Landscape by E.A. Keller and N. Pinter, 1996, Prentice-Hall, Inc.

Exercises in Active Tectonics, An Introduction to Earthquakes and Tectonic Geomorphology by N. Pinter, 1996, Prentice-Hall, Inc.

The Geology of Earthquakes by R.S. Yeats, K. Sieh, and C.R. Allen, 1997, Oxford University Press.

Also, McCalpin's new book on Paleoseismology.

Volume 18 Numbers 2/3, February–March 1996

ISSN 0191-8141

JOURNAL OF STRUCTURAL GEOLOGY

Special Issue

SCALING LAWS FOR FAULT AND FRACTURE POPULATIONS—ANALYSES AND APPLICATIONS

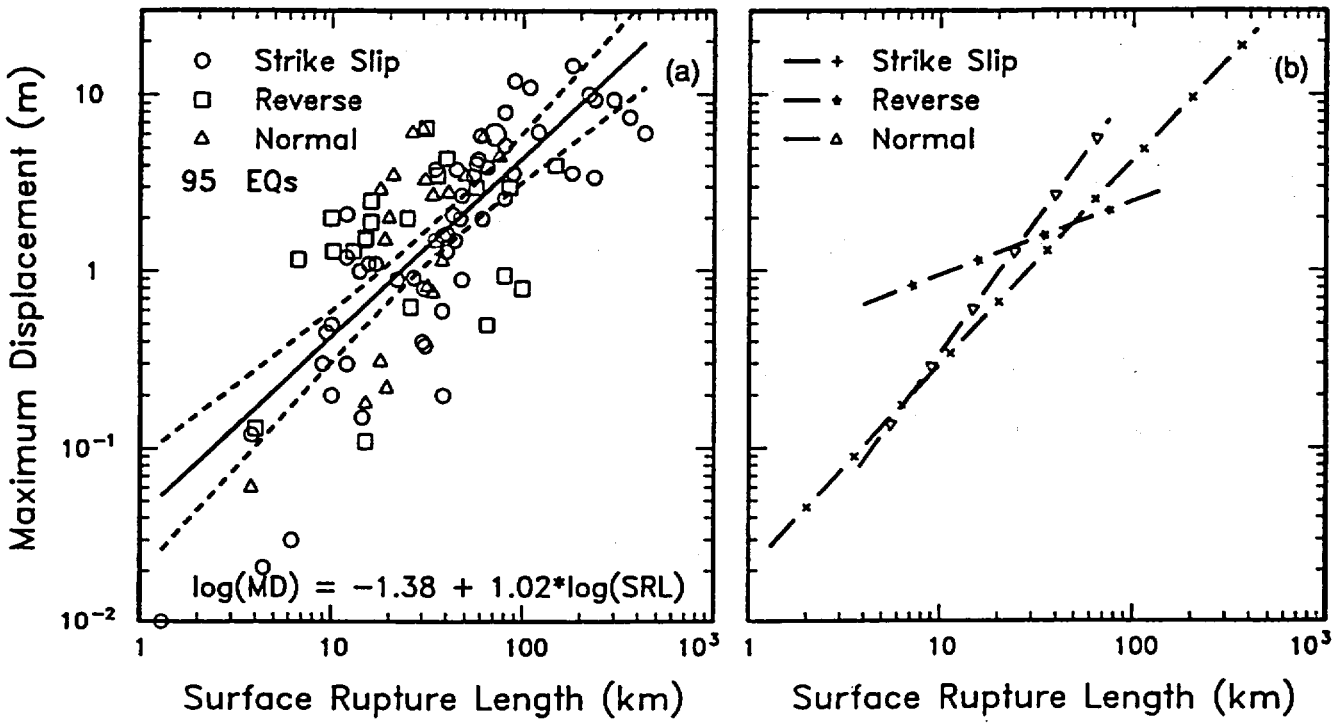

Figure 12. (a) Regression of surface rupture length on maximum displacement. Regression line shown for all-slip-type relationship. Short dashed line indicates 95% confidence interval. (b) Regression lines for strike-slip, reverse, and normal-slip relationships. See Table 2 for regression coefficients. Length of regression lines shows the range of data for each relationship.

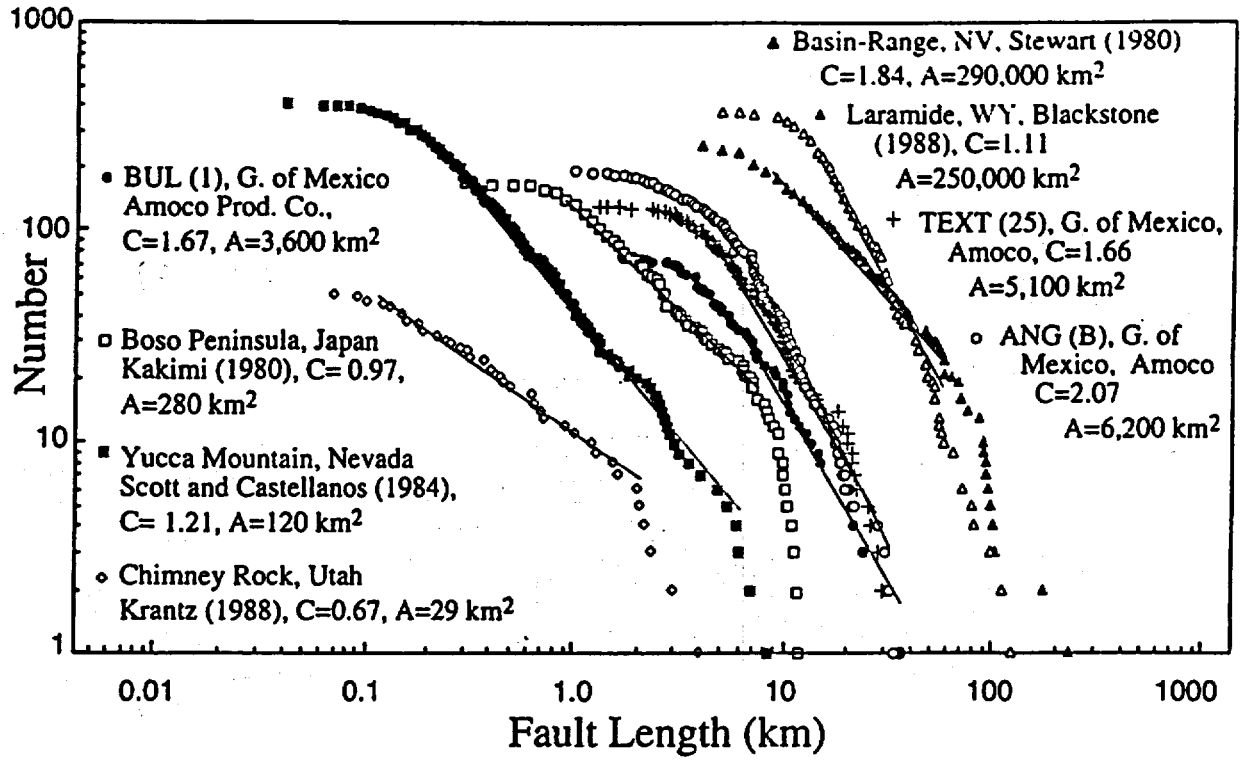

Fig. 1. Eight fault length data sets derived from the maps published in the references given on the figure. Thin lines show the portions of the curves which fit lines with slopes of C. Because these data were collected from two-dimensional samples of three-dimensional volumes, equation (1) and the data in Fig. 1 describe two-dimensional fault populations. The actual (three-dimensional) power-law exponent for small faults is $C + 1$ (Marrett & Allmendinger 1991). Also shown are the areas (A) in square kilometers of the maps from which the data were collected.

Total Displacement

Clark & Cox 1996

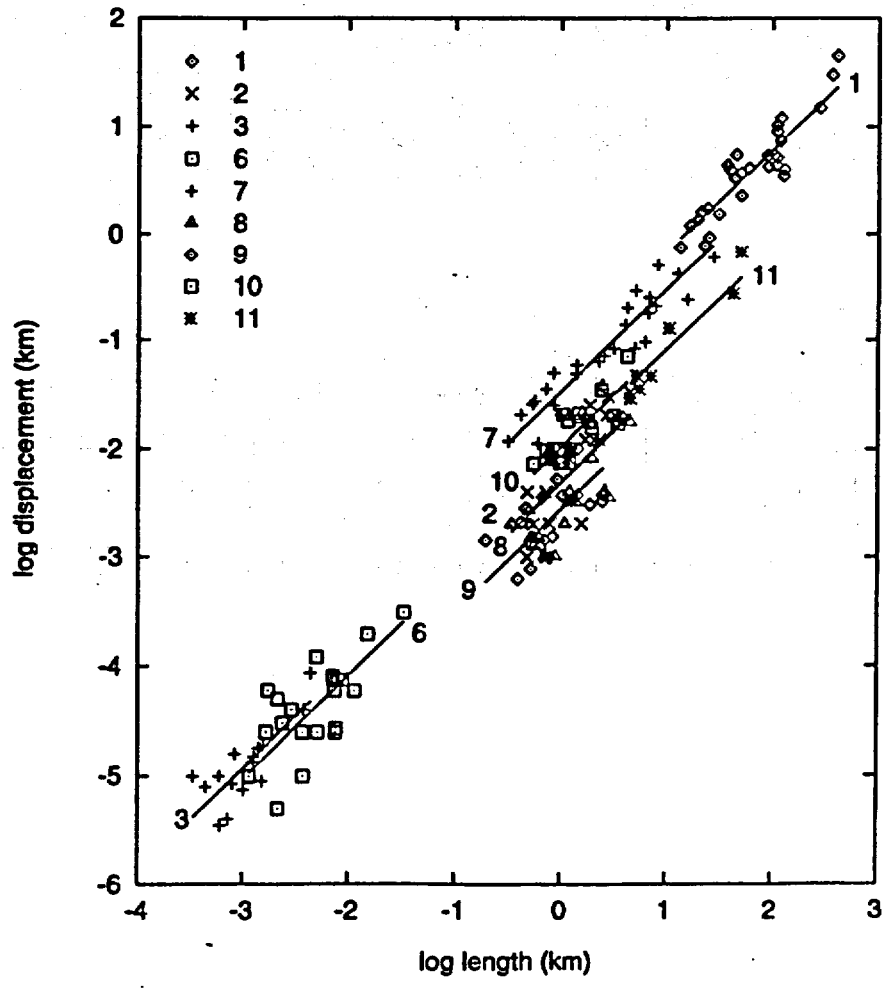

Fig. 1. Results of the combined analysis of nine data sets (lines), with the source data (symbols). Group numbers as in

Fossen & Gabrielsen (1996)

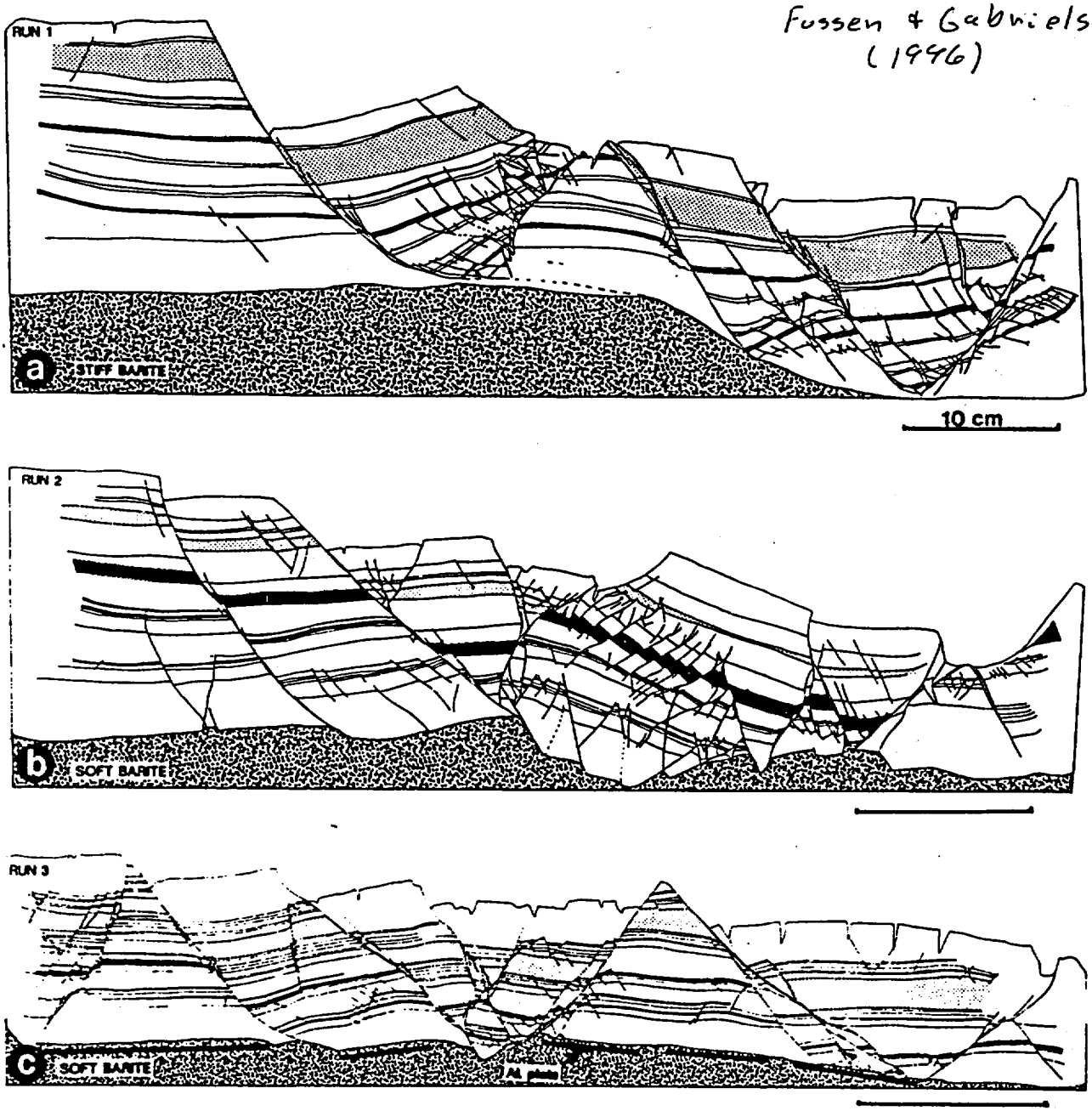

Fig. 5. Final stage of (a) run 1, (b) run 2 and (c) run 3. See text for discussion.

LÄGERDORF QUARRY FRACTURE MODEL

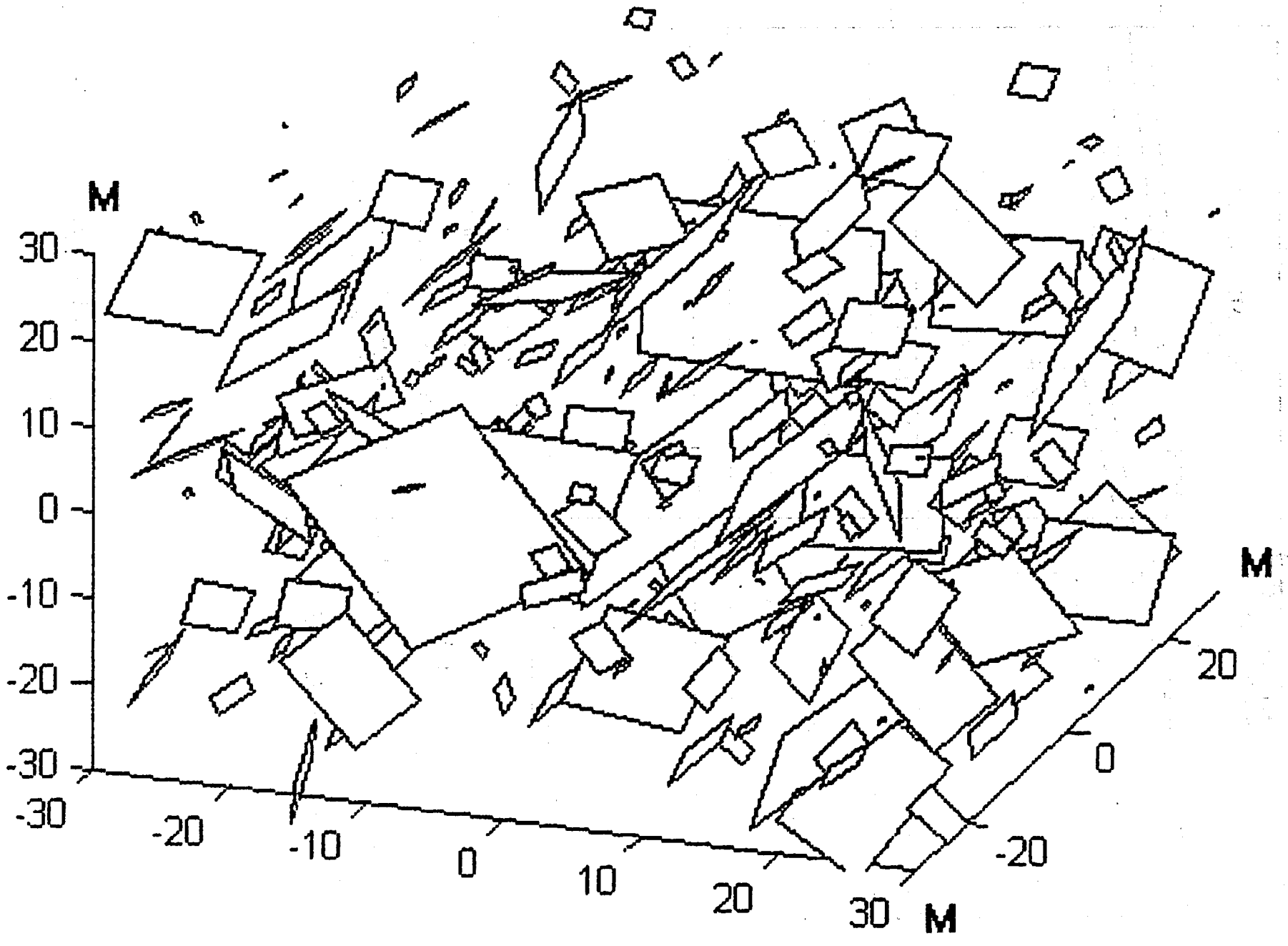

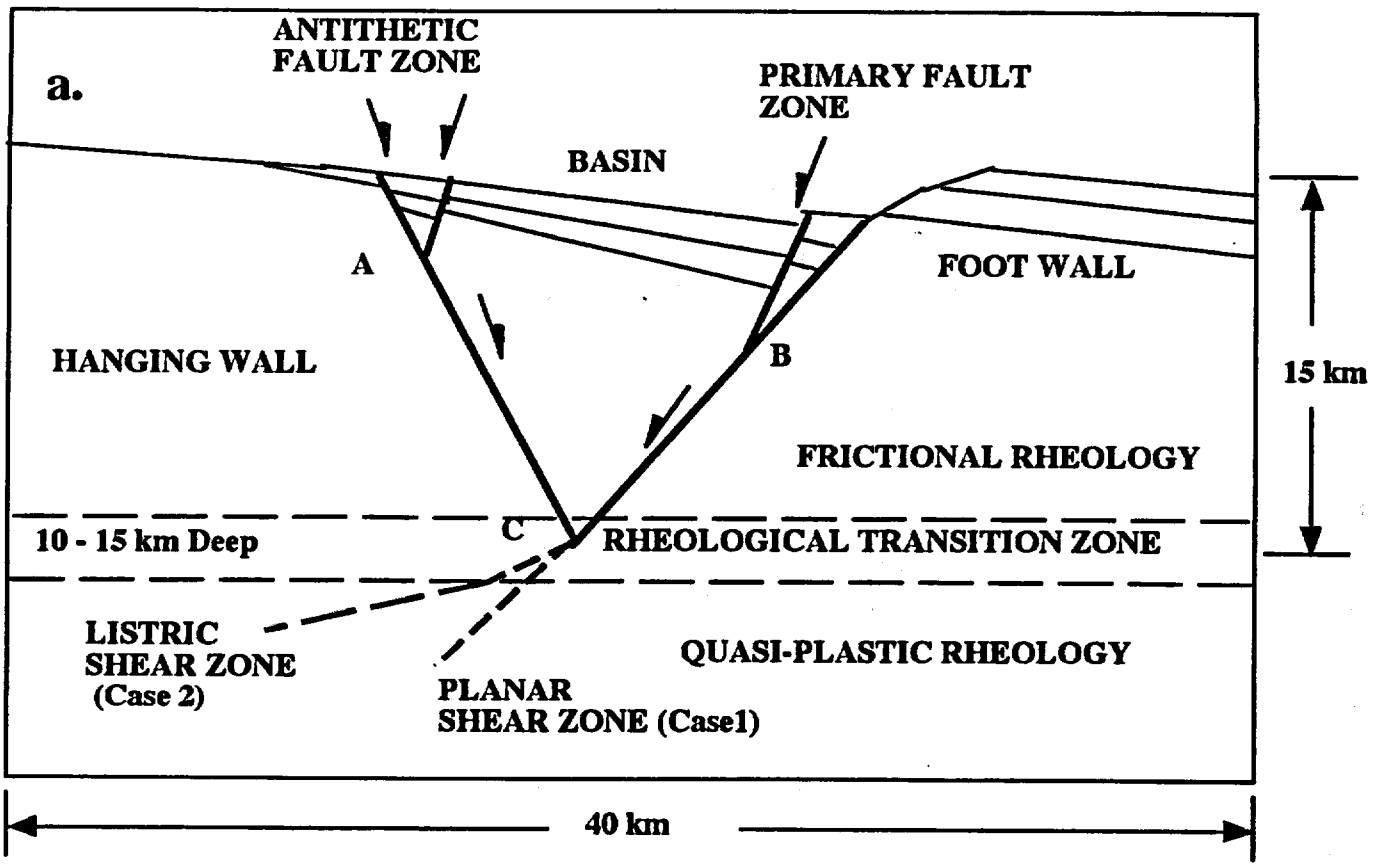

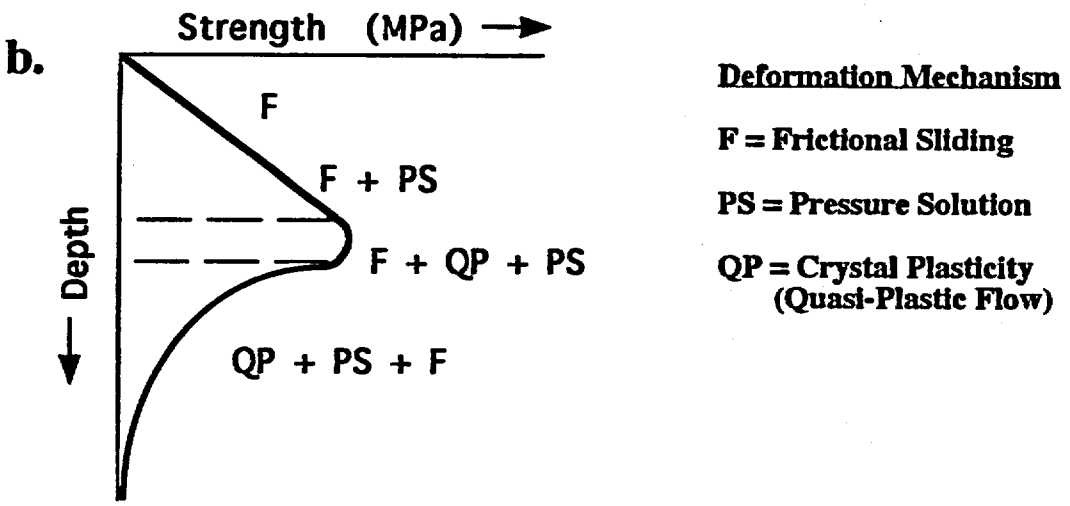

Deformation Mechanism

F = Frictional Sliding

PS = Pressure Solution

QP = Crystal Plasticity (Quasi-Plastic Flow)

Bruhn & Schulz

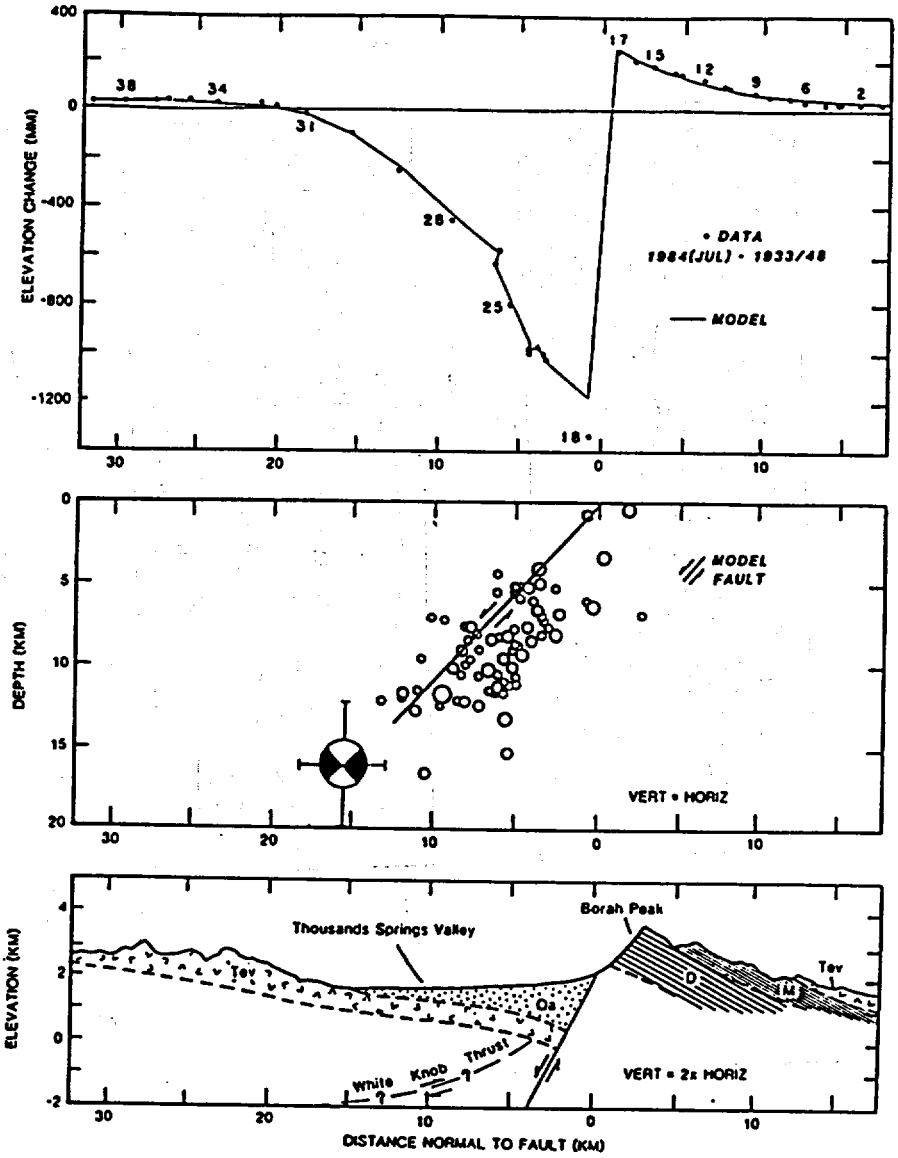

Figure 9–16. Cross sections of Borah Peak earthquake zone showing (top) observed coseismic elevation changes of benchmarks (dots) and the predicted changes based on a model of a planar fault, and mainshock and aftershocks near leveling line together with the location of the fault used in the geodetic model (middle), and a geological cross section including a low-angle thrust which was not reactivated during the earthquake. The distance along the cross section is with respect to the surface trace of the fault (bottom). After Stein and Barrientos (1985).

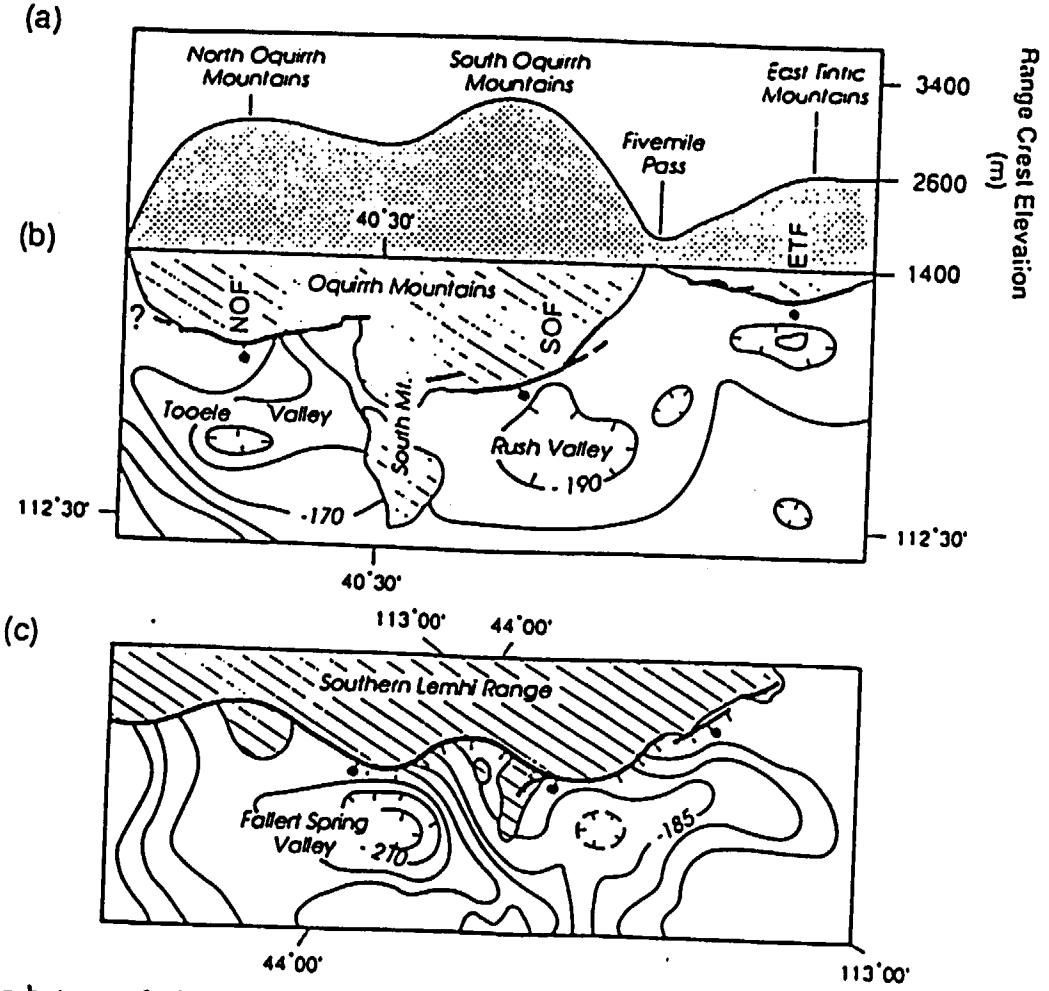

g. 16. Comparison between fault structures of Oquirrh–East Tintic Mountains normal fault zones and the southern mhi Range normal fault zone. (a) Elevation profile along the Oquirrh–East Tintic Mountains range crest. (b) Normal ılts along the western flank of the Oquirrh and East Tintic Mountains and complete Bouguer gravity contours in the jacent basin valleys (Cook *et al.* 1989), showing unlinked normal fault zones. SOF = South Oquirrh Mountains fault zone.)F = the North Oquirrh Mountains fault zone. ETF = the East Tintic Mountains fault zone. (c) Normal fault zone along : southwestern flank of the southern Lemhi Range and complete gravity contours (Bankey *et al.* 1985), showing the geometry of linked normal faults. Teeth marks are the late Quaternary fault scarps.

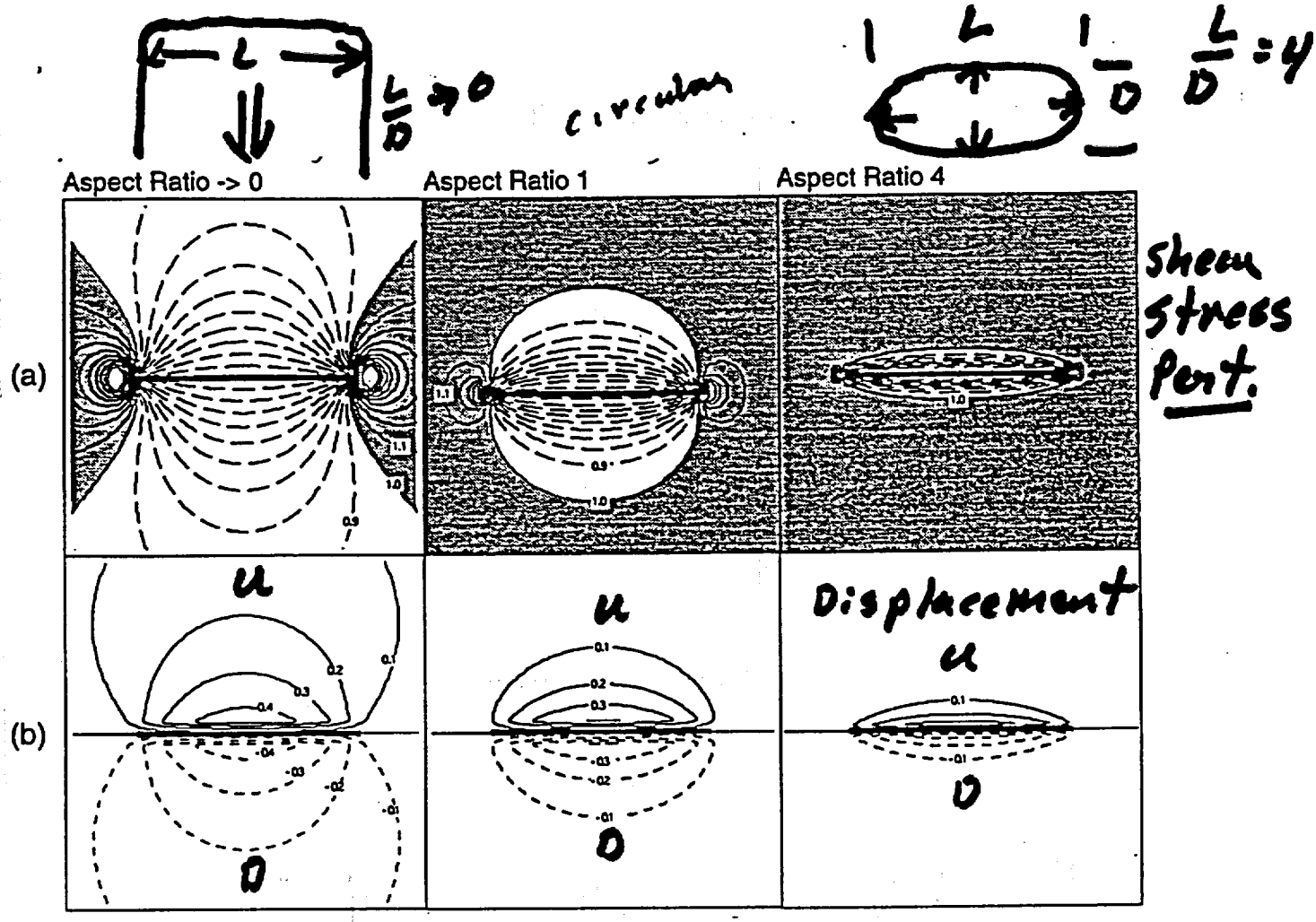

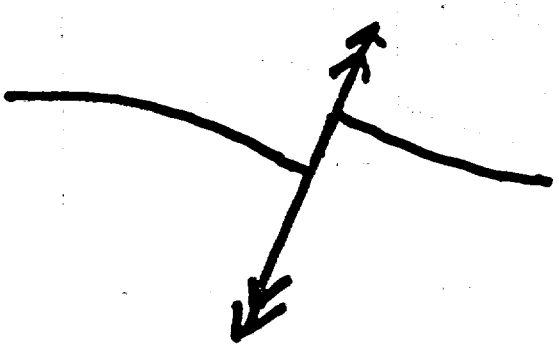

From Willemse & Pollard (96).

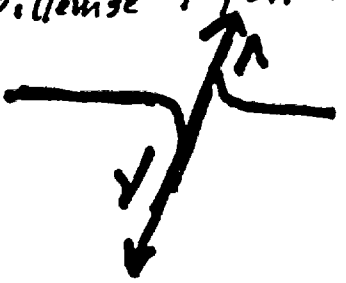

North of Little Rock Canyon - Springville Quadrangle

View along strike

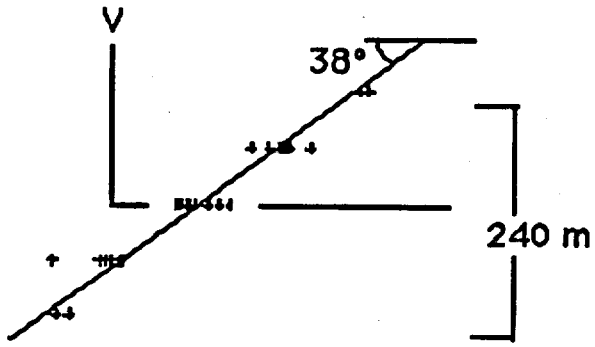

(30 data points)

Perspective View

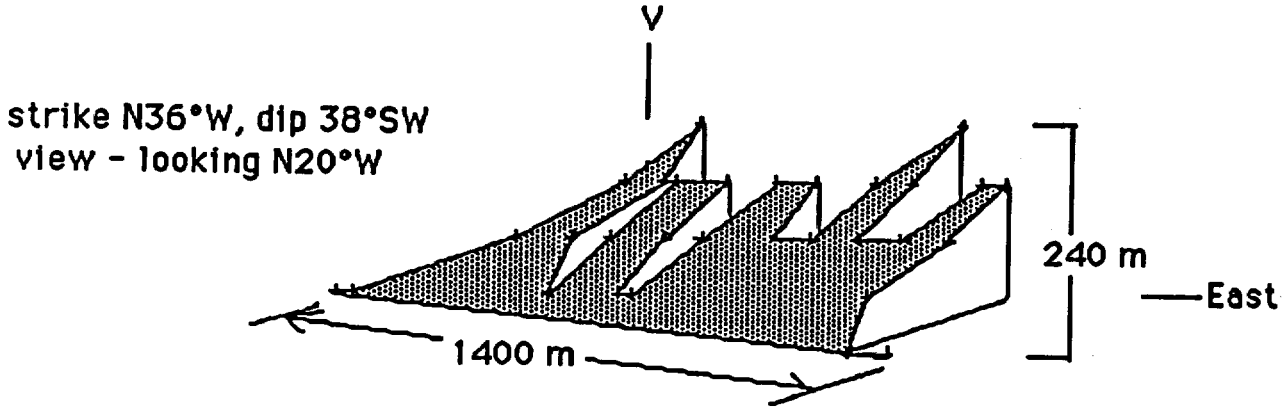

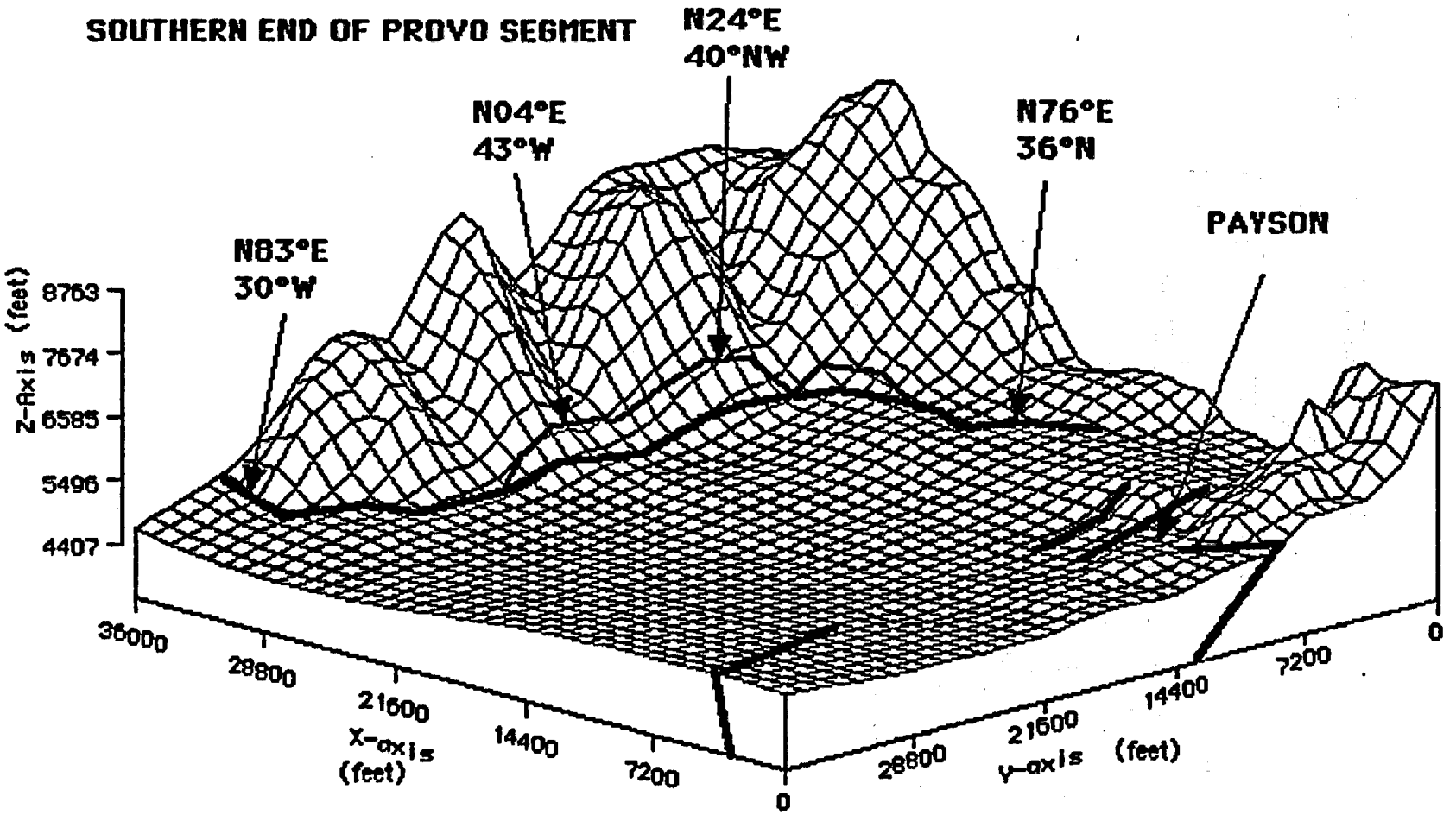
SOUTHERN END OF PROVO SEGMENT
N24°E
40°NW
N04°E
43°W
N76°E
36°N
N83°E
30°W
PAYSON
Z-Axis (feet)
8763
7674
6585
5496
4407
36000
28800
21600
14400
7200
0
X-axis
(feet)
28800
21600
14400
7200
0
Y-axis (feet)

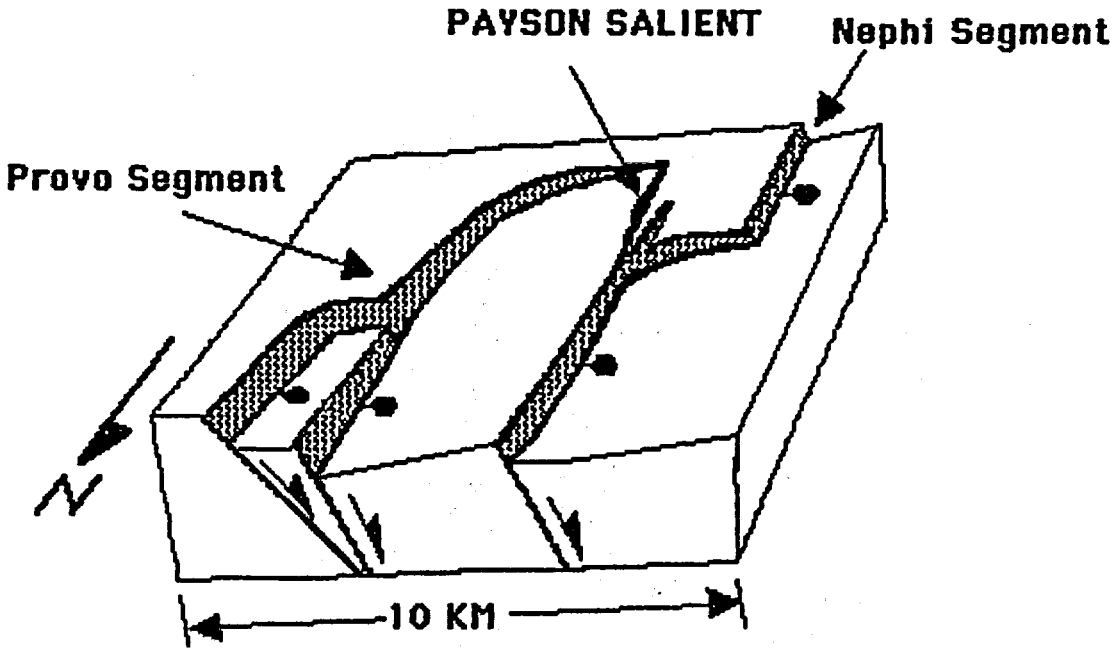
PAYSON SALIENT
Nephi Segment
Provo Segment
N
10 KM

READING THE RUPTURE
(Lesson #1)

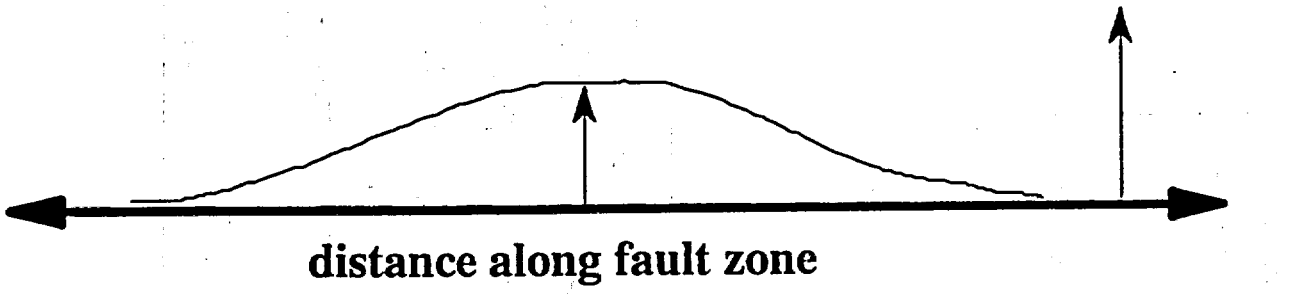

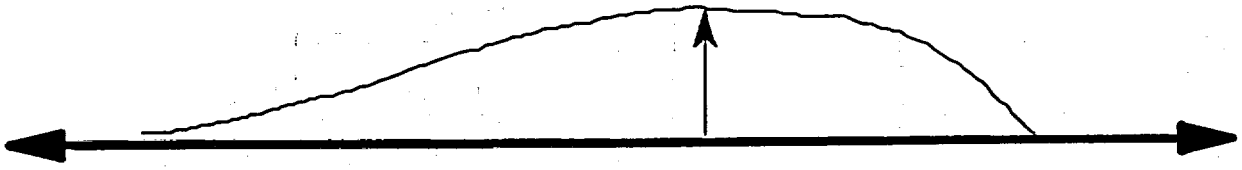

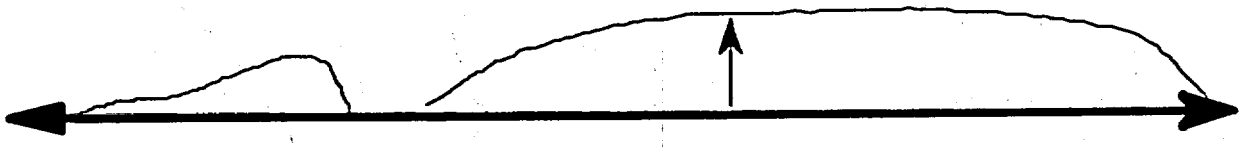

Case: One strong boundary, and a non-persistent termination point.

Case: No persistent termination point.

Case: A 'characteristic' rupture segment, and a non-persistent termination point.

R.L. Bruhn

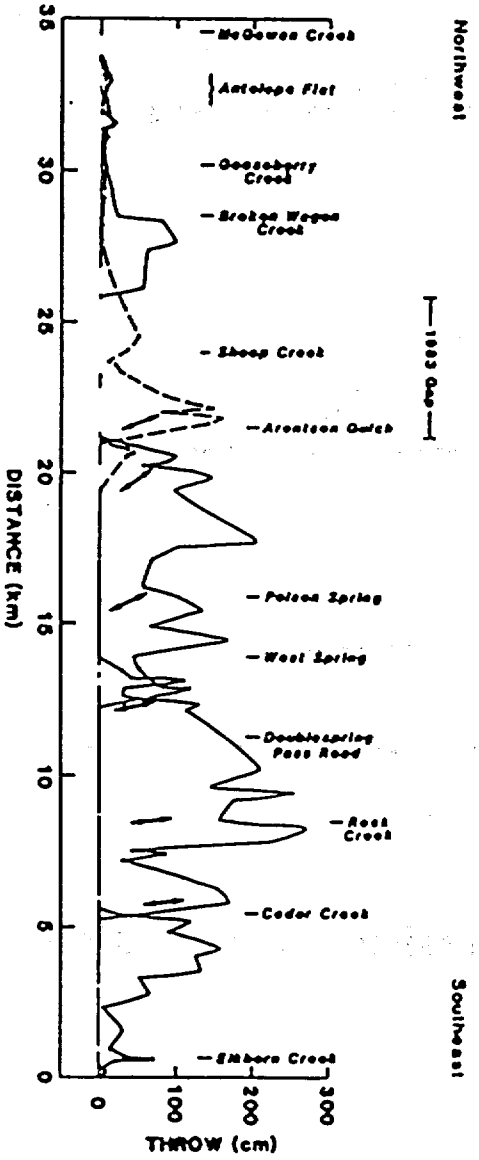

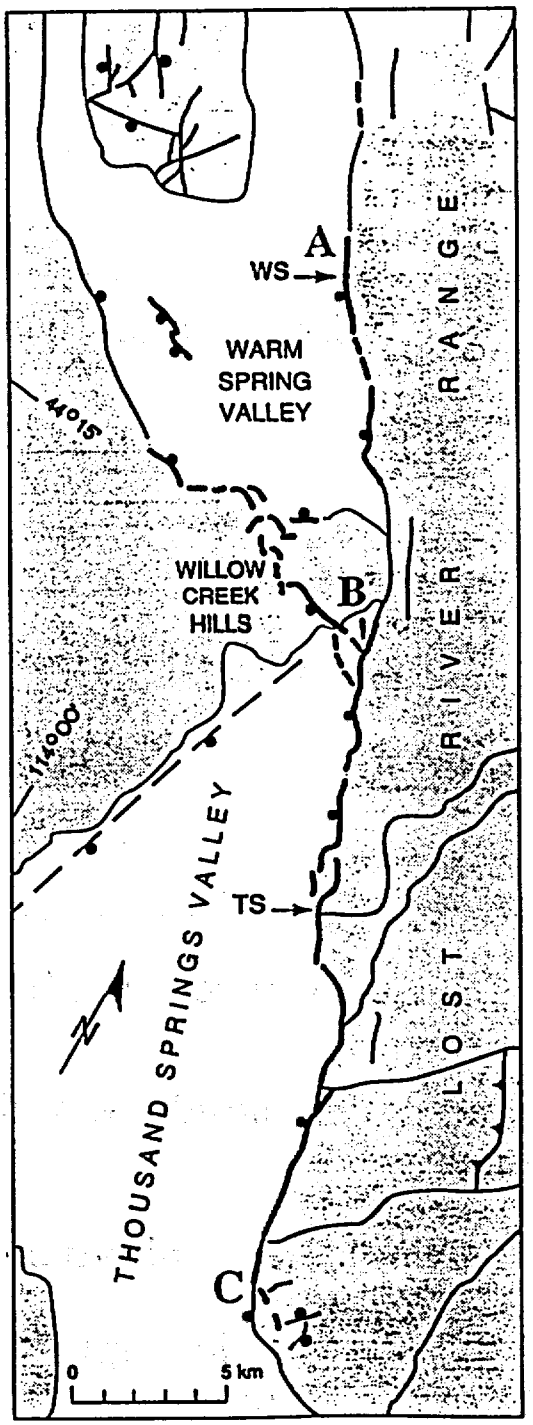

Figure 9–15. Map of fault scarps and ground rupture accompanying the 1983 Borah Peak earthquake (heavy lines, bar and ball on downthrown side). Shaded areas are mountains; alluviated valleys are unpatterned. After Crone et al. (1987) and Crone and Haller (1991).

Quaternary Fault Studies in the Site Area, with Emphasis on Fault Location and Geometry

C. MENGES

Objectives

- Describe previous studies
- Summarize results
  - Location
  - Planview patterns
  - Length
  - Surface expression
  - Fault geometry
  - Fault displacements and slip direction

Data from Chapter 4.2, Tectonic Synthesis Report

Fault Identification

- Photointerpretative Mapping
- Field investigations
  - Geologic mapping
  - Strip mapping along fault traces
  - Trenching studies
  - Geochronologic studies

Quaternary Fault Studies

- Mapping
  - Christiansen and Lipman, 1965
    - USGS quadrangle mapping
  - Scott and Bonk, 1984; Scott, 1992
    - Detailed geologic mapping
  - O'Neill and others, 1991
    - Systematic photointerpretation
  - Simonds and others, 1996
    - Detailed fault strip mapping
  - Day and others, 1995 to present
    - Very detailed geologic mapping of repository block

Quaternary Fault Studies

- Trenching investigations
  - Swadley, Hoover and Rosholt, 1984
    - Initial trenching
  - Addtional logging in the mid-late 1980's
  - Paleoseismic investigations, 1992-1996
    - Chapter 4, Tectonic synthesis report
- Results
  - 52 total trenches and enhanced exposures
    - 40 sites on Quaternary faults
    - 28 sites with evidence for Quaternary displacements

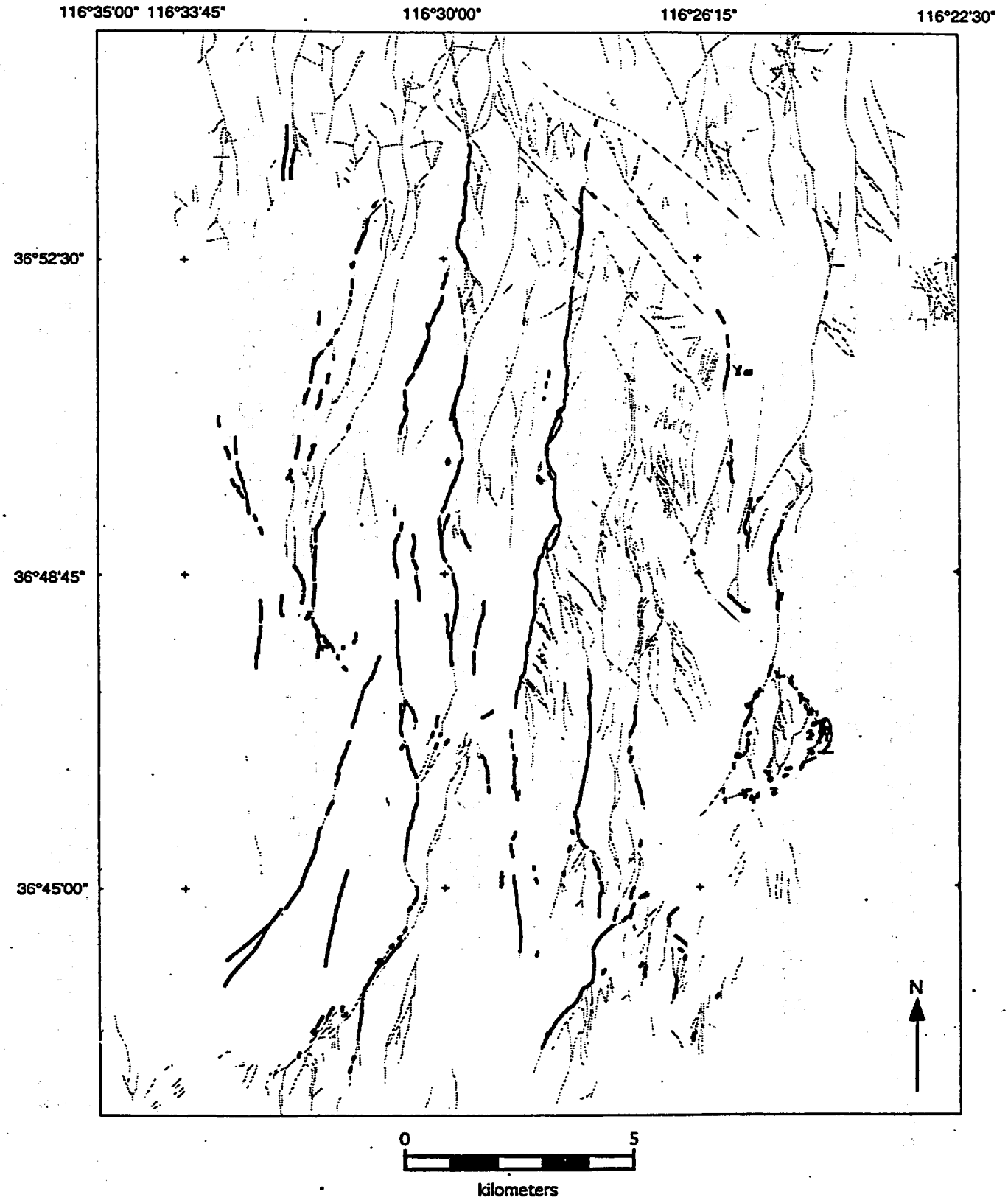

Figure 4.2.1 Map showing the distribution of fault traces in the Yucca Mountain area, simplified from Simmonds and others (1995). Quaternary and suspected Quaternary faults are shown in bold.

Fault Trace Patterns

- Great complexity
- Discontinuous surface traces
  - Gaps where buried by alluvium
  - Geophysical surveys for fault continuity
- High Density of closely-spaced faults
  - Separations commonly < 1-5 km
- Anastomosing pattern of fault intersections and bifurcations
  - Two basic fault systems evident
    - West and east side of mountains with possible interconnection

Fault Lengths

- Generally short lengths
  - Uncertainty as to exact lengths from discontinuous fault traces
- Individual continuous traces of <1km to 12 km
- Overall lengths of major faults of tens of kms
  - Minimum: 4km for Stagecoach Road fault
  - Maximum: 33 km for Paintbrush Canyon fault
  - Typically 10 to 20 km

Surface Expression of Faults

- At Yucca Mtn, major Quaternary faults at base of bedrock escarpments
  - West side, many fault-line scarps
    - Topographic enhancement of bedrock on footwall
  - East side, burial of fault by eolian and colluvial deposits (sand ramps)
- In Crater Flat, piedmont fault scarps in mid-late Quaternary alluvium

Fault Geometry

- Mostly surface data from mapping and trenches
  - Very limited subsurface data
    - Borehole, tunnel, geophysics
- General north to northeast orientations
  - Increasing NE strikes to south along Yucca Mountain
  - Exception: several NW trending faults
- Steep dips (>45 , commonly >60) mostly to west
  - Very steep (subvertical) dips common in alluvium in trenches
  - Dips remain steep in shallow subsurface
    - Bow Ridge fault >60 in ESF tunnel
    - Borehole data indicate Stagecoach Road fault >60 at 85 m depth

Fault Displacements and Sense of Slip

- Cumulative bedrock separations of 50-600 m
  - Majority of displacement late Miocene in age
- Very small cumulative vertical displacements in mid-late Quaternary
  - Commonly 1-2.5 m, maximum observed of 4-6m (Busted Butte)
- Sense of slip--normal, down to the west
  - Exceptions: proposed right lateral displacments on several NW trending faults
- Poor constraints on amount of lateral slip on major normal faults
  - Postulated as oblique normal slip with left-lateral component
    - Slickenlines with left-oblique rakes of >45 on many bedrock fault surfaces
    - Several similar left-oblique high-angle rakes (60 - 75) on possible slickenlines from carbonate coatings in Quaternary fault zones

Conclusions

- Large database on Quaternary site faults developed from many mapping and trenching studies
- Results on location and geometry of faults
  - Many closely-spaced faults in small area
  - Complex anastomosing fault pattern
  - Short lengths
  - Varied surface expressions
  - Faults trend NS-NE and dip steeply west
  - Small to moderate bedrock displacements and very small Quaternary displacements
  - Poorly-constrained but probably left-normal oblique sense of slip

LOCATION MAP OF MAJOR FAULTS AND TRENCHES AT YUCCA MOUNTAIN

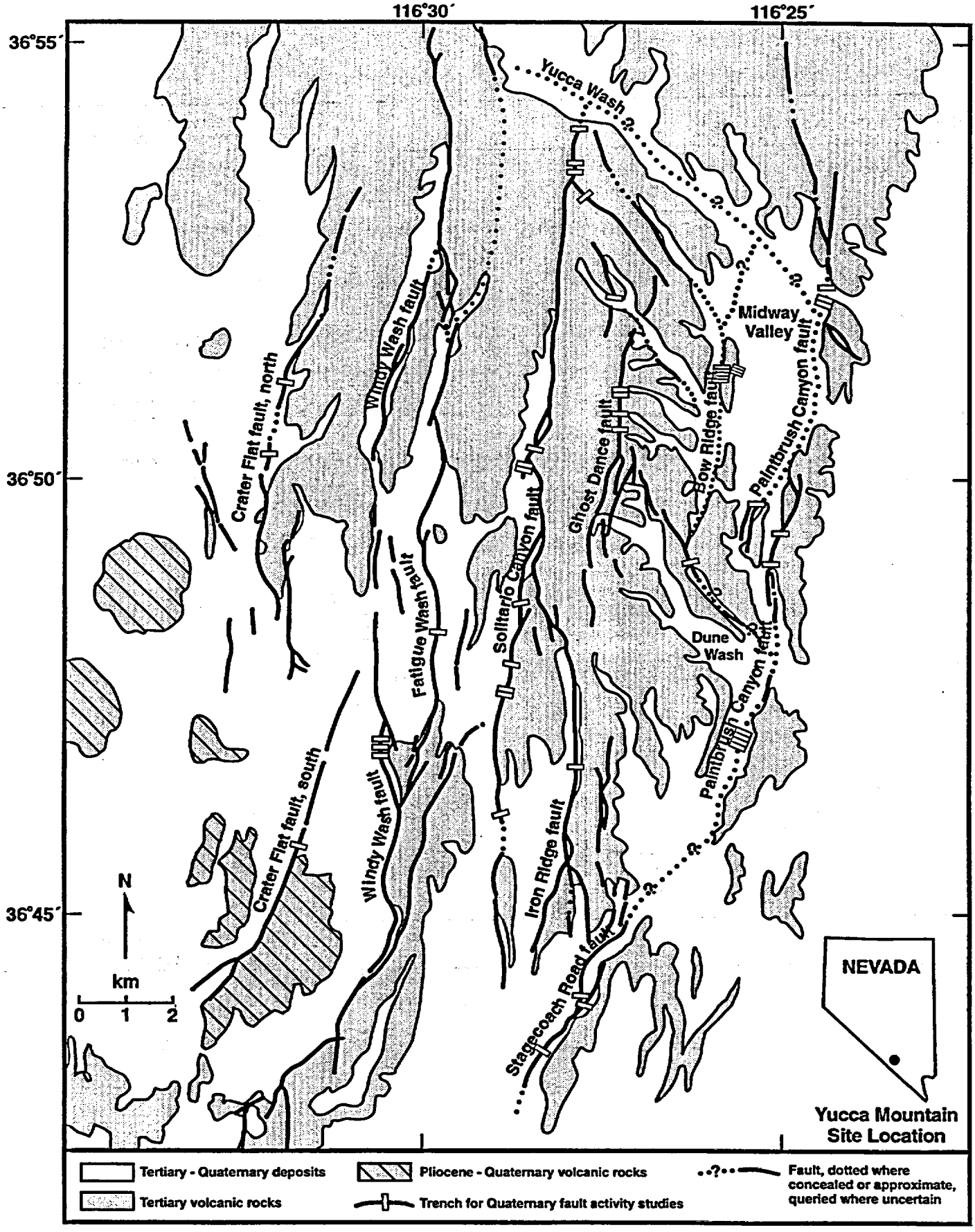

SOLITARIO CANYON FAULT DATA

EQUAL AREA
LOWER HEMISPHERE

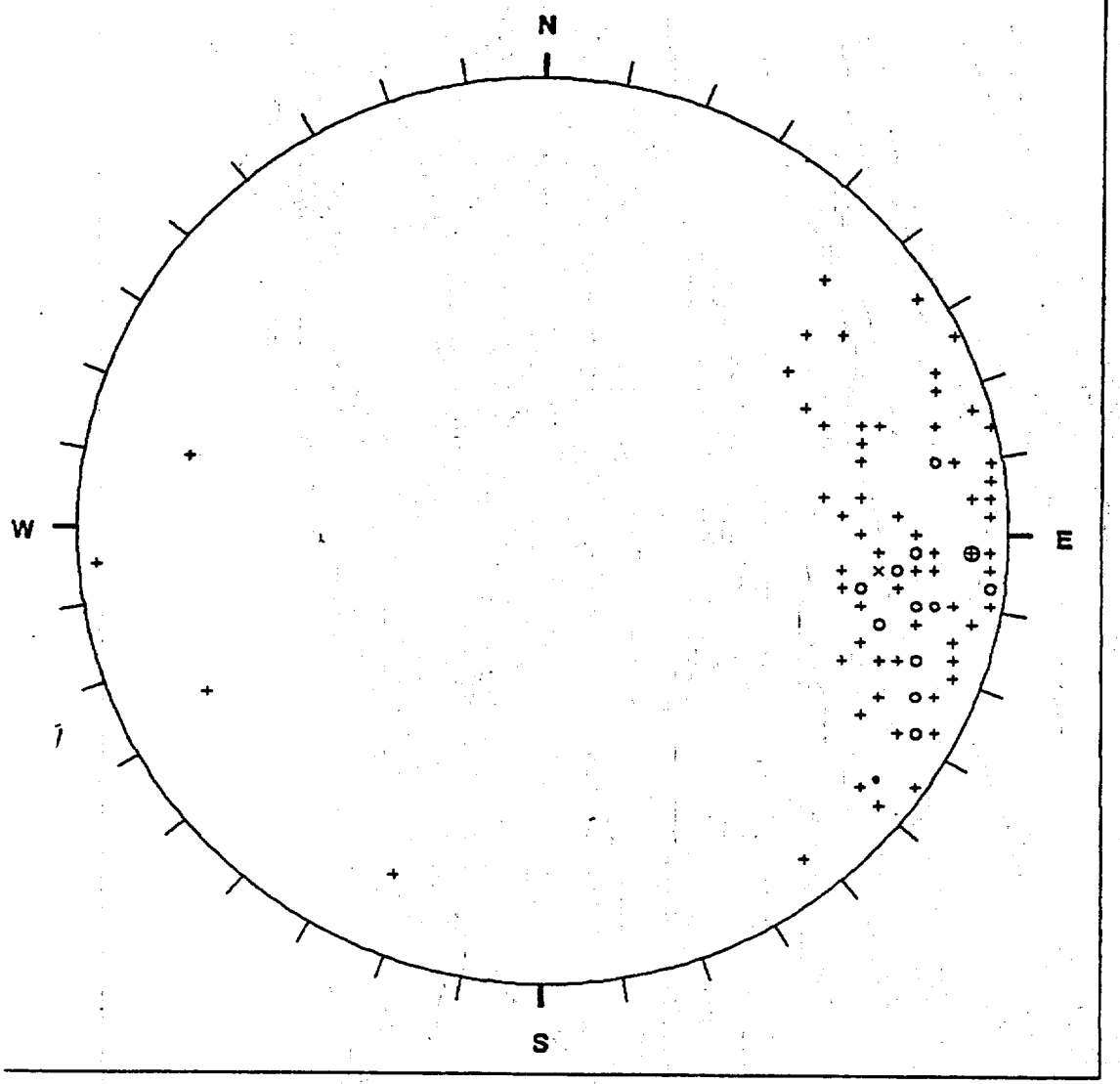

SCATTER PLOT

NUM. OF POLES

+	1 pole
o	2 poles
x	3 poles
X	4 poles
⊕	5 poles

STRIKE AND DIP DATA

93 Poles Plotted
93 Data Entries

Bare Mountain and Death Valley - Furnace Creek Faults

Larry W. Anderson
Bureau of Reclamation

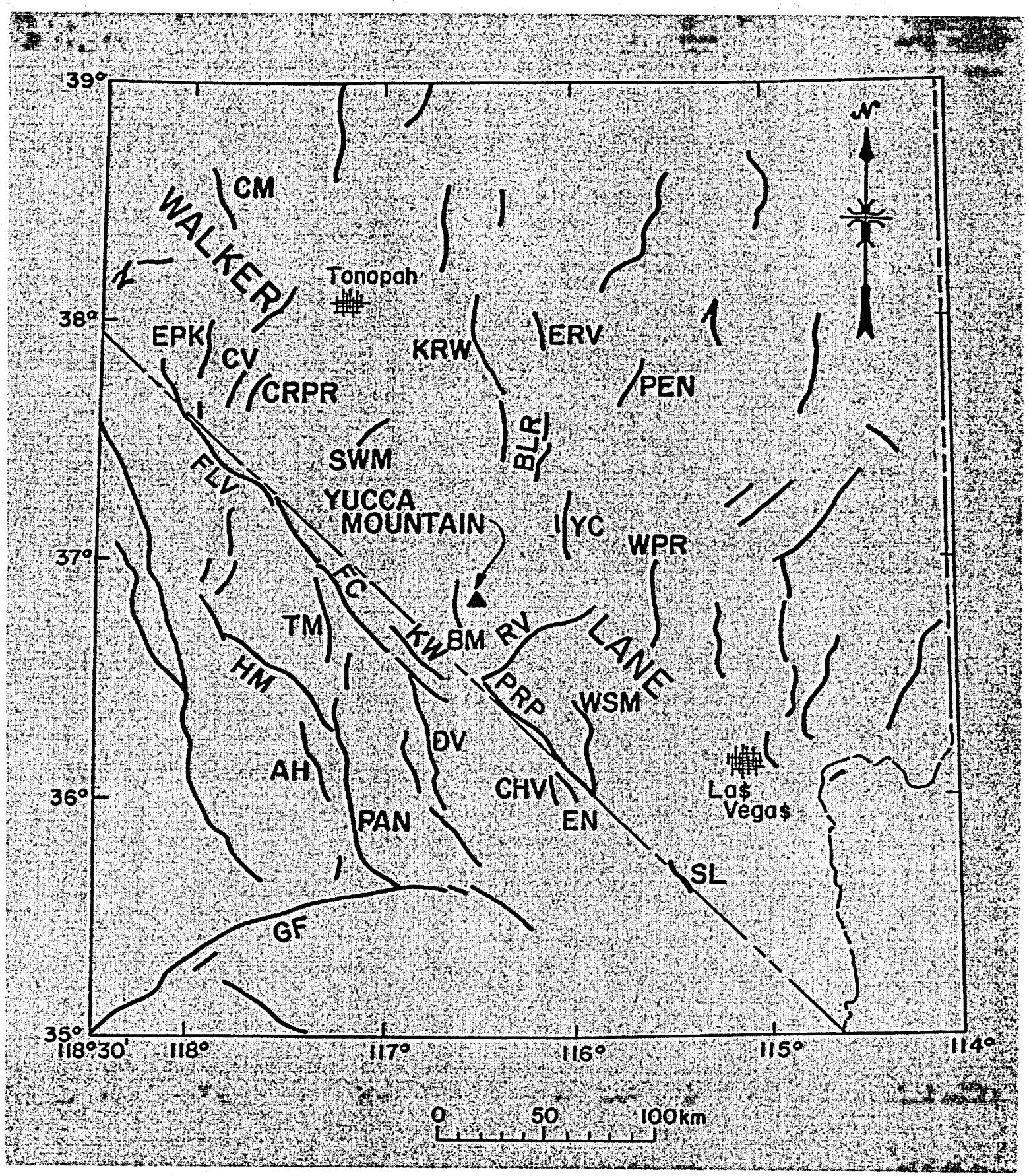
39°
38°
37°
36°
35°
118°30'
118°
117°
116°
115°
114°
CM
WALKER
Tonopah
EPK
CV
CRPR
KRW
ERV
PEN
SWM
BLR
FLV
YUCCA
MOUNTAIN
YC
WPR
EC
TM
KWBM
RY
LANE
HM
PRP
WSM
DV
AH
CHV
La$
Vega$
PAN
EN
SL
GF
0
50
100km

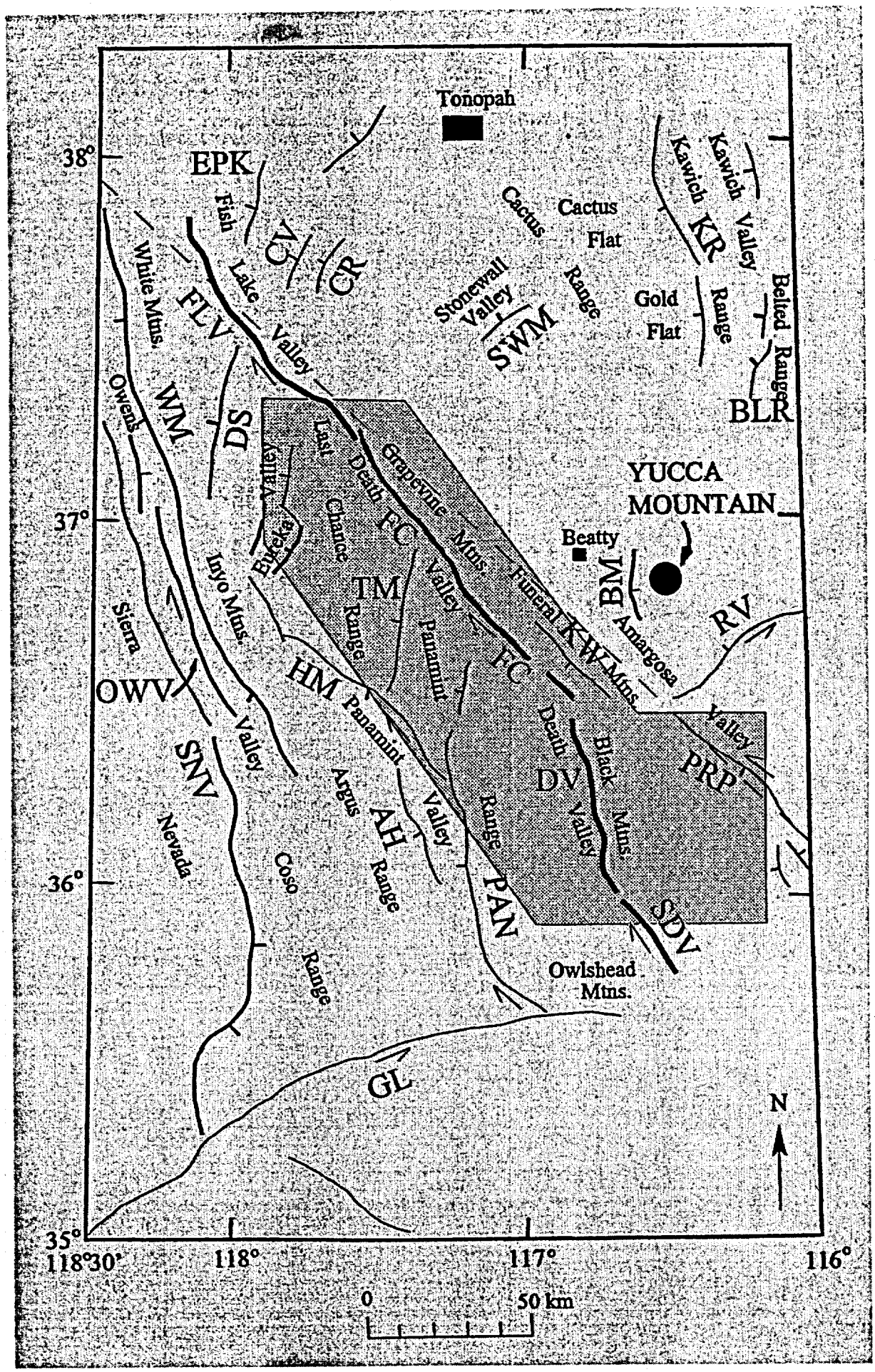
Tonopah
38°
EPK
Fish Lake Valley
White Mts.
FLV
Owens Valley
WM
DS
Last Chance Range
Death Valley
EC
Cactus Flat
Cactus Range
Stonewall Valley
SWM
Kawich Range
KR
Kawich Valley
Belted Range
BLR
Gold Flat
YUCCA MOUNTAIN
Beatty
BM
Amargosa Valley
RV
Funeral Mts.
KW
Crapevine Mts.
Panamint Valley
PV
TM
Panamint Range
HM
Inyo Mts.
Sierra Nevada
OWV
SNV
Argus Range
AH
Coso Range
PAN
Death Valley
DV
Black Mts.
PRP
SDV
Owlshead Mts.
GL
37°
36°
35°
118°30'
118°
117°
116°
N
0
50 km

Fault Parameters

	Length (km)	MRE (ka)	Disp/Event (m)	Recurrence (ka)	Slip Rate (mm/yr)
Bare Mtn Fault	20	> 14 - 24; <100	0.8 - 1.5	~100	<0.01
Death Valley Fault	45 - 60	> 0.2 ?	2.5 - 3.5	0.5 - 1.0	3 - 5
Furnace Creek Fault	105	> 0.2 ?	4.5	0.6 - 0.8	4 - 8; 8 - 10

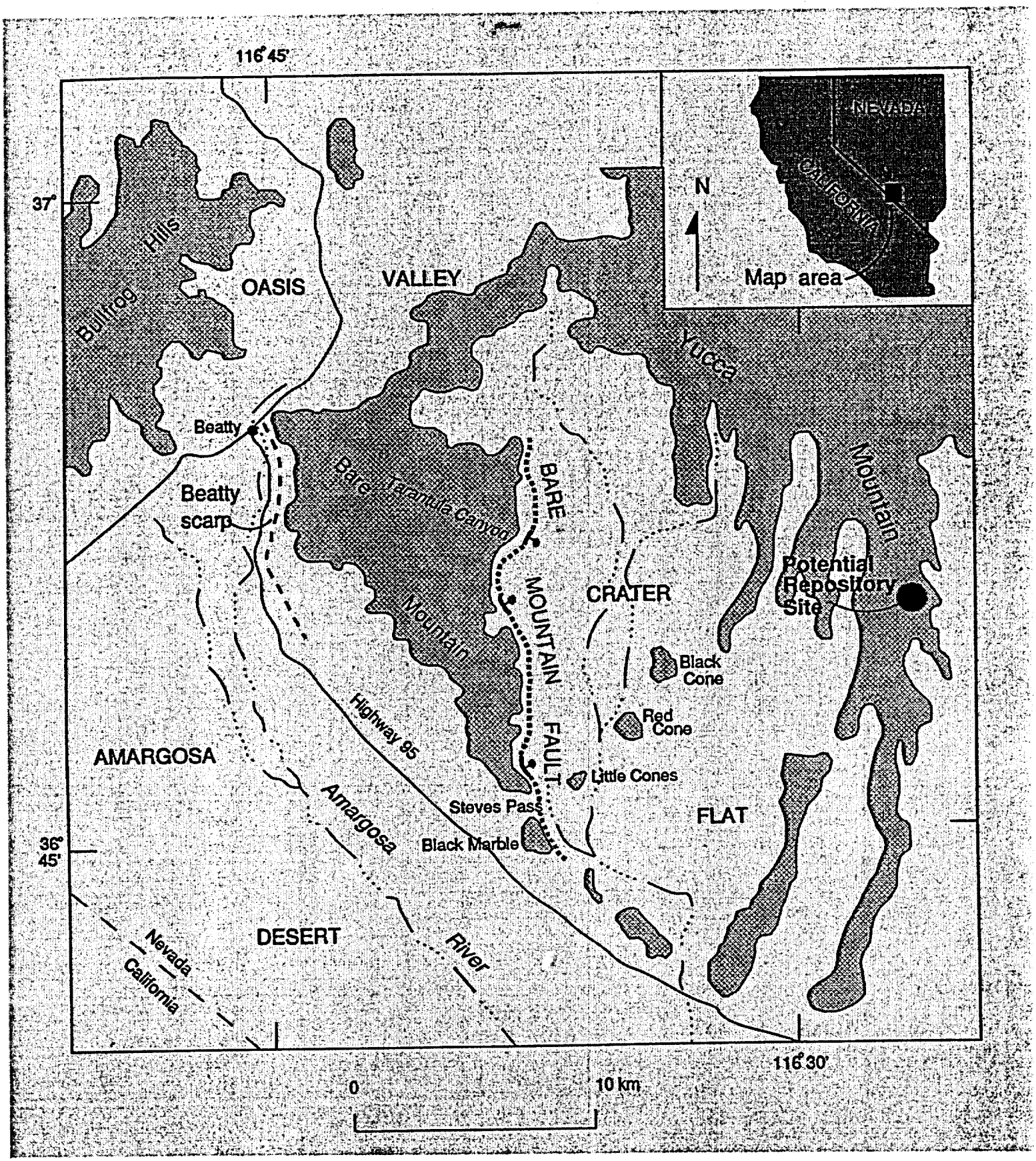
116°45'
37°
Bullfrog Hills
OASIS
VALLEY
Beatty
Beatty scarp
Bare Tarantula Canyon
BARE MOUNTAIN FAULT
Mountain
CRATER
Yucca
Mountain
Potential Repository Site
Black Cone
Red Cone
Little Cones
Highway 95
AMARGOSA
Amargosa
River
Steves Pass
Black Marble
FLAT
36° 45'
DESERT
Nevada
California
116°30'
0
10 km
N
NEVADA
CALIFORNIA
Map area

Correlation Chart for the Quarternary Alluvial Stratigraphy In the Vicinity of the Bare Mountain Fault

AGE	BARE MOUNTAIN			CRATER FLAT Peterson and Others, 1995	NEVADA TEST SITE Taylor and others, in press
	This Study	Swadley and Parrish, 1988	Mosen and others, 1992		
Holocene	Q5	Q1a Q1b (<0.14 ka)	Qyf	Modern Crater Flat (>0.3 to >1.3 ka)	Alluvium of Yucca Wash Alluvium of Topopah Spring
	Q4	Q1c (<10 ka)		Little Cones (>6 to >11 ka)	Alluvium of Jackass Flat
	Q3	Q2a	Qif	Late Black Cone (>17 to >30ka)	Alluvium of Fortymile Wash
Pleistocene	Q2	Q2b (145-160 ka)		Early Black Cone (>159 to >201 ka)	Alluvium of Sever Wash
	Q1	Q2c (270-430 ka) ?		Yucca (>375 ka)	Alluvium of Midway Valley
Pliocene	QTa	QTa (1100-2000 ka)	QTof	Solitario (>433 to >659 but <730 ka)	

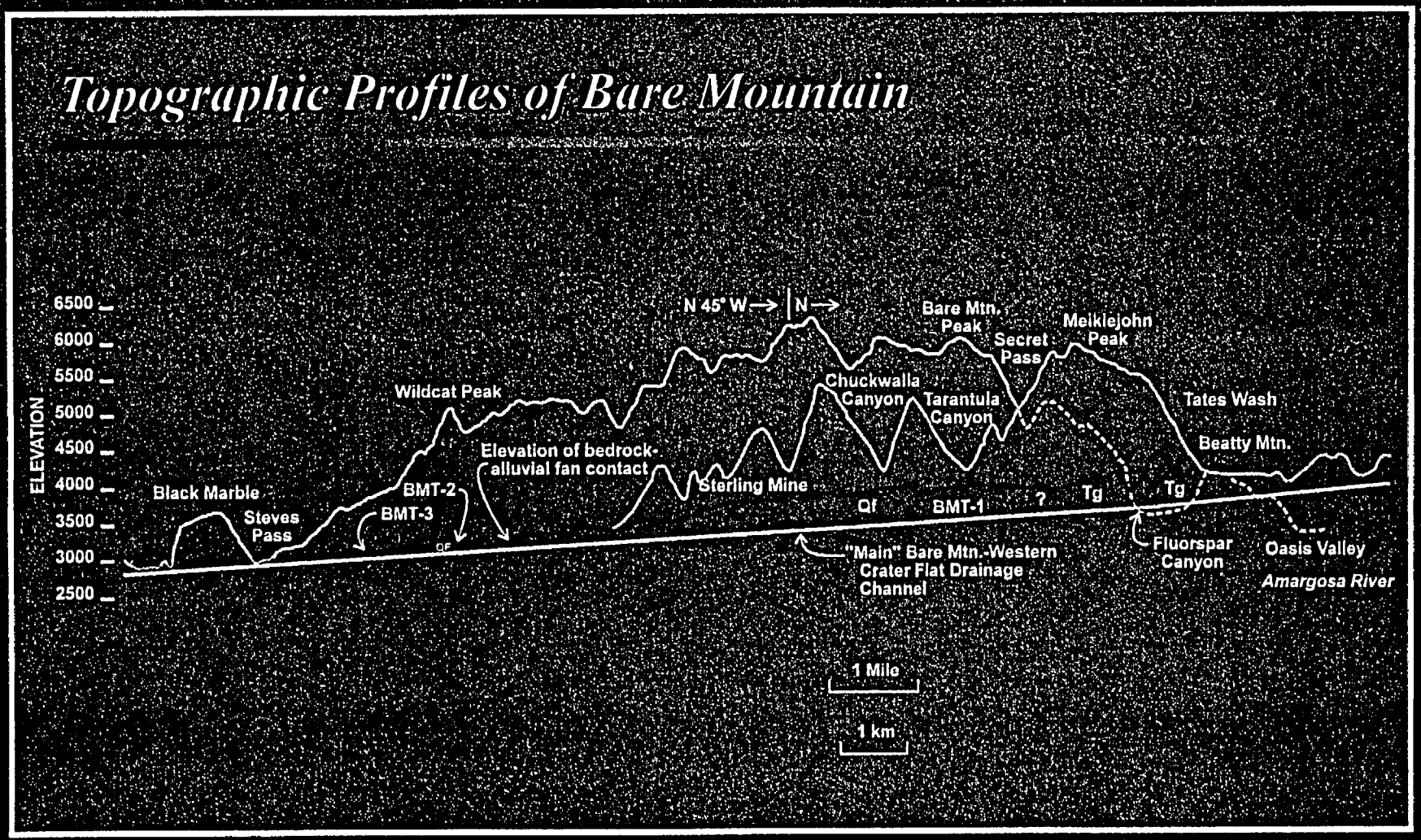
Topographic Profiles of Bare Mountain
ELEVATION
6500
6000
5500
5000
4500
4000
3500
3000
2500
N 45° W
N
Bare Mtn. Peak
Meiklejohn Peak
Secret Pass
Chuckwalla Canyon
Tarantula Canyon
Tates Wash
Beatty Mtn.
Wildcat Peak
Elevation of bedrock-alluvial fan contact
Black Marble
Steves Pass
BMT-2
BMT-3
QF
Sterling Mine
Qf
BMT-1
?
Tg
Tg
"Main" Bare Mtn.-Western Crater Flat Drainage Channel
Fluorspar Canyon
Oasis Valley
Amargosa River
1 Mile
1 km

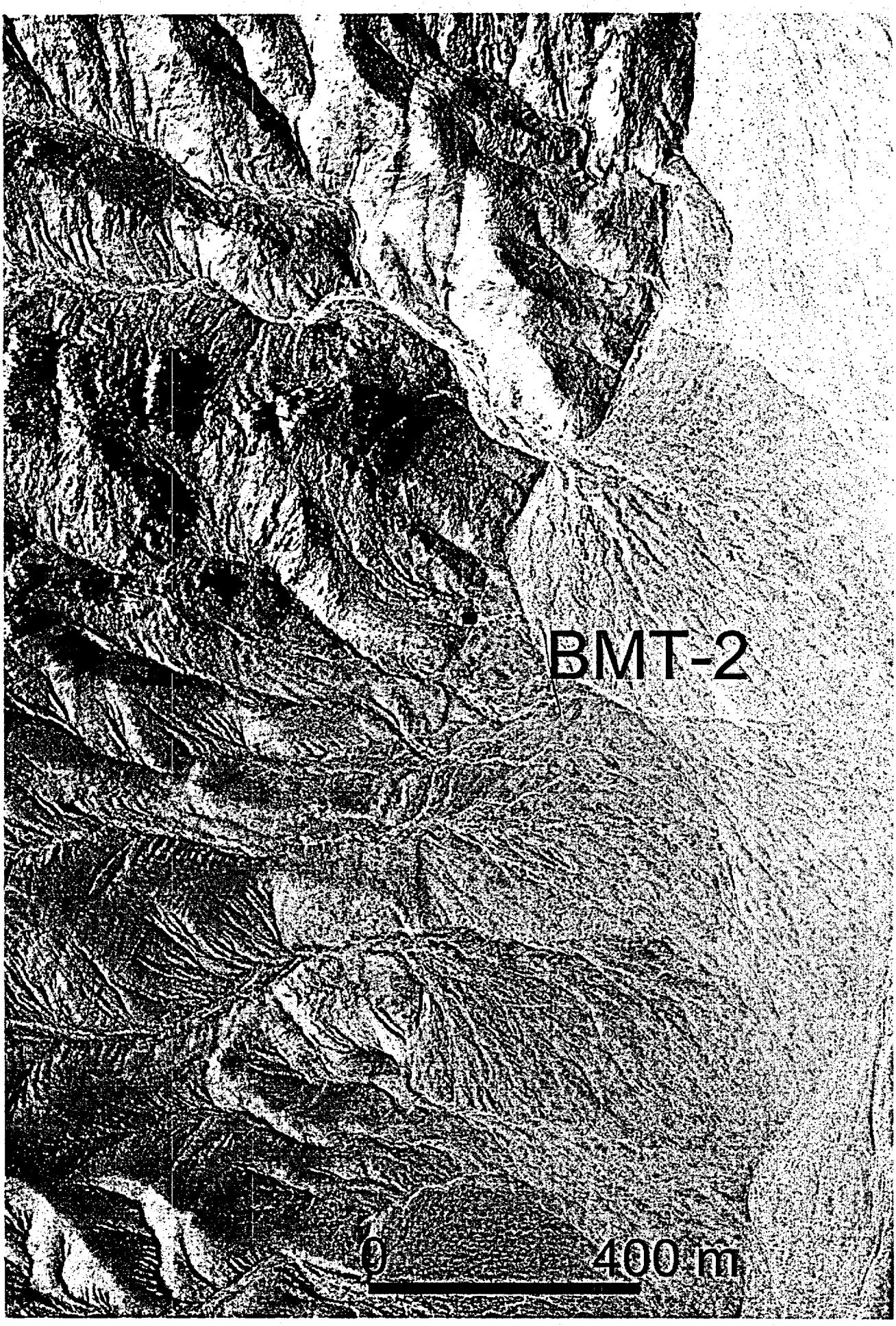
BMT-2
0
400 m

Geologic Map of the Wildcat Peak Site

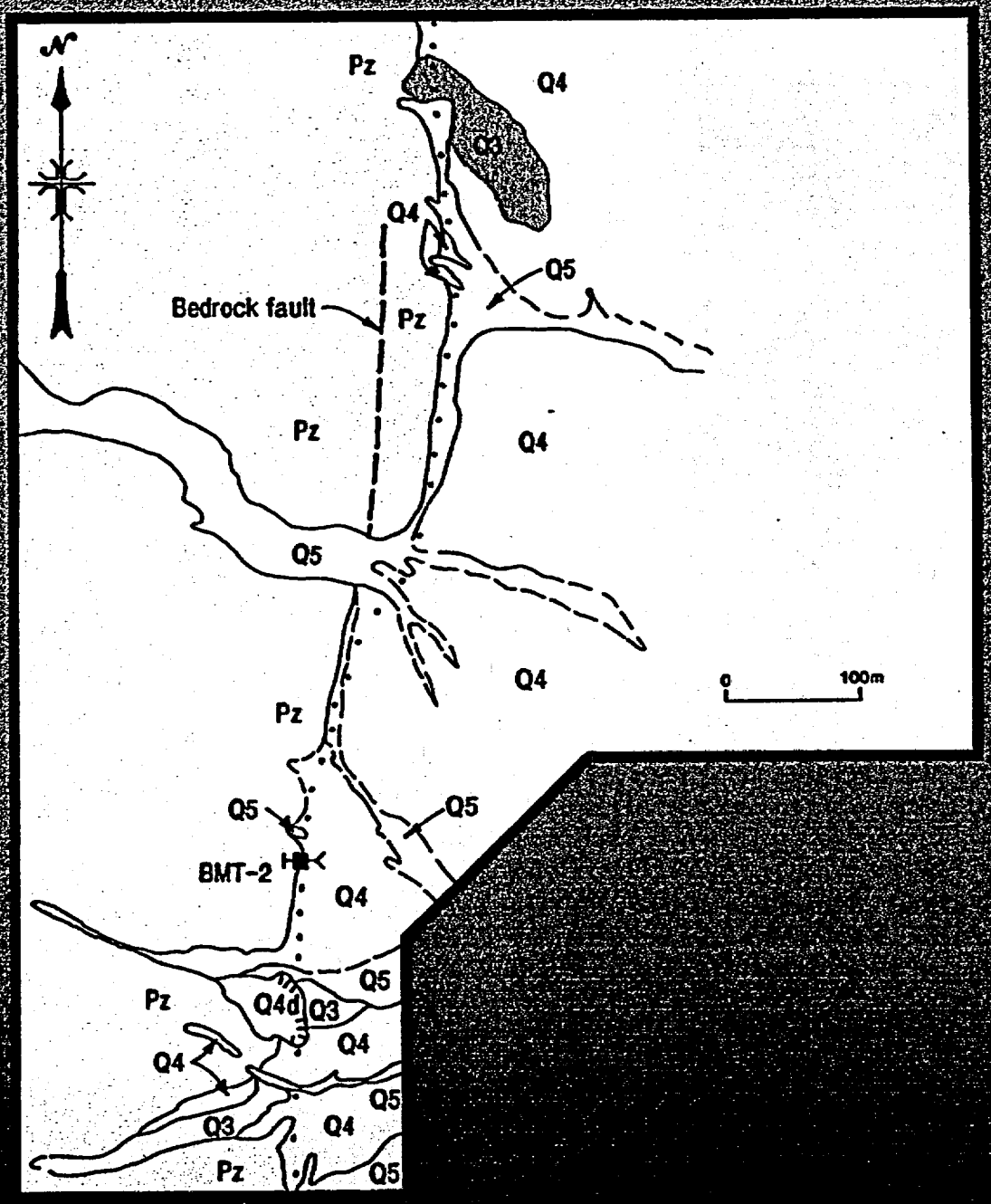

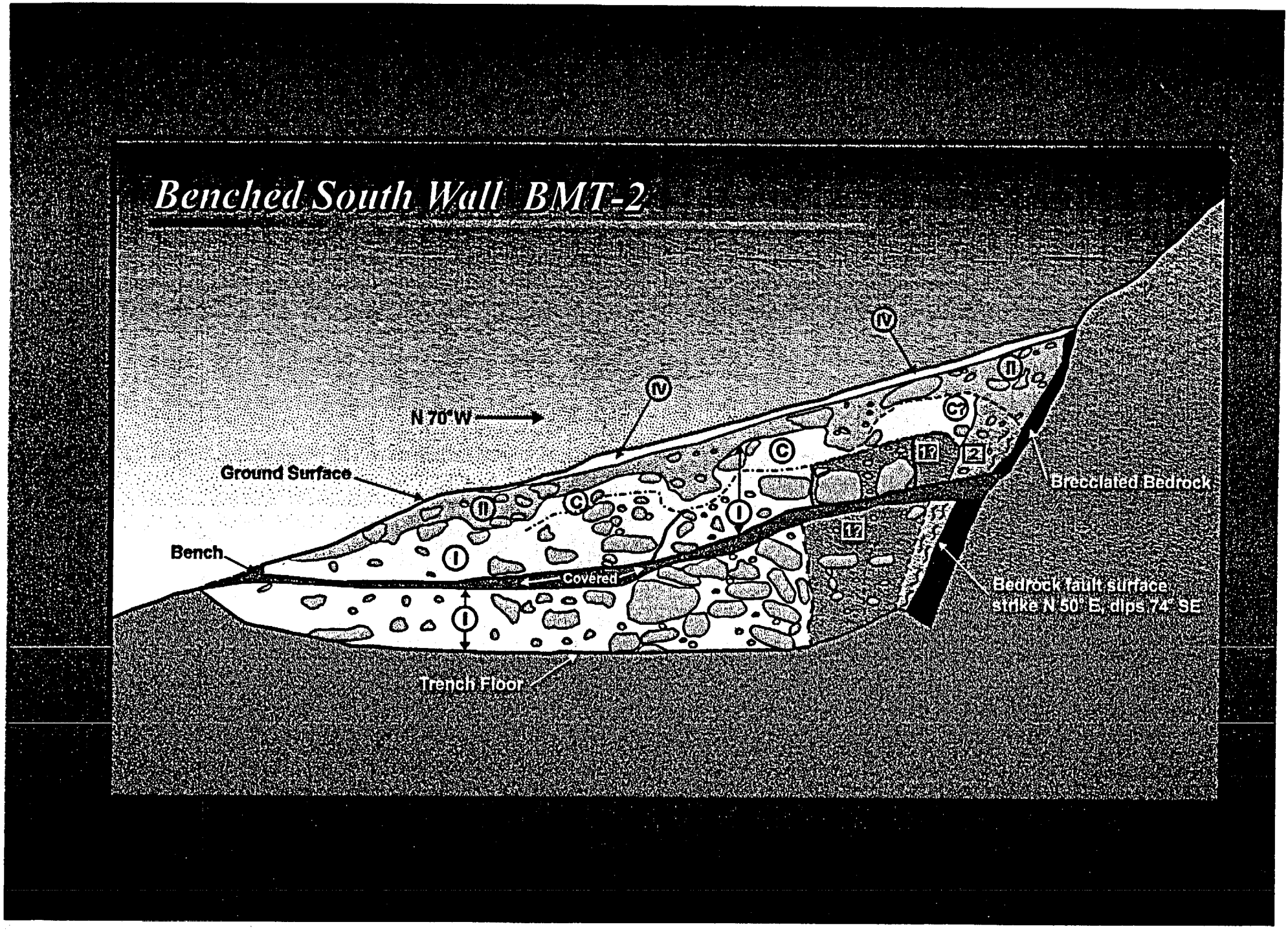
Benched South Wall BMT-2
N 70°W
Ground Surface
Bench
Covered
Trench Floor
Brecciated Bedrock
Bedrock fault surface
strike N 50° E, dips 74° SE
IV
II
C
I
1?
2

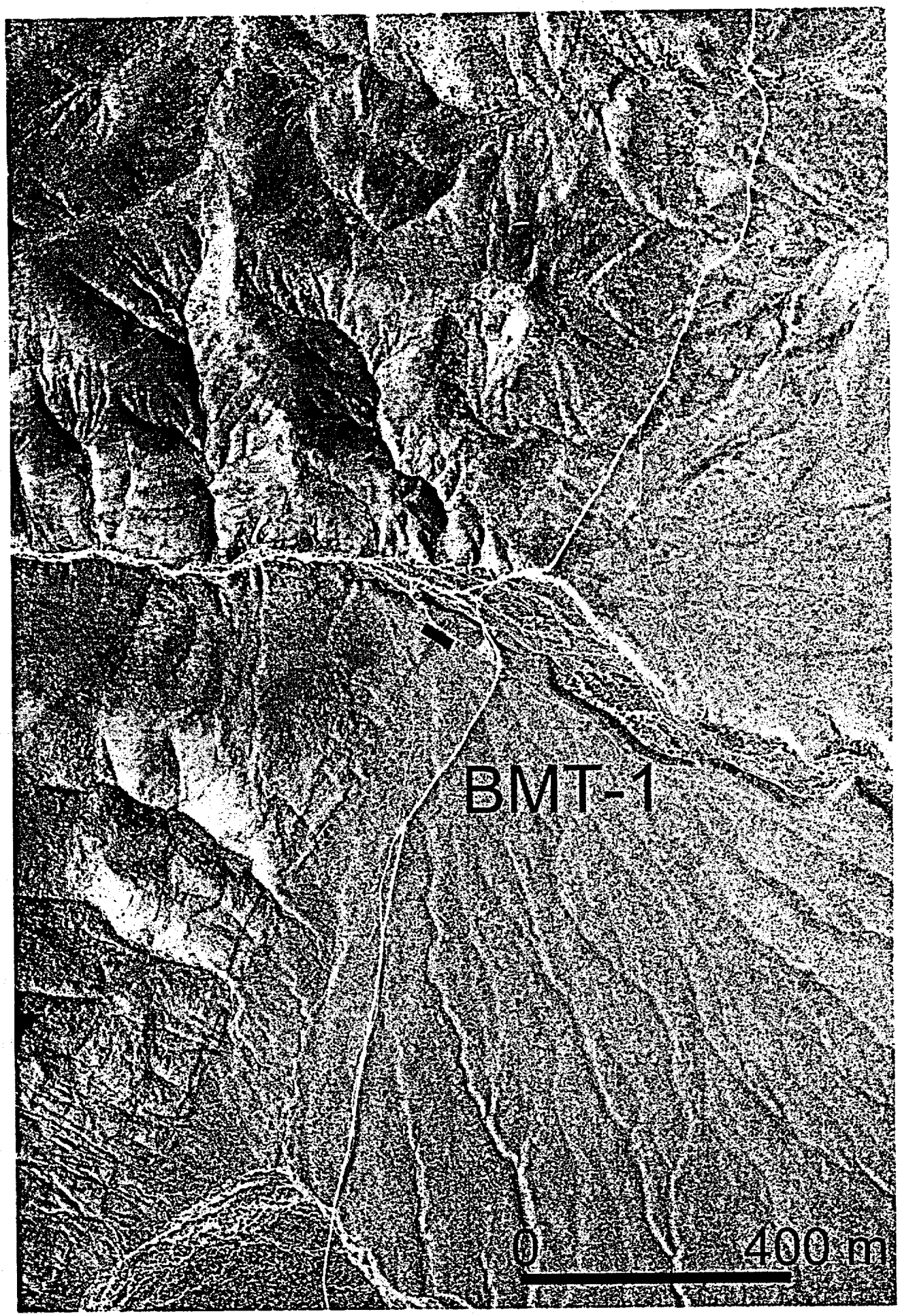
BMT-1
0
400 m

Geologic Map of the Tarantula Canyon Site

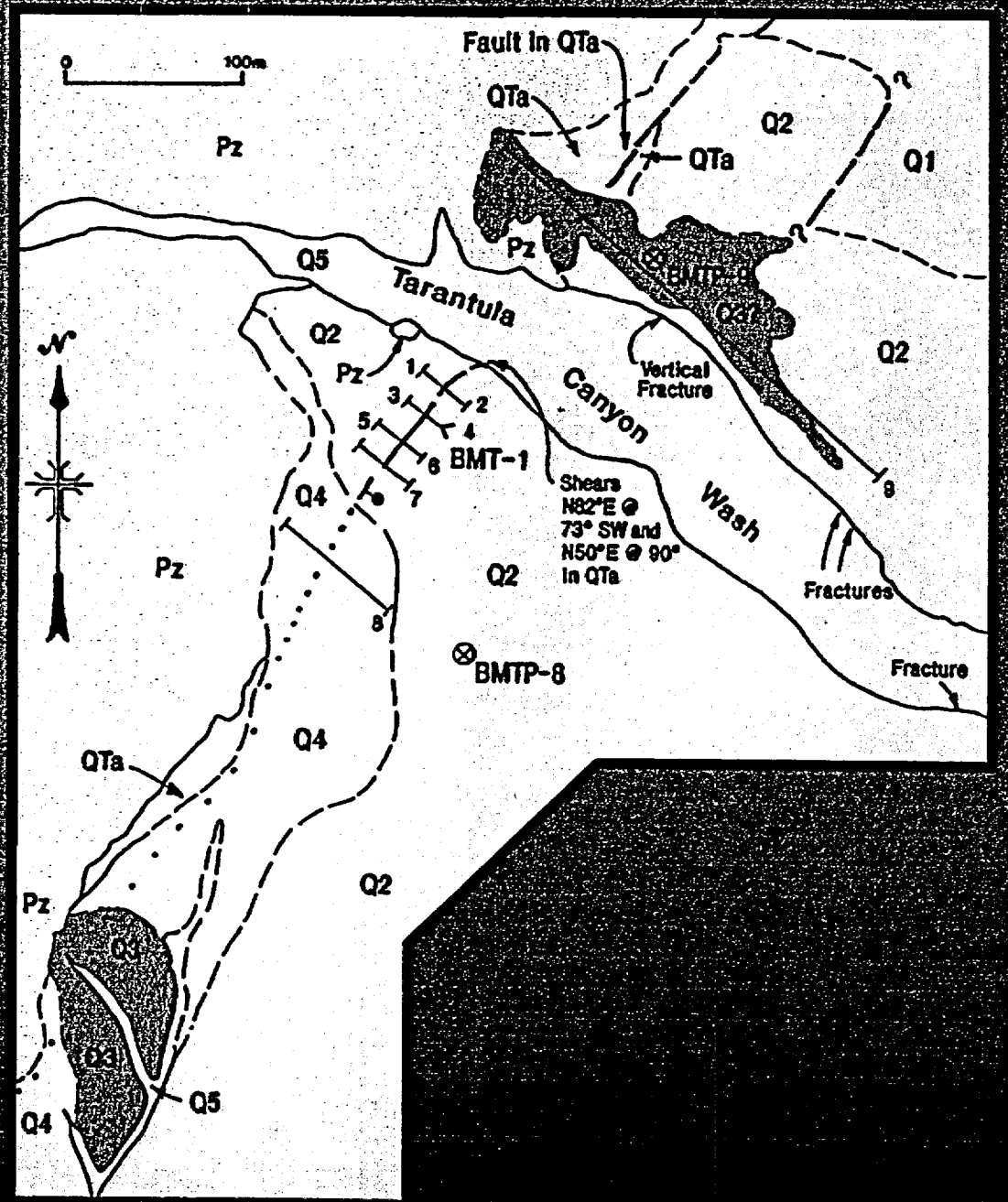

Scarp Heights and Maximum Scarp Angles

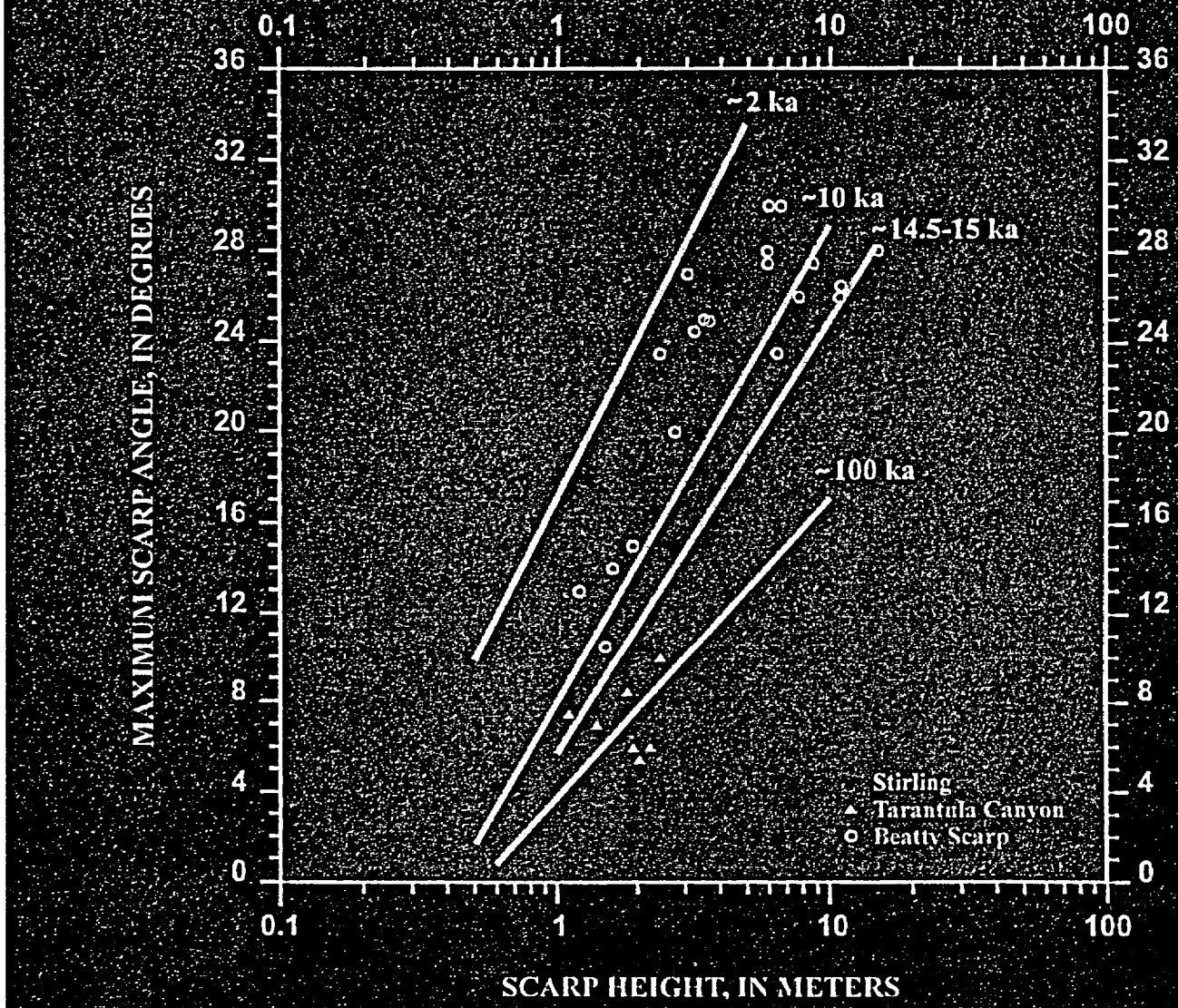

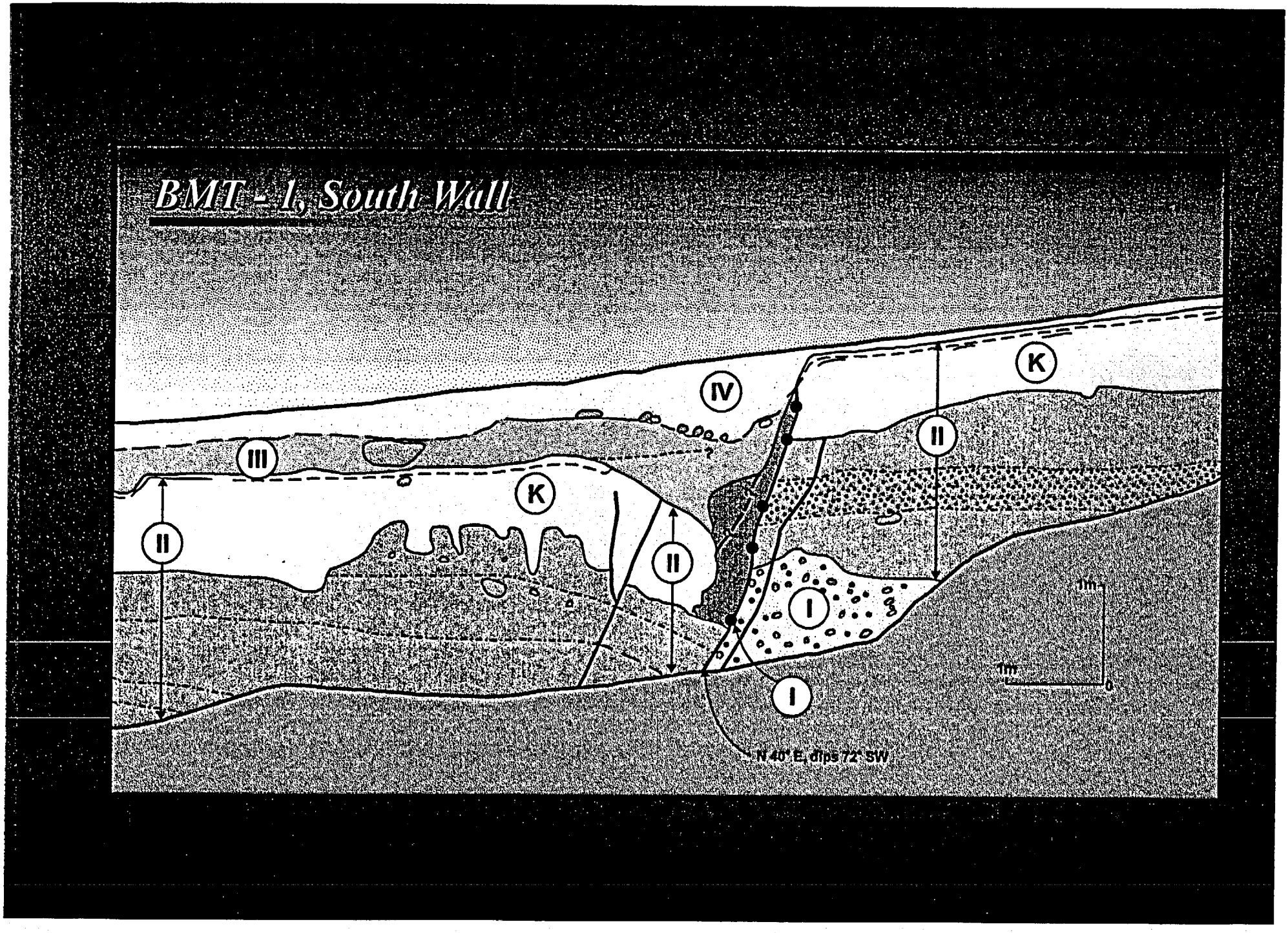
BMT - 1, South Wall
IV
K
III
II
K
II
II
I
I
1m
1m
0
N 40° E, dips 72° SW

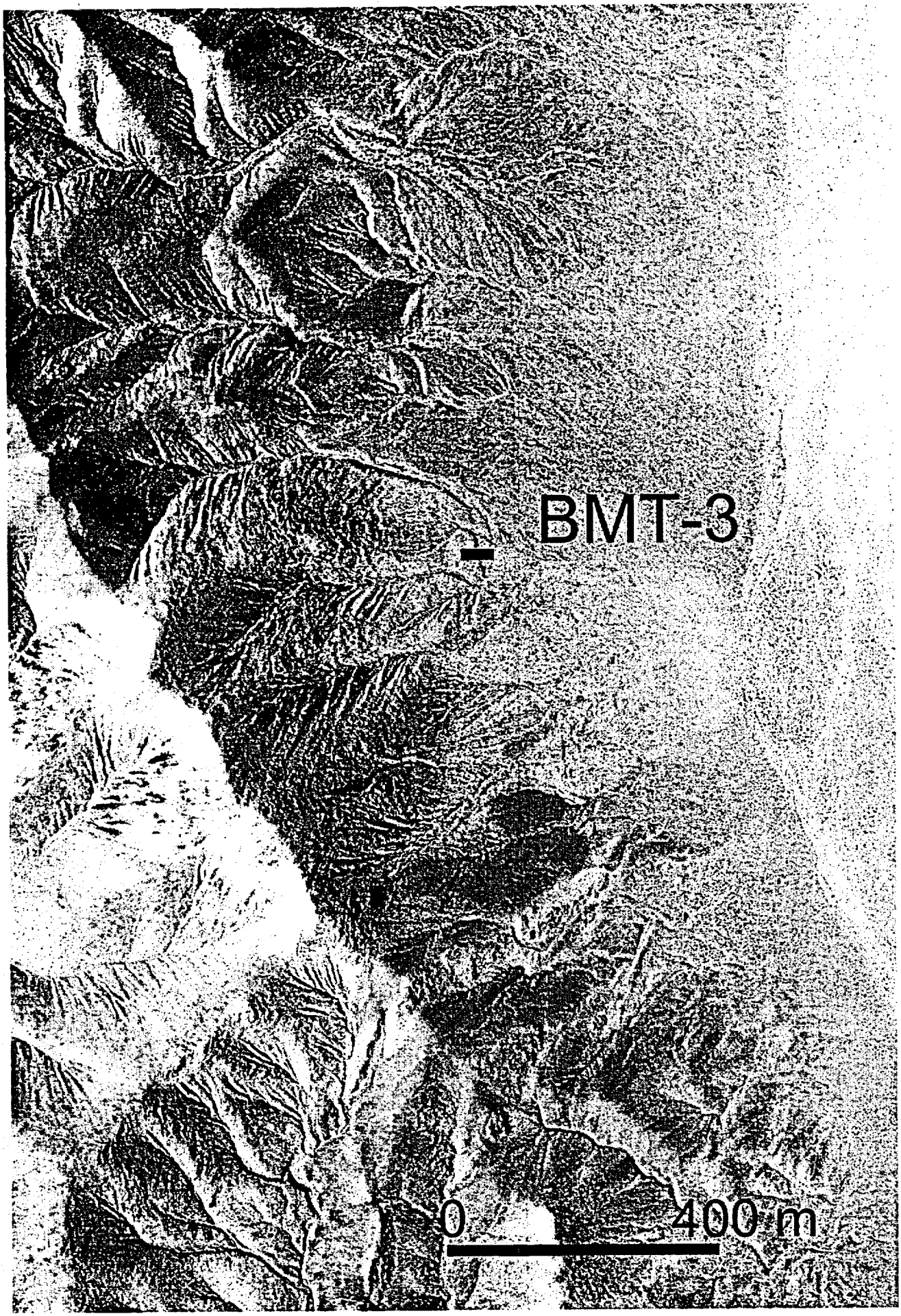
BMT-3
0
400 m

Geologic Map of the Stirling Site

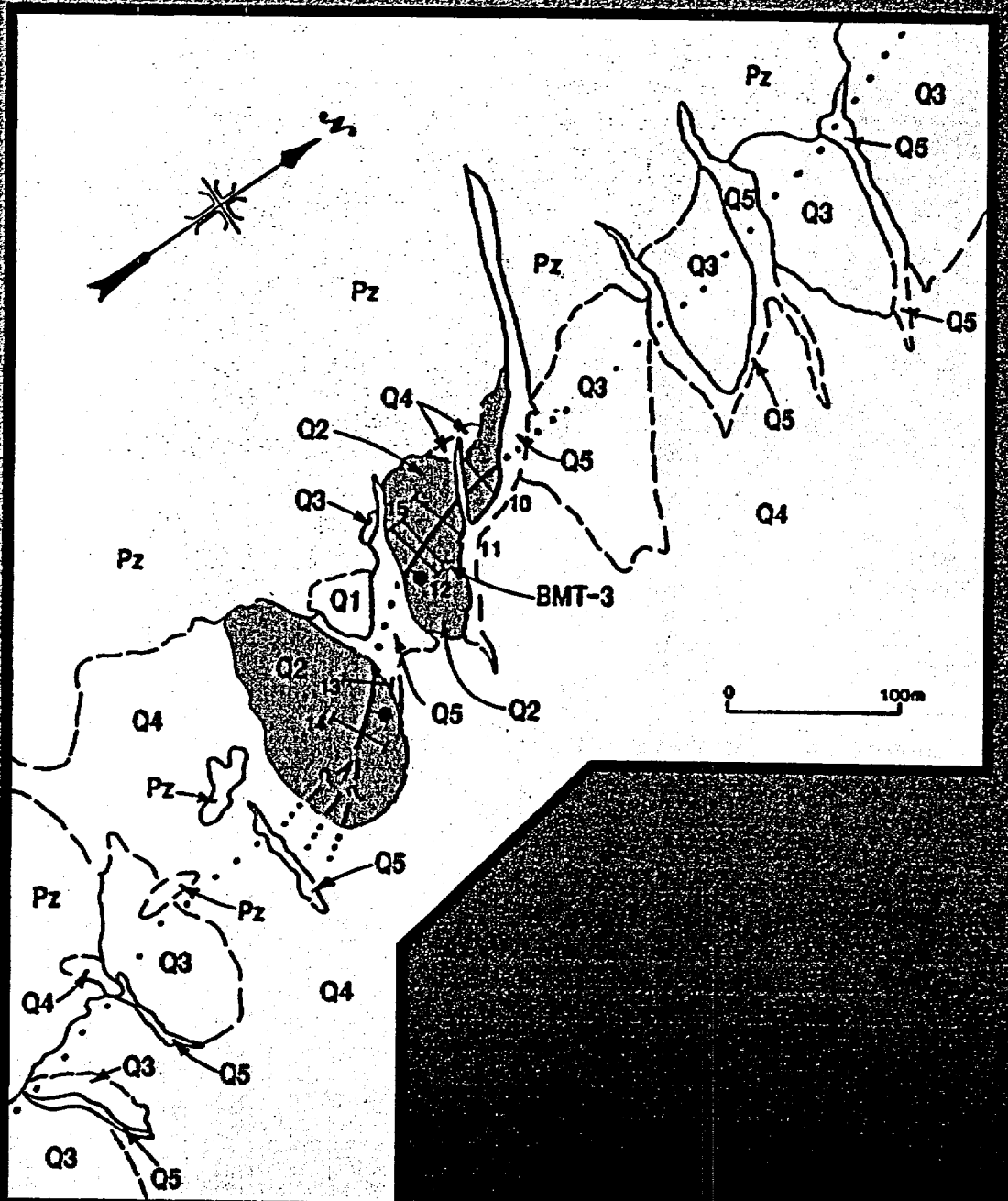

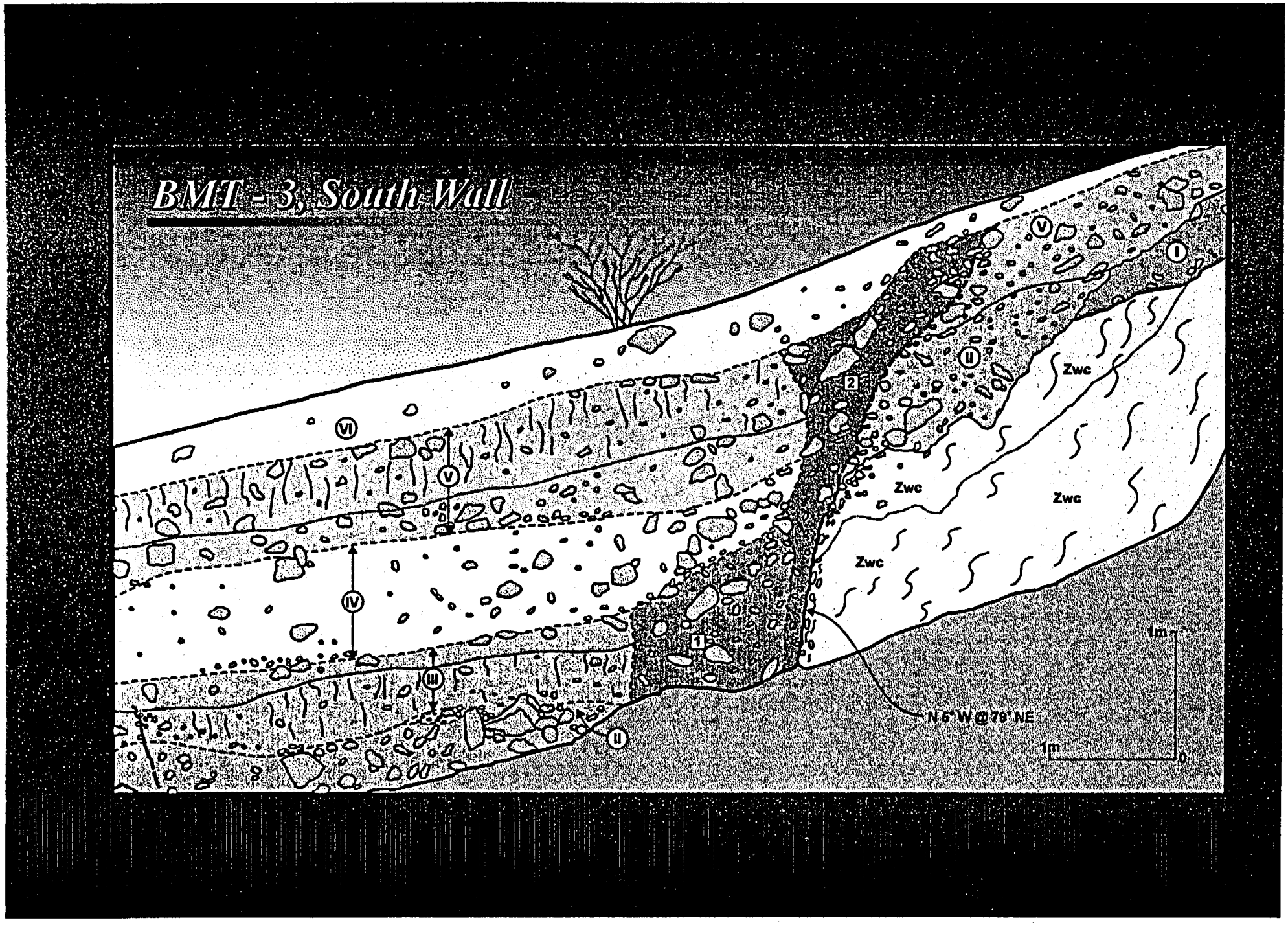
BMT - 3, South Wall
VI
V
IV
III
II
I
V
II
2
1
Zwc
Zwc
Zwc
Zwc
N 6° W @ 78° NE
1m
1m
0

Bare Mountain Fault

Length: 20 km - Unsegmented
Dip: 60 - 75°
Displacement/event: 0.8 - 1.5 m
MRE: > 14 - 24 ka; < 100 ka
Recurrence: ~ 100 ka
Slip Rate: < 0.01 mm/yr

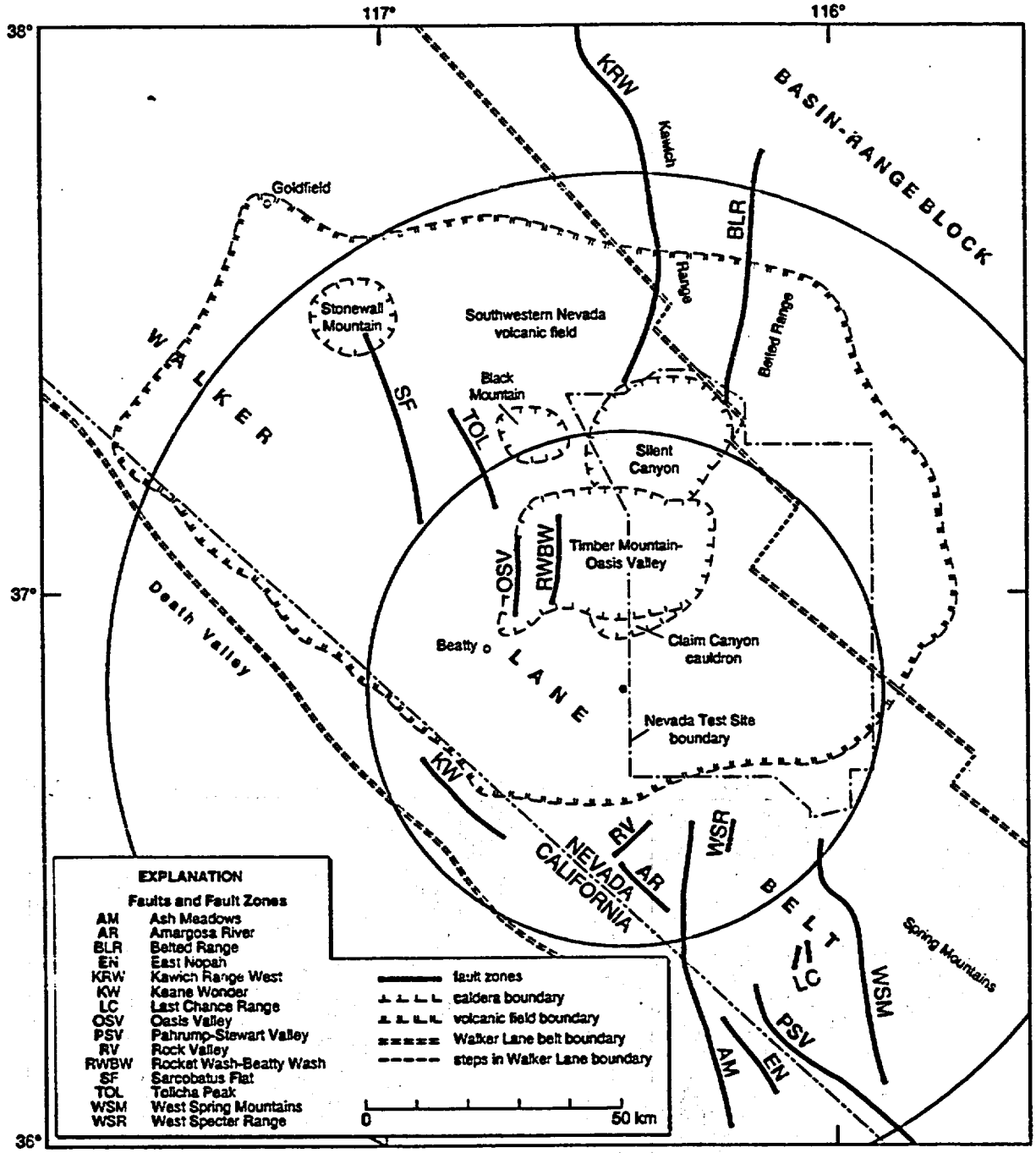

FIGURE 1. Map showing generalized traces of the regional faults studied under the two Memoranda of Agreement between the Yucca Mountain Project Branch and Branch of Earthquake and Landslide Hazards, U.S.G.S. Abbreviations in bold type identify faults described in this report, abbreviations in regular type identify faults described in a companion report (Anderson and others, 1995). Selected regional geologic features include Walker Lane belt, boundaries of the southern Nevada volcanic field, and some calderas within that field (modified from Carr, 1988). Dot at center of 50- and 100-km-radius circles marks location of proposed repository site. Most fault traces and abbreviations are from Pezzopane (1995).

Fig 1
E. Anderson

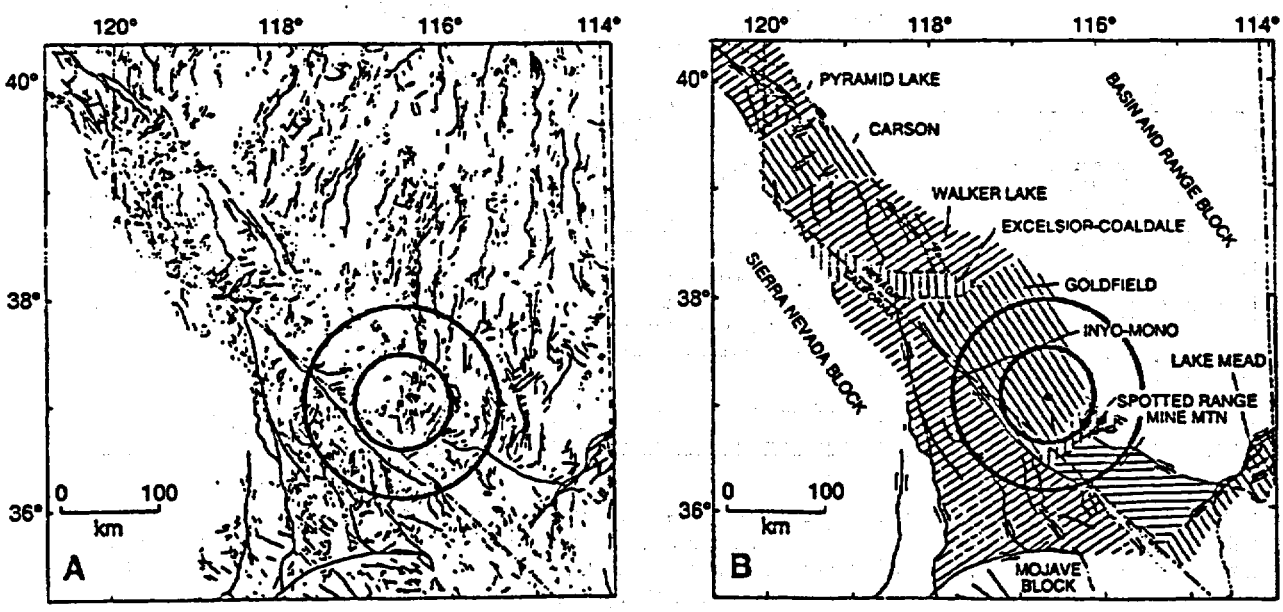

FIGURE 1. A, Map showing the Yucca Mountain site (dot at center of 50- and 100-km circles) relative to late Cenozoic faults in the western Great Basin (modified from Stewart, 1988). B, Same area as in A showing selected major faults and regional structural blocks (cross ruled) of the Walker Lane belt (from Stewart, 1988).

4

Fig. 2
E. Anderson

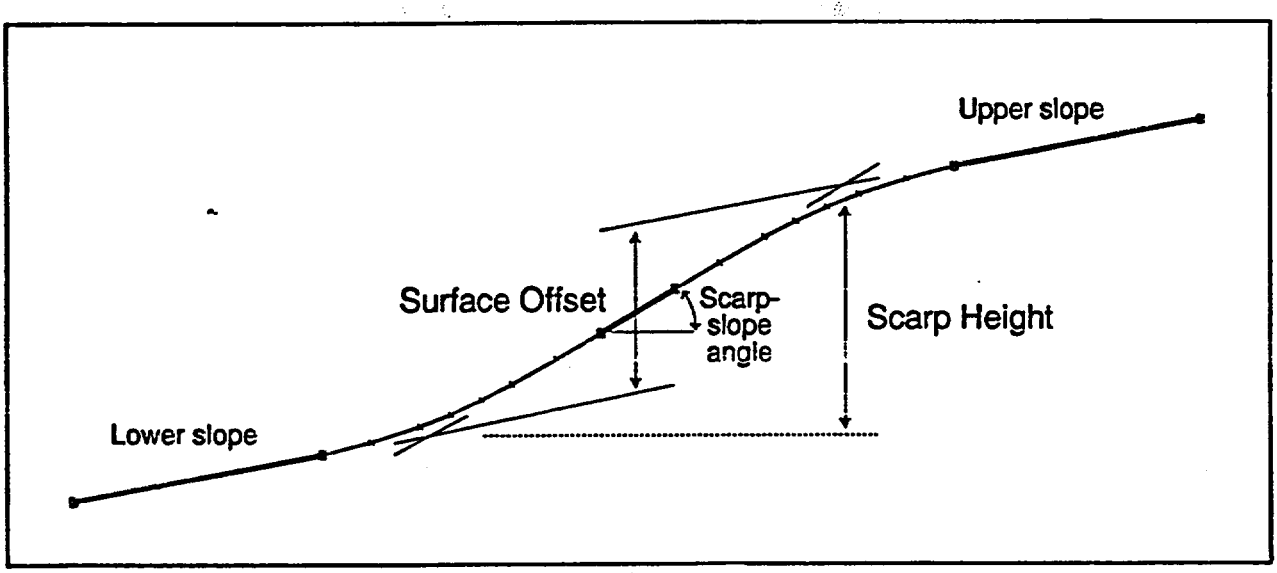

FIGURE 3. Definitions of scarp parameters. Upper and lower slope are intervals of the scarp profile that represent the prefaulting surfaces above and below the scarp. Scarp-slope angle is the steepest interval on the scarp face. Surface offset is the vertical distance between the projections of the upper and lower surfaces measured mid-way between the intersections of the steepest interval of the scarp face and the projections of the upper and lower surfaces; scarp height is the vertical relief between those intersections.

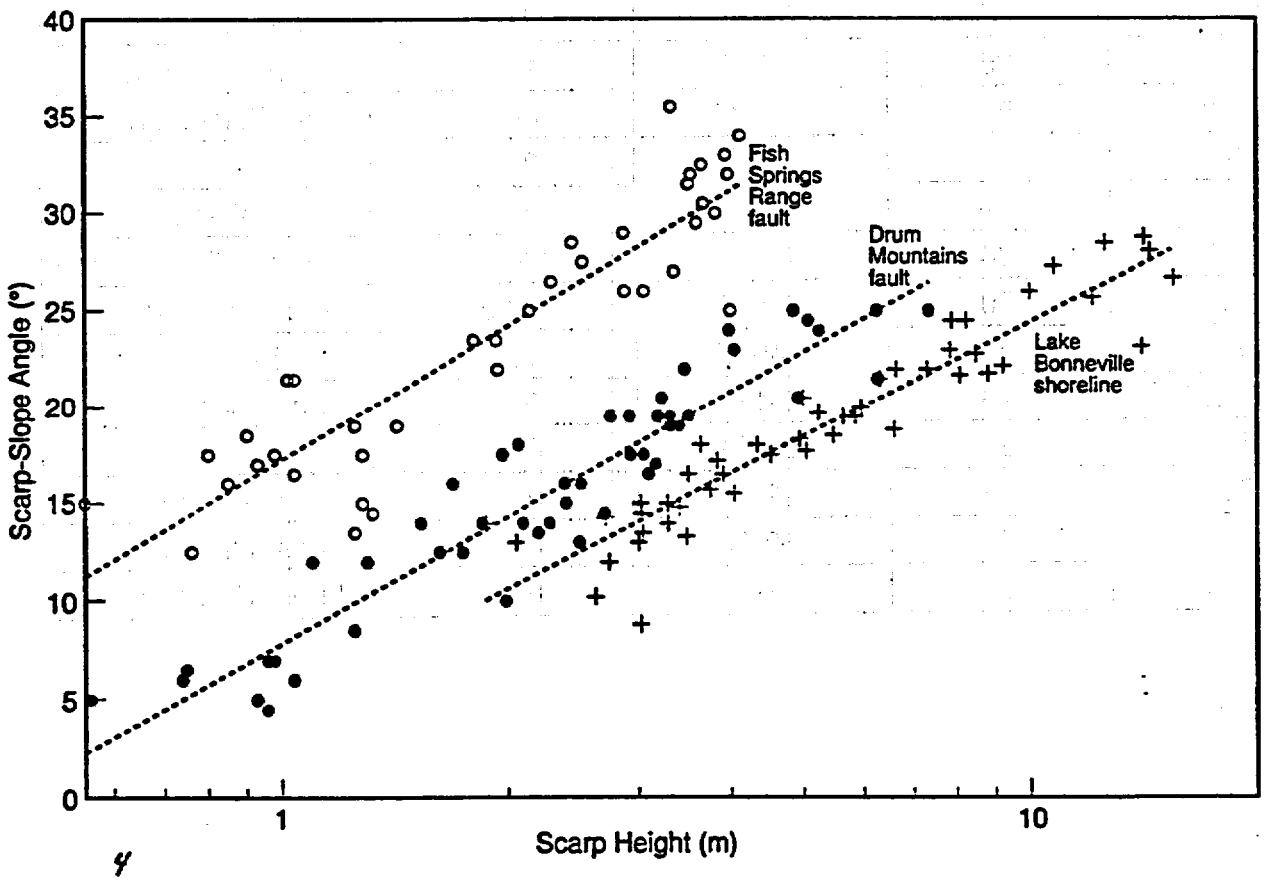

FIGURE 4. Scarp-slope angle versus log scarp-height data for single-event scarps in western Utah. The figure illustrates the resolution and variability of scarp-morphology data. Dotted lines are linear regressions to each of the sets of data. Open circles, fault scarp of Fish Springs Range (about 2 ka; Bucknam and others, 1989); solid circles, fault scarp of Drum Mountains (about 10 ka; Crone, 1983); crosses, shoreline scarp of Lake Bonneville (about 15 ka; Machette, 1989).

Figs 3, 4
E. Anderson

FAULT NAME	DISTANCE FROM YM	LENGTH (PIETY, 1994)	LENGTH (THIS STUDY)	TIMING OF MOST RECENT EVENT
AR	40	15	12	late Pleistocene
AM	34	30-60	30-49	late Pleistocene
BR	55	38-54	21	early Holocene
EN	85	17-19	19	m-l Pleistocene
KRW	57	80-84	4-7	late Pleistocene?
KW	43	25	0	
LC	—	—	2.4 & 2.8	m-l Pleistocene
OSV	24	20	0-2.5	pre mid Pleistocene
PSV	70	50-130	18.5	e-m Holocene
RV	27	32-65	16	late Pleistocene
RWBW	19	5-17	0	late Miocene
SF	52	27-51	0?	
TOL	42	22	0	prob Tertiary
WSM	53	30-60	31-48	latest Quaternary
WSR	33	—	8	latest Quaternary

Fig. 5
E. Anderson

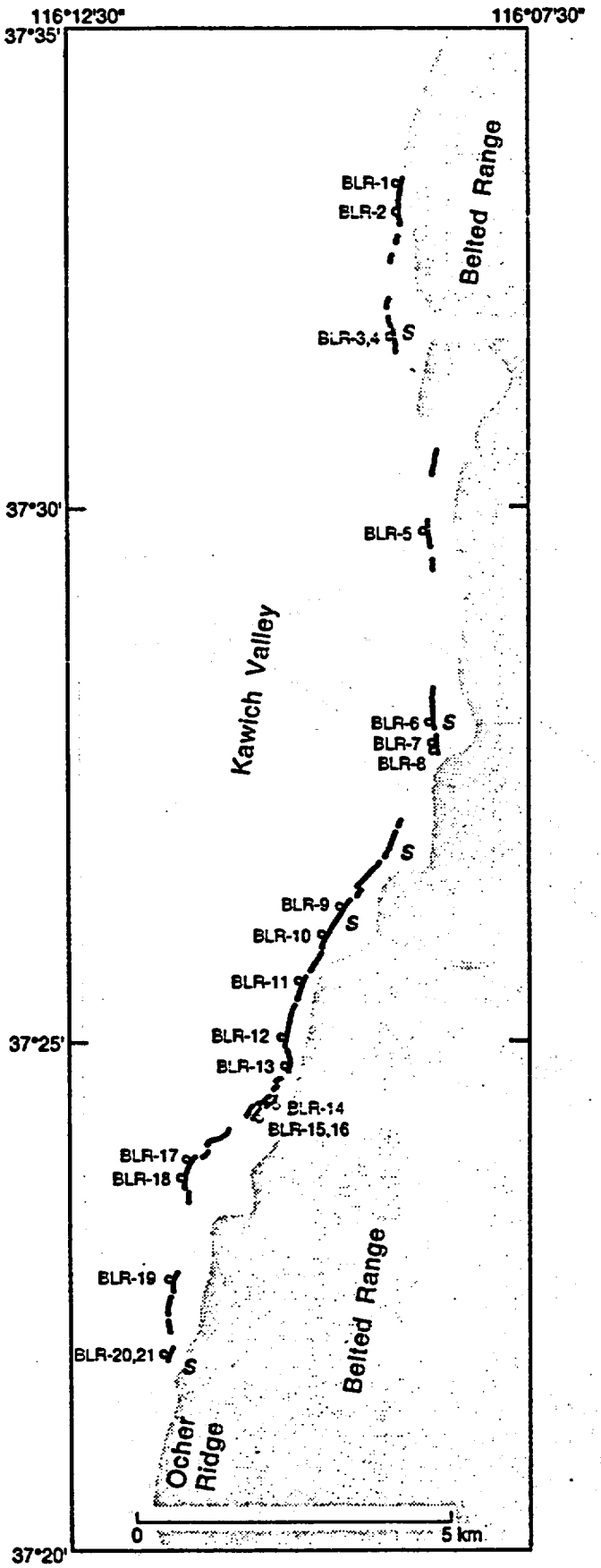

FIGURE 6. Map showing scarps on alluvium (solid lines) along Belted Range fault zone (BLR). Open circles show scarp-profile sites, numbered from north to south; *S*, site of probable single-event scarp. Range boundary drawn at approximate limit of exposed bedrock.

Fig. 6
E. Anderson

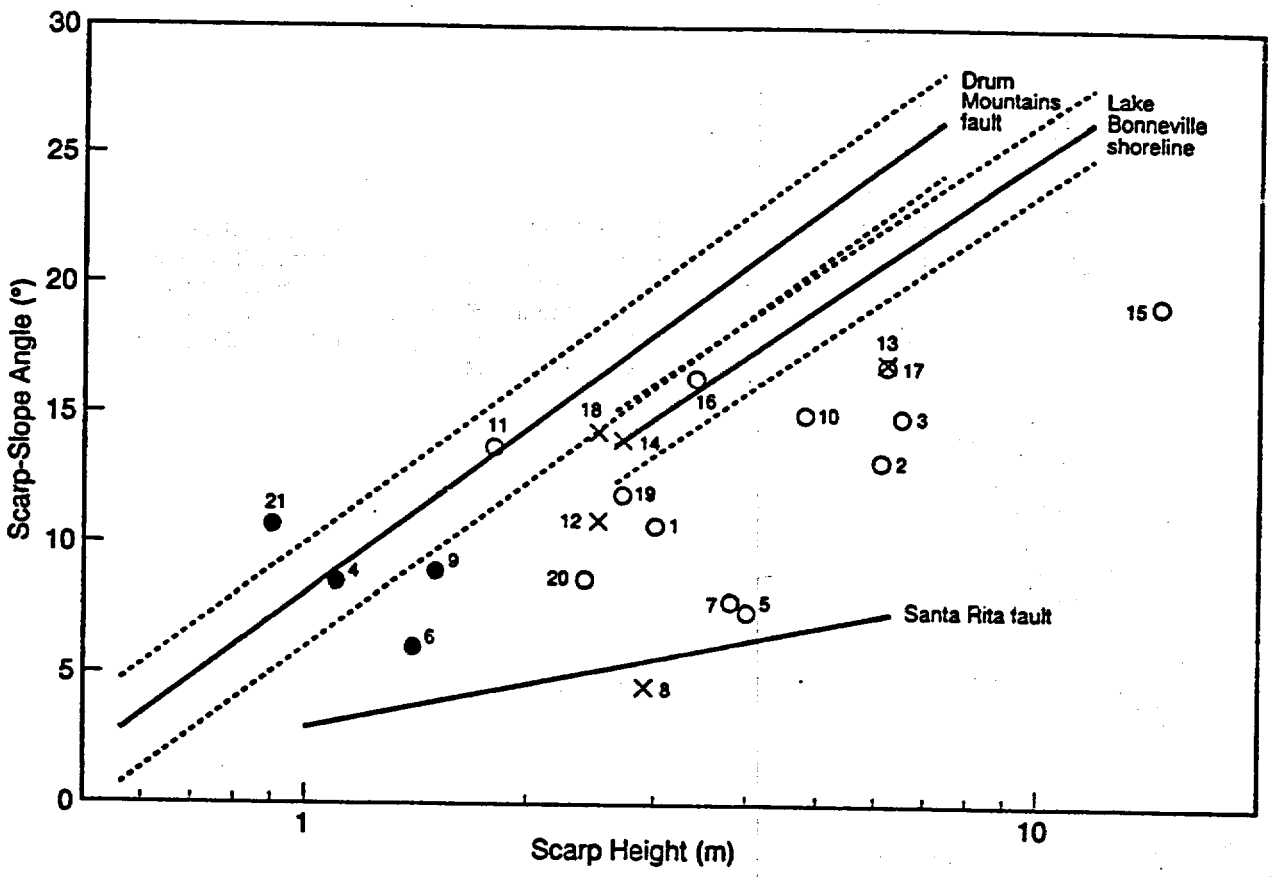

FIGURE 7. Plot of scarp-height—slope-angle values for scarps on alluvium along the Belted Range fault zone (BLR). Closed circles, probable single-event scarps; open circles, multiple-event scarps; x, large scarps that lack evidence of multiple periods of movement; numbers are BLR site numbers in figure 6 and table 3. Solid lines, regression lines for reference scarps; dotted lines, 1-σ limits for regressions. Lake Bonneville shoreline scarp (about 15 ka; Machette, 1989) and Drum Mountains fault scarp (about 10 ka; Crone, 1983) both from Bucknam and Anderson (1979); Santa Rita fault scarp (estimated age about 100 ka; Pearthree and Calvo, 1987). Points that plot above or below the 1-σ limits of a regression line suggest relative ages that are younger or older than those of the reference scarps, respectively.

Fig. 7
E. Anderson

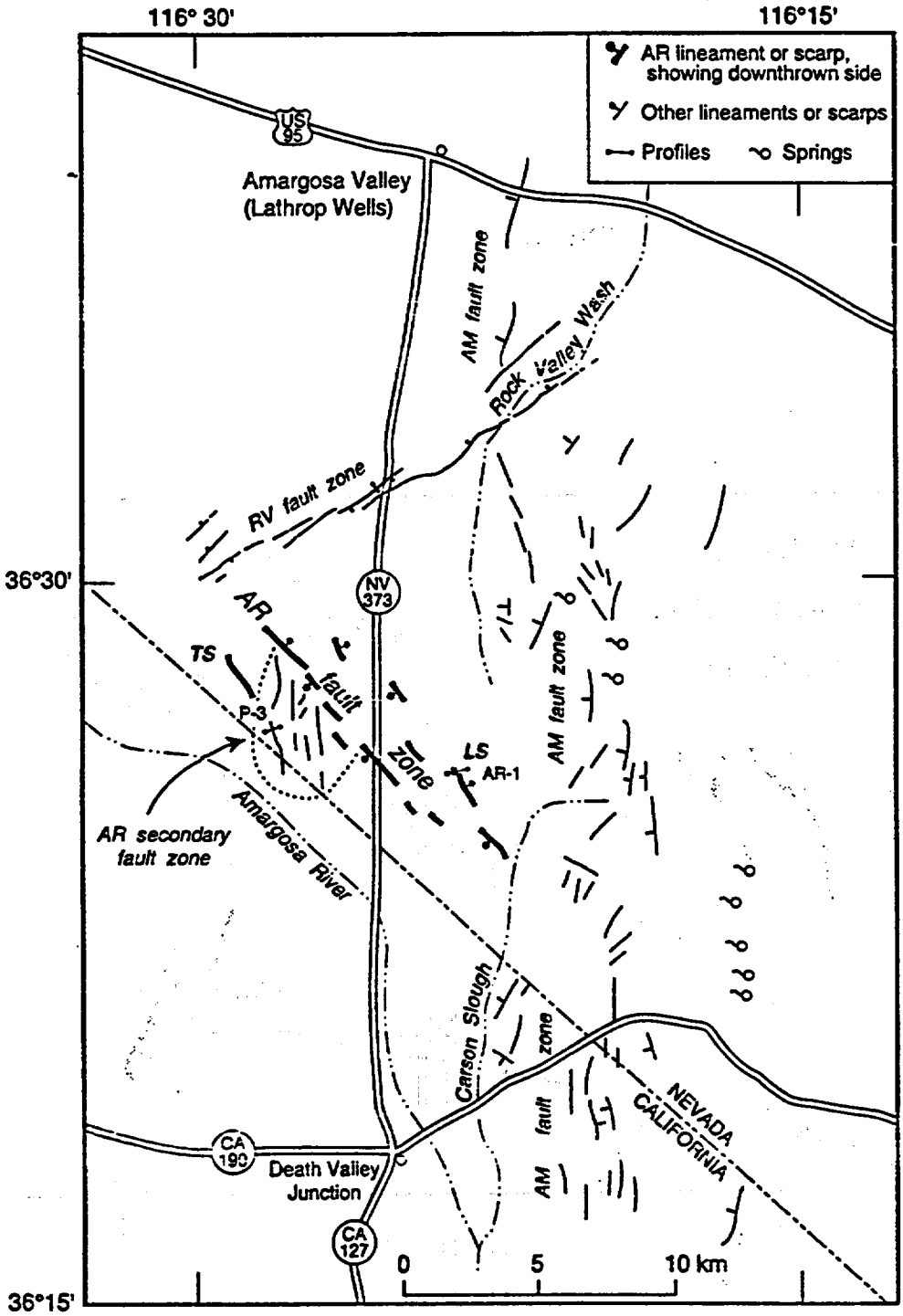

FIGURE 8. Map of the Amargosa River fault zone (AR) and selected geographic and cultural features in the Amargosa Valley. Features associated with Donovan's (1991) secondary fault zone are enclosed by dotted line. Abbreviations include *AM*, Ash Meadows fault zone and *RV*, Rock Valley fault zone, southwestern extension. Location of scarp profiles listed in table 3 are shown by bar symbol.

16

Fig. 8
E. Anderson

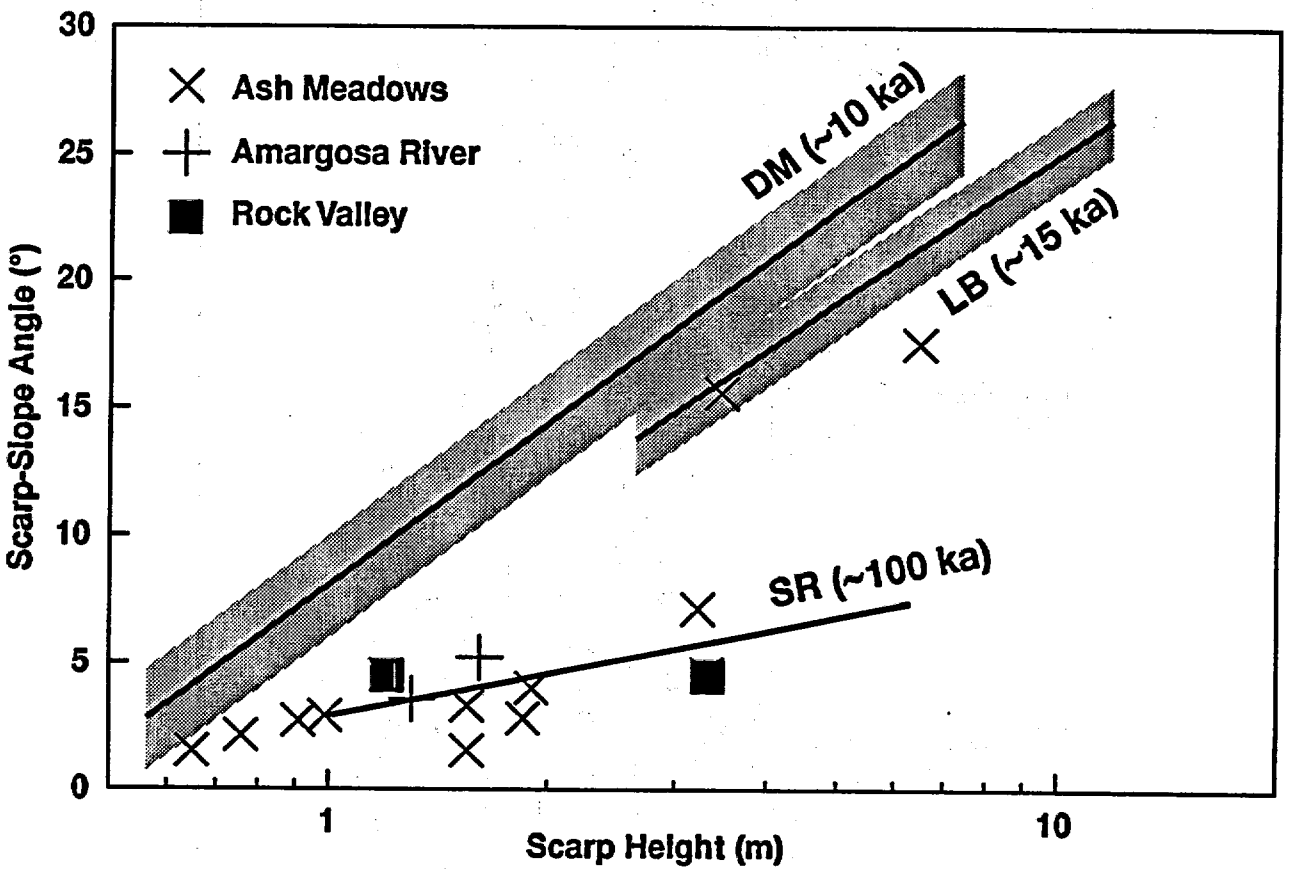

Fig. 9
E. Anderson

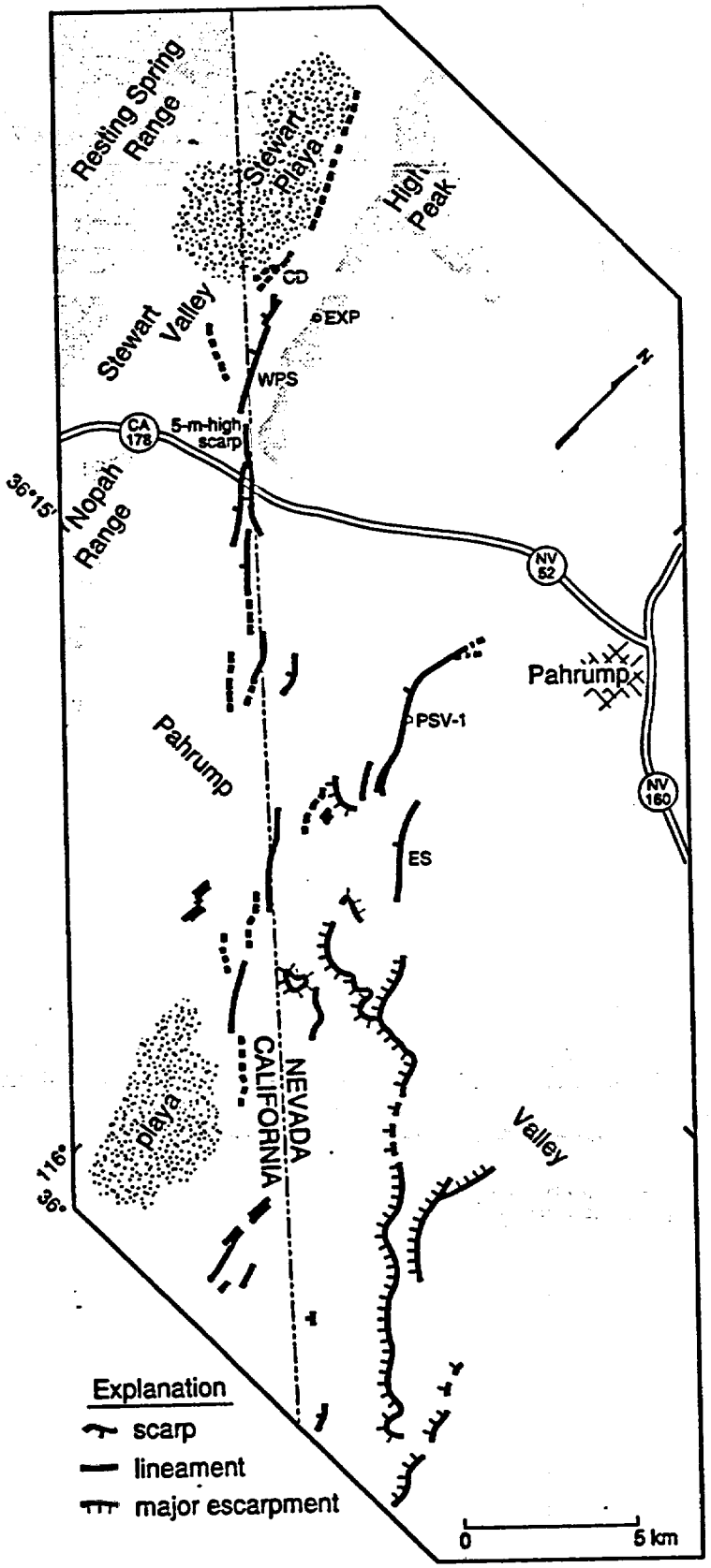

FIGURE 5. Map showing selected features of Pahrump-Stewart Valley fault zone (PSV) (after Hoffard, 1991). Locations discussed in the text include: CD, closed depression; ES, eroded scarp; EXP, exposure of Stewart Valley fault; PSV-1, profile site PSV-1; and WPS, warped playa sediment. Extent of mostly continuous bedrock shown by halftone fill. The most prominent scarps on late Quaternary deposits are in the Stewart Valley area, but the biggest escarpments associated with faulting are highly dissected and are restricted to the southern part of Pahrump Valley.

Figure 10
E. Anderson

Workshop #2

Need is to understand
a) available data bases
b) methodologies ~~for~~ available for characterizing each of these

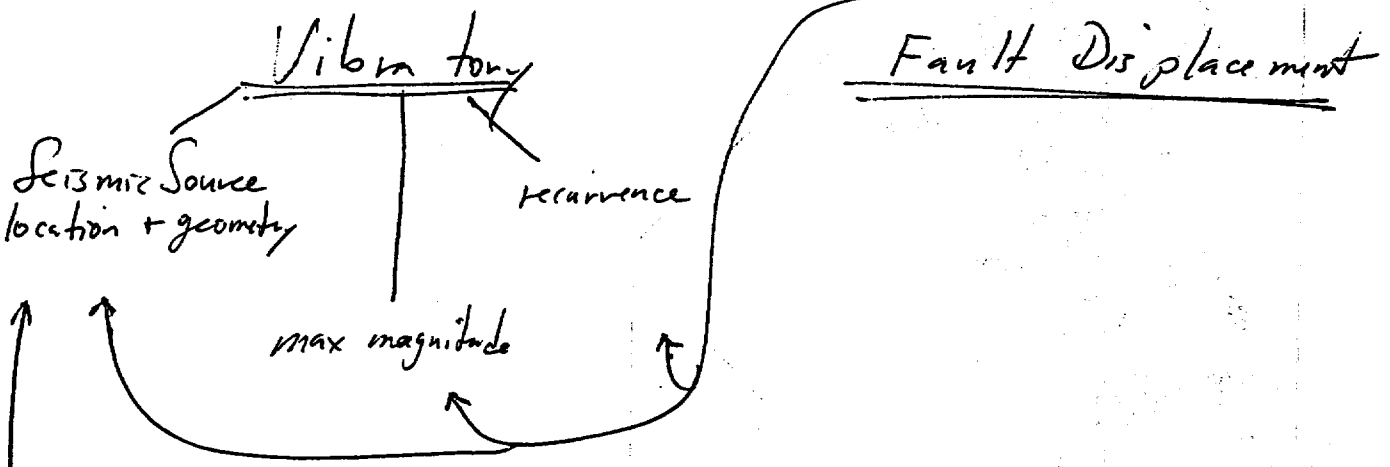

my talk is in this session & I'm asked to acknowledge uncertainties in the location and geometry

100 Pine Street, 10th Floor
San Francisco, CA 94111
(415) 434-9400 • FAX (415) 434-1365

GEOMATRIX

September 30, 1996

Dr. Ernie Anderson
U.S. Geological Survey
Denver Federal Center, MS 966
P.O. Box 25007
Denver, CO 80225

FAX #: (303) 273-8600

2 Pages Sent

Subject: Your Presentation at the Upcoming Seismic Source Characterization Workshop on Hazard Methodologies, October 16-18, 1996

Dear Ernie:

Welcome back to the Yucca Mountain seismic hazard analysis project! After a one-year hiatus, the seismic source characterization activities are starting back into action at a fast and furious pace. As you may recall, we conducted a workshop in 1995 that focused on the key technical issues that need to be addressed in characterizing seismic sources for vibratory ground motion and fault displacement hazard analysis. We then devoted a significant portion of the workshop to discussing the available data bases related to the seismic environment of Yucca Mountain.

Since last year, significant progress has been made gathering new field, compiling data bases into summary reports, and compiling analogue data regarding fault rupture processes. Therefore, we are able to take advantage of these efforts in providing data bases to each member of the seismic source characterization (SSC) expert panel.

In addition to providing additional data sets to the panel, a primary goal of the upcoming workshop (which is also termed Workshop #2, counting the 1995 workshop) is to identify *methods and approaches* to characterizing seismic sources for both vibratory ground motions and fault displacement hazard.

Shortly, you will receive the agenda for the upcoming workshop, which will identify all speakers and their time allotments. In the meantime, this letter is intended to provide you with information to help you prepare your presentation. The overall approach to presentations at the workshop is the following: SSC is first divided into two parts—vibratory ground motions and fault displacement— and general methods and approaches to characterizing each will be discussed. Second, ground motion hazard is divided into three parts—source geometry, maximum magnitude, earthquake recurrence—and approaches to assessing each are discussed. Third, the data bases pertinent to each of the three parts are discussed by a number of speakers. Likewise, the data bases related to fault displacement will be presented by several speakers. Through this format, we hope to update all of the experts on the available data, as well as

- continued -

GEOMATRIX

spark discussion of alternative approaches that are available to address ground motion and fault displacement hazard.

Ernie, your talk will occur in the session on the location and geometry of seismic sources. We would like for you and Larry to summarize the data bases that exist regarding the faults in the Yucca Mountain region. Although your talk will undoubtedly involve some presentation of *interpretations* as well as *data*, please remember that the next workshop (Workshop 3) is the real opportunity to present and debate alternative interpretations and models, and their consistency with the available data. Please include in your discussion an acknowledgment of the uncertainties that are involved in the assessment of the locations and geometries of regional faults, given the available data.

Many thanks for your participation in the workshop. We're looking for lively discussions and informative presentations. I will give you a call this week to answer any questions.

Best regards
GEOMATRIX CONSULTANTS, INC.

Kevin J. Coppersmith
SSC Facilitation Team Leader

KJC/nji

I:\PA\96P339\WK2-930L.DOC

AGENDA
SEISMIC SOURCE CHARACTERIZATION (SSC) HAZARD METHODOLOGIES WORKSHOP

October 16-18, 1996
Doubletree Hotel, Salt Lake City, Utah

GOAL OF THE WORKSHOP:

The workshop has two principal goals: to review the data that are available for the Yucca Mountain region, and to identify available methodologies for characterizing seismic sources for the Yucca Mountain seismic hazard analysis. The first goal is a follow-on to the first SSC workshop held in April of last year, because additional data have become available and/or synthesized in summary reports since that time.

APPROACH:

The approach used in this workshop to accomplish the above goals is to divide seismic source characterization into two parts: SSC related to vibratory ground motion hazard analysis and related to fault displacement hazard analysis. SSC is then divided into three components: seismic source location and geometry, maximum earthquake magnitude, and earthquake recurrence assessment. Each of these topics is first introduced by overview presentations that focus on the *methods and approaches* that are available to characterize them. These talks are then followed by a series of talks that describe the available *data bases and data interpretations* that relate to these topics. Although the presentations will undoubtedly entail some interpretations, the next workshop (Workshop #3 Alternative Models and Interpretations) will provide a forum for debating alternative interpretations of the available data. In the meantime, it is important that each member of the expert panel have an opportunity to understand the available methodologies and the available data bases for conducting the SSC.

WEDNESDAY, OCTOBER 16

8:30 - 10:00 **INTRODUCTION**

8:30 - 8:45 Welcome (T. Sullivan)

8:45 - 9:15 Yucca Mountain PSHA Project (C. Stepp)

9: 15 - 10:00 Overview of Process and Guidelines for Workshops (K. Coppersmith)

10:00 -10:15 BREAK

WEDNESDAY, OCTOBER 16 (CONT.)

10:15 - 4:15	**SEISMIC SOURCE CHARACTERIZATION FOR ASSESSING VIBRATORY GROUND MOTIONS—LOCATION AND GEOMETRY**
10:15 - 11:15	General Approach and Key Issues (W. Arabasz)
11:15 - 12:00	Methods for Assessing Location and Geometry of Seismic Sources (R. Bruhn)
12:00 - 1:00	**LUNCH**
1:00 - 1:45	Quaternary Fault Studies in the Site Area (C. Menges)
1:45 - 2:30	Quaternary Fault Studies in the Yucca Mountain Region (L. Anderson/E. Anderson)
2:30 - 2:45	**BREAK**
2:45 - 3:30	New Deep Seismic Reflection Line Data (T. Brocher)
3:30 - 4:15	Geometry Information from Seismicity Data (K. Smith)
4:15 - 4:30	Information on November Field Trip (K. Coppersmith)
4:30 - 5:00	**STATEMENTS FROM OBSERVERS**

THURSDAY, OCTOBER 17

8:30 - 11:45	**MAXIMUM EARTHQUAKE MAGNITUDE EVALUATION**
8:30 - 9:15	Methods for Assessing Maximum Magnitudes (K. Coppersmith)
9:15 - 10:00	Data Related to Segmentation and Displacement per Event on Site Area Faults (S. Pezzopane)
10:00 - 10:15	**BREAK**
10:15 - 11:00	Relation between Rupture Length, Slip Rate, and Magnitude (J. Anderson)
11:00 - 4:30	**EARTHQUAKE RECURRENCE EVALUATION**
11:00 - 11:45	Methods for Assessing Earthquake Recurrence (J. McCalpin)
11:45 - 12:45	**LUNCH**
12:45 - 1:30	Yucca Mountain Slip Rate and Recurrence Interval Data (J. Whitney)
1:30 - 2:15	Evidence for Temporal Clustering on the Solitario Canyon Fault (A. Ramelli)
2:15 - 3:00	CNWRA Fault Studies in the Yucca Mountain Region (J. Stamatakos)
3:00 - 3:15	**BREAK**
3:15 - 3:45	Global Positioning System Data (CNWRA data - J. Stamatakos; USGS data - S. Pezzopane)
3:45 - 4:30	Earthquake Catalog Analysis (I. Wong)
4:30 - 5:00	**STATEMENTS FROM OBSERVERS**

FRIDAY, OCTOBER 18

8:30 - 2:30	**SEISMIC SOURCE CHARACTERIZATION FOR FAULT DISPLACEMENT ANALYSIS**
8:30 - 9:30	Methods for Assessing Fault Displacement Hazard (R. Youngs)
9:30 - 10:15	Mapping of Yucca Mountain Block (W. Day)
10:15 - 10:30	**BREAK**
10:30 - 11:00	Fractures and Faults Mapped in the ESF (R. Lung)
11:00 - 11:45	Yucca Mountain Geophysical Data (E. Major)
11:45 - 12:15	Ghost Dance Fault Paleoseismic Data (J. Whitney)
12:15 - 1:15	**LUNCH**
1:15 - 1:45	Average and Maximum Fault Displacements (B. Slemmons)
1:45 - 2:30	Basin and Range Secondary Faulting Data (S. Pezzopane)
2:30 - 2:45	Where we go from here (K. Coppersmith)
2:45 - 3:00	**COMMENTS FROM OBSERVERS**

PROPOSED SCHEDU
SEISMIC HAZ

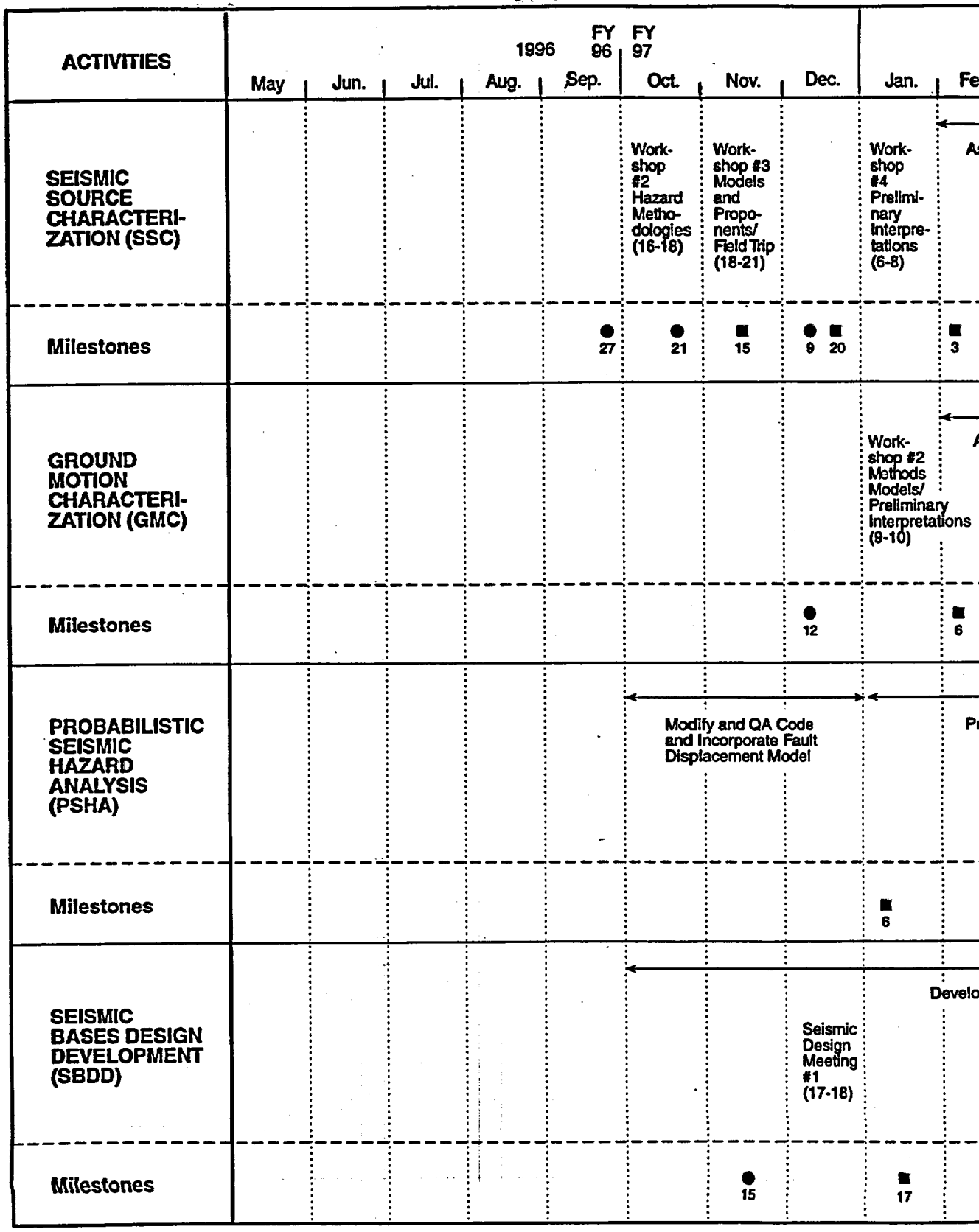

LEGEND:
- ● Work Plan
- ■ Letter Report
- △ Preliminary Interpretations to Facilitation Team
- ▲ Preliminary Interpretations to Calculations Team
- ◊ Final Interpretations to Facilitation Team
- ♦ Final Interpretations to Calculations Team

LE FOR YUCCA MOUNTAIN
ARD ASSESSMENT

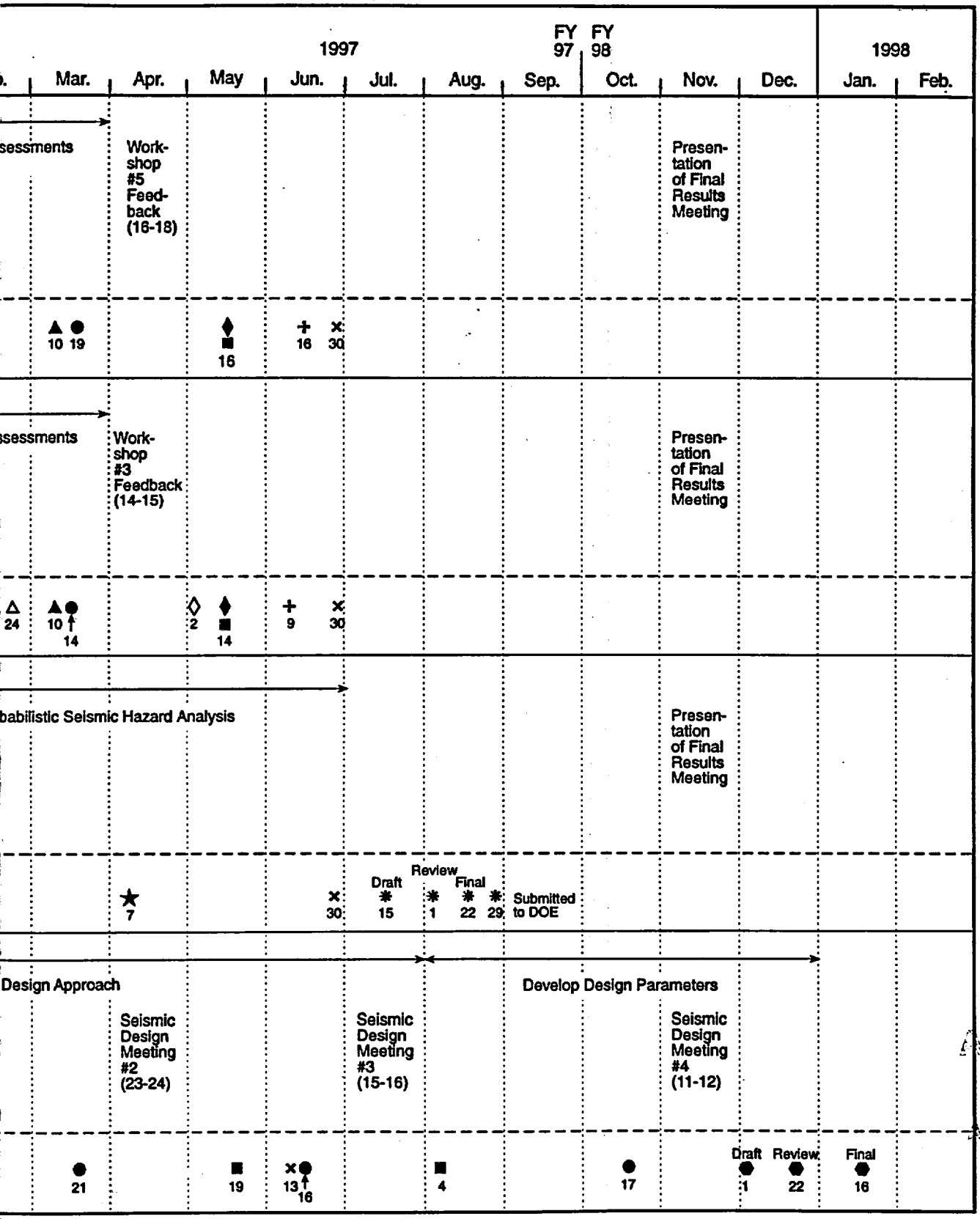

+ Expert Documentation to Facilitation Teams

× Activity Report

✱ PSHA Report

● Seismic Design Report (Topical #3)

★ Preliminary PSHA Calculations

9611260175-1

Seismic Source Characterization Hazard Methodologies Workshop

New Deep Seismic Reflection Lines

Tom Brocher, Clay Hunter, Vicki Langenheim

USGS

USGS/YMP

Talk Outline

Acquisition
Processing
Bare Mountain fault
Crater Flat east-dipping faults
Solitario C. - Ghost Dance f.
Faults east of Ghost Dance f.
Schematic structural models
Implications for seismic hazards
Summary

USGS/YMP

Regional Seismic Lines

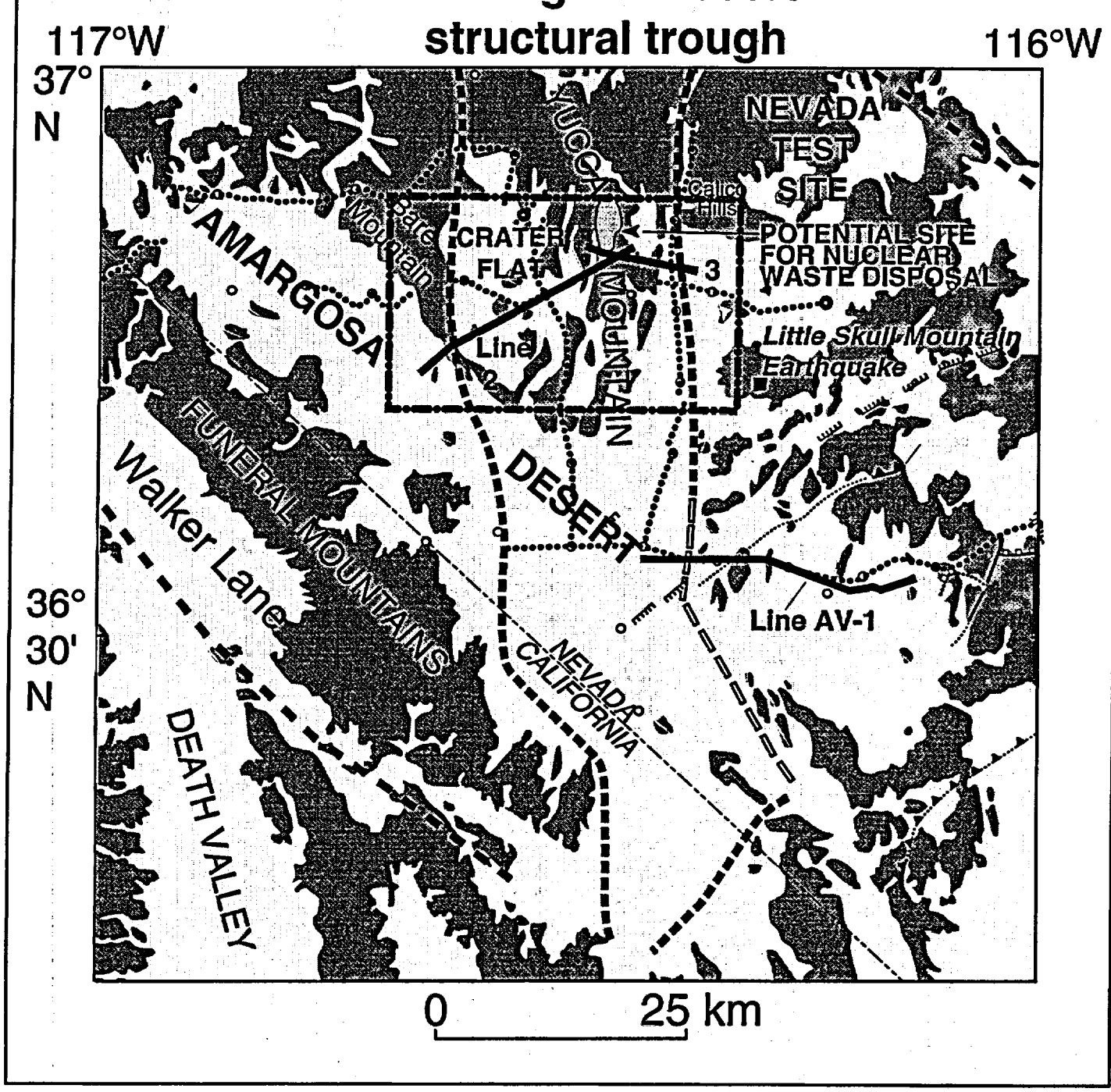

Simplified Stratigraphy

Several (4-5) km of Proterozoic/Paleozoic clastic and carbonate sedimentary rocks - highly-deformed with steep dips

2-3 km of bedded Mid-Miocene volcanic tuffs - generally low dips (<10 degrees)

Quaternary basaltic cones and flows within or on top of clastic sedimentary units

USGS/YMP

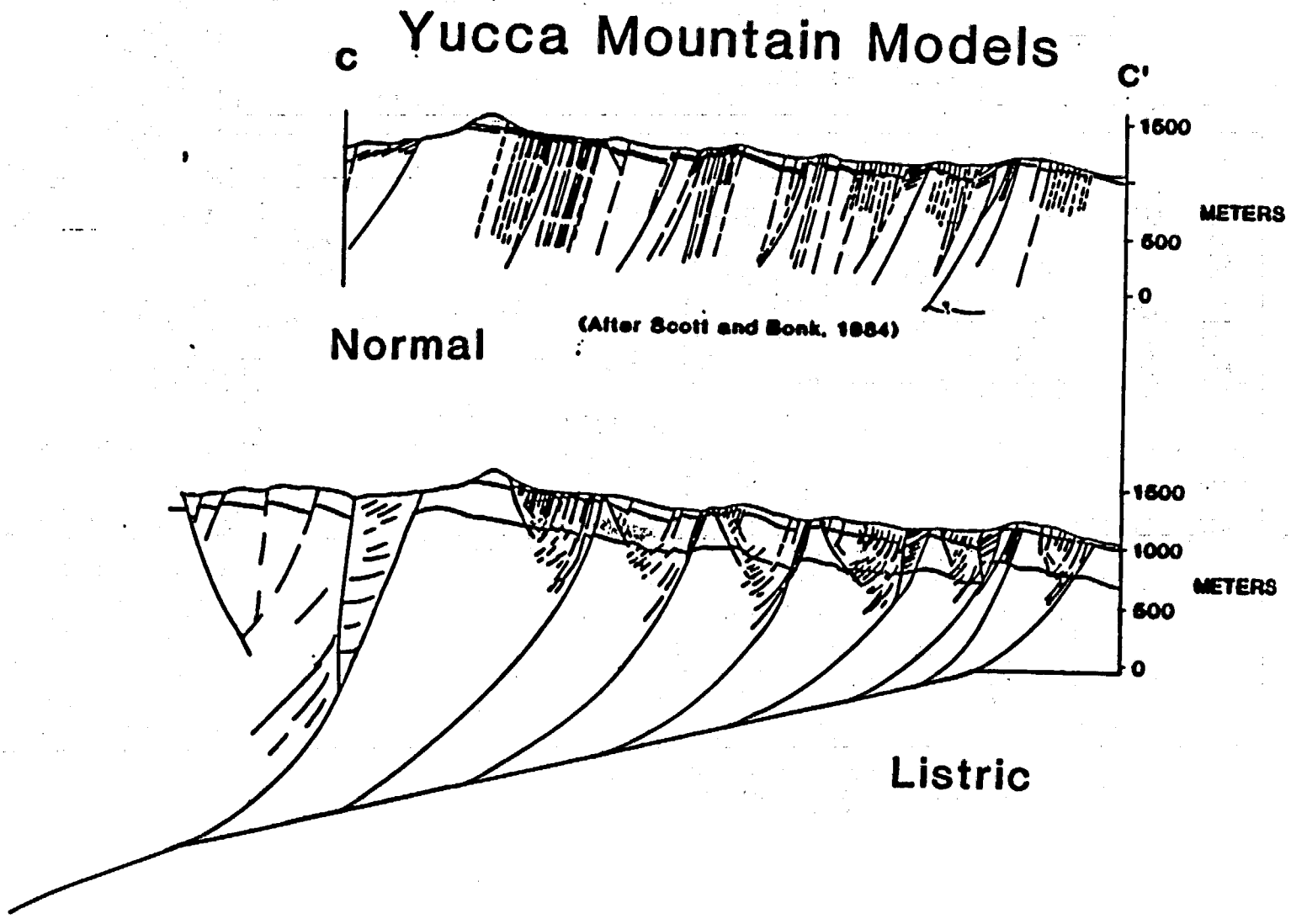
c
Yucca Mountain Models
C'
1500
500
0
METERS
Normal
(After Scott and Bonk, 1984)
1500
1000
500
0
METERS
Listric

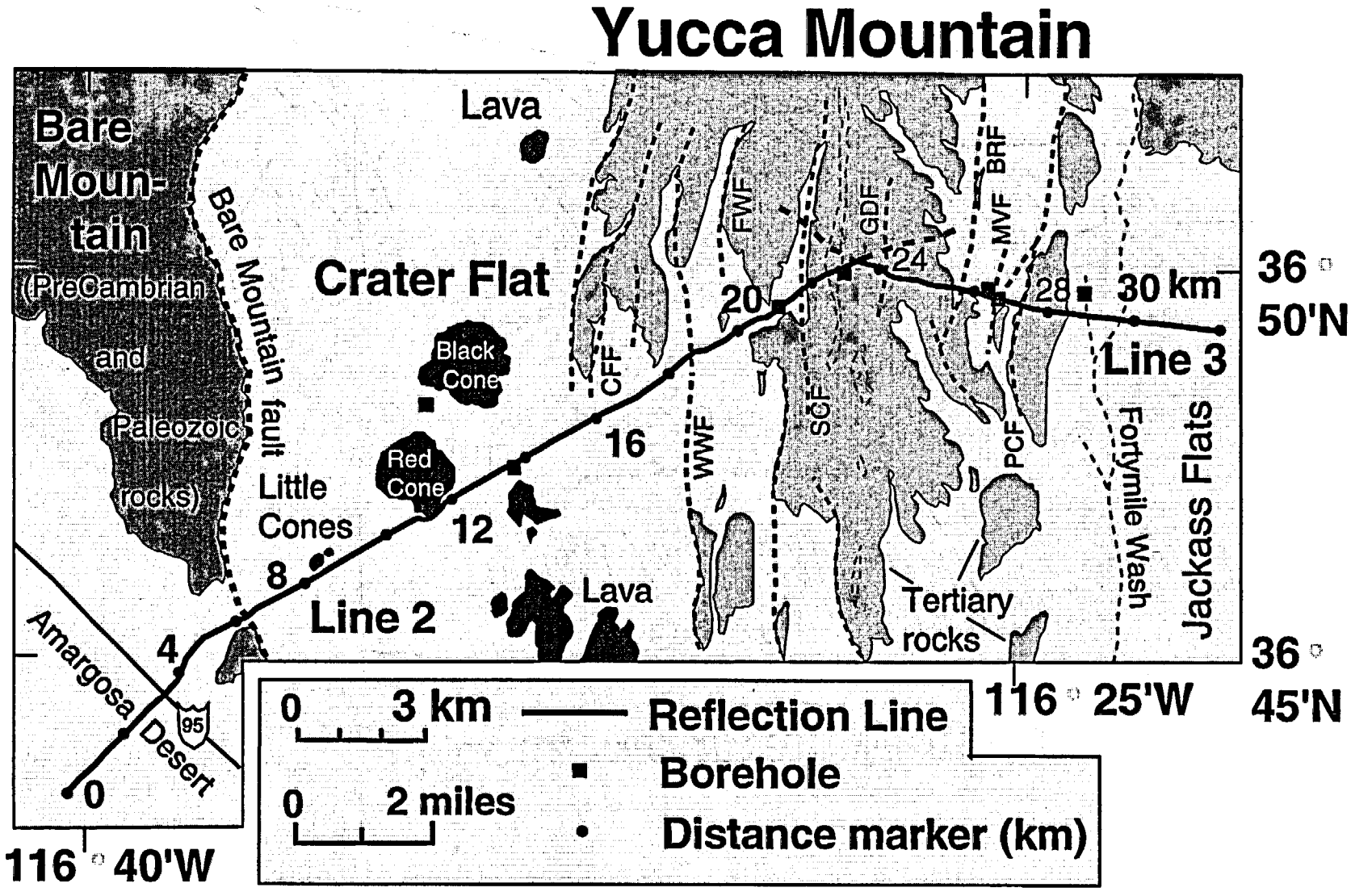
Yucca Mountain
Bare Mountain (PreCambrian and Paleozoic rocks)
Bare Mountain fault
Lava
Crater Flat
Black Cone
Red Cone
Little Cones
Line 2
Line 3
Lava
Tertiary rocks
Jackass Flats
Fortymile Wash
Amargosa Desert
95
CFF
FWF
GDF
BRF
MVF
WWF
SCF
PCF
0
4
8
12
16
20
24
28
30 km
36° 50'N
36° 45'N
116° 25'W
116° 40'W
0 3 km
0 2 miles
Reflection Line
Borehole
Distance marker (km)

Geophysical Databases

Crustal scale seismic reflection data - High-fold (60-125) - Vibrator, Poulter, Minihole sources

Ground magnetic and gravity data

Seismicity and focal mechanism data

Borehole and outcrop data

USGS/YMP

USGS OFR 96-28

by Brocher, Hart, Hunter, Langenheim

Data Acquisition

Data Processing

Preliminary Interpretation (now superceded)

Complete set of uninterpreted seismic lines

USGS/YMP

Seismic Data Acquisition

by Contractor

Upper Crust (0-5 s) - High-fold (60-125)
Vibrator, Poulter, Minihole Sources

Lower Crust (5-10 s) - Low-fold (1-8) Deep
Shothole Sources

480-channel recorder - split-spread - 25 m group -
12.5 m CMP spacing

USGS/YMP

Seismic Data Processing

by Contractor

Conventional CMP stacking - 2-D geometry

Phase compensation filtering of vibrator data to match it's phase to that of explosion data

Post-stack migration

Post-stack depth conversion

Limited pre-stack processing of Line 3

USGS/YMP

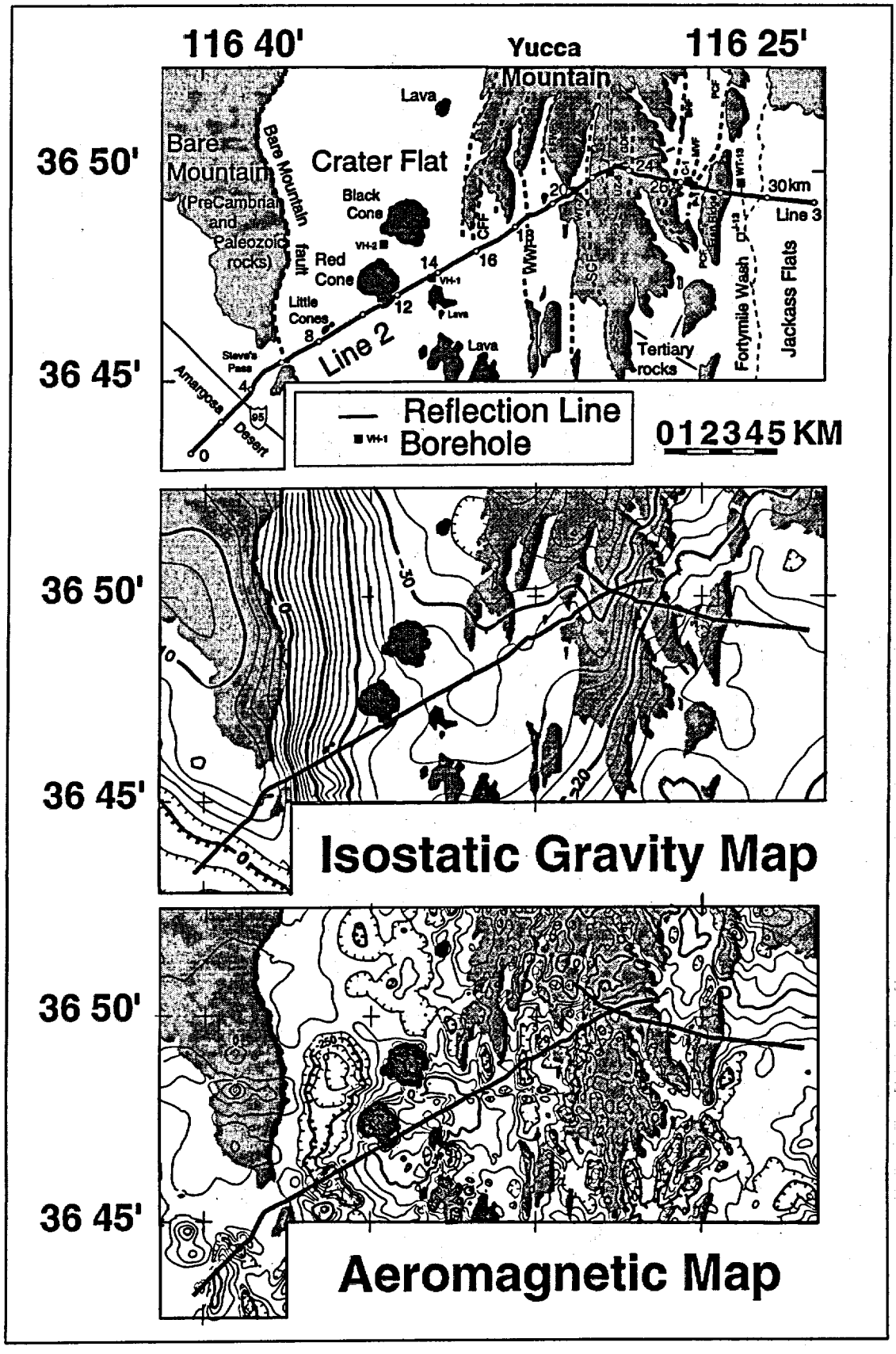
116 40'
Yucca
Mountain
116 25'
36 50'
36 45'
Lava
Bare
Mountain
(PreCambrian
and
Paleozoic
rocks)
Bare Mountain fault
Crater Flat
Black
Cone
Red
Cone
Little
Cones
Line 2
Steve's
Pass
Amargosa
Desert
95
Lava
Tertiary
rocks
Fortymile Wash
Jackass Flats
30km
Line 3
Reflection Line
Borehole
012345 KM
Isostatic Gravity Map
Aeromagnetic Map

Gravity Models

High-density Proterozoic/Paleozoic outcrops at Bare Mountain produce gravity high

Low-density Miocene tuffs at Yucca Mountain produce a gravity low

Tertiary fill beneath Crater Flat extends eastward under crest of Yucca Mountain

100-m offset of P/T boundary = 1 to 2 mGal

USGS/YMP

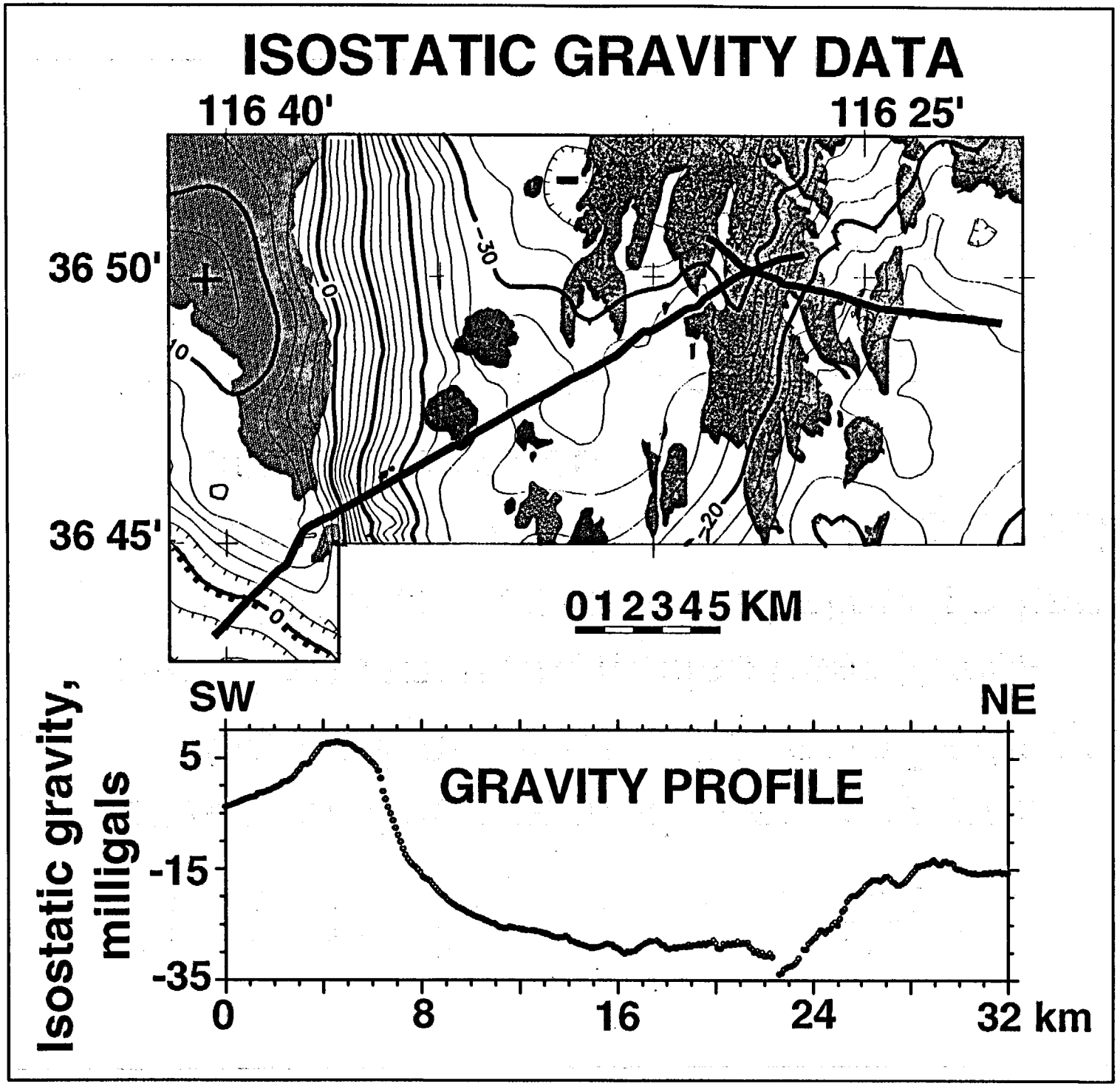
ISOSTATIC GRAVITY DATA
116 40'
116 25'
36 50'
36 45'
-30
-0
-10
-20
0
0
012345 KM
SW
NE
GRAVITY PROFILE
Isostatic gravity, milligals
5
-15
-35
0
8
16
24
32 km

Ground Magnetic Data

Broad positive magnetic anomaly over Crater Flat - source beneath Tertiary fill

High-frequency anomalies near Yucca Mountain - source in shallow Tertiary fill

Circular anomalies in Crater Flat over volcanic flows and cones

50 m of offset on Tpt = 20 to 50 nT

USGS/YMP

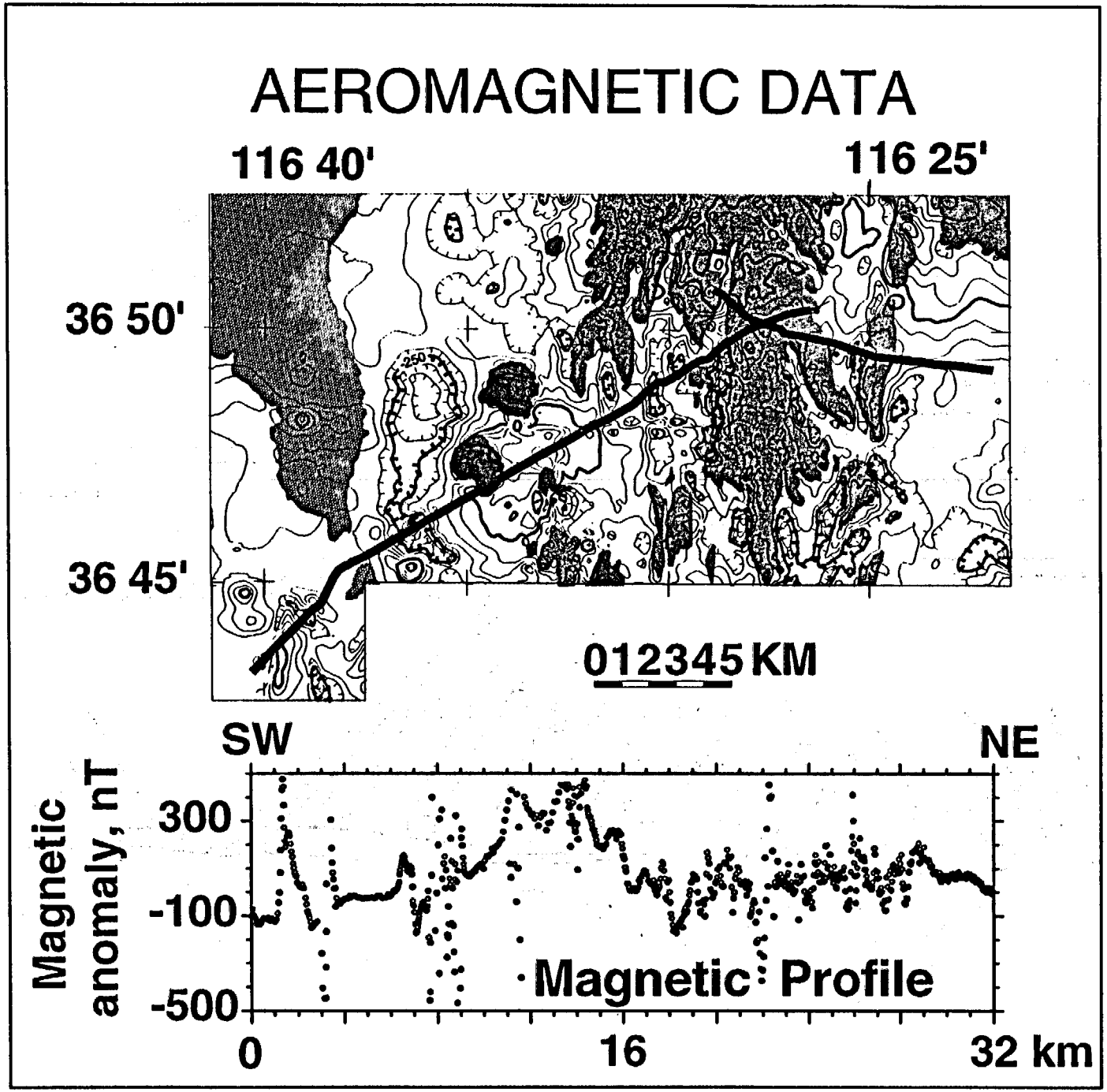
AEROMAGNETIC DATA
116 40'
116 25'
36 50'
36 45'
250
0
012345 KM
SW
NE
Magnetic anomaly, nT
300
-100
-500
Magnetic Profile
0
16
32 km

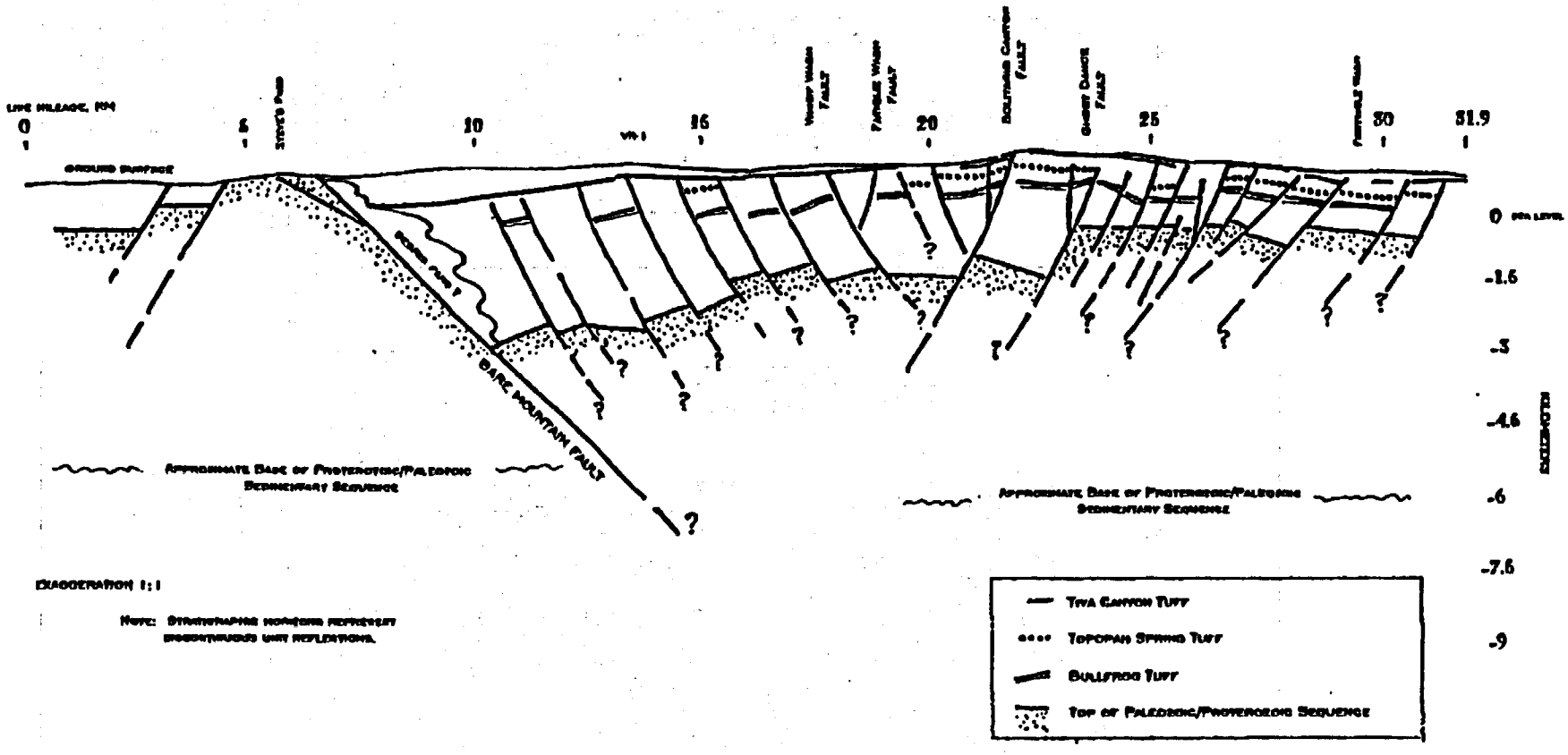
0
5
10
15
20
25
30
31.9
0
-1.6
-3
-4.6
-6
-7.6
-9
BARE MOUNTAIN FAULT
Tiva Canyon Tuff
Topopah Spring Tuff
Bullfrog Tuff
Top of Paleozoic/Proterozoic Sequence

Fig. 2d

Bare Mountain Fault

East-dipping (45°) range-front fault

True dip (65°)

Truncates distinctive zones of reflectivity (inferred 4-km-thick Proterozoic-Paleozoic sedimentary section) to depths of 6 to 7 km

USGS/YMP

SL = sea level units all in km

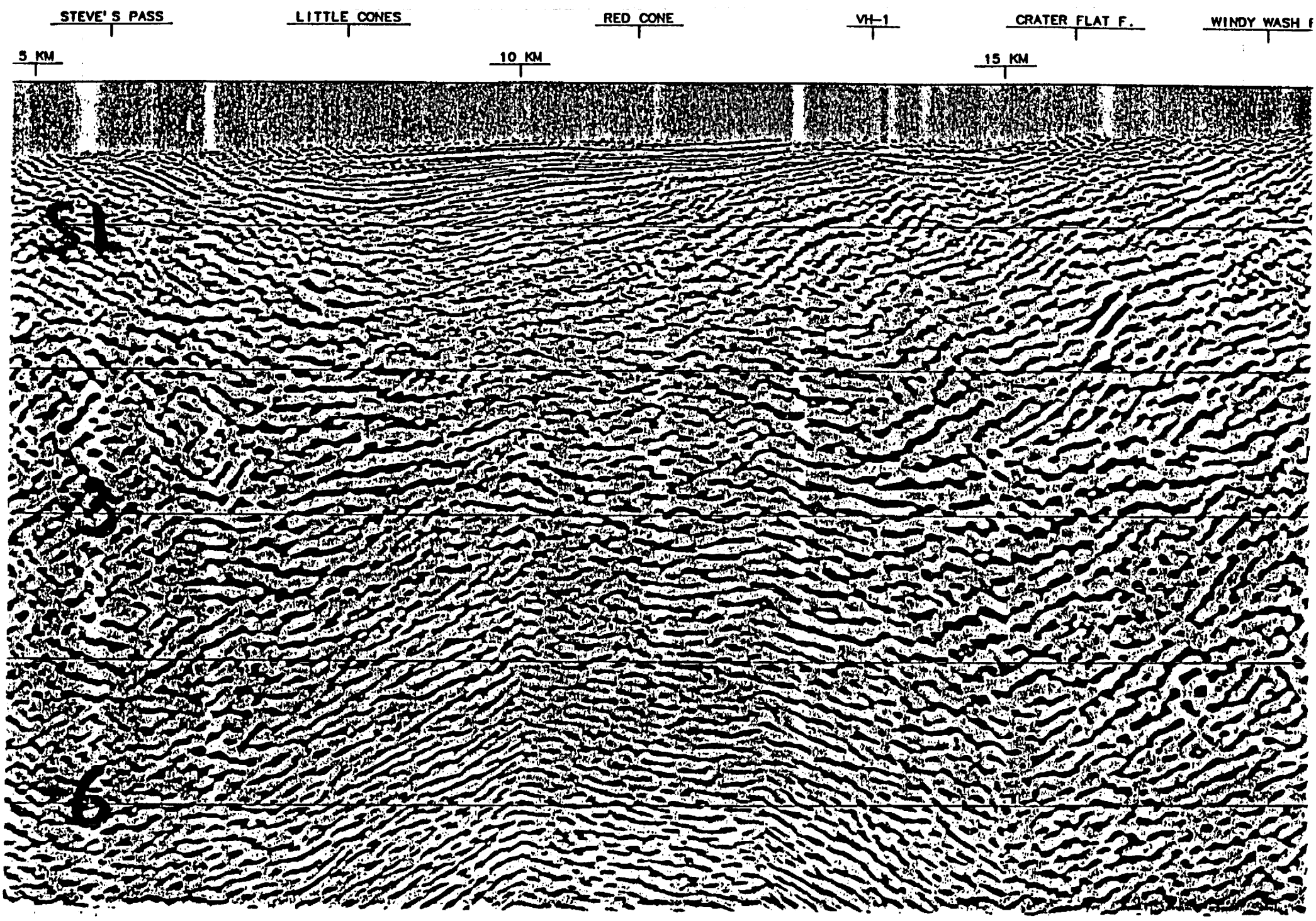

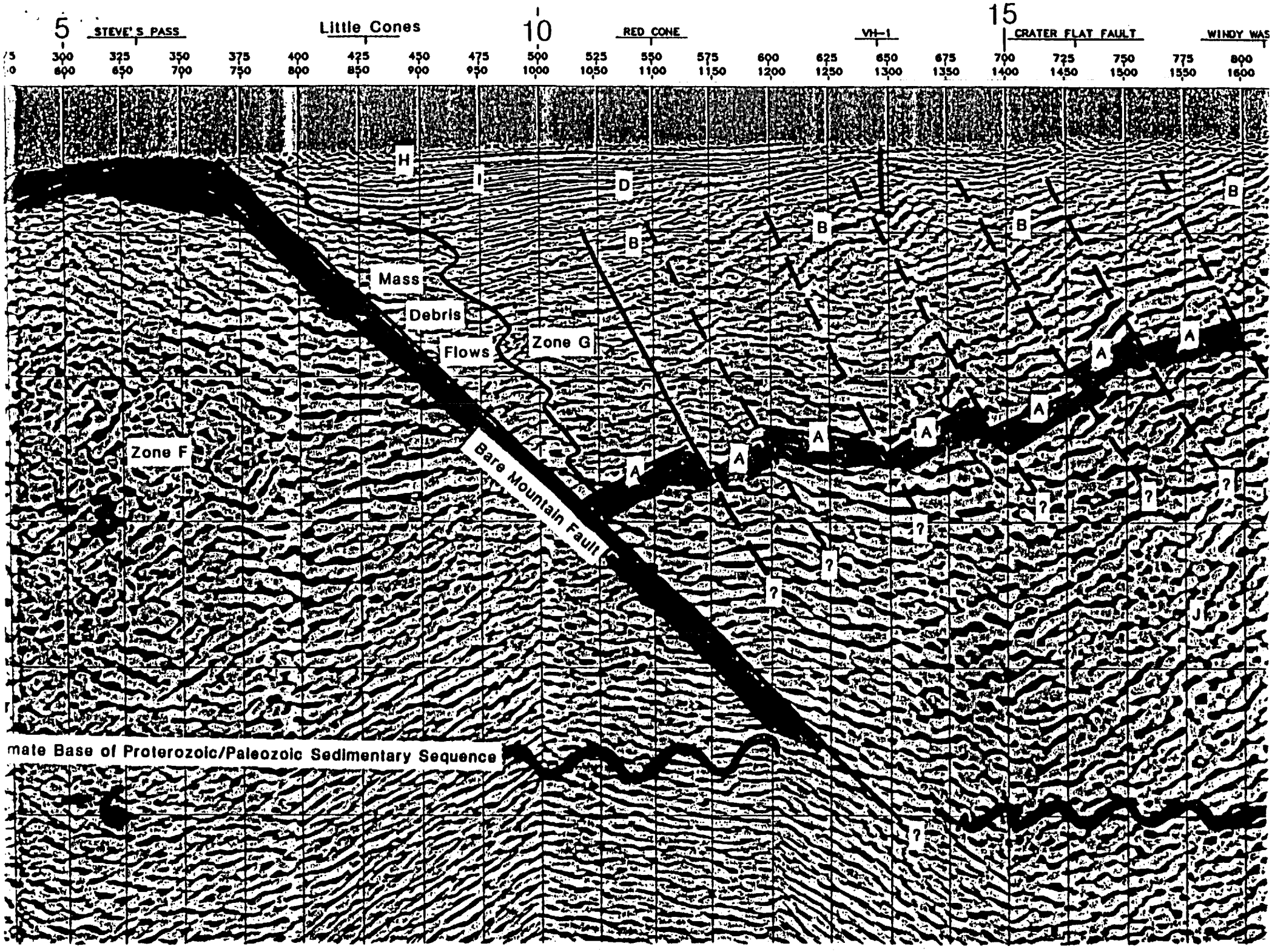
5
STEVE'S PASS
Little Cones
10
RED CONE
VH-1
15
CRATER FLAT FAULT
WINDY WAS
H
I
D
B
Mass
Debris
Flows
Zone G
Zone F
Bare Mountain Fault
A
?
J
mate Base of Proterozoic/Paleozoic Sedimentary Sequence

East-Dipping Faults Beneath Crater Flat

1) Geologic mapping of east-dipping faults

2) West-dipping Tertiary basin fill

3) Magnetic anomalies lie west of faults

USGS/YMP

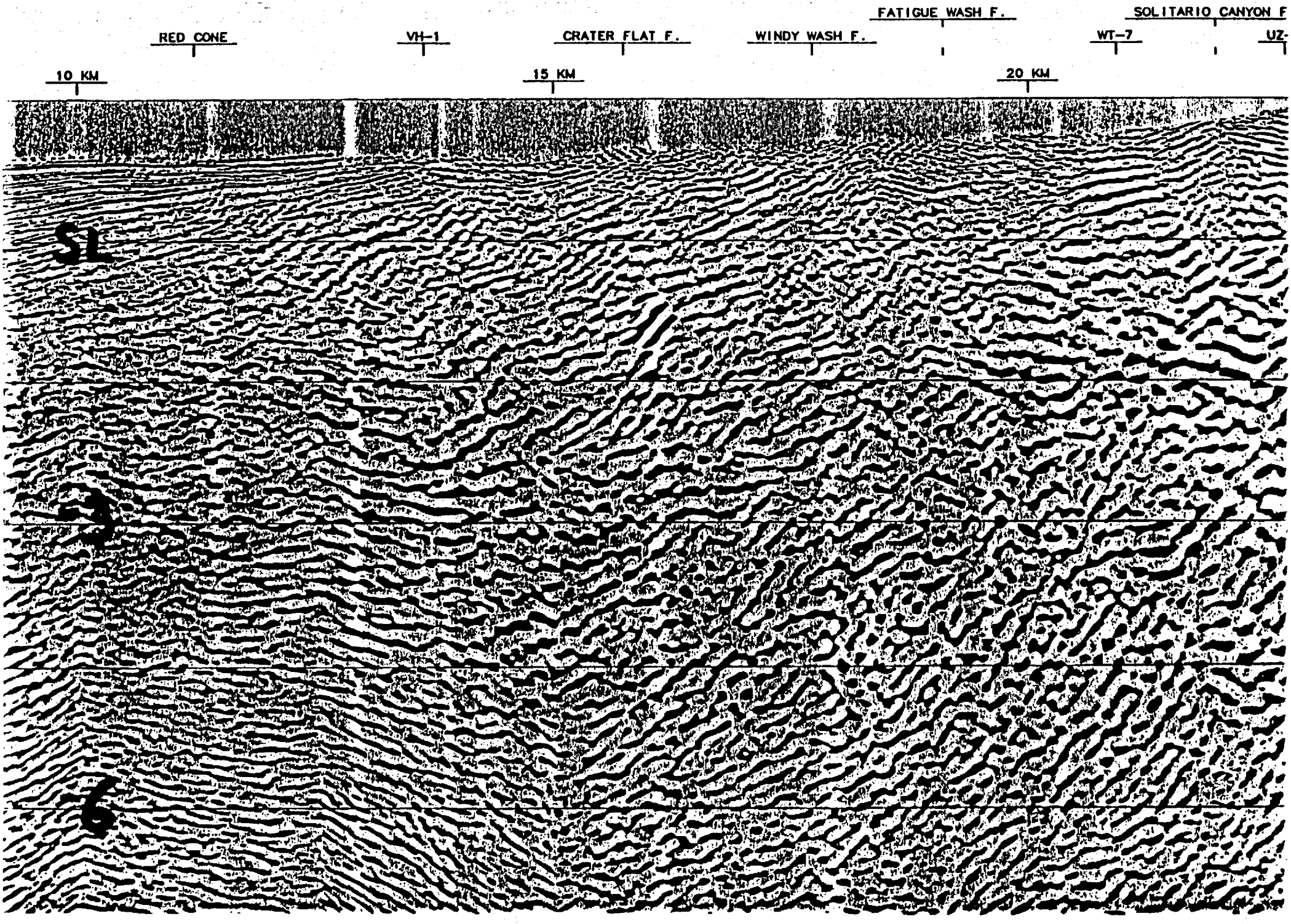
FATIGUE WASH F.
SOLITARIO CANYON F
RED CONE
VH-1
CRATER FLAT F.
WINDY WASH F.
WT-7
UZ-
10 KM
15 KM
20 KM
SL

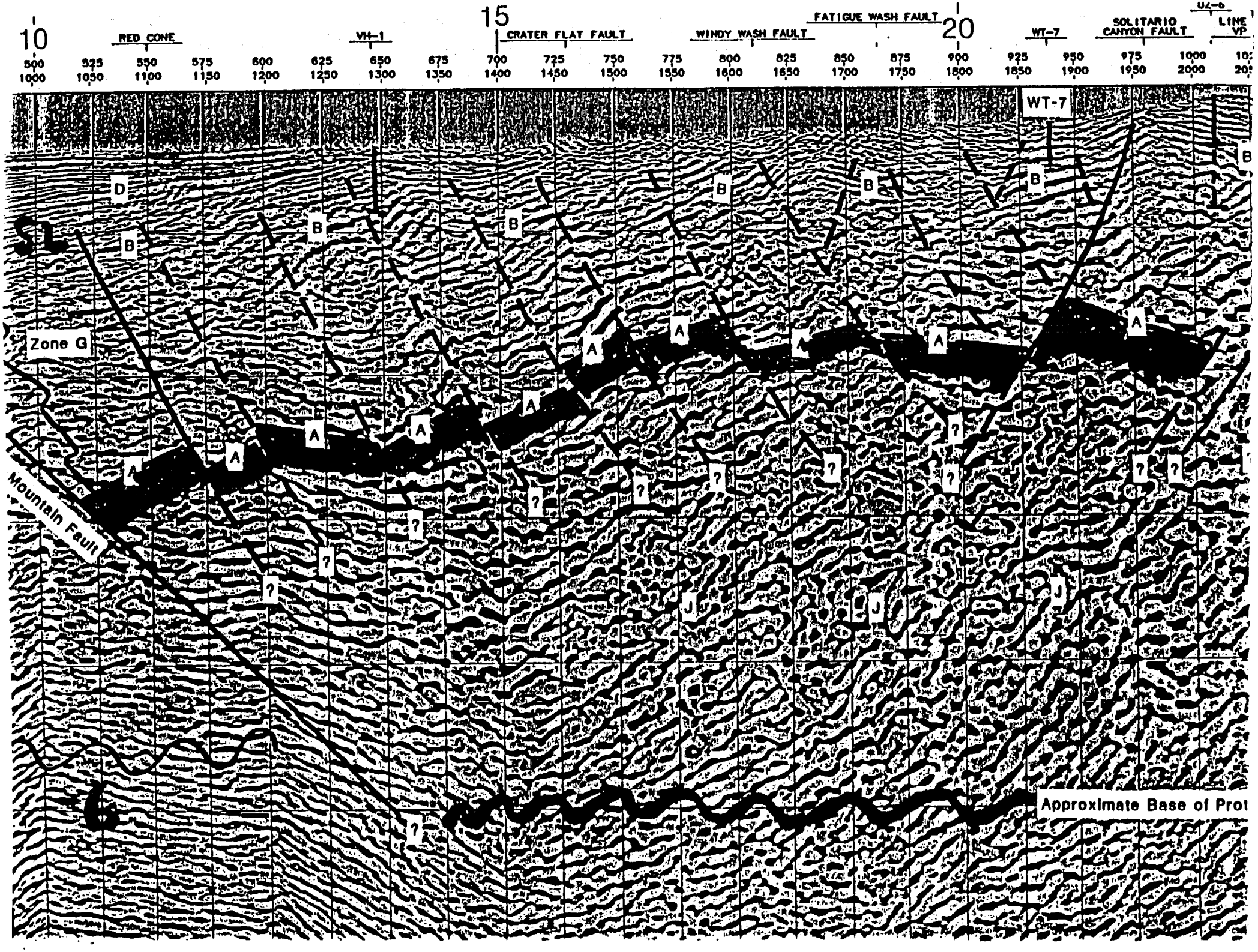
10
15
20
RED CONE
VH-1
CRATER FLAT FAULT
FATIGUE WASH FAULT
WINDY WASH FAULT
WT-7
SOLITARIO CANYON FAULT
LINE VP
500 525 550 575 600 625 650 675 700 725 750 775 800 825 850 875 900 925 950 975 1000
1000 1050 1100 1150 1200 1250 1300 1350 1400 1450 1500 1550 1600 1650 1700 1750 1800 1850 1900 1950 2000
WT-7
Zone G
Mountain Fault
Approximate Base of Prot

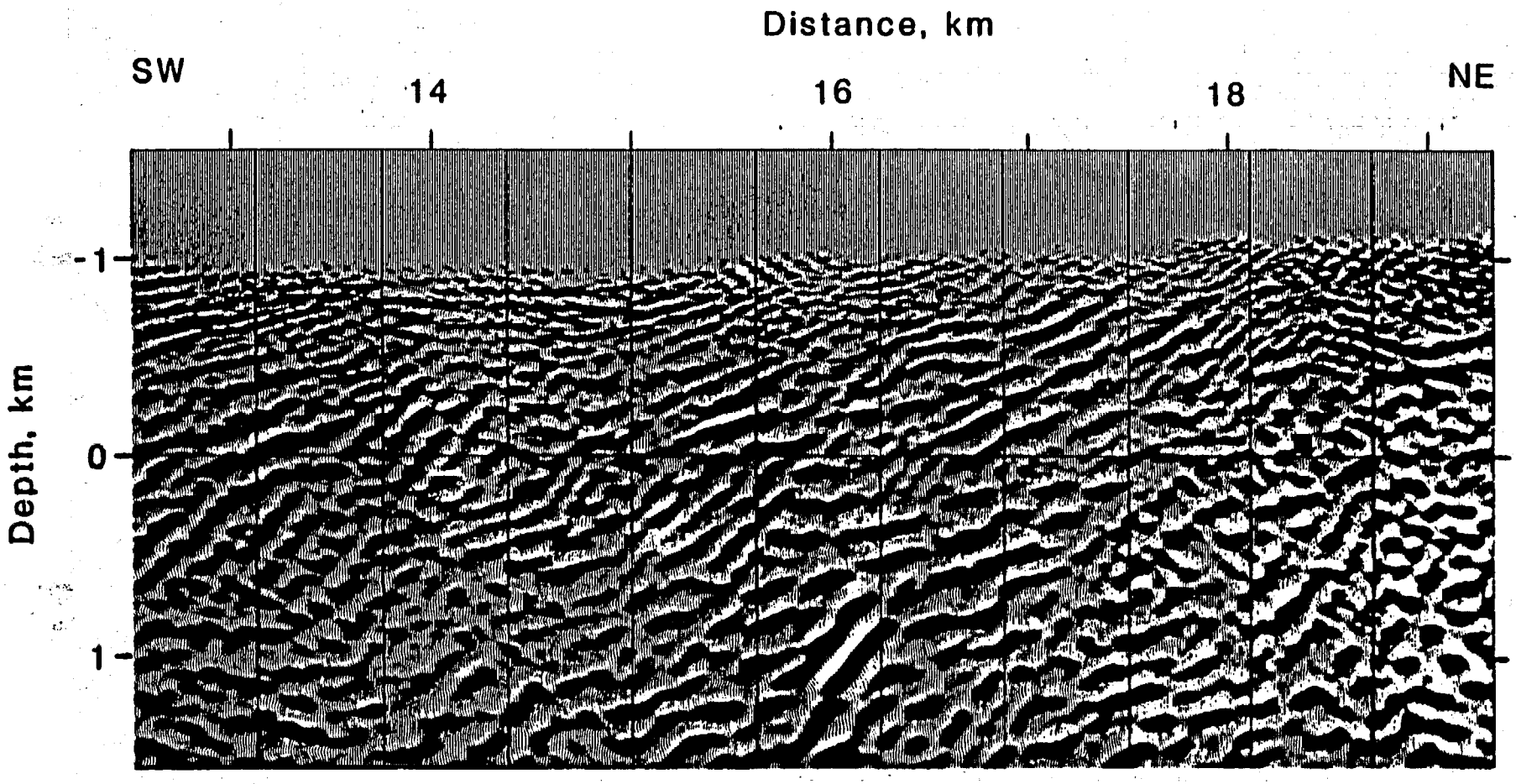
Distance, km
SW
14
16
18
NE
Depth, km
-1
0
1

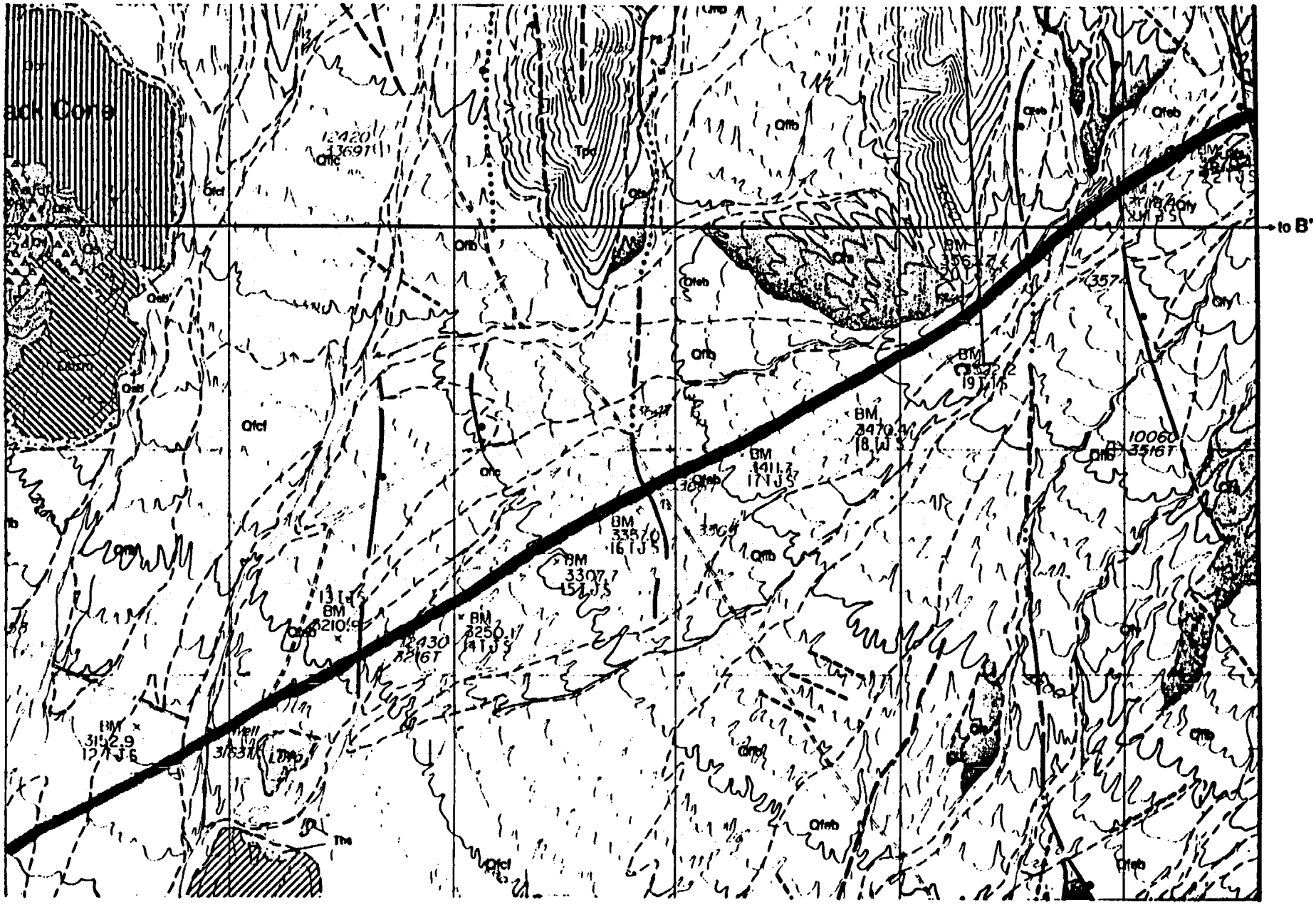

FAULDS AND OTHERS, 1994

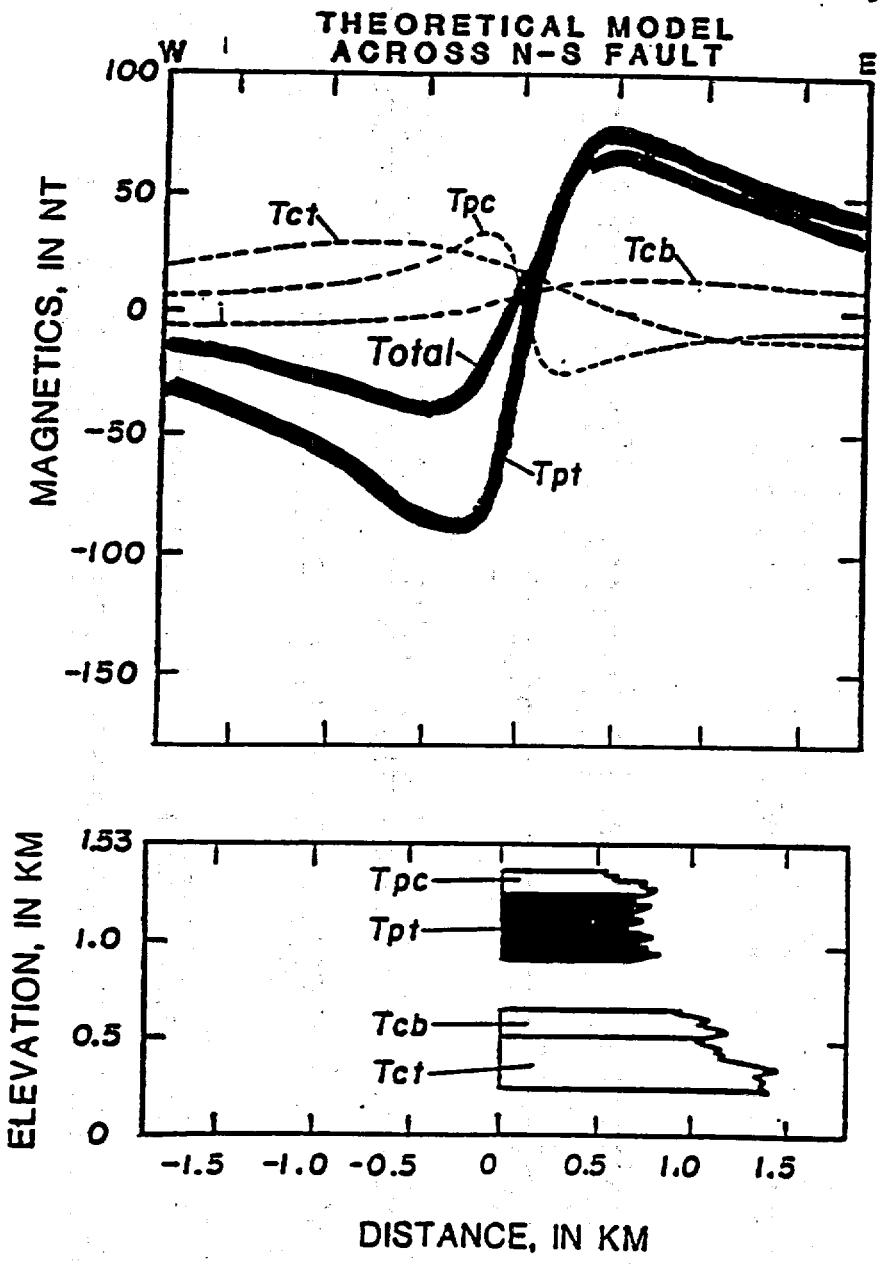

Figure 5. Theoretical magnetic anomaly from vertical offset of north-south trending fault (from Bath and Jahren, 1984). Geologic units and their modeled properties are described in tables 1 and 2, respectively.

Solitario Canyon Fault
Ghost Dance Fault

West-dipping faults with large offsets of the Paleozoic/Tertiary contact

Gravity model consistent with this interpretation to explain large gravity gradient under YM

Offset of Tiva Canyon Tuff across Ghost Dance fault at surface is less than 20 to 30 m

USGS/YMP

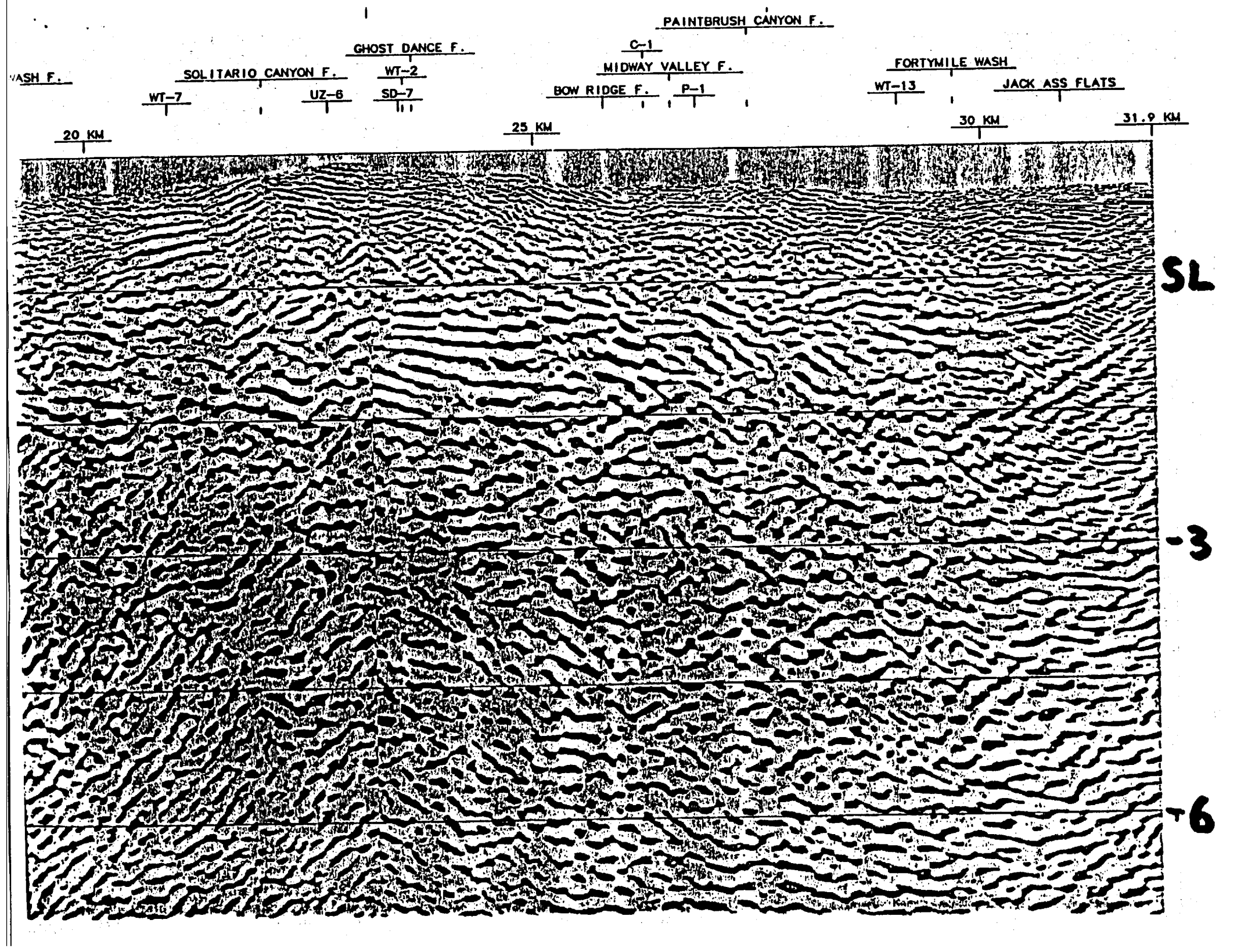
PAINTBRUSH CANYON F.
GHOST DANCE F.
C-1
MIDWAY VALLEY F.
FORTYMILE WASH
WASH F.
SOLITARIO CANYON F.
WT-2
WT-13
JACK ASS FLATS
WT-7
UZ-6
SD-7
BOW RIDGE F.
P-1
20 KM
25 KM
30 KM
31.9 KM
SL
-3
-6

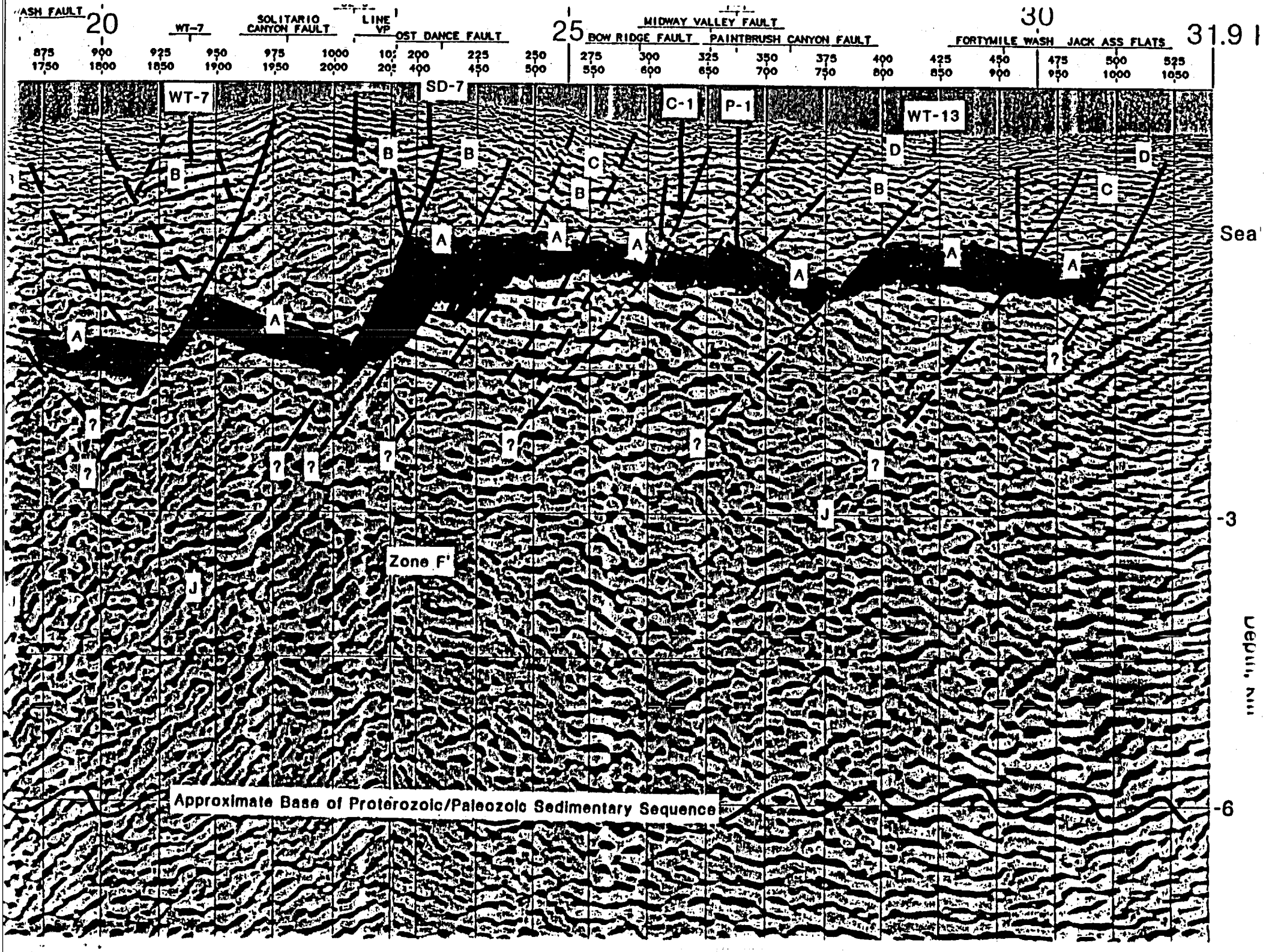
ASH FAULT
20
WT-7
SOLITARIO CANYON FAULT
LINE VP
OST DANCE FAULT
25
MIDWAY VALLEY FAULT
BOW RIDGE FAULT
PAINTBRUSH CANYON FAULT
30
FORTYMILE WASH
JACK ASS FLATS
31.9
875 900 925 950 975 1000 10 200 225 250 275 300 325 350 375 400 425 450 475 500 525
1750 1800 1850 1900 1950 2000 20 400 450 500 550 600 650 700 750 800 850 900 950 1000 1050
WT-7
SD-7
C-1
P-1
WT-13
Zone F'
Approximate Base of Proterozoic/Paleozoic Sedimentary Sequence
Sea
-3
-6
Depth, km

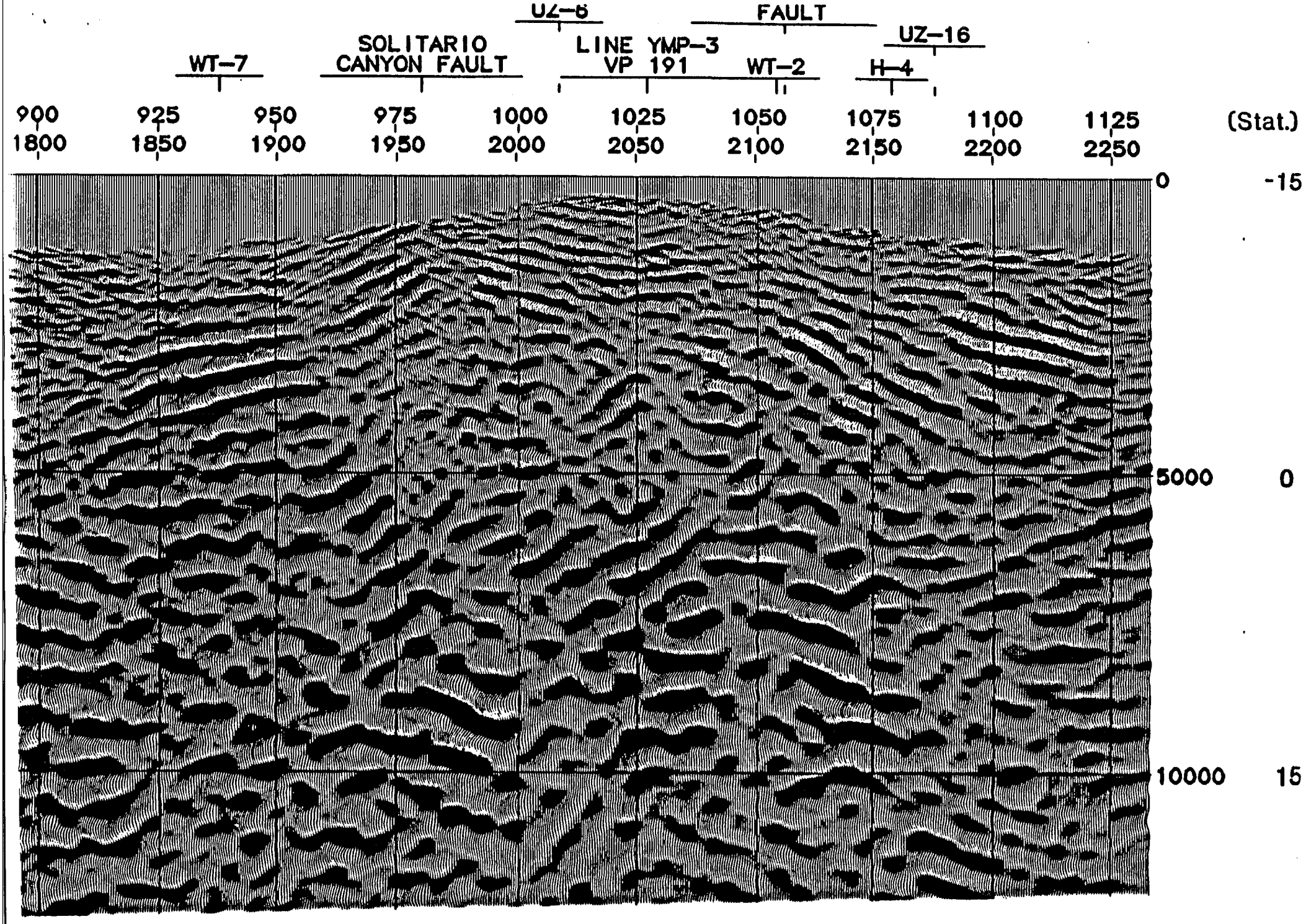
UZ-6
FAULT
UZ-16
SOLITARIO CANYON FAULT
LINE YMP-3 VP 191
WT-7
WT-2
H-4
900 925 950 975 1000 1025 1050 1075 1100 1125 (Stat.)
1800 1850 1900 1950 2000 2050 2100 2150 2200 2250
0 -15
5000 0
10000 15

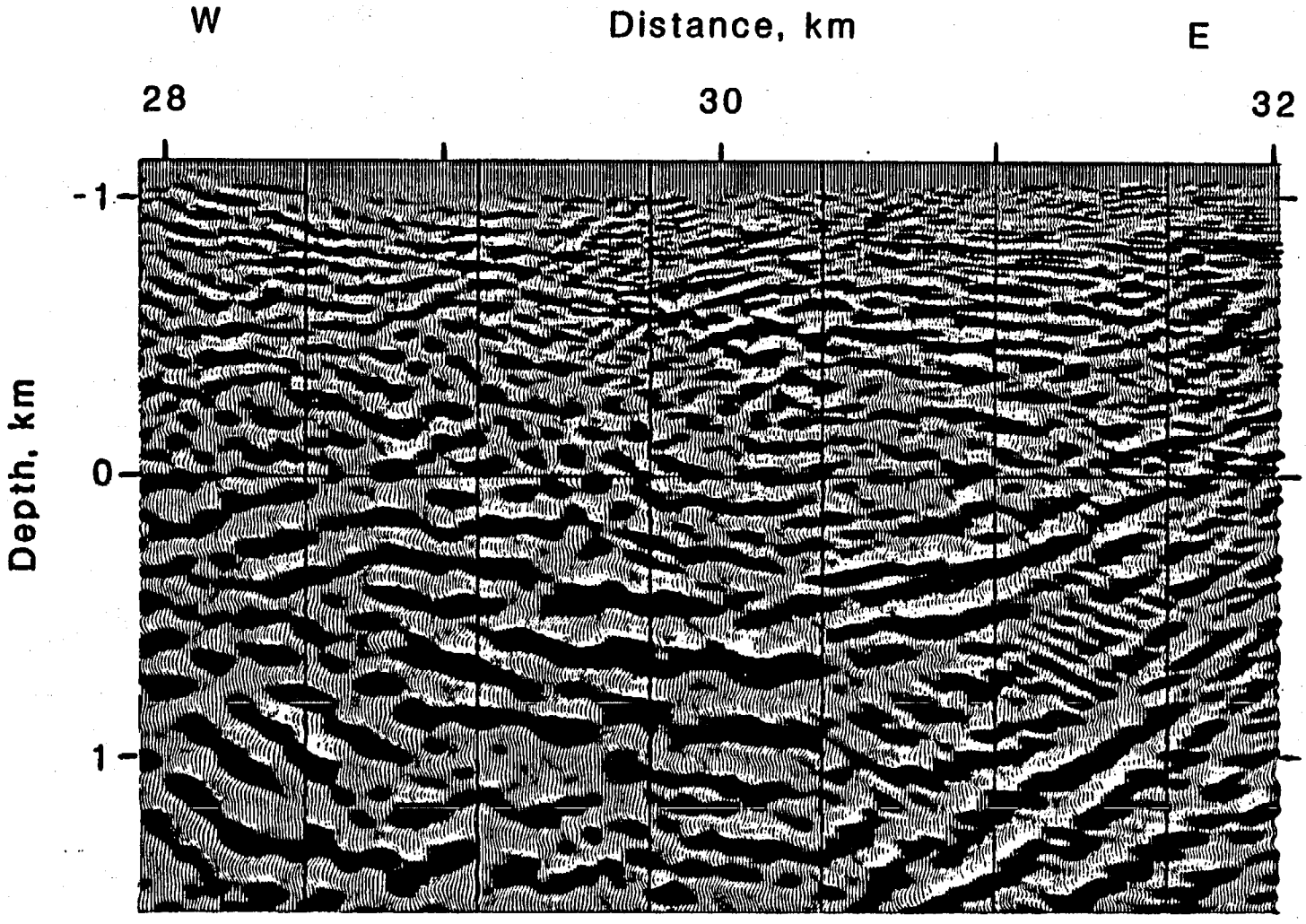
W
Distance, km
E
28
30
32
-1
0
1
Depth, km

Potential Field Models

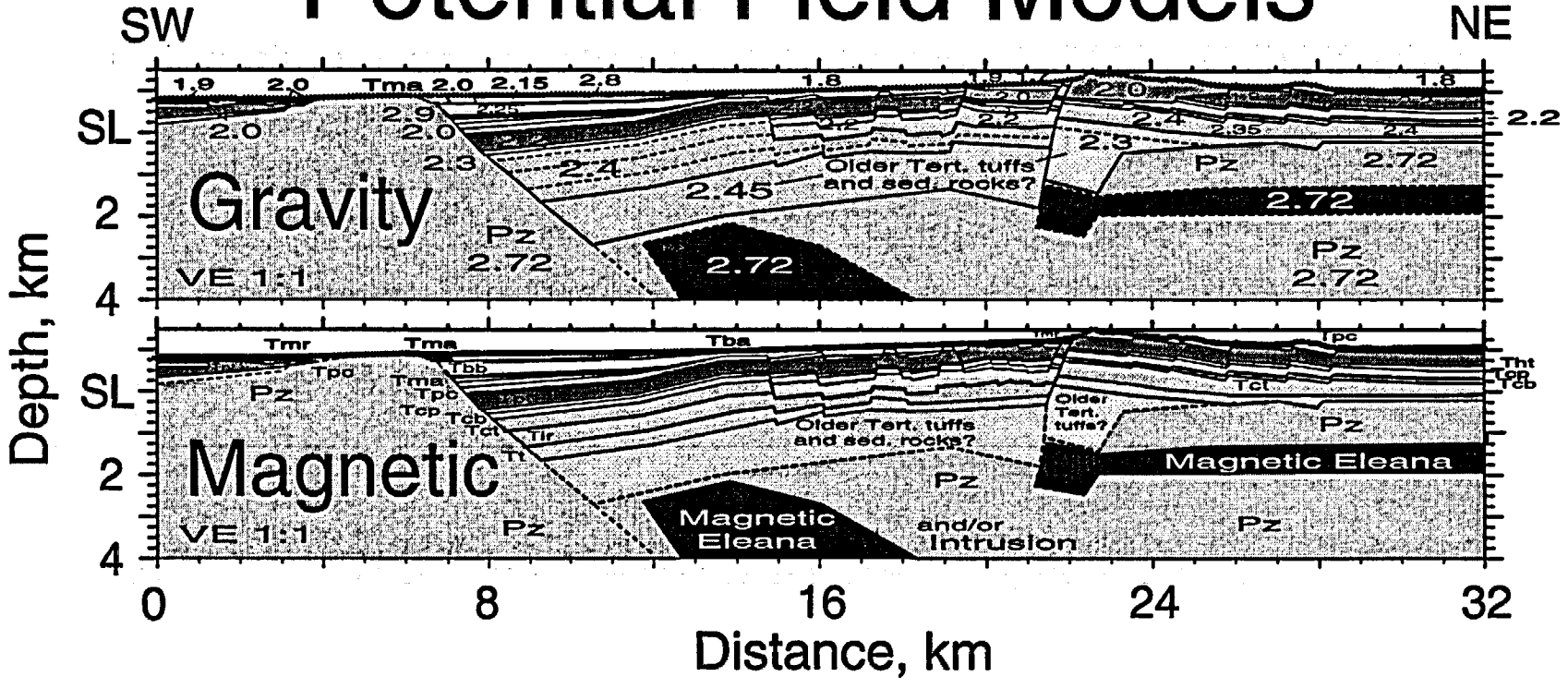

Modeling Philosophy

Fit of model to potential field data is a necessary requirement but is not sufficient to "prove" a structural model - but such modeling can rule out inconsistent structures

USGS/YMP

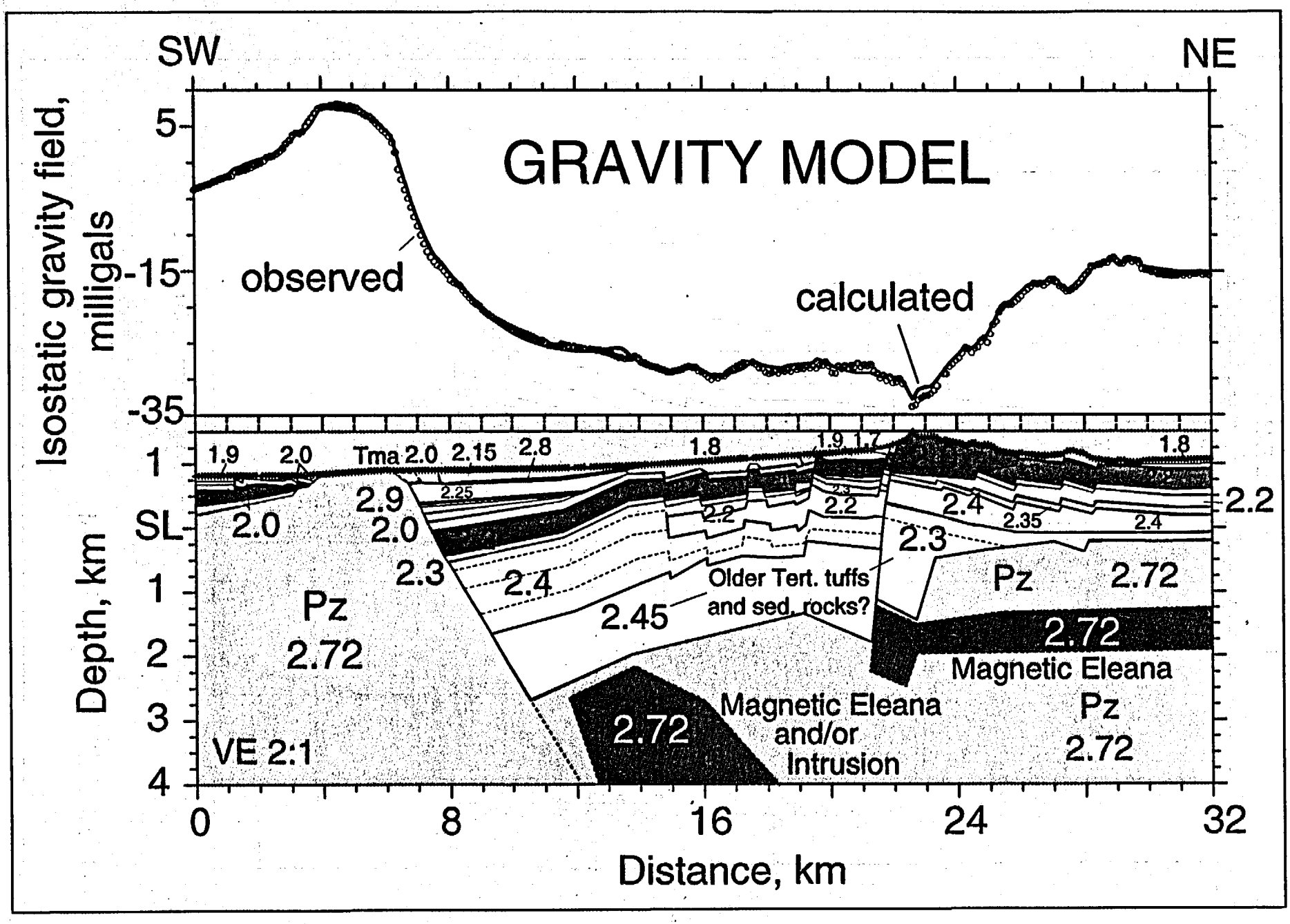
SW
NE
GRAVITY MODEL
Isostatic gravity field, milligals
5
-15
-35
observed
calculated
Depth, km
SL
1
2
3
4
0
8
16
24
32
Distance, km
VE 2:1
1.9
2.0
Tma
2.0
2.15
2.8
1.8
1.9
1.7
1.8
2.25
2.2
2.3
2.4
2.35
2.4
2.2
2.9
2.0
2.3
2.4
2.45
Older Tert. tuffs and sed. rocks?
Pz
2.72
Pz
2.72
2.72
Magnetic Eleana
2.72
Magnetic Eleana and/or Intrusion
Pz
2.72

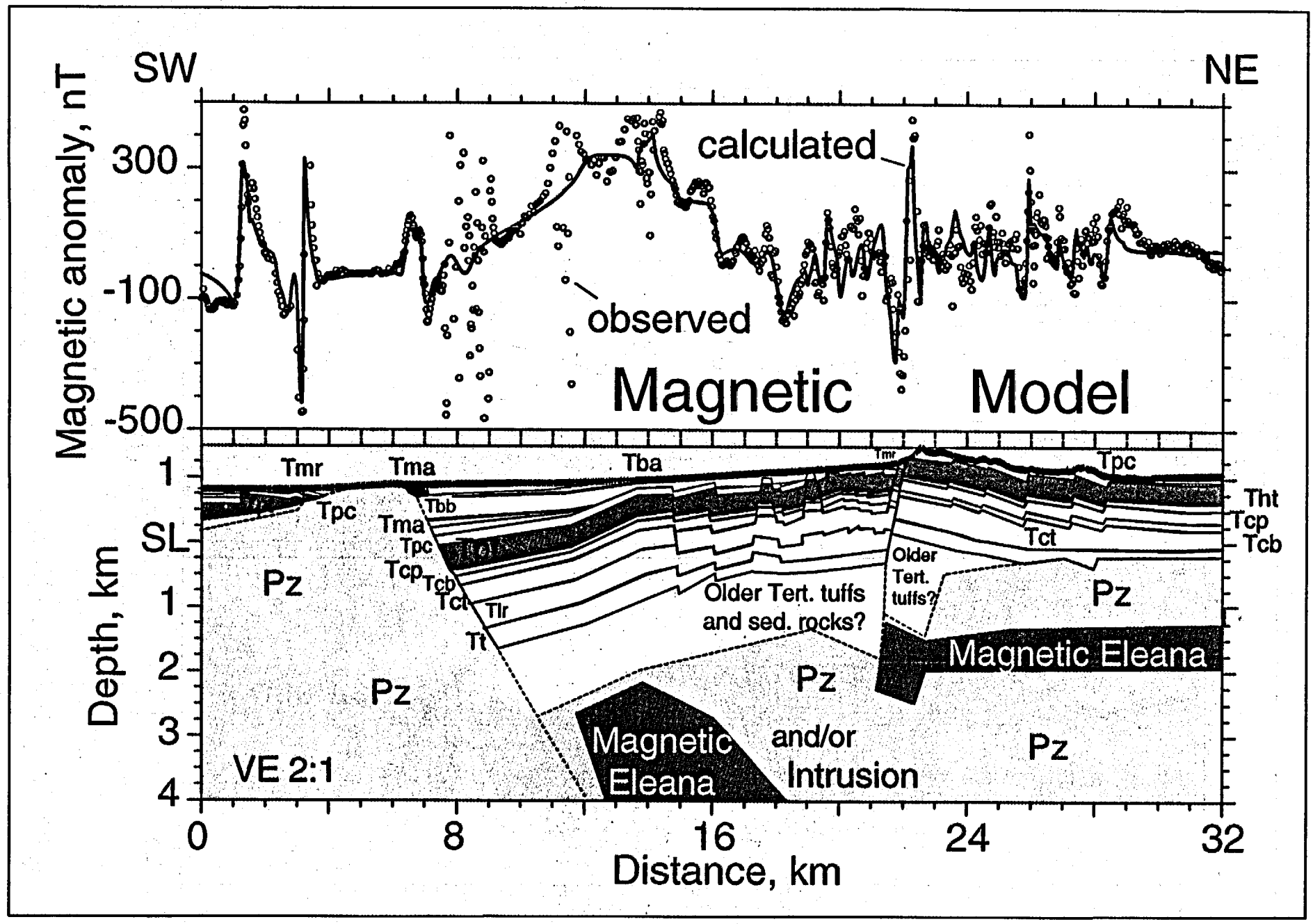
SW
NE
Magnetic anomaly, nT
300
-100
-500
calculated
observed
Magnetic Model
Tmr
Tma
Tba
Tmr
Tpc
Tht
Tcp
Tcb
Tbb
Tpc
Tma
Tpc
Tcp
Tcb
Tct
Tlr
Tt
Tct
Older Tert. tuffs and sed. rocks?
Older Tert. tuffs?
Pz
Pz
Pz
Pz
Magnetic Eleana
Magnetic Eleana
and/or Intrusion
VE 2:1
Depth, km
SL
1
1
2
3
4
0
8
16
24
32
Distance, km

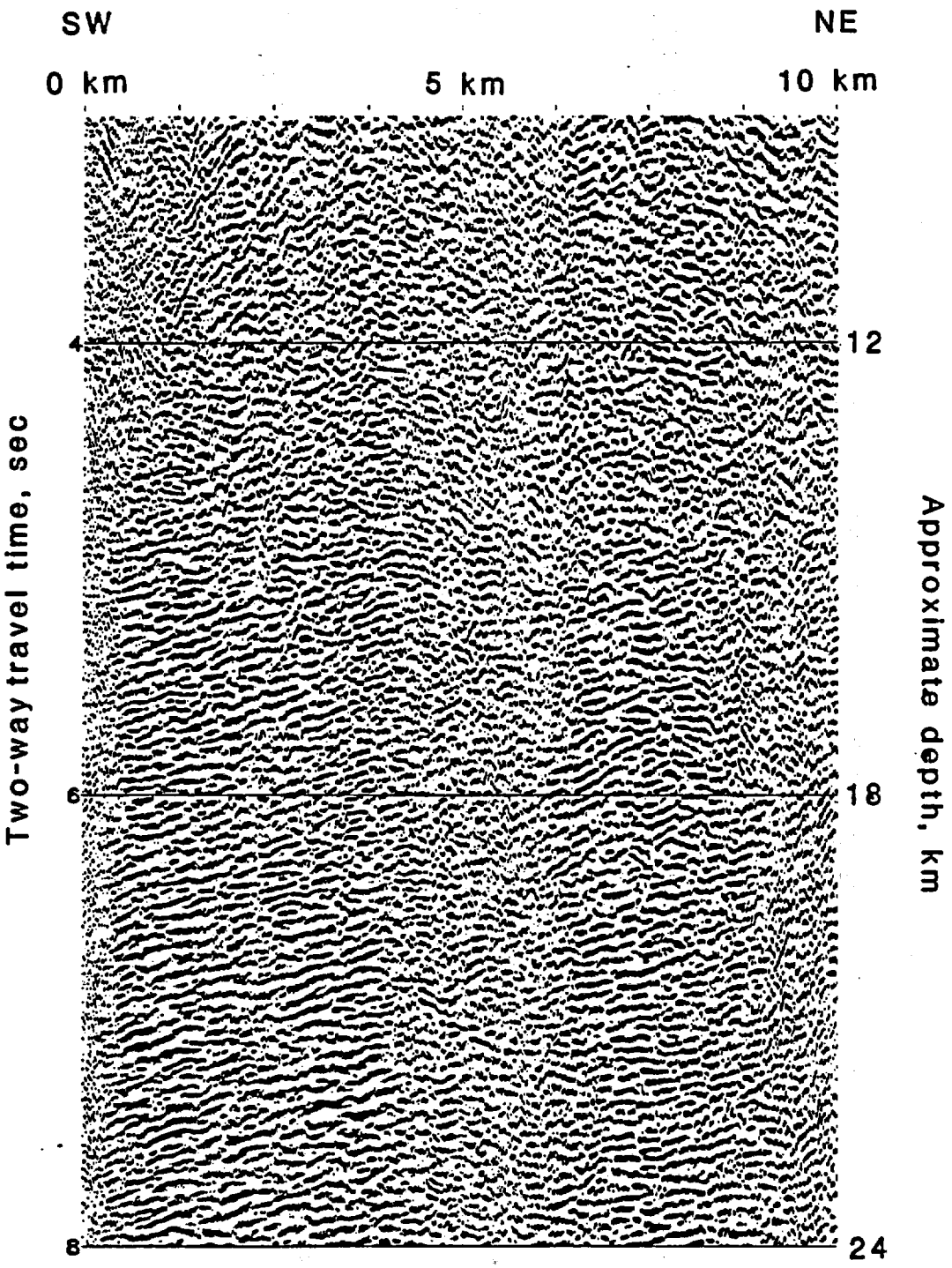
SW
NE
0 km
5 km
10 km
4
6
8
12
18
24
Two-way travel time, sec
Approximate depth, km

Fig. 5

OBSERVATIONS:

Bare Mountain fault is linear, moderate-angle fault to 6 or 7 km depth

Top of reflective lower crust nearly matches base of seismogenic crust (12 to 15 km)

Little Skull Mtn. earthquake ruptured at 10 km depth along 56° dipping fault plane

PRESENT DAY TECTONIC MODEL

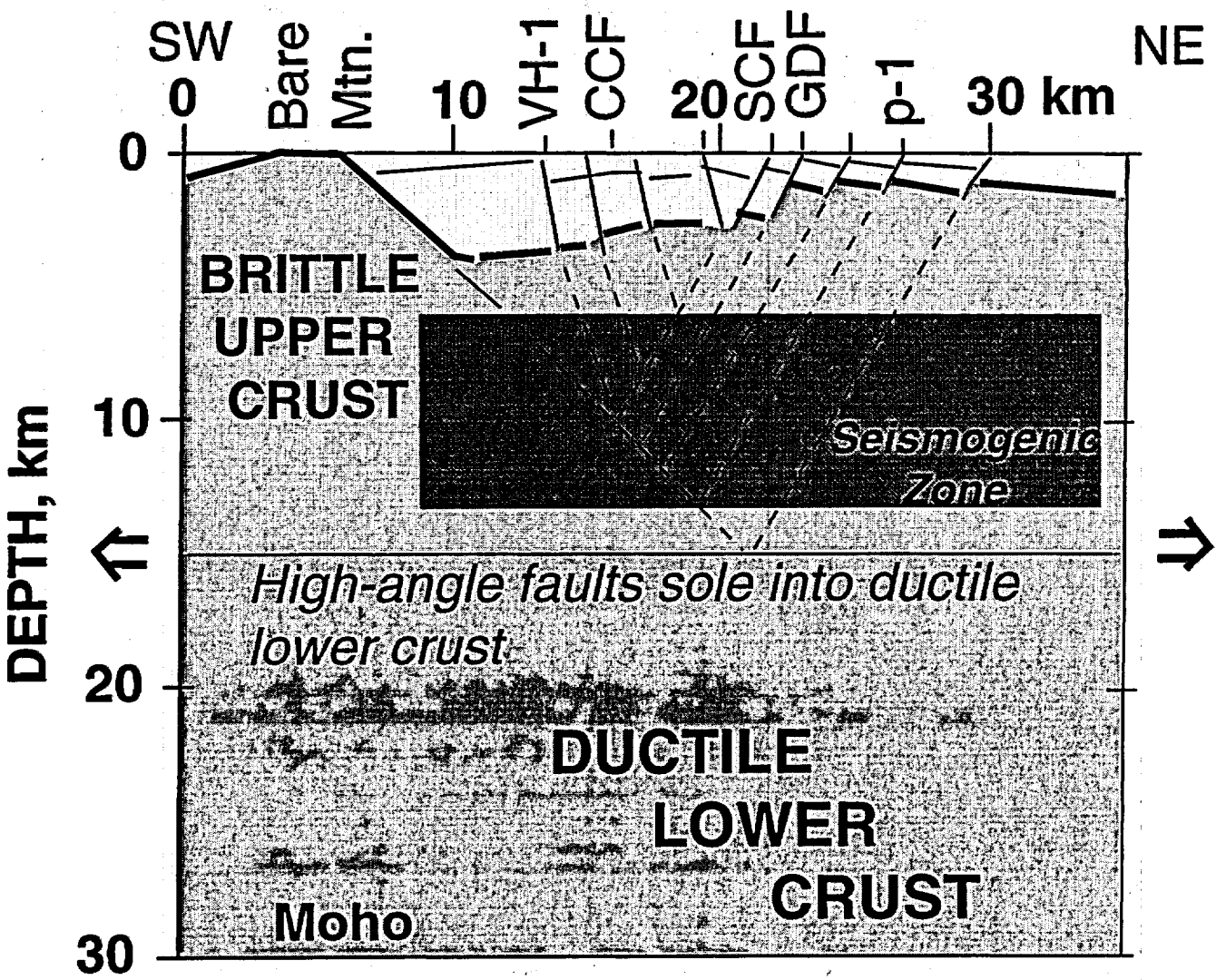

Hazard Implications

High- to moderate-angle faults dip beneath potential repository within 12 km

Schematic interpretation predicts relatively short spans within seismogenic crust under Crater flat

Faults dipping away from Yucca Mountain may direct energy towards YM during rupture

USGS/YMP

Model Uncertainties

Migration velocities (5° dip uncertainty)

Depth-conversion velocities

Mis-identification of reflections

Only 1-2 reflections within volcanic tuffs to constrain fault dips

USGS/YMP

Southern Great Basin Seismicity in the Vicinity of Yucca Mountain

October 18, 1996

Ken Smith

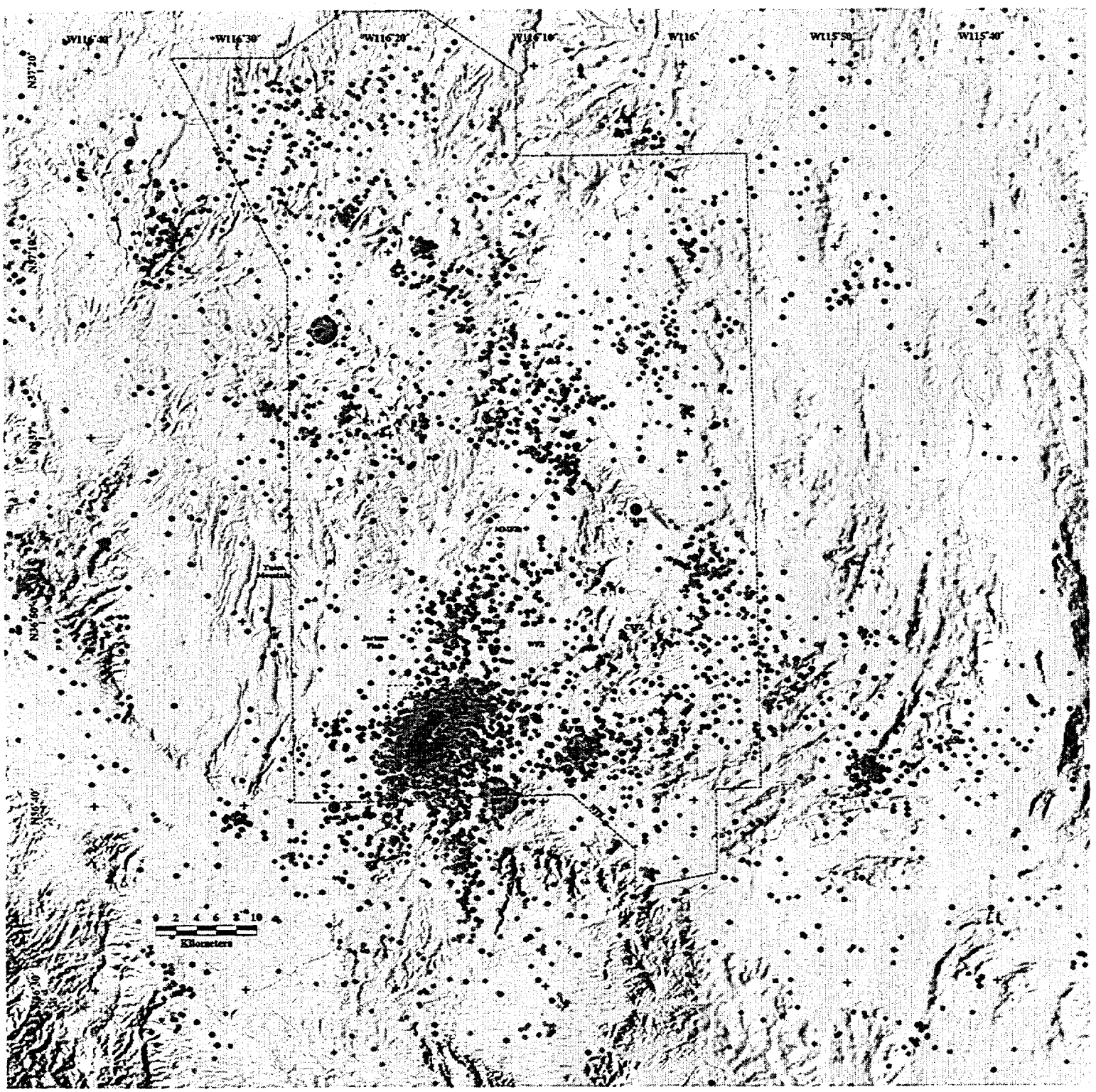
W116°40'
W116°30'
W116°20'
W116°10'
W116°
W115°50'
W115°40'
N37°20'
N37°10'
N37°
N36°50'
N36°40'
2 4 6 8 10
Kilometers

Earthquake Location Quality

Relation of Velocity Model to Real Earth
Station Distribution Relative to Earthquake Source
- **Near Source Stations**
  - **Stations within 1 focal depth**
  - **S-wave arrivals at stations within 1 focal depth**
- **Location Gap**

Quality of First Arrivals

- **P-waves**
- **S-waves**

Assessing Location Quality from Earthquake Catalogs

- **rms residual**
- **error H and Z**
- **near station**
- **Gap**
- **Number of phase readings**
- **Other quality measures**

First 21 stations of the SGBDSN

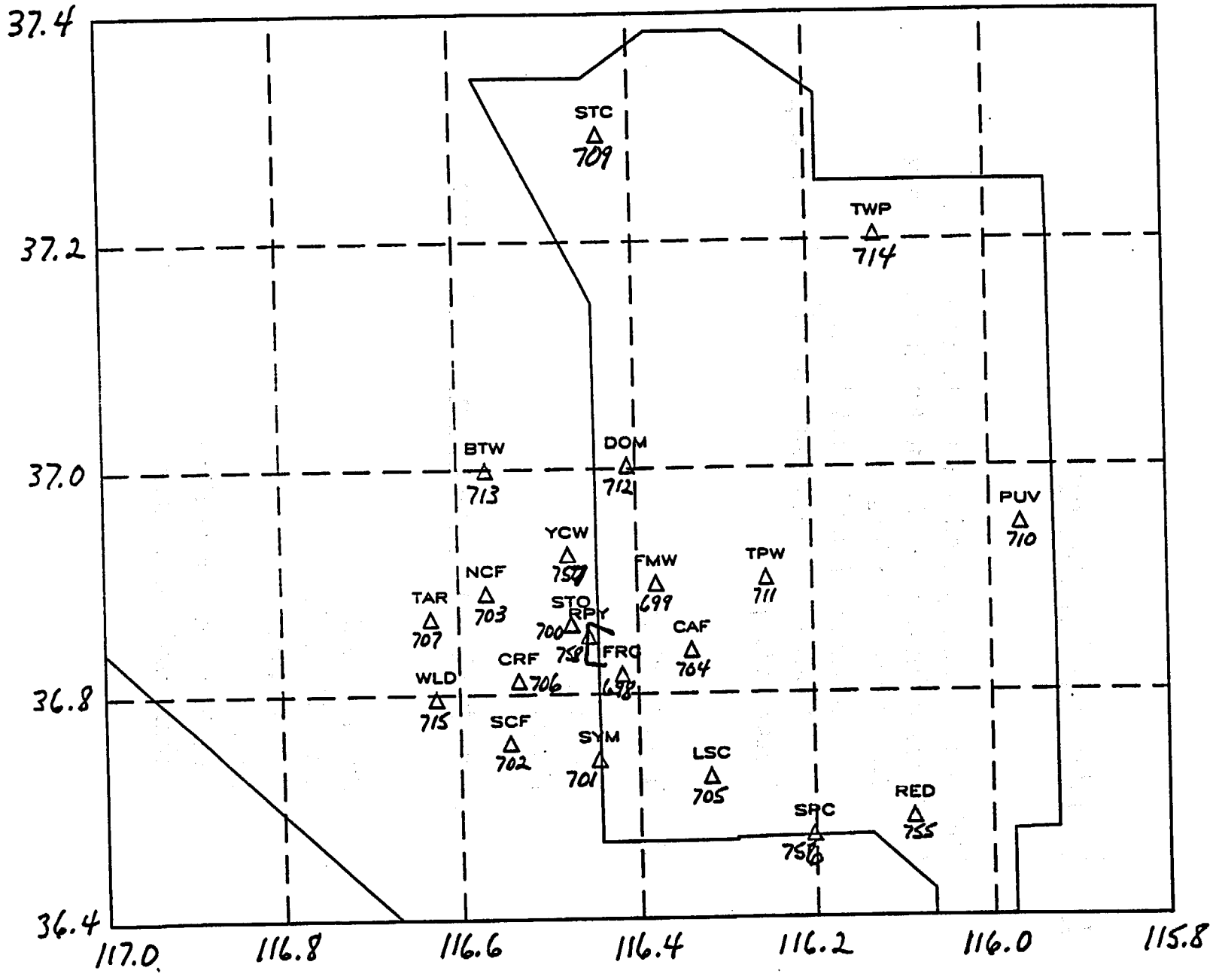

SGB Analog Stations

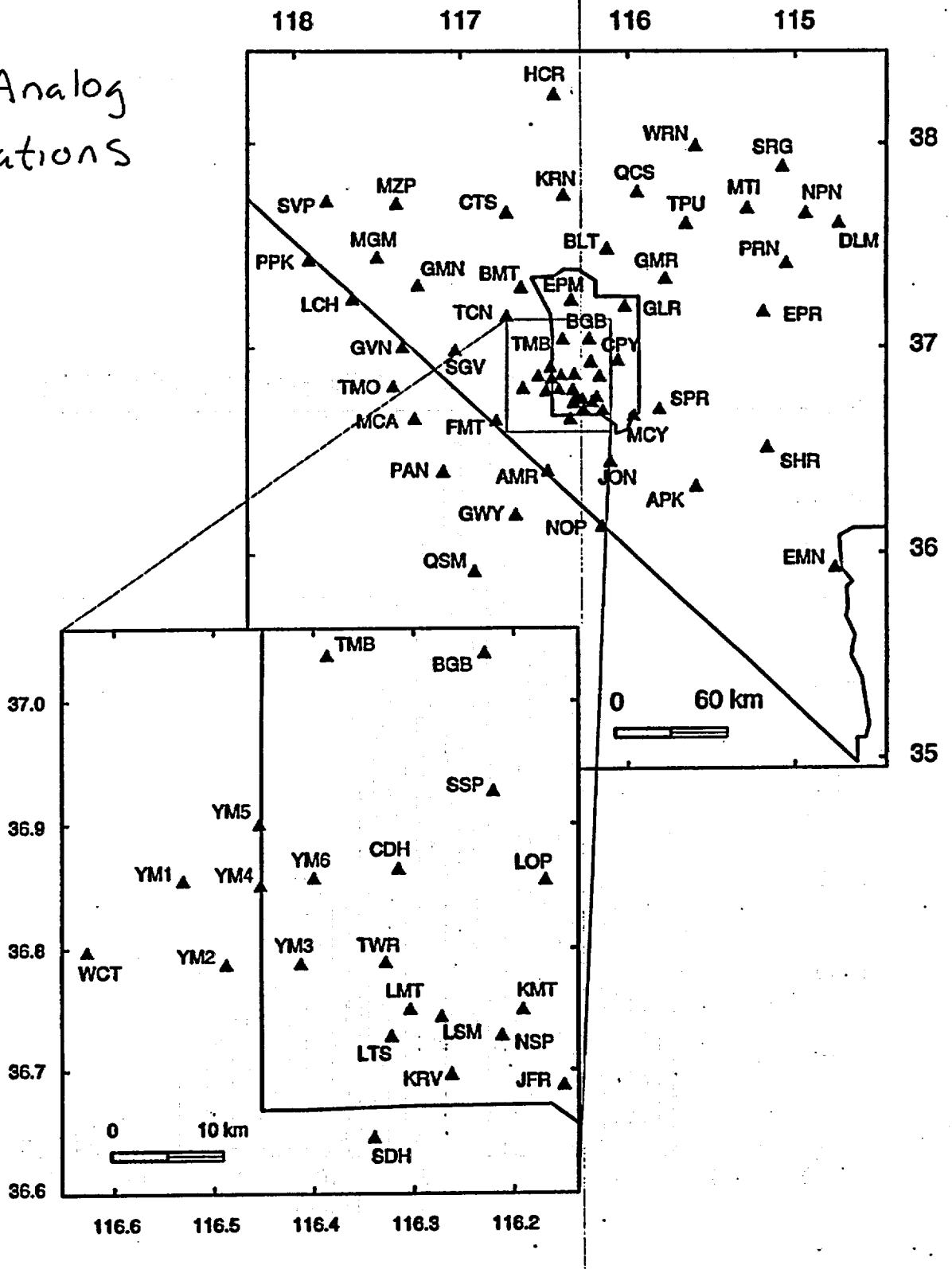

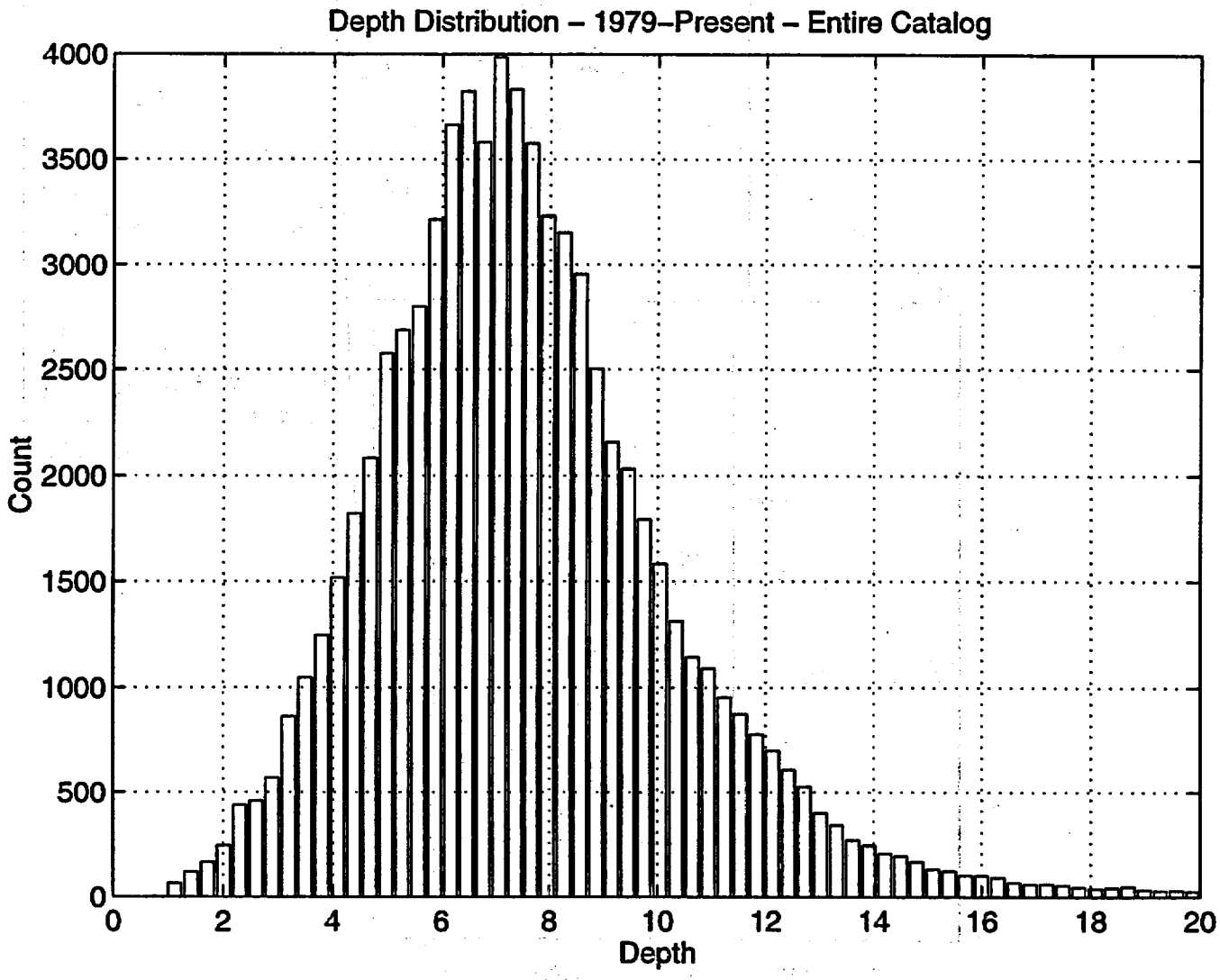
Depth Distribution – 1979–Present – Entire Catalog
Count
Depth
0
500
1000
1500
2000
2500
3000
3500
4000
0
2
4
6
8
10
12
14
16
18
20

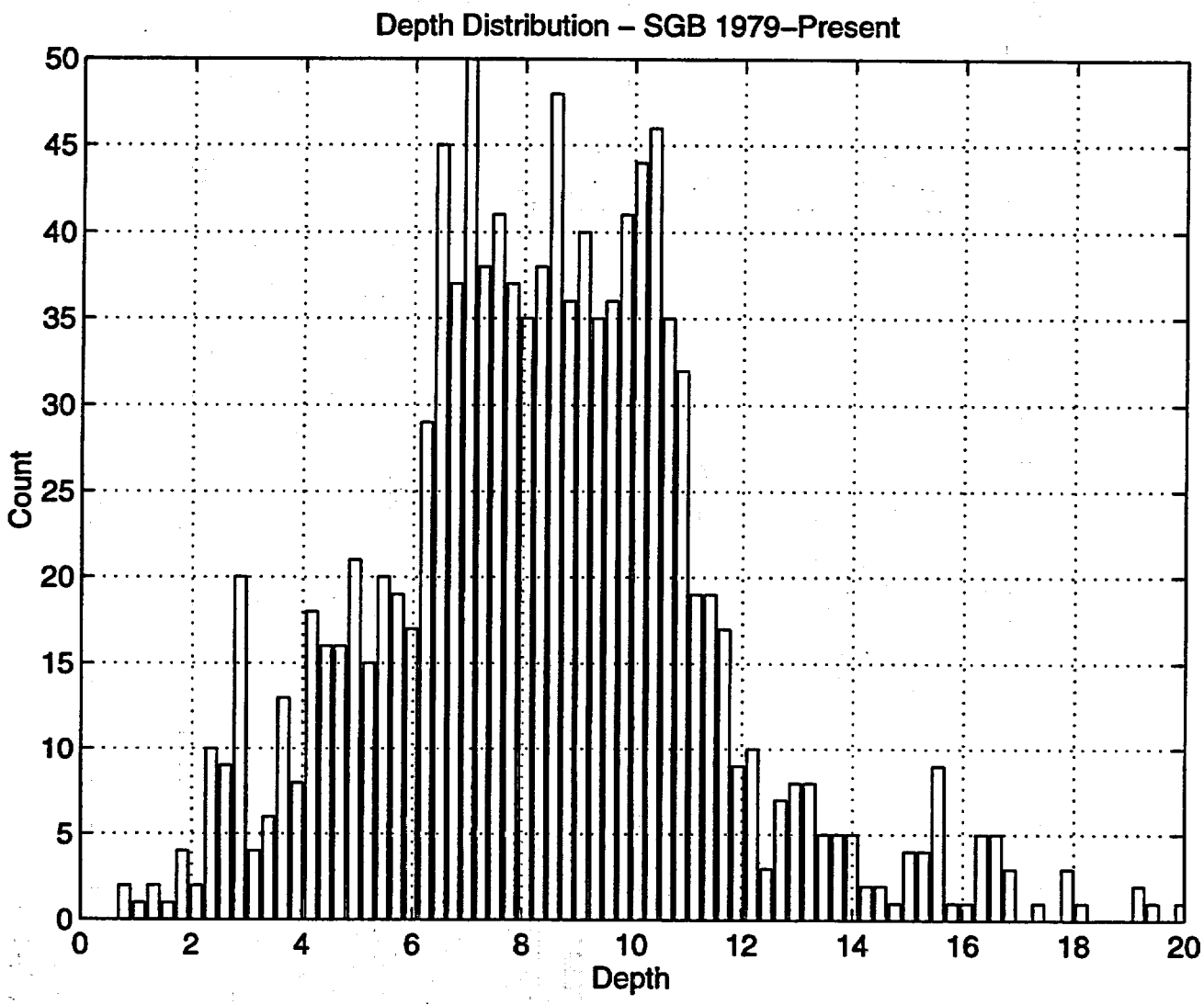
Depth Distribution – SGB 1979–Present
Count
Depth
0
5
10
15
20
25
30
35
40
45
50
0
2
4
6
8
10
12
14
16
18
20

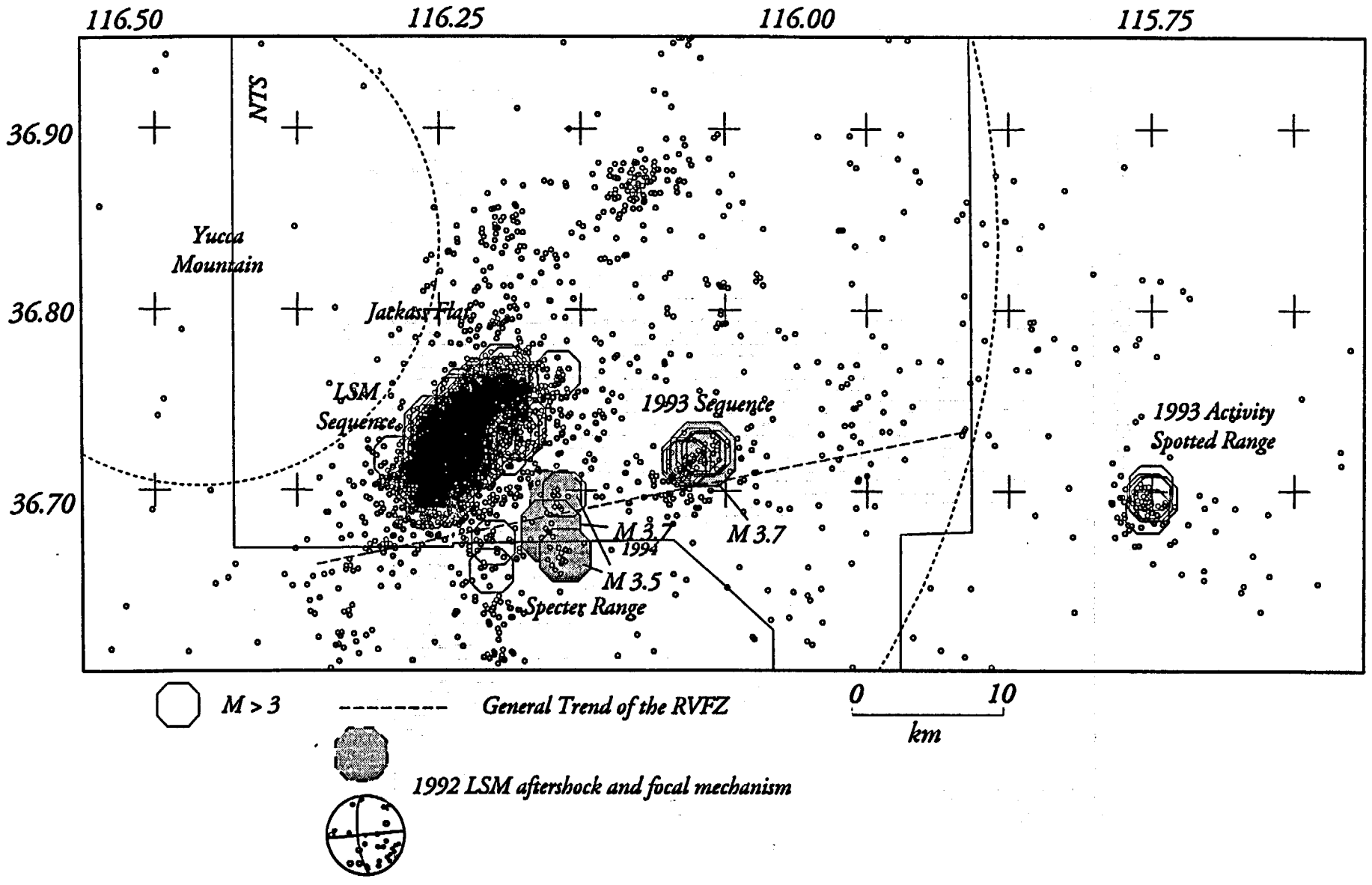
116.50
116.25
116.00
115.75
36.90
36.80
36.70
NTS
Yucca Mountain
Jackass Flats
LSM Sequence
1993 Sequence
1993 Activity Spotted Range
M 3.7
1994
M 3.7
M 3.5
Specter Range
M > 3
General Trend of the RVFZ
0
10
km
1992 LSM aftershock and focal mechanism

1992 Little Skull Mountain

Earthquake Sequence

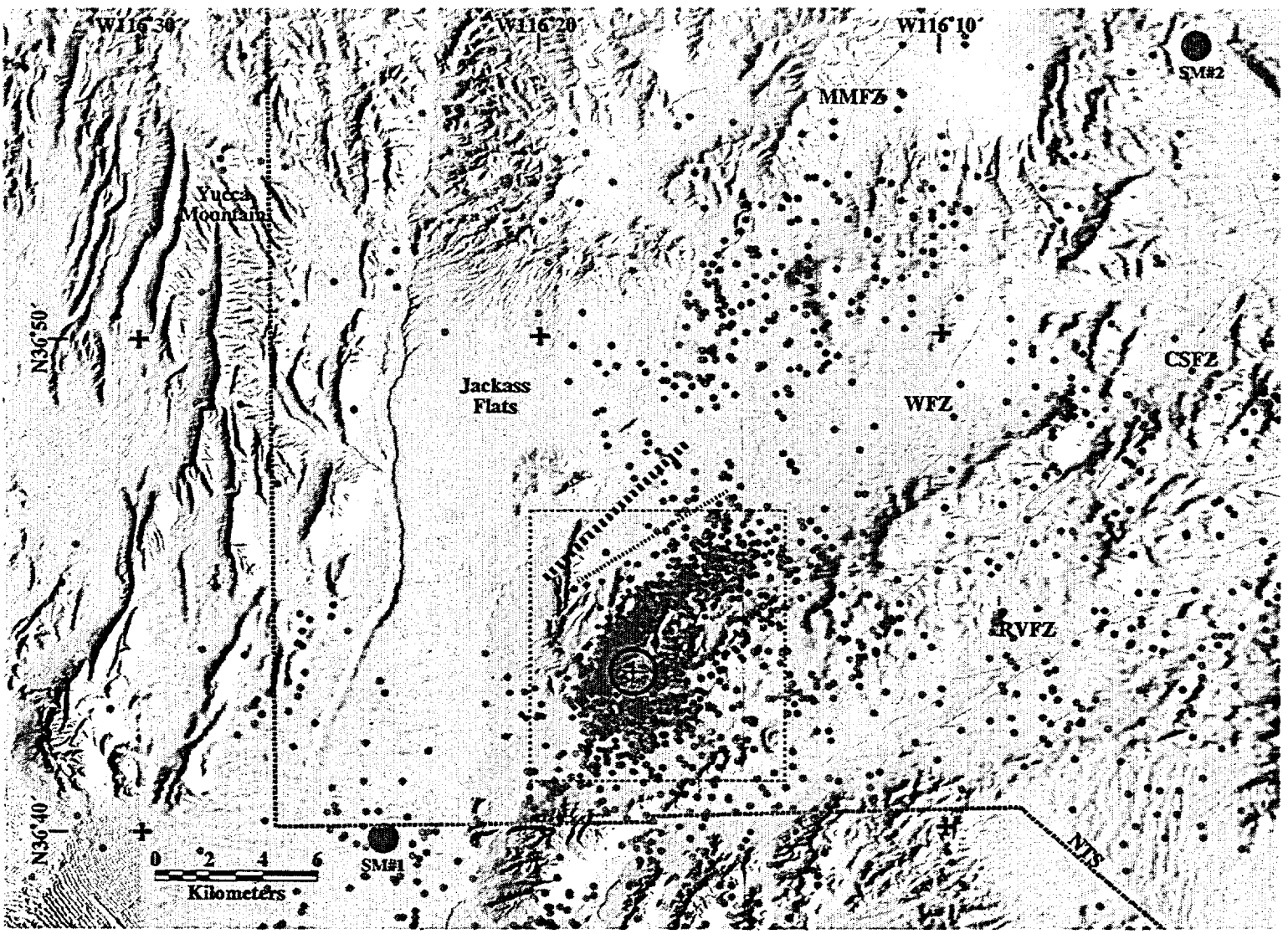
W116°30'
W116°20'
W116°10'
SM#2
MMFZ
Yucca
Mountain
N36°50'
Jackass
Flats
WFZ
CSFZ
RVFZ
N36°40'
0 2 4 6
Kilometers
SM#1
NTS

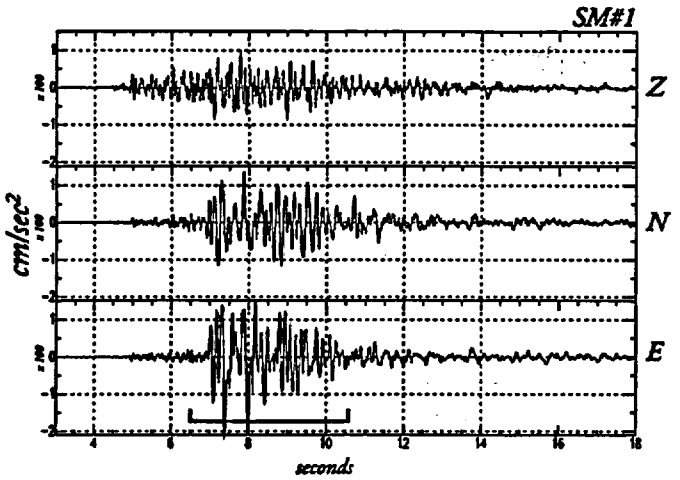

Lathrop Wells

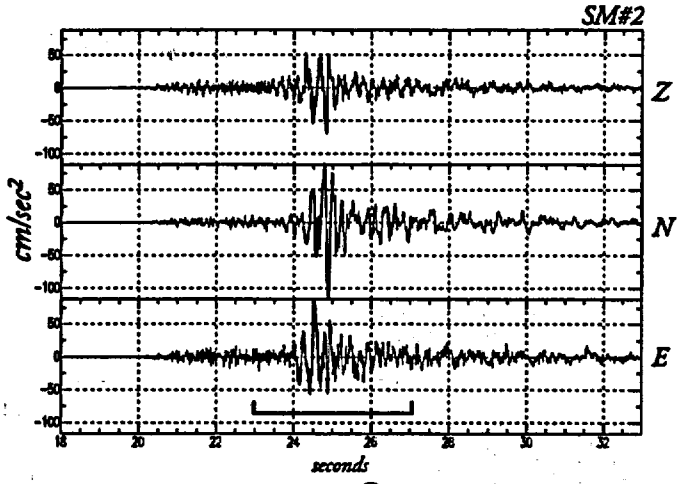

CP

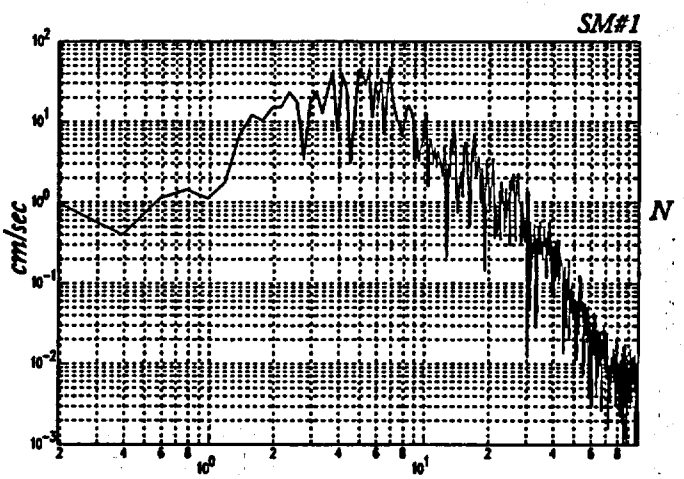

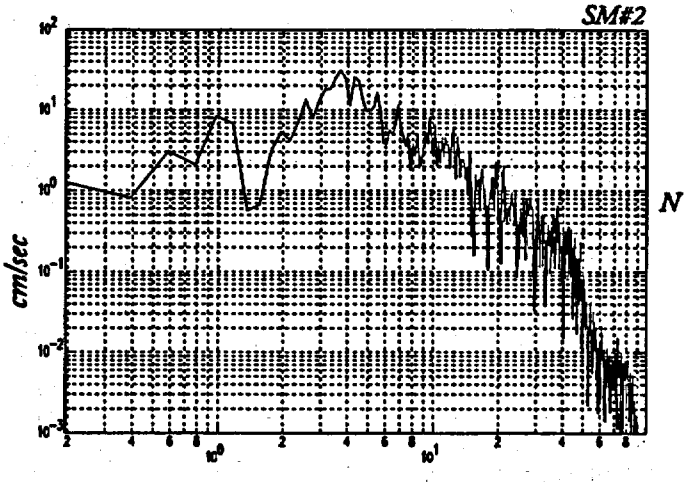

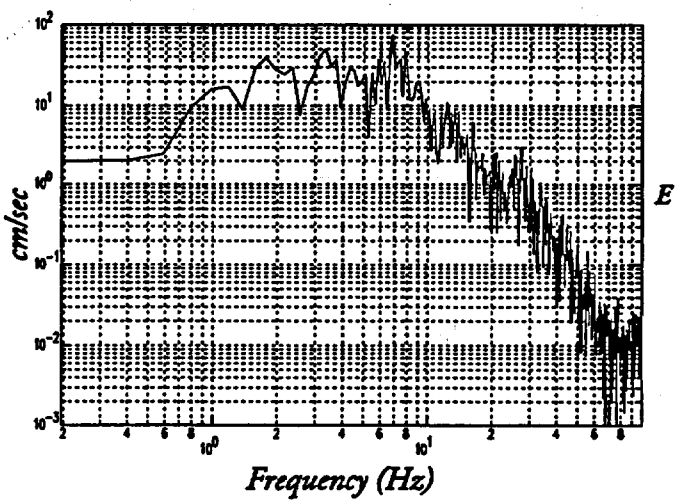

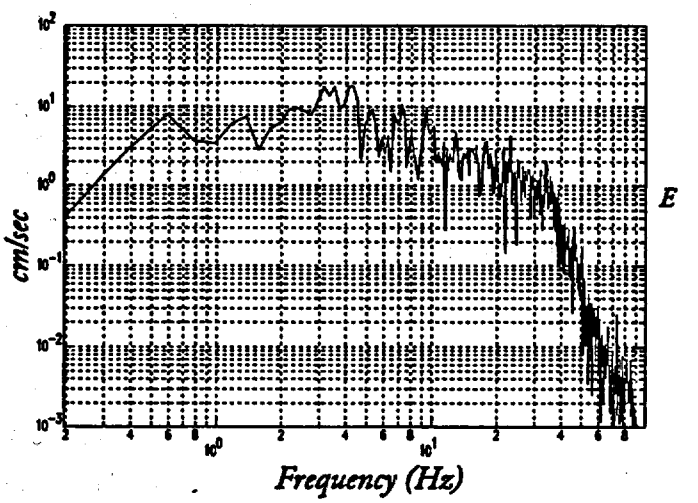

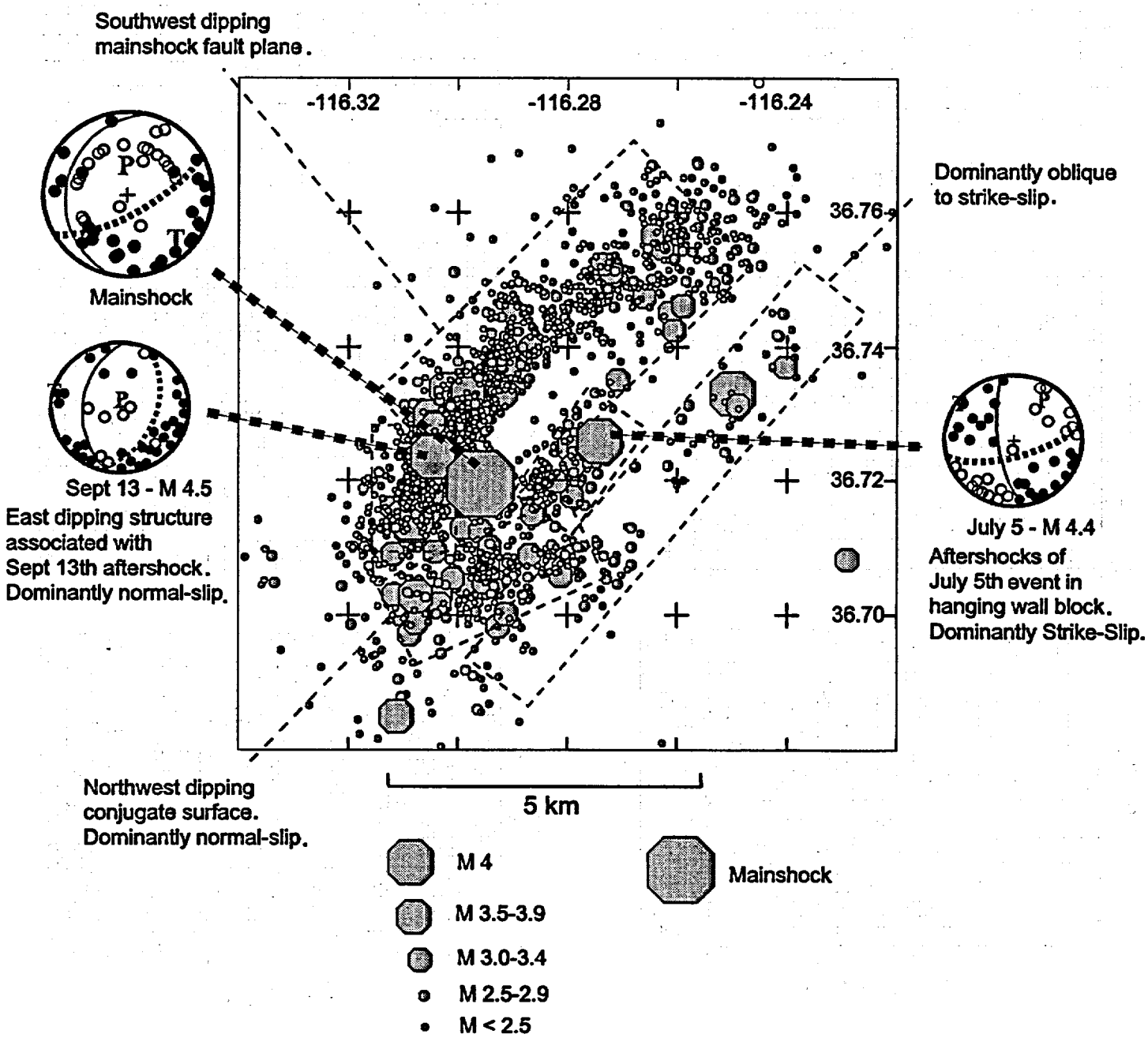
Southwest dipping
mainshock fault plane.
-116.32
-116.28
-116.24
36.76
36.74
36.72
36.70
P
T
Mainshock
Dominantly oblique
to strike-slip.
P
Sept 13 - M 4.5
East dipping structure
associated with
Sept 13th aftershock.
Dominantly normal-slip.
July 5 - M 4.4
Aftershocks of
July 5th event in
hanging wall block.
Dominantly Strike-Slip.
Northwest dipping
conjugate surface.
Dominantly normal-slip.
5 km
M 4
Mainshock
M 3.5-3.9
M 3.0-3.4
M 2.5-2.9
M < 2.5

First 38 Hours of the Sequence
1014 UTC 29 June - 30 June

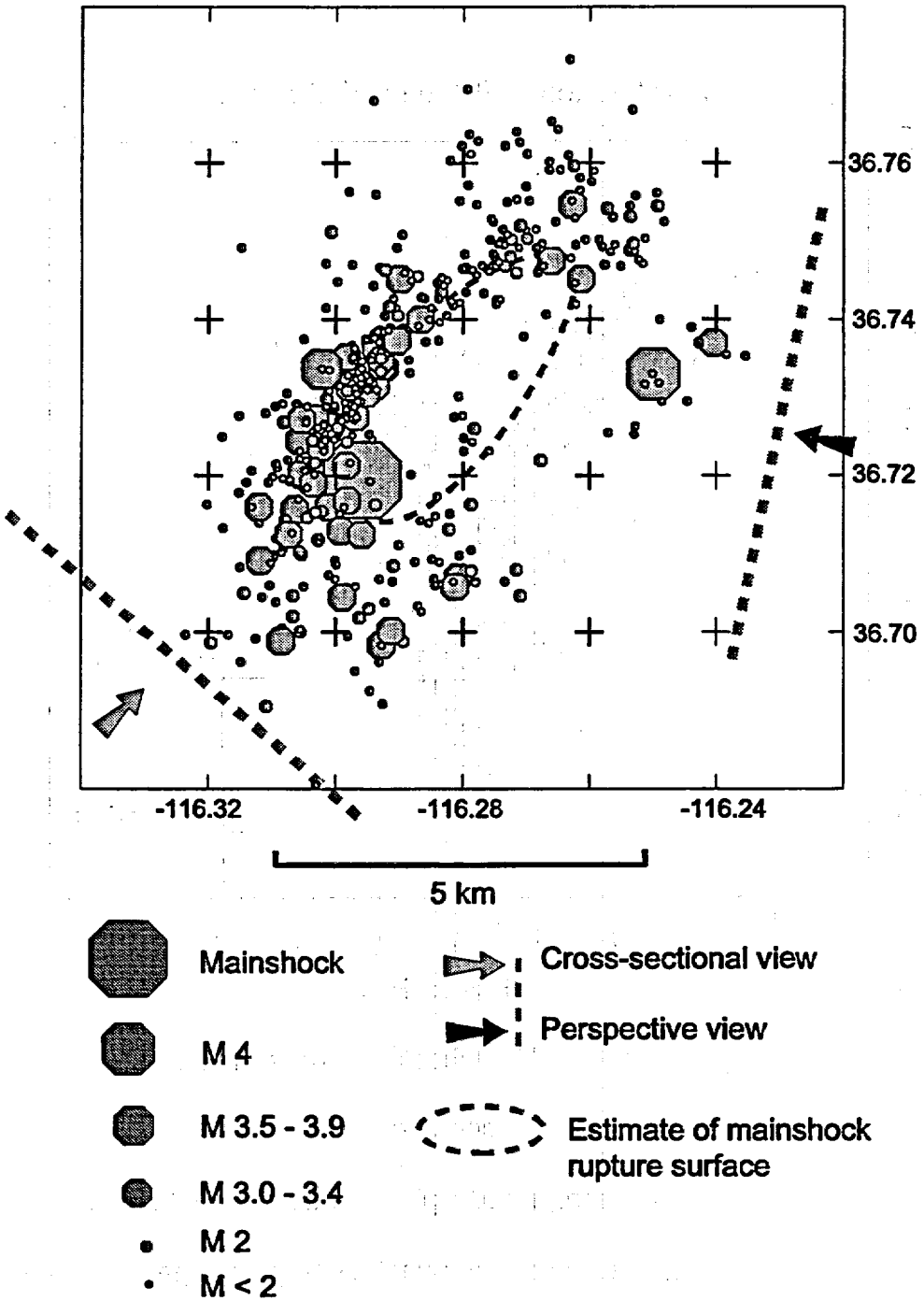

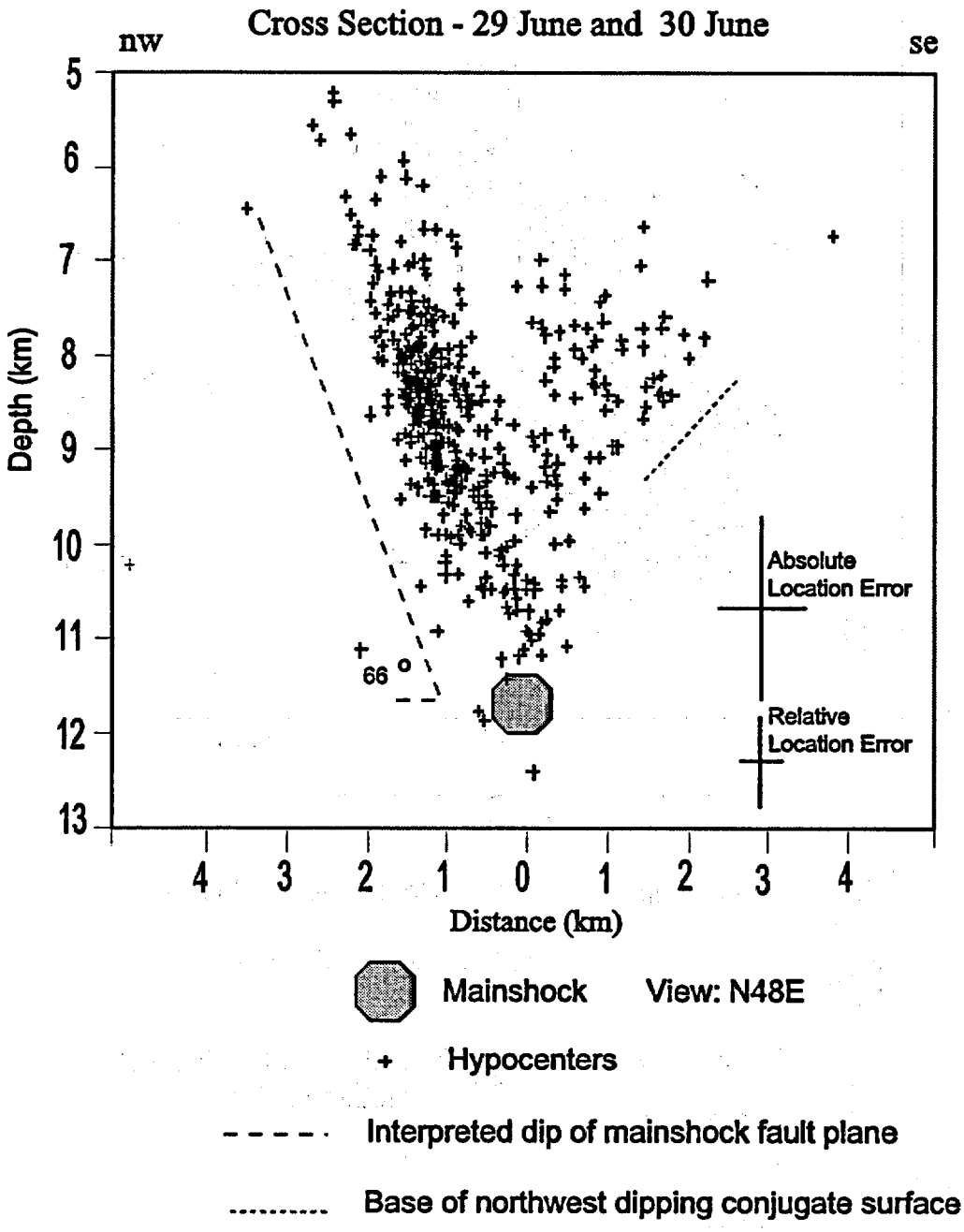
Cross Section - 29 June and 30 June
nw
se
5
6
7
8
9
10
11
12
13
Depth (km)
66
Absolute
Location Error
Relative
Location Error
4
3
2
1
0
1
2
3
4
Distance (km)
Mainshock
View: N48E
Hypocenters
Interpreted dip of mainshock fault plane
Base of northwest dipping conjugate surface

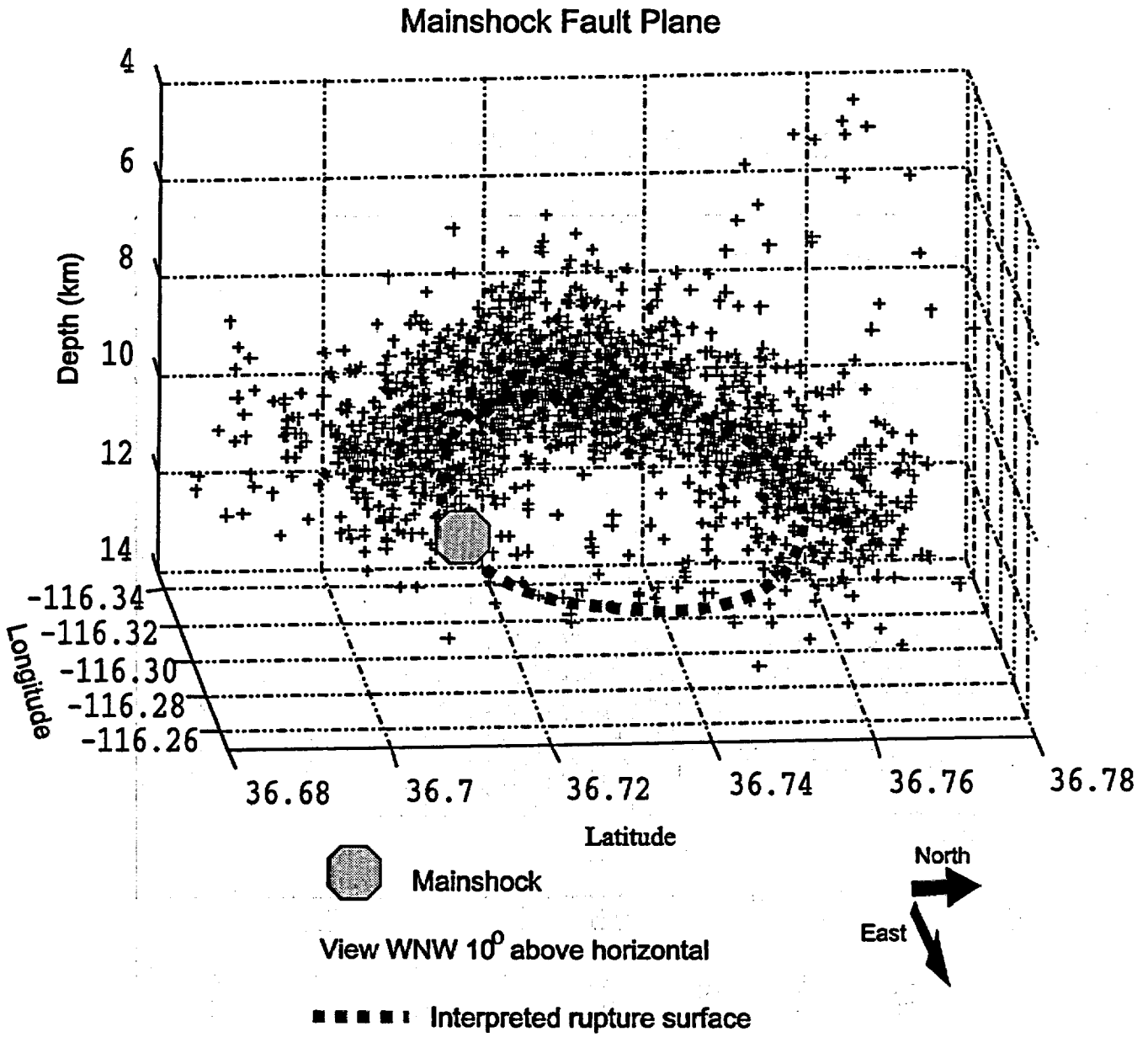
Mainshock Fault Plane
Depth (km)
4
6
8
10
12
14
Longitude
-116.34
-116.32
-116.30
-116.28
-116.26
36.68
36.7
36.72
36.74
36.76
36.78
Latitude
Mainshock
North
East
View WNW 10° above horizontal
Interpreted rupture surface

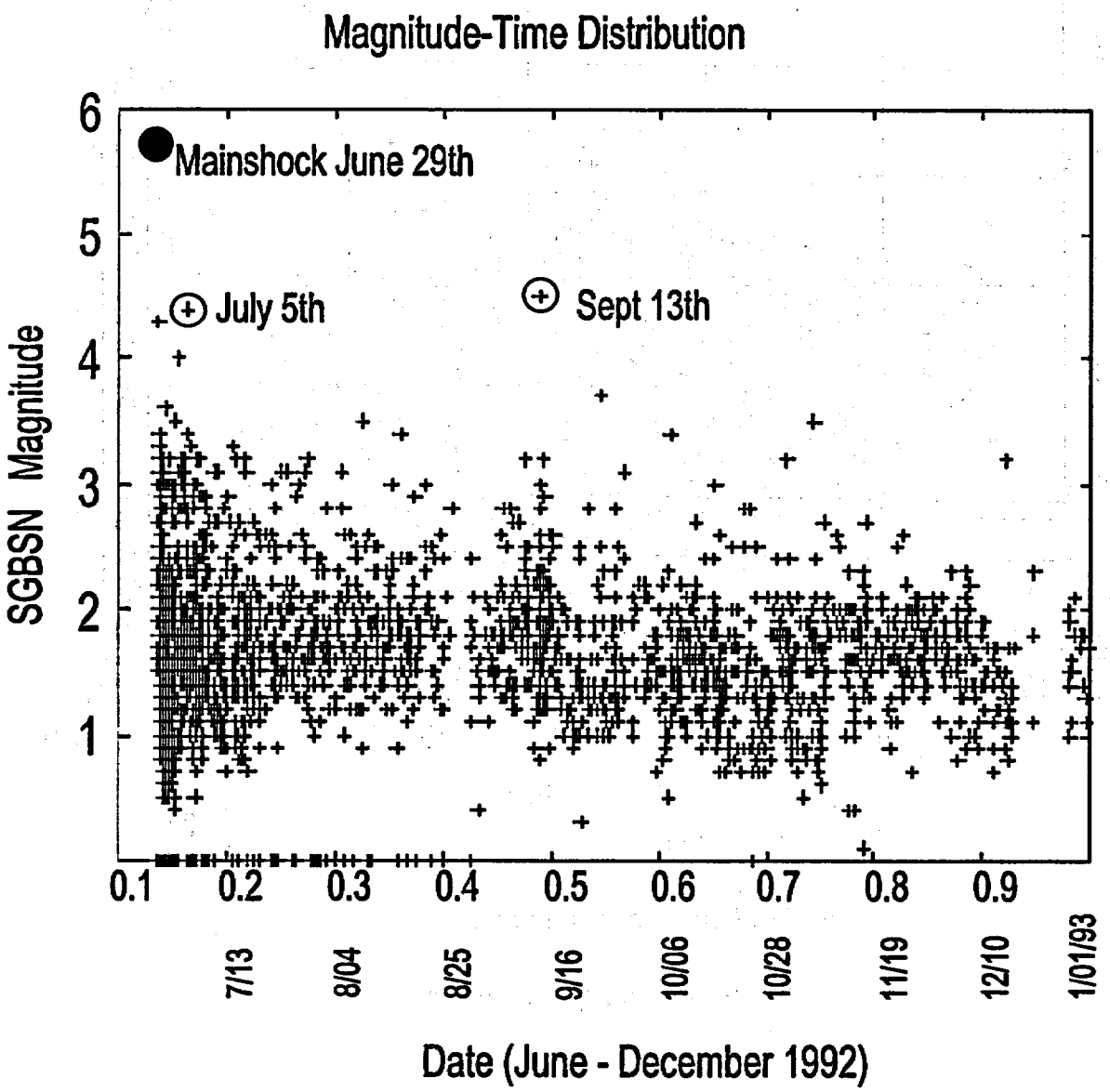
Magnitude-Time Distribution
Mainshock June 29th
July 5th
Sept 13th
SGBSN Magnitude
6
5
4
3
2
1
0.1
0.2
0.3
0.4
0.5
0.6
0.7
0.8
0.9
7/13
8/04
8/25
9/16
10/06
10/28
11/19
12/10
1/01/93
Date (June - December 1992)

Normal Focal Mechanisms

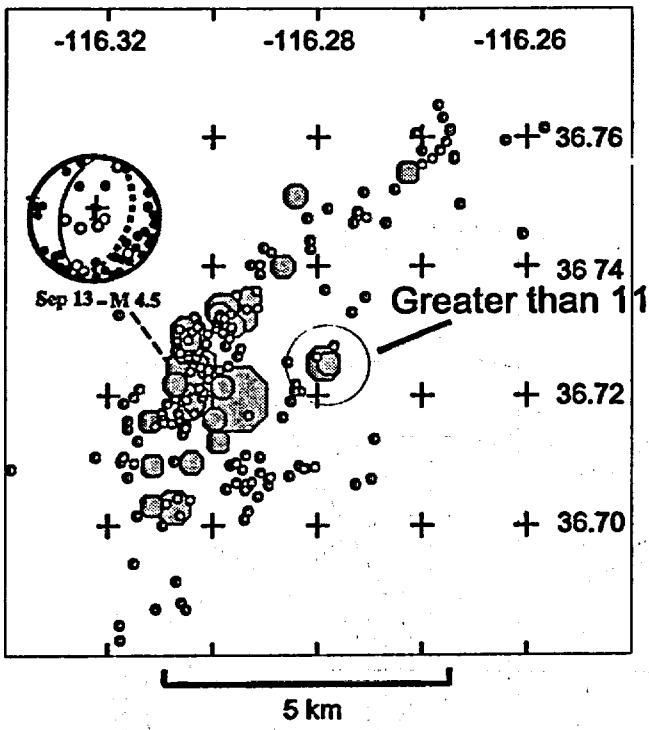

Strike Slip Focal Mechanisms

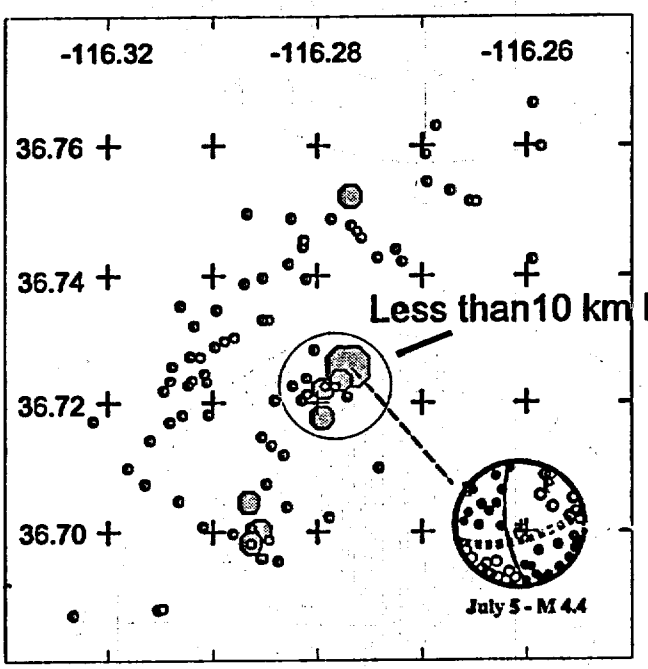

M 4
M 3.5 - 3.9
M 3.0 - 3.4
M < 3
Mainshock

Composite P and T Axes

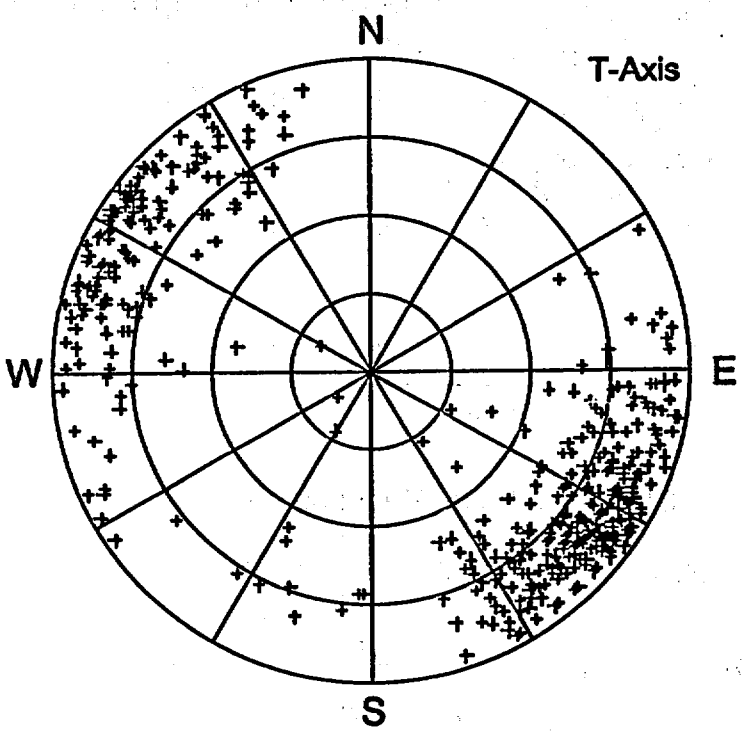

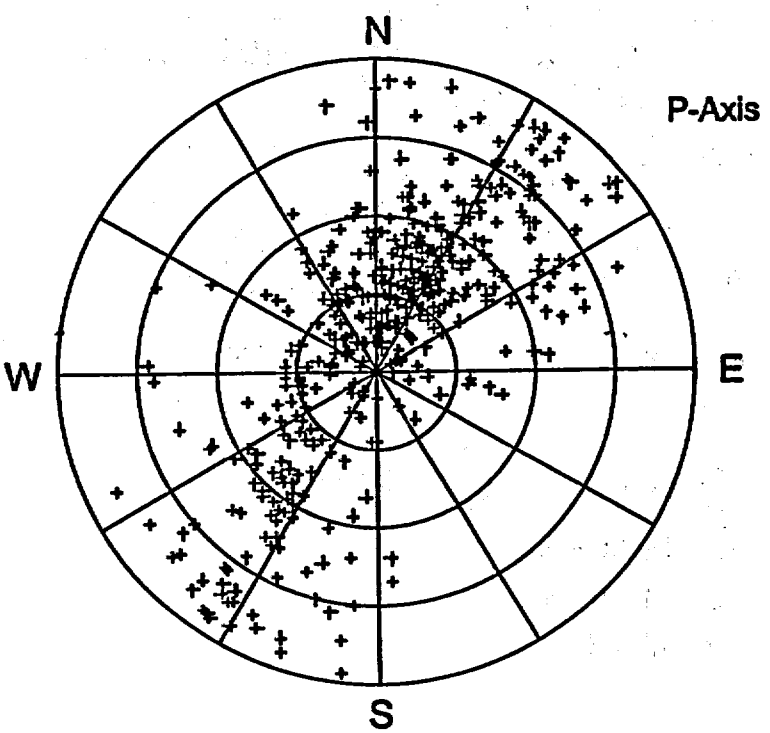

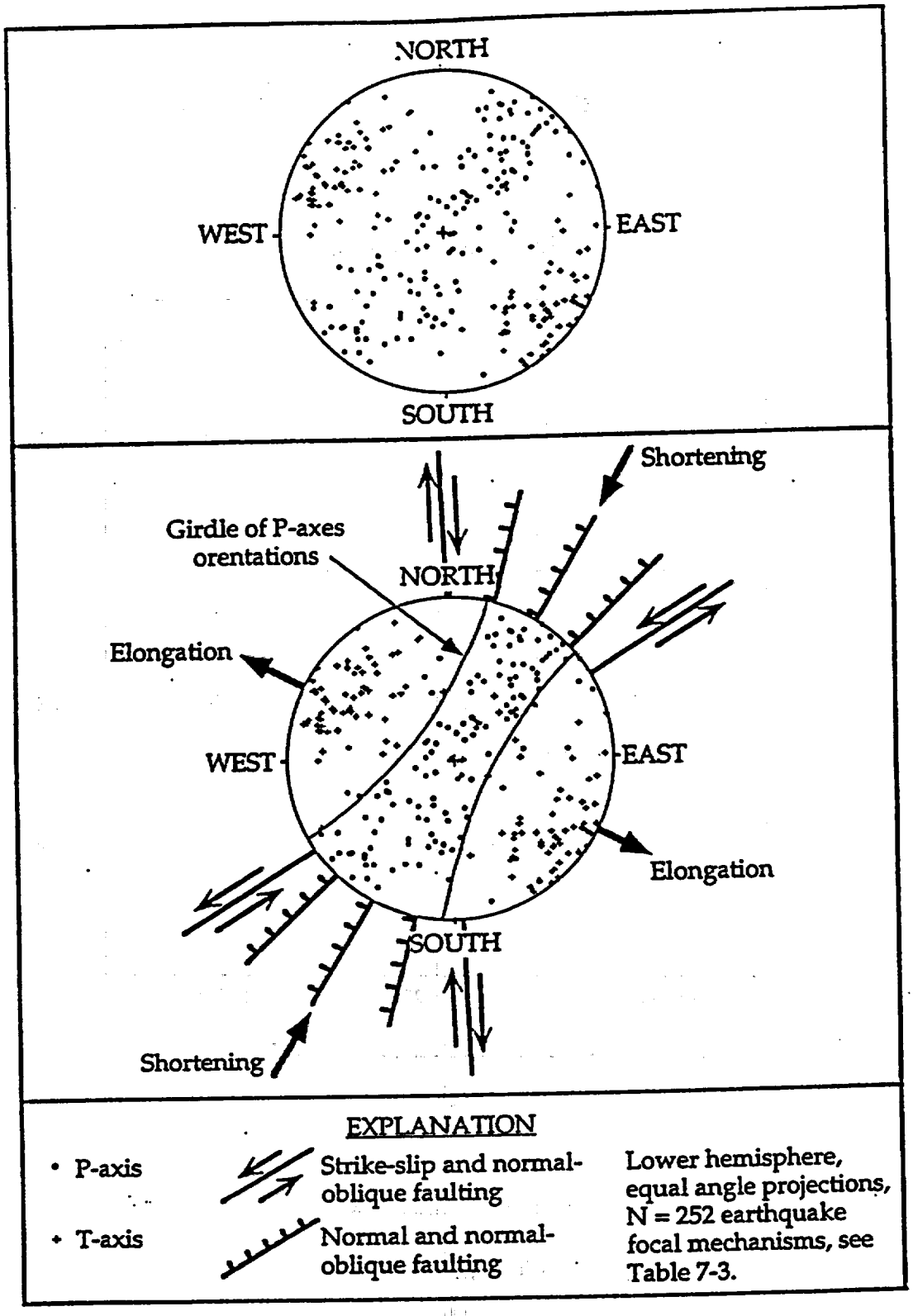

Figure 7-5. Lower-hemisphere equal-angle projection of the principal stress axes from focal mechanisms of earthquakes in the southern Great Basin. Upper plot shows the data, and the lower plot shows the inferred orientations of faulting consistent with the stress orientations. Maximum relative compression (P-) axes (• symbol) form a girdle from vertical to northeast-southwest orientations, whereas extensional (minimum relative compression) (T-) axes (+ symbol) trend northwest-southeast. Focal mechanism data are listed in table 7-1.

Foreshock Activity

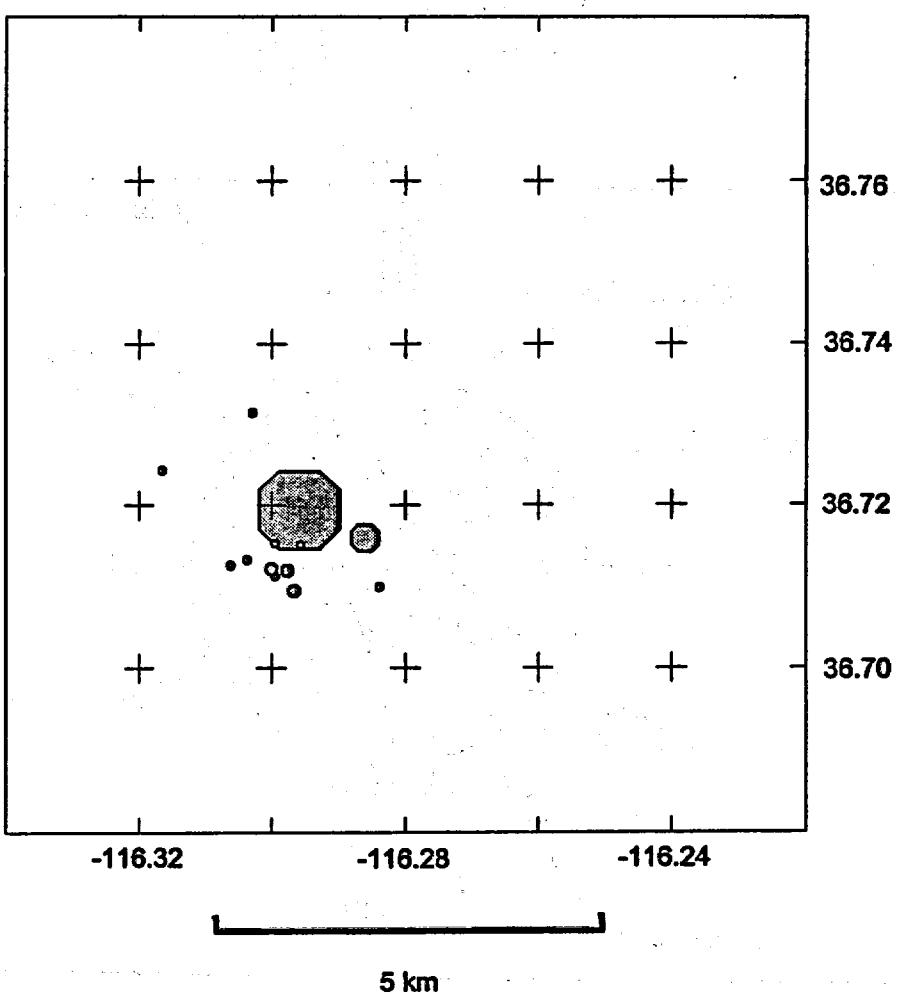

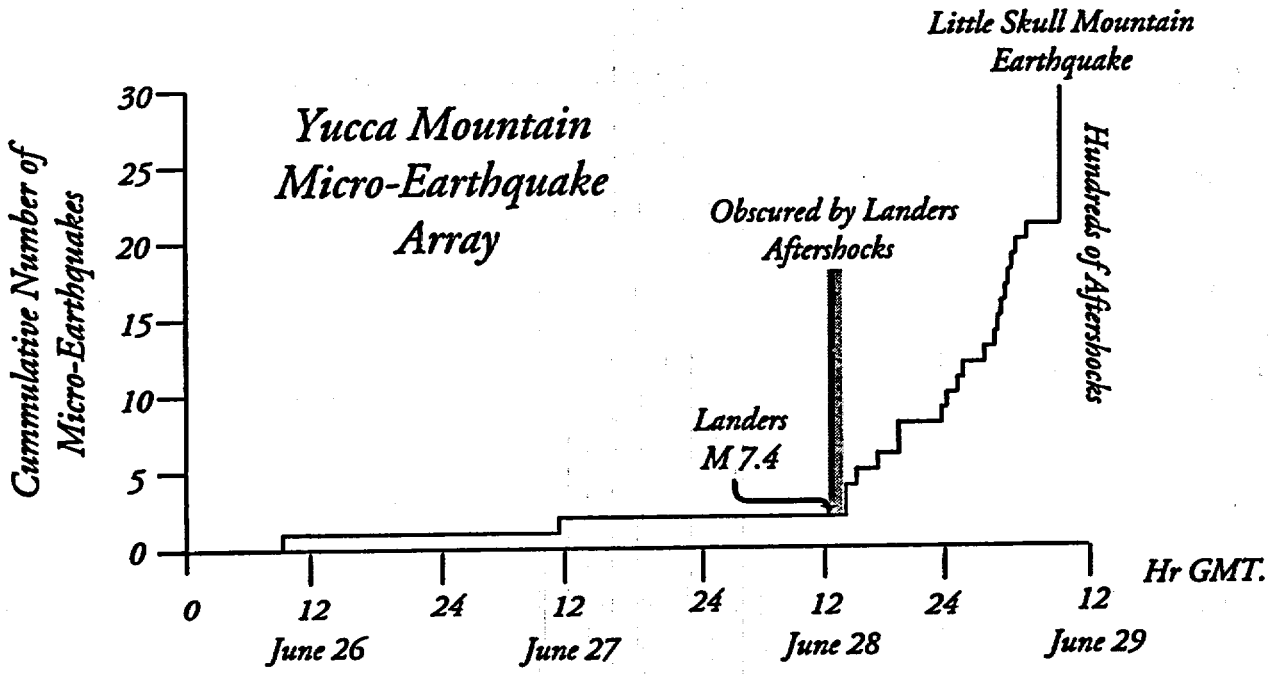
Little Skull Mountain Earthquake
Yucca Mountain Micro-Earthquake Array
Obscured by Landers Aftershocks
Hundreds of Aftershocks
Landers M 7.4
Cummulative Number of Micro-Earthquakes
30
25
20
15
10
5
0
0
12
24
12
24
12
24
12
Hr GMT.
June 26
June 27
June 28
June 29

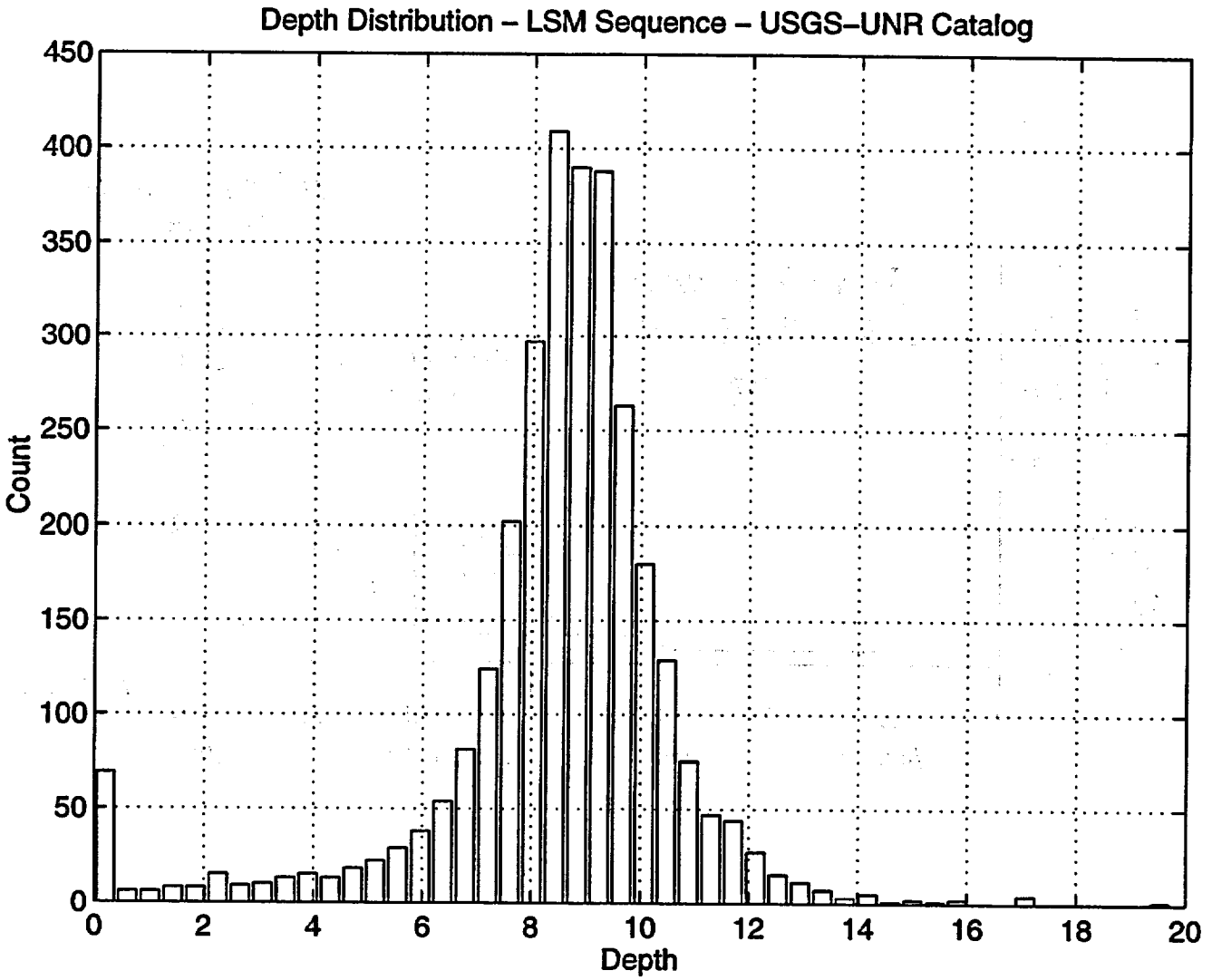
Depth Distribution – LSM Sequence – USGS–UNR Catalog
Count
Depth
0
50
100
150
200
250
300
350
400
450
0
2
4
6
8
10
12
14
16
18
20

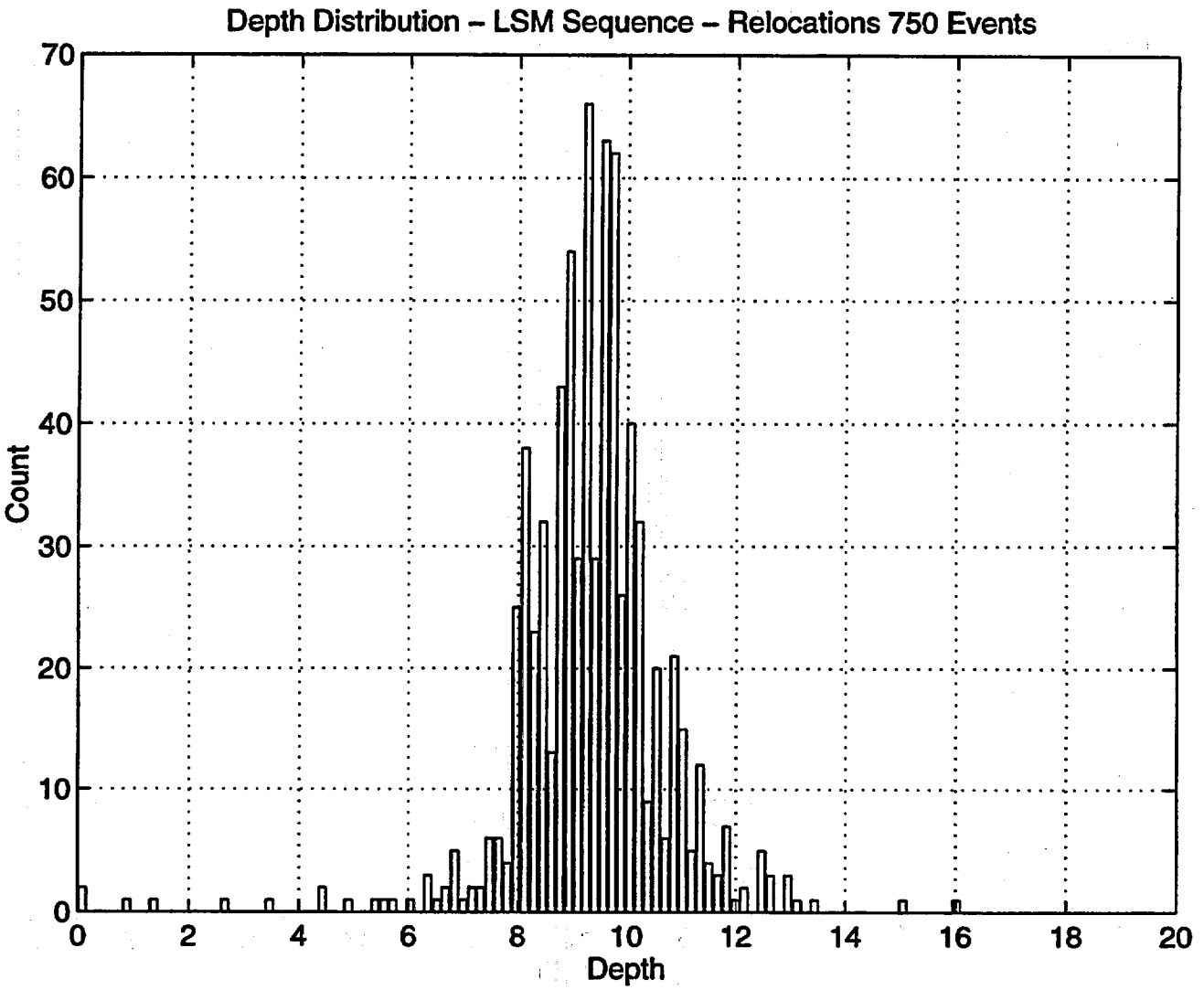
Depth Distribution – LSM Sequence – Relocations 750 Events
Count
Depth
0
10
20
30
40
50
60
70
0
2
4
6
8
10
12
14
16
18
20

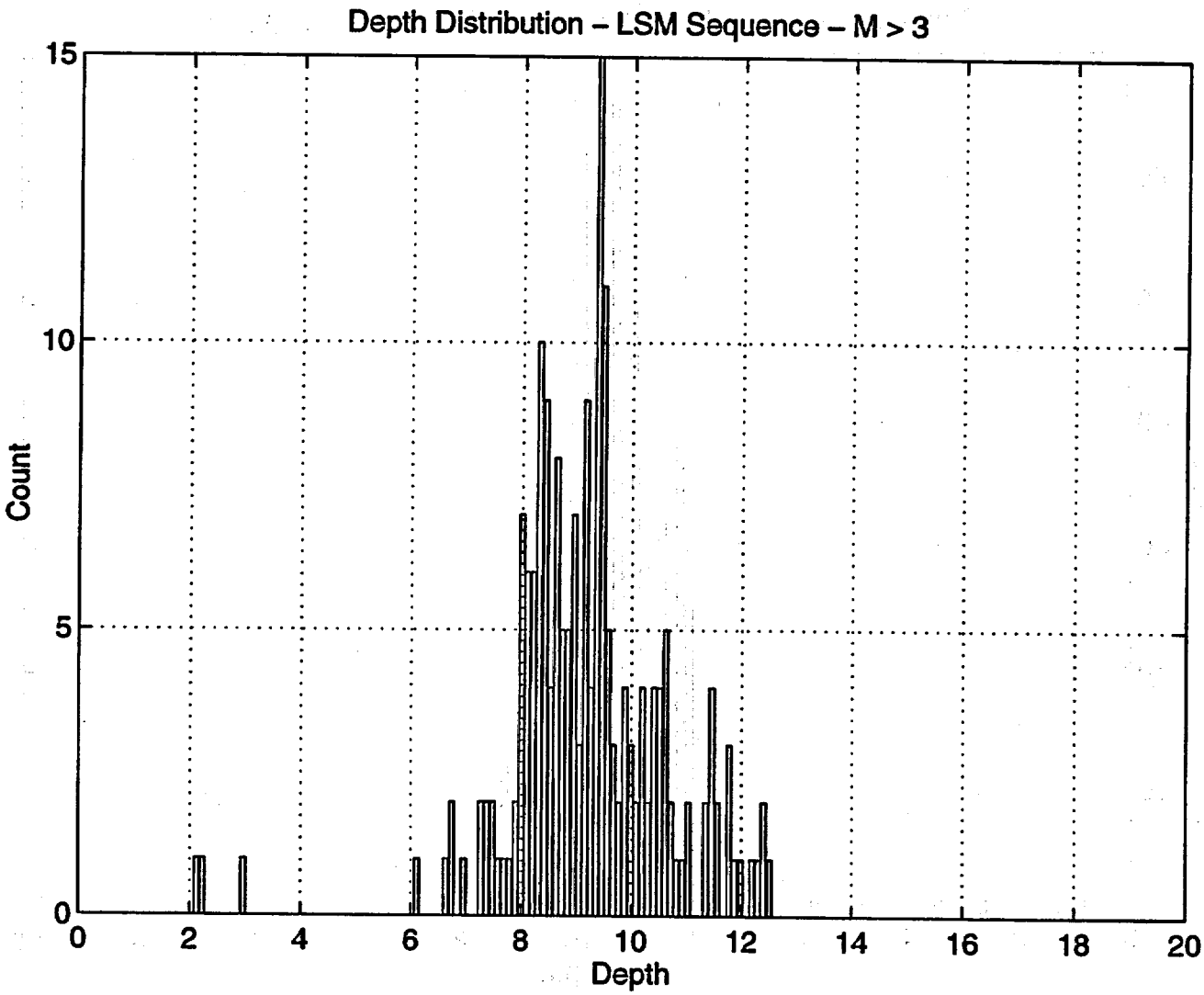
Depth Distribution – LSM Sequence – M > 3
Count
Depth
0
5
10
15
0
2
4
6
8
10
12
14
16
18
20

1993 Rock Valley

Earthquake Sequence

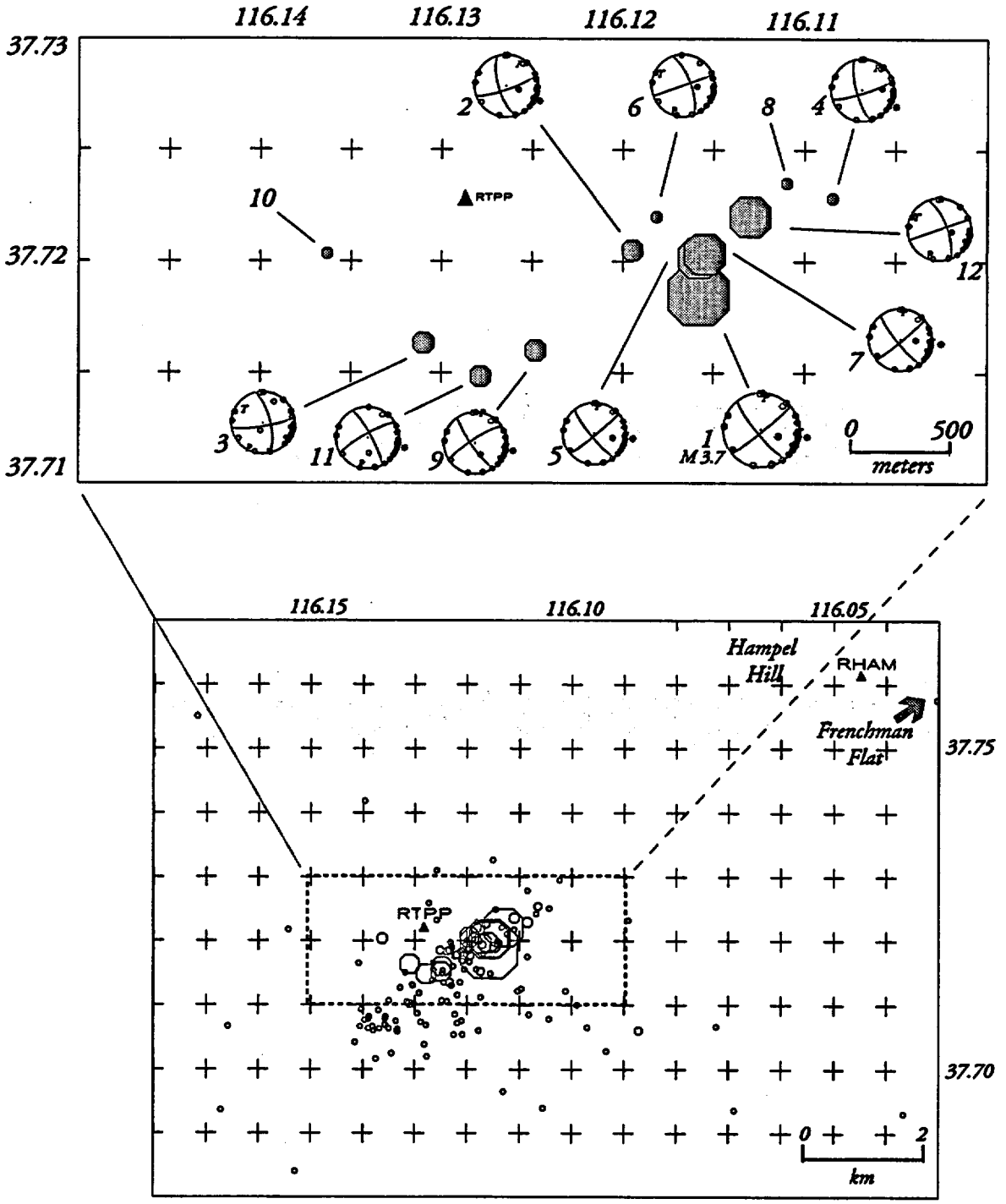

▲ *Portable Stations*

1993 Rock Valley Earthquakes

EV#	Origin Time	Lat°	Lon	Z	Z*	Md	gap	rms	S-P
1	93 530 1520 62.49	36 43.11	116 06.95	2.06	1.9	4.3	63	0.06	0.53
2.	93 531 315 79.97	36 43.23	116 07.17	1.91	1.9	3.2	62	0.06	0.50
3.	93 531 918 49.14	36 42.98	116 07.86	2.37	1.7	3.2	63	0.06	0.47
4.	93 531 1113 67.99	36 43.41	116 06.66	1.86	1.0	2.7	61	0.06	0.48
5.	93 531 1244 72.78	36 43.32	116 06.78	2.25	1.7	3.6	62	0.06	0.53
6.	93 531 2238 47.40	36 43.32	116 07.09	1.84	1.7	2.7	61	0.09	0.57
7.	93 6 1 1628 65.15	36 43.21	116 06.95	1.68	1.4	3.9	62	0.06	0.44
8.	93 6 3 835 70.40	36 43.37	116 06.51	0.71	1.4	2.6	61	0.08	0.53
9.	93 6 3 1720 32.89	36 42.96	116 07.49	1.80	1.7	3.3	63	0.07	0.47
10.	93 6 4 1623 37.38	36 43.22	116 08.18	0.85	0.9	2.5	61	0.10	0.31
11.	93 6 5 1323 71.33	36 42.89	116 07.67	1.63	1.1	3.4	70	0.06	0.39
12.	93 6 6 1531 43.82	36 43.22	116 06.93	2.45	1.8	3.6	83	0.07	0.55

EV# - Event number
Origin Time - Year-Month-Day-Hour-Minute-Second (UTC) that the earthquake occurred.
Z - Event depth (km) after relocation using layered velocity model.
Z*- Depth fixed by S minus P time at station RTPP and assuming a 3.0 km/sec P-wave velocity.
Md - Network duration magnitude.
gap - location gap in degrees.
rms - rms P-wave residual in seconds.
S-P - S minus P time (sec) at station RTPP.

1993 Rock Valley Focal Mechanisms

EV#	Strike	Dip	Rake
1.	50	85	-10
2.	70	80	-20
3.	80	80	20
4.	72	80	-15
5.	50	85	-10
6.	70	90	20
7.	50	85	-10
9.	237	80	10
12.	70	90	20

Strike, dip and rake angles of northeast striking fault plane (Aki and Richards, 1980, convention)

a.

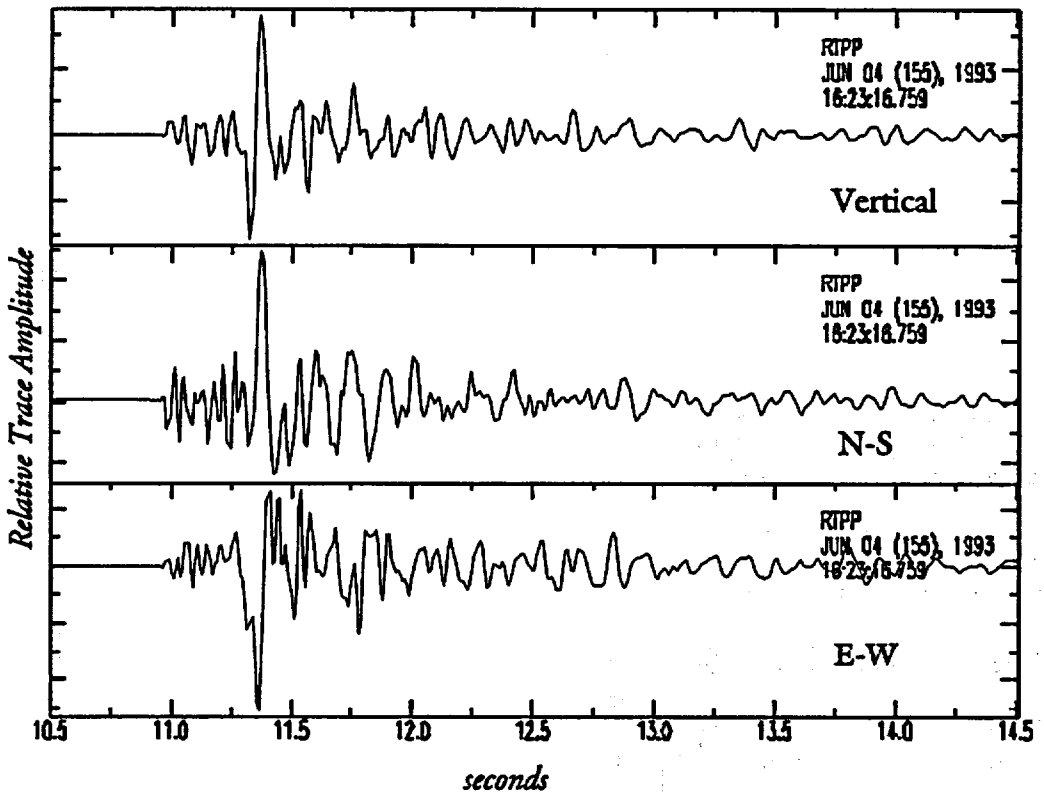
RTPP
JUN 04 (155), 1993
16:23:16.759
Vertical
RTPP
JUN 04 (155), 1993
16:23:16.759
N-S
RTPP
JUN 04 (155), 1993
16:23:16.759
E-W
Relative Trace Amplitude
10.5
11.0
11.5
12.0
12.5
13.0
13.5
14.0
14.5
seconds

b.

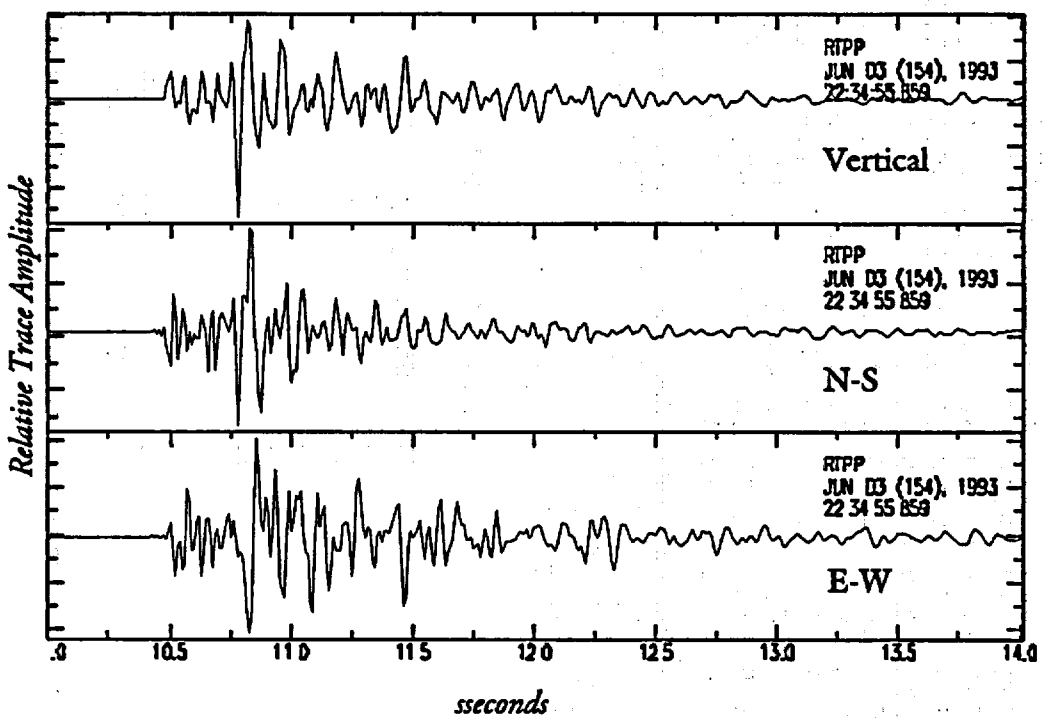
RTPP
JUN 03 (154), 1993
22:34:55.859
Vertical
RTPP
JUN 03 (154), 1993
22 34 55 859
N-S
RTPP
JUN 03 (154), 1993
22 34 55 859
E-W
Relative Trace Amplitude
.0
10.5
11.0
11.5
12.0
12.5
13.0
13.5
14.0
sseconds

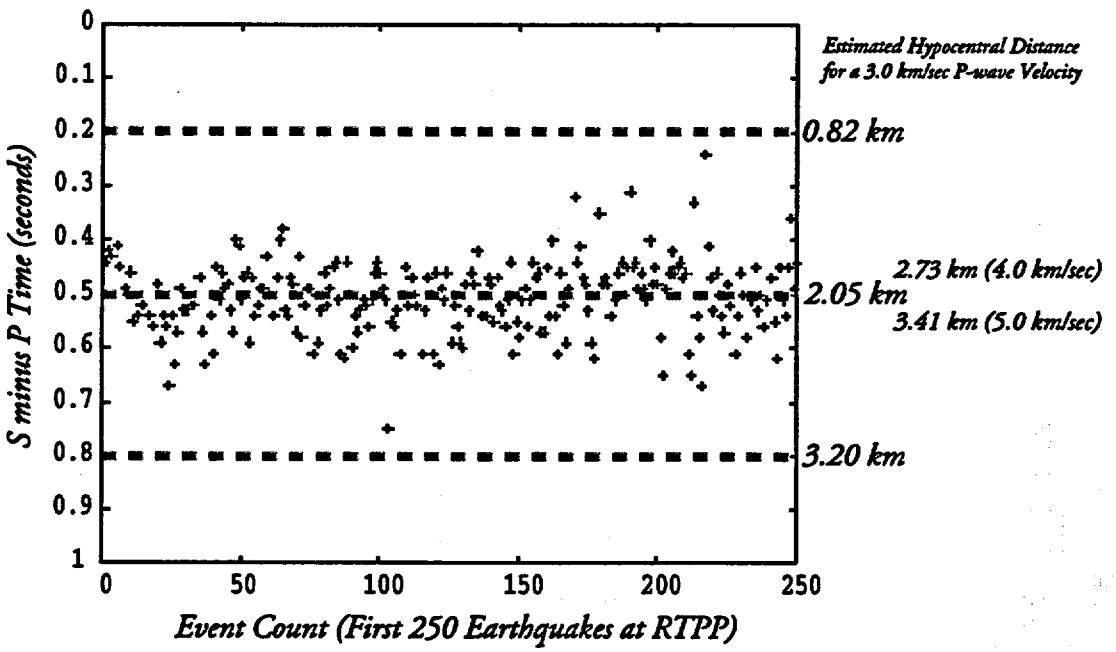
0
0.1
0.2
0.3
0.4
0.5
0.6
0.7
0.8
0.9
1
0
50
100
150
200
250
S minus P Time (seconds)
Event Count (First 250 Earthquakes at RTPP)
Estimated Hypocentral Distance
for a 3.0 km/sec P-wave Velocity
0.82 km
2.73 km (4.0 km/sec)
2.05 km
3.41 km (5.0 km/sec)
3.20 km

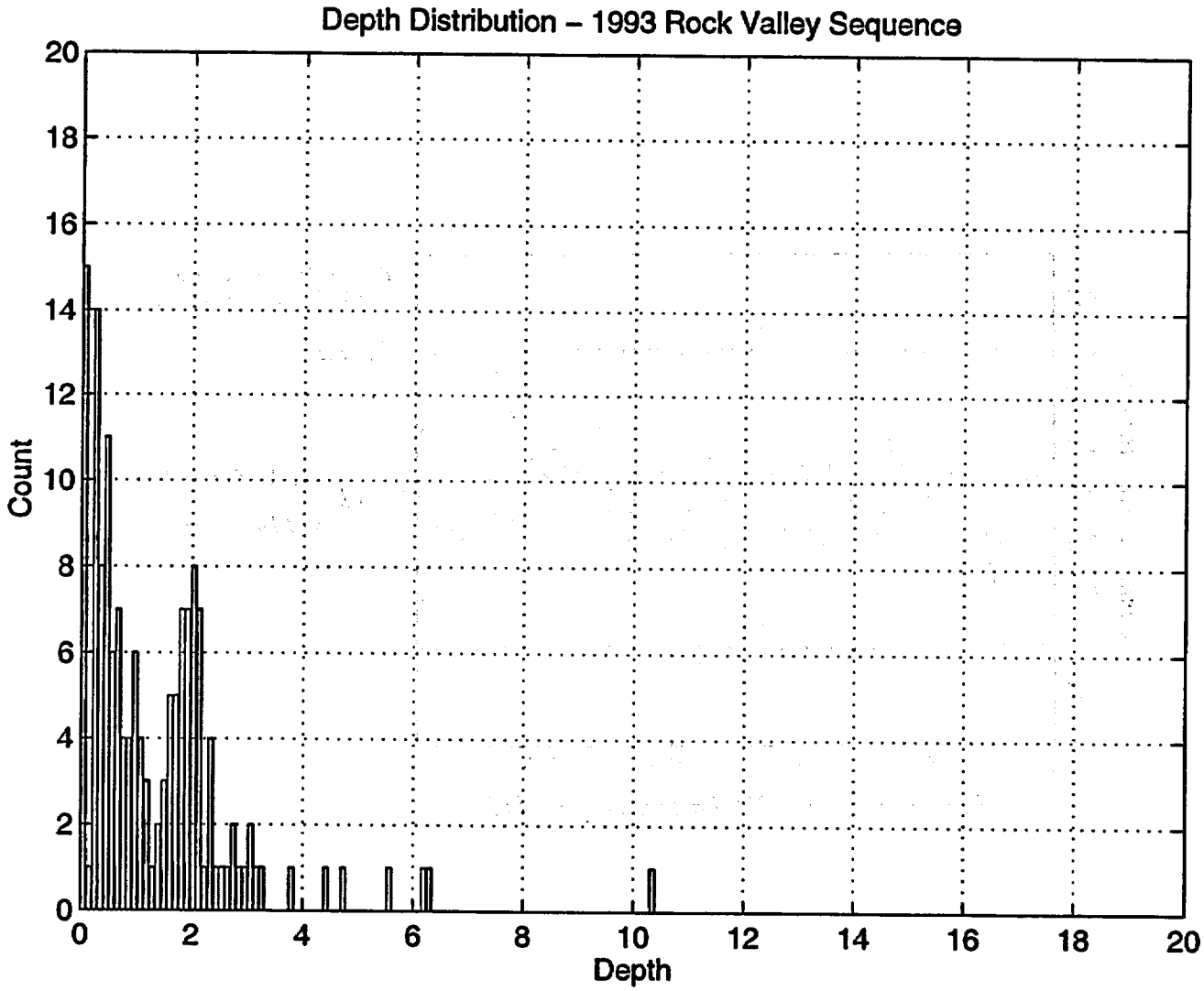
Depth Distribution – 1993 Rock Valley Sequence
Count
Depth
0
2
4
6
8
10
12
14
16
18
20

Recent Earthquakes

in the

Southern Great Basin

Rock Valley M 3.5 9/7/95

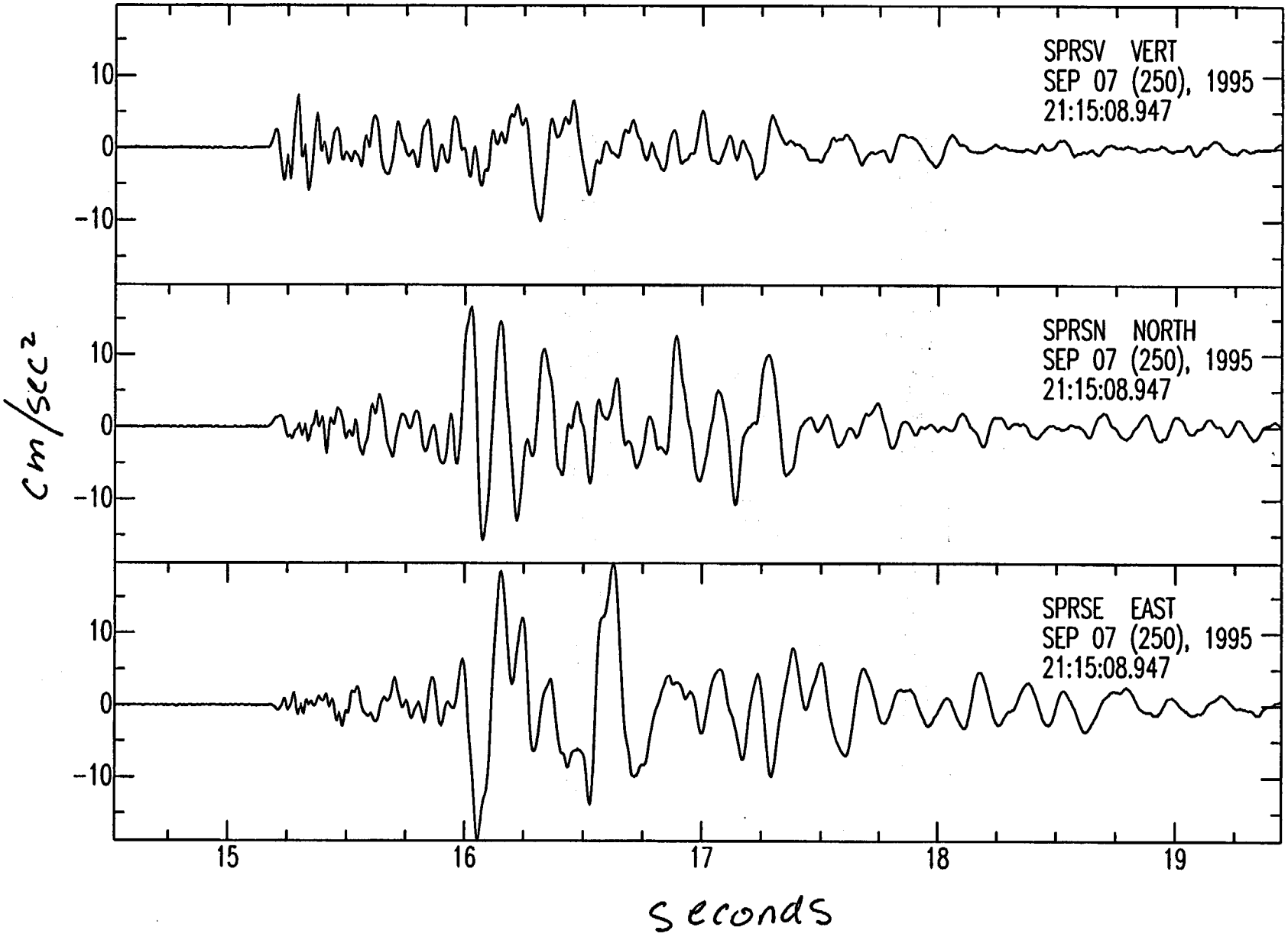

Rock Valley

950907 21:15 22.95
36-40.07 116-12.55
DEPTH = 3.84 KM
MAG = 3.40 A

RMS = 0.00 S
DMIN = 0 KM
AZM GAP = 0
FM = 47

ERH = 0.0 KM
ERZ = 0.0 KM
MISFIT = 0.05 (+.03)
STDR = 0.66

STRIKE UNCERTAINTY = 5
DIP UNCERTAINTY = 10
RAKE UNCERTAINTY = 5
% MACHINE PICKS = 0

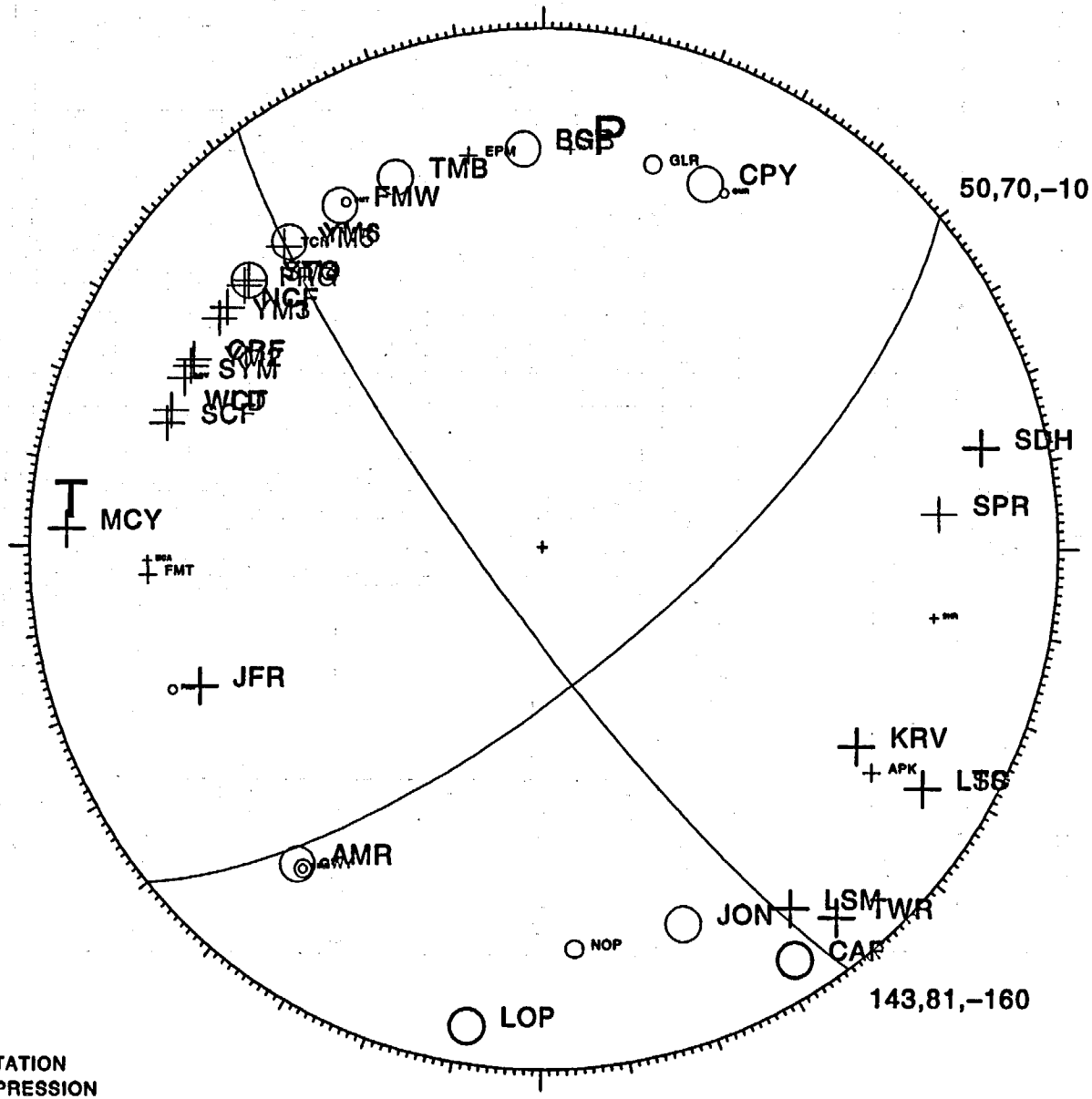

DISCREPANT OBSERVATIONS

STAT	DIST	AZM	AIN	PRMK
YM4	30	312	66	IPD0
EPM	63	349	66	IPU2
PAN	86	249	66	EPD3
BLT	91	4	66	EPU3

UP DWN
O O DILATATION
+ + COMPRESSION

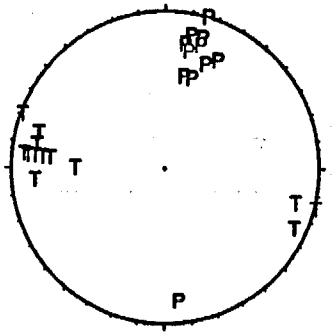

Thu Sep 7 17:25:42 1995

timber.lst

Timber Mountain

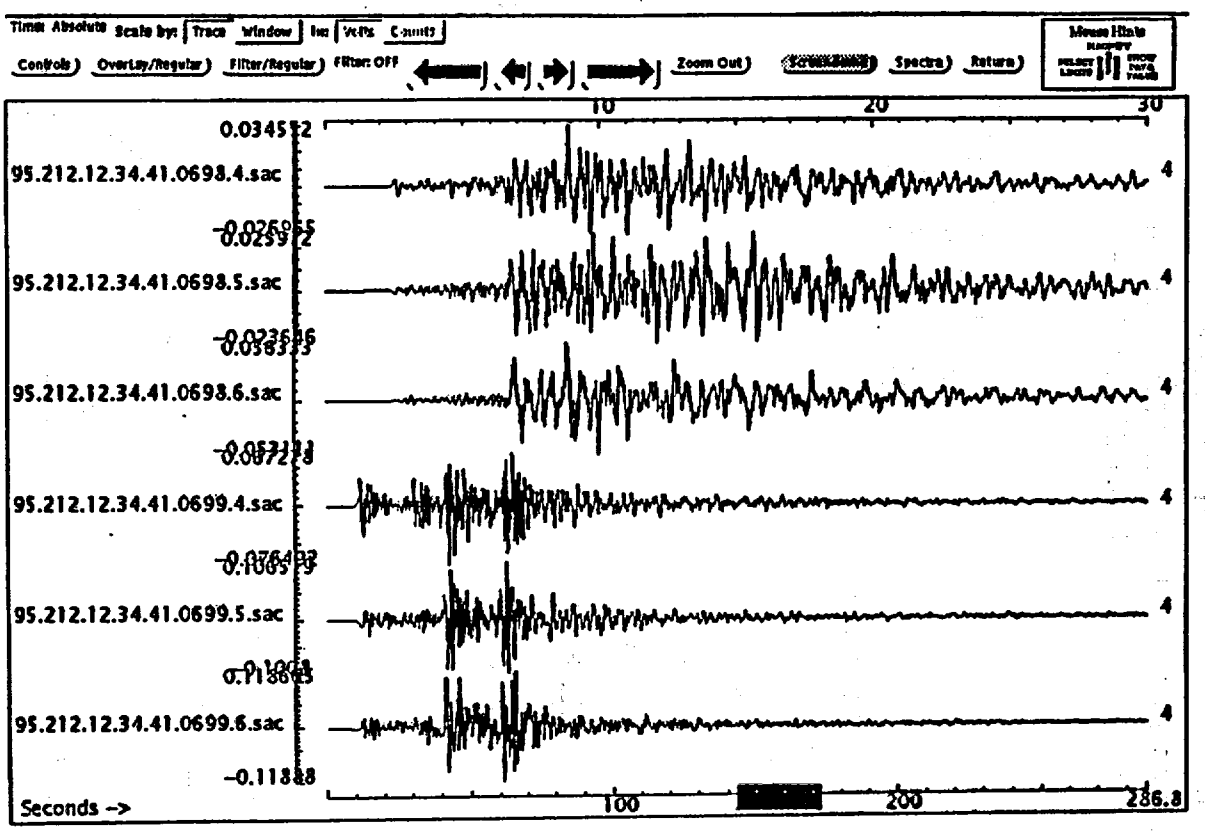

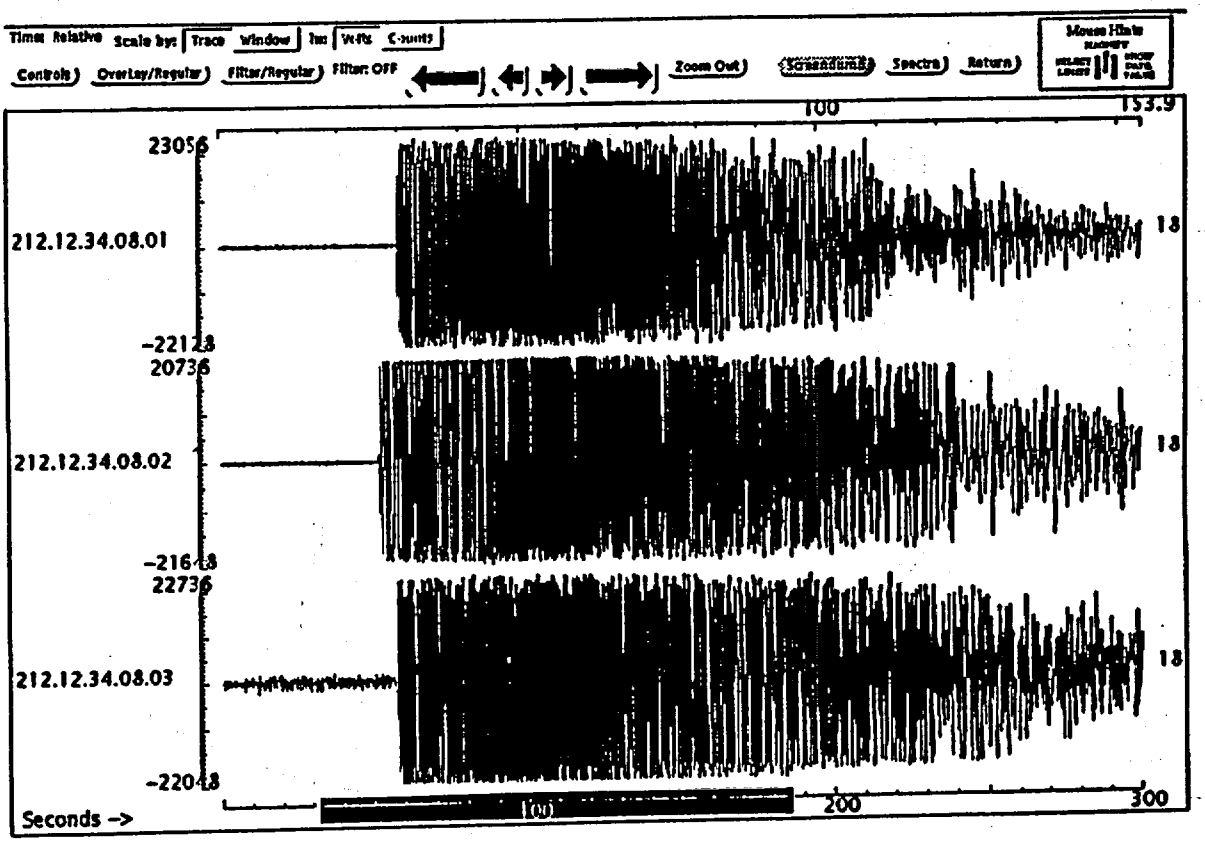

Timber Mountain

950731 12:34 46.83
37- 5.76 116-24.37
DEPTH = 15.71 KM
MAG = 4.10 A

RMS = 0.00 S
DMIN = 0 KM
AZM GAP = 0
FM = 61

ERH = 0.0 KM
ERZ = 0.0 KM
MISFIT = 0.02 (+.03)
STDR = 0.70

STRIKE UNCERTAINTY = 3
DIP UNCERTAINTY = 13
RAKE UNCERTAINTY = 20
% MACHINE PICKS = 0

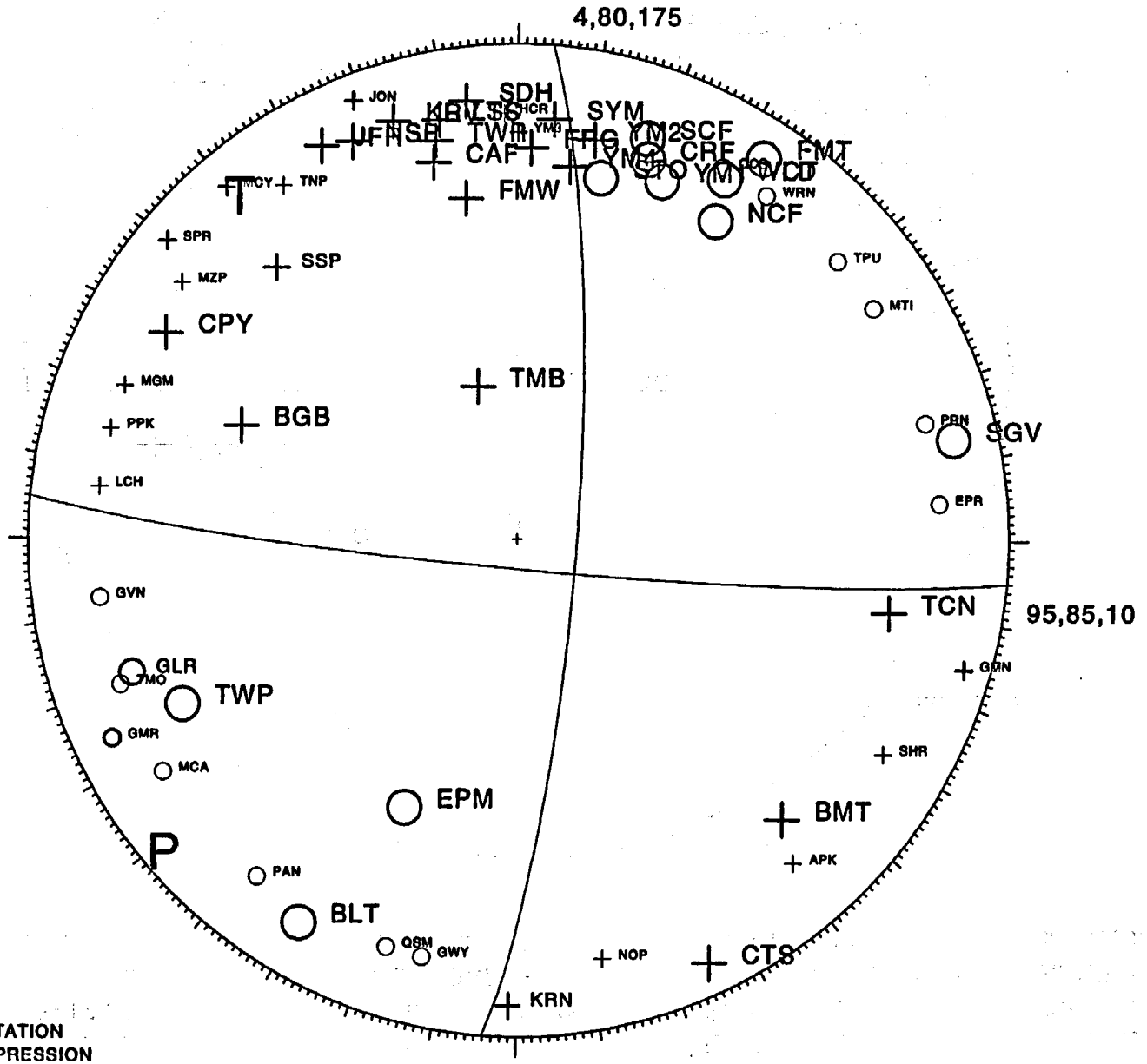

DISCREPANT OBSERVATIONS

STAT	DIST	AZM	AIN	PRMK
YM2	35	191	109	IPU0

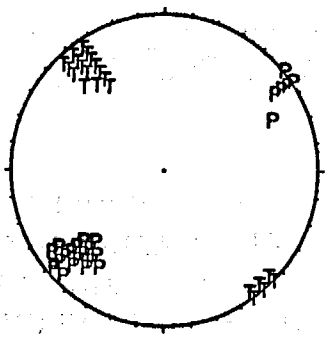

P & T 90% CONFIDENCE RANGE

UP DWN
O O DILATATION
+ + COMPRESSION

Thu Oct 10 16:07:18 1996

timber.lst

LSM Aftershock

960905 8:16 55.53
36–43.75 116–17.96
DEPTH = 9.79 KM
MAG = 3.50 A

RMS = 0.00 S
DMIN = 0 KM
AZM GAP = 0
FM = 20

ERH = 0.0 KM
ERZ = 0.0 KM
MISFIT = 0.05 (+.04)
STDR = 0.81

STRIKE UNCERTAINTY = 18
DIP UNCERTAINTY = 15
RAKE UNCERTAINTY = 10
% MACHINE PICKS = 0

DISCREPANT OBSERVATIONS

STAT	DIST	AZM	AIN	PRMK
LSC	2	259	168	IPU0

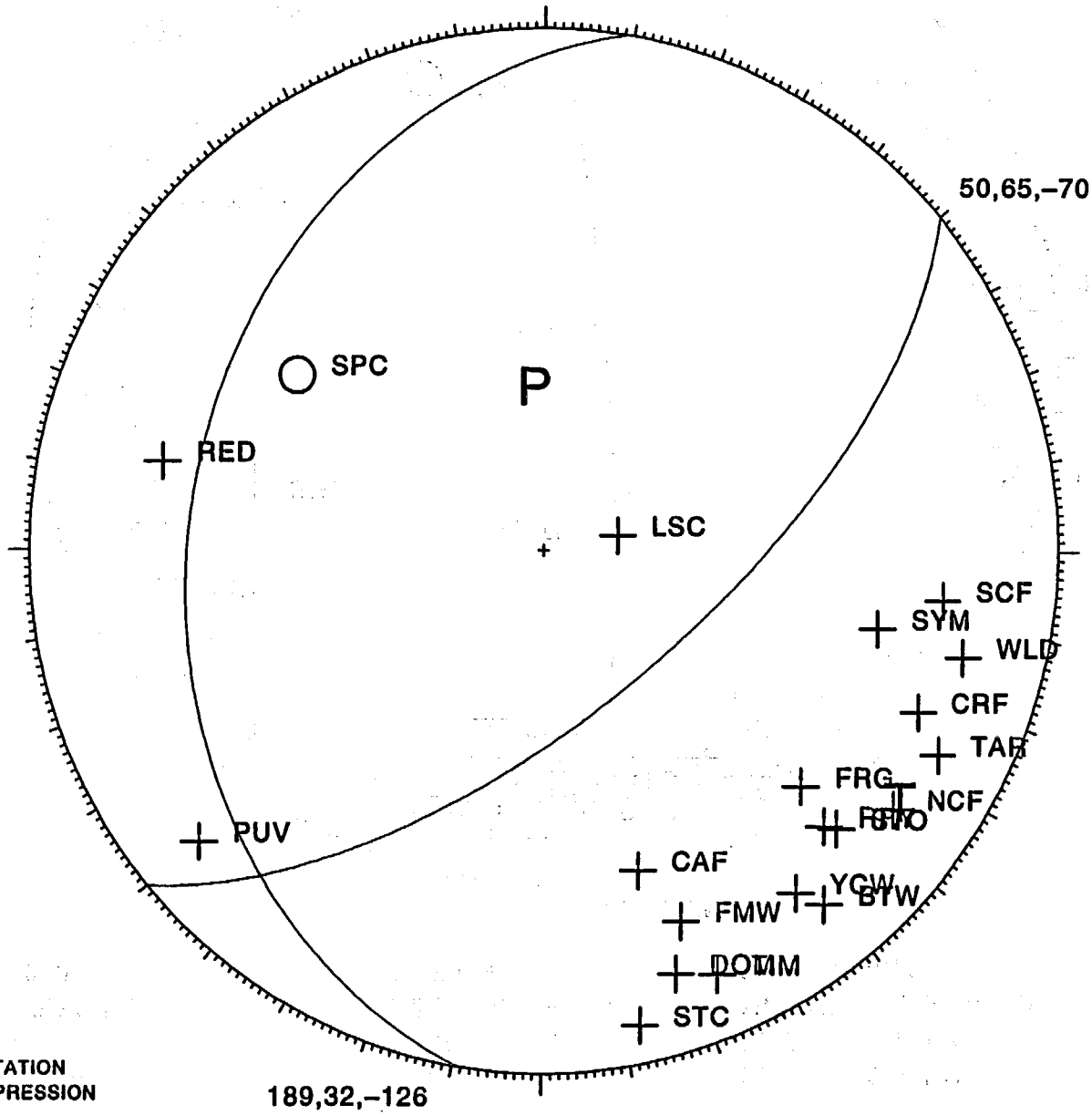

UP DWN
O O DILATATION
+ + COMPRESSION

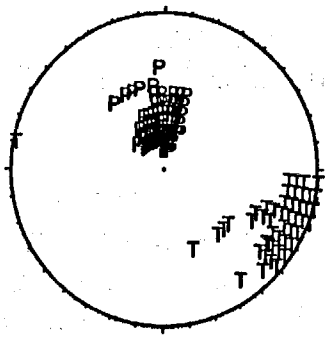

P & T 90% CONFIDENCE RANGE

Thu Sep 5 15:29:45 1996

timber.lst

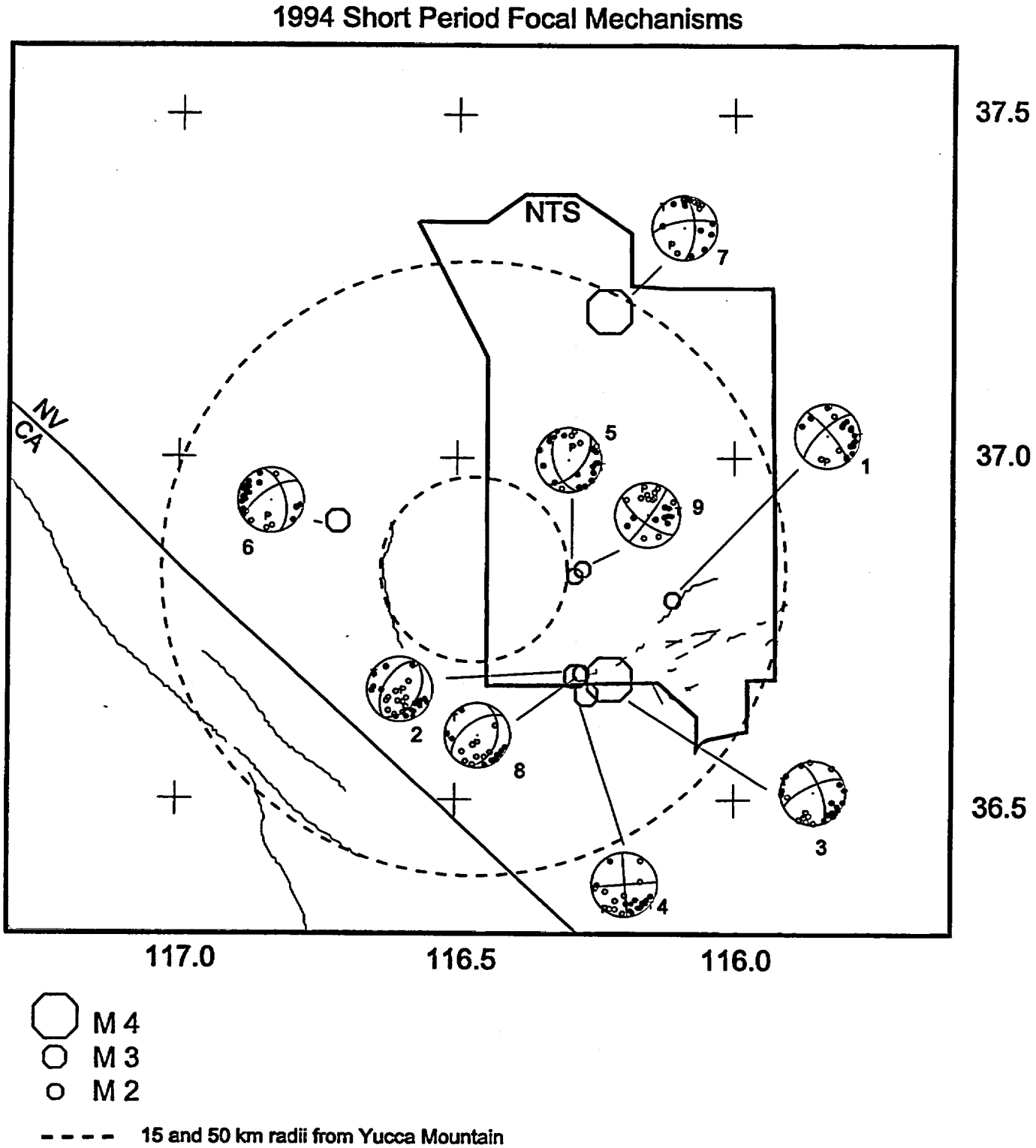

Figure 12. Lower hemisphere projections of reliably determined short period p-wave first motion focal mechanisms in the SGB druing 1994. See Table 3 for event desciptions and location information.

Small Earthquakes

at

Yucca Mountain

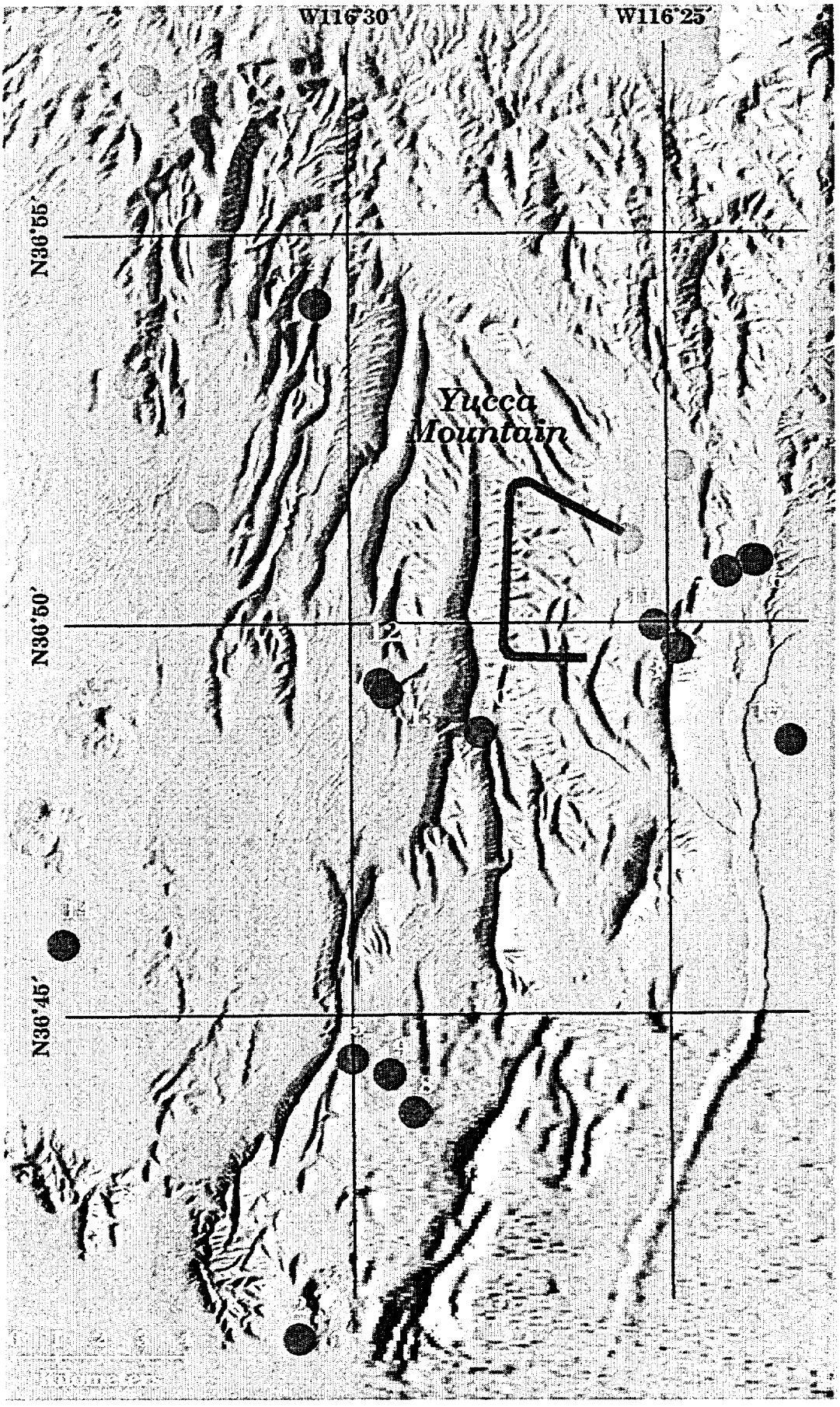
W116°30'
W116°25'
N36°55'
N36°50'
N36°45'
Yucca
Mountain

Fifteen Very Small Earthquakes in the Yucca Mountain Block May 1995 through Spetember 1996

Triggered at least 3 stations of Digital Network

#	Date	Origin Time	Lat	Lon	Depth	ML	#p	gap	near	rms	eh	ez	Q
1.	*95 5 5	1321 33.12	36N50.66	116W24.08	6.15	0.58	22	41	1.3	0.11	0.3	0.5	AA
2.	95 7 1	1526 56.69	36N40.84	116W30.88	8.65		13	242	5.7	0.13	1.0	0.9	BD
3.	95 7 7	759 -0.33	36N49.67	116W24.85	6.02	-0.27	16	94	1.3	0.11	0.3	0.4	AB
4.	95 728	618 51.42	36N54.10	116W30.52	4.80	-0.48	3	250	5.5	0.01	0.2	0.1	AD
5.	*95 9 4	1239 47.11	36N44.43	116W30.02	4.45	0.72	31	101	4.3	0.11	0.3	0.6	AB
6.	951119	2215 84.91	36N50.80	116W23.59	6.46	-0.25	5	115	4.1	0.06	0.5	0.7	AD
7.	951120	226 57.44	36N50.81	116W23.67	5.95	-0.43	5	114	4.0	0.06	0.5	1.1	AD
8.	9512 6	2327 15.90	36N43.74	116W29.06	7.80	0.29	10	210	3.7	0.12	0.7	0.6	AD
9.	96 129	1020 32.32	36N44.23	116W29.44	9.90		3	211	4.0	0.02	1.2	0.2	BD
10.	96 330	1957 28.63	36N48.60	116W27.98	7.24	-0.59	5	86	3.3	0.04	0.2	0.3	AA
11.	96 4 8	714 49.64	36N49.96	116W25.21	8.23	-0.58	5	147	1.8	0.06	0.5	0.5	AD
12.	*96 6 2	1645 75.18	36N49.11	116W29.44	9.61	0.01	6	171	2.1	0.04	0.7	0.5	AC
13.	96 6 2	1015 33.29	36N49.23	116W29.55	9.87	-0.69	14	63	3.8	0.11	0.3	0.4	AA
14.	96 731	357 37.30	36N45.91	116W34.54	8.55	-0.76	5	195	3.0	0.14	1.3	0.9	BD
15.	96 812	422 50.68	36N48.48	116W23.09	5.02	-0.62	3	237	3.3	0.00	0.1	0.1	AD

- referenced on figure.
Origin Time: Year-Month-Day-Hour-Minute-Second (UTC).
Depth: Event depth referenced to surface elevation.
* - triggered the older analog seismic network.

Diurnal Background Seismic Noise

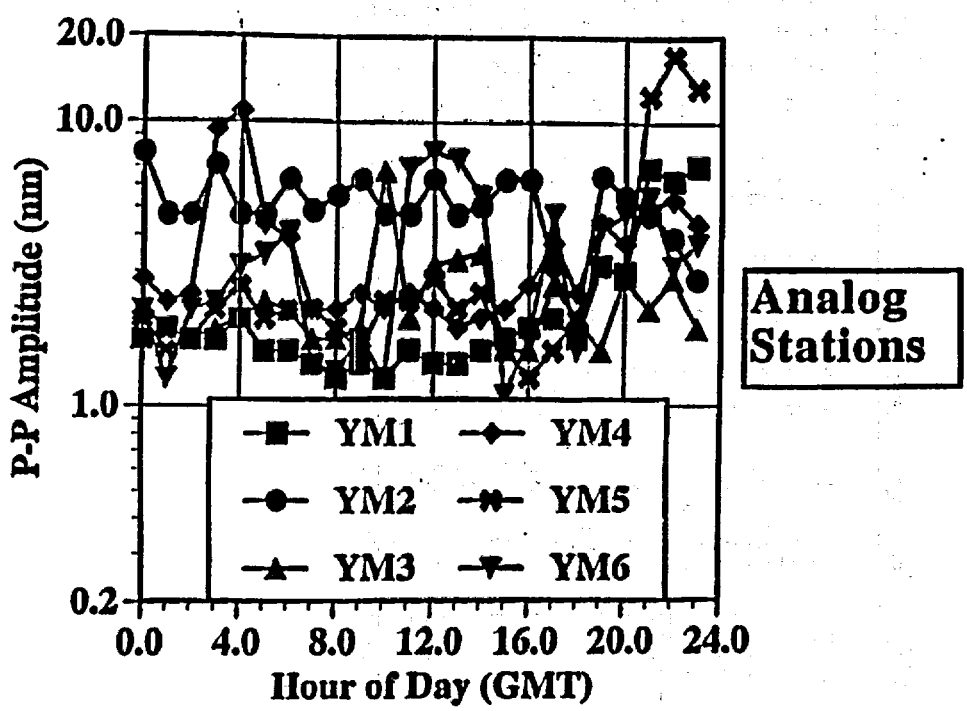

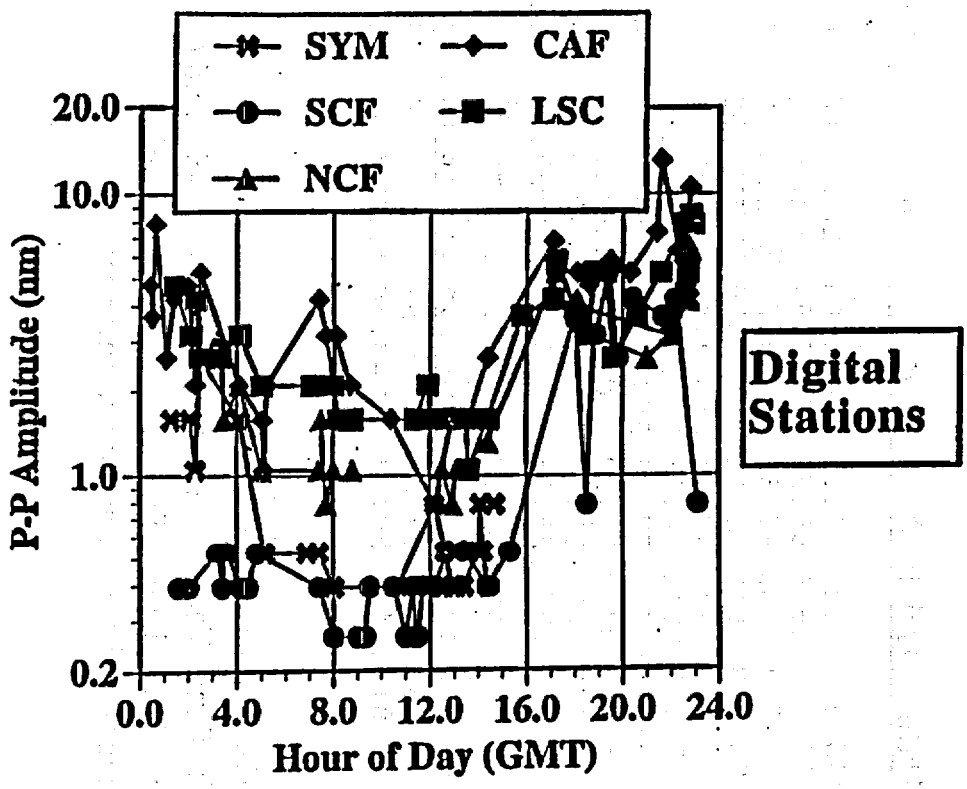

Near Alice Ridge

950505 13:21 33.11
36-50.83 116-23.91
DEPTH = 6.29 KM
MAG = 0.50 A

RMS = 0.00 S
DMIN = 0 KM
AZM GAP = 0
FM = 17

ERH = 0.0 KM
ERZ = 0.0 KM
MISFIT = 0.12 (+.05)
STDR = 0.60

STRIKE UNCERTAINTY = 10
DIP UNCERTAINTY = 10
RAKE UNCERTAINTY = 15
% MACHINE PICKS = 0

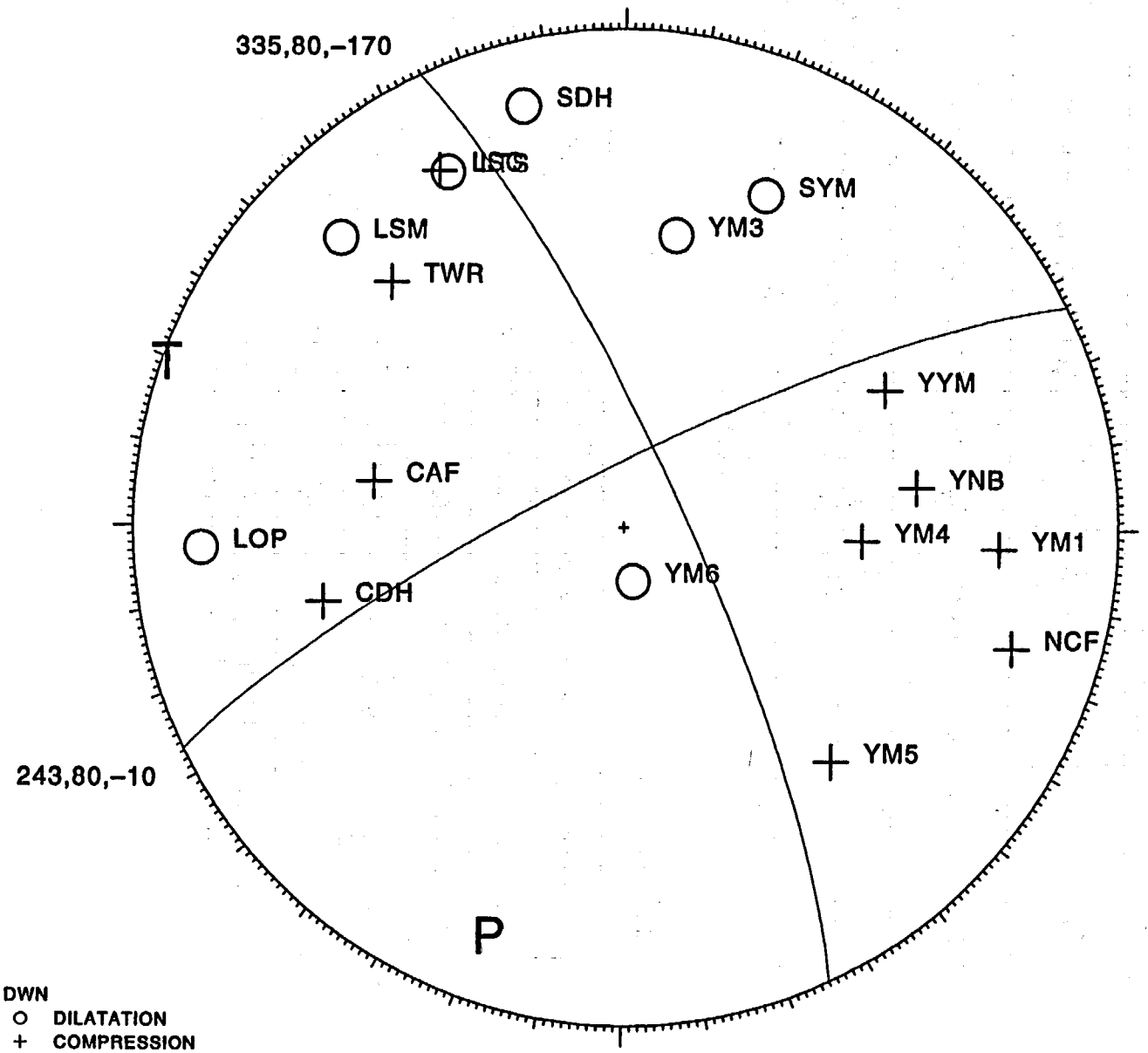

UP DWN
O O DILATATION
+ + COMPRESSION

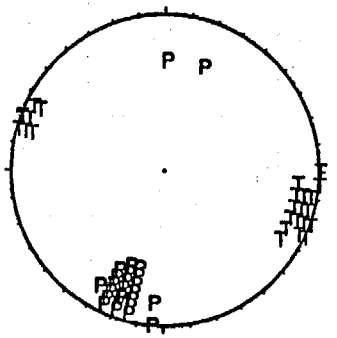

P & T 90% CONFIDENCE RANGE

Mon Oct 14 18:32:51 1996

timber.lst

July 7th Fran Ridge Event

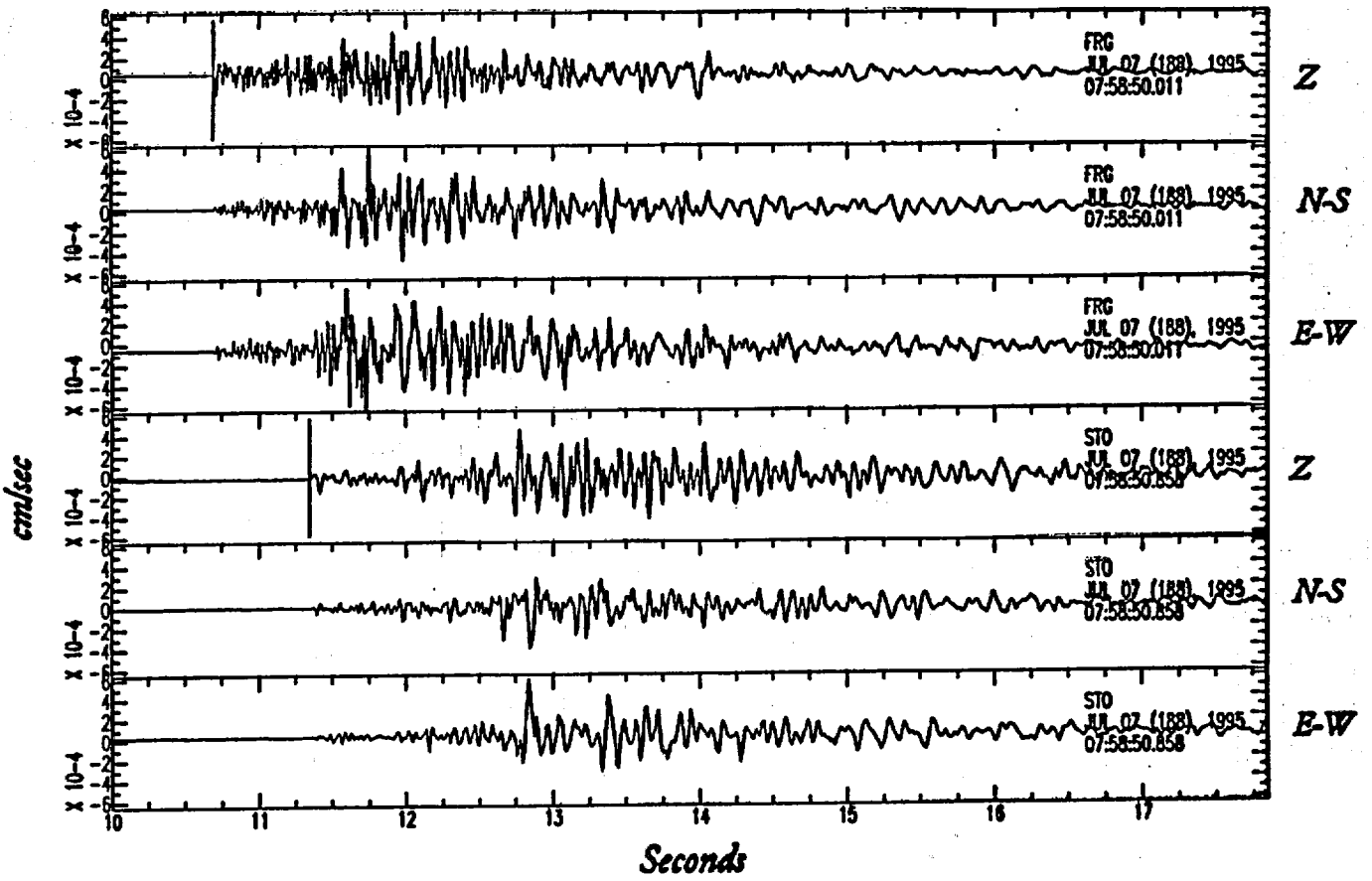

Filtered 1-5 Hz

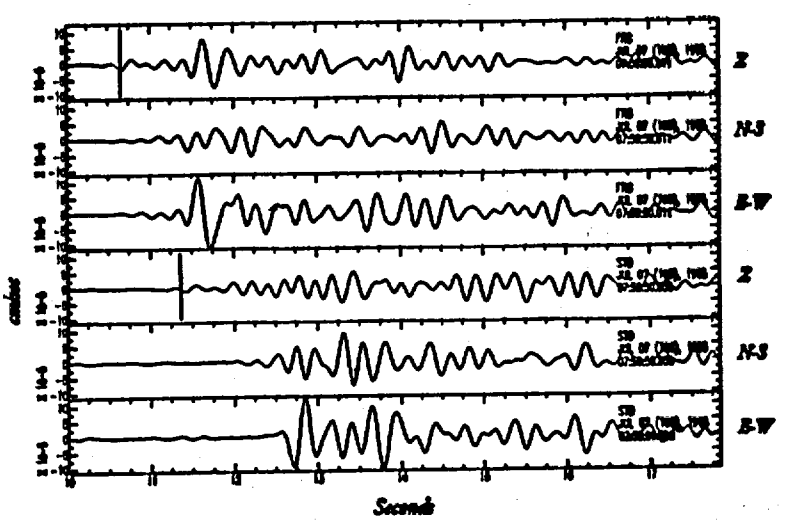

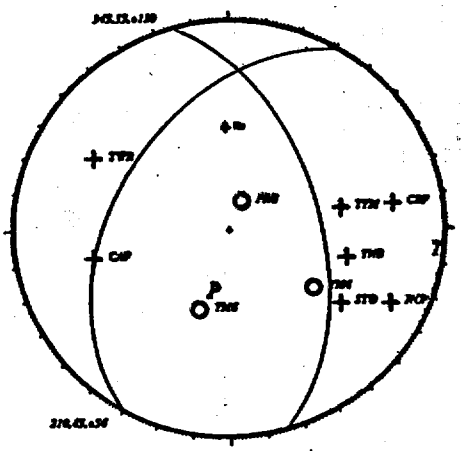

9/4/95 m ≈ 0.8 #5

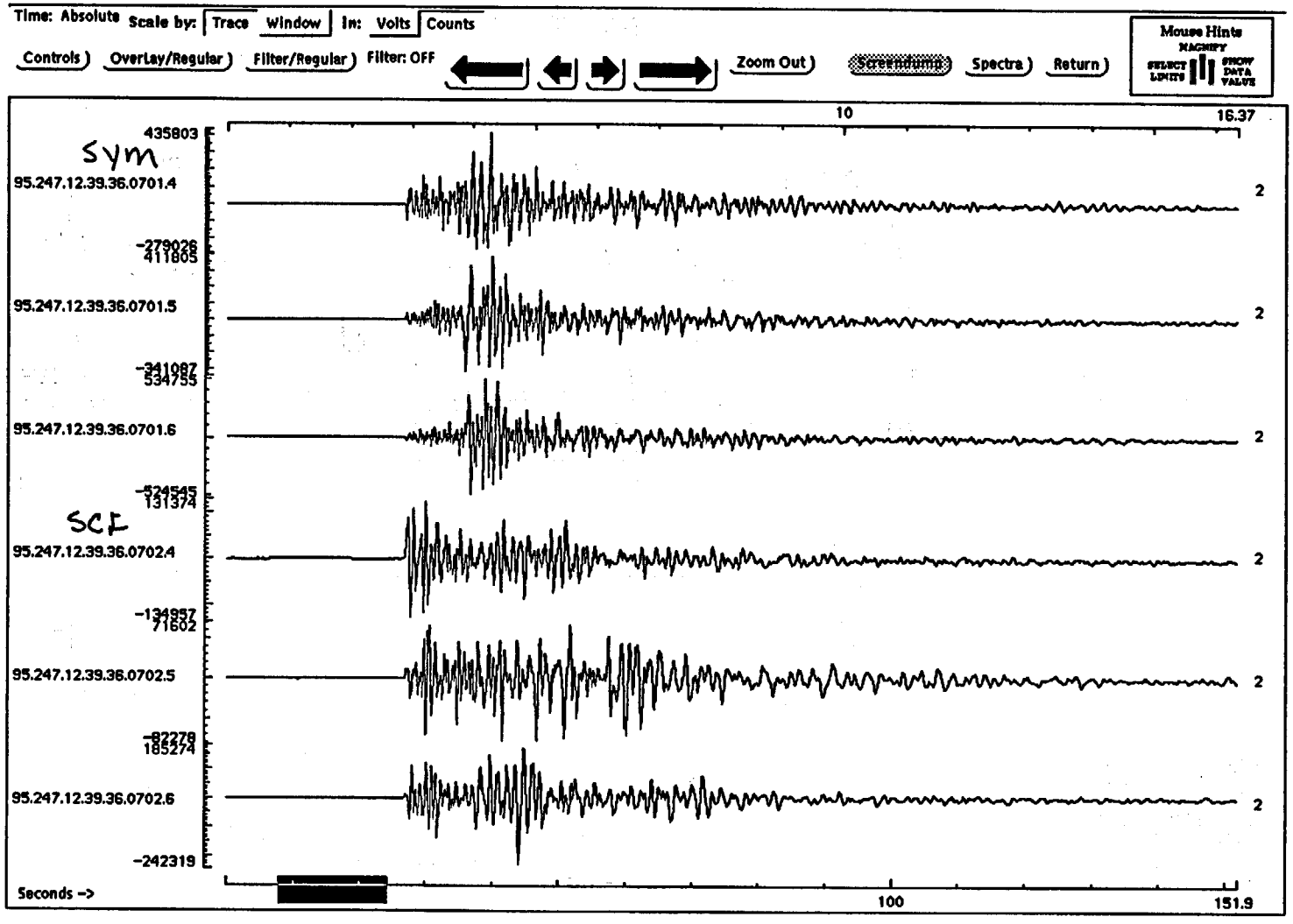
Time: Absolute
Scale by: Trace Window
In: Volts Counts
Controls
Overlay/Regular
Filter/Regular
Filter: OFF
Zoom Out
Screendump
Spectra
Return
Mouse Hints
MAGNIFY
SELECT LIMITS
SHOW DATA VALUE
10
16.37
435803
SYM
95.247.12.39.36.0701.4
-279026
411805
95.247.12.39.36.0701.5
-341087
534755
95.247.12.39.36.0701.6
-524545
131374
SCE
95.247.12.39.36.0702.4
-134857
71602
95.247.12.39.36.0702.5
-82278
185274
95.247.12.39.36.0702.6
-242319
2
Seconds ->
100
151.9

950904 12:39 47.10
36-44.57 116-29.92
DEPTH = 4.73 KM
MAG = 2.00 A

#5

RMS = 0.00 S
DMIN = 0 KM
AZM GAP = 0
FM = 29

ERH = 0.0 KM
ERZ = 0.0 KM
MISFIT = 0.06 (+.04)
STDR = 0.63

STRIKE UNCERTAINTY = 8
DIP UNCERTAINTY = 8
RAKE UNCERTAINTY = 10
% MACHINE PICKS = 0

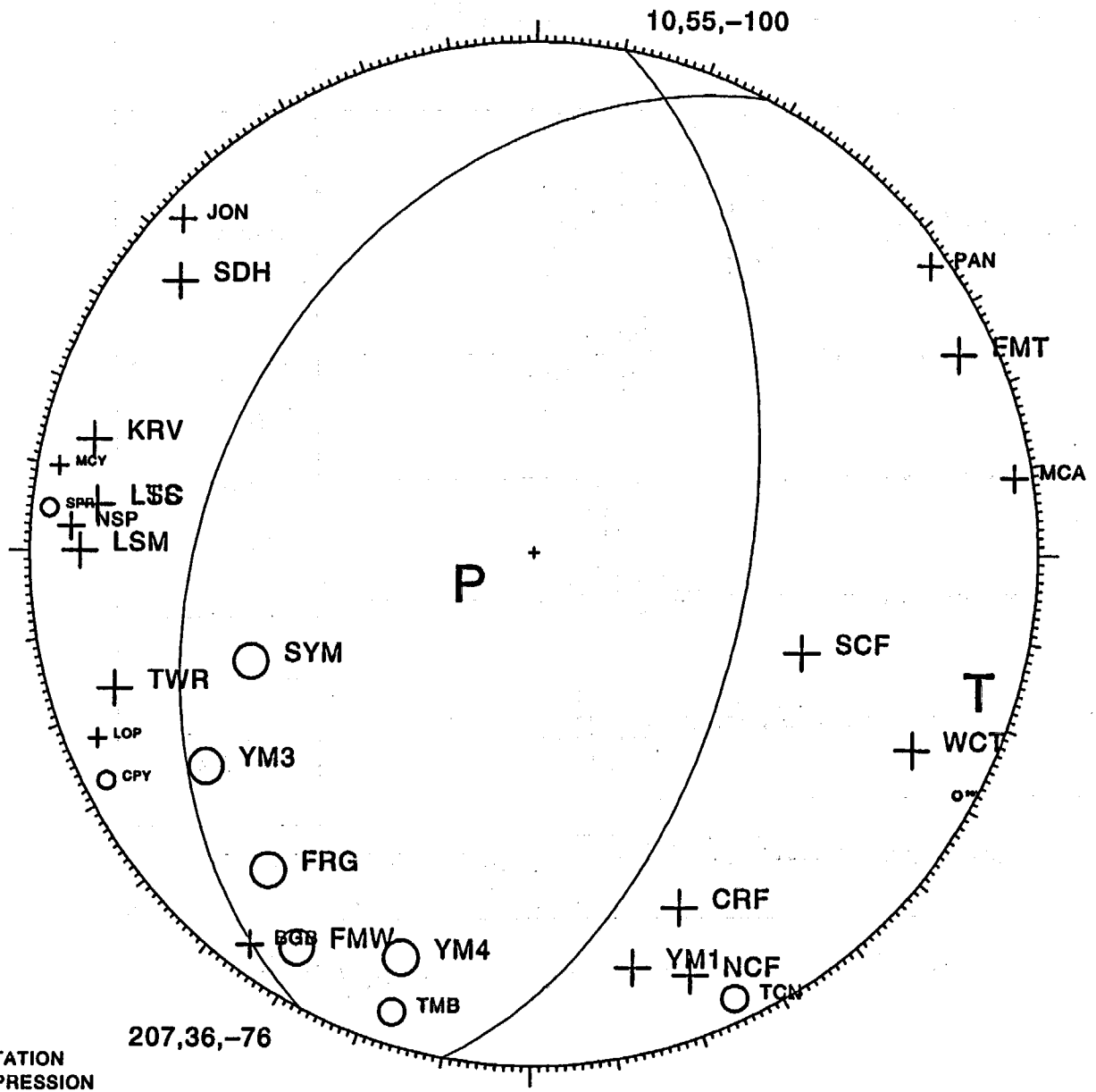

DISCREPANT OBSERVATIONS

STAT	DIST	AZM	AIN	PRMK
CPY	44	62	95	IPD2
TCN	49	335	95	EPD1
SGV	55	299	94	EPD3
SPR	62	95	94	EPD2

UP DWN
O O DILATATION
+ + COMPRESSION

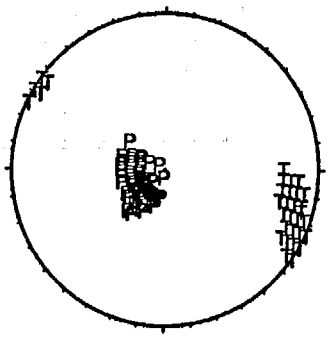

P & T 90% CONFIDENCE RANGE

Tue Oct 15 01:51:29 1996

timber.lst

6/2/96 M≈ -0.7 #13

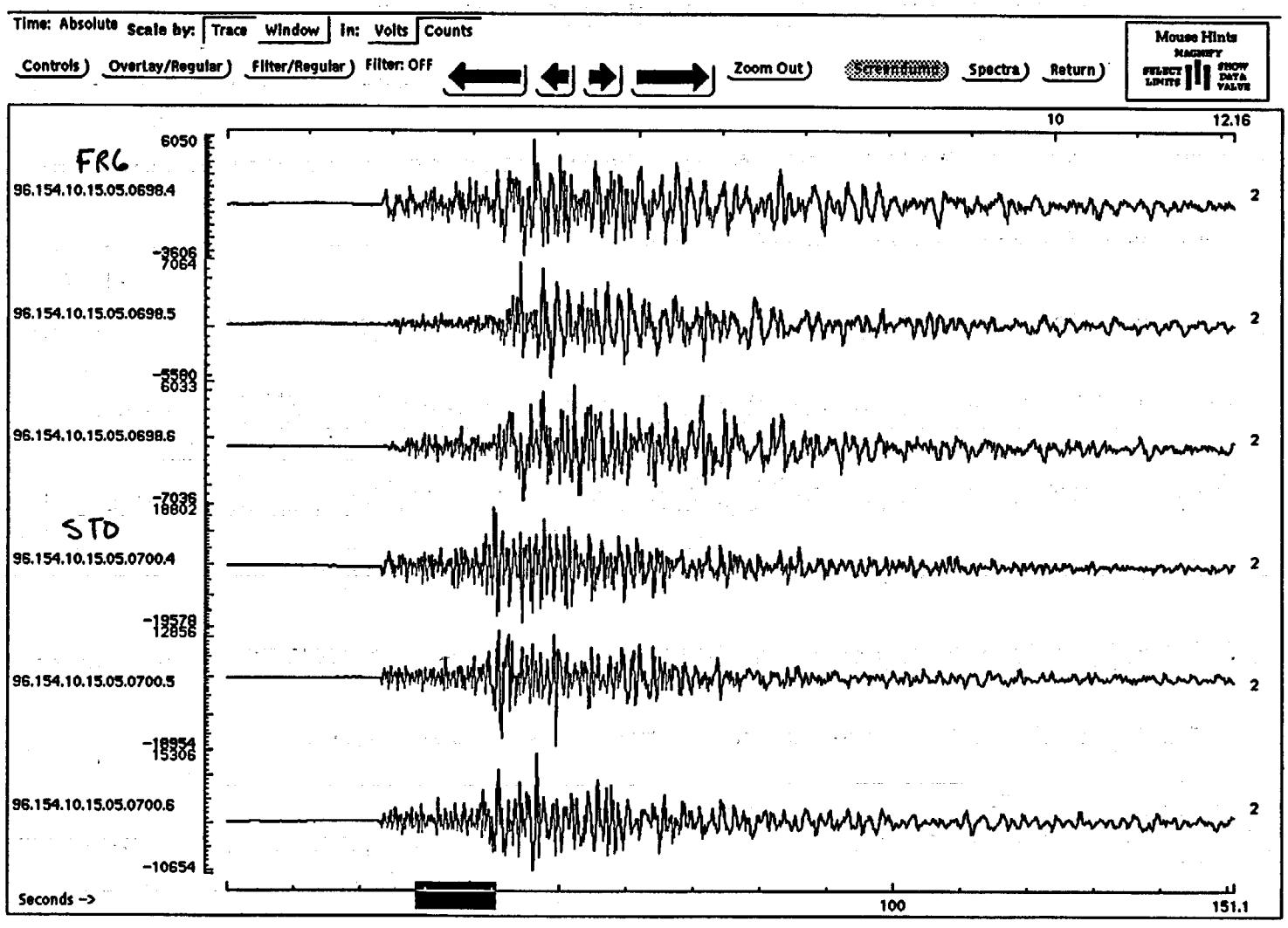
Time: Absolute
Scale by: Trace Window
In: Volts Counts
Controls
Overlay/Regular
Filter/Regular
Filter: OFF
Zoom Out
Screendump
Spectra
Return
Mouse Hints
10
12.16
FRG
6050
96.154.10.15.05.0698.4
-3606
7064
96.154.10.15.05.0698.5
-5580
6033
96.154.10.15.05.0698.6
-7036
18802
STD
96.154.10.15.05.0700.4
-19578
12856
96.154.10.15.05.0700.5
-18954
15306
96.154.10.15.05.0700.6
-10654
2
Seconds ->
100
151.1

7/31/96 # 14

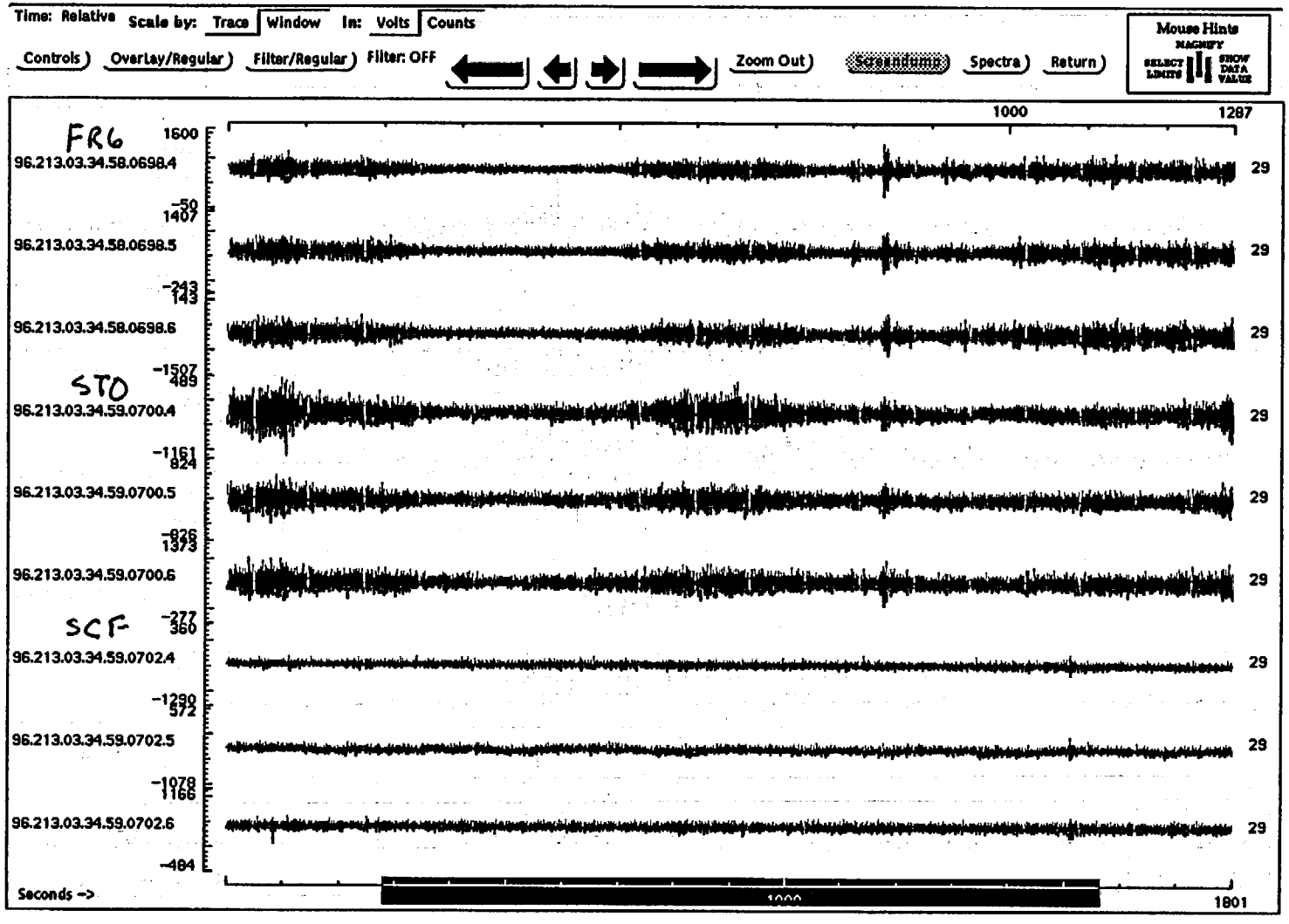
Time: Relative
Scale by: Trace Window In: Volts Counts
Controls
Overlay/Regular
Filter/Regular
Filter: OFF
Zoom Out
Spectra
Return
Mouse Hints
MAGNIFY
SELECT LIMITS
SHOW DATA VALUE
1000
1287
FR6
1600
96.213.03.34.58.0698.4
29
-50
1407
96.213.03.34.58.0698.5
29
-243
143
96.213.03.34.58.0698.6
29
STO
-1507
489
96.213.03.34.59.0700.4
29
-1161
824
96.213.03.34.59.0700.5
29
-826
1373
96.213.03.34.59.0700.6
29
SCF
-277
360
96.213.03.34.59.0702.4
29
-1290
572
96.213.03.34.59.0702.5
29
-1078
1166
96.213.03.34.59.0702.6
29
-484
Seconds ->
1000
1801

7/31/96 m ≈ -0.8 #14

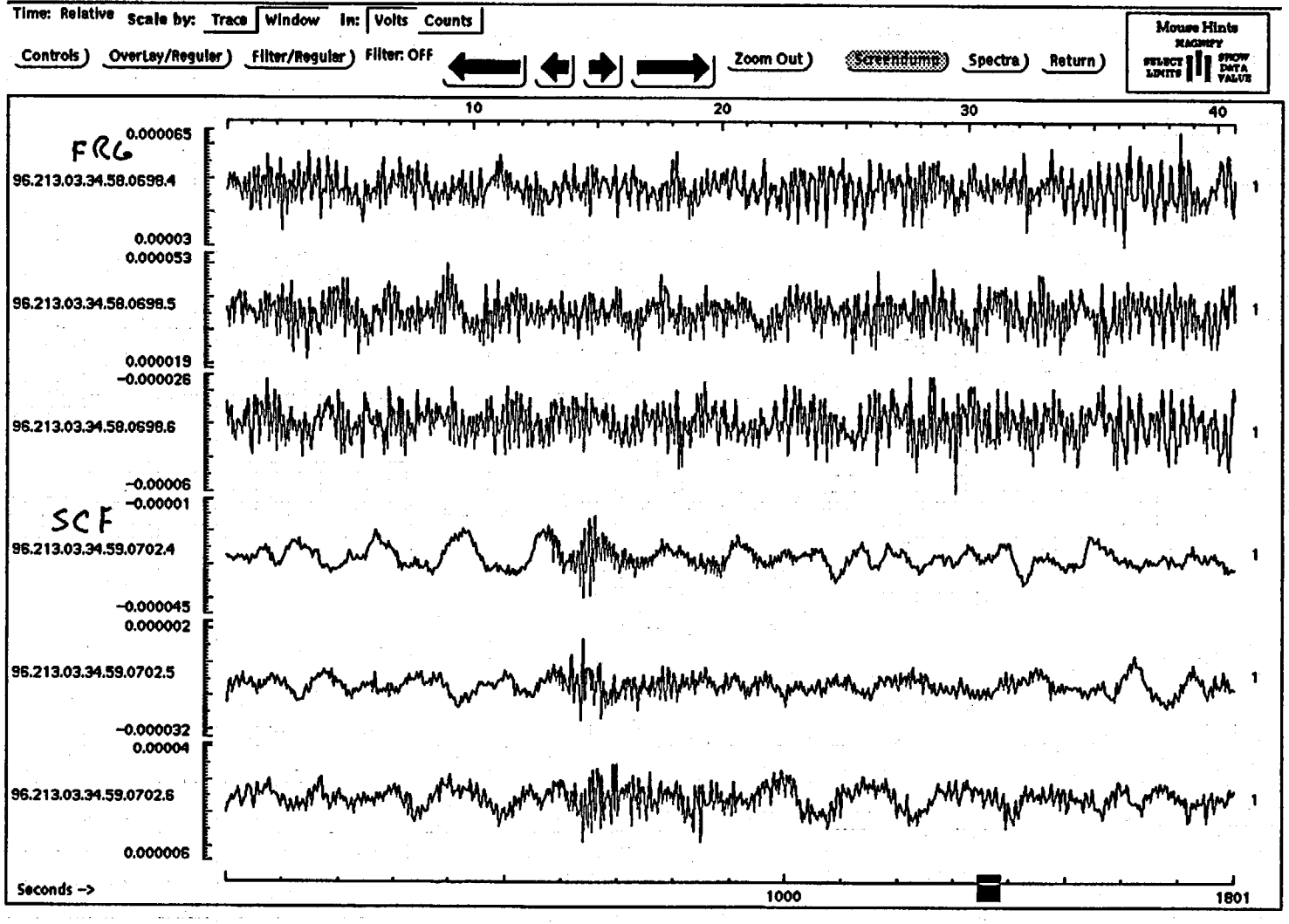
Time: Relative
Scale by: Trace Window In: Volts Counts
Controls
Overlay/Regular
Filter/Regular
Filter: OFF
Zoom Out
Screenfirms
Spectra
Return
Mouse Hints
MAGNIFY
SELECT LIMITS
SHOW DATA VALUE
10
20
30
40
FRG
0.000065
96.213.03.34.58.0698.4
0.00003
0.000053
96.213.03.34.58.0698.5
0.000019
-0.000026
96.213.03.34.58.0698.6
-0.00006
-0.00001
SCF
96.213.03.34.59.0702.4
-0.000045
0.000002
96.213.03.34.59.0702.5
-0.000032
0.00004
96.213.03.34.59.0702.6
0.000006
Seconds ->
1000
1801

Signal to Noise Values
-1
0
1
2
K&E
SEMI-LOGARITHMIC
5 CYCLES X 70 DIVISIONS
KEUFFEL & ESSER CO.
46 6213
MADE IN U.S.A.

Moment-Magnitude Scale for the Southern Great Basin

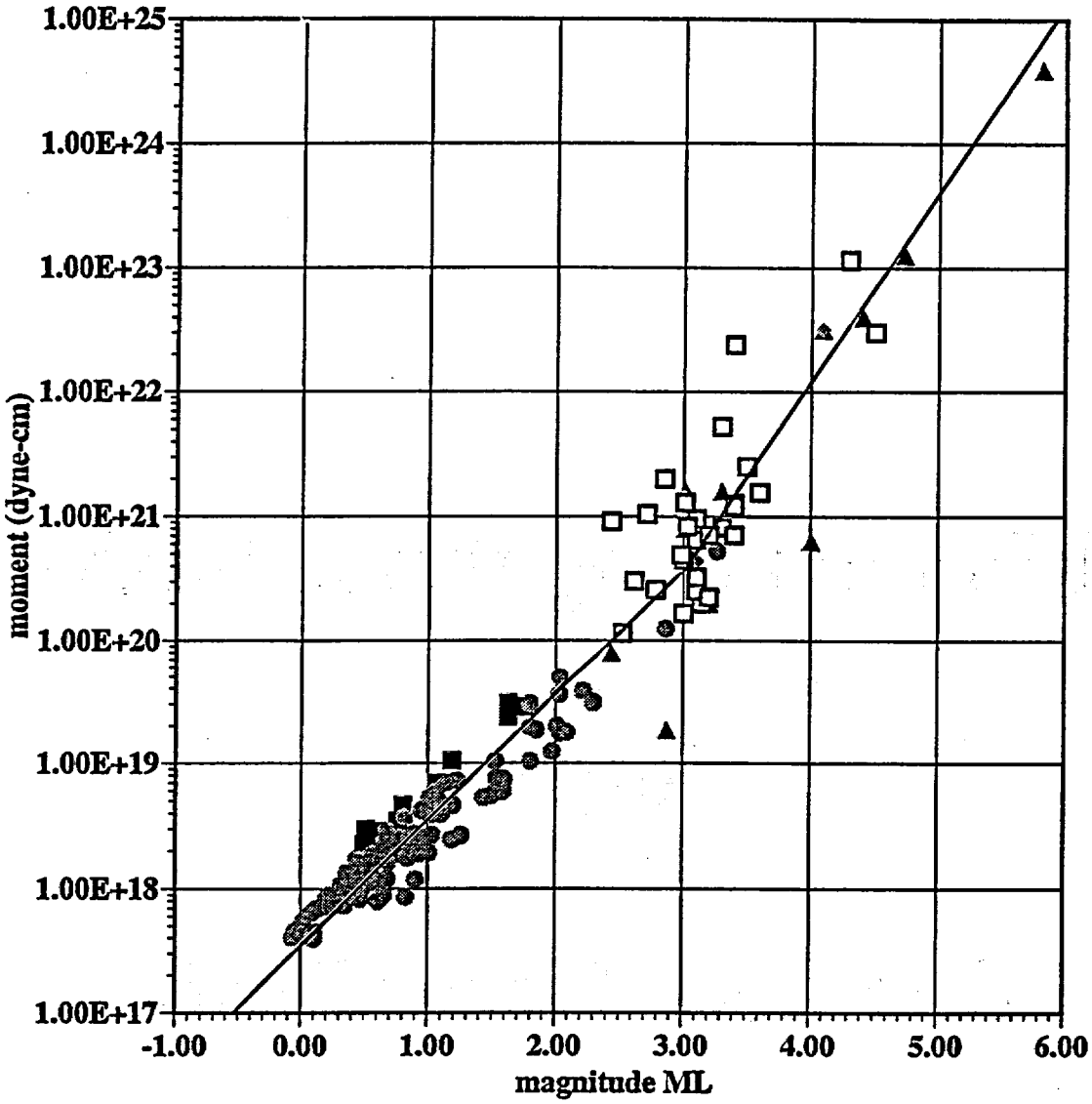

■	single-station (LSC) moment versus SGBSN ML
◍	SGBDSN moment versus SGBDSN ML
▲	Mayeda and Walters moment versus S & A or USGS ML
◆	Feng Su moment versus S&A or SGBSN ML
□	Deep Springs moment versus USGS ML

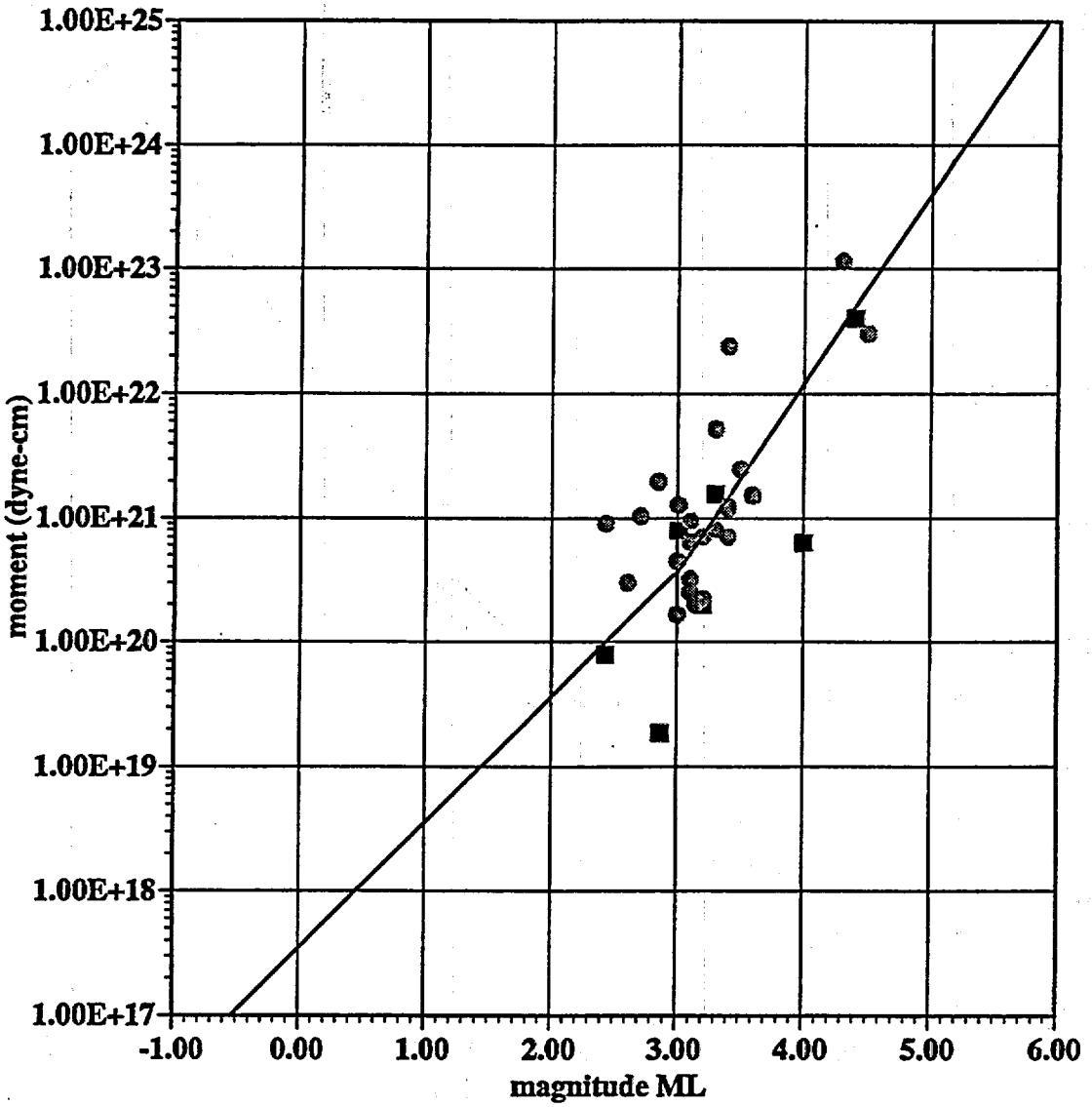

■	Mayeda and Walters moment versus USGS ML
●	Deep Springs moment versus USGS ML

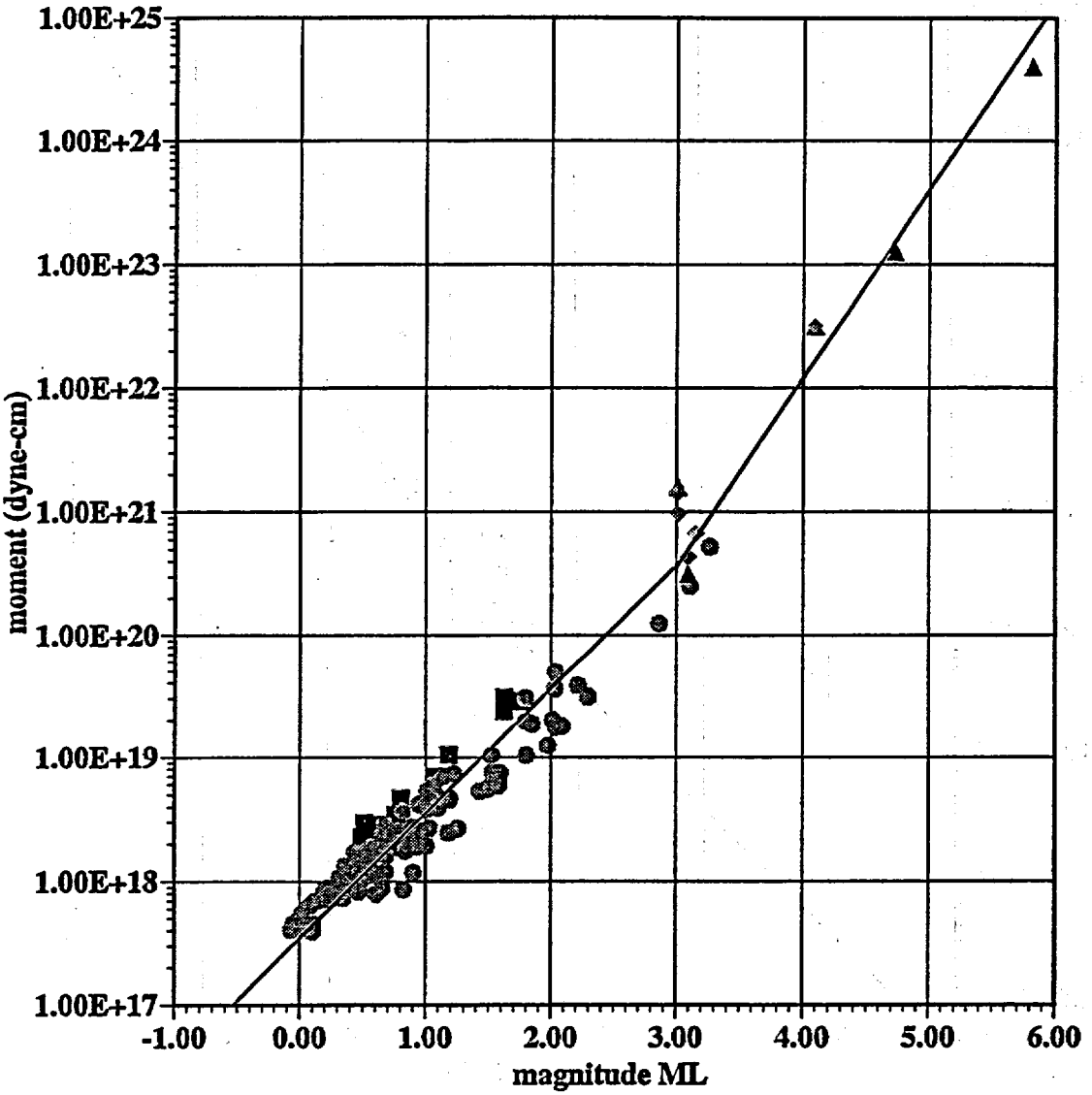

■	single-station (LSC) moment versus SGBSN ML
●	SGBDSN moment versus SGBDSN ML
▲	Mayeda and Walters moment versus S & A ML
◆	Feng Su moment versus S&A ML

METHODS FOR ESTIMATING MAXIMUM EARTHQUAKE MAGNITUDES

Kevin Coppersmith

Yucca Mountain Seismic Source Characterization Workshop #2

October 16-18, 1996
Salt Lake City, Utah

METHODS FOR ESTIMATING MAXIMUM EARTHQUAKE MAGNITUDES

MAXIMUM MAGNITUDE: the largest earthquake magnitude that a seismic source is capable of generating.

- Independent of frequency or time period
- Upper bound to recurrence relationship
- Uncertain (Mmax is rare relative to historical period of observation)

HOW IS Mmax ESTIMATED?

Every seismic source in a PSHA must be associated with a maximum magnitude, otherwise recurrence relationship is unbounded.

Constraints

- Historical seismicity
- Estimated rupture dimensions
- Analogy

Note: In western U.S. tectonic setting, seismic sources are usually faults and Mmax is usually estimated from rupture dimensions

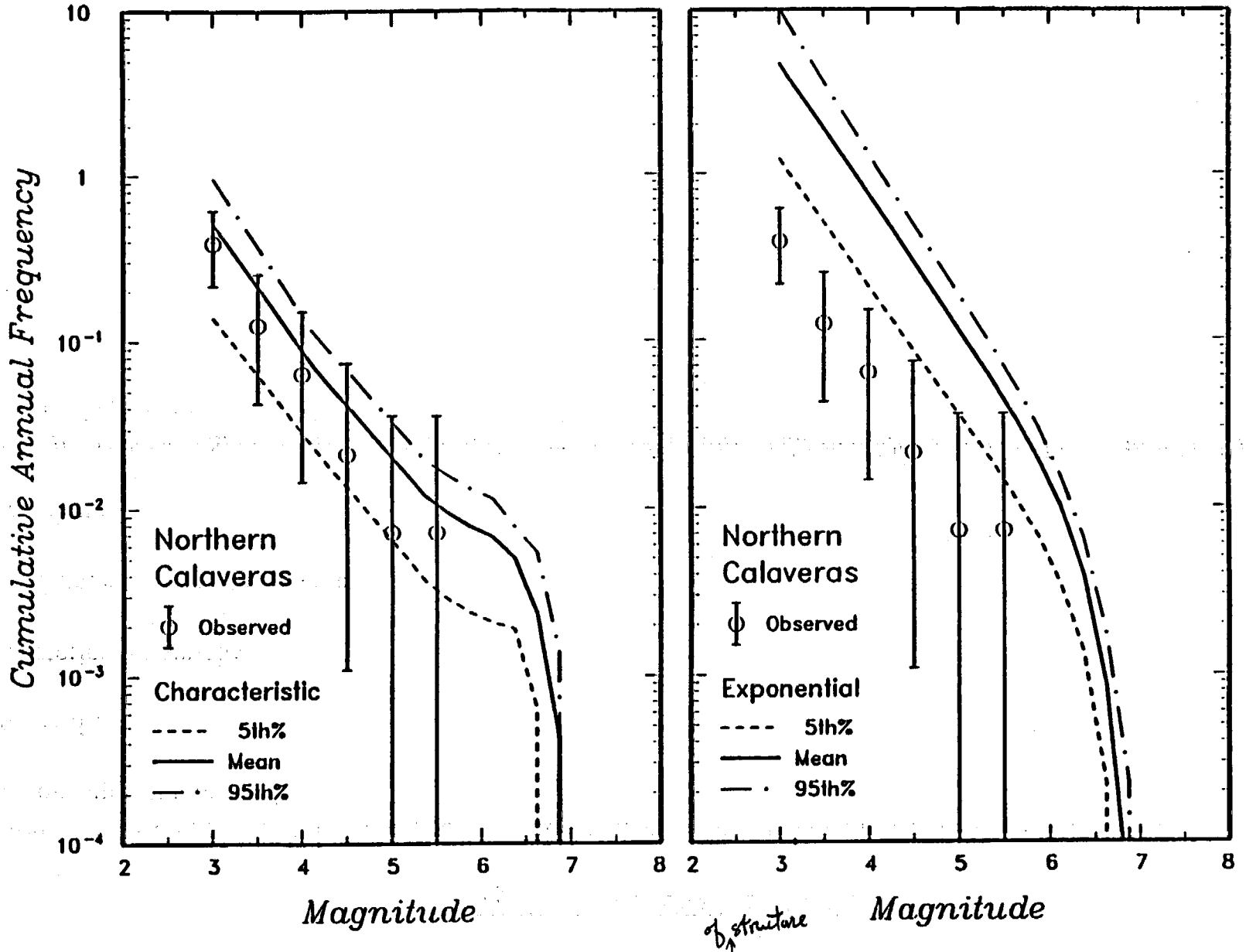

Figure 2-15 Comparison of recurrence rates developed from independent seismicity and from fault slip rates for the Northern Calaveras fault. Predicted recurrence rates are shown for the characteristic earthquake and exponential magnitude distribution models.

USING RUPTURE DIMENSIONS TO ESTIMATE Mmax

What is being estimated: the dimensions and magnitude of the maximum earthquake that can occur on a seismic source some time in the future.

Procedure:

1. Estimate the dimensions of rupture associated with a maximum event (e.g., rupture length, rupture area, displacement per event)

2. Using empirical correlations, estimate the magnitude associated with maximum rupture dimensions

3. Incorporate the uncertainties in the maximum rupture dimensions and in multiple estimates of the magnitude

ESTIMATING RUPTURE DIMENSIONS

Surface Rupture Length

Estimate the length of the largest future surface rupture, based on:

- Segmentation evidence: historical ruptures, timing of ruptures along length of fault, changes in behavior, geometric changes
- Fractional fault length

Subsurface Rupture Length

- Seismicity patterns (aftershocks)
- Identification of possible segmentation boundaries

Rupture Area

- Estimation of maximum downdip extent within seismogenic crust
- Seismogenic crustal thickness from focal depth distribution, heat flow, modeling

Maximum and Average Displacement Per Event

- Paleo-displacements from trenches, geomorphic evidence
- Distribution of slip along length of fault

Seismic Moment

- Distribution of slip along length of fault; relation to subsurface slip

Rupture Length, Slip Rate

- Late Quaternary slip rate

Table 2C
Regressions of Surface Rupture Length and Displacement

Equation*	Slip Type†	Number of Events	Coefficients and Standard Errors a(sa)	b(sb)	Standard Deviation s	Correlation Coefficient r	Displacement Range (m)	Rupture Length Range (km)
log (MD) = a + b * log (SRL)	SS	55	−1.69(0.16)	1.16(0.09)	0.36	0.86	0.01 to 14.6	1.3 to 432
	{R‡	*21*	*−0.44(0.34)*	*0.42(0.23)*	*0.43*	*0.38*	*0.11 to 6.5*	*4 to 148}*
	N	19	−1.98(0.50)	1.51(0.35)	0.41	0.73	0.06 to 6.4	3.8 to 75
	All	95	−1.38(0.15)	1.02(0.09)	0.41	0.75	0.01 to 14.6	1.3 to 432
log (SRL) = a + b * log (MD)	SS	55	1.49(0.04)	0.64(0.05)	0.27	0.86	0.01 to 14.6	1.3 to 432
	{R	*21*	*1.36(0.09)*	*0.35(0.19)*	*0.39*	*0.38*	*0.11 to 6.5*	*4 to 148}*
	N	19	1.36(0.05)	0.35(0.08)	0.20	0.73	0.06 to 6.4	3.8 to 75
	All	95	1.43(0.03)	0.56(0.05)	0.31	0.75	0.01 to 14.6	1.3 to 432
log (AD) = a + b * log (SRL)	SS	35	−1.70(0.23)	1.04(0.13)	0.32	0.82	0.10 to 8.0	3.8 to 432
	{R	*17*	*−0.60(0.39)*	*0.31(0.27)*	*0.40*	*0.28*	*0.06 to 2.6*	*6.7 to 148}*
	N	14	−1.99(0.72)	1.24(0.49)	0.37	0.59	0.08 to 2.1	15 to 75
	All	66	−1.43(0.18)	0.88(0.11)	0.36	0.71	0.06 to 8.0	3.8 to 432
log (SRL) = a + b * log (AD)	SS	35	1.68(0.04)	0.65(0.08)	0.26	0.82	0.10 to 8.0	3.8 to 432
	{R	*17*	*1.45(0.10)*	*0.26(0.23)*	*0.36*	*0.28*	*0.06 to 2.6*	*6.7 to 148}*
	N	14	1.52(0.05)	0.28(0.11)	0.17	0.59	0.08 to 2.1	15 to 75
	All	66	1.61(0.04)	0.57(0.07)	0.29	0.71	0.06 to 8.0	3.8 to 432

*SRL—surface rupture length (km); MD—maximum displacement (m); AD—average displacement (m).
§SS—strike slip; R—reverse; N—normal.
‡Regressions for reverse-slip relationships shown in italics and brackets are not significant at a 95% probability level.

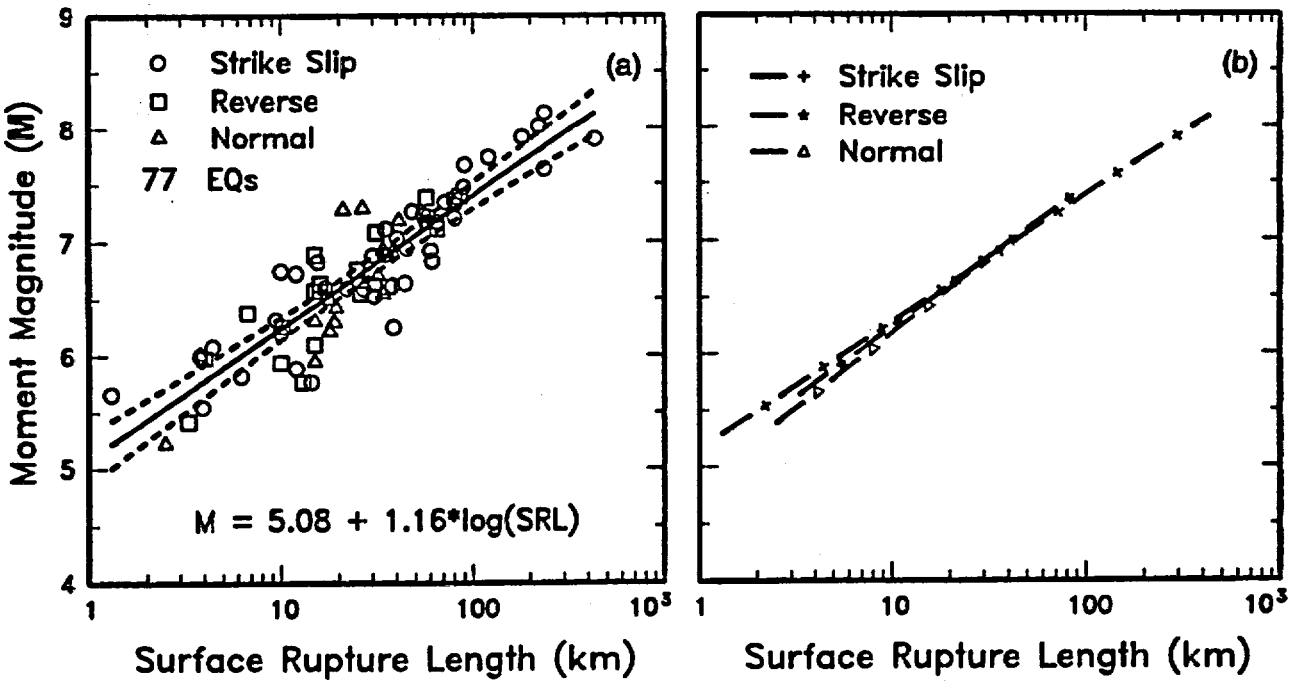

Figure 9. (a) Regression of surface rupture length on magnitude (M). Regression line shown for all-slip-type relationship. Short dashed line indicates 95% confidence interval. (b) Regression lines for strike-slip, reverse, and normal-slip relationships. See Table 2 for regression coefficients. Length of regression lines shows the range of data for each relationship.

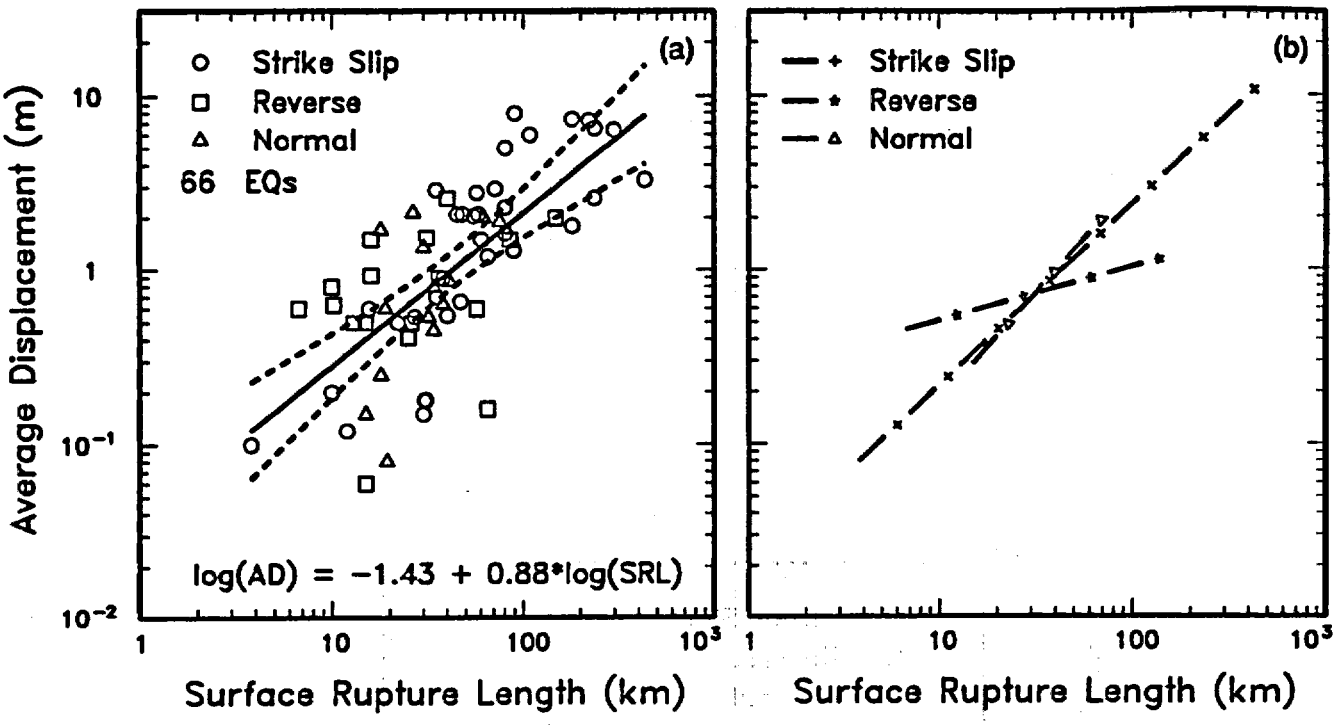

Figure 13. (a) Regression of surface rupture length on average displacement. Regression line shown for all-slip-type relationship. Short dashed line indicates 95% confidence interval. (b) Regression lines for strike-slip, reverse, and normal-slip relationships. See Table 2 for regression coefficients. Length of regression lines shows the range of data for each relationship.

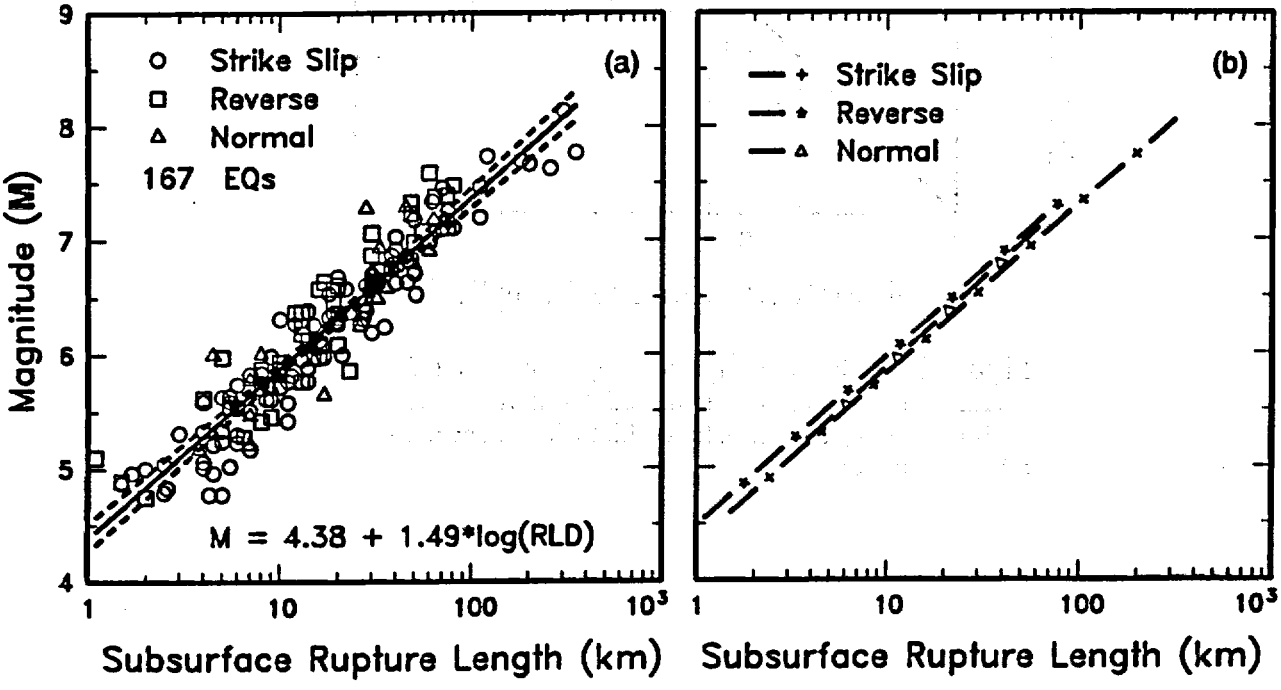

Figure 14. (a) Regression of subsurface rupture length on magnitude (M). Regression line shown for all-slip-type relationship. Short dashed line indicates 95% confidence interval. (b) Regression lines for strike-slip relationships. See Table 2 for regression coefficients. Length of regression lines shows the range of data for each relationship.

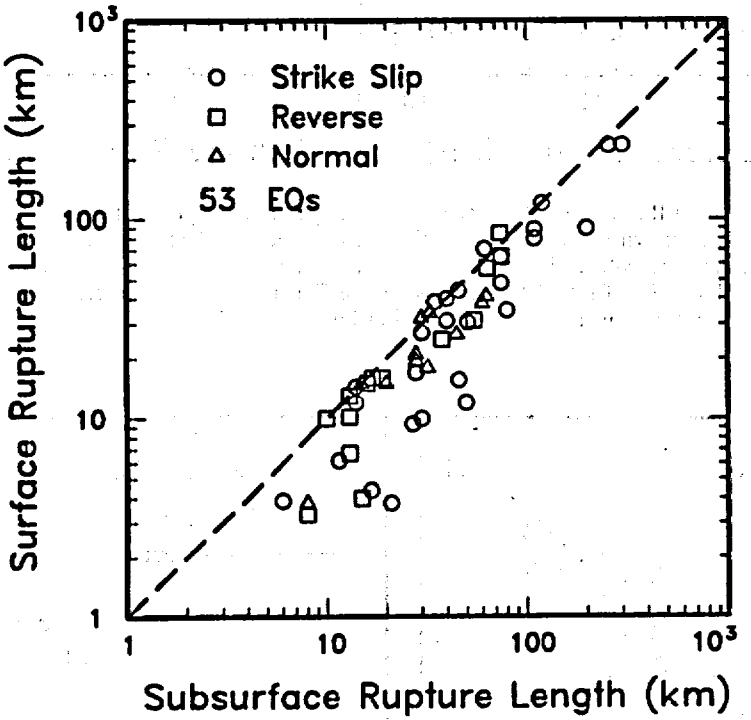

Figure 2. Surface rupture length versus subsurface rupture length estimated from the distribution of early aftershocks of historical continental earthquakes.

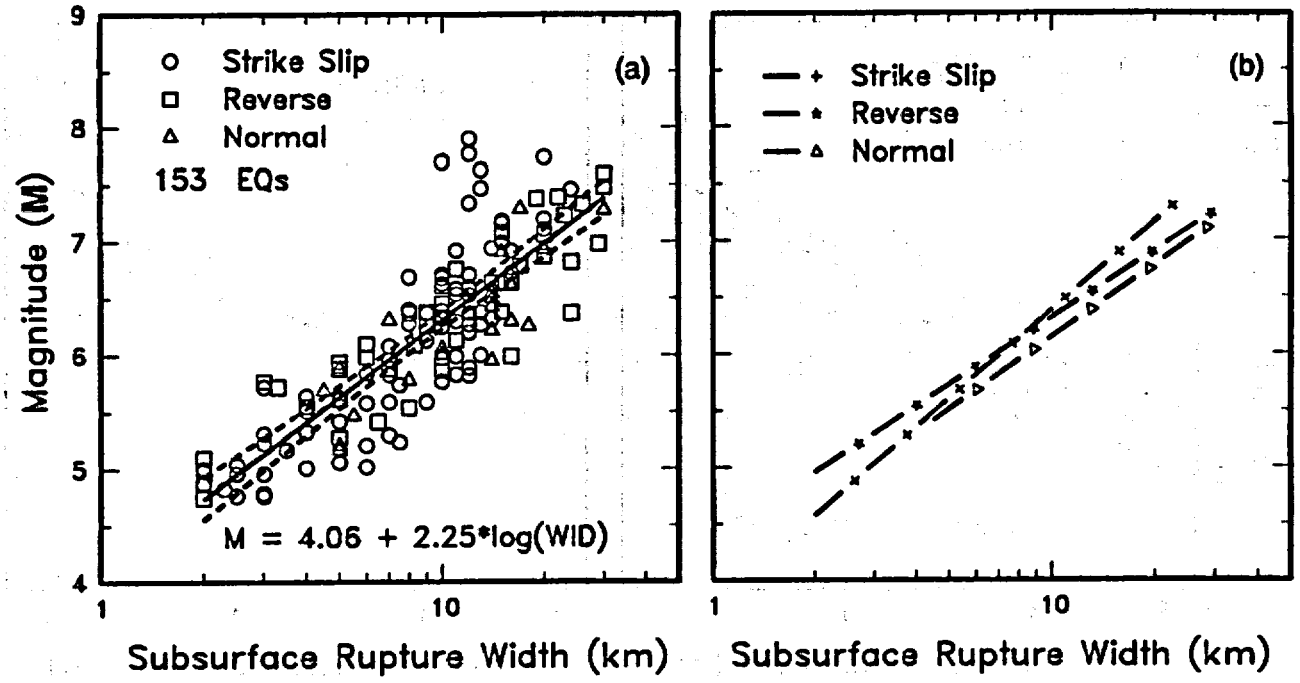

Figure 15. (a) Regression of downdip rupture width on magnitude (M). Regression line shown for all-slip-type relationship. Short dashed line indicates 95% confidence interval. (b) Regression lines for strike-slip, reverse, and normal-slip relationships. See Table 2 for regression coefficients. Length of regression lines shows the range of data for each relationship.

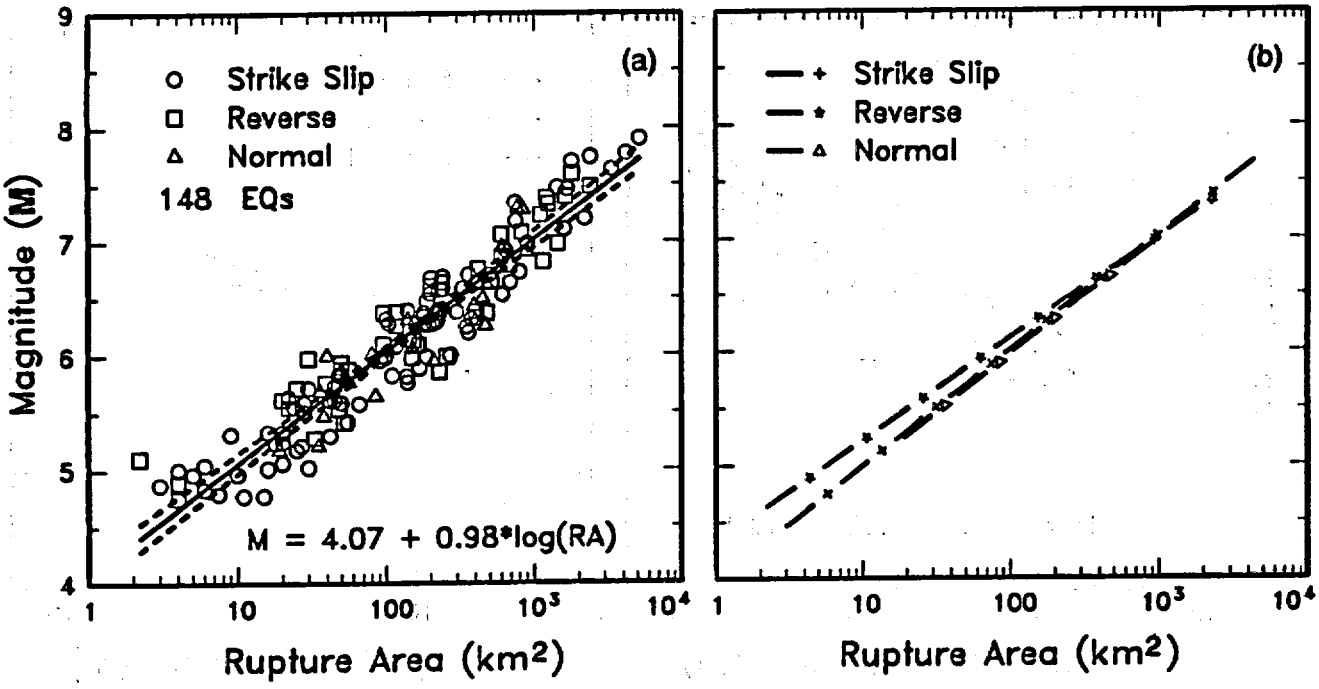

Figure 16. (a) Regression of rupture area on magnitude (M). Regression line shown for all-slip-type relationship. Short dashed line indicates 95% confidence interval. (b) Regression lines for strike-slip, reverse, and normal-slip relationships. See Table 2 for regression coefficients. Length of regression lines shows the range of data for each relationship.

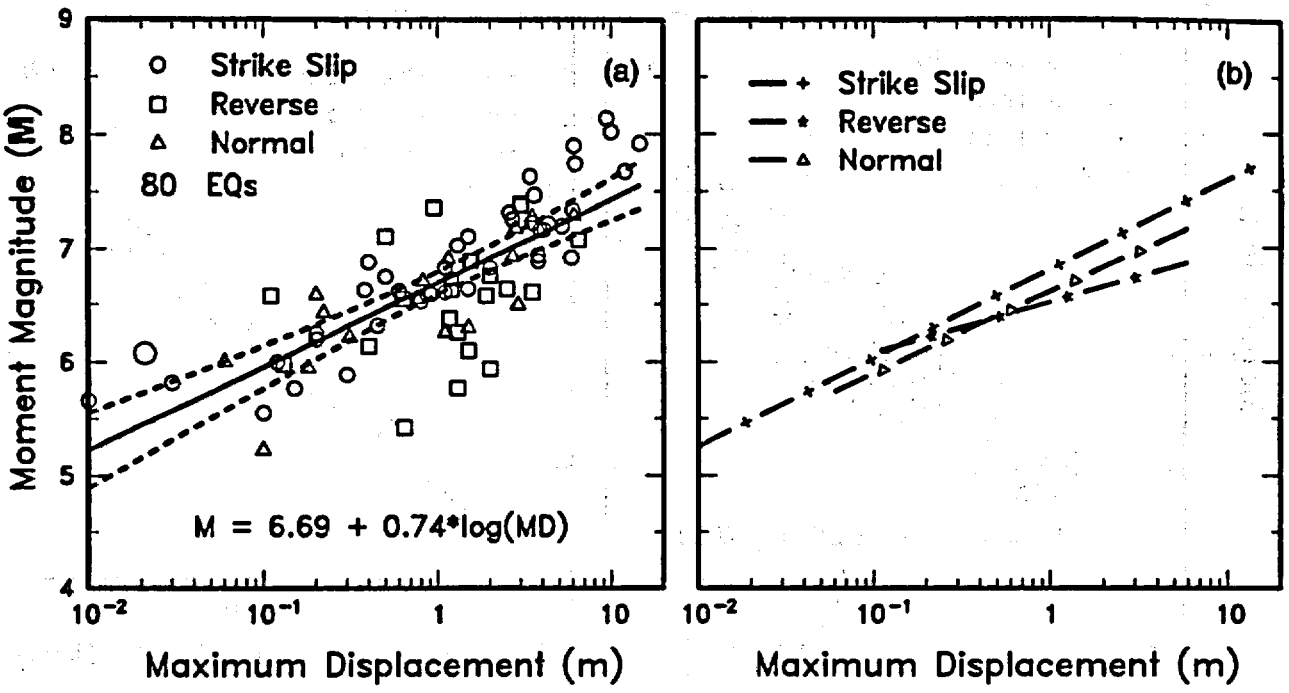

Figure 10. (a) Regression of maximum surface displacement on magnitude (M). Regression line shown for all-slip-type relationship. Short dashed line indicates 95% confidence interval. (b) Regression lines for strike-slip, reverse, and normal-slip relationships. See Table 2 for regression coefficients. Length of regression lines shows the range of data for each relationship.

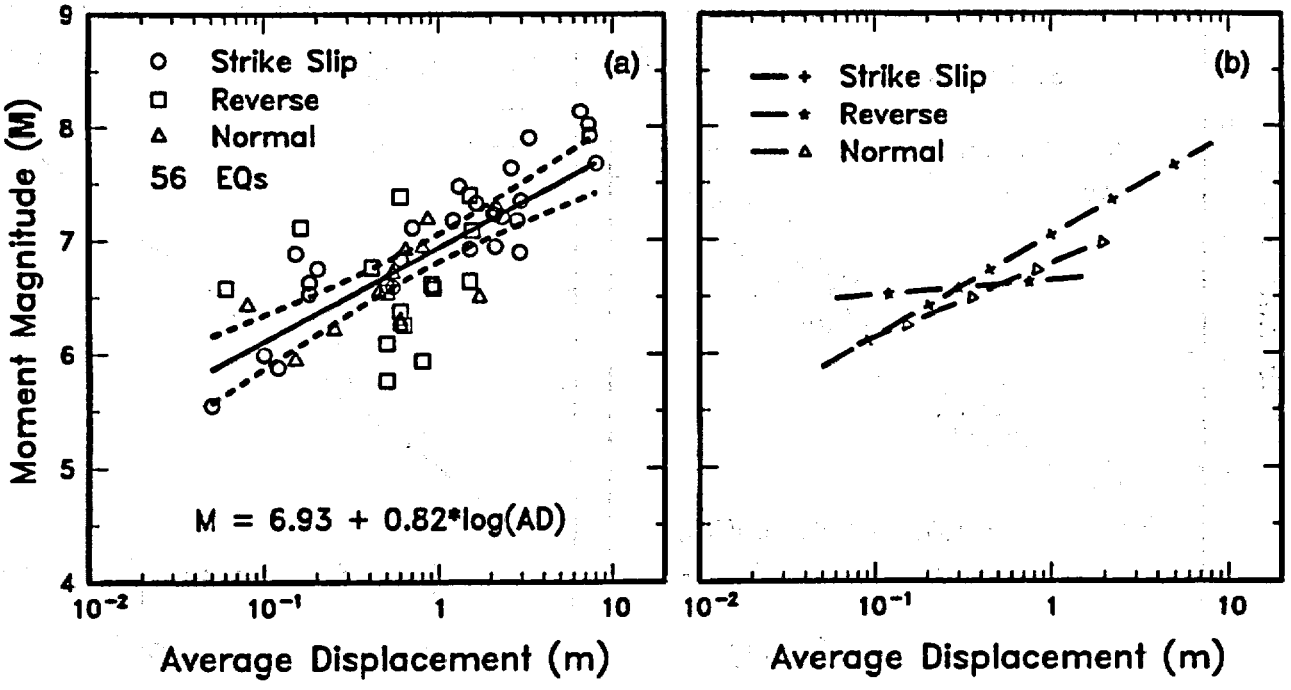

Figure 11. (a) Regression of average surface displacement on magnitude (M). Regression line shown for all-slip-type relationship. Short dashed line indicates 95% confidence interval. (b) Regression lines for strike-slip, reverse, and normal-slip relationships. See Table 2 for regression coefficients. Length of regression lines shows the range of data for each relationship.

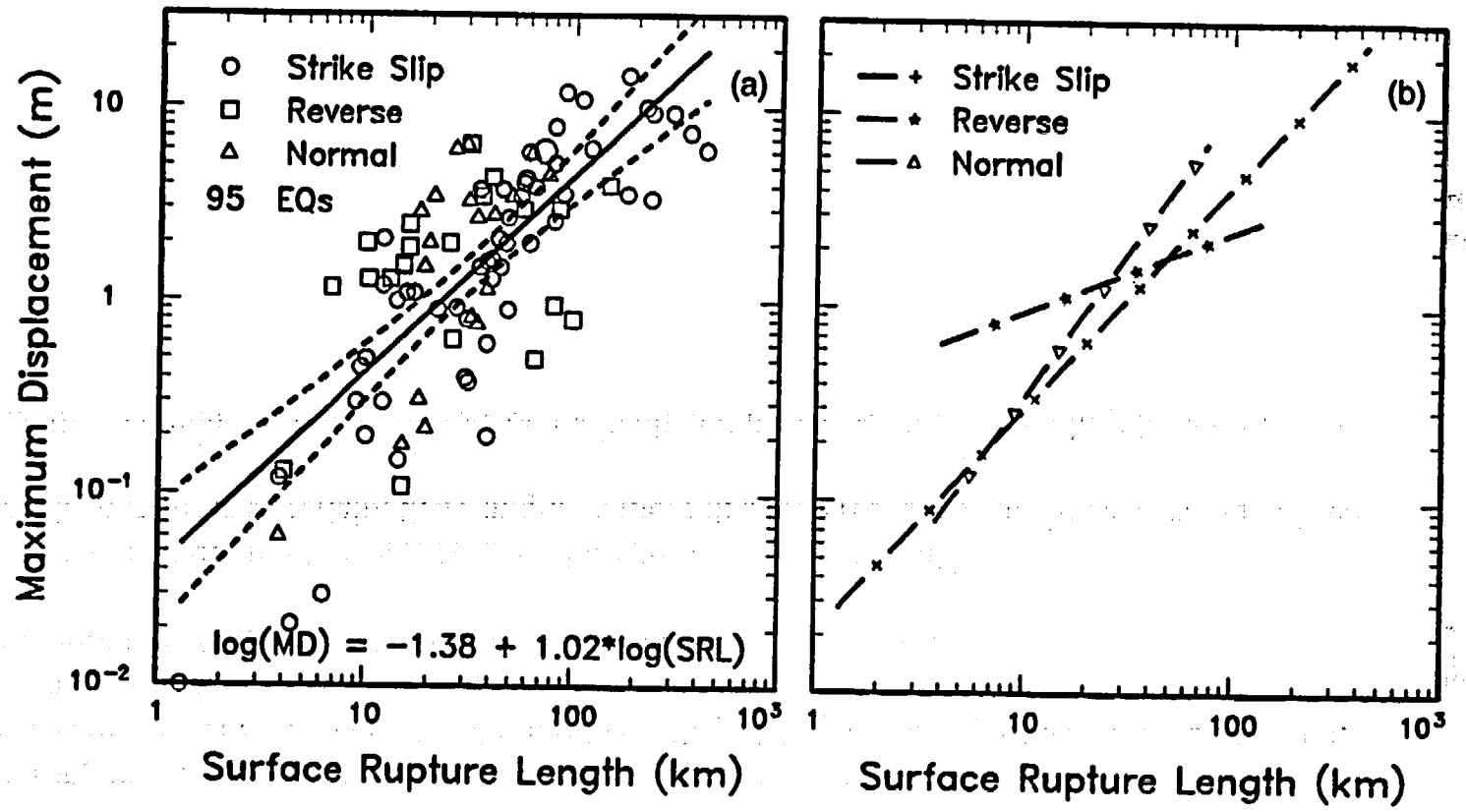

Figure 12. (a) Regression of surface rupture length on maximum displacement. Regression line shown for all-slip-type relationship. Short dashed line indicates 95% confidence interval. (b) Regression lines for strike-slip, reverse, and normal-slip relationships. See Table 2 for regression coefficients. Length of regression lines shows the range of data for each relationship.

COMMON MISTAKE IN ESTIMATING Mmax

1. Identify segments at a variety of scales (usually geometric segments)

2. Ask yourself wrong question: "Which of these segment lengths is most likely to occur?"
   - This is a *frequency* or *recurrence* question; reflects the relative frequency of occurrence of various size ruptures (magnitudes)
   - Shorter, more likely segments defines recurrence of sub-Mmax events

3. Instead: "Which segment defines the maximum rupture possible on this fault?"
   - Because the answer is uncertain, there might be more than one rupture segment scenario identified

4. Goal: To define the maximum rupture possible on the fault and the associated uncertainty in defining the maximum event.

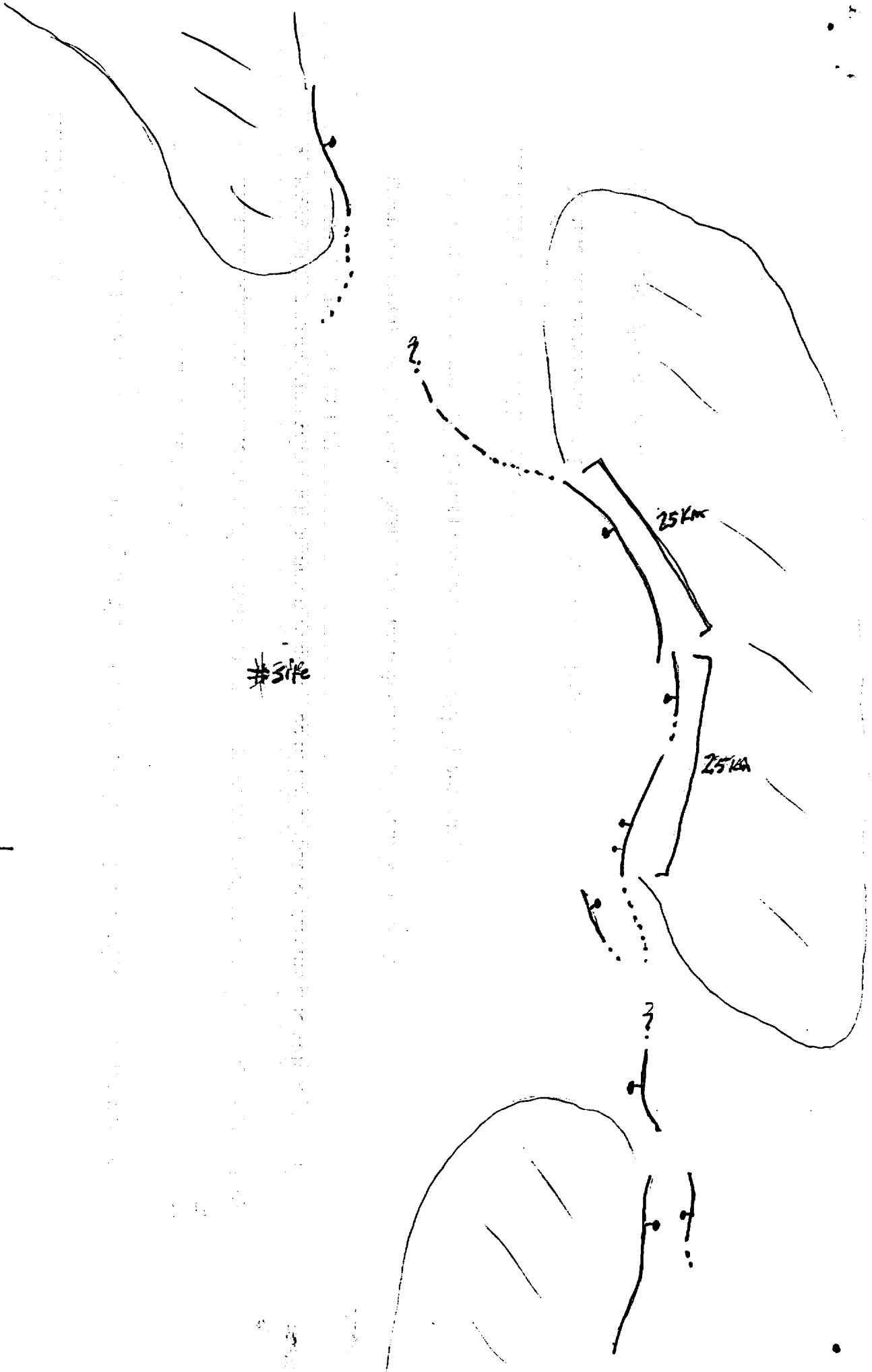

Scenarios

25 Km
50 Km
85 Km
105 Km

TOOLS FOR HANDLING UNCERTAINTIES IN Mmax

LOGIC TREES

- Can be used to express the uncertainty in alternative *approaches* and alternative *parameter values*.
- Elements of tree sequenced logically
- Branches represent discrete alternative 'states of nature' (mutually exclusive, collectively exhausitive)
- Probabilities associated with each branch reflect degree of belief that represents true value, given the available data (sum to 1.0)
- Documentation should provide basis for all branches and their relative weights
- (At Workshop #3 we will discuss methods for probability encoding)

CONTINUOUS DISTRIBUTIONS

- Continuous parameters can be expressed as distribution
- Can sample using simulation

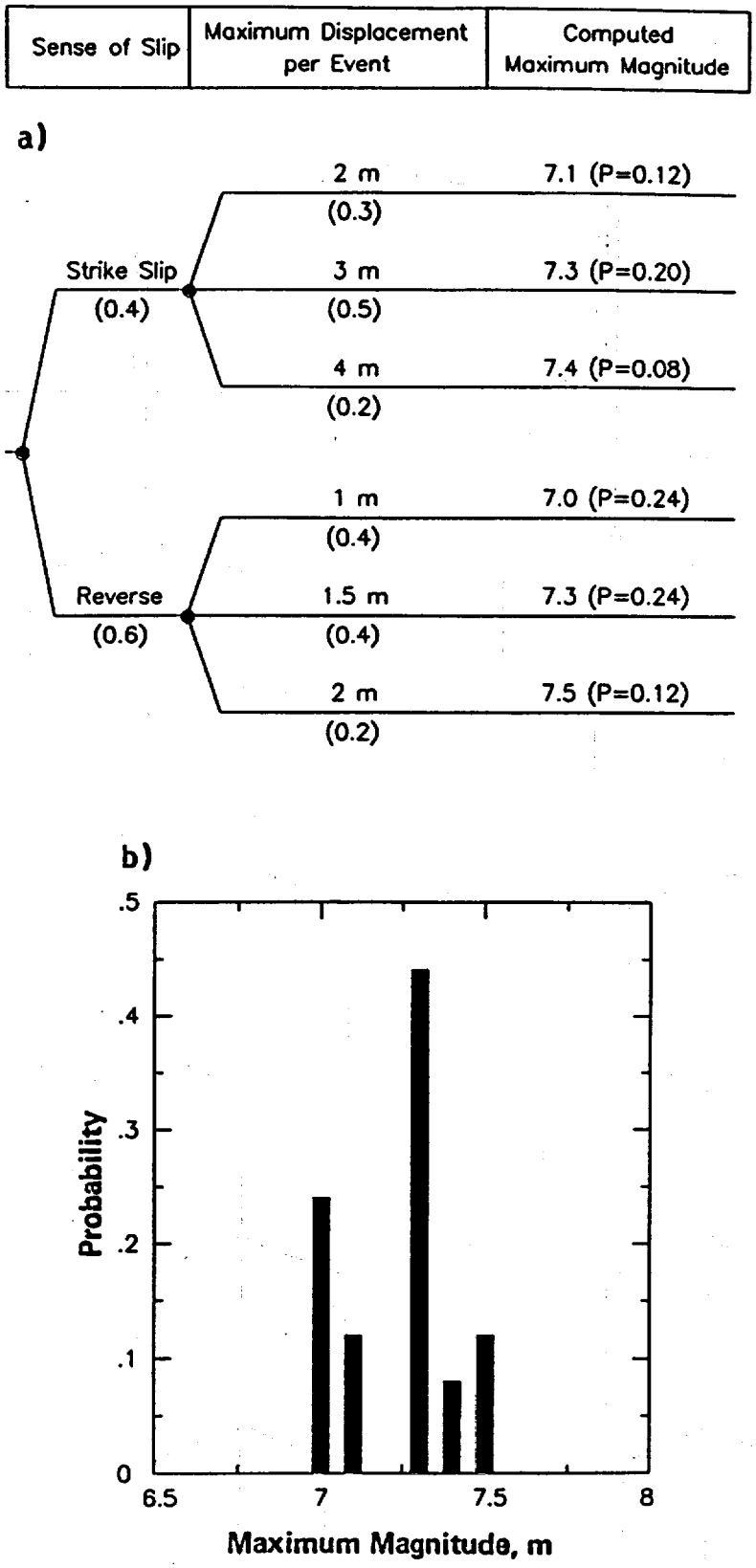

Figure 2. Example use of logic tree. (a) Example logic tree showing two parameters related to maximum magnitude: sense-of-slip and maximum rupture length. The resulting maximum-magnitude values are each associated with a probability that is the product of the conditional probabilities on the branches leading to each magnitude value. (b) Discrete distribution of maximum magnitude resulting from the logic tree assessments.

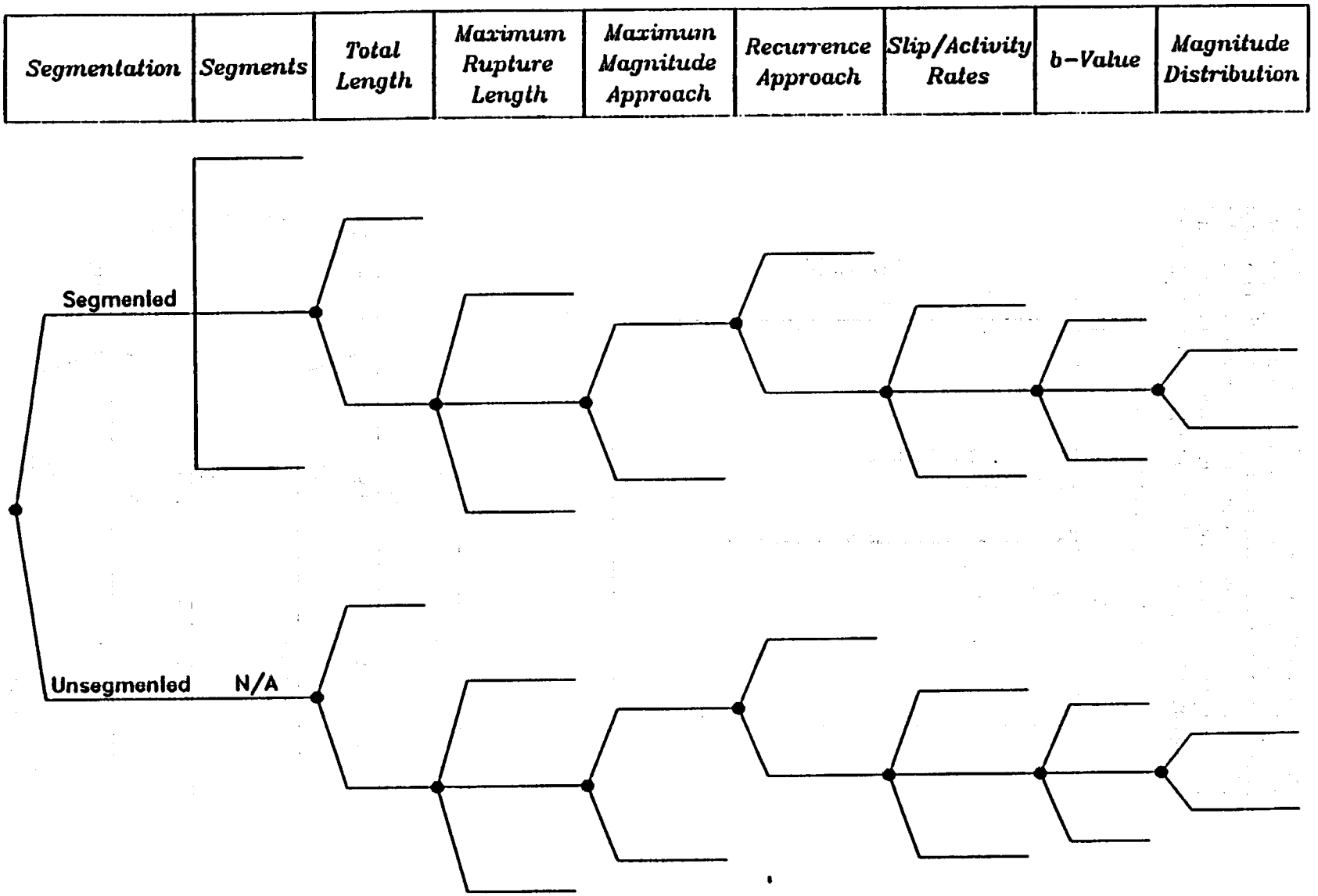

Figure 2-9 Generic logic tree used in this study to characterize seismic sources for probabilistic seismic hazard analysis.

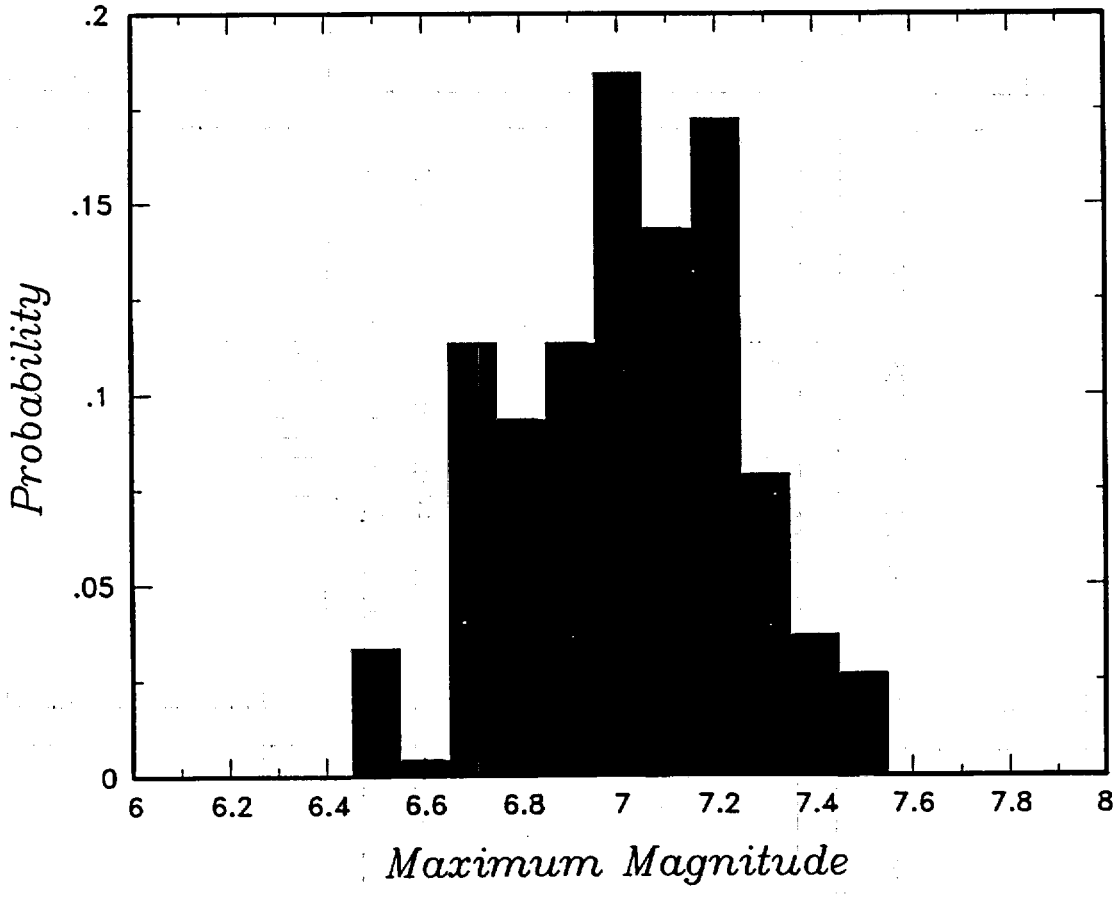

Figure 1 Maximum magnitude distribution for the Stansbury Fault (Mean Mmax = 7.0)

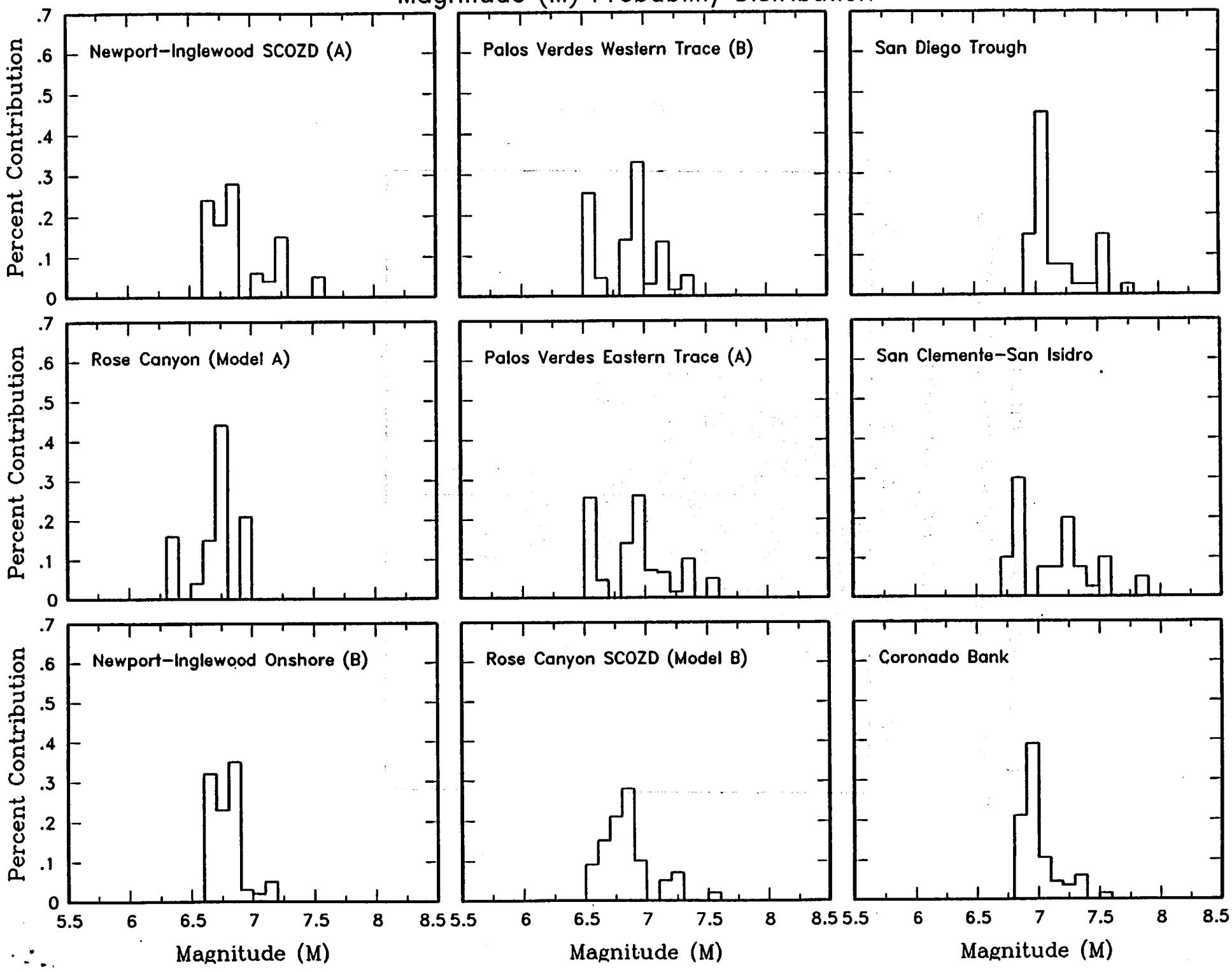
Magnitude (M) Probability Distribution
Newport-Inglewood SCOZD (A)
Palos Verdes Western Trace (B)
San Diego Trough
Rose Canyon (Model A)
Palos Verdes Eastern Trace (A)
San Clemente-San Isidro
Newport-Inglewood Onshore (B)
Rose Canyon SCOZD (Model B)
Coronado Bank
Percent Contribution
0
.1
.2
.3
.4
.5
.6
.7
5.5
6
6.5
7
7.5
8
8.5
Magnitude (M)

Maximum Earthquake Magnitudes at Yucca Mountain

Data Related to Fault Rupture Length, Fault Segmentation, and Displacement per Event on Yucca Mountain Faults

presented by

Silvio Pezzopane

U.S. Geological Survey

Yucca Mountain Project

Fault Rupture Length

- assume rupture of maximum fault length or some fraction of length
  - – indirect, inferential, assumptive
  - » ruptures not always simple and continuous along a single fault
  - » ruptures may step, splay, and form broad parallel zones
- identify faults or fault segments that ruptured at certain times
  - – most direct, credible
  - » timing of paleoevents
  - » trench locations
    - – constrains minimum rupture length
  - » displacement per event

Paleoseismic Timing Data

- Dating Techniques
  - » Thermoluminescence
  - » U-series
  - » Ash Correlation and Dating
  - » Correlation of Quaternary Deposits and Soils
  - » Archeological
- Revised Older (1980's) Trench Dates
  - » U-trend and older U-series
- in USGS Seismotectonic Report—Chapter 4
  - » Complete Catalog of Dates
  - » Description of Trench Data

Some Definitions

- Paleoevent—'Paleo Surface Rupture' recognized in one trench across one fault
  - » fracturing may or may not represent an individual paleoearthquake
  - » trench and study specific
- Rupture Scenario—Paleoevents of a <u>Similar Age</u> on one or more Faults
  - » probable paleoearthquakes
  - » minimum and maximum rupture length
  - » displacement per event
  - » accounts for distributed faulting

Paleoevent Timing Distributions

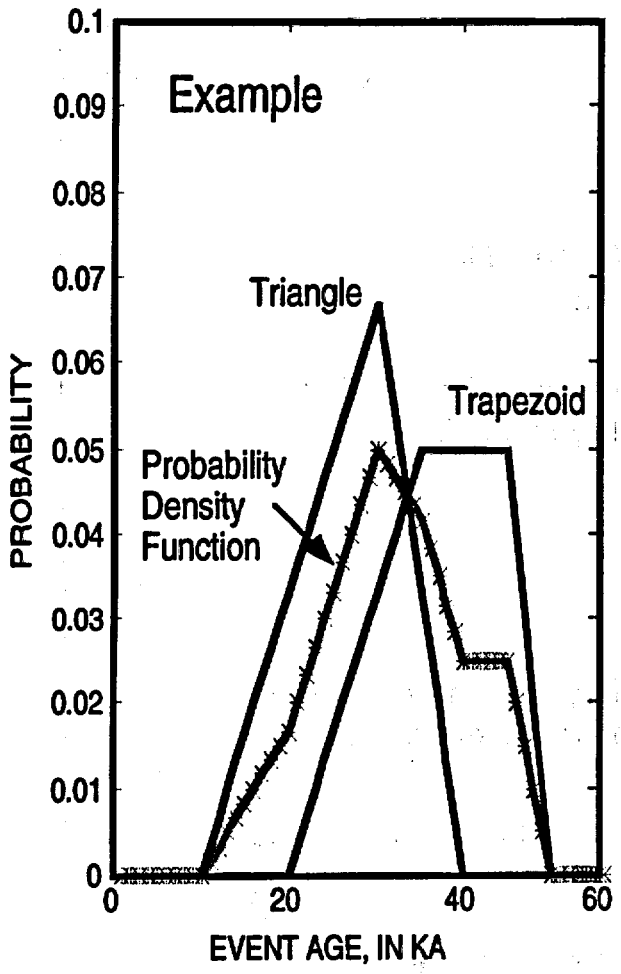

in USGS Seismotectonic Report—Chapter 5

- Example Timing Distribution Functions
  - » Triangle and Trapezoid
- Cross-hatched line is PDF for Event Age and Uncert.
- Paleoevents of Similar Age are Probable Paleo-Earthquake
- 9 Yucca Mtn Rupture Scenarios

Timing PDF of Rupture Scenario Z

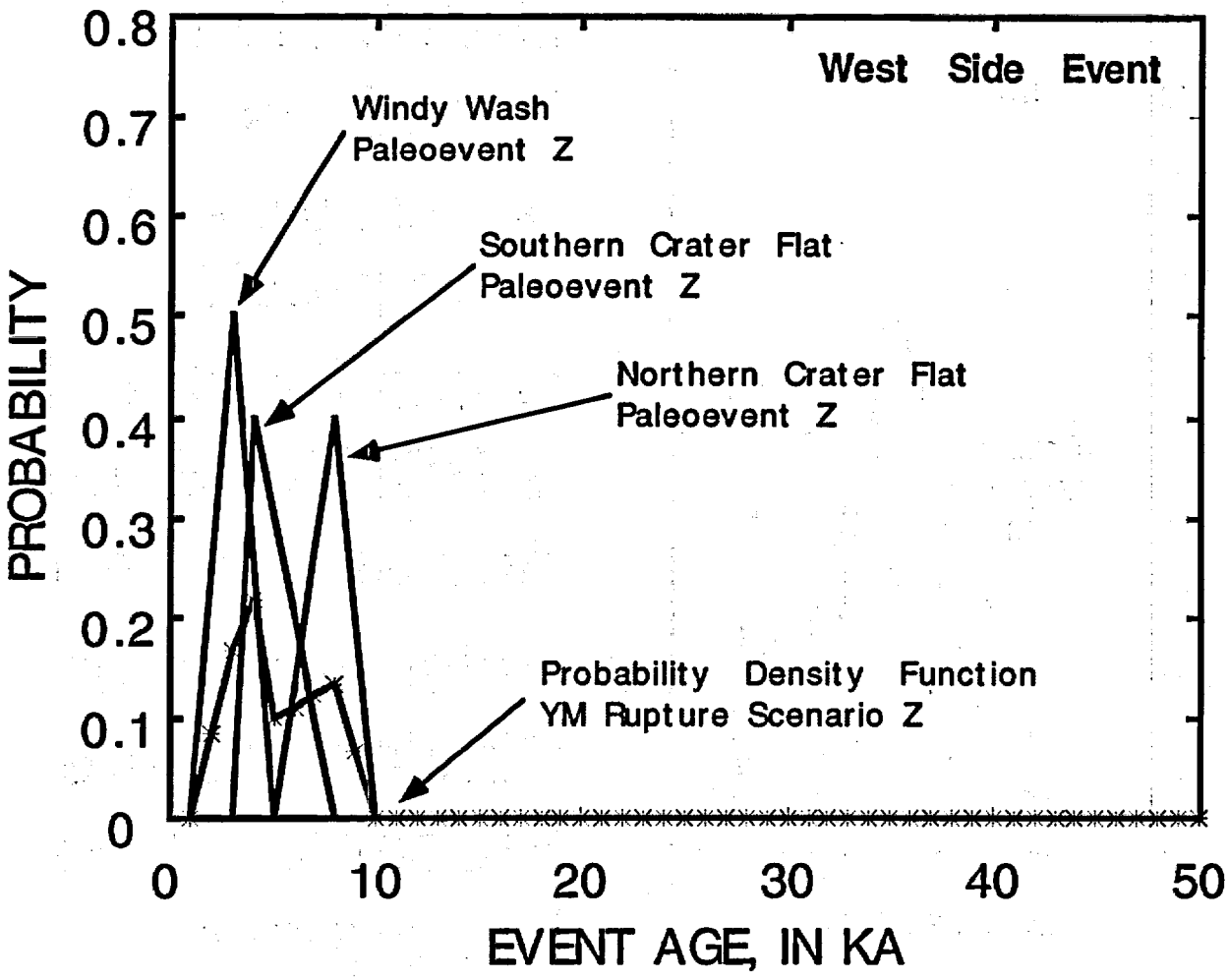

in USGS Seismotectonic Report—Chapter 5

Scenario Z

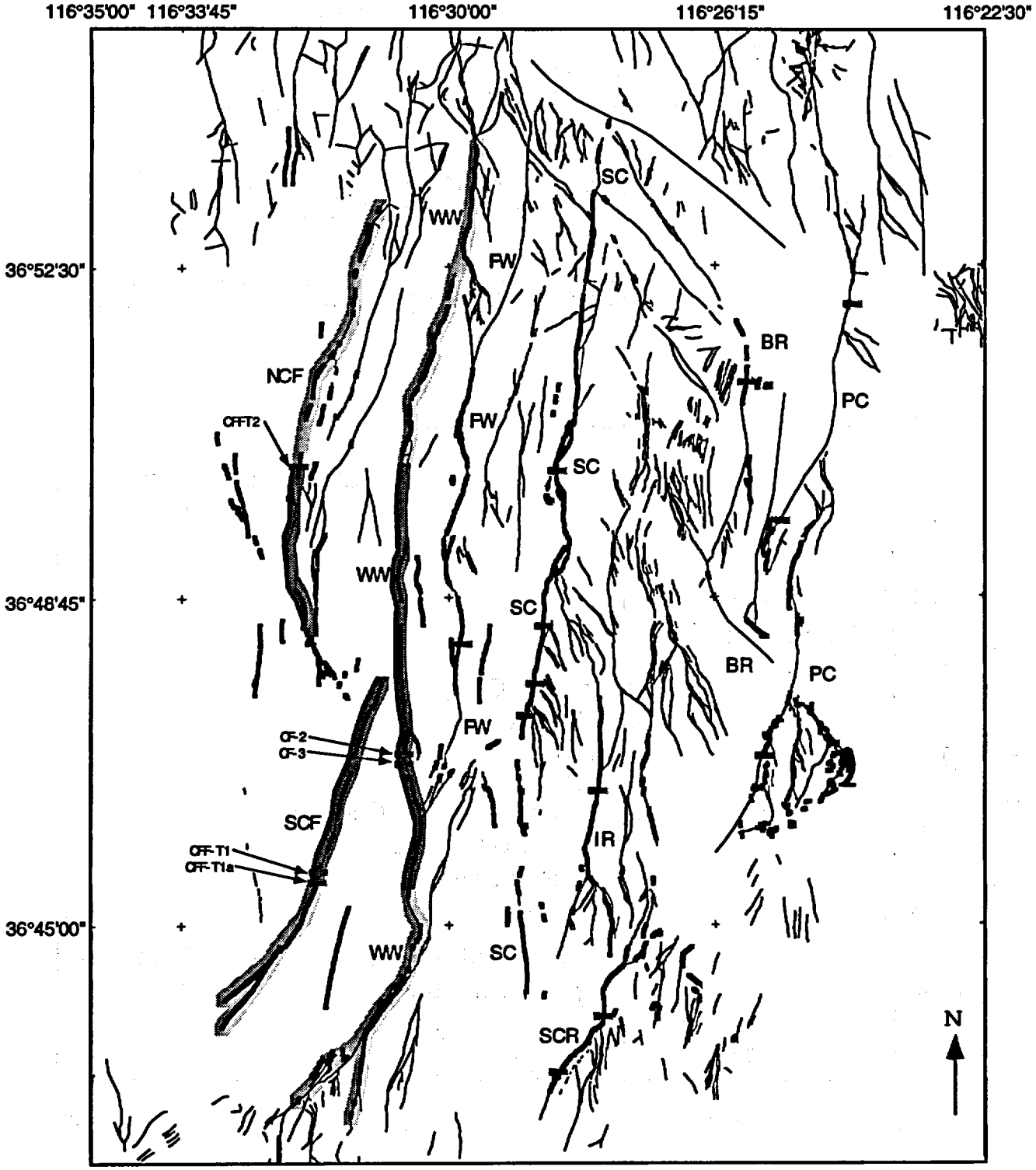

EXPLANATION

- Scenario Z minimum surface rupture length
- Scenario Z maximum surface rupture length
- Trench locations
- Faults; Quaternary and suspected Quaternary age of last movement
- Faults; pre-Quaternary or undetermined age of last movement

0 kilometers 5

Fault Abbreviations

BR = Bow Ridge	SC = Solitario Canyon
FW = Fatigue Wash	SCF = South Crater Flat
IR = Iron Ridge	SCR = Stagecoach Road
NCF = North Crater Flat	WW = Windy Wash
PC = Paintbrush Canyon	

Timing PDF of Rupture Scenario Y

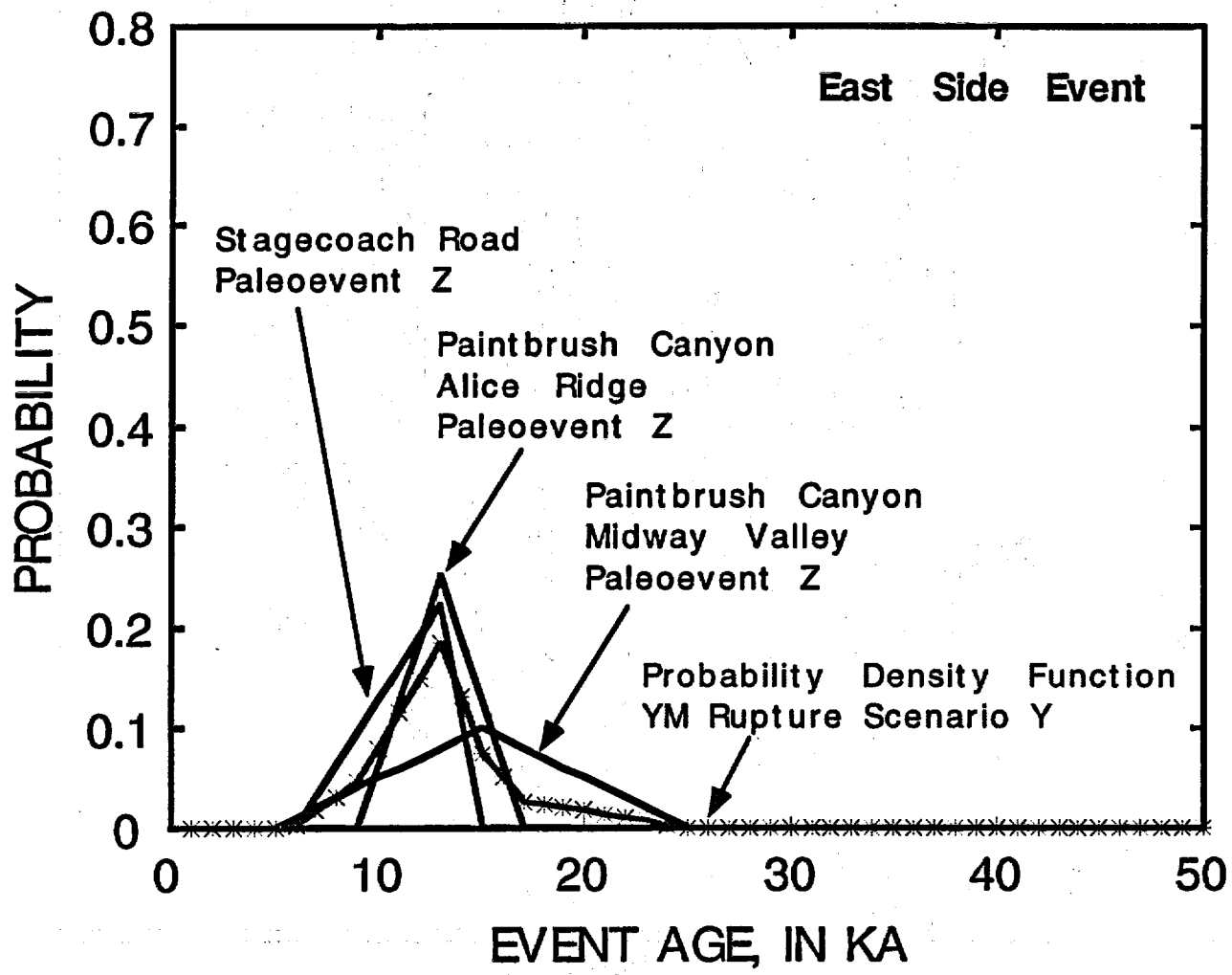

in USGS Seismotectonic Report—Chapter 5

Scenario Y

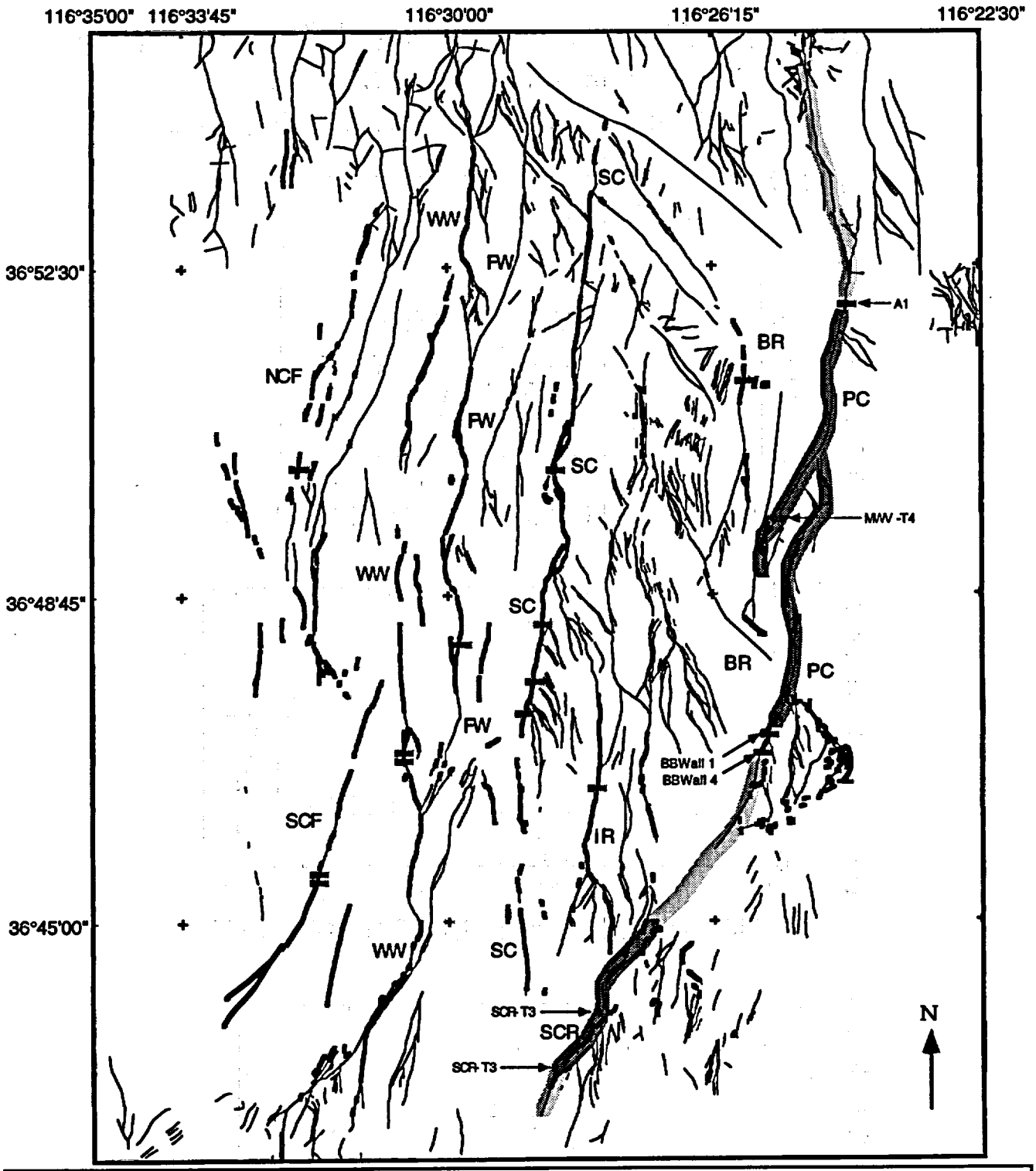

EXPLANATION

- Scenario Y minimum surface rupture length
- Scenario Y maximum surface rupture length
- Trench locations
- Faults; Quaternary and suspected Quaternary age of last movement
- Faults; pre-Quaternary or undetermined age of last movement

0 kilometers 5

Fault Abbreviations

BR = Bow Ridge	SC = Solitario Canyon
FW = Fatigue Wash	SCF = South Crater Flat
IR = Iron Ridge	SCR = Stagecoach Road
NCF = North Crater Flat	WW = Windy Wash
PC = Paintbrush Canyon	

Displacements per Event Along Fault Strike

Yucca Mountain Rupture Scenarios in USGS Seismotectonic Report—Chapter 5

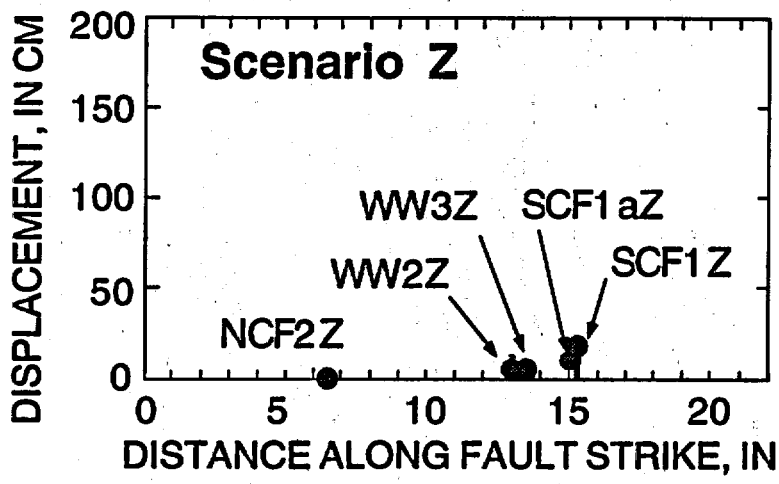

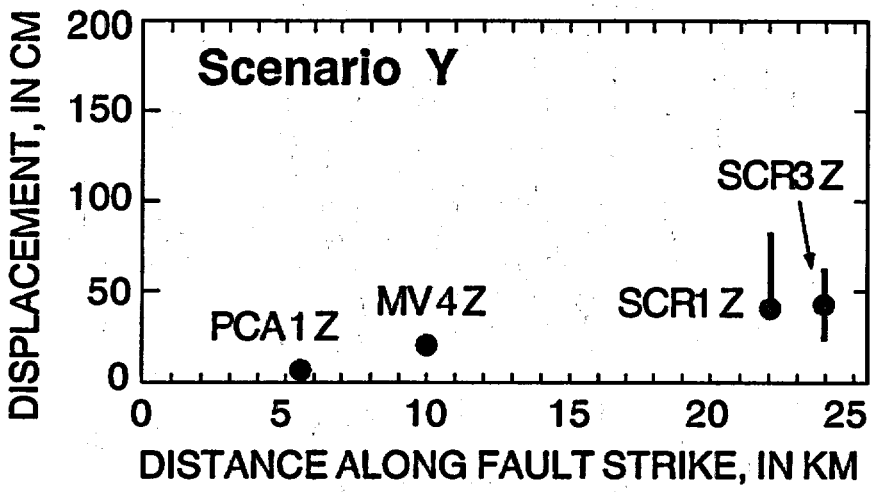

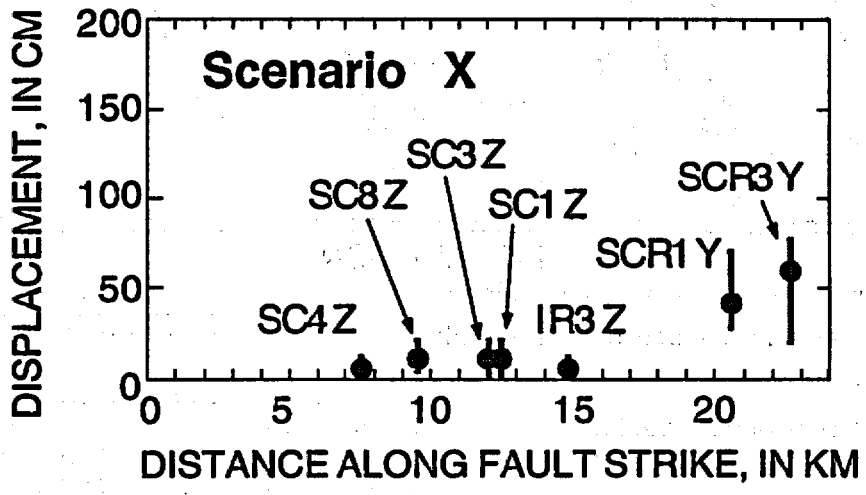

Timing PDF of Rupture Scenario U

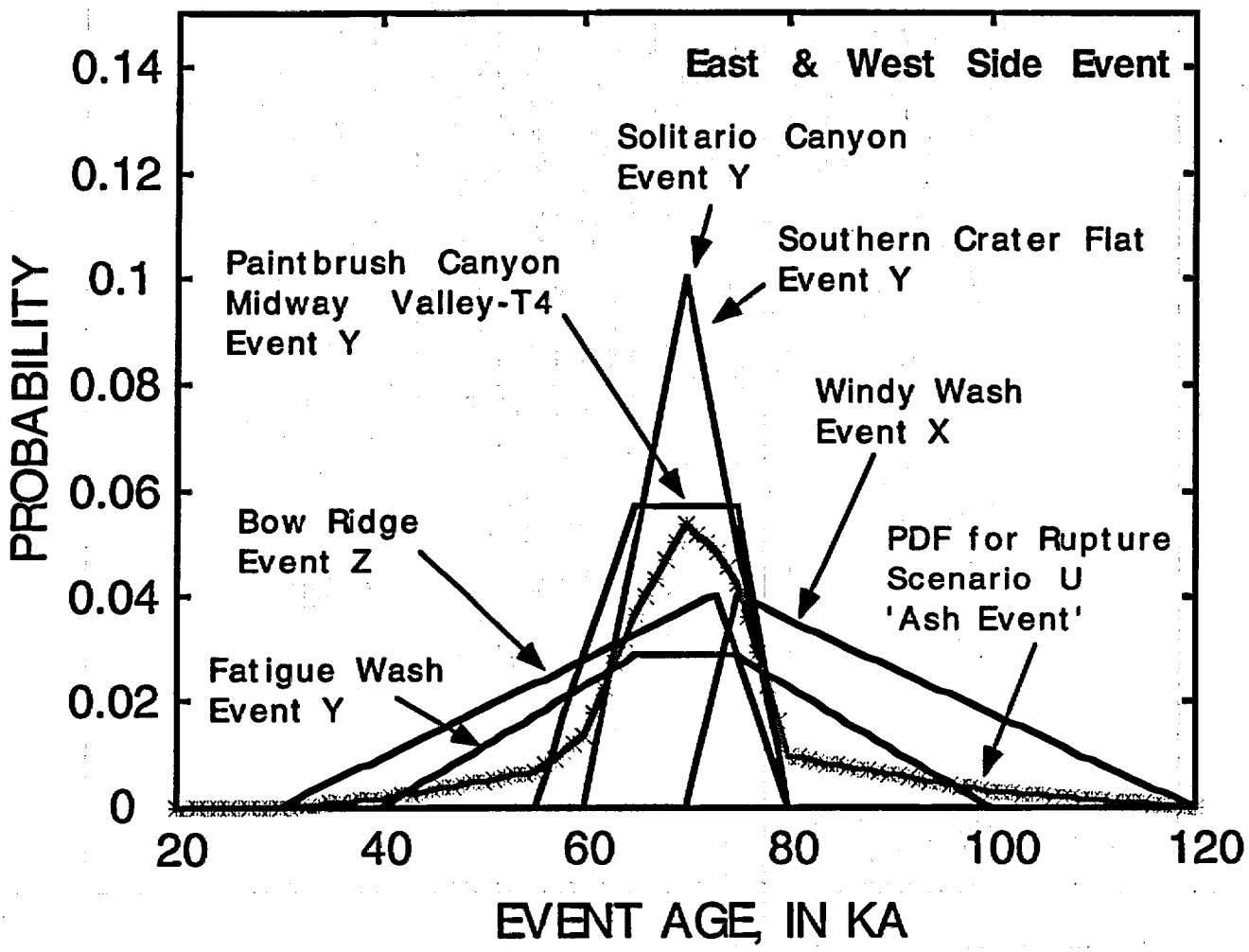

in USGS Seismotectonic Report—Chapter 5

Scenario U

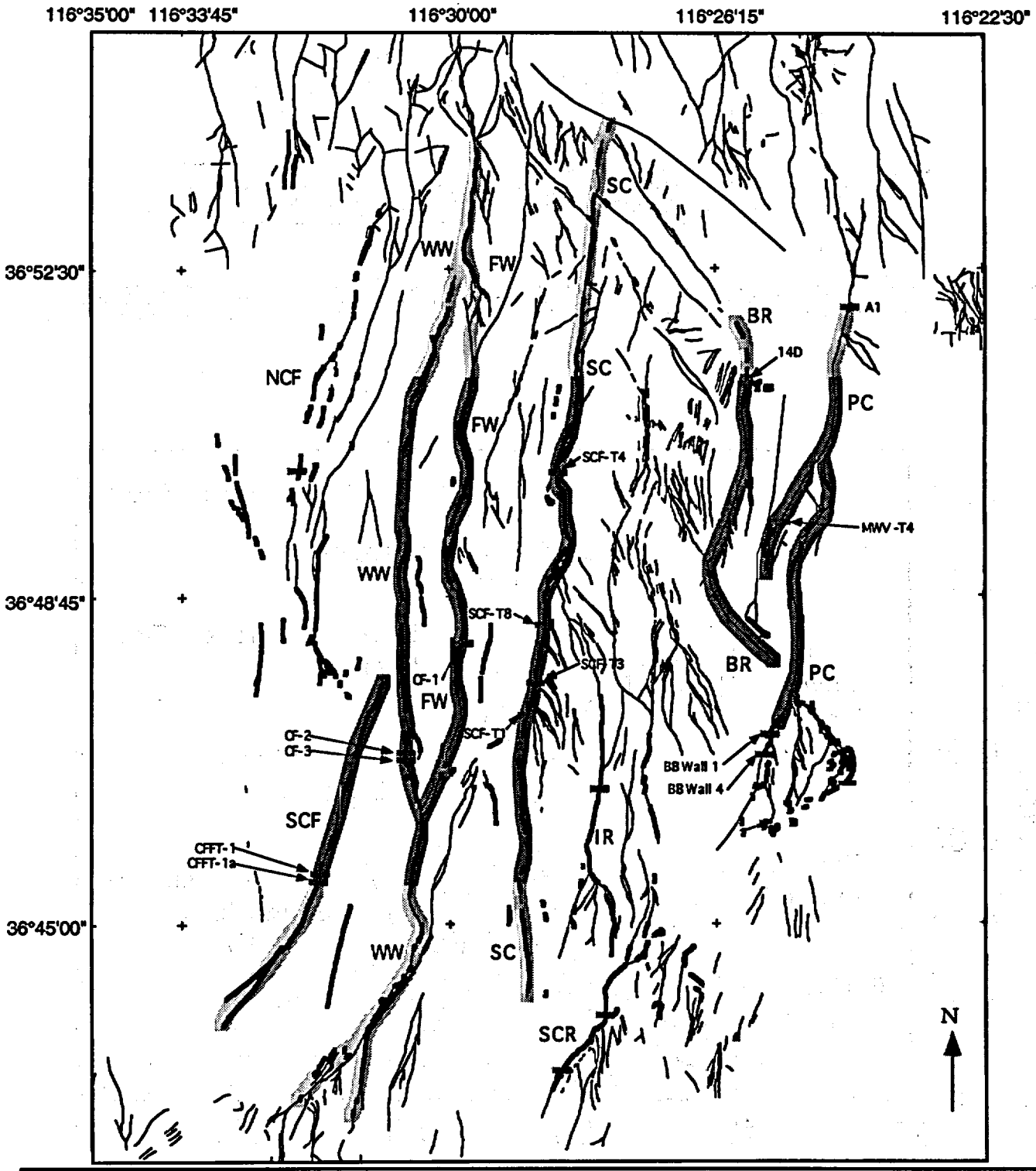

EXPLANATION

- Scenario U minimum surface rupture length
- Scenario U maximum surface rupture length
- Trench locations
- Faults; Quaternary and suspected Quaternary age of last movement
- Faults; pre-Quaternary or undetermined age of last movement

0 kilometers 5

Fault Abbreviations

BR = Bow Ridge	SC = Solitario Canyon
FW = Fatigue Wash	SCF = South Crater Flat
IR = Iron Ridge	SCR = Stagecoach Road
NCF = North Crater Flat	WW = Windy Wash
PC = Paintbrush Canyon	

Displacements for the Ash Event

Seismotectonic? or Volcanotectonic? or Both?

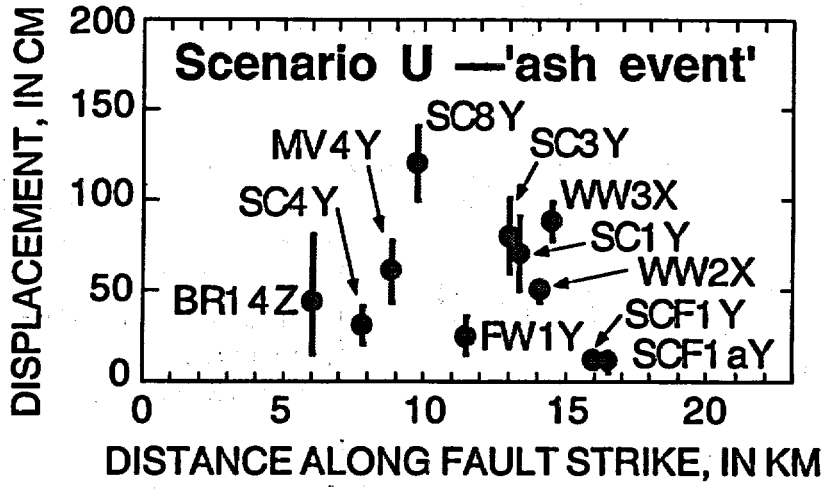

SOME HYPOTHETICAL STRUCTURAL SECTIONS

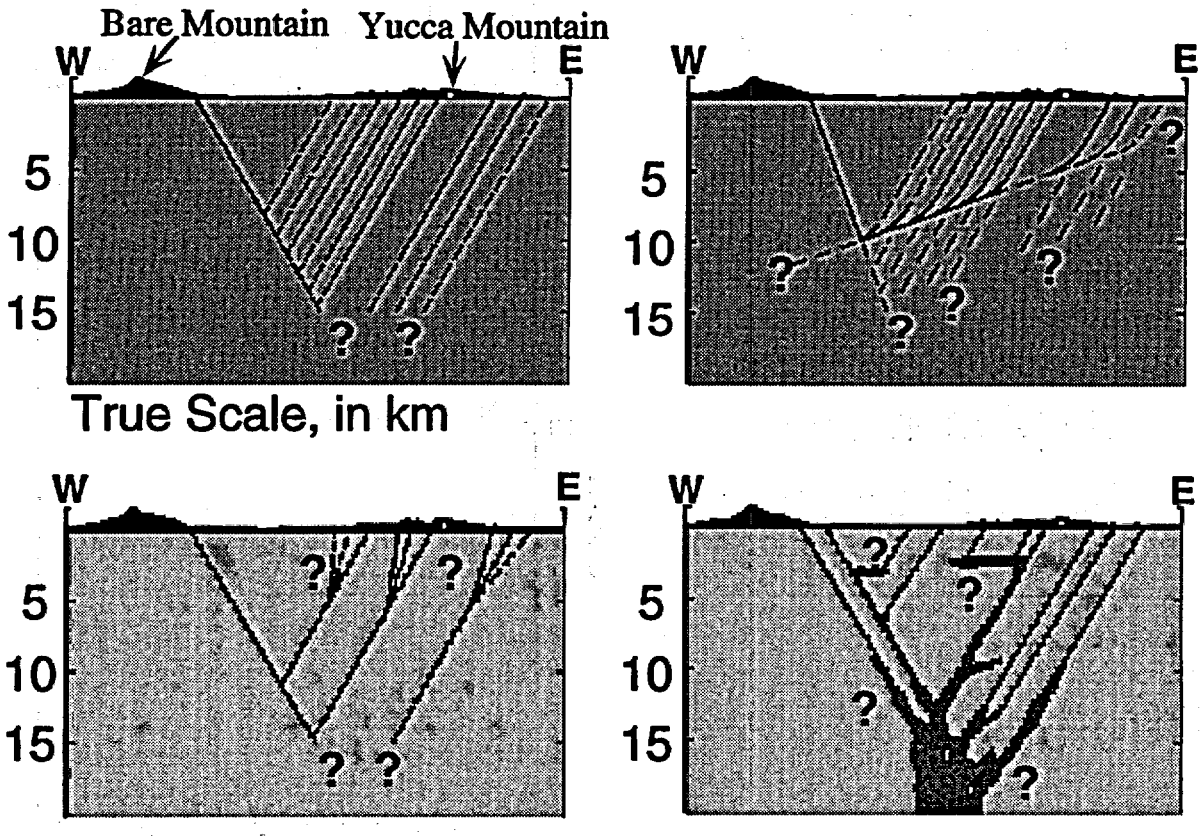

Displacement per Event

- Large-Displacement Paleoevents
  - » 12 Events
  - » M 6.4 to 6.9
  - » Many Paleoevents Overlap in Time
- All Paleoevents
  - » 39 Events
  - » M 5.6 to 6.9
  - » Includes Large-Displacements
  - » Many Paleoevents Overlap in Time
- Distributed Ruptures???

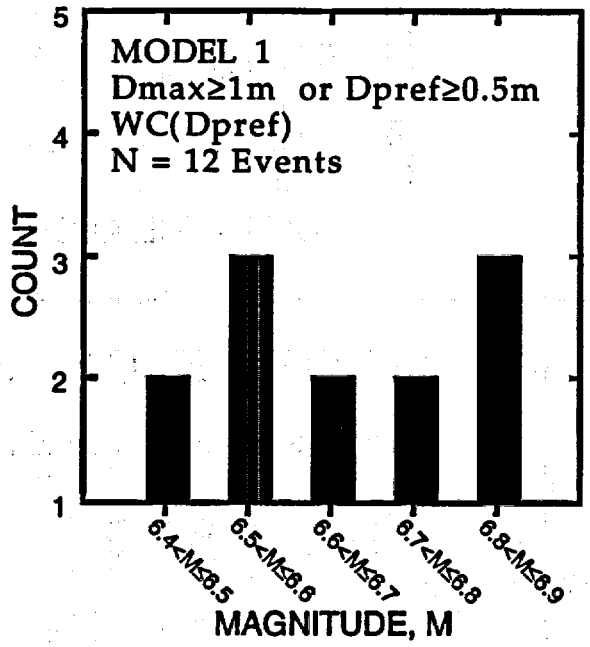

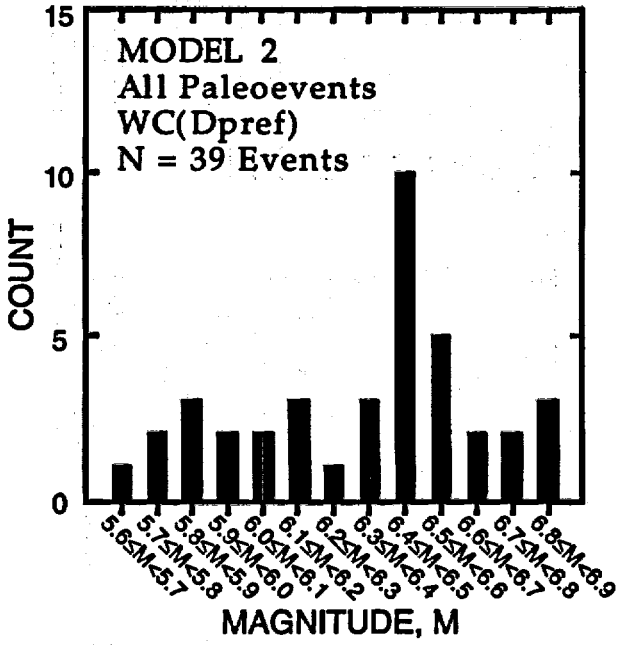

in USGS Seismotectonic Report—Chapter 5

Magnitude Comparison

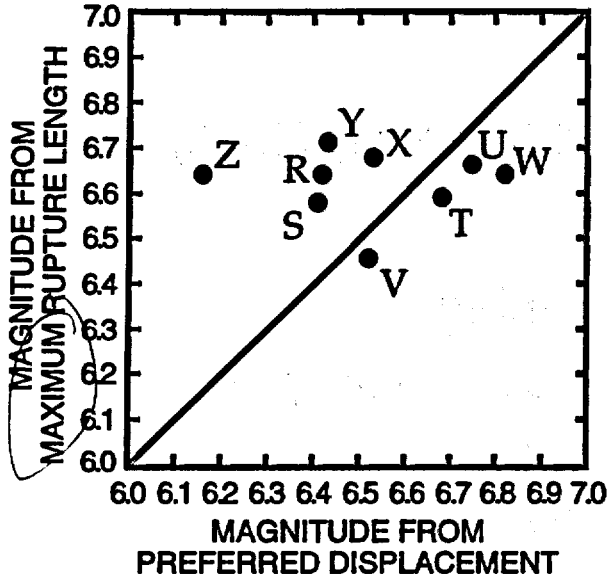

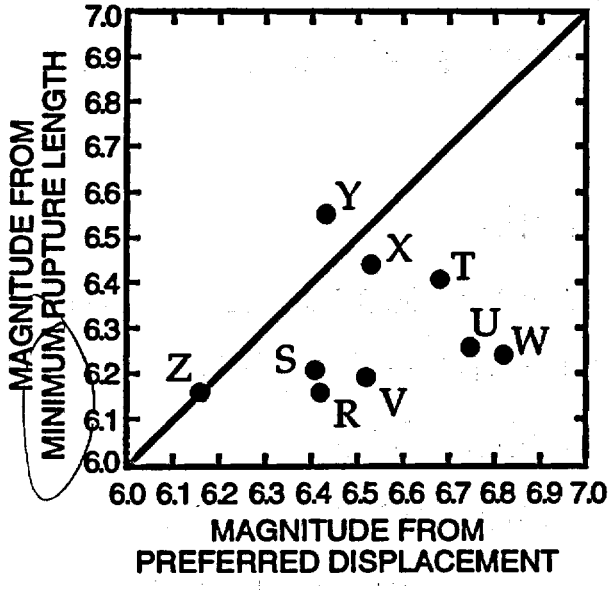

- Magnitudes Calculated from Preferred Displacements Compare Best with Magnitudes Calculated from Maximum Rupture Lengths
- Some Exceptions
  - » Max Rupture Lengths Too Long???
- Rupture Length and Displacement Data Need Further Evaluation

in USGS Seismotectonic Report—Chapter 5

—Summary—
Maximum Magnitude at Yucca Mountain

- Maximum Fault Lengths
  - » Quaternary Fault Maps
    - – Simonds and others (1995) & Piety (1996)
- Rupture Scenarios
  - » Paleoseismic Data and Timing
    - – USGS Seismotectonic Report—Chapter 4
  - » Min. & Max. Rupture Length
    - – USGS Seismotectonic Report—Chapter 5
  - » Displacement per Event
    - – USGS Seismotectonic Report—Chapters 4 & 5
- Uncertainties
  - » Interpretation of Paleoevents
    - – Are Fissures and Fractures Paleoearthquakes???
    - – Many Alternative Mechanisms—Chapters 5 and 9
  - » Correlation of Events—Timing Data
    - – Geochronology and Sample Context Errors
  - » Structural Model—Downdip Fault Geometry
    - – Sum Displacements??

Earthquake Size as a Function of Fault Slip Rate

John G. Anderson[1]

This presentation is based on the following publication:

John G. Anderson, Steven G. Wesnousky[2], and Mark W. Stirling[3] (1996). Earthquake Size as a Function of Fault Slip Rate, Bulletin of the Seismological Society of America 86, 683-690.

Presentation to Seismic Source Characterization
Workshop on Hazard Methodologies
October 16-18, 1996
Doubletree Hotel
Salt Lake City, Utah

[1] Seismological Laboratory and Department of Geological Sciences
University of Nevada, Reno, Nevada 89557
Tel: (702) 784-4265 FAX: (702) 784-1833 email: jga@seismo.unr.edu
[2] Center for Neotectonic Studies, Department of Geological Sciences
University of Nevada, Reno, Nevada 89557
Tel: (702) 784-6067 FAX: (702) 784-1382 email: stevew@seismo.unr.edu
[3] Center for Neotectonic Studies, Department of Geological Sciences
University of Nevada, Reno, Nevada 89557
Tel: (702) 784-1764 FAX: (702) 784-1382 email: stirling@seismo.unr.edu

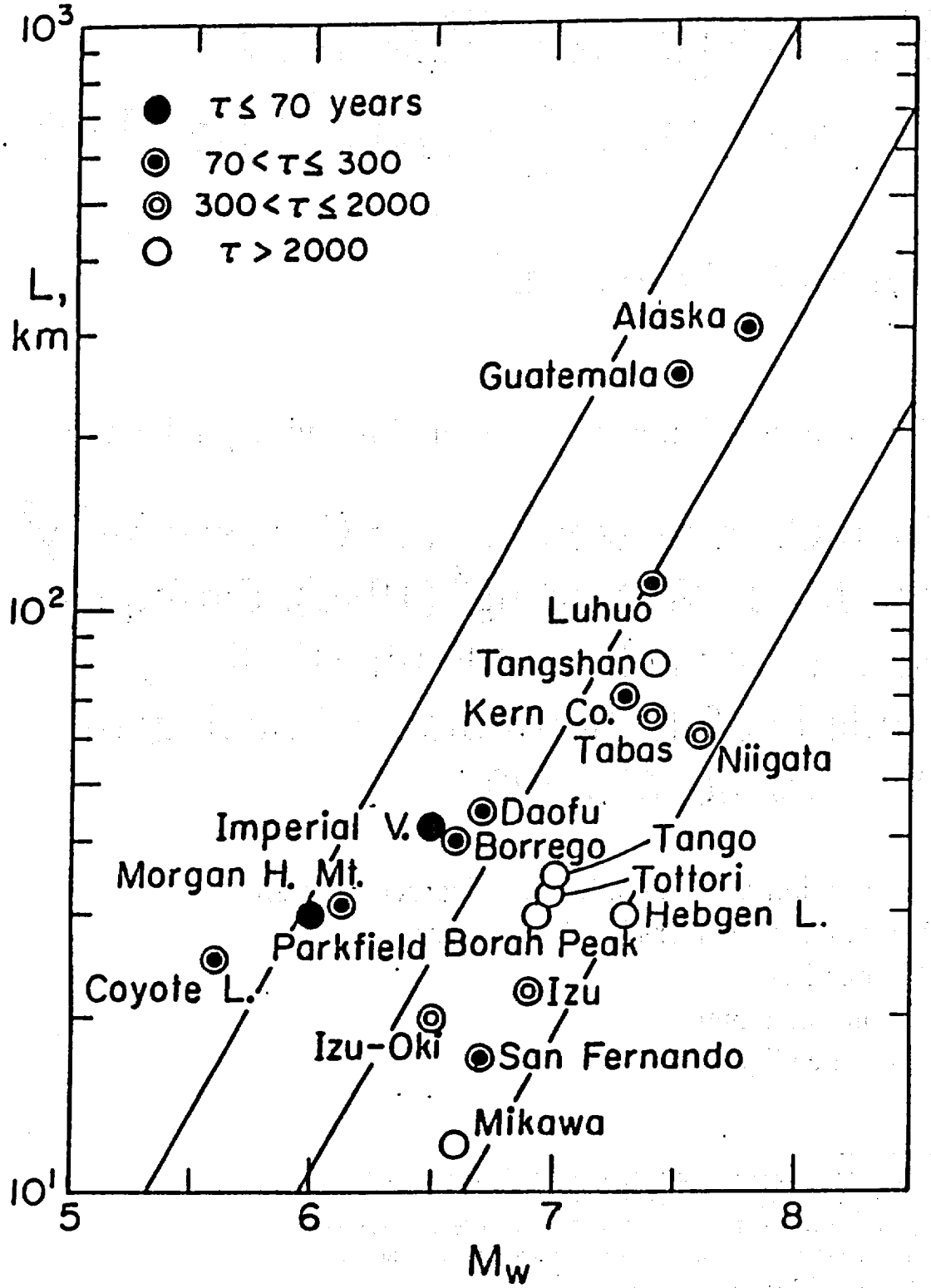

Fig. 2. The relations between the moment magnitude, M_W, and the fault length, L. The solid lines indicate the trend for a constant stress drop.

Kanamori and Allen, 1986

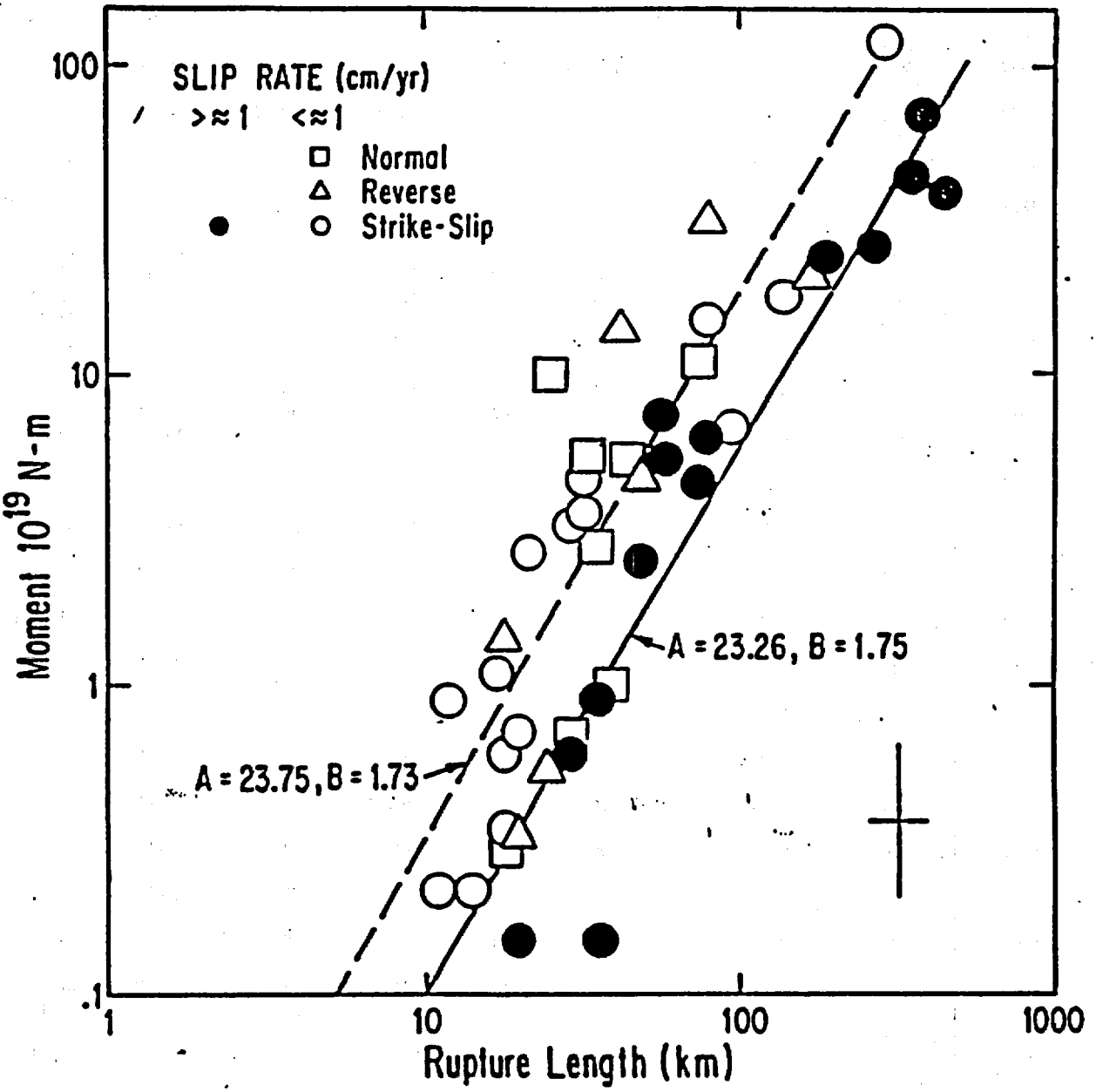

Fig 14. Earthquake rupture length versus earthquake moment, this figure distinguishes faults with slip rates above and below 1 cm/yr, and indicates the sense of displacement for the data points (from Wesnouski, 1986)

Table 1
Historical Earthquake Data

No.	Year	Location	M_0 ($\times 10^{26}$ dyne-cm)	M_w	Refs[a]	Length (km)	Refs[a]	Slip Rate (mm/yr)	Refs[a]
1	1811	New Madrid, Missouri	—	8.2[f]	86	60–250[h]	93, 70	0.01–2[f,m]	70, 93
2	1848	Marlborough, New Zealand	—	7.1[f]	88	95[g]	83	4–10[f]	5, 105
3	1857	Fort Tejon, California	53–87[a]	7.7–7.9[e]	1	360–400[g]	1, 16	16–43[f]	12
4	1868	Hayward, California	1.56[a]	6.8[e]	78	48[g]–52[i]	78, 108	8–10[f,n]	4
5	1872	Owens Valley, California	18–44[a]	7.4–7.7[e]	92	108[g]	92	1–3[f]	92
6	1888	Canterbury, New Zealand	—	7.0–7.3[f]	94	25–35[g]	87, 94	11–25[f]	18, 19, 87
7	1891	Nobi, Japan	−15[a]	7.4[e]	37	80[g]	39	1–10[f]	21
8	1896	Rikuu, Japan	14[a,b]	7.4[e]	39	36–50[h,i]	38, 39	0.1–1[f]	21
9	1906	San Francisco, California	35–43[a]	7.6–7.7[e]	1	420–470[g]	1, 62	15–28[f]	23, 24, 25, 26
10	1915	Pleasant Valley, Nevada	3–8[a]	6.9–7.2[e]	17, 78	34[g]	17	0.3–1[f]	27, 28
11	1927	Tango, Japan	4.6[a]	7.1[e]	40	33[h,i]	40	0.01–1[f]	21
12	1930	N. Izu, Japan	2.7[a,b]	6.9[e]	42	22[g,i]	36, 42	1–10[f]	21, 29
13	1933	Long Beach, California	0.41[c,d]	6.4[e]	78	23[h]	78	0.1–6[f]	12
14	1934	Parkfield, California	0.15[d]	6.1[e]	6	20[h]	7	29–39[f]	61
15	1939	Erzincan, Turkey	45[a]	7.7[e]	59	350[g]	30	5[f]–25[n]	31, 84, 107
16	1940	Imperial Valley, California	2.7[c,d]	6.9[e]	78	60[g]	8, 9	18–23[f]	32
17	1942	Erbaa Niksar, Turkey	2.5[a]	6.9[e]	59	50[g]	30	5[f]–25[n]	31, 84, 107
18	1944	Gerede-Bolu, Turkey	24[a]	7.6[e]	59	190[g]	30	5[f]–25[n]	31, 84, 107
19	1952	Kern County, California	11[a]	7.3[e]	10	75[f]	10	3–8.5[f]	10
20	1953	Golen-Yenice, Turkey	7.3[a]	7.2[e]	59	58[g]	30	5[f]–25[n]	31, 84, 107
21	1954	Fairview Peak, Nevada	6.4[c,d]	7.2[e]	78	46–64[g]	64	0.01–1[f]	103
22	1954	Dixie Valley, Nevada	2.9[c,d]	6.9[e]	78	46[g]	64	0.3–1[f]	27, 28
23	1956	San Miguel, Mexico	1.0[c,d]	6.6[e]	78	22[h]	78	0.1–0.5[f]	33
24	1959	Hebgen Lake, Montana	10.3[c]	7.3[e]	58	26[g]	20	0.8–2.5[f]	34
25	1964	Niigata, Japan	32[d]	7.6[e]	48	80[h]	48	0.01–1[f]	21
26	1966	Parkfield, California	0.15[d]	6.1[e]	2	37[g]	3	29–39[f]	6, 61
27	1967	Mudurnu Valley, Turkey	8.8[c]	7.3[e]	96	80[g]	30	5[f]–25[n]	31, 84, 107
28	1968	Borrego Mtn, California	1.2[c]	6.7[e]	11	30–45[g,h]	13, 14	1.4–5[f]	12, 106
29	1971	San Fernando, California	1.0[c,d]	6.6[e]	78	16[g]–17[h]	78	2–7.5[f]	35, 41
30	1973	Luhuo, China	19[c]	7.5[e]	72	89[g]–110[h]	78	5–10[f]	43
31	1979	Coyote Lake, California	0.051[c,d]	5.8[e]	78	14[h,j]	95, 73	15–19[f]	44
32	1979	Imperial Valley, California	0.6[d]	6.5[e]	52	30.5[g]	15	18–23[f]	32
33	1981	Daofu, China	1.3[c]	6.7[e]	75	46[h]	75	5–10[f]	43

(continued)

Table 1 (Continued)
Historical Earthquake Data

No.	Year	Location	M_0 ($\times 10^{26}$ dyne-cm)	M_w	Refs*	Length (km)	Refs*	Slip Rate (mm/yr)	Refs*
34	1983	Coalinga, California	0.54[d]	6.5[e]	60	25[h]	46	1–7[o]	45, 91
35	1983	Borah Peak, Idaho	2.1[c]–3.5[d]	6.8–7.0[e]	56, 57	30[h]–39.5[g]	90, 74	0.07–0.3[l]	34
36	1984	Morgan Hill, California	0.2[c,d]	6.2[e]	78	30[h]	67	3–6.4[l]	47, 49
37	1986	N. Palm Springs, California	0.16[c,d]	6.1[e]	78	9[g]–16[h]	78	14–25[l]	50
38	1987	Edgecumbe, New Zealand	0.63[c,d]	6.5[e]	78	18[g]–32[h]	78	1.3–2.8[l]	51
39	1987	Superstition Hills, California	1.1[c]	6.7[e]	68	27[g]	69	2–6[l]	12
40	1989	Loma Prieta, California	3.0[c]	7.0[e]	76	34[i]	77	12–28[l,o]	53, 24, 91
41	1990	Luzon, Philippines	39[c]	7.7[e]	65	110[g]–120[h]	66	10–20[l]	104
42	1992	Landers, California	6–11.5[c,d]	7.1–7.3[e]	97–101	70[g,h]	71, 82	0.08–2[l]	12, 54
43	1994	Northridge, California	0.76–2.6[c,d]	6.5–6.9[e]	22, 63, 79, 85, 89, 102	8–16[h,j,k]	80, 81, 22	1.4–1.7[l]	55

Explanation of Data

The superscripts beside each of the estimates of M_0, M_w, L, and slip rate represent the following:

M_0 estimated from (a) geological observations, (b) intensity data, (c) body waves, and (d) surface waves.

M_w estimated from (e) M_0, using the equation $\log M_0 = 16.1 + 1.5M$ (Hanks and Kanamori, 1979). If a range of M_0 is given, then the equivalent range of M_w is shown; (f) intensity data.

Length estimated from (g) geological observations, (h) aftershock distribution, (i) geodetic data, (j) broadband data, and (k) borehole-dilatational strainmeter data.

Slip rate estimated from (l) geological observations; (m) the equation $U^g = \dot{M}_0^g/\mu LW$, in which U^g is the slip rate, $\dot{M}_0^g$ is the seismic moment rate [New Madrid $\dot{M}_0^g$ is calculated by estimating the M_0 of the 1811 event from $\log M_0 = 16.1 + 1.5M$ (Hanks and Kanamori, 1979), and then dividing M_0 by return times estimated from paleoliquefaction studies], μ is the rigidity modulus, and L and W are the fault length and width; (n) geodetic data; and (o) slip partitioning studies.

*The references for the data sources are as follows:

1. Sieh (1978). 2. Tsai and Aki (1969). 3. Brown and Vedder (1967). 4. Lienkaemper *et al.* (1991). 5. Knuepfer (1992). 6. Bakun and McEvilly (1984). 7. Wilson (1936). 8. Brune and Allen (1967). 9. Trifunac (1972). 10. Stein and Thatcher (1981). 11. Petersen *et al.* (1991). 12. Petersen and Wesnousky (1994). 13. Clark (1972). 14. Hamilton (1972). 15. Sharp *et al.* (1982). 16. Hanks and Kanamori (1979). 17. Page (1935). 18. Van Dissen and Yeats (1991). Cowan and McGlone (1991). 20. Witkind (1964). 21. Research Group for Active Faults of Japan (1992). 22. Hudnut *et al.* (1994). 23. Prentice (1989). 24. Sims (1991). 25. Niemi and Hall (1992). 26. Clahan *et al.* (1994). 27. Wallace and Whitney (1984). 28. Bell and Katzer (1990). 29. Okada and Ikeda (1991). 30. Ambraseys (1970). 31. Straub and Kahle (1994). 32. Thomas and Rockwell (1996). 33. Hirabayashi *et al.* (1995). 34. Doser (1985a). 35. Sharp (1981). 36. Matsuda (1974). 37. Mikumo and Ando (1976). 38. Matsuda *et al.* (1980). 39. Thatcher *et al.* (1980). 40. Kanamori (1973). 42. Abe (1978). 43. Teng *et al.* (1983). 44. Savage *et al.* (1979). 45. Trumm *et al.* (1986). 46. Urhammer *et al.* (1983). 47. Galehouse (1991). 48. Abe (1975). 49. Bird and Kong (1994). 50. Hardin and Matti (1989). 51. Nairn and Beanland (1989). 52. Kanamori and Regan (1982). 53. Weber and Anderson (1990). 54. Jennings (1975). 55. Yeats and Huftile (1995). 56. Doser and Smith (1985). 57. Tanimoto and Kanamori (1986). 58. Doser (1985b). 59. Sykes and Quittmeyer (1981). 60. Kanamori (1983). 61. Sieh and Jahns (1984). 62. Thatcher (1975). 63. Thio and Kanamori (1994a). 64. Caskey *et al.* (1995). 65. Romanowicz (1992). 66. Yoshida and Abe (1992). 67. Bakun *et al.* (1984). 68. Bent *et al.* (1989). 69. Sharp *et al.* (1989). 70. Nuttli (1983). 71. Ad Hoc Working Group on the Probabilities of Future Large Earthquakes in Southern California (1992). 72. Zhou *et al.* (1983b). 73. Reasenberg and Ellsworth (1982). 74. Crone *et al.* (1987). 75. Zhou *et al.* (1983a). 76. Hanks and Krawinkler (1991). 77. Marshall *et al.* (1991). 78. Wells and Coppersmith (1994). 79. Zhao (1994). 80. Dreger *et al.* (1994). 81. Johnston and Linde (1994). 82. Sieh *et al.* (1993). 83. Lensen (1978). 84. Oral *et al.* (1995). 85. Wald and Heaton (1994b). 86. Johnston and Kanter (1990). 87. Cowan (1990). 88. Eiby (1973). 89. Thio and Kanamori (1994b). 90. Kanamori and Allen (1986). 91. Jones and Wesnousky (1992). 92. Beanland and Clark (1995). 93. Wesnousky and Leffler (1992). 94. Cowan (1991). 95. Bouchon (1982). 96. Hanks and Wyss (1972). 97. Freymueller (1994). 98. Johnson *et al.* (1994). 99. Wald and Heaton (1994a). 100. Cohee and Beroza (1994). 101. Dreger (1994). 102. Song *et al.* (1994). 103. J. Caskey, personal comm. 104. T. Nakata, personal comm. 105. Berryman (1979). 106. Gurrolo and Rockwell (1996). 107. Barka and Gulen (1988). 108. Yu and Segall (1995).

Proposed Regression Equation

$$M_W = A + B \log L + C \log S$$

Monte Carlo Method

10,000 Runs

M_W, L, S choosen at random within their bounds

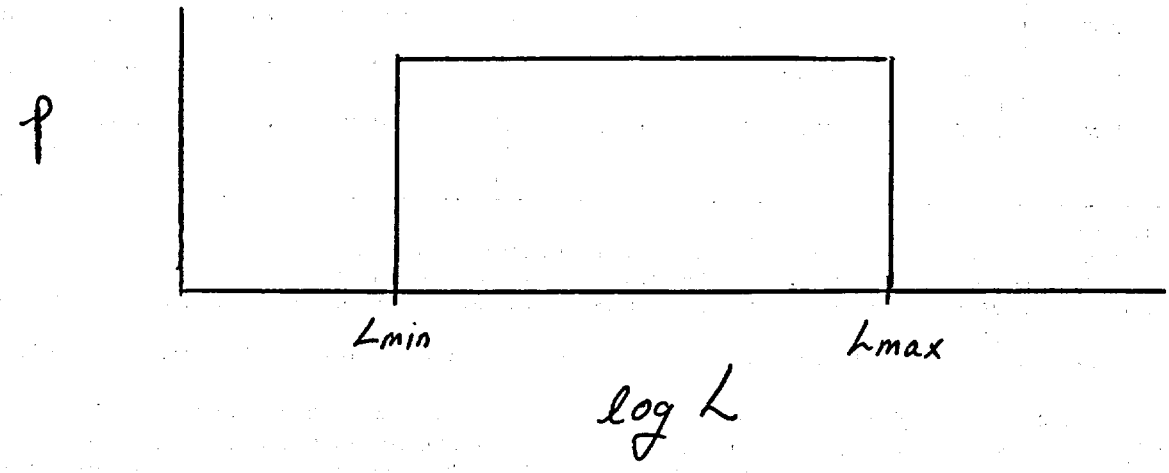

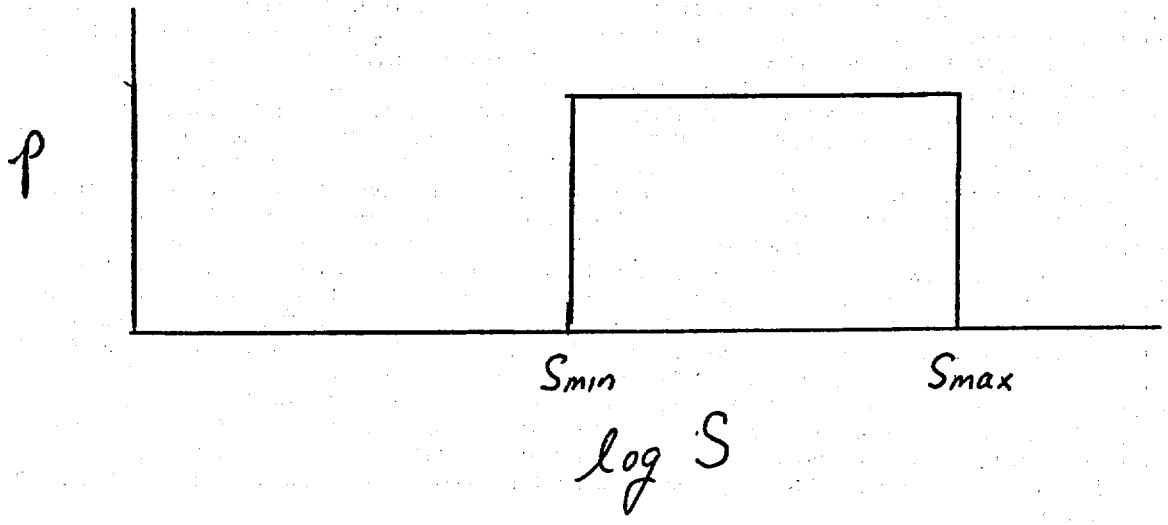

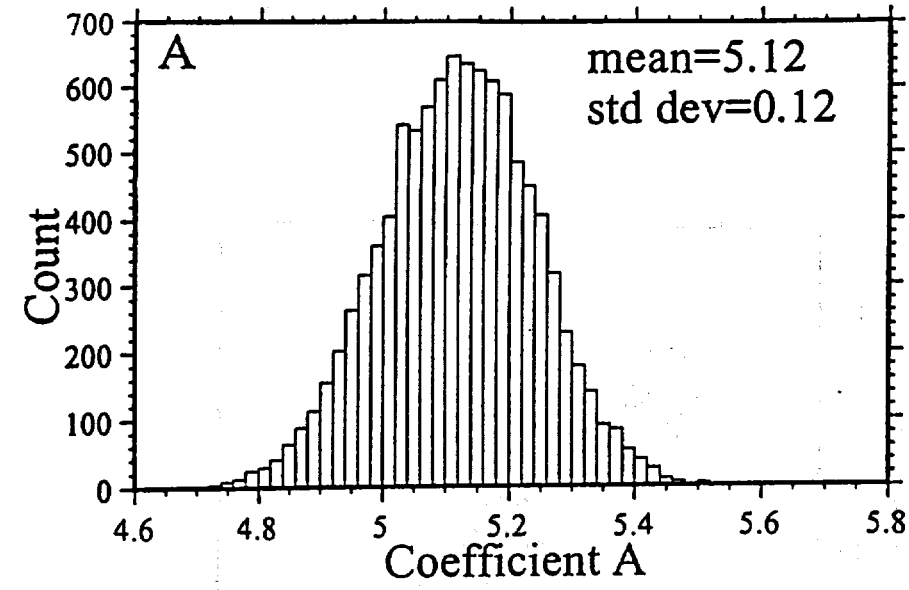
A
mean=5.12
std dev=0.12
Count
Coefficient A
700
600
500
400
300
200
100
0
4.6
4.8
5
5.2
5.4
5.6
5.8

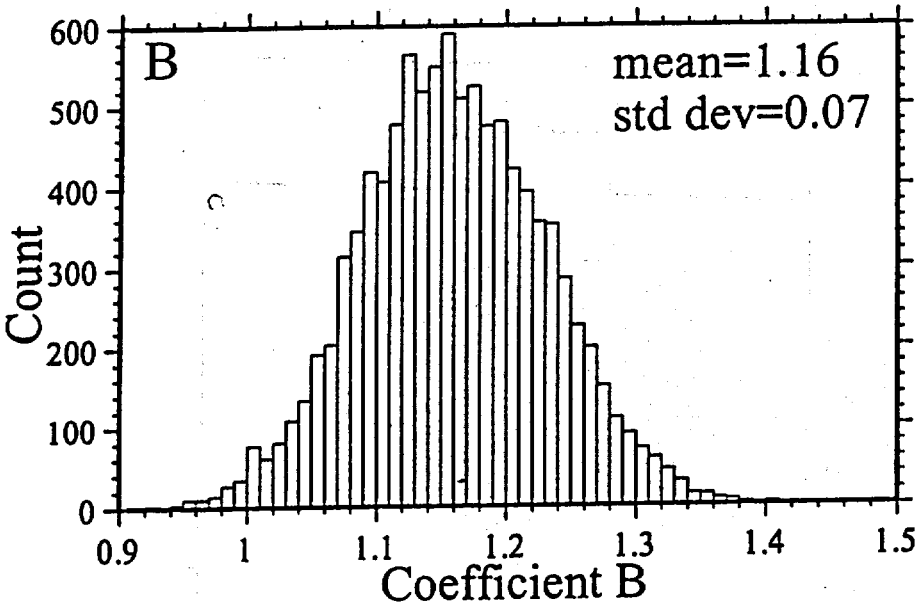
B
mean=1.16
std dev=0.07
Count
Coefficient B
600
500
400
300
200
100
0
0.9
1
1.1
1.2
1.3
1.4
1.5

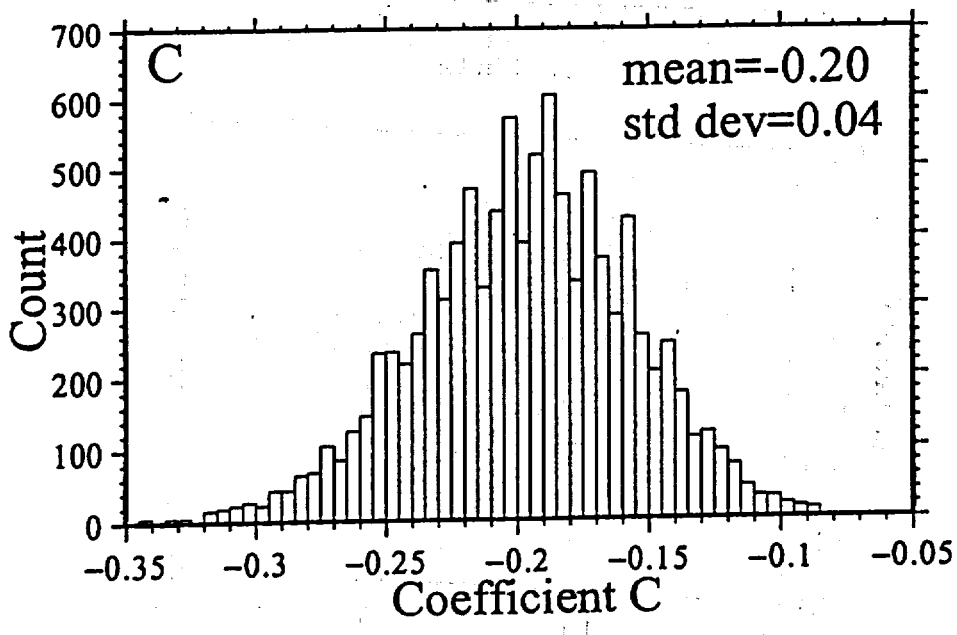
C
mean=-0.20
std dev=0.04
Count
Coefficient C
700
600
500
400
300
200
100
0
−0.35
−0.3
−0.25
−0.2
−0.15
−0.1
−0.05

Fig 2

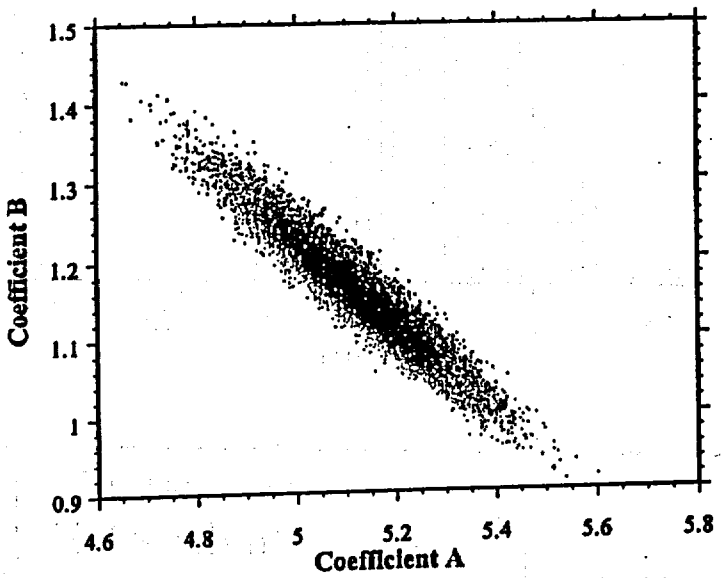
Coefficient B
1.5
1.4
1.3
1.2
1.1
1
0.9
4.6
4.8
5
5.2
5.4
5.6
5.8
Coefficient A

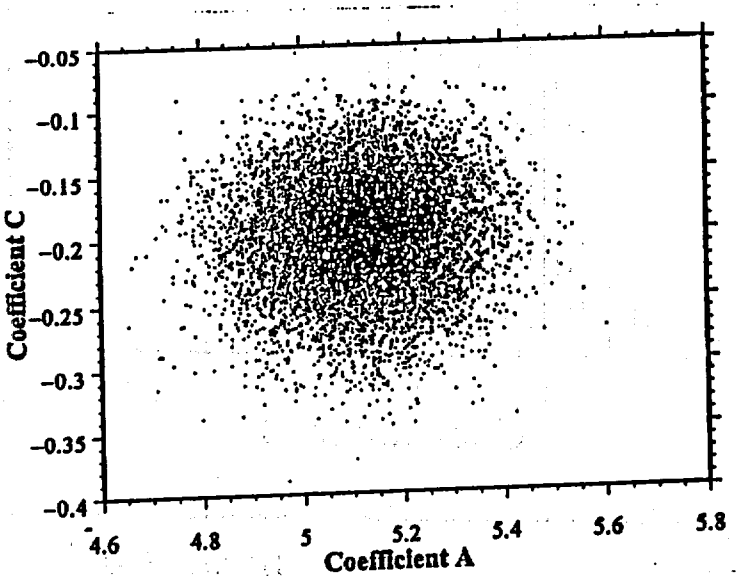
Coefficient C
-0.05
-0.1
-0.15
-0.2
-0.25
-0.3
-0.35
-0.4
4.6
4.8
5
5.2
5.4
5.6
5.8
Coefficient A

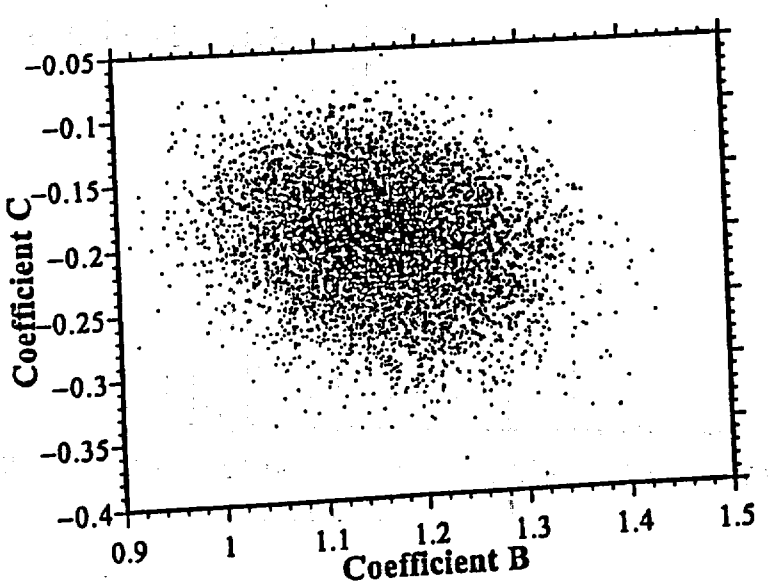
Coefficient C
-0.05
-0.1
-0.15
-0.2
-0.25
-0.3
-0.35
-0.4
0.9
1
1.1
1.2
1.3
1.4
1.5
Coefficient B

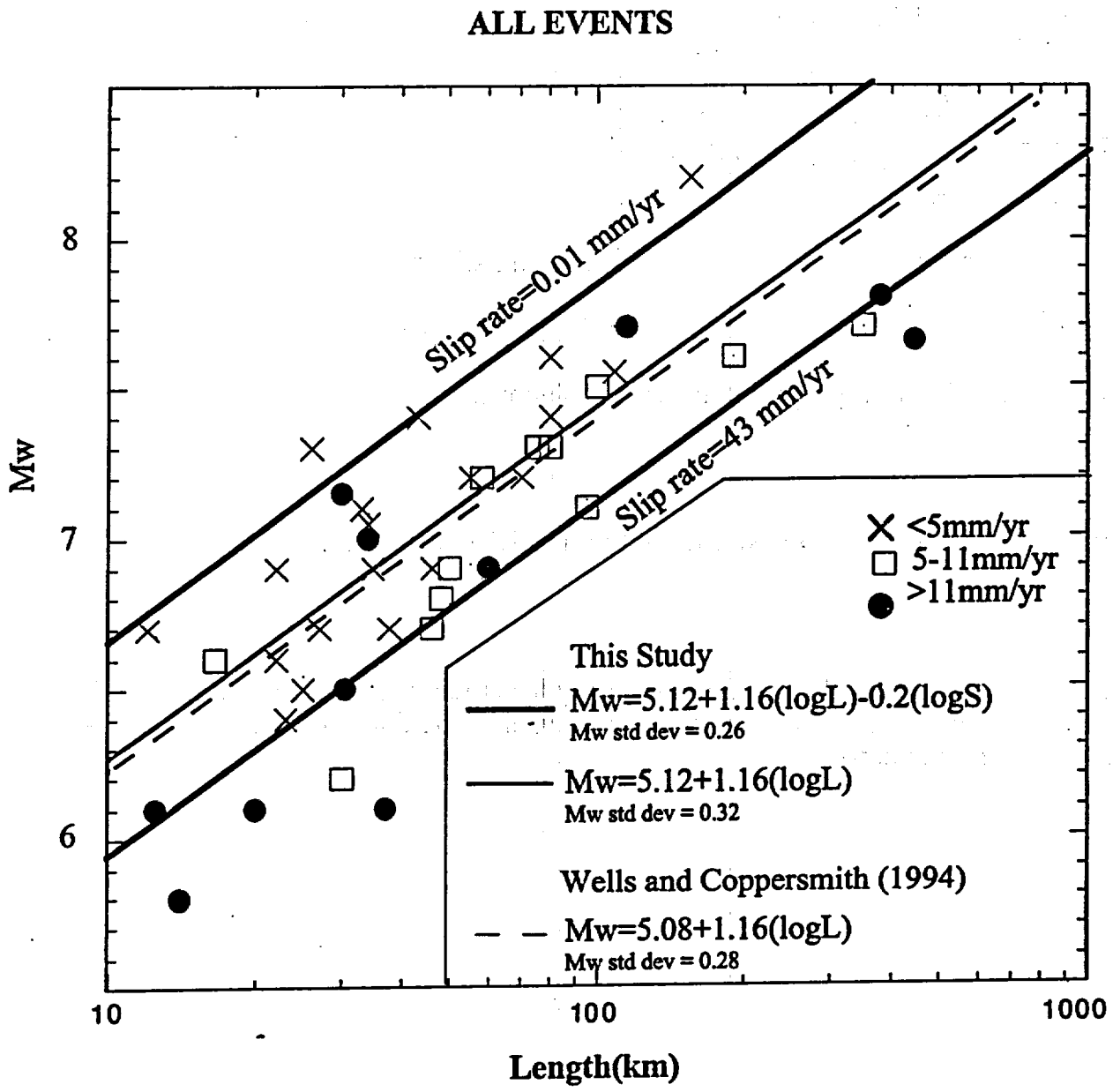
ALL EVENTS
Slip rate=0.01 mm/yr
Slip rate=43 mm/yr
<5mm/yr
5-11mm/yr
>11mm/yr
This Study
Mw=5.12+1.16(logL)-0.2(logS)
Mw std dev = 0.26
Mw=5.12+1.16(logL)
Mw std dev = 0.32
Wells and Coppersmith (1994)
Mw=5.08+1.16(logL)
Mw std dev = 0.28
Mw
8
7
6
10
100
1000
Length(km)

Variance Reduction

L2 Norm (Standard Deviation)

$$\sigma = \left\{ \frac{1}{N} \sum_{i=1}^{N} (M_i - \hat{M}_i)^2 \right\}^{1/2}$$

Excluding slip rate: $\sigma = 0.32$

Including slip rate: $\sigma = 0.26$

This variance reduction is significant with 75% confidence.

L1 norm: variance reduction is significant with 95% confidence.

C is never closer to zero than -0.05, indicating less than one chance in 10^4 of finding a set of parameters, within the specified ranges of the data, for which the coefficient on slip rate is zero.

Seismic moment

$$M_o = \mu L W D$$

Moment magnitude

$$M_W = 2/3(\log M_o - 16)$$

Combining relations:

$$M_W = 2/3 \log L + 2/3 \log D + 2/3(\log \mu + \log W - 16)$$

For our data, W has a narrow range so the last term is nearly constant.

If $D \propto W$, B should be 0.67. (W model)

If $D \propto L$, B should be 1.33. (L model)

In our regression, $B = 1.16 \pm 0.07$. This is closer to the L model, but it differs from the L model prediction by over twice its standard deviation.

ALL EVENTS

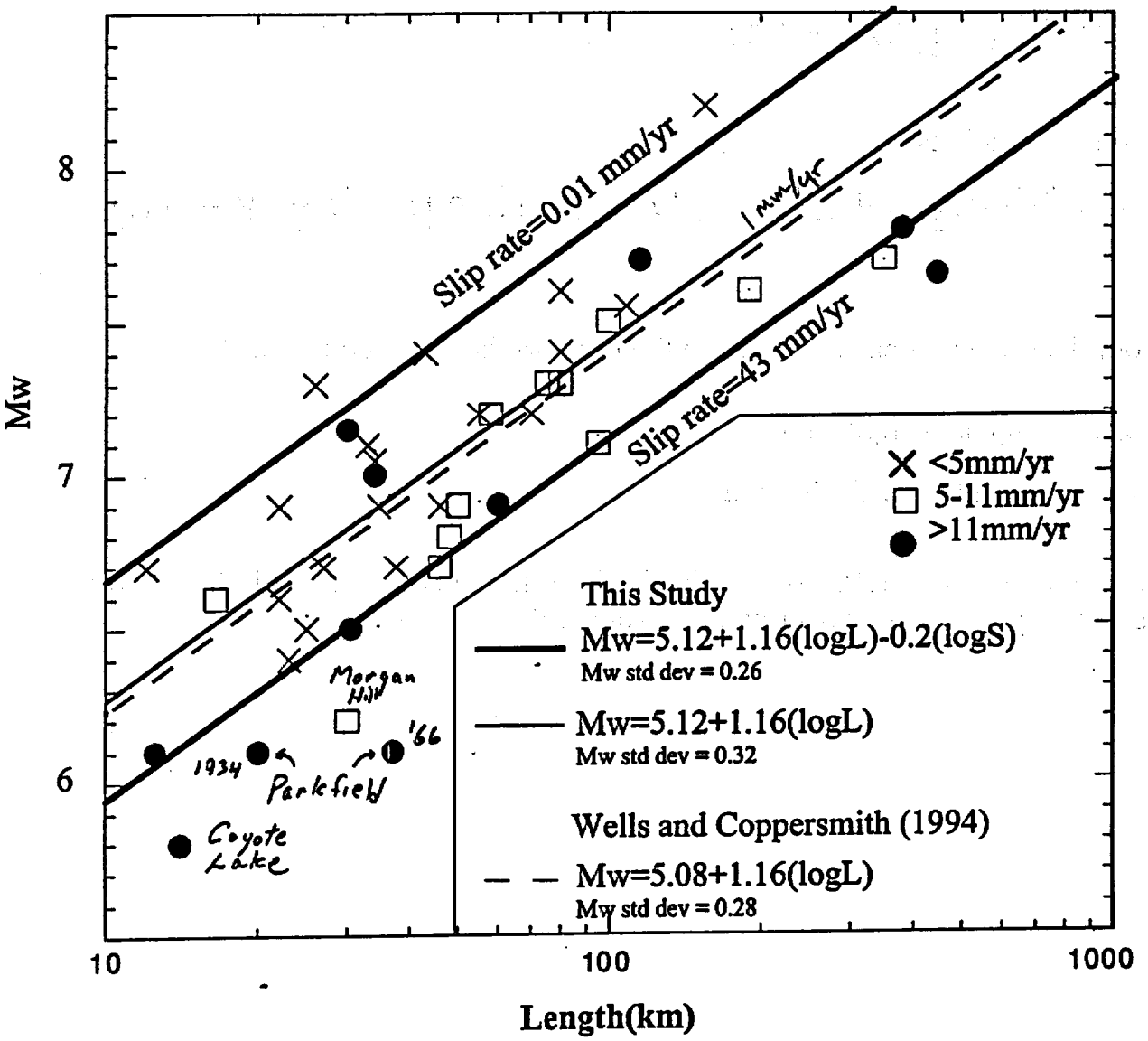

Events that adjoin creeping sections are marked

MLS Table for Normal Faults									
		Range	Used	Range		Used		Pred.	
			M	L	S	L	S	Magnitude	Residual
10	Pleasant Valley, Neva	6.9-7.2	7.05	34	.3-1	34	0.6	6.95	0.10
21	Fairview Peak	7.2	7.2	46-64	.01-1	55	0.1	7.36	-0.16
22	Dixie Valley	6.9	6.9	46	.3-1	46	0.6	7.10	-0.20
24	Hebgen Lake	7.3	7.3	26	.8-2.5	26	1.4	6.73	0.57
35	Borah Peak	6.8-7.0	6.9	30-39.5	.07-.3	35	0.14	7.10	-0.20
38	Edgecumbe, NZ	6.5	6.5	18-32	1.3-2.8	25	1.9	6.68	-0.18
							Average Residual		-0.01
							Standard deviation		0.31
MLS for extensional environments									
5	Owens Valley	7.4-7.7	7.55	108	3-Jan	108	2	7.41	0.14
10	Pleasant Valley, Neva	6.9-7.2	7.05	34	.3-1	34	0.6	6.95	0.10
16	Imperial Valley 1940	6.9	6.9	60	18-23	60	21.5	6.89	0.01
21	Fairview Peak	7.2	7.2	46-64	.01-1	55	0.1	7.36	-0.16
22	Dixie Valley	6.9	6.9	46	.3-1	46	0.6	7.10	-0.20
24	Hebgen Lake	7.3	7.3	26	.8-2.5	26	1.4	6.73	0.57
32	Imperial Valley 1979	6.5	6.5	30.5	18-23	30.5	21.5	6.55	-0.05
35	Borah Peak	6.8-7.0	6.9	30-39.5	.07-.3	35	0.14	7.10	-0.20
38	Edgecumbe, NZ	6.5	6.5	18-32	1.3-2.8	25	1.9	6.68	-0.18
							Average Residual		0.00
							Standard deviation		0.25

Conclusions

The distribution of coefficient C shows that a regression that does not include slip rate as a parameter will systematically overestimate the expected magnitudes on the fastest slipping faults, and will systematically underestimate the expected magnitudes on the slowest slipping faults.

Faults with slower slip rates tend to fail in earthquakes with higher static stress drop.

Bulletin of the Seismological Society of America, Vol. 86, No. 3, pp. 683–690, June 1996

Earthquake Size as a Function of Fault Slip Rate

by John G. Anderson, Steven G. Wesnousky, and Mark W. Stirling

Abstract Estimates of the potential size of earthquakes on mapped active faults are generally based on regressions of earthquake magnitude (M_w) versus length (L) of fault rupture for historical earthquakes. The fault slip rate (S) has been ignored in formal prediction equations, but more accurate predictions of future earthquake magnitudes on mapped faults may be obtained when it is included. A least-squares regression for a data set of 43 earthquakes occurring on faults for which slip rates are reported shows $M_w = 5.12 + 1.16 \log L - 0.20 \log S$, where L is in units of Km and S is in units of mm/yr. The result indicates that the largest earthquakes will occur on the slowest slipping faults if the rupture length is held constant.

Introduction

The estimate of earthquake size on mapped faults is fundamental to seismic hazard analysis. As a result, there is a long history of efforts to use historical data to develop regressions between earthquake size (magnitude or seismic moment) and earthquake rupture length, area, or fault displacement. A thorough review of past efforts, a synthesis of new observations, and the development of new regressions has recently been put forth by Wells and Coppersmith (1994). The slip rate of the fault on which an earthquake occurs has been generally ignored in such regressions when applied to seismic hazard analysis, except by Wesnousky (1986) who sorted the faults into high and low slip rate categories. However, within the community of seismologists concerned with the mechanics of faulting, it has been previously established that there also exists a dependency of earthquake size on earthquake return time and the tectonic environment in which earthquakes occur (e.g., Kanamori and Allen, 1986; Scholz *et al.*, 1986). Here, we use observations from 43 earthquakes that occurred on faults for which slip rates are reported and develop a regression for moment magnitude (M_w; Hanks and Kanamori, 1979) as a function of surface rupture length (L) and fault slip rate (S). Our result shows that the inclusion of fault slip rate in such regressions reduces the misfit between predicted and observed values of M_w as compared with regressions based solely on L and, hence, can yield more accurate predictions of future earthquake magnitudes on active faults.

Data and Analysis

We start with a list of 43 historical earthquakes for which there exist estimates of the moment magnitude M_w, the fault rupture length L, and the slip rate S of the respective fault on which the earthquake occurred (Table 1). The data are the result of a global search of observations, limited to earthquakes that occur in regions where the seismogenic depth is 15 to 20 km. The distribution of the data is shown in Figure 1.

The regression we develop has the form

$$M_w = A + B \log L + C \log S, \qquad (1)$$

where A, B, and C are constants to be determined by the regression. We avoid assuming a preferred slip rate or rupture length for each fault in our study by using a Monte Carlo approach. Values of S for each fault were chosen at random, assuming the probability density of $\log S$ is constant between the minimum and maximum estimates. Likewise, in setting up each regression, we chose L at random, assuming the probability density of $\log L$ is constant between its minimum and maximum values or between a range of $\pm 20\%$ of the rupture length if minimum and maximum values are absent in Table 1. This range is the average of rupture length ranges shown in Table 1. M_w is similarly chosen at random between the minimum and maximum values, or between the range of $M_w - 0.3$ and $M_w + 0.3$ if the minimum and maximum values are absent in Table 1. The width of the interval on the magnitude (± 0.3) is chosen to represent an uncertainty on the moment of plus or minus a factor of 3, which we believe to be conservative in most cases.

We generated 10,000 Monte Carlo realizations consistent with the above ranges of data, and for each we used a standard least-squares technique (e.g., Menke, 1989) to find A, B, and C. The distribution of values for A, B, and C is shown in Figure 2. There is almost no correlation between B and C in the Monte Carlo simulations (Fig. 3), indicating that the rupture length and slip rate act independently. The mean values and standard deviations of these distributions may be taken for regression coefficients:

$$M_w = (5.12 \pm 0.12) + (1.16 \pm 0.07)\log L - (0.20 \pm 0.04)\log S. \qquad (2)$$

Table 1
Historical Earthquake Data

No.	Year	Location	M_0 ($\times 10^{26}$ dyne-cm)	M_w	Refs*	Length (km)	Refs*	Slip Rate (mm/yr)	Refs*
1	1811	New Madrid, Missouri	—	8.2[f]	86	60–250[h]	93, 70	0.01–2[i,m]	70, 93
2	1848	Marlborough, New Zealand	—	7.1[f]	88	95[g]	83	4–10[j]	5, 105
3	1857	Fort Tejon, California	53–87[a]	7.7–7.9[e]	1	360–400[g]	1, 16	16–43[j]	12
4	1868	Hayward, California	1.56[a]	6.8[e]	78	48[g]–52[i]	78, 108	8–10[i,n]	4
5	1872	Owens Valley, California	18–44[a]	7.4–7.7[e]	92	108[g]	92	1–3[j]	92
6	1888	Canterbury, New Zealand	—	7.0–7.3[f]	94	25–35[g]	87, 94	11–25[j]	18, 19, 87
7	1891	Nobi, Japan	−15[a]	7.4[e]	37	80[g]	39	1–10[j]	21
8	1896	Rikuu, Japan	14[a,b]	7.4[e]	39	36–50[h,i]	38, 39	0.1–1[j]	21
9	1906	San Francisco, California	35–43[a]	7.6–7.7[e]	1	420–470[g]	1, 62	15–28[j]	23, 24, 25, 26
10	1915	Pleasant Valley, Nevada	3–8[a]	6.9–7.2[e]	17, 78	34[g]	17	0.3–1[j]	27, 28
11	1927	Tango, Japan	4.6[a]	7.1[e]	40	33[h,i]	40	0.01–1[j]	21
12	1930	N. Izu, Japan	2.7[a,b]	6.9[e]	42	22[g,i]	36, 42	1–10[j]	21, 29
13	1933	Long Beach, California	0.41[c,d]	6.4[e]	78	23[h]	78	0.1–6[j]	12
14	1934	Parkfield, California	0.15[d]	6.1[e]	6	20[h]	7	29–39[j]	61
15	1939	Erzincan, Turkey	45[a]	7.7[e]	59	350[g]	30	5[j]–25[n]	31, 84, 107
16	1940	Imperial Valley, California	2.7[c,d]	6.9[e]	78	60[g]	8, 9	18–23[j]	32
17	1942	Erbaa Niksar, Turkey	2.5[a]	6.9[e]	59	50[g]	30	5[j]–25[n]	31, 84, 107
18	1944	Gerede-Bolu, Turkey	24[a]	7.6[e]	59	190[g]	30	5[j]–25[n]	31, 84, 107
19	1952	Kern County, California	11[a]	7.3[e]	10	75[i]	10	3–8.5[j]	10
20	1953	Golen-Yenice, Turkey	7.3[a]	7.2[e]	59	58[g]	30	5[j]–25[n]	31, 84, 107
21	1954	Fairview Peak, Nevada	6.4[c,d]	7.2[e]	78	46–64[g]	64	0.01–1[j]	103
22	1954	Dixie Valley, Nevada	2.9[c,d]	6.9[e]	78	46[g]	64	0.3–1[j]	27, 28
23	1956	San Miguel, Mexico	1.0[c,d]	6.6[e]	78	22[h]	78	0.1–0.5[j]	33
24	1959	Hebgen Lake, Montana	10.3[c]	7.3[e]	58	26[g]	20	0.8–2.5[j]	34
25	1964	Niigata, Japan	32[d]	7.6[e]	48	80[h]	48	0.01–1[j]	21
26	1966	Parkfield, California	0.15[d]	6.1[e]	2	37[g]	3	29–39[j]	6, 61
27	1967	Mudurnu Valley, Turkey	8.8[c]	7.3[e]	96	80[g]	30	5[j]–25[n]	31, 84, 107
28	1968	Borrego Mtn, California	1.2[c]	6.7[e]	11	30–45[g,h]	13, 14	1.4–5[j]	12, 106
29	1971	San Fernando, California	1.0[c,d]	6.6[e]	78	16[g]–17[h]	78	2–7.5[j]	35, 41
30	1973	Luhuo, China	19[c]	7.5[e]	72	89[g]–110[h]	78	5–10[j]	43
31	1979	Coyote Lake, California	0.051[c,d]	5.8[e]	78	14[h,i]	95, 73	15–19[j]	44
32	1979	Imperial Valley, California	0.6[d]	6.5[e]	52	30.5[g]	15	18–23[j]	32
33	1981	Daofu, China	1.3[c]	6.7[e]	75	46[h]	75	5–10[j]	43

(continued)

Table 1 (Continued)
Historical Earthquake Data

No.	Year	Location	M_o ($\times 10^{26}$ dyne-cm)	M_w	Refs*	Length (km)	Refs*	Slip Rate (mm/yr)	Refs*
34	1983	Coalinga, California	0.54[d]	6.5[e]	60	25[h]	46	1–7[o]	45, 91
35	1983	Borah Peak, Idaho	2.1[c]–3.5[d]	6.8–7.0[e]	56, 57	30[h]–39.5[g]	90, 74	0.07–0.3[j]	34
36	1984	Morgan Hill, California	0.2[c,d]	6.2[e]	78	30[h]	67	3–6.4[j]	47, 49
37	1986	N. Palm Springs, California	0.16[c,d]	6.1[e]	78	9[g]–16[h]	78	14–25[j]	50
38	1987	Edgecumbe, New Zealand	0.63[c,d]	6.5[e]	78	18[g]–32[h]	78	1.3–2.8[j]	51
39	1987	Superstition Hills, California	1.1[c]	6.7[e]	68	27[g]	69	2–6[j]	12
40	1989	Loma Prieta, California	3.0[c]	7.0[e]	76	34[i]	77	12–28[l,o]	53, 24, 91
41	1990	Luzon, Philippines	39[c]	7.7[e]	65	110[g]–120[h]	66	10–20[j]	104
42	1992	Landers, California	6–11.5[c,d]	7.1–7.3[e]	97–101	70[g,h]	71, 82	0.08–2[j]	12, 54
43	1994	Northridge, California	0.76–2.6[c,d]	6.5–6.9[e]	22, 63, 79, 85, 89, 102	8–16[h,i,k]	80, 81, 22	1.4–1.7[j]	55

Explanation of Data

The superscripts beside each of the estimates of M_o, M_w, L, and slip rate represent the following:

M_o estimated from (a) geological observations, (b) intensity data, (c) body waves, and (d) surface waves.

M_w estimated from (e) M_o, using the equation $\log M_o = 16.1 + 1.5M$ (Hanks and Kanamori, 1979). If a range of M_o is given, then the equivalent range of M_w is shown; (f) intensity data.

Length estimated from (g) geological observations, (h) aftershock distribution, (i) geodetic data, (j) broadband data, and (k) borehole-dilatational strainmeter data.

Slip rate estimated from (l) geological observations; (m) the equation $U^s = \dot{M}_0^s/\mu LW$, in which U^s is the slip rate, $\dot{M}_0^s$ is the seismic moment rate [New Madrid $\dot{M}_0^s$ is calculated by estimating the M_0 of the 1811 event from $\log M_0 = 16.1 + 1.5M$ (Hanks and Kanamori, 1979), and then dividing M_0 by return times estimated from paleoliquefaction studies], μ is the rigidity modulus, and L and W are the fault length and width; (n) geodetic data; and (o) slip partitioning studies.

*The references for the data sources are as follows:

1. Sieh (1978). 2. Tsai and Aki (1969). 3. Brown and Vedder (1967). 4. Lienkaemper *et al.* (1991). 5. Knuepfer (1992). 6. Bakun and McEvilly (1984). 7. Wilson (1936). 8. Brune and Allen (1967). 9. Trifunac (1972). 10. Stein and Thatcher (1981). 11. Petersen *et al.* (1991). 12. Petersen and Wesnousky (1994), 13. Clark (1972). 14. Hamilton (1972). 15. Sharp *et al.* (1982). 16. Hanks and Kanamori (1979). 17. Page (1935). 18. Van Dissen and Yeats (1991). Cowan and McGlone (1991). 20. Witkind (1964). 21. Research Group for Active Faults of Japan (1992). 22. Hudnut *et al.* (1994). 23. Prentice (1989). 24. Sims (1991). 25. Niemi and Hall (1992). 26. Clahan *et al.* (1994). 27. Wallace and Whitney (1984). 28. Bell and Katzer (1990). 29. Okada and Ikeda (1991). 30. Ambraseys (1970). 31. Straub and Kahle (1994). 32. Thomas and Rockwell (1996). 33. Hirabayashi *et al.* (1995). 34. Doser (1985a). 35. Sharp (1981). 36. Matsuda (1974). 37. Mikumo and Ando (1976). 38. Matsuda *et al.* (1980). 39. Thatcher *et al.* (1980). 40. Kanamori (1973). 42. Abe (1978). 43. Teng *et al.* (1983). 44. Savage *et al.* (1979). 45. Trumm *et al.* (1986). 46. Urhammer *et al.* (1983). 47. Galehouse (1991). 48. Abe (1975). 49. Bird and Kong (1994). 50. Hardin and Matti (1989). 51. Nairn and Beanland (1989). 52. Kanamori and Regan (1982). 53. Weber and Anderson (1990). 54. Jennings (1975). 55. Yeats and Huftile (1995). 56. Doser and Smith (1985). 57. Tanimoto and Kanamori (1986). 58. Doser (1985b). 59. Sykes and Quittmeyer (1981). 60. Kanamori (1983). 61. Sieh and Jahns (1984). 62. Thatcher (1975). 63. Thio and Kanamori (1994a). 64. Caskey *et al.* (1995). 65. Romanowicz (1992). 66. Yoshida and Abe (1992). 67. Bakun *et al.* (1984). 68. Bent *et al.* (1989). 69. Sharp *et al.* (1989). 70. Nuttli (1983). 71. Ad Hoc Working Group on the Probabilities of Future Large Earthquakes in Southern California (1992). 72. Zhou *et al.* (1983b). 73. Reasenberg and Ellsworth (1982). 74. Crone *et al.* (1987). 75. Zhou *et al.* (1983a). 76. Hanks and Krawinkler (1991). 77. Marshall *et al.* (1991). 78. Wells and Coppersmith (1994). 79. Zhao (1994). 80. Dreger *et al.* (1994). 81. Johnston and Linde (1994). 82. Sieh *et al.* (1993). 83. Lensen (1978). 84. Oral *et al.* (1995). 85. Wald and Heaton (1994b). 86. Johnston and Kanter (1990). 87. Cowan (1990). 88. Eiby (1973). 89. Thio and Kanamori (1994b). 90. Kanamori and Allen (1986). 91. Jones and Wesnousky (1992). 92. Beanland and Clark (1995). 93. Wesnousky and Leffler (1992). 94. Cowan (1991). 95. Bouchon (1982). 96. Hanks and Wyss (1972). 97. Freymueller (1994). 98. Johnson *et al.* (1994). 99. Wald and Heaton (1994a). 100. Cohee and Beroza (1994). 101. Dreger (1994). 102. Song *et al.* (1994). 103. J. Caskey, personal comm. 104. T. Nakata, personal comm. 105. Berryman (1979). 106. Gurrolo and Rockwell (1996). 107. Barka and Gulen (1988). 108. Yu and Segall (1995).

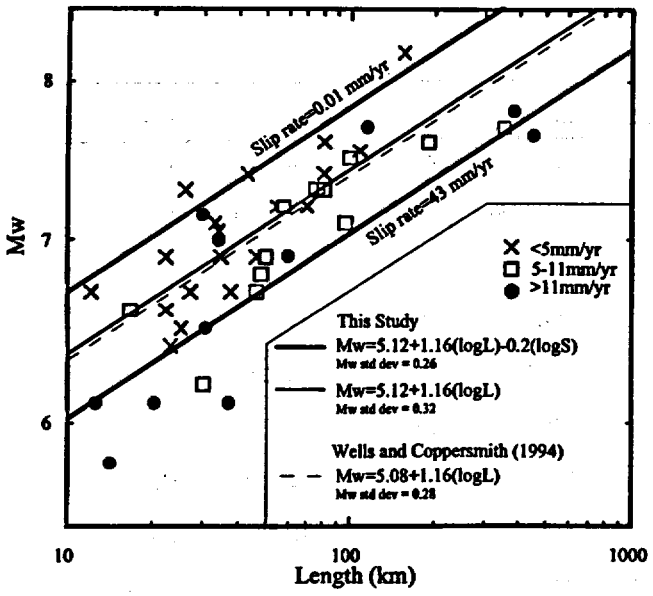

Figure 1. Relationship between magnitude, rupture length, and slip rate. Data are shown as points (mean values of length and M_w), with different symbols depending on the range of fault slip rate. The heavy lines are from equation (2), which includes slip rate, and are shown for slip rates of 0.01 mm/yr and 43 mm/yr, as labeled on the graph. The light solid line is the prediction from equation (3) in which slip rate is not included as a parameter. The dashed line shows regression results of Wells and Coppersmith (1994) for magnitude as a function of surface rupture length.

Predicted magnitudes using equation (2) are shown in Figure 1. For comparison, we also determined the regression relationship between only magnitude and fault rupture length to equal

$$M_w = (5.12 \pm 0.12) + (1.16 \pm 0.07)\log L \quad (3)$$

Equation (3) is shown by the thin line on Figure 1.

The sample standard deviation is defined by

$$\sigma = \left\{\frac{1}{N}\sum(M_i - \hat{M}_i)^2\right\}^{1/2},$$

where M_i is the observation and $\hat{M}_i$ is the predicted magnitude, and the sum is over all observations. For equation (2), we found $\sigma = 0.26$ magnitude units. For the predictions of equation (3), $\sigma = 0.32$ magnitude units. Although the F-test (e.g., Mason *et al.*, 1989) indicates that this error reduction is significant at only 75% confidence, equation (2) is better than equation (3) with 95% confidence when an $L1$ norm (e.g., Menke, 1989) is used to measure the misfit. More importantly, the coefficient, C, on slip rate, in distribution on Figure 2, is never closer to zero than -0.05, indicating much less than 1 chance in 10,000 of finding a set of parameters, within the specified ranges, for which the coefficient on slip rate is zero. That is to say, the distribution on coefficient C shows that a regression that does not include slip rate as a parameter will systematically overestimate the expected magnitude of earthquakes on the fastest slipping faults and, conversely, will systematically underestimate the expected magnitude of earthquakes on the slowest slipping faults. It is on these bases that we assert that inclusion of slip rate leads to meaningful improvement in the fit to the data.

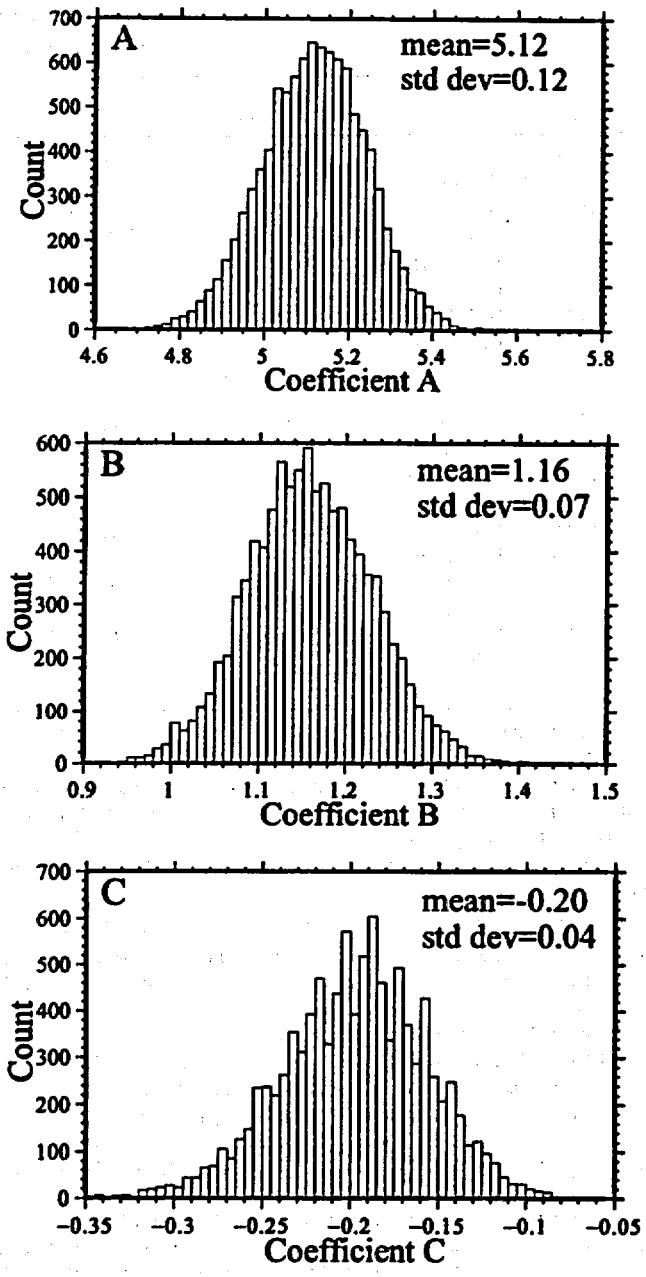

Figure 2. Distribution of coefficients A, B, and C (equation 1) in 10,000 runs in which the slip rate and rupture length on each fault and M_w are chosen at random from a uniform distribution within a range of allowed values, as discussed in the text. Specifically, log S and log L are given uniform distributions between their minimum and maximum values.

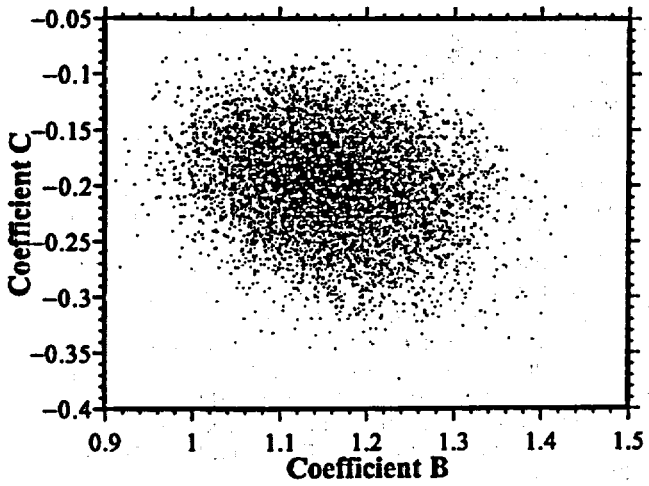

Figure 3. Scatter plot of coefficients B and C for 10,000 individual runs in the Monte Carlo calculations.

Discussion

Because we have considered only faults for which slip rate estimates exist, our data set is much smaller than used in the recent summary and regression analyses of Wells and Coppersmith (1994). Nonetheless, Figure 1 shows that equation (3) is virtually identical to the Wells and Coppersmith regression. It thus appears that our data are not obviously biased in any significant manner relative to the data used by Wells and Coppersmith.

For any given fault length, the curve for the slowest slip rate in Table 1 (S = 0.01 mm/yr) yields estimates of magnitude about 0.7 magnitude units greater than the curve for the fastest slip rate in Table 1 (S = 43 mm/yr curve), a difference twice the standard deviation of the curve fit. The regression of M_w on L that ignores slip rate (equation 3) would agree with the regression in equation (2) for S = 1 mm/yr. The comparison of curves illustrates that simple regressions of M_w on L that ignore fault slip rate appear to underestimate the magnitude of earthquakes on the relatively slow slipping faults. That is to say, information useful to making accurate estimates of future earthquake size is being ignored when fault slip rate is not considered in estimating potential earthquake size on active faults.

It is also useful to briefly consider our results in the context of the definition of seismic moment. The seismic moment is defined as $M_0 = \mu LWD$, in which L is fault length, W is fault width, D is average slip, and μ is the shear modulus, which is about 3×10^{11} dyne/cm^2. The relationship between seismic moment and magnitude is $M_w = (2/3)(\log M_0 - 16)$, where M_0 is in units of dyne-cm (Hanks and Kanamori, 1979). Combining the two relationships yields

$$M_w = \frac{2}{3}\log L + \frac{2}{3}\log D + \frac{2}{3}(\log \mu + \log W - 16).$$

We may consider W approximately constant because our data set is limited to earthquakes with moderate to high dip and in regions where the seismogenic depth is limited to the upper 15 to 20 km. Thus, M_w will be primarily dependent on L and D. If $D \propto W$ (the W model), B should equal 2/3. If $D \propto L$ (the L model), as suggested by Scholz (1982) and approximately confirmed by the data set of Wells and Coppersmith (1994), then M_w = 4/3 Log L + const. The value we obtain for B (equation 2) is between these two values. If only faults with $L > 30$ km are included in the regression to assure that L is greater than the fault width, the coefficient B is 1.18, which is about the same as the result with the full data set. Thus, B is much closer to the prediction of the L model than it is to the prediction of the W model, but it is significantly different from either one.

The reduction of magnitude with a higher slip rate is consistent with a physical model in which, as the time from the last earthquake increases, geological processes strengthen the fault (Kanamori and Allen, 1986; Scholz *et al.*, 1986). Stated another way, a fault with a slow slip rate tends to have earthquakes with a greater static stress drop and greater average slip than a fault with a faster slip rate. The compilation of Wells and Coppersmith (1994) suggested that dip-slip faults tend to have a larger average slip per event (magnitude held constant) than strike-slip faults. To test this, the data were divided into faults with strike-slip mechanisms and faults with dip-slip mechanisms. The regression on strike-slip data gave similar coefficients to those in equation (2). The dip-slip data cover only a small range of slip rates, and consequently, the coefficient on slip rate is smaller. Nonetheless, the regression on dip-slip faults alone predicts similar magnitudes as equation (2) for the slip rates spanned by the data. Hence, fault mechanism does not appear to be as important a factor as the slip rate on the fault on which the earthquake occurs when trying to estimate the earthquake size or stress drop as a function of fault length.

In the context of the physical model, it is interesting to consider some of the events that are conspicuously below the prediction curves in Figure 1. Four events with $L < 50$ km fall between 0.2 and 0.5 magnitude units below the curve for 43 mm/yr. All are from central or northern California: 1934 Parkfield; 1966 Parkfield; 1984 Morgan Hill; 1979 Coyote Lake. An interesting feature of all of these events is that they occurred adjacent to creeping sections of the San Andreas system. Considering that fault strength is probably significantly below average on the creeping sections, it is plausible that strength for all of these segments is somewhat lower than average, contributing to the anomalies.

It is plausible that amplitudes of dynamic strong ground motions correlate with static stress drop. If so, our observations predict that strong ground motion amplitudes are inversely related to fault slip rate. Recently, Boore *et al.* (1995) observed that reverse faults have larger ground motions than strike-slip faults. The result is probably consistent with our result because most of the reverse faults in their data set are characterized by low slip rate. In other words, it is reasonable

that fault slip rate has more influence on dynamic strong ground motion than does fault mechanism and that estimation techniques for the dynamic ground motions from earthquakes might be improved by incorporating slip rate.

Conclusions

We conclude that a regression for moment magnitude (M_w) as a function of surface rupture length (L) and fault slip rate (S) reduces the uncertainty in estimating the potential size of future earthquakes on mapped faults as compared to the standard regressions of M_w on L that are commonly used in seismic hazard analysis. The results of the regression indicate that faults with slower slip rates tend to fail in earthquakes with higher static stress drop.

Acknowledgments

Takashi Nakata and John Caskey supplied unpublished slip-rate data for the Philippines and Dixie Valley faults, respectively. Michael P. Sleeman and Takashi Kumamoto helped with some initial data gathering and analysis. We thank Donald Wells and an anonymous reviewer for their helpful comments. This research was supported by the U.S. Geological Survey (Grants 1434-94-G-2460 and 1434-94-G-2479) and the Southern California Earthquake Center. Center for Neotectonic Studies Contribution No. 14.

References

Abe, K. (1975). Reexamination of the fault model for the Niigata earthquake of 1964. *J. Phys. Earth* **23**, 394–366.

Abe, K. (1978). Dislocations, source dimensions and stresses associated with earthquakes in the Izu Peninsula, Japan, *J. Phys. Earth* **26**, 253–274.

Ad Hoc Working Group on the Probabilities of Future Large Earthquakes in Southern California (1992). *Future Seismic Hazards in Southern California; Phase I: Implications of the 1992 Landers Earthquake Sequence*, National Earthquake Prediction Evaluation council, California Earthquake Prediction Evaluation council, and Southern California Earthquake Center technical report, 42 pp.

Ambraseys, N. (1970). Some characteristic features of the Anatolian fault zone, *Tectonophysics* **9**, 143–165.

Bakun, W. H., M. M. Clark, R. S. Cockerham, W. L. Ellsworth, A. G. Lindh, W. H. Prescott, A. F. Shakal, and P. Spudich (1984). The 1984 Morgan Hill, California, earthquake, *Science* **225**, 288–291.

Bakun, W. H. and T. V. McEvilly (1984). Recurrence models and Parkfield earthquakes, *J. Geophys. Res.* **89**, 3051–3058.

Barka, A. A. and L. Gulen (1988). New constraints on age and total offset of North Anatolian fault zone: implications for tectonics of the eastern Mediterranean region, in *Special Publication of the Middle East Technological University 1987. Meloh Tokay Geology Symposium*, Ankara, Turkey.

Beanland, S. and M. M. Clark (1995). The Owens Valley fault zone, eastern California, and surface faulting associated with the 1872 earthquake, *U.S. Geol. Soc. Bull.* **1982**, 29 pp.

Bell, J. W. and T. Katzer (1990). Timing of late Quaternary faulting in the 1954 Dixie Valley earthquake area, central Nevada, *Geology* **18**, 622–625.

Bent, A. L., D. V. Helmberger, R. J. Stead, and P. Ho-Liu (1989). Waveform modeling of the November 1987 Superstition Hills earthquakes, *Bull. Seism. Soc. Am.* **79**, 500–514.

Berryman, K. R. (1979). Active faulting and derived PHS directions in the South Island, New Zealand, *Roy. Soc. New Zealand Bull.* **18**, 29–34.

Bird, P. and X. Kong (1994). Computer simulations of California tectonics confirm very low strength of major faults, *Geol. Soc. Am. Bull.* **106**, no. 2, 159–174.

Bonilla, M. G. (1973). Trench exposures across surface fault ruptures associated with San Fernando earthquake, in San Fernando, California, earthquake of February 9, 1971, 3, pp. 173–182, United States Department of Commerce, Washington, D.C.

Boore, D. M., W. B. Joyner, and T. E. Fumal (1995). Ground motion estimates for strike- and reverse-slip faults (preprint).

Bouchon, M. (1982). The rupture mechanism of the Coyote Lake earthquake of August 6, 1979 inferred from near field data, *Bull. Seism. Soc. Am.* **72**, 745–757.

Brown, R. D., Jr. and J. G. Vedder (1967). The Parkfield-Cholame, California, earthquakes of June–August 1966: surface tectonic fractures along the San Andreas Fault, *U.S. Geol. Surv. Profess. Paper 579.*

Brune, J. N. and C. R. Allen (1967). A low stress-drop, low-magnitude earthquake with surface faulting: the Imperial, California, earthquake of March 4, 1966, *Bull. Seism. Soc. Am.* **57**, 501–514.

Canitez, N. and M. N. Toksoz (1972). Static and dynamic study of earthquake source mechanism: San Fernando Earthquake, *J. Geophys. Res.* **77**, 2583–2594.

Caskey, S. J., S. G. Wesnousky, P. Zhang, and D. B. Slemmons (1995). Surface faulting of the 1954 Fairview Peak (Ms = 7.2) and Dixie Valley (Ms = 6.9) earthquakes, Central Nevada, *Bull. Seism. Soc. Am.* **85**, 000–000.

Clahan, K. B., N. T. Hall, and R. H. Wright (1994). Preliminary late Holocene slip rate for the San Francisco Peninsula segment of the San Andreas fault (abstracts with programs), *Geol. Surv. Am.* **26**, no. 2.

Clark, M. M. (1972). Surface rupture along the Coyote Creek fault, the Borrego Mountain Earthquake of April 9, 1968, *U.S. Geol. Surv. Profess. Paper 787*, 55–57.

Cohee, B. P. and G. C. Beroza (1994). Slip distribution of the 1992 Landers earthquake and its implications for earthquake source mechanics, *Bull. Seism. Soc. Am.* **84**, 692–712.

Cowan, H. A. (1990). Late Quaternary displacements on the Hope fault at Glynn Wye, North Canterbury, *New Zealand J. Geol. Geophys.* **33**, 285–294.

Cowan, H. A. (1991). The North Canterbury earthquake of September 1, 1888, *J. Roy. Soc. New Zealand* **21**, 1–12.

Cowan, H. A. and M. S. McGlone (1991). Late Holocene displacements and characteristic earthquakes on the Hope River segment of the Hope fault, New Zealand, *J. Roy. Soc. New Zealand* **21**, 373–384.

Crone, A. J., M. N. Machette, M. G. Bonilla, J. J. Lienkaemper, K. L. Pierce, W. E. Scott and R. C. Bucknam (1987). Surface faulting accompanying the Borah Peak earthquake and segmentation of the Lost River fault, central Idaho, *Bull. Seism. Soc. Am.* **77**, 739–770.

Doser, D. I. (1985a). The 1983 Borah Peak, Idaho and 1959 Hebgen Lake, Montana earthquakes: models for normal fault earthquakes in the Intermountain Seismic Belt, in *Proceedings of Workshop XXVIII, on the Borah Peak, Idaho earthquake, U.S. Geol. Surv. Open-File Rept.* **85–290.**

Doser, D. I. (1985b). Source parameters and faulting processes of the 1959 Hebgen Lake, Montana earthquake sequence, *J. Geophys. Res.* **90**, 4537–4555.

Doser, D. I. and R. B. Smith (1985). Source parameters of the 28 October 1983 Borah Peak, Idaho, earthquake from body wave analysis, *Bull. Seism. Soc. Am.* **90**, 1041–1051.

Dreger, D. S. (1994). Investigation of the rupture process of the 28 June 1994 Landers Earthquake Utilizing TERRAscope, *Bull. Seism. Soc. Am.* **84**, 713–714.

Dreger, D., M. Pasyanos, S. Loper, R. McKenzie, N. Gregor and B. Romanowicz (1994). The January 17, 1994 Northridge earthquake: a regional perspective, *Program for Northridge Abstracts, 89th Seismological Society of America Meeting.*

Eiby, G. A. (1973). A descriptive catalog of New Zealand earthquakes, *New Zealand J. Geol. Geophys.* **16**, 857–907.

Freymueller, J. (1994). The co-seismic slip distribution of the Landers earthquake, *Bull. Seism. Soc. Am.* **84**, 646–659.

Galehouse, J. S. (1991). Creep rates on the Bay Area faults during the past decade, *Seism. Res. Lett.* **62**, 12.

Gurrola, L. D. and T. K. Rockwell (1996). Timing and slip for prehistoric

earthquakes on the Superstition Mountain fault, Imperial Valley, southern California, *J. Geophys. Res.* (in press).

Hamilton, R. M. (1972). Aftershocks of the Borrego Mountain earthquake from April 12 to June 12, 1968, The Borrego Mountain Earthquake of April 9, 1968, *U.S. Geol. Surv. Profess. Paper 787.*

Hanks, T. and H. Kanamori (1979). A moment magnitude scale, *J. Geophys. Res.* **84**, 2348–2350.

Hanks, T. C. and H. Krawinkler (1991). The 1989 Loma Prieta earthquake and its effects: introduction to the special issue, *Bull. Seism. Soc. Am.* **81**, 1415–1423.

Hanks, T. C. and M. Wyss (1972). The use of body-wave spectra in the determination of seismic-source parameters, *Bull. Seism. Soc. Am.* **62**, 561–589.

Harden, J. W. and J. C. Matti (1989). Holocene and late Pleistocene slip rates on the San Andreas Fault in Yucaipa, California, using displaced alluvial-fan deposits and soil chronology, *Geol. Soc. Am. Bull.* **101**, 1107–1117.

Hirabayashi, K. C. and T. K. Rockwell (1996). A neotectonic study of the San Miguel-Vallecitos fault, Baja California, Mexico, *Bull. Seism. Soc. Am.* **86**, 000–000.

Hudnut, K. W., M. H. Murray, A. Donnellan, Y. Bock, P. Fang, M. Cline, Y. Feng, Z. Shen, B. Hager, T. Herring, and R. King (1994). Coseismic displacements of the 1994 Northridge, California, earthquake, *The 89th Annual Meeting of the Seismological Society of America.*

Hudnut, K. W. and K. E. Sieh (1989). Behavior of the Superstition Hills Fault during the past 330 years, *Bull. Seism. Soc. Am.* **79**, 304–329.

Hudnut, K. W., M. H. Murray, A. Donnellan, Y. Bock, P. Fang, M. Cline, Y. Feng, Z. Shen, B. Hager, T. Herring, and R. King (1994). Coseismic displacements of the 1994 Northridge, California, earthquake, Program for Northridge abstracts, *89th Seismological Society of America Meeting.*

Jennings, C. W. (1975). Fault map of California, California geologic data map series, Department of Conservation, San Francisco, California.

Johnson, H. O., D. C. Agnew, and K. Hudnut (1994). Bounds on earthquake movement from geodetic data: application to the Landers earthquake, *Bull. Seism. Soc. Am.* **84**, 660–667.

Johnston, A. C. and L. R. Kanter (1990). Earthquakes in stable continental crust, *Scientific Am.* **262**, 68–75.

Johnston, M. J. S. and A. T. Linde (1994). Continuous borehole strain before, during and after the Jan 17, 1994, M6.7 Northridge, California, earthquake, Program for Northridge abstracts. *89th Seismological Society of America Meeting.*

Jones, C. H. and S. G. Wesnousky (1992). Variations in strength and slip rate along the San Andreas Fault System, *Science* **256**, 83–86.

Kanamori, H. (1973). Mode of strain release associated with major earthquakes, in Japan, *Annu. Rev. Earth Planet Sci.* **1**, 213–239.

Kanamori, H. (1983). Mechanism of the 1983 Coalinga earthquake determined from long-period surface waves, *Calif. Div. Mines Geol. Spec. Publ.* **66**, 233–240.

Kanamori, H. and C. R. Allen (1986). Earthquake repeat time and average stress drop, *Earthquake Source Mechanics* S. Das, J. Boatwright, and C. H. Scholz (Editors), *Geophysical Monograph* **37**, 227–235.

Kanamori, H. and J. Regan (1982). Long-period surface waves, *U.S. Geol. Surv. Profess. Pap. 1254*, 55–58.

Knuepfer, P. L. (1992). Temporal variations in latest Quaternary slip across the Australian-Pacific plate boundary, northeastern South Island, New Zealand, *Tectonics* **11**, no. 3, 449–464.

Lensen, G. J. (1960). A 12 mile lateral drag along the Awatere fault, Abstract for the 9th Science Congress, Royal Society of New Zealand, 47.

Lensen, G. J. (1978). Historic tectonic earth deformation, in *The Geology of New Zealand,* R. P. Suggate, G. R. Stevens, and M. T. TePunga (Editors), Government Printer. Wellington, 33–37.

Lienkaemper, J. J., G. Borchardt, and M. Lisowski (1991). Historic creep rate and potential for seismic slip along the Hayward fault, California, *J. Geophys. Res.* **96**, 18261–18283.

Marshall, G. A., R. S. Stein, and W. Thatcher (1991). Faulting Geometry and slip from co-seismic elevation changes: the 18 October 1989, Loma Prieta, California, earthquake, *Bull. Seism. Soc. Am.* **81**, 1660–1693.

Mason, R. L., R. F. Gunst, and J. L. Hess (1989). *Statistical Design and Analysis of Experiments,* John Wiley & Sons, New York, 692 pp.

Matsuda, T. (1974). Surface faults associated with Novi (mino-Owari) earthquake of 1891, Japan, *Bull. Seism. Soc. Am.* **13**, 85–126.

Matsuda, T. (1975). Magnitude and recurrence interval of earthquakes from a fault, *J. Seism. Soc. Japan, Series 2,* **28**, 269–283.

Matsuda, T., H. Yamazaki, T. Nakata, and T. Imaizumi (1980). The surface faults associated with the Rikuu earthquake of 1896, *Bull. Earthquake Res. Inst. Univ. Tokyo* **55**, 795–855.

Menke, W. (1989). *Geophysical Data Analysis: Discrete Inverse Theory,* Academic Press, San Diego, 289 pp.

Mikumo, T. and M. Ando (1976). A search into the faulting mechanism of the 1891 great Nobi earthquake, *J. Phys. Earth* **24**, 63–87.

Nairn, I. A. and S. Beanland (1989). Geological setting of the 1987 Edgecumbe earthquake, New Zealand, *New Zealand J. Geol. Geophys.* **32**, 1–13.

Niemi, T. M. and N. T. Hall (1992). Late Holocene slip rate and recurrence of great earthquakes on the San Andreas fault in northern California, *Geology* **20**, no. 3, 195–198.

Nuttli, O. W. (1983). Average seismic source parameter relations for mid-plate earthquakes, *Bull. Seism. Soc. Am.* **73**, 519–535.

Okada, A. and Y. Ikeda (1991). Active faults and neotectonics in Japan, *Quaternary Res.* **30**, 161–174.

Oral, M. B., M. Reilinger, T. Nafi, R. W. King, A. A. Barka, K. Ibrahim, and O. Lenk (1995). Global positioning system offers evidence of plate motions in eastern Mediterranean, *EOS* **76**, no. 2, 9–11.

Page, B. M. (1935). Basin-Range faulting in Pleasant Valley, Nevada, *J. Geol.* **43**, 690–707.

Petersen, M. D., L. Seeber, L. R. Sykes, J. F. Nabelek, J. Armbruster, J. Pacheco, and K. W. Hudnut (1991). Seismicity and fault interaction, southern San Jacinto fault, southern California: implications for seismic hazard, *Tectonics* **10**, 1187–1203.

Petersen, M. D. and S. G. Wesnousky (1994). Fault slip rates and earthquake histories for active faults in southern California, *Bull. Seism. Soc. Am.* **84**, no. 5, 1608–1649.

Prentice, C. S. (1989). Earthquake geology of the northern San Andreas fault near Point Arena, California, *Ph.D. Thesis.* California Institute of Technology, Pasadena, California.

Reasenberg, P. and W. L. Ellsworth (1982). Aftershocks of the Coyote Lake, California, earthquake of August 6, 1979, *J. Geophys. Res.* **87**, 10637–10655.

Research Group for Active Faults of Japan (1992). Map of Active Faults in Japan with an Explanatory Text, University of Tokyo Press.

Romanowicz, B. (1992). Strike-slip earthquakes on quasi-vertical transcurrent faults: inferences for general scaling relations, *Geophys. Res. Lett.* **19**, 481–484.

Savage, J. C., W. H. Prescott, M. Lisowski and N. King (1979). Geodetic measurements of deformation near Hollister, California, 1971–1978, *J. Geophys. Res.* **84**, 7599–7615.

Scholz, C. H. (1982). Scaling laws for large earthquakes: consequences for physical models, *Bull. Seism. Soc. Am.* **72**, 1–14.

Scholz, C. H., C. A. Aviles, and S. G. Wesnousky (1986). Scaling differences between large intraplate and interplate earthquakes, *Bull. Seism. Soc. Am.* **76**, 65–70.

Sharp, R. V. (1981). Displacements on tectonic ruptures in the San Fernando earthquake of February 9, 1971: discussion and some implications. *U.S. Geol. Surv. Open-File Rept. 81-668.*

Sharp, R. V., K. E. Budding, J. Boatright, M. J. Ader, M. G. Bonilla, M. M. Clark, T. E. Fumal, K. K. Harms, J. J. Lienkaemper, D. M. Morton, B. J. O'Niel, C. L. Ostergren, D. J. Ponti, M. J. Rymer, J. L. Saxton, and J. D. Sims (1989). Surface faulting along the Superstition Hills fault zone and nearby faults associated with the earthquakes of 24 November 1987, *Bull. Seism. Soc. Am.* **79**, 252–281.

Sharp, R. V., J. J. Lienkaemper, M. G. Bonilla, D. B. Burke, B. F. Cox, D. G. Herd, D. M. Miller, D. M. Morton, D. J. Ponti, M. J. Rymer, J. C. Tinsley, J. C. Yount, J. F. Kahle, E. W. Hart, and K. E. Sieh (1982).

Surface faulting in central Imperial Valley, California, earthquake of October 15, 1979, in the Imperial Valley, California, earthquake of October 15, 1979, *U.S. Geol. Surv. Profess. Pap.* **1254**, 119–143.

Sieh, K., L. Jones, E. Hauksson, K. Hudnut, D. Eberhart-Phillips, T. Heaton, S. Hough, K. Hutton, H. Kanamori, A. Lilje, S. Lindvall, S. F. McGill, J. Mori, C. Rubin, J. A. Spotila, J. Stock, H. Thio, J. Treiman, B. Wernicke, and J. Zachariasen (1993). Near-field investigations of the Landers earthquake sequence, April to July 1992, *Science* **260**, 171–176.

Sieh, K. E. (1978). Slip along the San Andreas fault associated with the great 1857 earthquake, *Bull. Seism. Soc. Am.* **68**, 1421–1448.

Sieh, K. E. and R. H. Jahns (1984). Holocene activity of the San Andreas Fault at Wallace Creek, California, *Geol. Soc. Am. Bull.* **95**, 883–896.

Sieh, K., L. Jones, E. Hauksson, and K. Hudnut (1993). Near-field investigations of the Landers earthquake sequence, April to July, 1992, *Science* **260**, 171–176.

Sims, J. D. (1991). Distribution and rate of slip across the San Andreas transform boundary, Hollister area, central California, *Geol. Soc. Am.* (abstracts with programs), **23**, no. 2, 98.

Song, X., L. E. Jones, and D. Helmberger (1994). Source characteristics of the January 17, 1994 Northridge California earthquake from regional broadband modeling, Program for Northridge abstracts. *89th Seismological Society of America Meeting.*

Stein, R. S. and W. Thatcher (1981). Seismic and aseismic deformation associated with the 1952 Kern County, California, earthquake and relationship to Quaternary history of the White Wolf fault, *J. Geophys. Res.* **86**, 4913–4928.

Straub, C. and H. Kahle (1994). Global Positioning System (GPS) estimates of crustal deformation in the Marmara Sea region, northwestern Anatolia, *Earth Planet. Sci. Lett.* **121**, 495–502.

Sykes, L. R. and R. C. Quittmeyer (1981). Repeat times of great earthquakes along simple plate boundaries, in *Earthquake Prediction: An International Review, Maurice Ewing Series 4*, D. W. Simpson and P. G. Richards (Editors), American Geophysical Union, Washington, D.C., 217–247.

Tanimoto, T. and H. Kanamori (1986). Linear programming approach to moment tensor inversion of earthquake sources and some tests on the three-dimensional structure of the upper mantle, *Geophys. J. R. Astr. Soc.* **84**, 413–430.

Teng, R., Z. Huang, H. Qian, T. Deng, L. Jiang, P. Ge, S. Liu, Y. Cao, and C. Zhang (1983). On the recent tectonic activity and earthquakes of the Xianshuihe fault zone in *A Collection of Papers of International Symposium on Continental Seismicity and Earthquake Prediction*, Seismological Press, Beijing.

Thatcher, W. (1975). Strain accumulation and release mechanism of the 1906 San Francisco earthquake, *J. Geophys. Res.* **80**, 4862–4872.

Thatcher, W., T. Matsuda, and J. B. Rundle (1980). Lithospheric loading by the 1896 Rikuu earthquake in northern Japan: implications for plate flexure and asthenospheric rheology, *J. Geophys. Res.* **85**, 6429–6435.

Thio, H. K. and H. Kanamori (1994a). Source complexity of the 1994 Northridge earthquake, Program for Northridge Abstracts, *89th Seismological Society of America Meeting.*

Thio, H. K. and H. Kanamori (1994b). Moment tensor solutions for the Northridge earthquake sequence, Program for Northridge Abstracts, *89th Seismological Society of America Meeting.*

Thomas, A. P. and T. K. Rockwell (1996). Slip on the Imperial fault in the past 300 years at the U.S.-Mexico international border based on trenching, *Bull. Seism. Soc. Am.* **86**, (in press).

Trifunac, M. D. (1972). Tectonic stress and the source mechanism of the Imperial Valley, California, earthquake of 1940, *Bull. Seism. Soc. Am.* **62**, 1283–1302.

Trumm, D. A., J. C. Tinsley, and R. S. Stein (1986). Holocene fold deformation and earthquake recurrence at Coalinga anticline, California: fluvial stratigraphic analysis, *EOS* **67**, 1222.

Tsai, Y. B. and K. Aki (1969). Simultaneous determination of the seismic moment and attenuation of seismic surface waves, *Bull. Seism. Soc. Am.* **59**, 275–287.

Urhammer, R. A., Darragh, R. D. and B. Bolt (1983). The 1983 Coalinga earthquake sequence: May 2 through Aug. 1, *Spec. Rept. Calif. Div. Mines Geol.* **66**, 221–232.

Van Dissen, R. J. and R. S. Yeats (1991). Hope fault, Jorden thrust, and uplift of the Seaward Kaikoura Range, New Zealand, *Geology* **19**, 393–396.

Wald, D. J. and T. H. Heaton (1994a). A multidisciplinary source analysis of the 1994 (Mw6.7) Northridge earthquake using strong motion, teleseismic, and geodetic data, Program for Northridge Abstracts, *89th Seismological Society of America Meeting.*

Wald, D. J. and T. H. Heaton (1994b). Spatial and temporal distribution of slip for the 1992 Landers, California, earthquake, *Bull. Seism. Soc. New Zealand* **84**, 668–692.

Wallace, R. E. and R. A. Whitney (1984). Late Quaternary history of the Stillwater seismic gap, Nevada, *Bull. Seism. Soc. Am.* **74**, 301–314.

Weber, G. E. and R. S. Anderson (1990). Marine terrace deformation pattern: its implications for repeat times of Loma Prieta earthquakes and for the long term evolution of the Santa Cruz mountains, *U.S. Geol. Surv. Open-File Rept. 90–274.*

Wells, D. G. and K. J. Coppersmith (1994). New empirical relationships among magnitude, rupture length, rupture width, rupture area, and surface displacement, *Bull. Seism. Soc. Am.* **84**, 974–1002.

Wesnousky, S. G. (1986). Earthquakes, Quaternary faults, and seismic hazard in California, *J. Geophys. Res.* **91**, 12587–12631.

Wesnousky, S. G. and L. M. Leffler (1992). The repeat time of the 1811 and 1812 New Madrid earthquakes: a geological perspective, *Bull. Seism. Soc. Am.* **82**, 1756–1785.

Wilson, J. T. (1936). Foreshocks and aftershocks of the Nevada earthquake of December 20, 1932, and the Parkfield earthquake of June 7, 1934, *Bull. Seism. Soc. Am.* **26**, 189–194.

Witkind, I. J. (1964). Reactivated faults north of Hebgen Lake, *U.S. Geol. Surv. Profess. Pap.* **435**, 37–50.

Yeats, R. S. and G. J. Huftile (1995). The Oak Ridge fault system and the 1994 Northridge earthquake, *Nature* **373**, 418–420.

Yoshida, Y. and K. Abe (1992). Source Mechanism of the Luzon, Philippines Earthquake of July 16, 1990, *Geophys. Res. Lett.* **19**, 545–548.

Yu, E. and P. Segall (1995). Slip in the 1868 Hayward earthquake from the analysis of historical triangulation data, *EOS* **76**, no. 46, 406.

Zhao, L. (1994). Regional waveform modeling of the main shock of 17 January 1994 Northridge, California earthquakes, Program for Northridge Abstracts. *89th Seismological Society of America Meeting.*

Zhou, H., Liu, H. L. and H. Kanamori (1983a). Source processes of large earthquakes along the Xianshuihe fault in Southwestern China, *Bull. Seism. Soc. Am.* **73**, 537–551.

Zhou, H. L., C. R. Allen and H. Kanamori (1983b). Rupture complexity of the 1970 Tonghai and the 1973 Luhuo earthquakes, China, from P-wave inversion and relationship to surface faulting, *Bull. Seism. Soc. Am.* **73**, 1585–1597.

Seismological Laboratory and Department of Geological Sciences
Mackay School of Mines
University of Nevada
Reno, Nevada 89557
E-mail: jga@seismo.unr.edu
(J.G.A.)

Center for Neotectonic Studies and Department of Geological Sciences
Mackay School of Mines
Reno, Nevada 89557
(S.G.W., M.W.S.)

Manuscript received 29 June 1995.

METHODS FOR ASSESSING EARTHQUAKE RECURRENCE

By: James P. McCalpin
GEO-HAZ Consulting, Inc.

For: Yucca Mountain Seismic Hazard Workshop #2
Oct. 16-18, 1996

Note: Page numbers refer to the book "Paleoseismology".

1. AREAL SOURCES

1.1 Simple extrapolation of the historical "b" value from an area, to large magnitudes (M>6)

Problem: M>6 EQs can come from a few large structures, but the bulk of smaller historical EQs (and the "b" value) probably come from many smaller structures. If these 2 groups of sources obey different "b" values, extrapolated recurrence at M>6 will be invaild.

2. FAULT SOURCES

2.1 Simple extrapolation of the historical "b" value for a single fault, to large magnitudes (M>6)

Problem: for most Quaternary faults, there aren't enough historical EQs that can be unambiguously assigned to a given fault

Problem: even if one can derive a "b" value for a given fault, based on M<6 EQs, it may not be valid to extrapolate that "b" value to M>6 to estimate recurrence (Schwartz and Coppersmith, 1984 Fig.)

2.2 Geologic Method #1--Direct Method (p.457-458)

$$RI = D/(S-C)$$

where: RI= recurrence interval (yr)

D= displacement per faulting event (mm)

S= coseismic slip rate (mm/yr)

C= creep rate (mm/yr)

2.3 Geologic method #2--Geologic Method (i.e., dating individual morphogenic paleoearthquakes)

1st Question: what is the magnitude of the morphogenic EQs that we are dating?

A--a range of morphogenic EQs? (M6-7.5)

B--smaller range of characteristic EQs ?(M7-7.5)

C--maximum EQs only ?(M7.5)

Problem: most paleoearthquake dating comes from individual trench sites, but it is hard to estimate paleo-magnitude from a single site, due to spatial variations in displacement during each event.

2.3.1 Dating PaleoEQs by Dating Displaced Geomorphic Surfaces (p. 139-141, 460-461)

(Example of different fault scarp heights on 2 different age surfaces; p. 108-109)

Uncertainties: 1) in the exact ages of the surfaces offset

2) in the uniformity of recurrence

3) even given perfectly uniform recurrence, a range of recurrences is permissible

2.3.2 Dating PaleoEQs by Dating Displaced Deposits (p. 144-145)

Uncertainties: 1) analytical uncertainties

2) calibration uncertainties-- what time scale are dates on?

3) sample context uncertainties (how does the date relate to the timing of the paleoEQ?)

Result= SPACE-TIME DIAGRAM (p. 464-465)

3. VARIATIONS IN RECURRENCE

3.1 Variations in recurrence are closely tied to the magnitude range of characteristic earthquakes. E.g., the slip-predictable model predicts variation in recurrence if magnitudes (stress drops) vary. (Fig.)

3.2 Visualize paleoEQs as points on a time line; recurrence is the gaps between the points (p. 483)

3.3 Probablity Distributions of Recurrence on Single Faults, and on Groups of Faults

3.3.1 Gaussian; COV=sigma/RI=0.3-0.5?

Ex.: if COV=0.3 and RI=1000 yrs, then sigma=300 yrs.
At 1 sigma, RI ranges from 700-1000-1300 yrs
At 2 sigma, RI ranges from 400-1000-1600 yrs

3.3.2 Lognormal distribution (center of mass skewed to left; long tail to right)
Ex.: grouped plate-boundary megaEQs (Nishenko)

3.3.3 Weibull distribution (Pallett Creek, Sieh; 5 central segments of Wasatch fault, McC. and Nishenko) (FIG).

4. TEMPORAL CLUSTERING

(caused by anomalously short recurrence interval(s) compared to the mean)

4.1 On a single fault-- should not happen between maximum, or even characteristic, EQs. Could happen to a degree if all size morphogenic EQs are dated (M 6-7.5)

4.2 On a system of faults or fault segments--(p. 482-487)

--harder to see in a space-time diagran; easier to see on a composite paleoEQ history (all PaleoEQS transferred to a single time line)

--caused by "contagion" ?, i.e. the transfer of stress from one failed segment to the next, which then shortens the time to failure in that segment

--HOWEVER, apparent temporal clustering among faults or segments can easily arise from random coincidences among completely independent faults. THEREFORE, all tests for contagion must be framed in terms of probablities that the cluster is not a fortuitous occurrence.

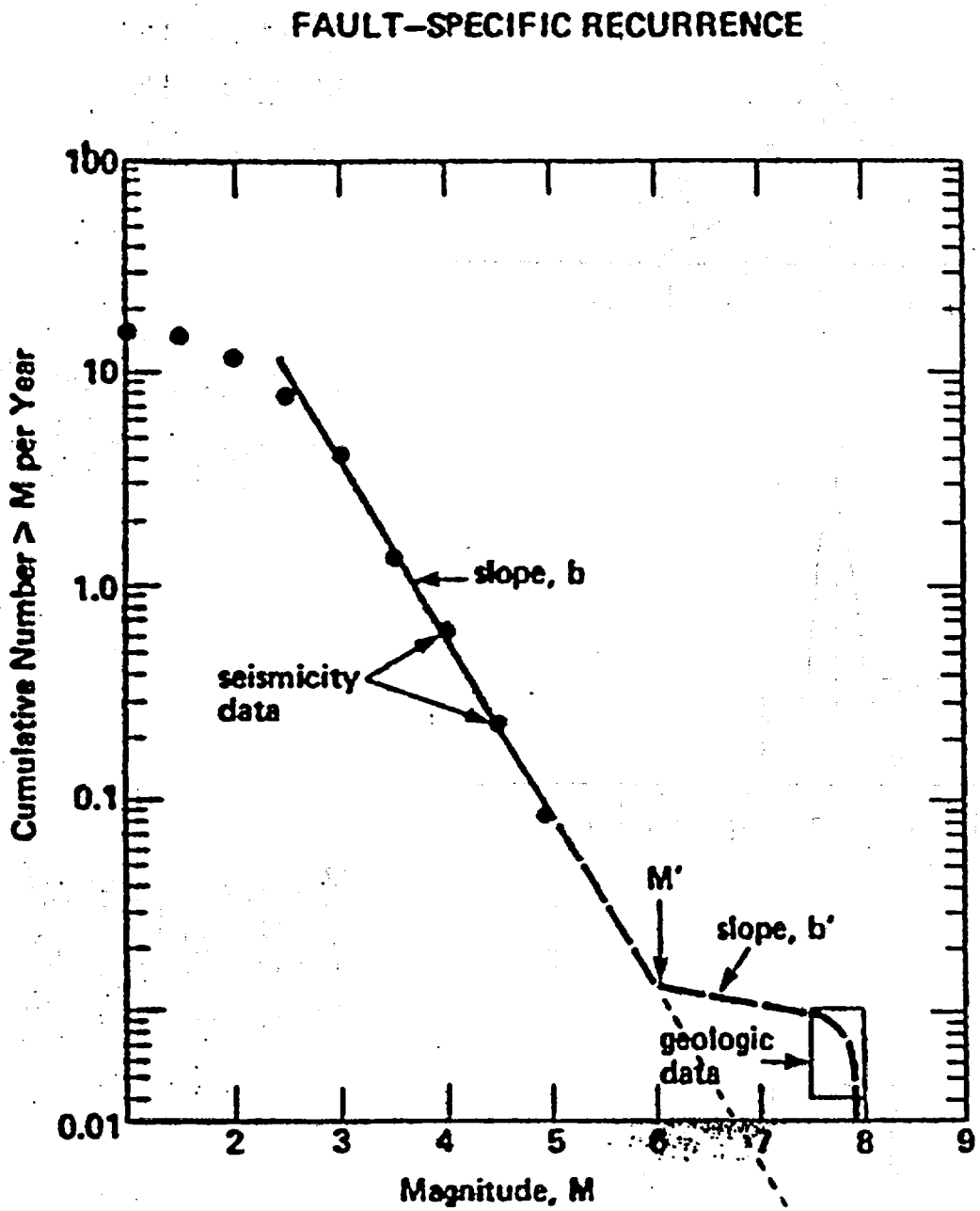

Fig. 15. Diagrammatic cumulative frequency-magnitude recurrence relationship for an individual fault or fault segment. Above magnitude M' a low b value (b') is required to reconcile the small-magnitude recurrence with geologic recurrence, which is represented by the box.

the mismatch between the position of the recurrence curve

and the
must be
rectly fr
long or l
Recur
have be
Greece.
and coa
segment
earthqu
characte
occurs l
relativel
and gen
et al. [19
It has
contribu
an earth
crease t
frequenc
a full cy
earthqu
foreshoc
adjacent
aftersho
[*Agnew*
have be

GIVEN: a land-form is displaced, with 2 age dates = 10.2, 13.6 ka

Q: what is uncertainty in age?

ASSUME

2 ages represent 1σ range; Distrib. = Gauss

$\bar{X}$ = 11.9 ka

RANGE = 3.4 ka

σ = 1.7 ka

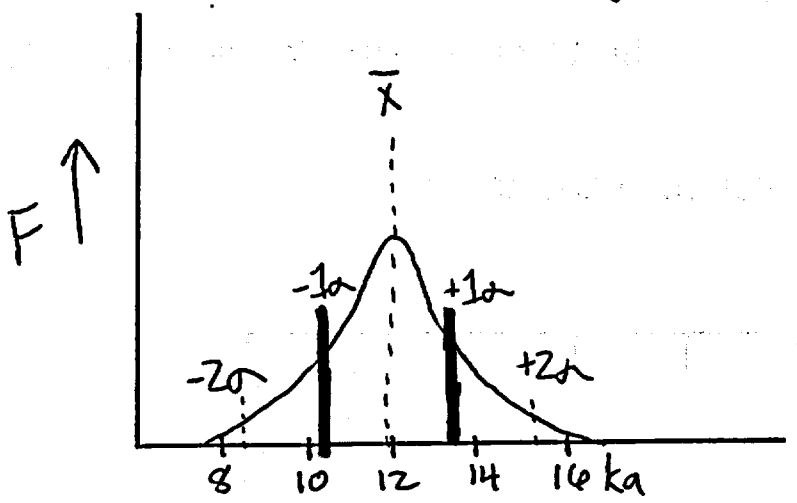

2 ages represent 2σ range; Distrib. = Gauss

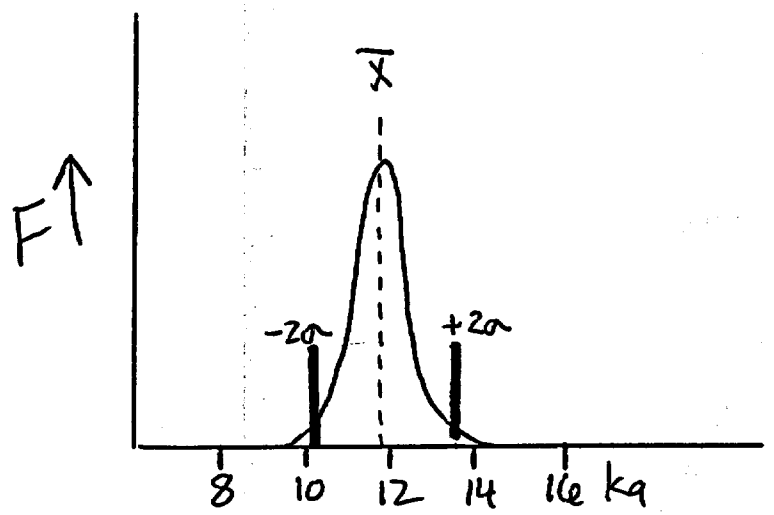

2 ages represent absolute Min + Max; Distrib = DISCRETE UNIFORM

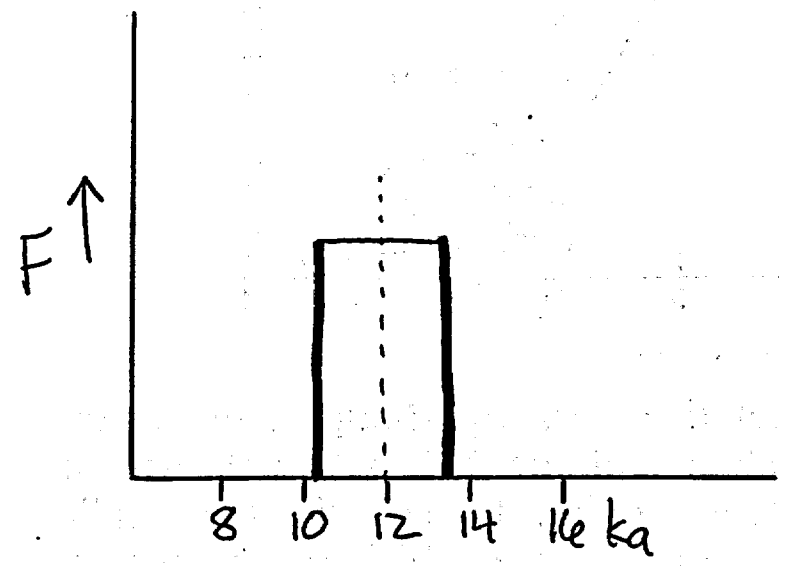

offset by multiple earthquake ruptures. The slip per event is more difficult to estimate from reconnaissance studies, but can be estimated from the maximum or average slip observed during large historic earthquakes, or from the smallest consistent offsets of geomorphic features.

In general, slip rate may be calculated (after Wallace, 1970) as:

$$\mathrm{RI} = D/(S - C), \tag{9.1}$$

where

RI = mean recurrence interval
D = displacement during a single, typical faulting event
S = coseismic slip rate
C = creep slip rate (assumed to be zero for most faults unless historic creep has been documented).

Estimates of displacement per event and slip rate will contain uncertainties that arise from (1) the field measurements of paleoseismic offset and (2) errors in dating offset landforms and deposits, as described in Chapters 3, 5, and 6. It is critical that these uncertainties be carried throughout any computation of slip rate (e.g., Niemi and Hall, 1992). For example, a landform may be offset 50 ± 5 m and be bracketed by limiting ages of 15 and 23 ka. Uncertainties in net offset are often presumed to follow a Gaussian distribution (Sec. 6.2.3), with (in our example) 50 m representing a "best estimate" of offset and 5 m presumed to capture most (95%) of the measurement uncertainty (i.e., 2σ). Uncertainties in landform age likewise arise from the (typically) limited number of numerical ages, and uncertainty about how tightly those ages bracket true landform age. For example, if we deem it unlikely that true landform age is outside of the bracketing ages, we may presume that bracketing ages define $\pm 2\sigma$ limits on the probability distribution of age. In the example cited above, such an assumption implies mean age μ = 19 ka and σ = 2 ka. In contrast, if we consider the ages as not so closely bracketing, we may consider them to constitute $\pm 1\sigma$ limits on the age distribution, in which case our example values would be μ = 19 ka and σ = 4 ka.

In the less closely bracketed scenario above, slip rate is calculated as:

$$\frac{\text{Net offset}}{\text{Landform age}} = \frac{50 \pm 5\ \text{m}}{19 \pm 4\ \text{ka}}. \tag{9.2}$$

RI = mean recurrence interval
D = displacement during a single, typical faulting event
S = coseismic slip rate
C = creep slip rate (assumed to be zero for most faults unless historic creep has been documented).

Estimates of displacement per event and slip rate will contain uncertainties that arise from (1) the field measurements of paleoseismic offset and (2) errors in dating offset landforms and deposits, as described in Chapters 3, 5, and 6. It is critical that these uncertainties be carried throughout any computation of slip rate (e.g., Niemi and Hall, 1992). For example, a landform may be offset 50 ± 5 m and be bracketed by limiting ages of 15 and 23 ka. Uncertainties in net offset are often presumed to follow a Gaussian distribution (Sec. 6.2.3), with (in our example) 50 m representing a "best estimate" of offset and 5 m presumed to capture most (95%) of the measurement uncertainty (i.e., 2σ). Uncertainties in landform age likewise arise from the (typically) limited number of numerical ages, and uncertainty about how tightly those ages bracket true landform age. For example, if we deem it unlikely that true landform age is outside of the bracketing ages, we may presume that bracketing ages define $\pm 2\sigma$ limits on the probability distribution of age. In the example cited above, such an assumption implies mean age $\mu = 19$ ka and $\sigma = 2$ ka. In contrast, if we consider the ages as not so closely bracketing, we may consider them to constitute $\pm 1\sigma$ limits on the age distribution, in which case our example values would be $\mu = 19$ ka and $\sigma = 4$ ka.

In the less closely bracketed scenario above, slip rate is calculated as:

$$\frac{\text{Net offset}}{\text{Landform age}} = \frac{50 \pm 5 \text{ m}}{19 \pm 4 \text{ ka}}. \tag{9.2}$$

According to the division rule for values with unequal standard deviations (Geyh and Schliecher, 1990):

$$t^* \pm \sigma^* = \frac{t_1}{t_2} \pm t^* \sqrt{\left(\frac{\sigma_1^2}{t_1^2}\right) + \left(\frac{\sigma_2^2}{t_2^2}\right)} \tag{9.3}$$

Substituting the values from Eq. (9.2) into Eq. (9.3); we obtain:

$$\frac{50 \pm 5 \text{ m}}{19 \pm 4 \text{ ka}} = 2.63 \pm 0.61 \text{ m/ka} \quad \text{or} \quad 2.63 \pm 0.61 \text{ mm/yr.}$$

The slip rate calculated in Eq. (9.4) thus retains the elements of uncerta associated with the input variables. The 2-σ limits on slip rate from Eq (1.41 to 3.85 m/ka) bound 95% of the probability distribution and are sir to the minimum and maximum cross-quotients derived from the values in (9.2) (1.96 to 3.67 m/ka).

In a similar manner, estimates of displacement per event carry uncertai based on the field measurements of landforms or strata offset in indivi paleoearthquakes. To continue with our example, suppose our hypothe fault had a typical (characteristic) displacement of 5.5 ± 1.5 m per e which we assume to be normally distributed. Recurrence interval is calculated via Eq. (9.1) as:

$$\text{RI} = \frac{5.5 \pm 1.5 \text{ m}}{2.63 \pm 0.61 \text{ m/ka}} = 2.09 \pm 0.75 \text{ ka} \quad \text{or} \quad 2090 \pm 750 \text{ yr.}$$

This recurrence interval incorporates the uncertainties in net offset, landf age, and slip per event, making the assumption that each of those varia is normally distributed. The 2-σ limits on the recurrence interval from (9.5) (590 to 3590 yr) are somewhat greater than the minimum and maxi cross-quotients (1234 to 3465 yr).

The paleoseismic input variables of net offset, landform age, and slip event may also be assumed to follow other probability distributions. An ous distribution is the discrete uniform distribution, in which all values bet the bracketing (field) values are assumed to have equal probability. distribution might be appropriate, for example, if only two field measurem of a parameter can be collected (such as the landform ages cited in example) and they both seem equally likely. The mean (μ) and variance of a discrete uniform probability distribution can be calculated from the data and the equations:

$$\mu = \frac{\sum_{i=1}^{k} x_i}{k}$$

an over several hundred years. In the first model, termed *time predi*
g. 9.14B), earthquakes occur at a constant critical stress level (T1), b
ss drop and magnitude vary. Thus the time of the next earthquake
es can be predicted based on the slip in the previous earthquake,
ume a constant slip rate through time. The second model makes a co
ertion, that earthquakes fail back to a given stress level (T2) regardl
ir size, and thus slip in the next earthquake can be predicted from the
e the previous earthquake; this is termed the *slip-predictable mode*
The discovery that slip varies along strike during earthquakes necessi
anding these one-dimensional models to include a second dimension
lt strike. Two-dimensional behavior models were initially formulated
along-strike slip patterns in historic earthquakes (see examples in Cha
id 6), and were later expanded to include slip patterns for paleoearthq
ed on geomorphic offsets (e.g. Schwartz and Coppersmith, 1984). M
be classified into two broad groups, the variable slip models an
form slip models.

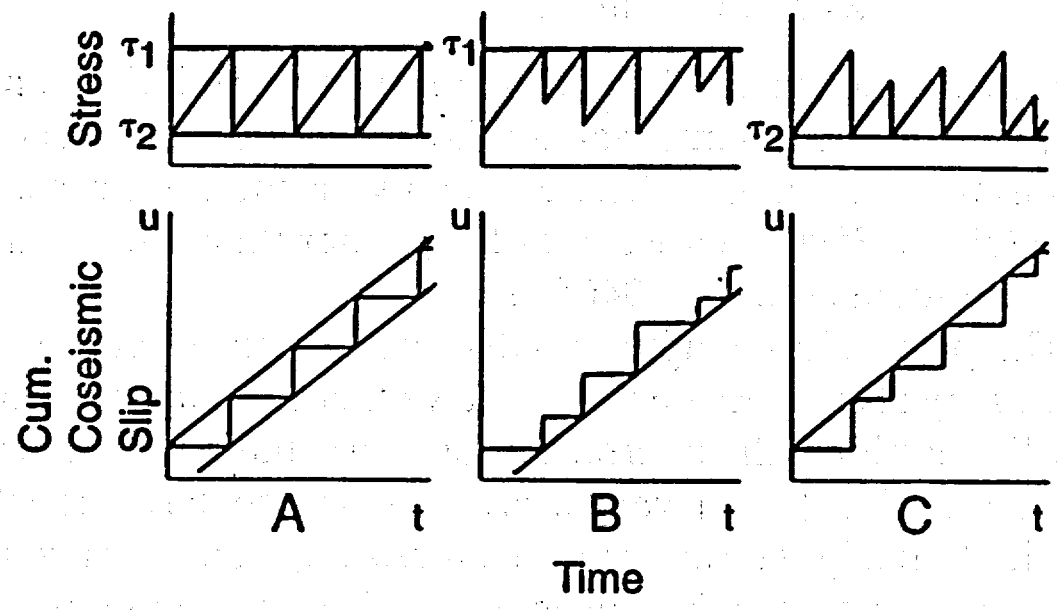

Figure 9.14 Diagram contrasting (A) the perfectly periodic model, (B) the time-pred
el, and (C) the slip-predictable model of earthquake recurrence. Upper figures show p
ress drop with time, lower figures show patterns of fault slip through time. [From
0); reprinted with permission of Cambridge University Press.]

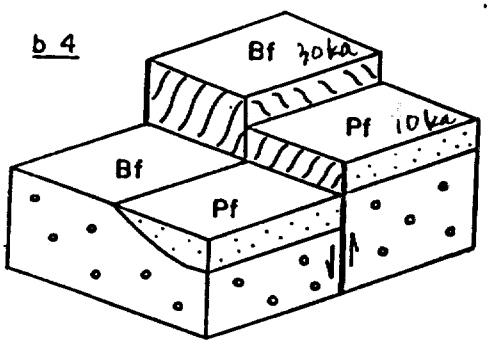

Case 1: 2 paleoearthquakes, neither age known

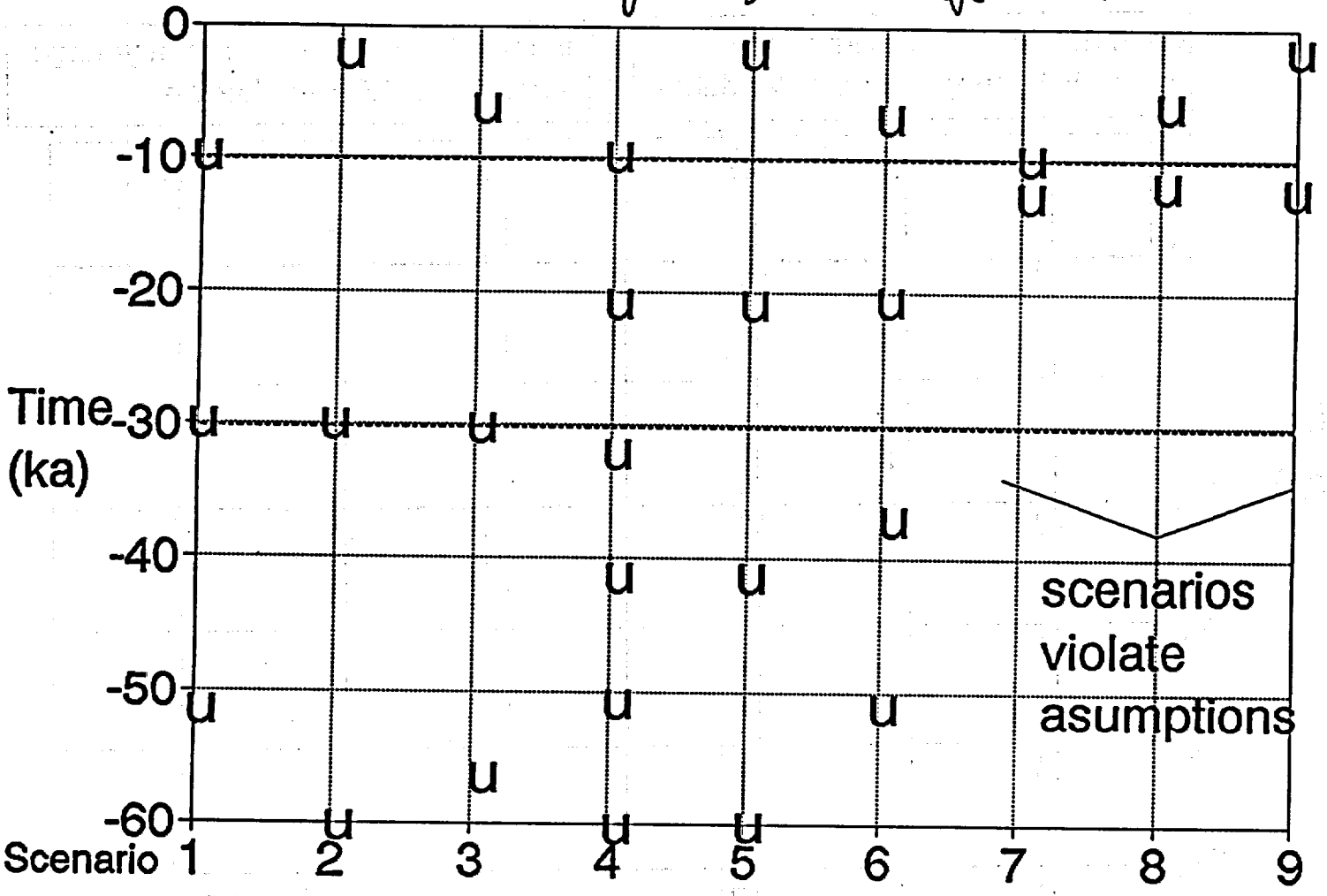

Scenario	1	2	3	4	5	6	7	8	9
Recurrence	20	30	25	10	20	15 ka			
Interval (ka)	AVG	MAX		MIN	AVG				

uniform recurrence

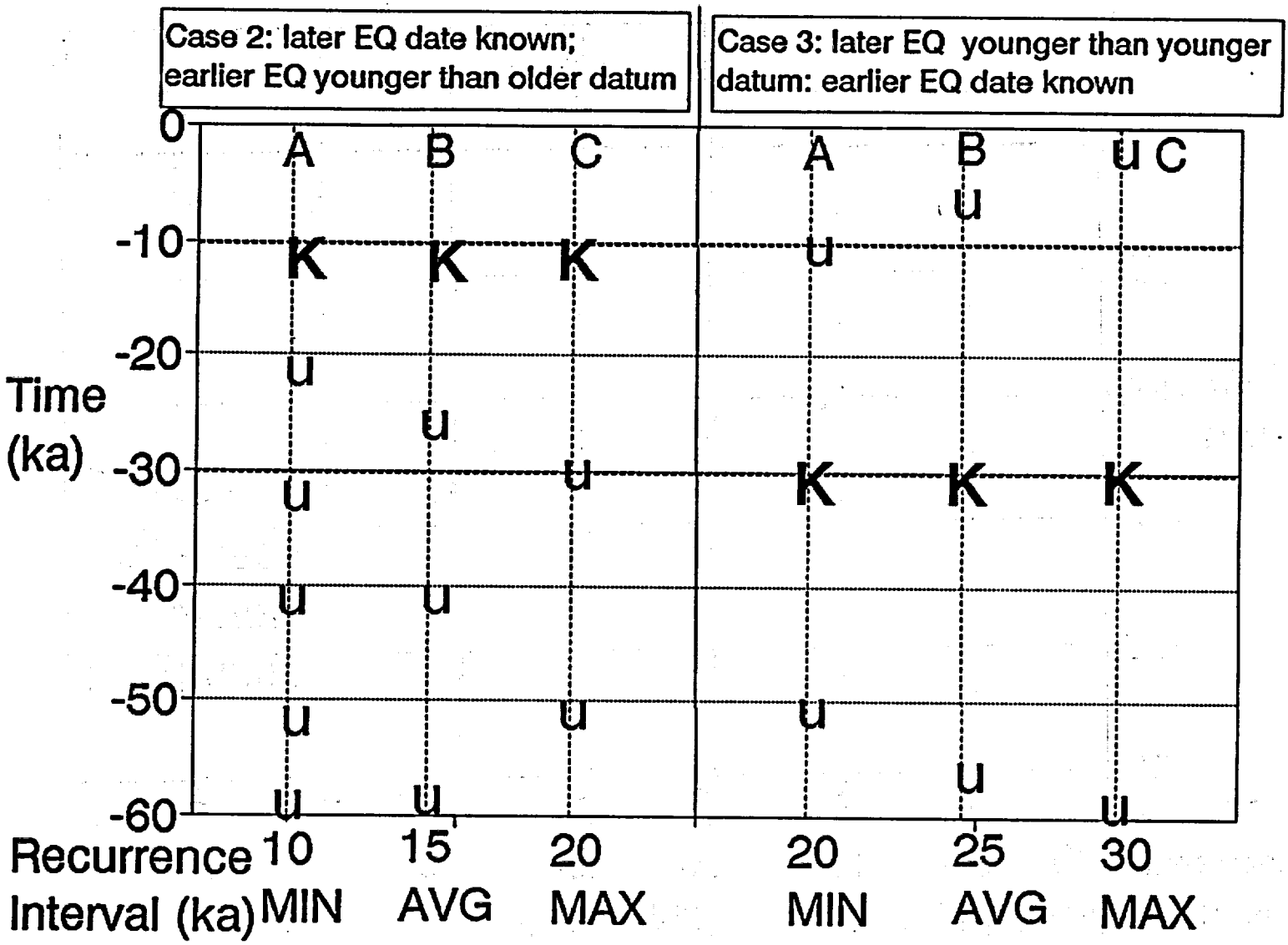
Case 2: later EQ date known; earlier EQ younger than older datum
Case 3: later EQ younger than younger datum: earlier EQ date known
0
-10
-20
-30
-40
-50
-60
Time (ka)
A
B
C
A
B
C
K
K
K
K
K
K
u
u
u
u
u
u
u
u
u
u
u
u
u
u
u
u
u
u
Recurrence Interval (ka)
10 MIN
15 AVG
20 MAX
20 MIN
25 AVG
30 MAX

b 4

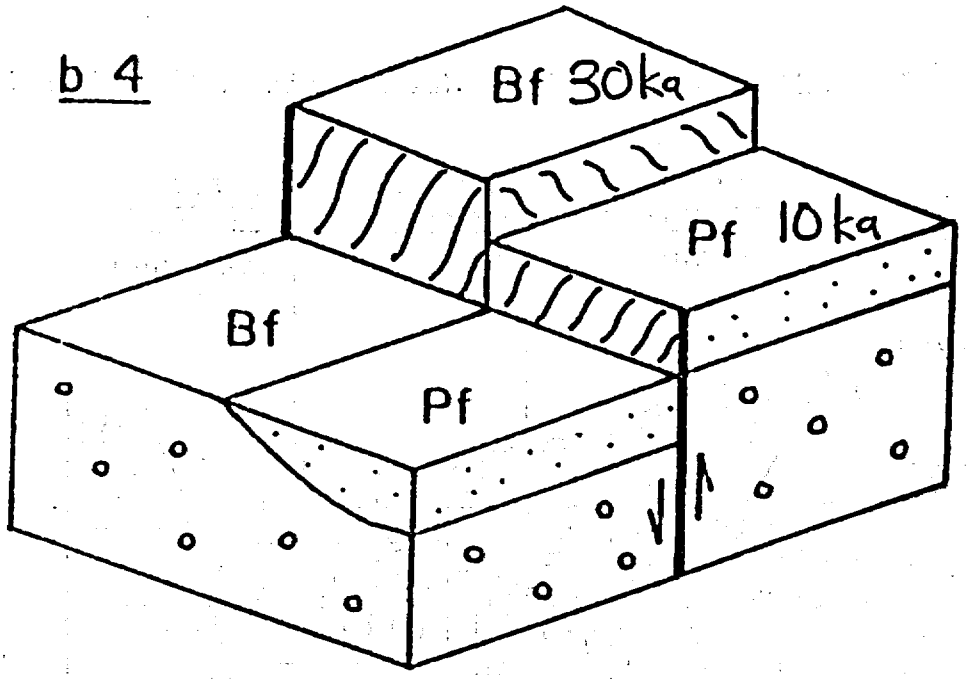

L: 2 paleoearthquakes, neither age k

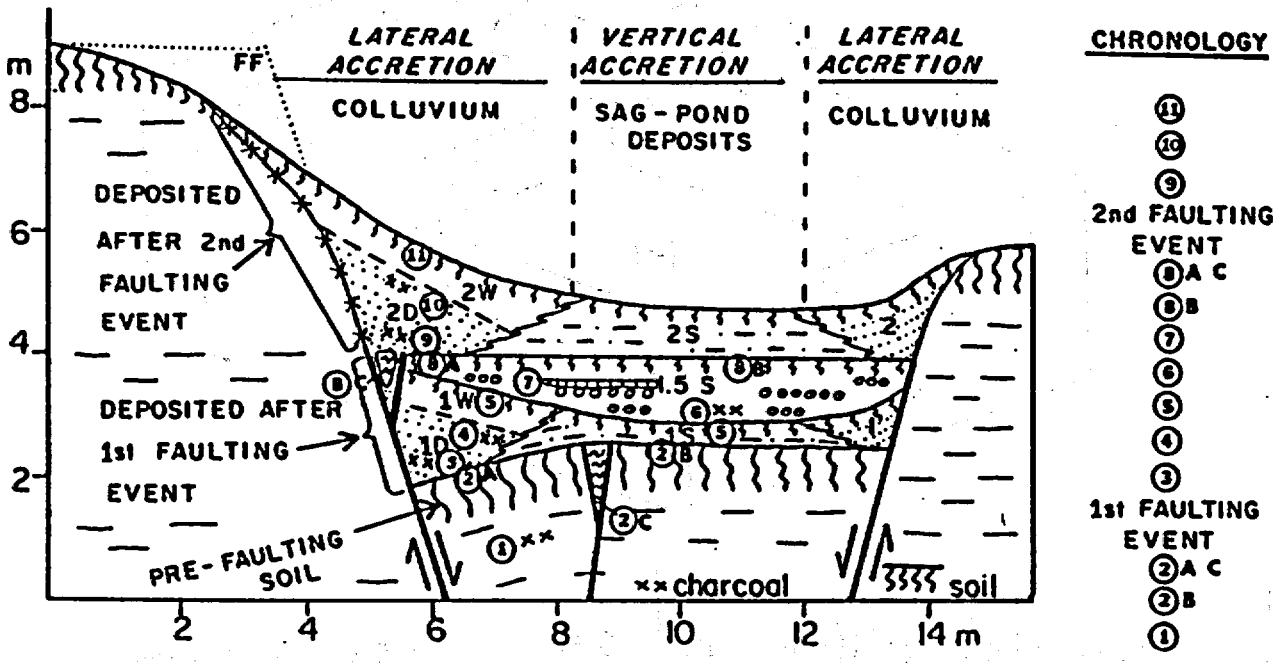

Figure 2. Schematic cross section through a normal fault scarp and graben formed by two surface-faulting events; this is a composite section showing features observed in many trenches across the WFZ. Colluvium shed from the main scarp (at left) is divided into debris facies (D) and wash facies (W); both facies grade into coeval sag pond deposits (1S, 2S). Between faulting events a fluvial deposit (1.5S), containing lenses of gravel (circles), completely filled the graben. Circled numbers indicate potential sites for obtaining radiocarbon samples, and the chronology at right shows which samples most closely constrain the times of the faulting events. Debris facies colluvium is deposited immediately after faulting, whereas sag pond deposition may be climatically controlled and postdate faulting by decades. Radiocarbon dates from sites 2A and 8A have traditionally been interpreted as the closest maximum limiting ages on faulting, as shown on the chronology at right. However, if radiocarbon ages from soils 2 and 8 are mean residence time corrected to reflect the age of soil burial, they become minimum age constraints on faulting, with the closest constraint closest to the fault. Most of the numerical ages in Table 1 are from positions 2A/8A or 2C/8C. Ages labeled "min" in Table 1 are from positions such as 3 and 9. Samples from wash facies colluvium (5, 11) and interbedded fluvial deposits (6, 7) do not provide close age constraints on faulting.

that most closely constrain the times of earthquakes. Paleoearthquake studies on the WFZ can be d into three time periods. Between 1977 and 1984, ward-Clyde Consultants identified and trenched each of ntral fault segments [*Swan et al.*, 1980, 1981a, b; *n and Schwartz*, 1982; *Schwartz et al.*, 1983; *Schwartz oppersmith*, 1984]. Most ^{14}C ages from these trenches derived from charcoal, either detrital or in situ burns. oal fragments have the advantage of containing carbon a short age span (unlike soils) but the disadvantage of lly not lying near the event horizon. Buried soils and ic fissure fills nearer to the event horizons were mapped ere generally not dated (compare work by *Swan et al.*] with work by *McCalpin et al.* [1994]), because rs at the time were uncertain how to interpret ^{14}C ages l organics of mixed origins and ages. Thus most of the ges from these early studies provided only approximate dating of several facies was also begun [*Forman et al.*, 19 1991; *McCalpin and Forman*, 1991]. All the numerical ag from the USGS trenches (but not from earlier Woodwa Clyde trenches) are inventoried by *Machette et al.* [199 Appendix], who list 55 ages (38 ^{14}C, 17 thermoluminescen

From 1989 to present, additional trench studies ha continued under USGS funding. These include 14 trench across a zone of distributed fault scarps in the Brigham C segment [*McCalpin and Forman*, 1993], one trench on t Weber segment [*McCalpin et al.*, 1994], and eight trenches the Salt Lake City segment [*Lund*, 1992; *Black and Lu* 1995; *Black et al.*, 1995]. Data from these studies are eit published only in abstracts [e.g., *Lund et al.*, 1990; *Osten* 1990] or are unpublished, so we obtained the original labo tory ages and trench logs from the authors (Table 1).

We next examined the logs of sampled trenches to ident those samples whose stratigraphic position most clos

		cm)	
P. McCalpin (unpublished data, 1994, from Rock Creek fault, Wyoming)	in a 40 cm-thick horizon, roughly linear age trend of 0.3 mm/yr between 2260 and 3280 ^{14}C year BP (Figure 3)	4.1	1 series of 4
lean age trend in debris acies soils[b]		4.6 (range 3.7-6.7)	

Described as the number of series (vertical transects) followed by the number of samples within each series
For a 10-cm-thick sample, the difference between the age of the center of the sample and the top of the sample (upper horizon contact) be calculated as the product of age trend times 50 mm, yielding a range of 185-335 years (mean 230 years). We assume that the 150- r spread between age estimates roughly represents ±2σ uncertainty associated with mean residence time correction.

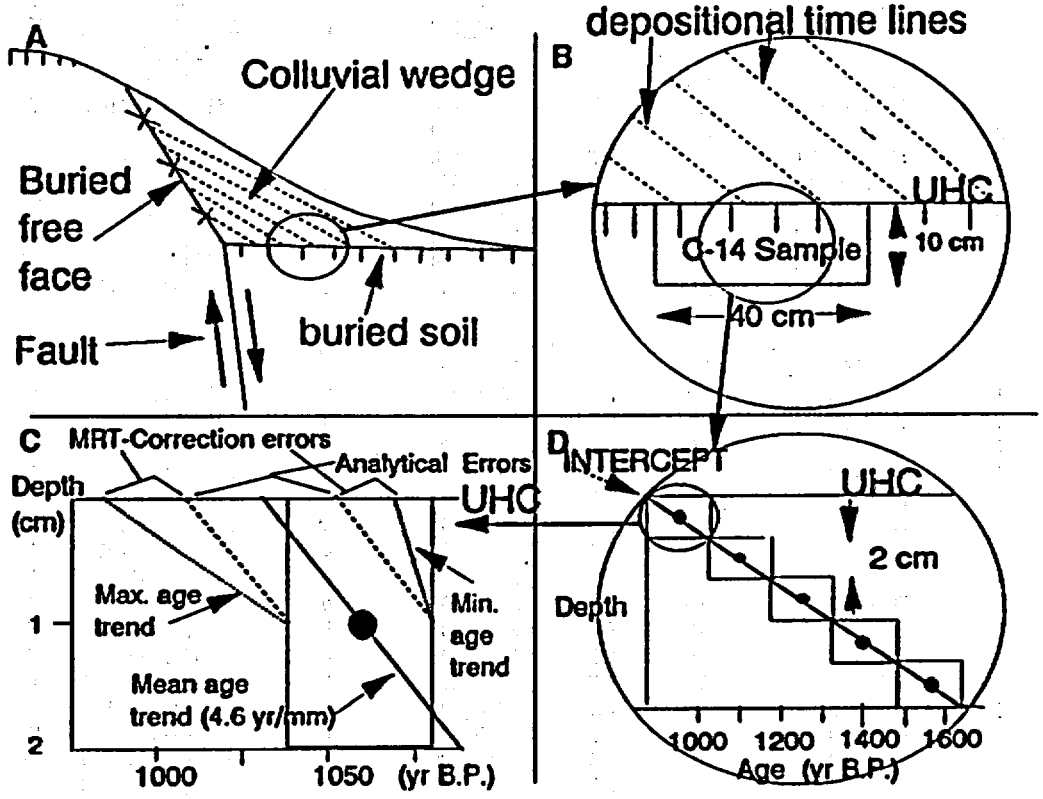

Figure 3. Idealized diagrams of a single-event normal fault scarp showing various sources of uncertainty in relating numerical ages to the time of paleoearthquakes. (a) simplified cross-section of the colluvial wedge. Dashed lines show depositional time lines in colluvium. (b) close-up view of a typical radiocarbon sample, emphasizing the time-transgressive nature of the event horizon (i.e., burial of the upper horizon contact of the soil). (d) close-up of the 10 cm-thick radiocarbon sample, showing the trend of increasing age with depth (compare to Figure 4) and the principle of extrapolating the age of the upper horizon contact. (c) close-up of how age uncertainties are calculated for the event horizon (upper horizon contact) immediately above the dated sample. Cross shows mean radiocarbon ages with 2σ limits; solid square shows dendro-corrected radiocarbon age, with 2σ limits shown by the horizontal dimension of the surrounding box. Vertical dimension of the box indicates sample thickness. Solid line shows a least-squares regression lines through the dendro-corrected mean ages. The top of the graph represents the upper horizon contact of the soil. The total 2σ error range on age of the upper horizon contact is composed of an analytical component and a sample context component. The analytical component is defined by extrapolations of the mean age trend (4.6 yr/mm) from the ±2σ limits on the age of the uppermost 10 cm-thick sample (dashed lines). The sample context component is defined by extrapolations of the maximum age trend (6.7 yr/mm) from the -2σ age limit and the minimum age trend (3.7 yr/mm) from the +2σ age limit (dotted lines).

Table 1. (continued)

Trench[a]	Source[b]	Lab No.[c]	Material[d]	Geologic Unit[e]	Lab 14C age (14C yr B.P. or TL age[f] (cal yr B.P.)	CAS/ MRT (cal yr BP)[g]	MRT-Corrected Age of Event Horizon	Paleo-earthquake Constrained[h]
				Weber Segment				
K-88	1	B-29901	Ab	DC	900±80	b	917(683)550	Z
GC	2	NSRL-523	Ab	PC	990±80	b	978(821)587	Z
EO-2	3	PITT-0096	Ab	PC	1065±30	b	954(882)602	Z
K-88	1	B-29902	Ab	DC	1130±70	b	1140(920)784	Z
EO-2	3	PITT-0098	Ab	PC	1365±40	d	1228(1098)943	Z
EO-1	3	ITL-47	A	DC	1200±200	-	1200±200	Z
K-88	1	B-38680	A	CF	2220±50	e	3145(2821)2465	Y, min
GC	2	NSRL-520	Ab	PC	2490±100	f	2725(2588,2521, 2413)2224	Y
EO-2	3	ITL-74	Ab	PC	3200±300	-	3200±300	Y
EO-2	3	PITT-104	Ab	PC	3295±130	g	3818(3450)3165	Y
EO-2	3	ITL-80	Ab	L	4000±400	-	4000±400	X
EO-2	3	USGS-2499	C	DF	4100±180	-	5045(4564)4087	X
EO-2	3	PITT-0094	Ab	DF	4505±65	a	5032(4755)4471	X
EO-1	3	ITL-138	L	DF	4600±400	-	4600±400	X
K-88	1	ITL-150,171	Ab	DC	5850±636	-	5850±636	W
K-88	1	ITL-150,171	Ab	DC	6100±404	-	6100±404	W
K-88	1	B-29900	Ab	DC	5780±90	a	6651(6389)6116	W
				Salt Lake City Segment[k]				
DC-2	3	B-21303	Ab	PC	1170±60	c[l]	1103(862)700	Z
DC-1	1	B-54646	Ab	PC	930±60	b	912(741)579	Z
DC2-2	2	B-77139	OM	CF	1570±60	h	1393(1146)927	Z
DC2-3	2	B-77141	Ab	PC	1420±60	b	1349(1227)1103	Z
DC2-4	2	B-79188	OM	CF	1620±60	h	1446(1193)958	Z
DC2-1	2	B-80845	Ab	PC	1850±60	i	1797(1632)1415	Z
DC-2	1	B-28320	Ab	PC	1640±50	c[l]	1508(1318)1136	Z
DC-1	3	B-21304	Ab	PC	1830±80	c	1785(1564)1279	Z
DG-1	1	B-50879	Ab	PC	1760±60	b	1738(1559)1381	Z
DG-1	1	B-50880	Ab	PC	2370±70	b	2600(2277)2103	Y
DG-1	1	B-54017	Ab	PC	2410±60	b	2621(2303)2164	Y
DC2-5	2	B-79184	Ab	PC	2940±60	i	3177(2932)2691	Y
DC2-4	2	B-79920	OM	CF	3760±80	h	4172(3794)3480	X
DC2-2	2	B-77140	Ab	PC	3810±90	j	4304(4035)3748	X
DC-1	1	B-54649	Ab	PC	4520±60	b	5300(5114)4812	W
DC-1	3	B-21300	Ab	PC	4910±100	c[l]	5745(5452)5140	W
DC-2	3	B-21302	Ab	PC	4710±90	c	5516(5214)4958	W
DC-1	3	B-21299	Ab	PC	5230±80	c[l]	6074(5790)5545	W
				Provo Segment[m]				
Map.N1	1	PITT-0191	C	DF	330±50	-	502(425,392,319) 287	Z, min
AmFk.2	2	ITL-3	S	SP	500±200	-	500±200	Z, min
Map.N1	1	B-21306	C	L	445±70	-	551(505)311	Z, min
Map.N1	1	PITT-0188	C	L	490±65	-	635(517)334	Z, min
RockCr.	2	PITT-0091	Ab	DF	455±35	k	666(606)549	Z, min
RockCr.	3	-	Ab	DF	-	l	590±90	Z, min
WC 1	4	B-23781	C	PC	320±120	-	542(403)0	Z
AmFk.1	2	ITL-23	Ab	PC	400±100	-	400±100	Z
AmFk.2	2	USGS-2533	Ab	PC	620±150	k	760(494)221	Z
Map.N1	1	PITT-0189	C	PC	730±40	-	715(664)576	Z
AmFk.1	2	USGS-2532	Ab	PC	980±70	a	905(696)468	Z
Map.N2	1	B-21733	C	PC	770±100	-	919(672)547	Z
WC 1	4	B-23779	C	DF	890±60	-	931(782)671	Z
WC 1	4	B-23778	C	DF	950±60	-	961(909,800)724	Z
RockCr.	2	DIC-3236	A	PC	1110±50	e	985(806)670	Z
RockCr.	3	-	Ab	DF	-	m	810±130	Z
AmFk.1	2	USGS-2531	Ab	PC	2620±70	a	2723(2545)2293	Y
AmFk.1	2	ITL-16	Ab	PC	2700±200	-	2700±200	Y
Map.S1	1	B-26117	Ab	PC	2890±80	d	3128(2807)2550	Y

Table 3. Limiting Numerical Ages, Weighted Mean Age Estimates, and Recurrence Intervals for Paleoearthquakes on Central Wasatch Fault Zone

Segment	Event	Limiting Ages,[a] cal years B. P.		Weighted Interevent Time,[c] Mean ±2σ, cal years
		No.	Mean[b]±2σ	
Brigham City	Z	4	2125±104	1309±176
	Y	3	3434±142	1240±220
	X	3	4674±108	1296±294
	W[d]	1	5970±242	1330±426
	V[d]	1	7300±350	1218±488
	U[d]	2	8518±340	4492±412
	T[d]	1	13,010	mean[e]= 1282±138
Weber	Z	6	1016±62	2048±130
	Y	3	3064±114	1339±108
	X	4	4403±122	1729±188
	W[d]	3	6132±144	mean[e]=1782±102
Salt Lake City	Z	9	1230±62	1269±152
	Y	3	2499±138	1442±258
	X	2	3940±216	1440±256
	W	4	5381±136	mean[e]=1441±182
Provo	Z	10	618±30[f]	2224±78
	Y	5	2842±72	2639±168
	X	2	5481±152	mean[e]=2297±70
Nephi	Z	7	1148±68	2716±248
	Y	5	3864±238	Mean[e]=2716±248
Totals		76	mean[e]=1918 years	

[a] Number of close limiting ages from Table 1; does not include less closely limiting minimum ages marked as "min" inTable 1.
[b] Mean weighted by the standard deviation.
[c] Interevent times and their uncertainties are computed by the weighting procedure to the nearest year but should be rounded off to the nearest decade for any derivative calculations.
[d] These earthquakes predate 5.6 ka and are not used in the synthetic modeling.
[e] Weighted mean±2σ over the past 5600 years, the period in

B.P.). *Mache*
to indicate th
occur in clus
however, the
central WFZ
Schwartz [19
nonpersistenc
may reflect th
on the fault
systems exhi
coupled syst
Figure 4 is j
on completel

Distingui
temporal clu
seismic haza
earthquakes
recurrence h
segment [e.g
Probabilities
of regional c
between segr
of the likelih
stress states
[e.g., *Cornel*
quakes has
Below we c
paleoseismic
paleoseismic
(Using stanc
distribution
histories wc
arrangement
earthquake
interactions
1981; *Ward*,
test the stren
seismic his
environment

The term
characteristic
previous lit
commonly b

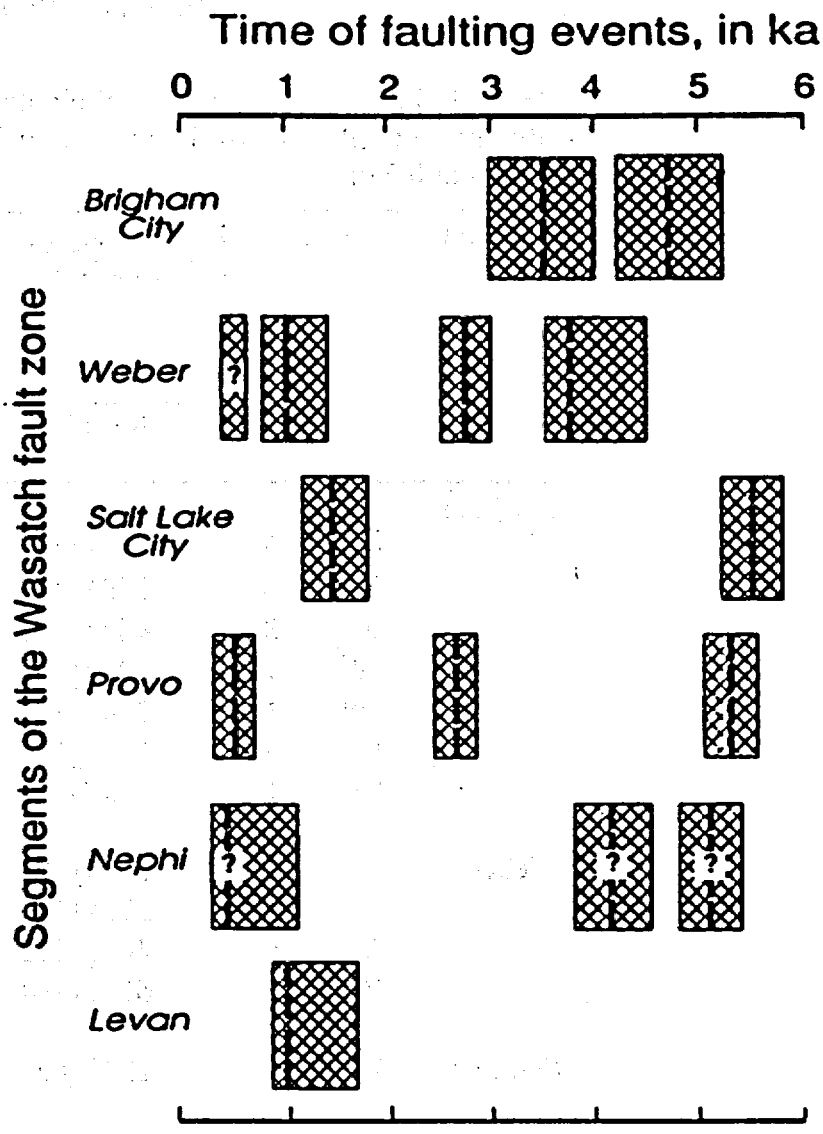

Figure 9.9 Example of a space–time diagram; estimated timing of major pa on the Wasatch fault zone (Utah) in the past 6 ka. Dashed vertical lines indic the most probable time of faulting (queried or missing where timing is uncertain) patterns indicate permissible limits for faulting events as determined from a calibrated ^{14}C and thermoluminescence age estimates. [From Machette *et al.*, (1 with permission from *Annales Tectonicae.*]

The symbols representing earthquakes in a space–time diagr represent temporal probabilities of occurrence. If an earthquake by only two numerical ages, these ages define the limits of a box within which the probability of earthquake occurrence must be

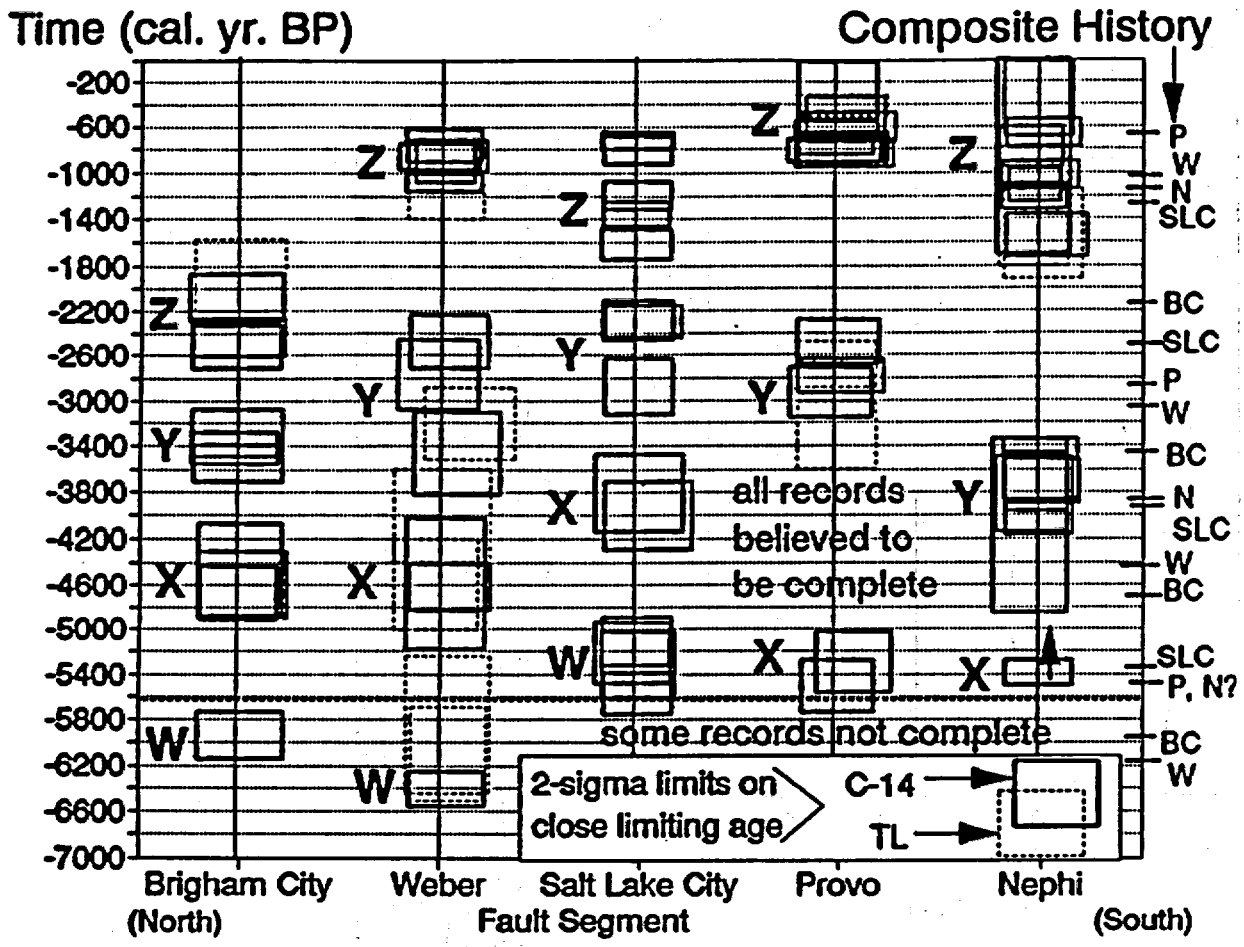

Space–time diagram of the Wasatch fault zone (same segments and time span ɔut with axes transposed and all of the close limiting numerical ages plotted instead ible limits for faulting. Vertical dimensions of each box span the 2-σ age limits. ages are from similar stratigraphic positions immediately beneath event horizons ht to date each earthquake closely (see Sec. 3.4.5). The composite paleoseismic nargin) shows the mean of limiting ages for each paleoearthquake, identified by diagram includes three paleoearthquakes (event Z on Brigham City, events X and :e City) that were identified after Fig. 9.9 was published. [From McCalpin and 6); reprinted with permission of the American Geophysical Union.]

Rates

ın be calculated from the cumulative displacement of dated land-

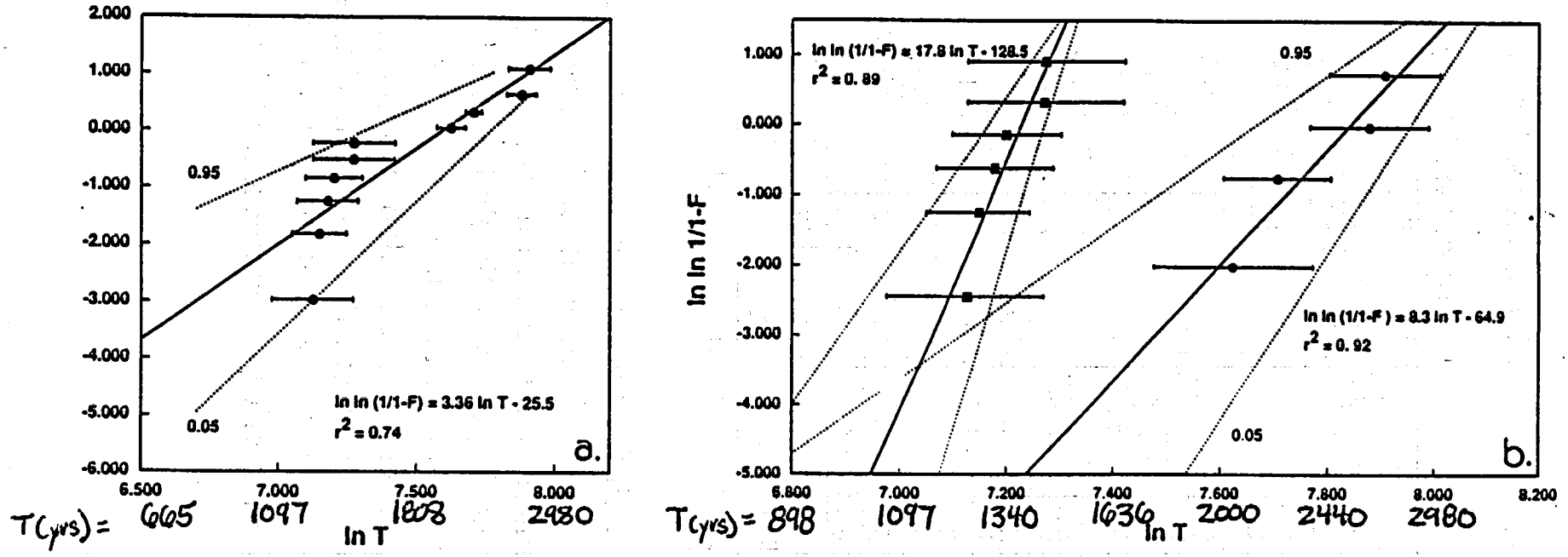

Figure 8. Cumulative Weibull plots of ln ln [1/ 1-$F(T)$] versus ln T for Holocene earthquake repeat times along the central five segments of the WFZ. Horizontal error bars shown for interevent times are 90% confidence intervals (see Table 6). Cumulative distributions are plotted according to a $(n_i$-1/2)/N plotting rule. Least squares fit to the data (solid lines) define the Weibull distribution parameters. Dotted lines show 0.05 and 0.95 confidence interval estimates to the distribution. (a) All interevent times in the past 5.6 kyr (grouped data); β=3.36, mean repeat time=1775$\pm$291 years (2σ range). Two subgroups of interevent times appear, those with ln T<7.5 and ln T>7.5, suggesting bimodal recurrence behavior. (b) Data from Figure 8a replotted to emphasize the short-recurrence (ln T<7.5) and long-recurrence (ln T>7.5) groups. For the short-recurrence group, β=17.8 and mean repeat time=1328$\pm$104 years (2σ range). For the long-recurrence group, β=8.3 and mean repeat time=2346$\pm$448 years (2σ range).

GIVEN: 10 FAULTS, each has Gaussian recurrence, $\bar{RI} = 10ka$, $\sigma = 3ka$, COV = 0.3

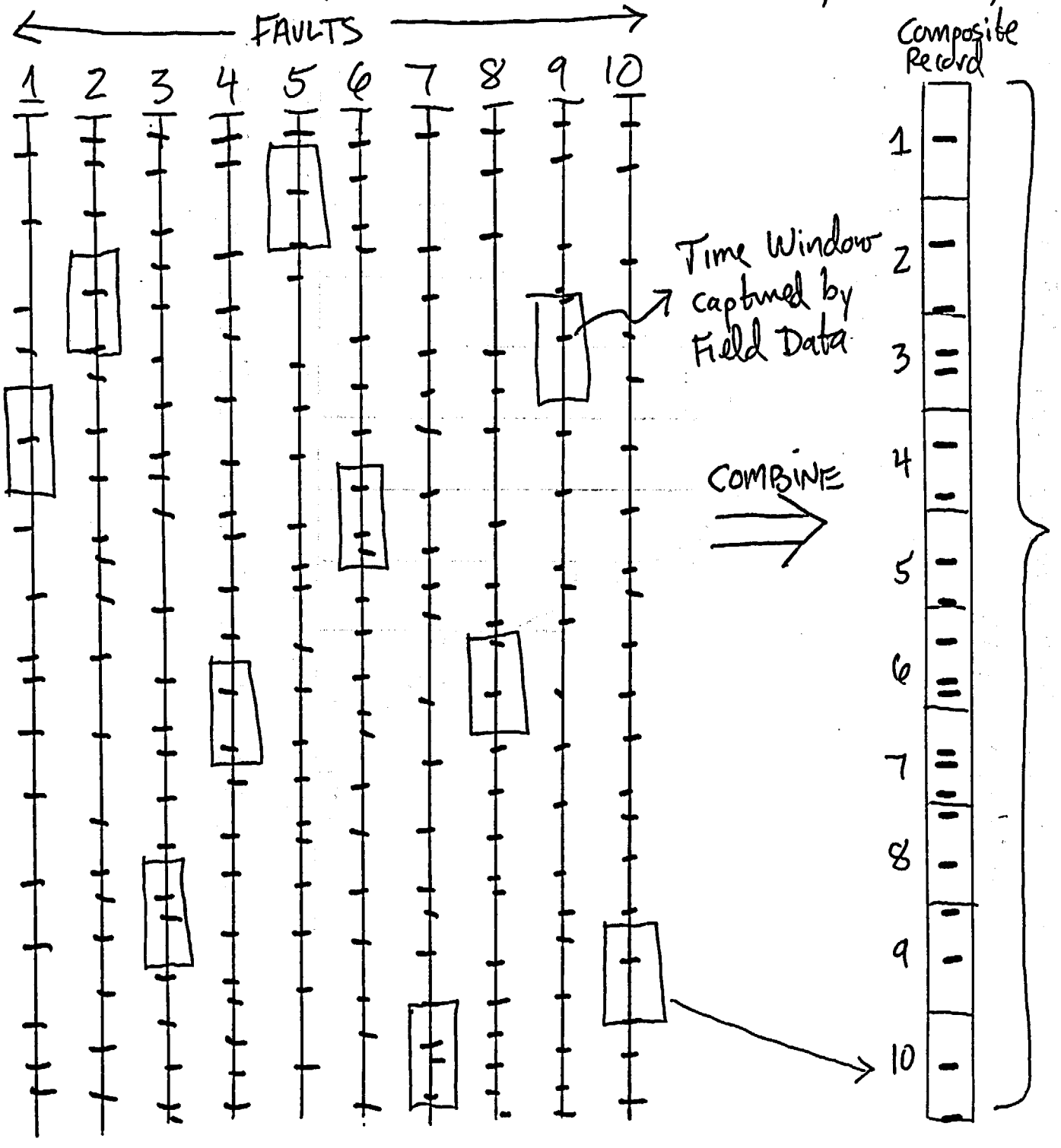

THE RECURRENCE HISTORY OF THIS COMBINED RECORD SHOULD ALSO HAVE:

$\bar{RI} = 10ka$

$\sigma = 3ka$

Distrib. = Gaussian

The histogram of $b(x; 15, 0.4)$ and the corresponding superi
which is completely determined by its mean and varian
Figure 6.21.

The exact probability that the binomial random variable X a
x is equal to the area whose base is centered at x. For example
that X assumes the value 4 is equal to the area of the rectangle
$x = 4$. Using Table A.1, we find this area to be

$$P(X = 4) = b(4; 15, 0.4) = 0.1268,$$

which is approximately equal to the area of the shaded reg
curve between the two ordinates $x_1 = 3.5$ and $x_2 = 4.5$ in Fi
to z-values, we have

$$z_1 = \frac{3.5 - 6}{1.897} = -1.32$$

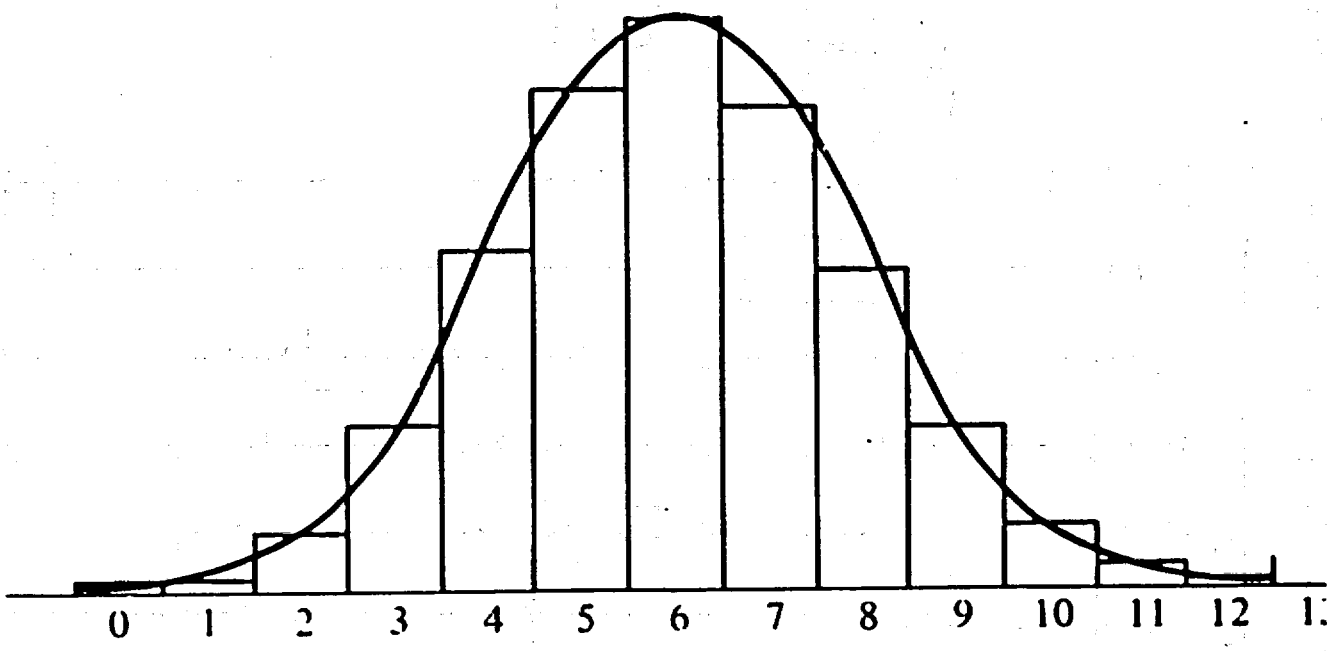

FIGURE 6.21 Normal approximation of $b(x; 15, 0.4)$.

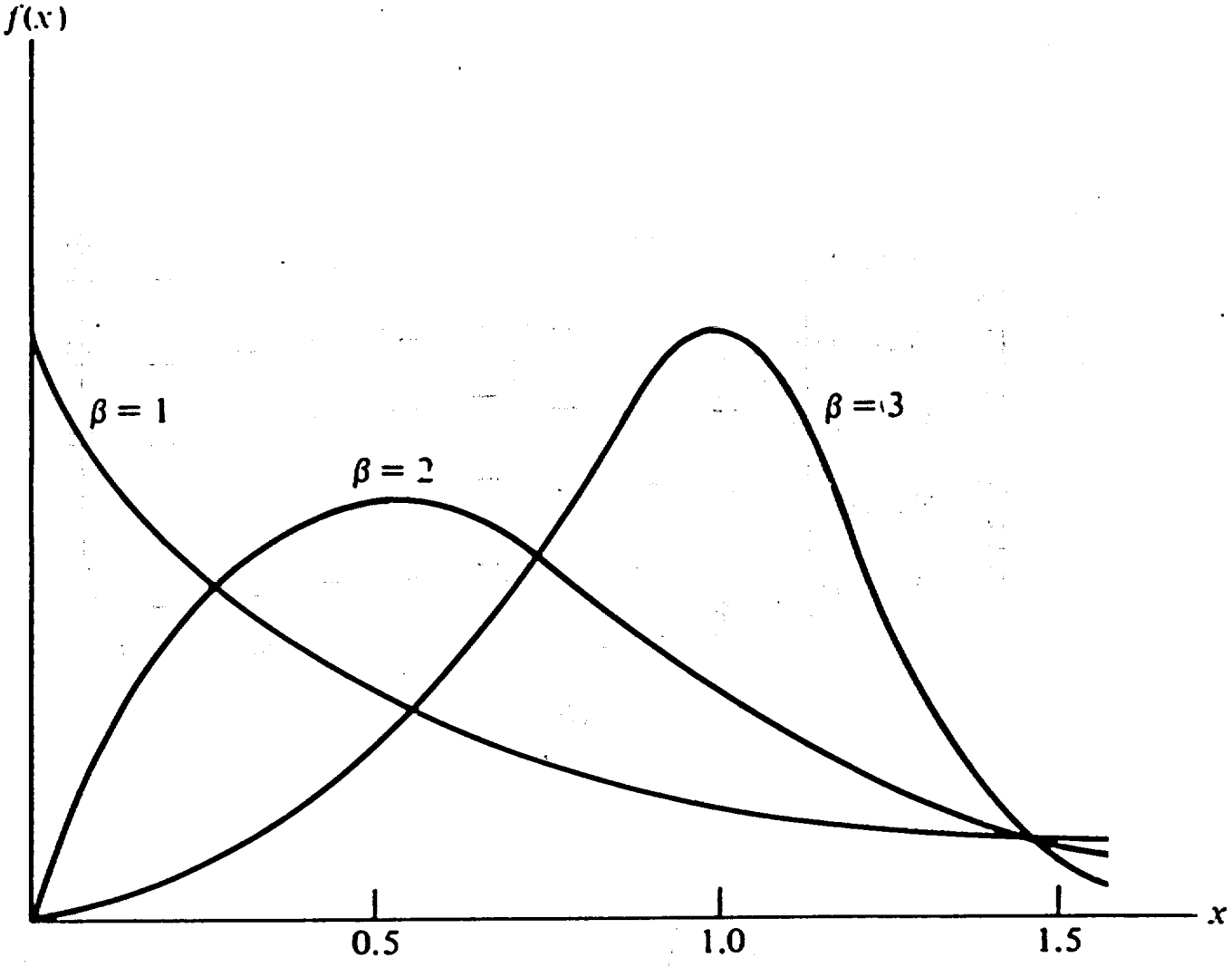

FIGURE 6.28 Weibull distributions ($\alpha = 1$).

where $F(t)$ is the cumulative distribution of T. The conditional component will fail in the interval from $T = t$ to $T = t + \Delta t$, giv to time t, is given by

$$\frac{F(t + \Delta t) - F(t)}{R(t)}.$$

Dividing this ratio by Δt and taking the limit as $\Delta t \to 0$, we ge denoted by $Z(t)$. Hence

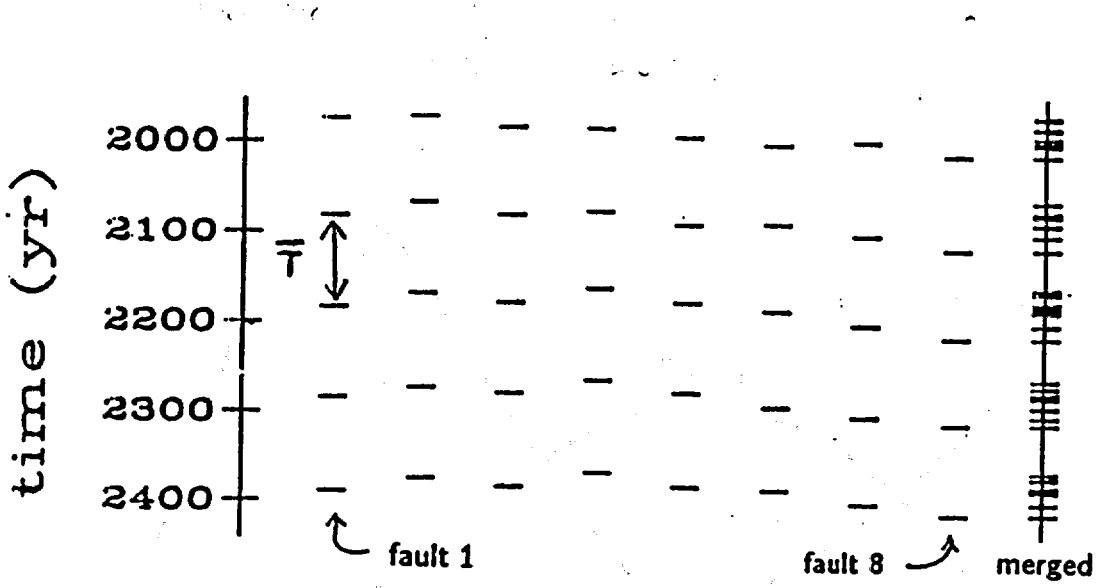
time (yr)
2000
2100
2200
2300
2400
$\bar{T}$
fault 1
fault 8
merged

a.

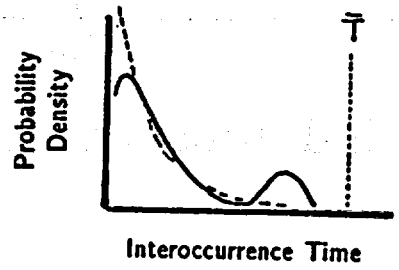
Probability Density
$\bar{T}$
Interoccurrence Time

b.

Fig. 9-~~Mb~~ 14

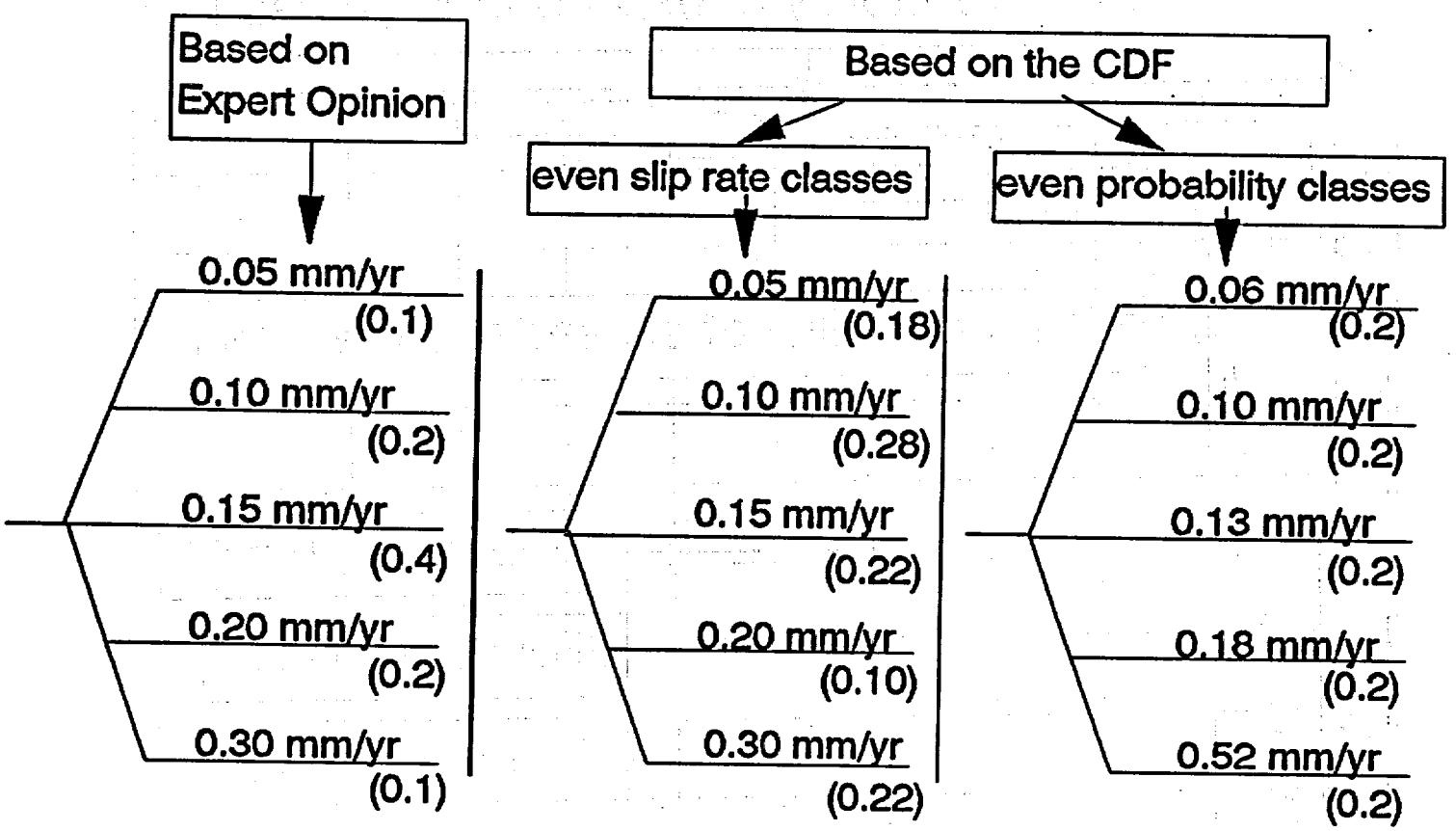
Based on
Expert Opinion
0.05 mm/yr
(0.1)
0.10 mm/yr
(0.2)
0.15 mm/yr
(0.4)
0.20 mm/yr
(0.2)
0.30 mm/yr
(0.1)
Based on the CDF
even slip rate classes
0.05 mm/yr
(0.18)
0.10 mm/yr
(0.28)
0.15 mm/yr
(0.22)
0.20 mm/yr
(0.10)
0.30 mm/yr
(0.22)
even probability classes
0.06 mm/yr
(0.2)
0.10 mm/yr
(0.2)
0.13 mm/yr
(0.2)
0.18 mm/yr
(0.2)
0.52 mm/yr
(0.2)

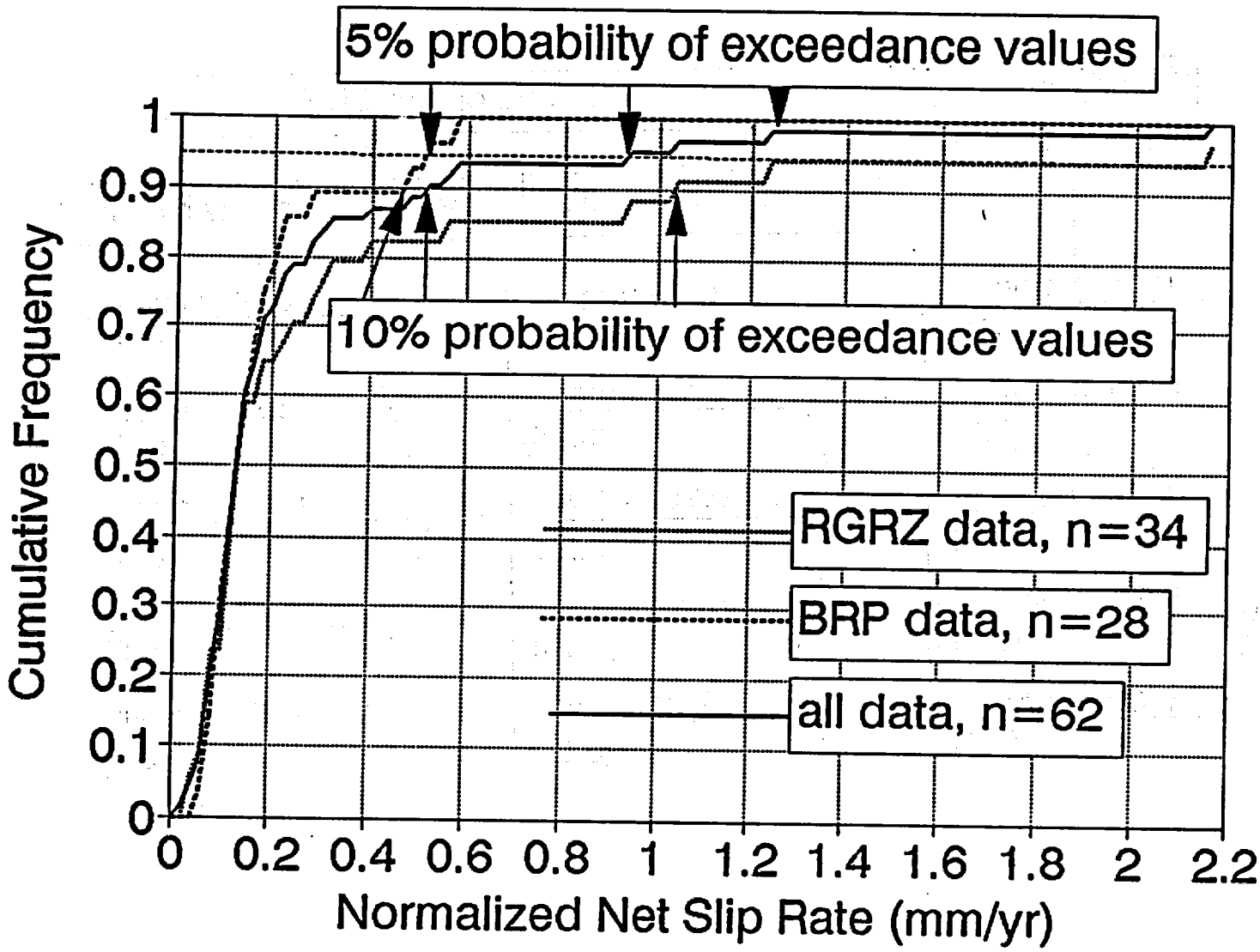
5% probability of exceedance values
10% probability of exceedance values
RGRZ data, n=34
BRP data, n=28
all data, n=62
Cumulative Frequency
0
0.1
0.2
0.3
0.4
0.5
0.6
0.7
0.8
0.9
1
0
0.2
0.4
0.6
0.8
1
1.2
1.4
1.6
1.8
2
2.2
Normalized Net Slip Rate (mm/yr)

Earthquake Recurrence Evaluation

Yucca Mountain Slip Rate and Recurrence Interval Data

presented by

John Whitney
US Geological Survey

Yucca Mountain Slip Rate Data

- **Measured Offset on Oldest, Dated Deposit**
  - » **Dating Uncertainties**
    - – U-series, TL, Volcanic Ashes, Soils
  - » **Increased Left-lateral Component of Slip Southward (0° - 30°)**
  - » **Possible Erosion of Footwall Deposits**
    - – High Confidence with Offset Soils
  - » **Average Slip Rate Variations Over Time**
    - – Late Quaternary vs. Early Quaternary

Known and Suspected Quaternary Faults near Yucca Mountain

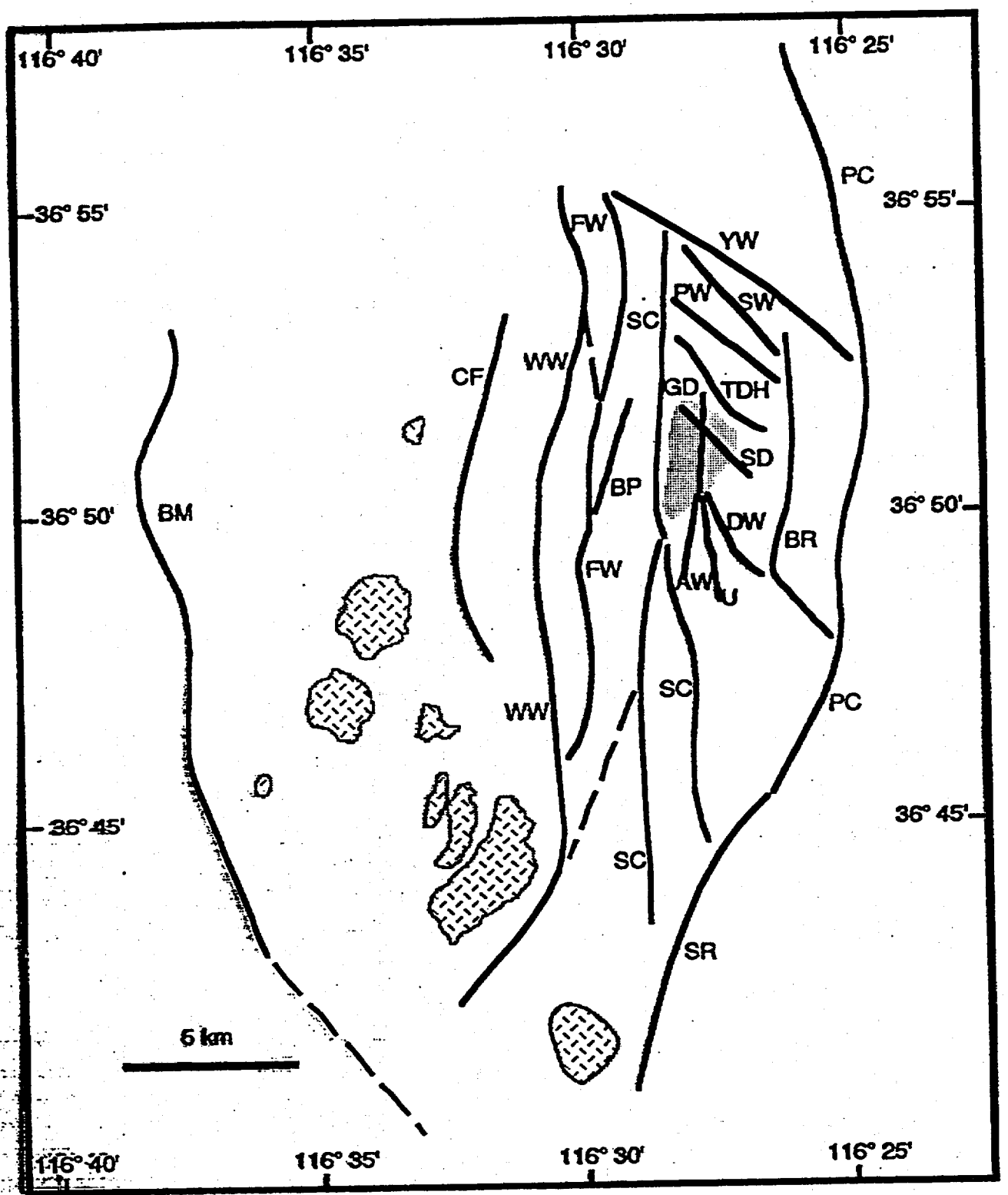


93-52
1636 13
HAP-83F
590

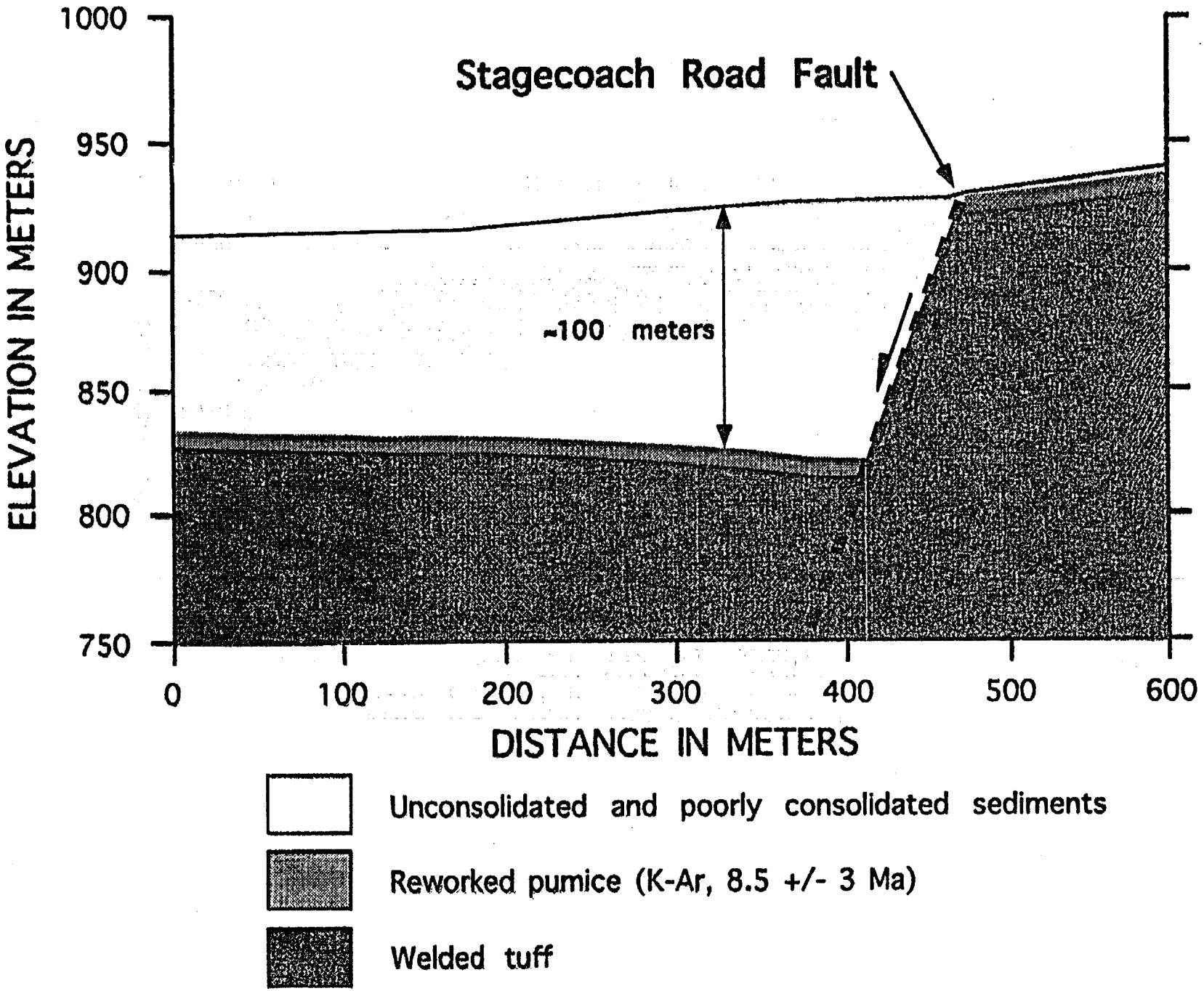
Stagecoach Road Fault
~100 meters
ELEVATION IN METERS
1000
950
900
850
800
750
0
100
200
300
400
500
600
DISTANCE IN METERS
Unconsolidated and poorly consolidated sediments
Reworked pumice (K-Ar, 8.5 +/- 3 Ma)
Welded tuff

SEISMIC LINE PERPENDICULAR TO WINDY WASH FAULT

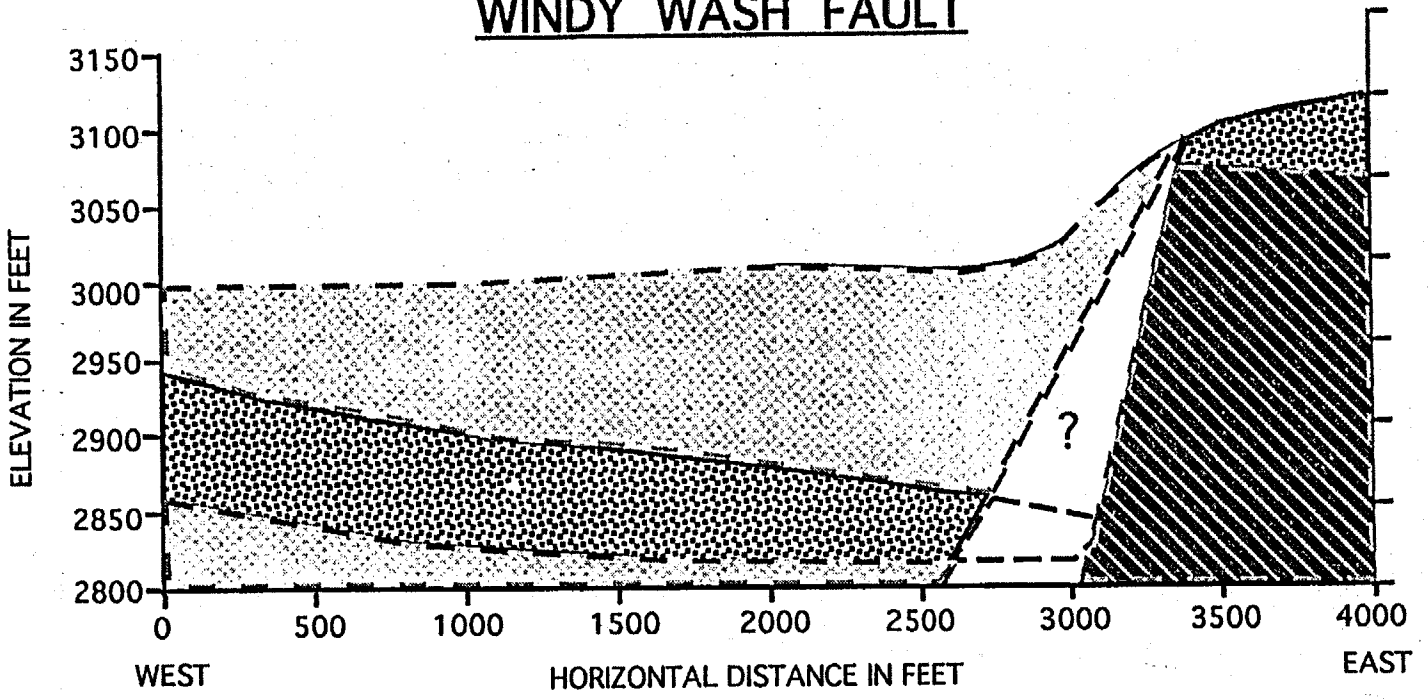

Photograph of

Solitario Canyon

and

Fatigue Wash

Fault Scarps

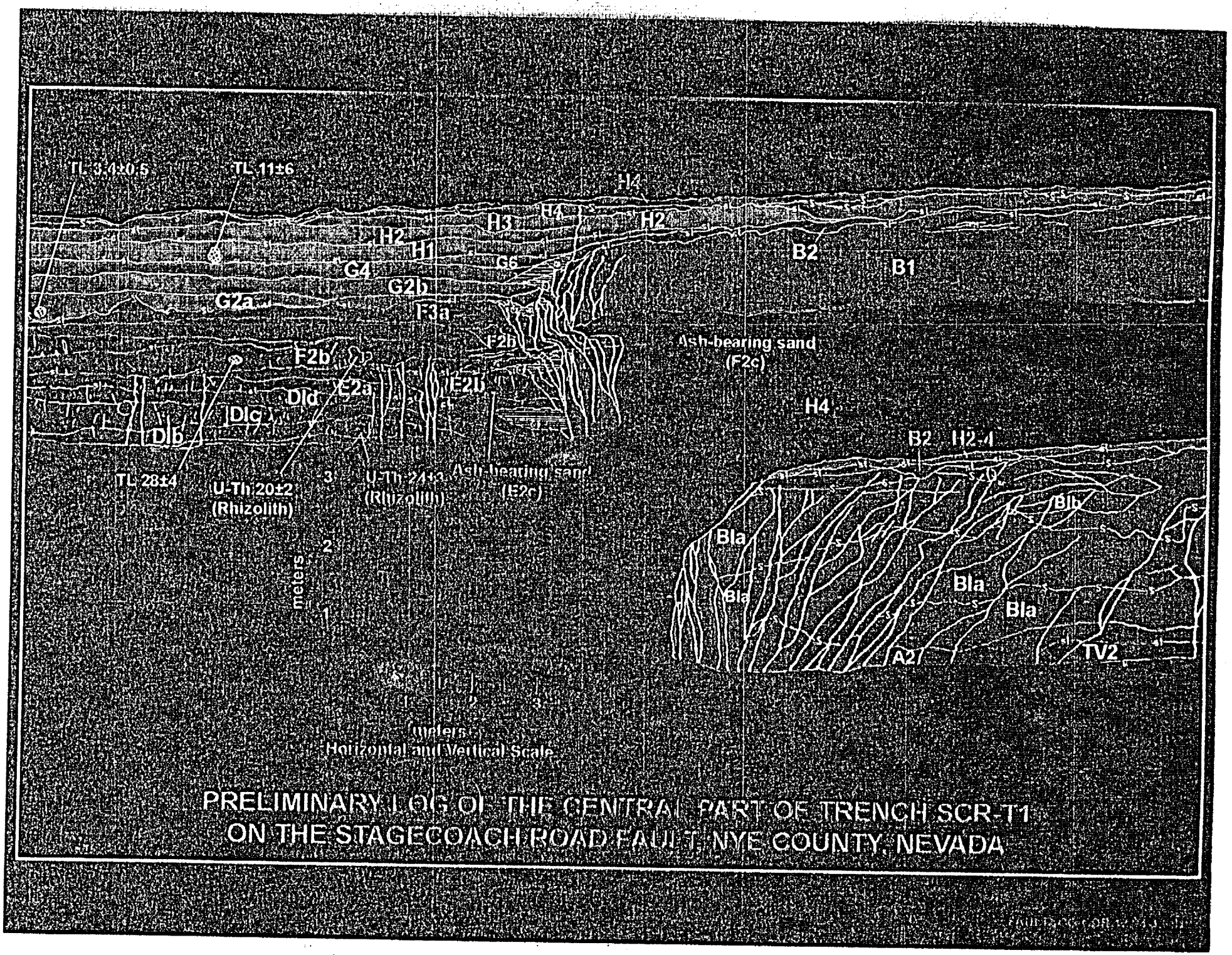

PRELIMINARY LOG OF THE CENTRAL PART OF TRENCH SCR-T1
ON THE STAGECOACH ROAD FAULT, NYE COUNTY, NEVADA

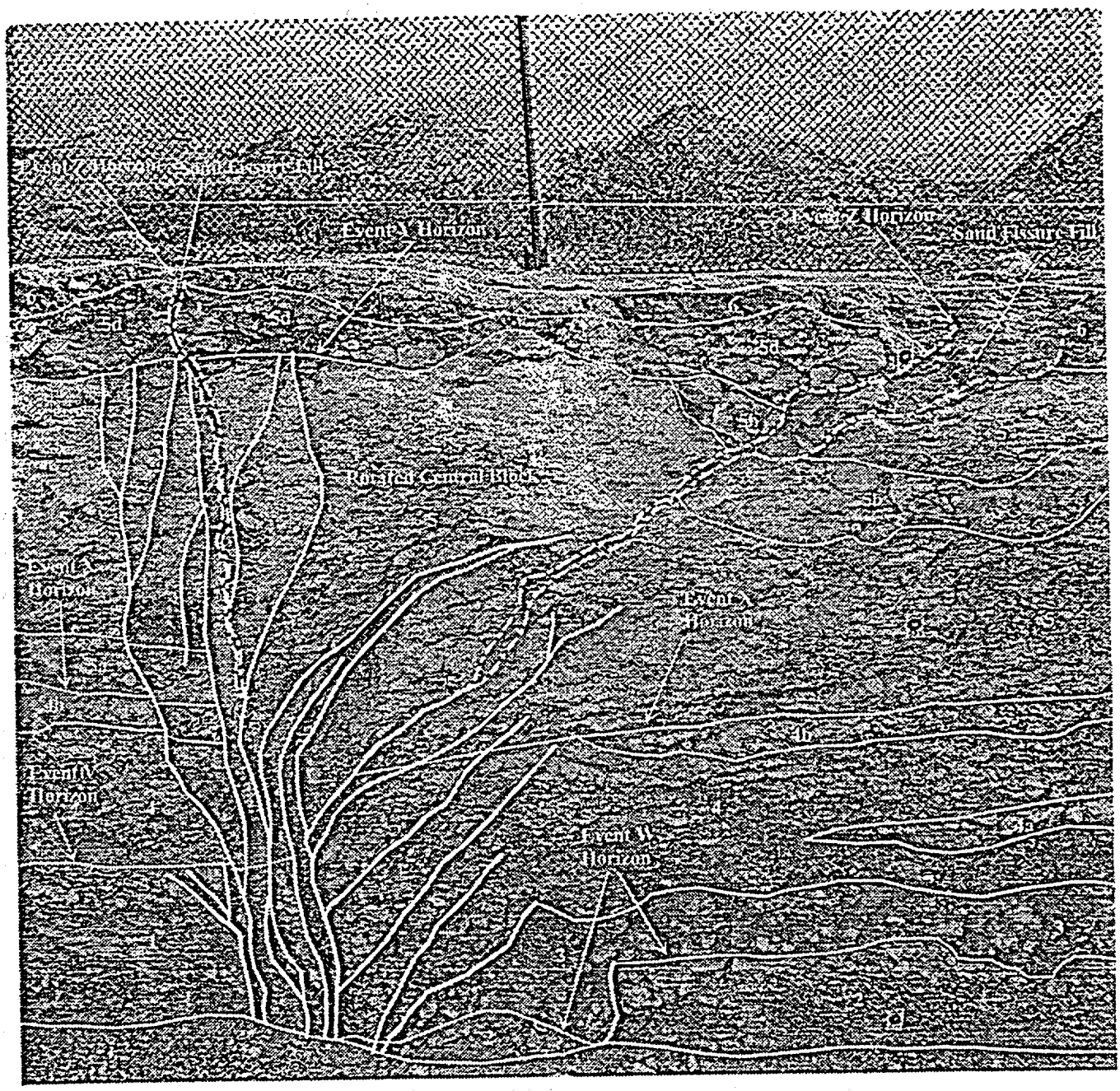

Northern Crater Flat Fault, Trench CFFT2a, Main Fault, South Wall, Event Horizons

Figure 4.11.3.

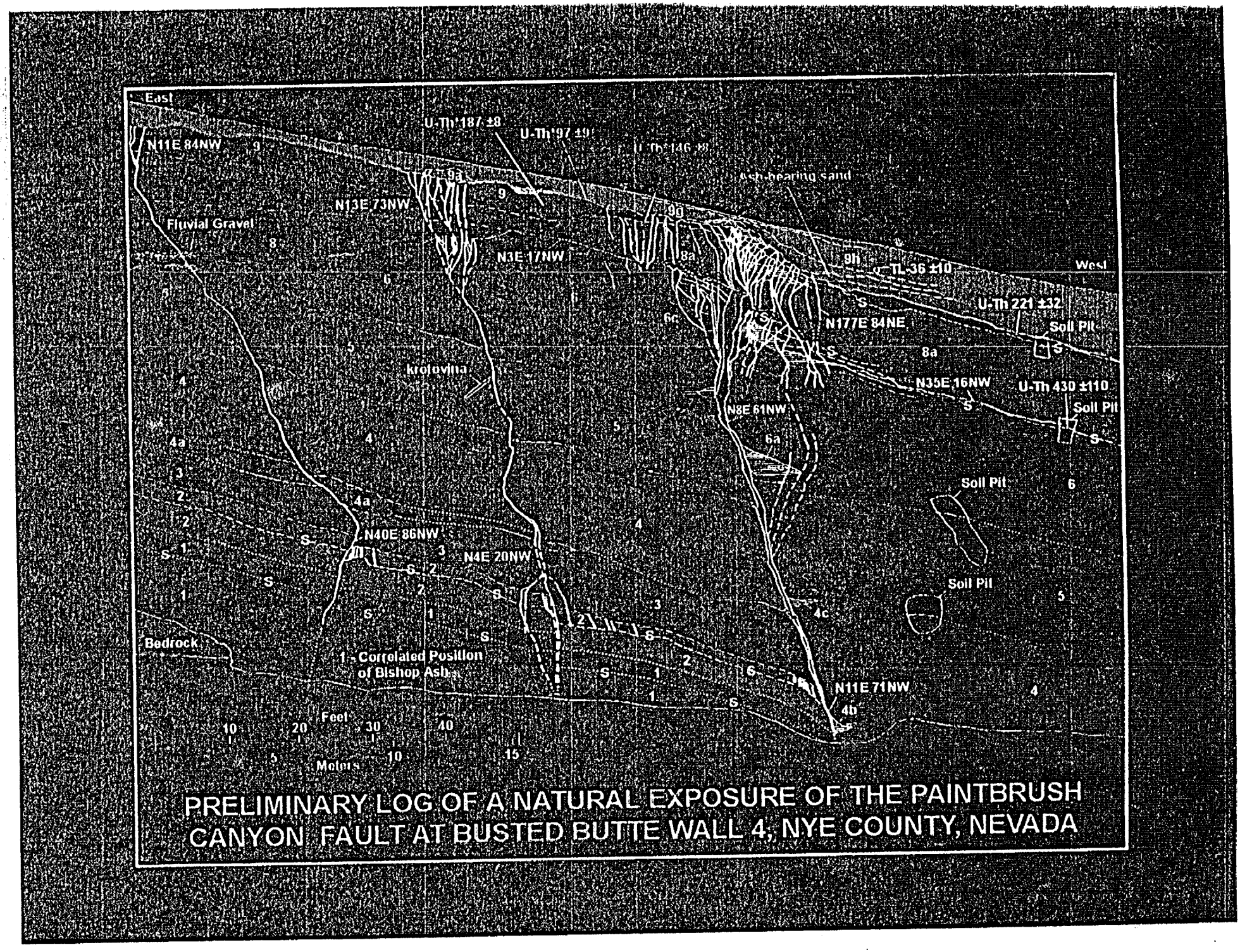
East
West
N11E 84NW
U-Th 187 ±8
U-Th 197 ±9
U-Th 146 ±8
ash-bearing sand
N13E 73NW
Fluvial Gravel
N3E 17NW
9h
TL 36 ±10
U-Th 221 ±32
Soil Pit
N177E 84NE
krotovina
N35E 16NW
U-Th 430 ±110
Soil Pit
N8E 61NW
Soil Pit
N40E 86NW
N4E 20NW
Soil Pit
Bedrock
1 - Correlated Position of Bishop Ash
N11E 71NW
Feet
Meters
PRELIMINARY LOG OF A NATURAL EXPOSURE OF THE PAINTBRUSH CANYON FAULT AT BUSTED BUTTE WALL 4, NYE COUNTY, NEVADA

Calculated and Estimated ( ) Slip Rates on Faults in the Yucca Mountain Area

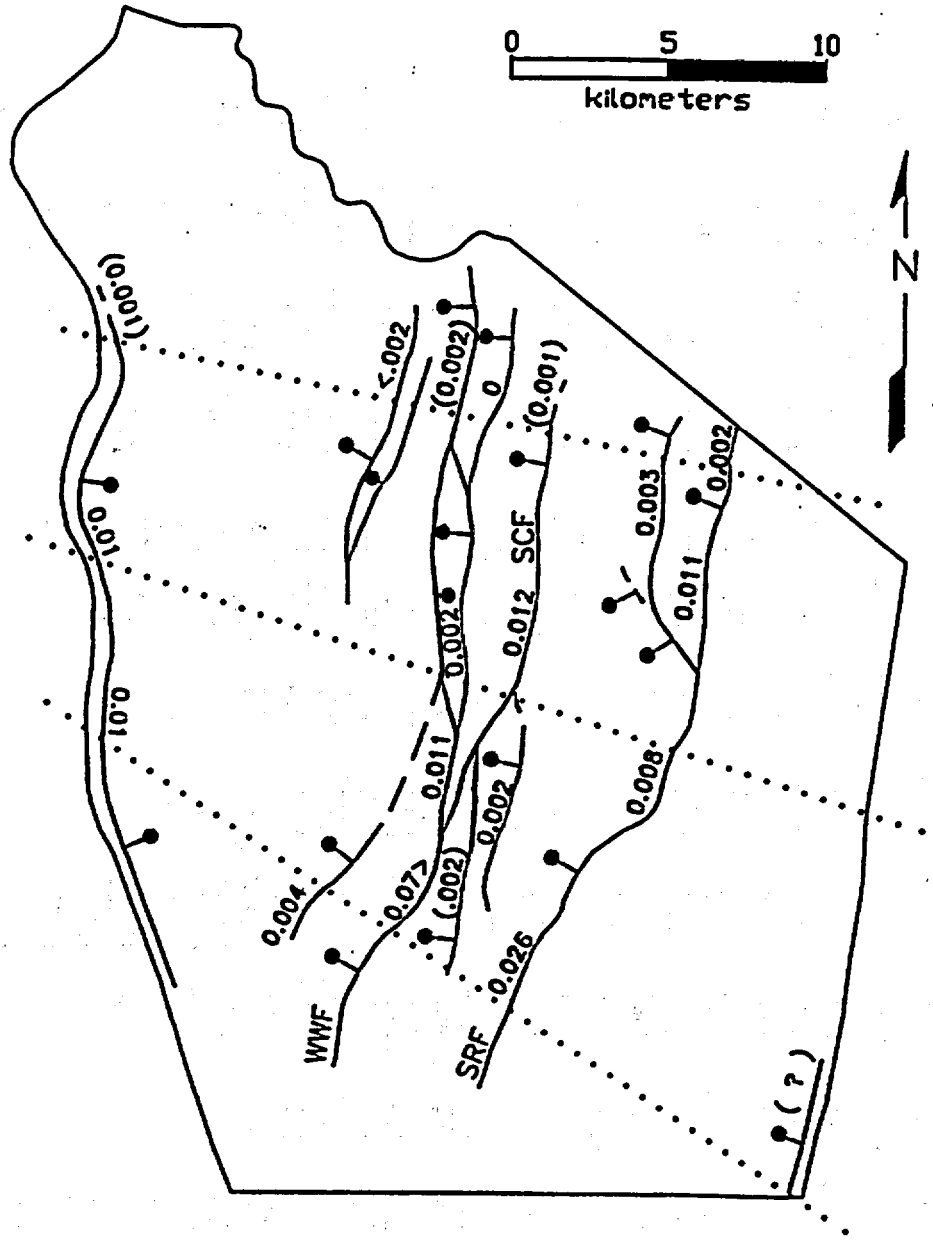

From: USGS Seismotectonic Report - Chapter 2

Some Definitions

- Paleoevent—'Paleo Surface Rupture' recognized in one trench across one fault
  - » fracturing may or may not represent an individual paleoearthquake
  - » trench and study specific
- Rupture Scenario—Paleoevents of a Similar Age on one or more Faults
  - » probable paleoearthquakes
  - » minimum and maximum rupture length
  - » displacement per event
  - » accounts for distributed faulting

Paleoearthquake Recurrence Data — Rupture Scenarios

Large Displacement Events

- Criteria:
  - » Preferred Displacements ≥50 cm, or Maximum Displacements ≥100 cm
  - » Smaller Displacements (<50 cm) are Secondary Faulting
- 500 kyr/ 12 Events = 44 (+10, -7) kyr
- 150 kyr/8 Events = 19 (+8,-4) kyr

in USGS Seismotectonic Report—Chapter 5

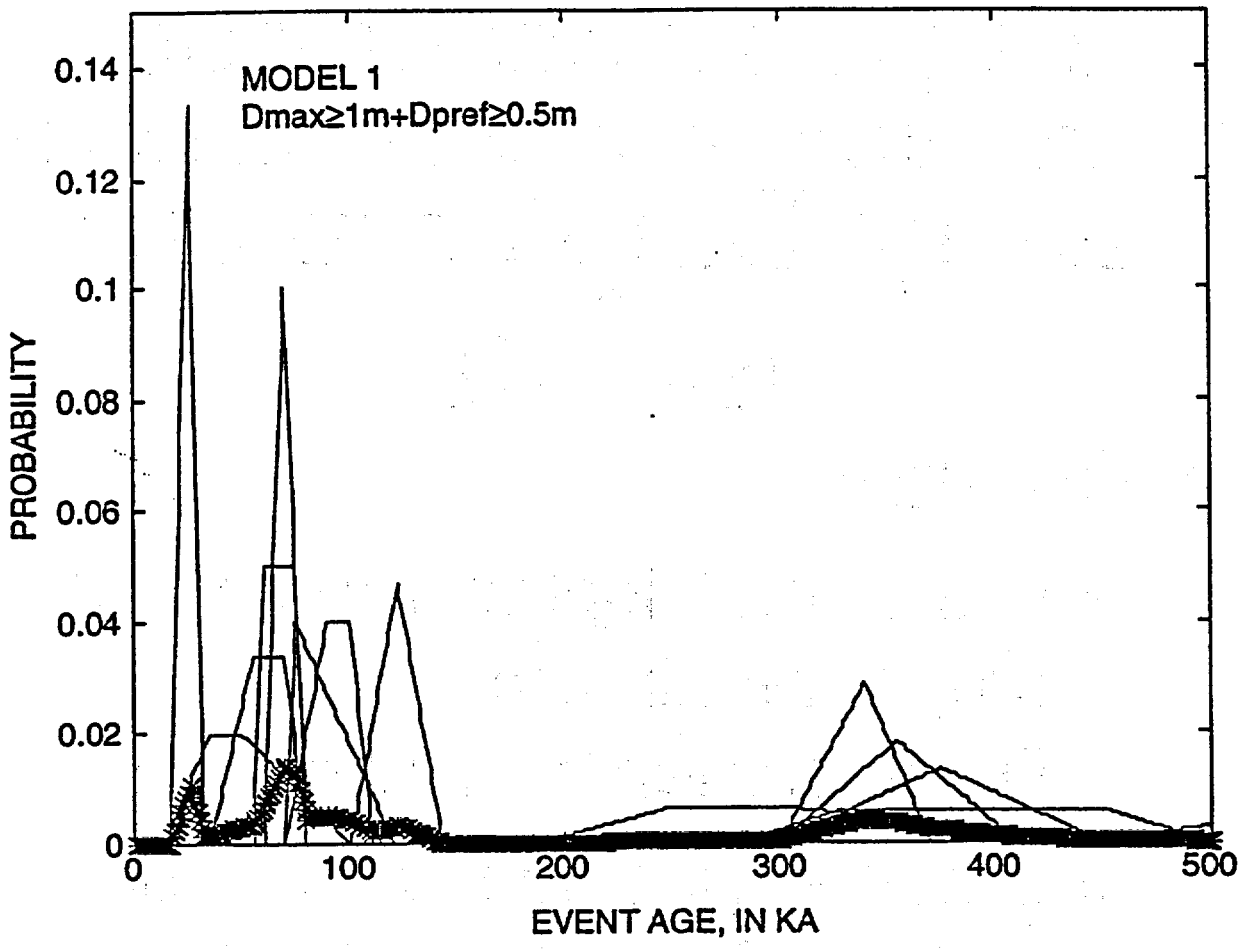
MODEL 1
Dmax≥1m+Dpref≥0.5m
PROBABILITY
0.14
0.12
0.1
0.08
0.06
0.04
0.02
0
0
100
200
300
400
500
EVENT AGE, IN KA

fig. 5-3

Paleoearthquake Recurrence Data — Rupture Scenarios

All Events Scenario

- All 39 Paleoevents are Individual Paleo Ruptures
  - » Temporal Uncertainties
    - – Dating Deposits, Not 'Events'
  - » Missed Paleo Surface Ruptures (< 25 cm)
    - – Erosion of Fault-Related Deposits due to Low Depositional Rates
- 500 kyr/ 39 (-10,+20) Events = 13 ± 5? kyr

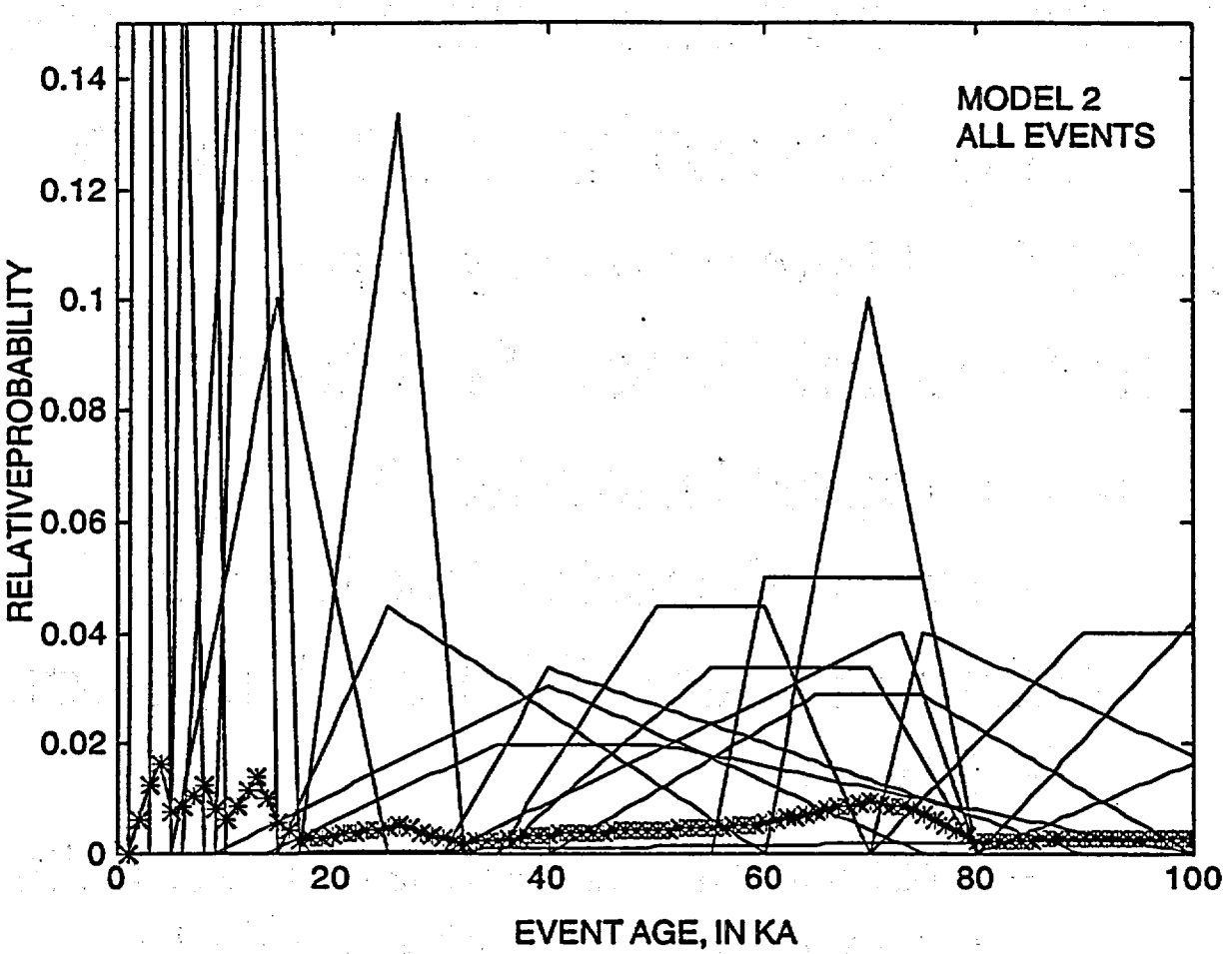
MODEL 2
ALL EVENTS
RELATIVEPROBABILITY
0.14
0.12
0.1
0.08
0.06
0.04
0.02
0
0
20
40
60
80
100
EVENT AGE, IN KA

figure 5-4-C

Paleoearthquake Recurrence Data — Rupture Scenarios

All Events Scenario (continued)

- 26 Paleoevents in last 150 (+ 10, -20) ka
  - » Cracking and Small Displacements are Counted as Individual Paleoearthquakes
  - » Geologic Record in Trenches Complete Only for Last 130 - 160 ka
- 150 kyr/ 26 Events = 5.8 (+ 0.4, - 0.8) kyr
  - » Recurrence increases if 2-4 paleoevents are 1 paleoearthquake

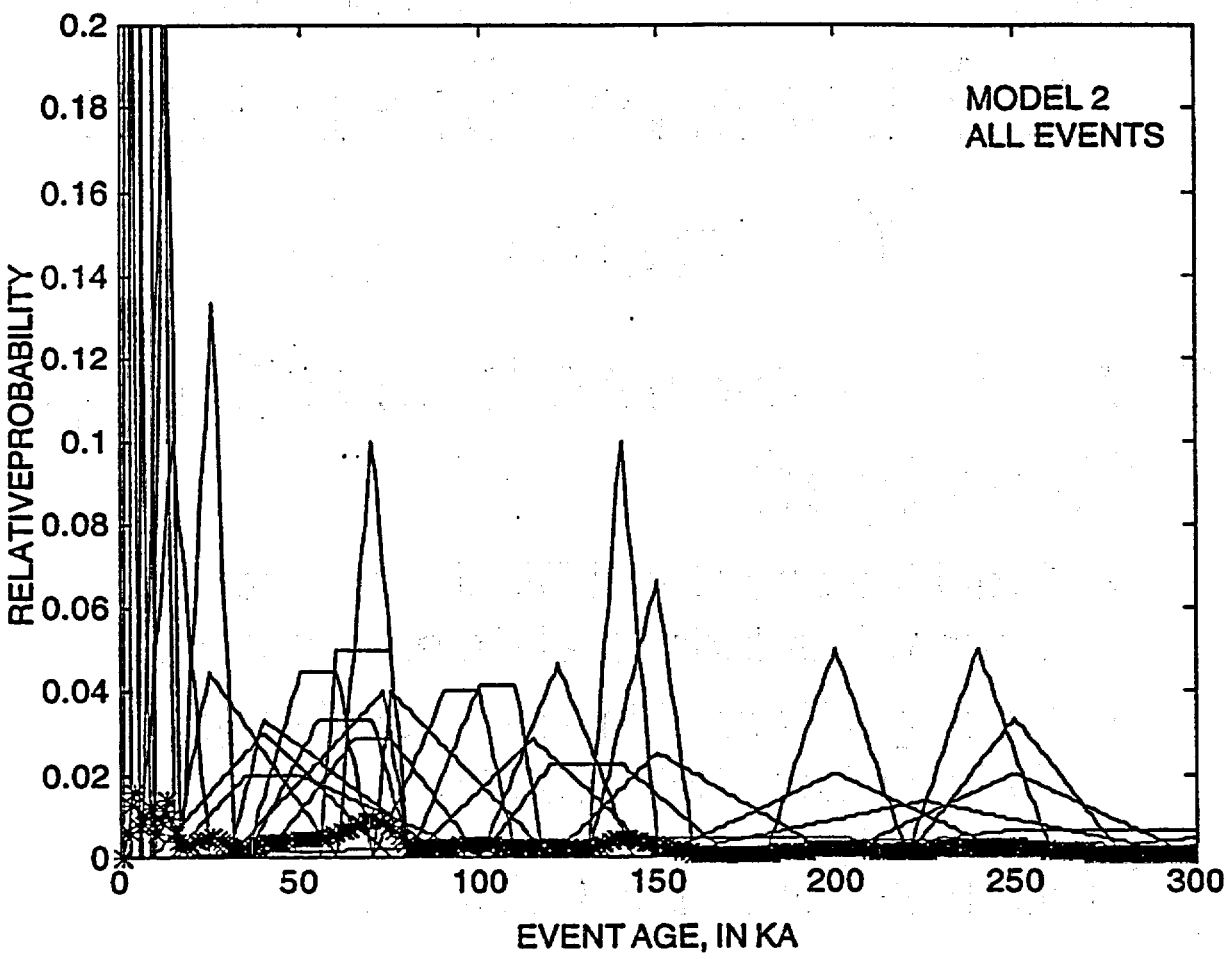
MODEL 2
ALL EVENTS
RELATIVEPROBABILITY
0.2
0.18
0.16
0.14
0.12
0.1
0.08
0.06
0.04
0.02
0
0
50
100
150
200
250
300
EVENT AGE, IN KA

figure 5-4-B

Paleoearthquake Recurrence Data — Rupture Scenarios

Rupture Scenarios

- Correlate Events in Time
  - » Use Stratigraphic and Geochronological Constraints
- 9 Rupture Scenarios Based on Timing Distributions
- 150 kyr/ 9 Events = 17 kyr ± 5 kyr

Paleoearthquake Recurrence Data — Rupture Scenarios

Rupture Scenarios Recurrence

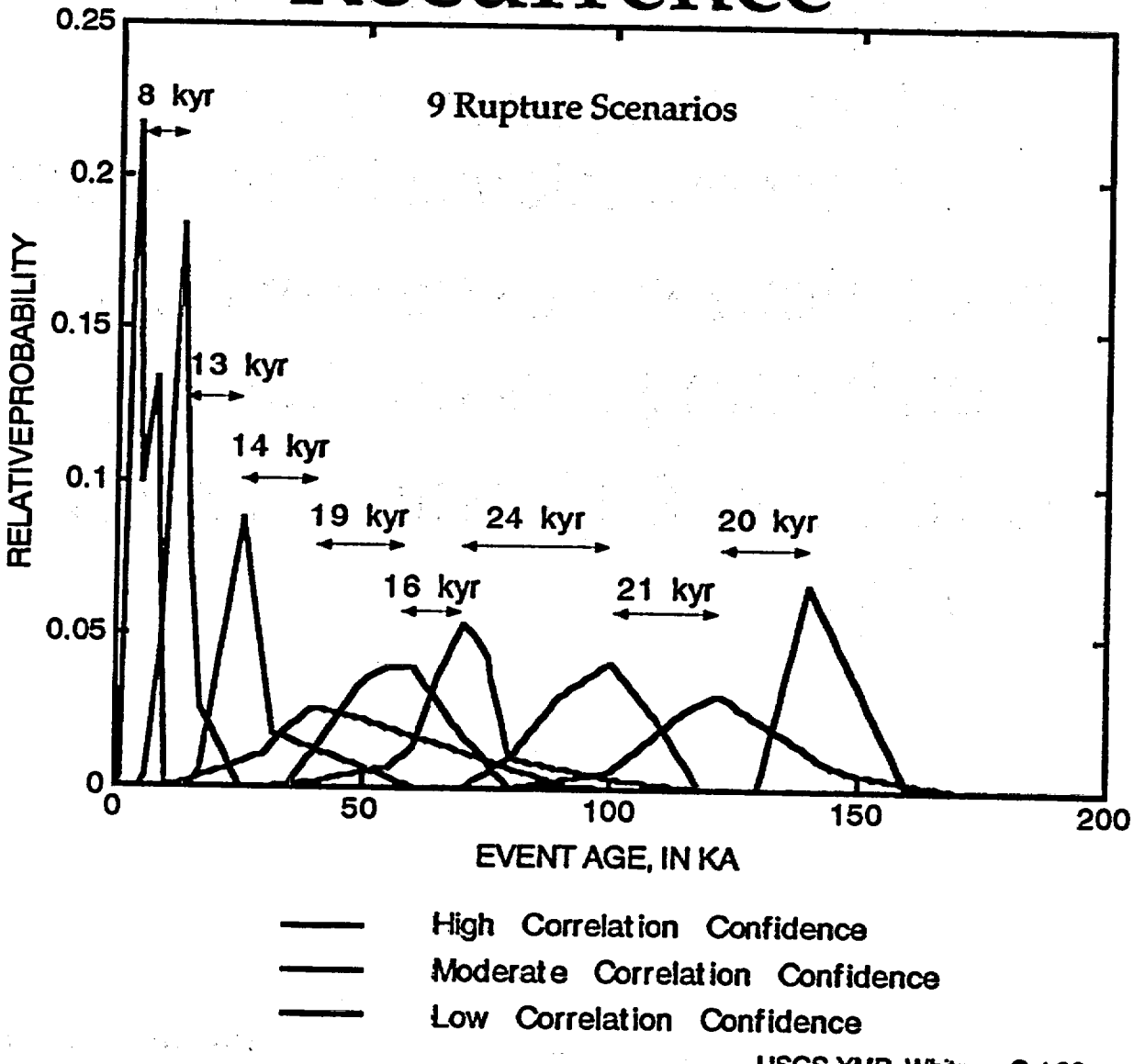

USGS-YMP Whitney Oct 96

in USGS Seismotectonic Report—Chapter 5

Results of the Earthquake Magnitude and Recurrence Models for Yucca Mountain Faults.

Recurrence Model	Number of Paleoevents	Average Recurrence Interval (kyr)
(Dmax ≥ 1 m & Dpref ≥ 0.5 m)		
1 (<500 kyr)	12	44 (+10, -7)
1 (<150 kyr)	8	19 (+8, -4)
(all events)		
2 (<500 kyr)	39	13 (± 5?)
2a (<500 kyr)	10-20?	35 (+15, -10)
2b (<150 kyr)*	26	5.8 (+0.4, -0.8)
*Recurrence increases if 2-4 paleoevents (distributed ruptures) are 1 paleoearthquake		
(rupture scenarios)		
3 (<150 kyr)	9	17 ± 5?

from: Seismotectonic Framework of Yucca Mountain, Chapter 5: Earthquake Magnitude and Recurrence

Presentation to the Yucca Mountain
Seismic Source Characterization Workshop #2:
Hazard Methodologies,
October 16-18, 1996

PALEOSEISMIC STUDIES OF THE SOLITARIO CANYON FAULT (SCF)

Alan R. Ramelli
Research Geologist
Nevada Bureau of Mines and Geology
University of Nevada
Reno, NV

I. Setting/rupture pattern

- Solitario Canyon fault (SCF) is one of several principal faults of an interconnected, anastomosing fault system ('Yucca Mt. fault system')

- Low, subdued fault scarp extends fairly continuously along SCF for at least 14 km; this is the longest continuous scarp at Yucca Mt., but not the most active fault

  - northern end of SCF scarp is adjacent to subsurface facilities area
  - southern end is poorly defined due to burial by young deposits

- SCF can be divided into four sections based on activity, each section is 4-5 km long (listed below in order of decreasing activity)

  1) south-central section has largest displacements and was primary focus of study
  2) southern section has smaller displacements than, and is separated from, section #1 by a bend in the SCF coincident with a splay connecting the SCF with the southern Windy Wash fault
  3) north-central section bounds subsurface facilities area; is separated from section #1 by a 1-km right step, and has relatively small displacement
  4) northern section has negligible Quaternary activity, although study at "Mile-high mesa" by Pezzopane indicates possible minor Pleistocene offsets

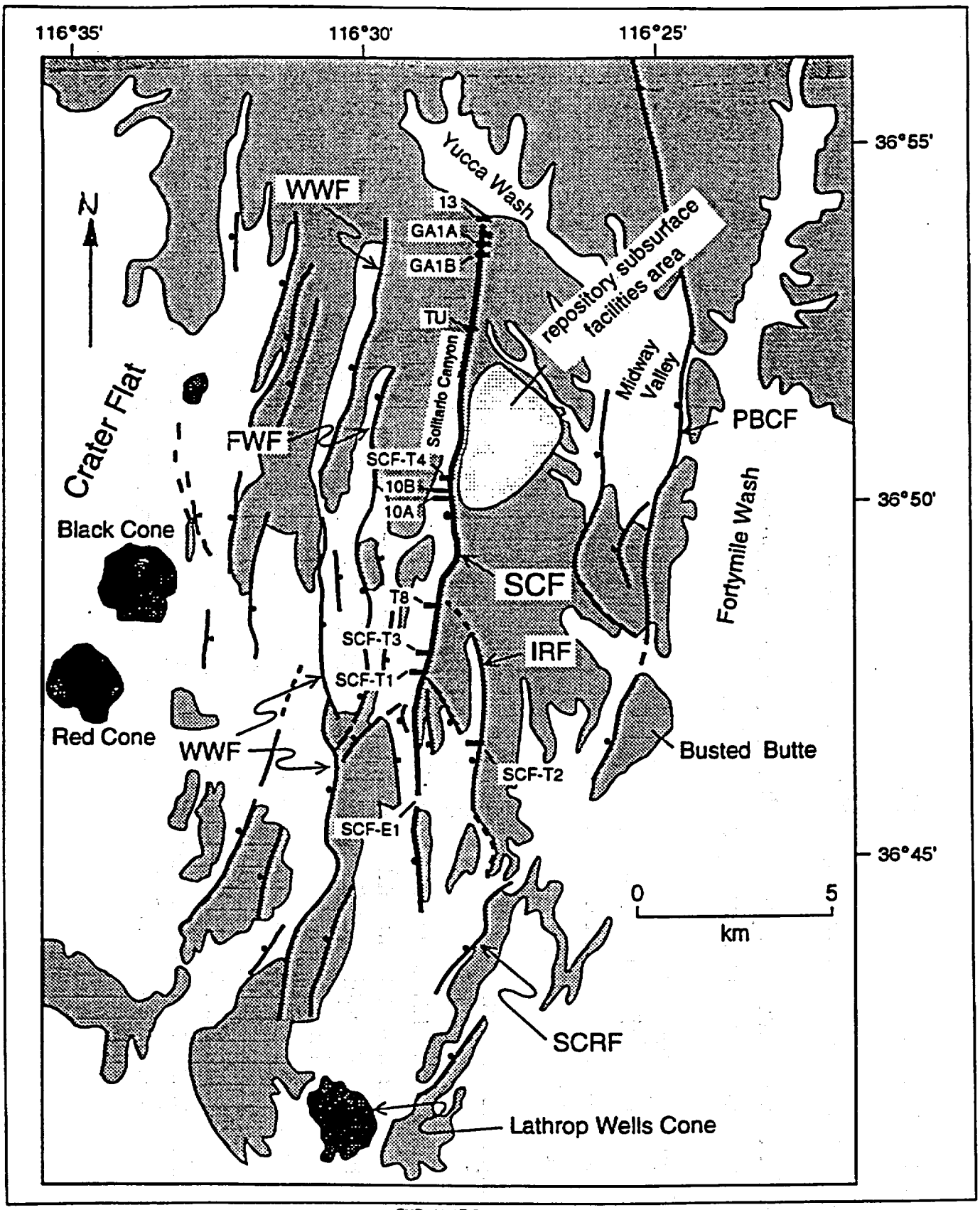

Figure 4.7.1 Generalized map of the Solitario Canyon fault and other nearby Quaternary faults at Yucca Mountain, with locations of exploratory trenches

II. Solitario Canyon fault trench: T8

- Originally excavated in early 1980's; deepened for this study

- Of all SCF trenches, apparently has largest displacements and most complete record of mid- to late Quaternary surface faulting

- Exposes gravels entirely engulfed in carbonate (unit 1); these deposits are >500 ka in age (possibly 1 Ma or older), and comprise much of alluvial fan surface and most of the adjacent downthrown colluvial surfaces, indicating low rate of Quaternary activity

- Sequence of events:
  - F1 - carbonate-cemented fault zone; fabric obliterated; juxtaposed against unit 1
  - F2 - gravel-filled fissure cut by 2-cm thick silica veins
  - F3 - earliest, and second largest, event cutting mid- to late Quaternary deposits
  - F4 - small, equivocal fissure; U-series age (HD1072, 118 $\pm$ 6 ka) is apparent minimum
  - F5 - largest event; 60-70 cm wide fissure containing basaltic ash; U-series ages (HD1070, 37 to 56 ka; HD1466, 47 $\pm$ 9 ka and 66 $\pm$ 23 ka) and one TL age (TL-30, 36 $\pm$ 5 ka) are apparent minimums
  - F6 - small ash-bearing fissure (north wall) and dragged ash (south wall); U-series age (HD1071, 15.5 $\pm$ 1.6 ka) is apparent minimum

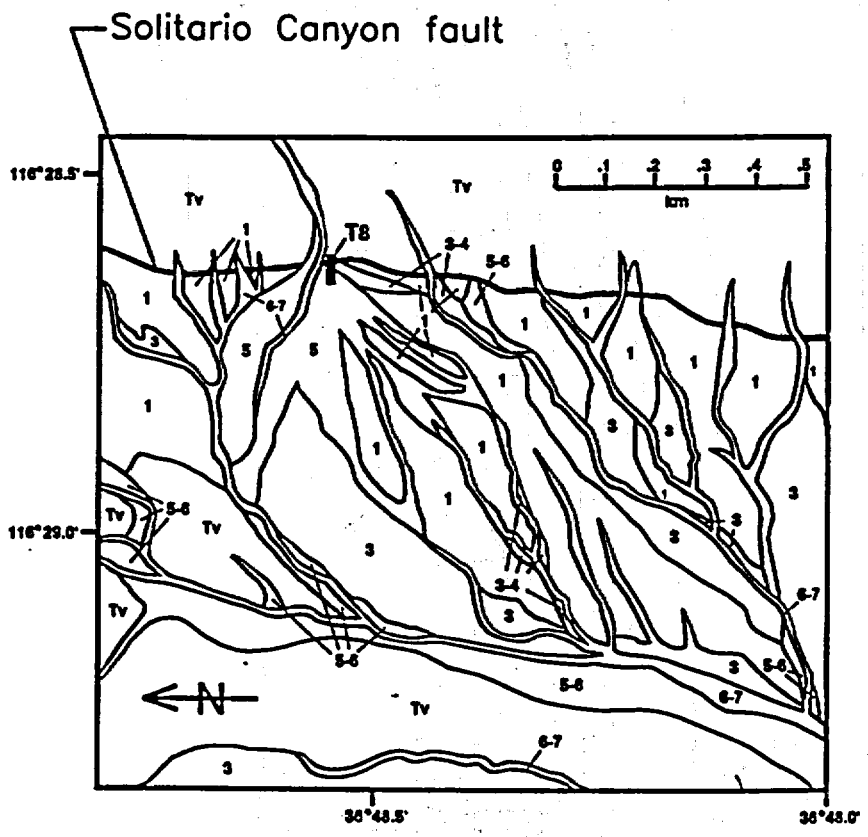

Figure 4.7.2. Preliminary map of the surficial geology at the T8 site along the Solitario Canyon fault

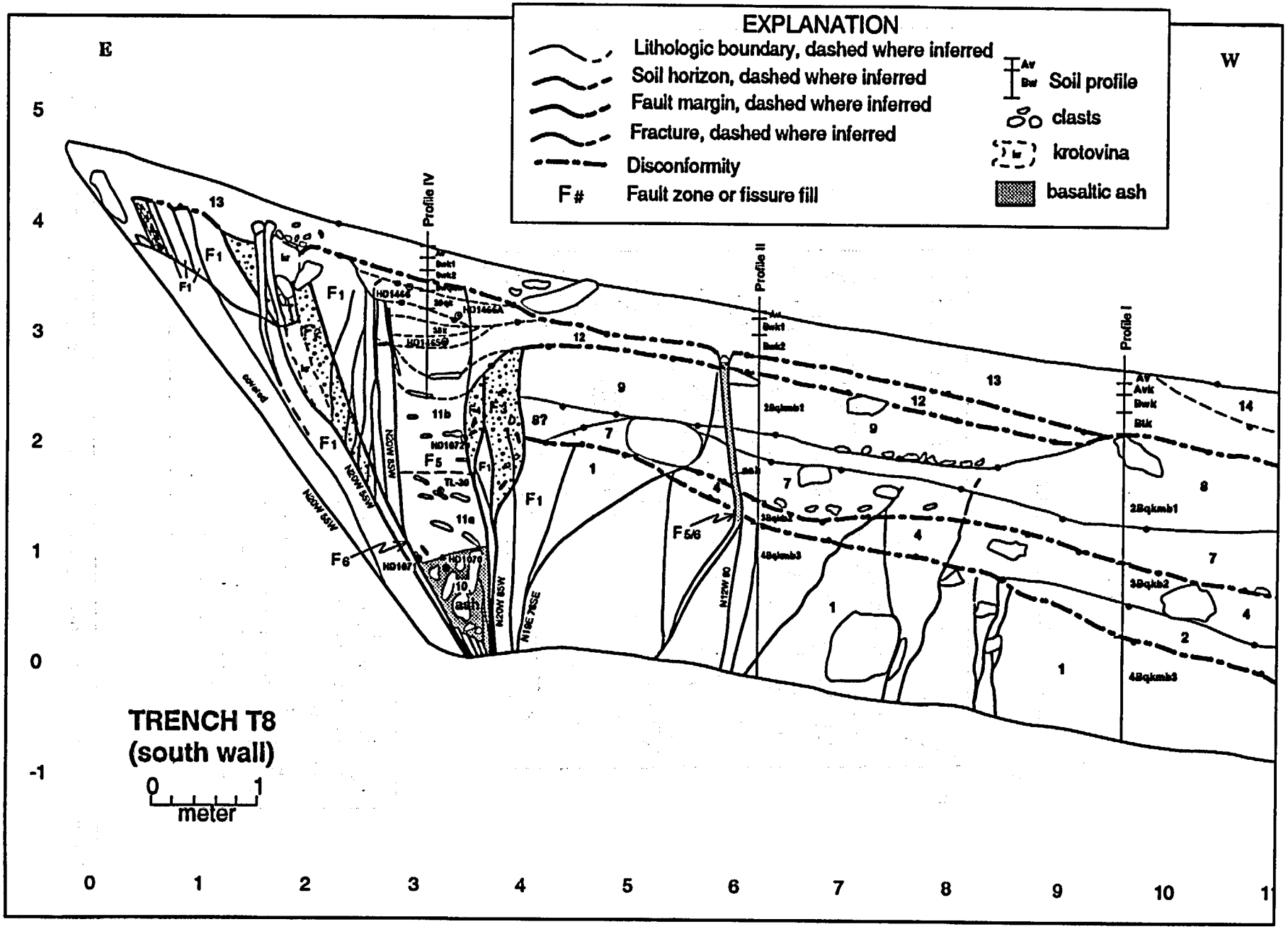
EXPLANATION
Lithologic boundary, dashed where inferred
Soil horizon, dashed where inferred
Fault margin, dashed where inferred
Fracture, dashed where inferred
Disconformity
F# Fault zone or fissure fill
Soil profile
clasts
krotovina
basaltic ash
E
W
Profile IV
Profile II
Profile I
TRENCH T8
(south wall)
0 1
meter
F1
F5
F5/6
F6
11a
11b
10
ash
2Bqkmb1
3Bqkb2
4Bqkmb3
0 1 2 3 4 5 6 7 8 9 10 11

III. Solitario Canyon fault trench: SCF-T3

- Located on colluvial slope in the hope it would provide a more complete record of surface faulting, but this did not turn out to be the case

- Massively-cemented ($CaCO_3$ Stage IV-V) colluvial deposits (units 8-9) are present near the surface on the downthrown side of the fault; these deposits yielded U-series ages of 700-900 ka, and are displaced only by mid- to late Quaternary events, providing the strongest evidence for temporal clustering

- Sequence of events:
  - F1 - massive $CaCO_3$ & $CaCO_3$-cemented gravels; includes gravel juxtaposed against massive $CaCO_3$ across fault @ 4.5 m; capped by unit 9, thus predating above U-series ages
  - F2 - cannot be discriminated from F1
  - F3 - 20-cm wide gravel- and silt-filled fissure; poss. related to wedge-shaped deposit (unit 10); crosscut by dipping F5 fissure
  - F4 - not recognized, although possibly bounding eastern F5 fissure
  - F5 - two prominent basaltic ash-filled fissures; 30-60 cm summed width; tops erosionally truncated
  - F6 - carbonate-filled fractures cutting eastern F5 fissure

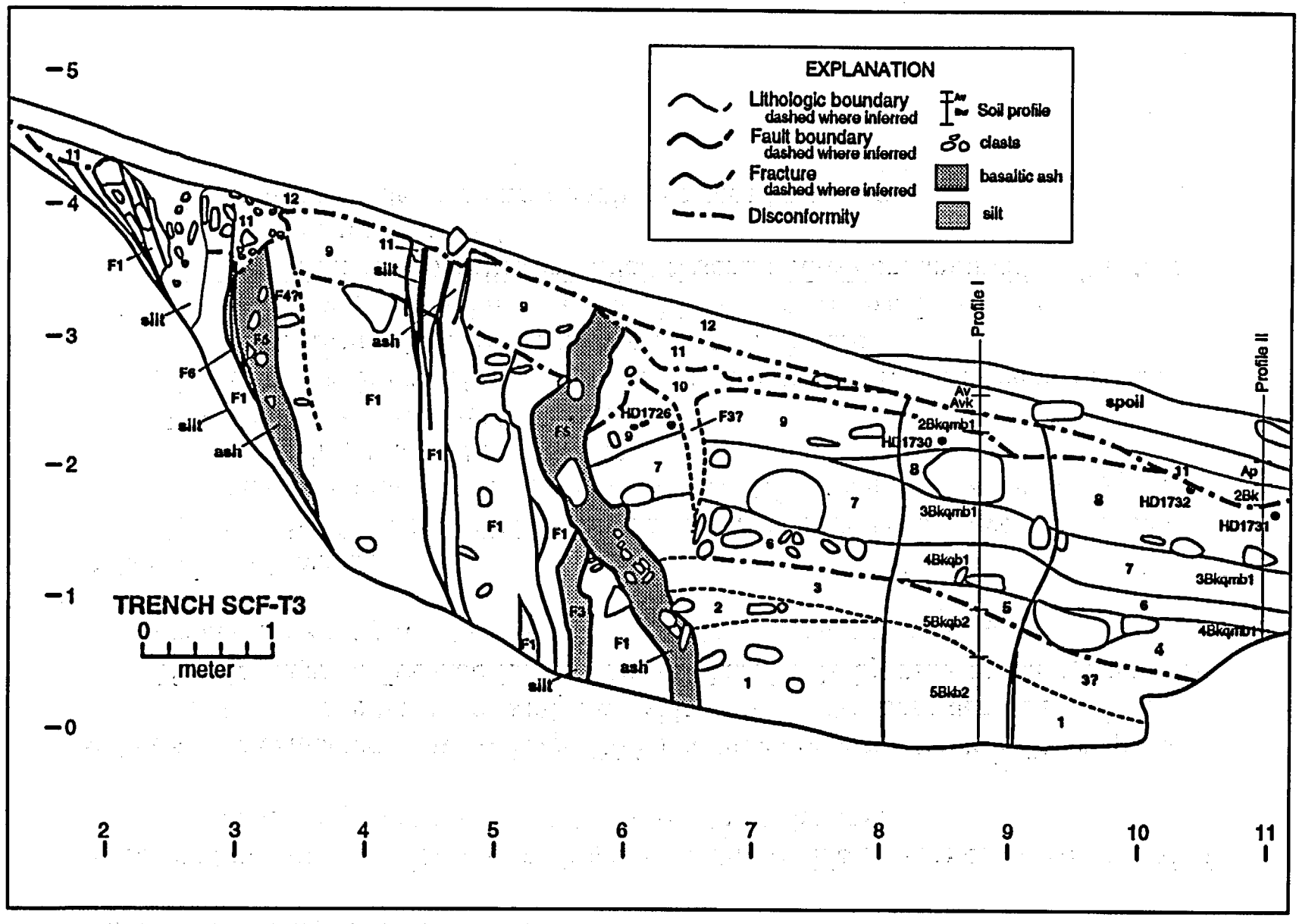
EXPLANATION
Lithologic boundary
dashed where inferred
Fault boundary
dashed where inferred
Fracture
dashed where inferred
Disconformity
Soil profile
clasts
basaltic ash
silt
TRENCH SCF-T3
0
1
meter
Profile I
Profile II
spoil
silt
ash
F1
F2?
F3
F4?
F5
F6
F37
HD1726
HD1730
HD1731
HD1732
2Bkqmb1
3Bkqmb1
4Bkqb1
5Bkqb2
5Bkb2
4Bkqmb1
Av
Avk
Ap
2Bk
−5
−4
−3
−2
−1
−0
2
3
4
5
6
7
8
9
10
11

IV. Solitario Canyon fault trench: SCF-T1

- Excavated across lineament/apparent small scarp on latest Pleistocene/early Holocene alluvial fan surface; surficial deposits determined to be unfaulted

- Incomplete record of faulting due to erosive environment

- Cementation of units 7-8 (Stage IV-V) is comparable to deposits in SCF-T3 yielding 700-900 ka U-series ages

- U-series samples from SCF-T1 have not been analyzed

- Sequence of events:

  F1 - evidenced by faulting/backtilting of units 1-4
  F2 - likely part of progressive offset of units 5-7 (shown schematically; relations obscured by $CaCO_3$ overprinting)
  F3/4 - cannot be discriminated; poss. slip along main fault zone cutting unit 8 and/or fracturing of units 7-8 between 18.5 & 20 m on log
  F5 - two prominent basaltic ash-filled fissures (about 16.5 & 19 m on log); slip along main fault cannot be ruled out
  F6 - minimal cementation of probable small colluvial wedge (unit 17), suggests this event may have occurred along main fault zone prior to deposition of unit 19 containing argillic soil

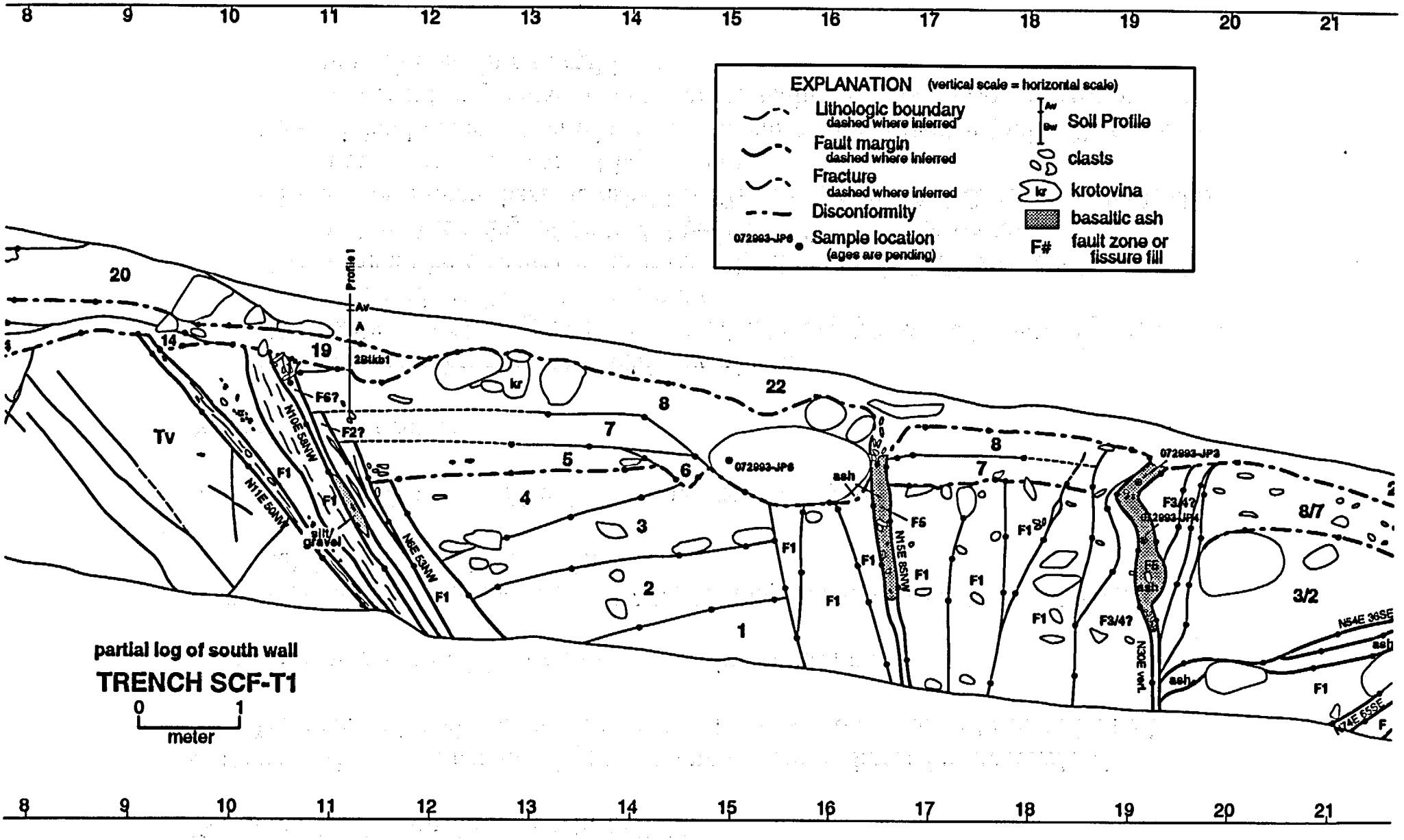
8 9 10 11 12 13 14 15 16 17 18 19 20 21
EXPLANATION (vertical scale = horizontal scale)
Lithologic boundary dashed where inferred
Fault margin dashed where inferred
Fracture dashed where inferred
Disconformity
072993-JP6 Sample location (ages are pending)
Soil Profile
clasts
kr krotovina
basaltic ash
F# fault zone or fissure fill
Profile 1
Av
A
2Btkb1
kr
F6?
F2?
Tv
N10E 58NW
N11E 50NW
N6E 53NW
N15E 85NW
N3E Ver.
N5AE 36SE
N7AE 65SE
F1
F2
F3/4?
F5
F6
ash
silty gravel
072993-JP6
072993-JP3
072993-JP4
20
19
14
22
8
7
6
5
4
3
2
1
8/7
3/2
partial log of south wall
TRENCH SCF-T1
0 1
meter

V. Solitario Canyon fault trench: SCF-T4

- Excavated into eroded remnant of hillslope colluvium to assess activity of SCF adjacent to subsurface facilities area of proposed repository

- Similar to other SCF trenches, mid- to late Quaternary surface faulting expressed as subvertical, extensional fissure openings

- Much less displacement than trenches T8, SCF-T3, & SCF-T1; Quaternary deposits downthrown against fault are <3 m thick, and mid- to late Quaternary events formed a zone of fissuring only 20-30 cm wide

- Sequence of events:

  F1 - Faulting of units 2-3 and formation of apparent colluvial wedge (unit 4)
  F2 - Fissure ≤ 10 cm wide cuts unit 4; capped by cemented deposits (units 5-6)
  F3 - Cemented fissure 5-10 cm wide cutting units 5-6
  F4 - Not recognized
  F5 - Basaltic ash-filled fissure; apparently accounts for most of mid- to late Quaternary displacment
  F6 - $CaCO_3$-cemented fractures cutting F5 fissure

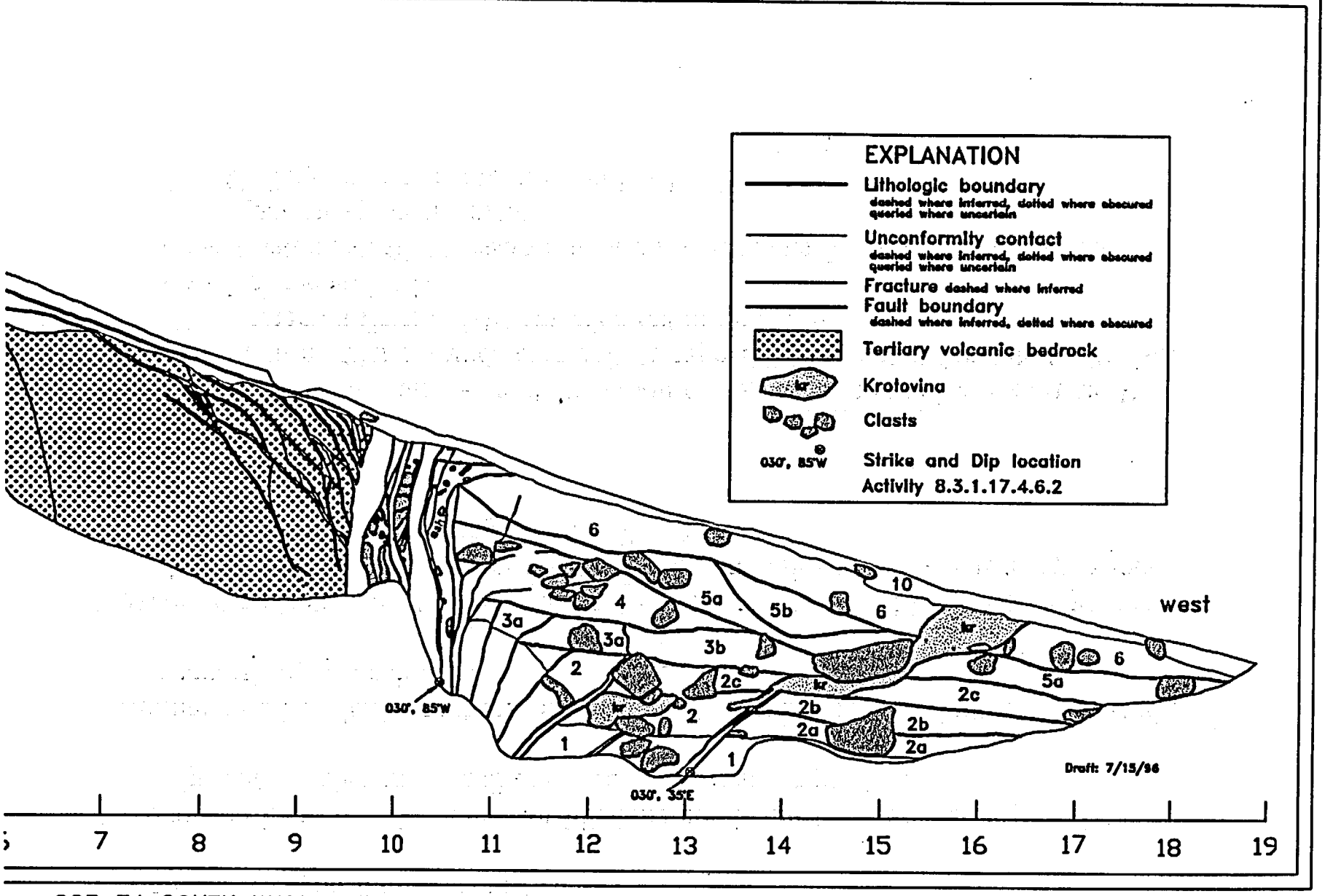

SCF-T4 SOUTH WALL, Solitario Canyon Fault
by A. Ramelli, J. Oswald, and G. Vadurro
March, 1994
Figure 4.7.8

VI. Mid- to late Quaternary sequence of events on SCF followed a hiatus in activity

- Surface ruptures along SCF can be reasonably correlated between trenches; relations are consistent with a sequence of events over the mid- to late Quaternary (last 200 ka or so) that followed a hiatus in activity lasting for several hundred thousand years or more.

- Deposits engulfed in carbonate and silica are present on the downthrown side of the fault at or near the surface at all sites; at SCF-T3, these deposits cap the older fault zone and yielded U-series ages on silica rinds of 700-900 ka

- Two events account for most of the mid- to late Quaternary offset; fissures containing abundant basaltic ash at all sites are almost certainly correlative and indicate offsets at least twice as large as any other event; all trenches except SCF-T1, which has an incomplete record, indicate an earlier event with about half the offset as that containing the ash; expression of smaller events, with displacements of no more than a few 10's of cm, are variable and in some cases equivocal.

- At least two fracturing events postdate the most recent event with definable displacement; older, similar features would be impossible to discriminate; the origin(s) of these fractures are problematic, and could include both tectonic and nontectonic causes.

Table 4.7.3 Estimated displacements associated with mid- to late Quaternary surface faulting events along the Solitario Canyon fault

Event	Age (ka)	SCF-T4	T8	SCF-T3	SCF-T1	Comments
?	5-15	np	0?	0?	np	Silt-filled openings
?	15-25	np?	0	np?	np?	Cemented fracture
Z	20-30	0-10?	10-20	0-10?	?	Minor fissure; fracturs in event Y fissure fill; dragged event Y ash
Y	70-80	20-40	110-130	60-120	50-120	Largest event; fissures contain basaltic ash
X	120-200	np?	20-40	?	?	15 cm wide fissure in T8
W	150-250	15-30	30-60	20-40	?	Second largest event
cumulative offset		60-80	180-260	80-130	150-250	

VII. Possible association of faulting and basaltic volcanism

- In all SCF trenches, the largest fissures contain enough basaltic ash to appear black, and at T8, nearly-pure, angular basalt fragments fill the bottom meter of the fissure; these relations indicate ash was emplaced shortly after fissure opening, and strongly suggest that faulting and volcanism were somehow associated.

- Available data are permissive of, but do not prove, an association between the the mid- to late Quaternary activity on the SCF and eruptive activity at the Lathrop Wells cinder cone: 1) fissures both predating and postdating the prominent ash-bearing fissure contain lesser amounts of ash, but in neither case can reworking of ash be precluded; 2) the time span of eruptive activity approximately coincides with the sequence of mid- to late Quaternary faulting; and 3) temporal coincidence of faulting and volcanism during multiple events are permissive given available age constraints.

- Although the downdip extension of the southern SCF could intersect the feeder dike of the Lathrop Wells cinder cone, the largest surface offsets (central part of the fault) are spatially removed from the eruptive center.

VIII. Yucca Mt. faults are unlikely to behave independently

- Individual fault traces are generally short and highly interconnected.
- Of Quaternary faults rupturing the surface, the most active are NNE-striking, west-facing faults in the southern part of the area, including Stagecoach Road, Windy Wash, and Crater Flat faults; the central part includes numerous, less-active faults, including Solitario Canyon, Fatigue Wash, and several east-facing faults; faults in the northern part are mostly west-facing and exhibit only minor Quaternary activity.
- The northward decrease in activity suggests that activity is 'driven' from the south.
- The apparent association of spatially-separated surface faulting and volcanism may indicate both are related to broader deformation and/or slip on buried structures.